Imperial College London

The influence of salt tectonics in the evolution of the Subalpine chains, Haute-Provence, France

A thesis submitted to

Imperial College London

For the degree of

Doctor of Philosophy (PhD)

Lajos Adam Csicsek

Department of Earth Science and Engineering

Imperial College London

Statement of originality

I certify that the research presented in this thesis is my own PhD research carried out under the supervision of Dr Lidia Lonergan and Prof. Rodney Graham. The results presented here have not been previously submitted to Imperial College London or any other academic institution for a degree or diploma, or any other certification.

Lajos Adam Csicsek

December 2023

Copyright declaration

The copyright of this thesis rests with the author. Unless otherwise indicated, its contents are licensed under a Creative Commons Attribution-Non Commercial 4.0 International Licence (CC BY-NC).

Under this licence, you may copy and redistribute the material in any medium or format. You may also create and distribute modified versions of the work. This is on the condition that: you credit the author and do not use it, or any derivative works, for a commercial purpose.

When reusing or sharing this work, ensure you make the licence terms clear to others by naming the licence and linking to the licence text. Where a work has been adapted, you should indicate that the work has been changed and describe those changes.

Please seek permission from the copyright holder for uses of this work that are not included in this licence or permitted under UK Copyright Law.

Abstract

The Subalpine chains of Haute Provence have been studied for over 100 years. Upper Triassic evaporites are known to be the basal detachment surface for thin-skinned Alpine compression and diapirs have been also identified. However, the importance of salt tectonics during Tethyan rifting and the passive margin subsidence which followed it, and the influence of precursor salt structures in the evolution of the Alpine fold and thrust belt have been underestimated. This work describes pre-Alpine salt structures in the Subalpine chains in more detail and discusses in depth the effects of salt tectonics in the evolution of the fold and thrust belt.

The initiation of salt tectonics was triggered by the Early-Middle Jurassic Tethyan rifting. First generation salt structures developed north of the Provençal platform in the slope and basin palaeogeographical domains. Passive diapirism dominated during the subsequent passive margin phase leading to the formation of a polygonal primary minibasin and salt-ridge system.

Salt tectonic activity culminated in the extrusion of evaporites onto the seafloor during the Albian-Cenomanian and coincided with the deposition of black shales. Allochthonous salt sheets were emplaced from mature diapirs, and extrusive sheets coalesced to form a salt canopy which covered large areas of the primary minibasin and salt-ridge system and the Tethyan margin. A second generation of salt structures developed above the canopy, and they bounded elongated secondary minibasins.

From the Late Cretaceous onwards, Alpine compression led to the squeezing of the first-generation salt structures and depletion of the canopy. Secondary minibasins were carried as piggyback basins in the actively deforming fold and thrust belt and the interaction of salt tectonics and thrusting resulted in the formation of asymmetric hybrid basins.

The geometry of the pre-Alpine salt structures and adjacent minibasins strongly influenced the structural style of the fold and thrust belt.

Acknowledgements

First, I would like to thank my supervisors, Lidia Lonergan and Rod Graham for their guidance, proficiency, and advice throughout these long years. Finishing of the thesis would not have been possible without your help. I am extremely grateful for your endless support when I was confronting the hardship of my underlying health conditions.

Many thanks to Sam Brooke-Barnett. We started to understand local and regional scale problems together and without your ideas and help, I could not solve the mysteries of salt tectonics around Castellane and Barrême.

Thanks to our French colleagues, Jean-Paul Callot, Naïm Célini and Jean-Claude Ringenbach, for their ideas, support, and friendship. They helped me to get a better understanding of salt tectonics both in Haute-Provence and in the Sivas basin.

I am grateful for the financial support of NERC and Imperial College London through the CDT in Oil & Gas programme.

I am grateful for the financial support of Imperial College London's COVID stipend extension scheme. I would like to the thanks to CASP for their Research Award for Geological Fieldwork, which made my first visit to Haute-Provence possible in 2017.

I am deeply thankful to Amanda Allotey, Saskia Goes, Lorna Morrow and Emma Watson for their contribution and guidance with administration.

I want to thank all my friends and all the lovely people in the department for the inclusive culture and environment.

I am thankful for my friends who willingly helped me as field assistants in the Subalpine chains, from the mountain tops to the bottom of the gorges. Thanks to Soma Budai, Gábor Csillag, Herkules Gábor Héja, Vencel Lovrity, Tamás Müller and Éva Oravecz who were always helpful and reliable during those long days in the mountains.

The Communauté de Communes Alpes Provence Verdon is thanked for providing the drone image of the area surrounding the village of Barrême.

And, of course, I am extremely grateful for the endless support and patience of my fiancé, Amália Nagyillés. I also thank to my family for their support. They helped me through my long journey from Hungary to London and France and back again.

Table of Contents

ABSTRACT 3

ACKNOWLEDGEMENTS 4

TABLE OF CONTENTS 5

TABLE OF FIGURES 8

CHAPTER 1: GENERAL INTRODUCTION 32

1.1. AIM OF THE WORK 33

1.2 ORGANIZATION OF THE THESIS 34

1.3 INTRODUCTION TO SALT TECTONICS 35

1.3.1 'Salt, the viscous rock' *35*

1.3.2 Processes of salt movement and diapir growth. Salt structures *36*

1.3.3 Minibasins: Depocenters subsiding into salt *39*

1.3.4 Internal deformation within minibasins and salt-sediment interactions *43*

1.3.5 Welds: structures marking vanished salt bodies *48*

1.3.6 Salt tectonics in compressional settings and folded belts *49*

1.4 DATA/METHODOLOGY/FIELDWORK 56

CHAPTER 2: GEOLOGICAL SETTING AND STRATIGRAPHY 57

CHAPTER 3: PREVIOUSLY RECOGNISED SALT RELATED STRUCTURES AND SALT TECTONICS IN THE SUBALPINE CHAINS 72

3.1 BARLES FLAP 74

3.2 LA ROBINE UNIT 75

3.3 VÉLODROME MINIBASIN 76

3.4 LA CINE FAULT 77

3.5 GÉVAUDAN DIAPIR 79

3.6 ST-JURS 'DIAPIRIC INTRUSION' 79

3.7 ROUAINE-DALUIS FAULT SYSTEM AND THE DALUIS DIAPIR 81

3.8 VALBERG-BEUIL WELD 84

3.9 PUGET-THÉNIERS DIAPIR 85

3.10 CONCLUSION 86

CHAPTER 4: JURASSIC-EARLY CRETACEOUS MINIBASIN FORMATION ABOVE THE AUTOCHTHONOUS EVAPORITE LEVEL 88

4.1 JURASSIC-EARLY CRETACEOUS SALT TECTONICS IN THE SOUTHERN STRUCTURAL DOMAIN, AROUND BLIEUX AND CASTELLANE.

OBSERVATIONS, STRUCTURAL AND STRATAL GEOMETRIES 90

4.1.1. The Taloire syncline, the Porte de St-Jean syncline and the Taulanne syncline: depocenters and their bounding salt structures of the southern structural domain *91*

4.1.1.1. The St Vincent diapir and the la Grau anticline. Structural and stratigraphic observations 95

4.1.1.2. The Taulanne syncline. Structural and stratigraphic observations 98
4.1.1.3. The Chasteuil salt structure 103
4.1.1.4. The Port de St-Jean syncline 108
4.1.1.5. An overturned flap at Brayal, the Crête de Colle Bernaiche section 113
4.1.1.6. The Taloire syncline and the la Crotte-Deneiras area 115
4.1.1.7. Newly identified minibasins and salt structures: Interpretation of the Taulanne syncline, the Porte de St-Jean syncline and Taloire syncline and their bounding salt structures 121
4.1.2. The Destourbes thrust sheet, the Teillon thrust sheet and the southern part of the la Blache-Castellane thrust sheet. The eastern part of the southern structural domain 136
4.1.2.1. The Destourbes thrust sheet. Stratal and structural observations 139
4.1.2.2. The salt structures and intervening synclines of the Teillon thrust sheet. Stratigraphic and structural observations 141
4.1.2.3 The southern part of the la Blache-Castellane thrust sheet 151
4.1.2.4 Interpretation of the Destourbes thrust sheet, the Teillon thrust sheet and the southern part of the la Blache-Castellane thrust sheet 155
4.1.3 The Petit Mourre diapir and the adjacent synclines of the southern structural domain 165
4.1.3.1 The la Gondole syncline. Structural and stratigraphic observations 168
4.1.3.2 The Petit Mourre diapiric structure and adjacent synclines: the le Chiran, Grande Plaine and Blieux synclines 169
4.1.3.3 Interpretation of the la Gondole, le Chiran, the Grande Plaine synclines, the Blieux syncline and their bounding structures 183
4.1.4 Interpretation of the Jurassic-Early Cretaceous salt related structures of the southern structural domain 195
4.2 Jurassic-Early Cretaceous salt tectonics in the northern structural domain around Barrême. Observations, structural and stratal geometries 198
4.2.1 The Gévaudan diapir and its flanking strata: the Clavoune and the Col de la Pierre Plantée sections 202
4.2.2 Interpretation of the Gévaudan diapir and its flanking sections 208
4.3 Conclusion of the chapter 212

CHAPTER 5. AN ALBIAN-CENOMANIAN SALT CANOPY AND SECONDARY MINIBASINS IN THE SUB-ALPINE FOLD AND THRUST BELT OF HAUTE PROVENCE, FRANCE 214

Key Points 216
Abstract 217
1. Introduction 218
2. Geological setting of the Southern Subalpine chains of Haute Provence 219
3. Evidence for allochthonous salt emplacement into higher stratigraphic levels during the Albian-Cenomanian 224
3.1 Data and observations 224
3.1.1 Stratigraphic and structural relationships around Gévaudan diapir (northern region) 224
3.1.1.1 Flanking strata of the Gévaudan diapir: the Clavoune, Fontaine Salée and Font Chaude sections 225
3.1.2 Stratigraphic and structural relationships around the la Grau anticline and Castellane diapir (southern region) 229
3.1.2.1 The la Grau salt-cored anticline 229
3.1.2.2 The Castellane diapir 231
3.2 Interpretation 233
4 Indirect evidence for the existence of an Albian-Cenomanian salt canopy on the Tethyan margin 236
4.1 Data and observations 236

4.2 Interpretation *240*
5 DISCUSSION 243
5.1 Cretaceous structural evolution *244*
5.1.1 Albian-Cenomanian emplacement of Keuper evaporites into higher stratigraphic levels: extrusion from feeder diapirs 244
5.1.2 The formation and possible extent of the Albian-Cenomanian salt canopy and secondary minibasin formation above the allochthonous salt 244
5.2 The Alpine modification of the salt tectonic system of the Subalpine chains. How the canopy and the secondary minibasins were incorporated into the fold and thrust belt *246*
5.2.1 Pre-Priabonian (Pre-Nummulitic) structural evolution of the salt tectonic system 247
5.2.2 The Eocene-Oligocene (Priabonian-Chattian) structural evolution of the salt tectonic system 249
5.2.3 The Miocene-Pliocene evolution of the salt tectonic system 253
5.3 Salt canopy and associated secondary minibasins in fold and thrust belts *254*
6 CONCLUSION 257
CHAPTER 6. CONCLUSIONS AND FUTURE WORK 259
6.1 KEY CONCLUSIONS 260
6.2 FUTURE WORK 263
REFERENCES 266

Table of Figures

Chapter 1

Fig. 1.1 Physical properties of salt compared to other lithologies (Warren, 2016). 36

Fig. 1.2 Schematic shapes of salt structures in cross-section view and map view. Redrawn and modified after Jackson & Talbot (1991) and Jackson & Hudec (2017). 37

Fig. 1.3 Different modes of diapir piercement of the overburden (Hudec & Jackson (2007), colours changed). 38

Fig. 1.4 Schematic salt geometries, minibasin types and types of structures in the Gulf of Mexico. Redrawn and modified after Pilcher et al. (2011). 40

Fig. 1.5 (a) Map view of primary minibasins from the Southern Subalpine Chains, France. The La Robine unit consists of three Liassic depocenters separated by salt walls (Célini et al., 2020). (b) Example of primary and secondary minibasins from the Sivas basin, Turkey. The two generations of minibasins are separated by an allochthonous salt canopy (Kergaravat et al., 2016). 41

Fig. 1.6 Mechanisms of minibasin subsidence and key criteria to describe them (Hudec et al., 2009), (colours changed). 42

Fig. 1.7 Three-dimensional physical model shows reactive diapirs developed above footwall of basement faults during thick-skinned extension. Minibasins are located between emerging diapirs (Dooley et al., 2005). 43

Fig. 1.8 Two examples of megaflaps. (a) A megaflap adjacent to Diapir C in the Atwater Foldbelt, northern Gulf of Mexico. The megaflap formed on the basinward side of the diapir due to contraction during the gravity spreading of the margin. The vertical relief of the megaflap is more than 5 km. (Rowan et al. (2016), colours changed). (b) Overturned flap of the Barre de Chine, Southern Subalpine Chains, France. The flap comprises a condensed and overturned section of Lower and Middle Jurassic rocks originally forming the flank of the Barles diapir. The overturning of the megaflap is related to the emplacement of an allochthonous salt sheet during the deposition the Callovian-Oxfordian Terres Noires formation. The allochthonous salt reached the surface and extruded as a salt nappe to the seabed. After Graham et al. (2012). 44

Fig. 1.9 Sequential evolution model of megaflap formation. (a) Formation of a basal megaflap along a passive diapir. Modified after Schultz-Ela (2003) and Jackson & Hudec (2017), colours changed. (b) Cartoon evolution of the Barre de Chine flap. Modified after Graham et al. (2012). 45

Fig. 1.10 Schematic sections showing halokinetic sequences (HS) and composite halokinetic sequences (CHS) forming adjacent to passive diapirs. (a) Hook halokinetic sequence. (b) Wedge halokinetic sequence. (c) Tabular composite halokinetic sequence. (d) Tapered composite halokinetic sequence. Modified after Giles & Rowan (2012). 46

Fig. 1.11 Hook and wedge halokinetic sequences in the Sivas basin, Turkey (Ribes et al. (2015), colours changed). 47

Fig. 1.12 (a) Outcrop example of a weld, SW of the Emirhan minibasin, Sivas basin, Turkey. The lower segment of the weld is completely welded. The upper segment of the weld is

incomplete and contains a few meters of remnant gypsum (Jackson & Hudec, 2017; Kergaravat et al., 2017). Photo by Lajos Adam Csicsek. (b) Cross-section view of a subvertical secondary weld, La Popa basin, Mexico (Rowan et al. (2012), colours changed). 48

Fig. 1.13 Structural style in shortened regions which contain salt depends on the thickness of the evaporite level, its overburden, and the absence (a) or presence (b) of precursor salt structures (Hudec & Jackson (2007) and Jackson & Hudec (2017), colours changed)..... 50

Fig. 1.14 (a) Structural configuration of a diapir province where isolated salt stocks and walls are surrounded by synkinematic sediments (blue strata). Green strata represent thin roof (dark green) and thick roof (light green) of the salt structures and adjacent sediments. Block diagrams show how isolated diapiric provinces responding to regional shortening with thin cover (b) and thick cover (c) (Duffy et al. (2018), colours changed). 51

Fig. 1.15 Three mechanism of allochthonous salt sheet emplacement and evolutionary histories of the sheets (Hudec & Jackson (2006), colours changed). 52

Fig. 1.16 Schematic evolution of two generations of minibasins below and above an allochthonous salt canopy in compressional setting. Salt sheets extruded over first generation of minibasins from mushroom shaped diapirs and amalgamated into an allochthonous evaporite canopy. Modified after Kergaravat et al. (2016). 53

Fig. 1.17 Conceptual models showing structural styles and processes in shortened isolated minibasin provinces. Minibasins subsided into a single salt layer, and they were not welded at their base before the onset of the regional shortening. a) Low regional shortening strain. (b) High regional shortening strain (Duffy et al. (2021), colours changed). 55

Chapter 2

Fig. 2.1 Tectonic map of the Western Alps modified after Schmid et al. (2004). (b) Simplified geological map of Subalpine chains after Rouire et al. (1979) and Kerckhove et al. (1980). The study area subdivided into two structural domains, the northern domain and southern domain, respectively. (c) Regional cross-section of the study area. Numbers showing salt structures of the autochthonous salt layer. (1) 'the anticline at the lake', (2) Dôme de Châteauredon, (3) pedestal of the Gévaudan diapir, (4) pedestal of the la Cine salt wall..... 58

Fig. 2.2 Lithostratigraphic column of the study area and major tectonic events in the Western Alps. In the text, on maps and cross-sections I refer the lithostratigraphic units as they are shown in this column (Data from Kerckhove & Roux (1976a); Kerckhove & Roux (1978a); Campredon et al. (1980b); De Graciansky et al. (1981)). 59

Fig. 2.3 Cargneule breccia from the Castellane diapir. Note the coin for scale..... 60

Fig. 2.4 Syn-rift tectonic framework of the Western Alps (De Graciansky et al., 2010). Two different trends of faults (NW-SE and NE-SW) developed during the rifting of the margin. D. = Daluis fault. External crystalline massifs: Arg. = Argentera, Bell. = Belledonne, MtB. = Mont blanc, Pelv. = Pelvoux, Rdf. = Rouaine-Daluis fault..... 61

Fig. 2.5 Simplified section from the Provençale platform to the Dauphinois - Vocontian basin west of Castellane, highlighting facies variations in the Tithonian - Valanginian section. Modified after Cotillon (1994). 63

Fig. 2.6 Facies distribution maps of the Southern Subalpine chains during the Mesozoic. (a) Liassic facies distribution map. (b) Late Jurassic facies distribution map. (c) Cretaceous facies distribution map. The maps are not palinspastically restored. The northern and southern

structural domains are shown together here. Locations of stratigraphic logs (RL1-5) shown on Fig. 2.7 are indicated by their code. Black dashed lines mark the approximate strike of the boundaries between the facies zones during the Mesozoic and define the edge of the Provençal platform. Modified from Ganeval (1973); Kerckhove & Roux (1976a); Kerckhove & Roux (1978a); De Graciansky et al. (1981); Dumont (1988) and Roux et al. (1988). 65

Fig. 2.7 Generalised stratigraphic sections from the Provençal platform to the Dauphinois and Vocontian basins intersecting the mixed or slope facies zone. Data from Kerckhove & Roux (1976a); Kerckhove & Roux (1978a); De Graciansky et al. (1981); Dumont (1988) and Roux et al. (1988). The sections illustrate facies and thickness variations of the Mesozoic stratigraphy. See Fig. 2.6 for location of the logs..... 66

Fig. 2.8 Liassic and Middle Jurassic tectonic framework of the external Alpine domain (Kerckhove & Roux, 1978a; Dardeau, 1988). The solid red lines between Nice and the Dauphine domain represents a normal fault system which defined the northern edge of the Provençal platform. Black-dotted areas represent horts and half-horsts. Redrawn after Dardeau (1988). 67

Fig. 2.9 Chronostratigraphic diagram of Eocene and Oligocene formations of the foreland basin system of Southern Subalpine chains (Evans et al. (2004), colours modified). Stratigraphic codes of the unites are (e.g, eC or e7 are used in figures, maps etc. in following chapters). For the location of the Barrême and Douroulles synclines see Fig. 2.1b. Note that the Argens-Allons syncline, the Cordoeil-Chamatte anticline and the Annot syncline are situated E of the study area. They are out of scope of the work presented here and not shown on Fig. 2.1b and c..... 68

Chapter 3

Fig. 3.1 Geological map of the Subalpine Chains showing examples of known salt structures: B = Barre de Chine flap, C = La Cine fault, D = Daluis diapir, G = Gévaudan diapir, Lr = La Robine unit, P = Puget-Théniers diapir, R = Rouaine-Daluis fault system, S = St-Jurs diapiric intrusion, V = Vélodrome minibasin, Va = Valberg-Beuil weld. Data from (Kerckhove & Roux, 1978a; Kerckhove & Roux, 1978b; Rouire et al., 1979; Kerckhove et al., 1980; Mascle et al., 1988; Dardeau & De Graciansky, 1990; Lickorish & Ford, 1998; Graham et al., 2012; Brooke-Barnett et al., 2019; Célini et al., 2020; Célini, 2020; Graham & Csicsek, 2020; Brooke-Barnett et al., 2021; Brooke-Barnett, 2022; Célini et al., 2022). 73

Fig. 3.2 The overturned flap of the Barre de Chine adjacent to the Barles diapir (shown here as Triassic cargneule) (Graham et al., 2012)..... 74

Fig. 3.3 Section showing abrupt thickness changes, unconformities in the Jurassic sections and bounding salt structures in the La Robine unit (Célini et al., 2020). 75

Fig. 3.4 Uninterpreted (a) and interpreted (b) photo panorama of the Vélodrome syncline (Célini, 2020; Célini et al., 2022) highlighting the overturned edges of the syncline. Angular unconformities and thickness changes occurred within the Oligocene and Mio-Pliocene fill of the secondary minibasin below the overriding Digne Nappe and La Robine unit..... 76

Fig. 3.5 Cross section across the la Cine weld, north of the Barrême syncline, showing thickness changes and unconformities in the Mesozoic section along the weld. The salt wall is completely welded in its central segment and remnant gypsum shown below a thin Liassic roof section in the upper part (Célini, 2020). 78

Fig. 3.6 Cross-section of Lickorish & Ford (1998) in Jackson & Hudec (2017). 79

Fig. 3.7 Geological map showing the diapiric intrusion at the village of St-Jurs (Kerckhove & Roux, 1978a). Triassic gypsum is shown as tG. Upper Jurassic-Lower Cretaceous succession of the St-Jurs imbricates is shown in blue and green colours. Mio-Pliocene sediments of the Valensole basin and Quaternary cover are shown in pale brown colours..... 80

Fig. 3.8 Composite section showing the Daluis diapir during the deposition of the Tithonian limestone (Mascle et al., 1988; Brooke-Barnett, 2022). Thinning of the Jurassic section, slumping, local unconformities and syn-sedimetary faults occurred on the flank of the diapir. 82

Fig. 3.9 Bedding parallel Triassic gypsum (T_G) and mineralised caprock within the Aptian-Albian black marls, observed south-west of the Daluis diapir (Brooke-Barnett, 2022). 83

Fig. 3.10 Interpreted photo panorama of the western segment of the Valberg-Beuil weld (Brooke-Barnett, 2022). Syn-sedmientary normal faults crosscut the Liassic-Middle Jurassic section south of the weld and sealed here by Middle Jurassic sediments. Geological key: T_K + T_C = Triassic Keuper and cargneule breccia; J_{L1} + J_{L2} + J_L = Lower Jurassic; J_M = Bajocian-Bathonian; J_{C-O}= Callovian-Oxfordian. The weld is indicated by a dashed line and a pair of black dots. 84

Fig. 3.11 (a). Section crossing the Puget-Théniers diapir. (b). Late Cretaceous restoration of the diapir and surrounding sediments. Redrawn after Dardeau & De Graciansky (1990). Note the thickness changes of the Jurassic-Cretaceous section, local unconformities and normal faults sealed by the Upper Cretaceous sediments on the flank of the salt body. See Fig. 2.2b for geological key. 86

Chapter 4

Fig. 4.1 Simplified geological map of eastern part of the southern structural domain, in the vicinity of Blieux and Castellane. Redrawn after Kerckhove & Roux (1976a) and Kerckhove & Roux (1978a). See Fig. 4.2 for the structural explanation. 93

Fig. 4.2 Structural map of the eastern part of the southern structural domain showing synclines, their bounding Alpine structures or pre-Alpine salt structures and their Mesozoic palaeogeographic position. Data from Kerckhove & Roux (1976a) and Kerckhove & Roux (1978a). For geological map see Fig. 4.1. 94

Fig. 4.3 Detailed geological map of the St-Vincent diapir and the northern part of the Taulanne syncline. See Fig. 4.1 for location. See Fig. 4.2 for structural map and explanation of the area. 95

Fig. 4.4 Photo panorama of St-Vincent diapir, the la Grau anticline and the bounding Taulanne syncline, looking to SSE. See Fig. 4.3 for key and viewpoint location. 96

Fig. 4.5 Cross section (S9-S9') from the Provençal Platform to the basinal Lambruisse-Lauppe thrust sheet, intersecting Taloire syncline, the Porte de St-Jean syncline and the Taulanne syncline of the Mesozoic slope facies zone and the Haute Sionne syncline and the la Blache-Castellane thrust sheet. See Fig. 4.1 for cross section location. Note that the northern segment of the section is not shown on Fig. 4.1. 97

Fig. 4.6 Detailed geological map of the Taulanne syncline. See Fig. 4.1 for location. See Fig. 4.2 for structural map and explanation of the area. 100

Fig. 4.7 Transect showing thickness variations between the core of the Taulanne syncline and the flanking Cadiéres de Brandis and la Grau sections. Note that thicknesses are inferred in

the core of the Taulenne sycnline. See Fig. 4.2 location of the logs and Fig. 4.6 for geological key. 101

Fig. 4.8 Detailed geological map of the Chasteuil salt structure, the southern part of the Taulanne syncline, the Porte de St-Jean syncline and the northern part of the Taloire syncline. See Fig. 4.1 for location. See Fig. 4.2 for structural map and explanation of the area. 104

Fig. 4.9 Uninterpreted (a) and interpreted (b) photo panorama of the western sector of the Brandis syncline and the Chasteuil salt structure, the Porte de St-Jean syncline and the merging Taloire syncline in the background, in the vicinity of the village of Chasteuil. The photo presents an oblique cross section view of the welded Chasteuil salt structure. Black epsilons indicate younging direction. See Fig. 4.8 for geological key and viewpoint location. 106

Fig. 4.10 Uninterpreted (a) and interpreted (b) photo panorama of the western sector of the Brandis syncline and the Chasteuil salt structure, the Porte de St-Jean syncline and the merging Taloire syncline, N of the village of Chasteuil, looking to NW. Black epsilons indicate younging direction. See Fig. 4.8 for geological key and Fig. 4.9 viewpoint location. 107

Fig. 4.11 Uninterpreted (a) and interpreted (b) photo panorama of eastern sector the the Porte de St-Jean syncline and the bounding Brans thrust and the Chasteuil salt structure. The black epsilons indicate younging direction. See Fig. 4.8 for geological key and viewpoint location. 108

Fig. 4.12 Zoom of the S10 cross section (S10a – S10a') through the Taloire syncline, the Chasteuil salt structure and the bounding Porte de St-Jean syncline and the Taulanne

syncline, illustrating gradual thickness changes, local unconformities and multidirectional tilting of independent depocenters. See Fig. 4.8 for cross section location..... 109

Fig. 4.13 Large-scale slump fold in the Berriasian-Lower Valanginian (n1 and n2a) section of the Porte de St-Jean syncline, at the village of Chasteuil. The orientaion of the slump fold suggests transport towards to SE. White dashed line marks the unconformity at the base of the Lover Valanginian marl and limestone formation (n2b). See Fig. 4.9 and Fig. 4.10 for viewpoint location..... 111

Fig. 4.14 The contact of the Tithonian limestone and the Lower Valanginian marl on the northern flank of the Port de St-Jean syncline, NE of the village of Chasteuil. The Lower Valanginian marl is right way up and the Tithonian limestone is overturned to SW. Note boudins and sheared layers in the Lower Valanginian marl. Note the field notebook for the scale. See Fig. 4.9 and Fig. 4.10 for viewpoint location..... 112

Fig. 4.15 Uninterpreted (a) and interpreted (b) photo panorama of the overturned section at the Crête de Colle Bernaiche, E of the Chasteuil salt structure, on SW flank of the Taulanne syncline. Black epsilons indicate younging direction. See Fig. 4.8 for geological key and viewpoint location..... 113

Fig. 4.16 Zoom of the S10 cross section (S10b-S10b') showing the Chasteuil salt structure and the overturned section of the Crête de Colle Bernaiche. See Fig. 4.8 for cross section location and Fig. 4.12 for key..... 115

Fig. 4.17 Detailed geological map of the western part of the Taloire syncline, the la Gondole syncline and the esatern part of the Blieux syncline. See Fig. 4.2 for structural map and explanation of the area..... 116

Fig. 4.18 Interpreted (a) and uninterpreted (b) photo panorama of the la Crotte area and Deneiras section of the Taloire syncline and the eastern termintaion of the la Gondole syncline. Black epsilons indicate younging direction. See Fig. 4.2 for structural explanation. See Fig. 4.17 for geological key and viewpoint location..... 119

Fig. 4.19 Sequential evolution of the south-western limb of the Taulanne syncline (Crête de Colle Bernaiche section), from Bajocian (a) to Cenomanian (d) (not to scale). Note that sediments younger than Valanginian are not preserved on the flanks of the Taulanne syncline. Stratal and structural geometries of Hauterivian-Cenomanian formations shown here are highly speculative. 124

Fig. 4.20 Sequential evolution of the Porte de St-Jean minbasin and its bounding salt salt structures, the Chasteuil salt structure and the Brans diapir, from Bajocian (a) to Valanginian (c) (not to scale). (d). Zoom of the northern flank of the Porte de St-Jean minibasin. Note that the pedestal of Brans diapir possibly located in the subsurface, below the Cadiéres de Brandis section, along the Alpine basal detachment at the depth of 3 km. 127

Fig. 4.21 Sequential evolution of the SW flank of the Taloire minibasin and its bounding structure, the Berbené salt wall, at the la Crotte section, from the Bajocian to the Valanginian. The absence of sediments younger than Lower Valanginian in the la Crotte section of the Taloire minibasin mean that the complete Early Cretaceous and Late Cretaceous history of the basin cannot be ascertained. Not to scale. 131

Fig. 4.22 Normal faulting occured along the SE flank of the Berbené salt wall, during the Early Valanginian, and led to the failure of the flanking strata. See Fig. 4.21 for key. Not to scale. 133

Fig. 4.23 Simplified map view of the Taloire minibasin, the Porte de St-Jean minibasin, the Taulanne minibasin and the salt structures which bounded these depocenters. The map is not restored and only showing the approximate palinspastic position of the minibasins and their bounding salt structures. Note that all the minibasins were located between the Provençal platform and the pelagic domain of the Dauphinois and Vocontian basins. Additional salt structures and minibasins to the WNW and ESE along the Provençal platform are not shown here. 134

Fig. 4.24 Simplified geological map of the eastern part of the southern structural domain, in the vicinity of Blieux and Castellane. Redrawn after Kerckhove & Roux (1976a) and Kerckhove & Roux (1978a). See Fig. 4.25 for the structural explanation. 137

Fig. 4.25 Structural map of the eastern part of southern structural domain, showing synclines, their bounding Alpine structures or pre-Alpine salt structures and their Mesozoic palaeogeographic position. Data from Kerckhove & Roux (1976a) and Kerckhove & Roux (1978a). 138

Fig. 4.26 Detailed geological map of the Destourbes and Teillon thrust sheets of the slope palaeogeographic domain. The thrust sheets overthrusted the edge of the Provençal platform and they are overriden by the basinal la Blache-Castellane thrust sheet (Fig. 4.25). See Fig. 4.24 for location and Fig. 4.25 for structural explanation. 140

Fig. 4.27 Uninterpreted (a) and interpreted (b) photo panorama of the Teillon diapir and the Crête de Rus anticline with the bounding la Lagne and les Combes synclines, looking to E. See Fig. 4.26 for key and viewpoint location. 145

Fig. 4.28 Uninterpreted (a) and interpreted photo panorama of the Teillon diapir and the la Lagne syncline, looking to SE and showing the overtunred flank of the syncline and the gently dipping top of the mushroom shaped diapir. Black epsilons indicate younging direction. See Fig. 4.26 for key and viewpoint location. 147

Fig. 4.29 Regional cross section (S12-S12') from the Provençal platform to the basinal Lambruisse-Lauppe thrust sheet through the Teillon thrust sheet which represents the Mesozoic slope palaeogeographic domain. See Fig. 4.24, Fig. 4.25 and Fig. 4.26 for cross section location. The location of basement involved extensional faults is highly specualtive. These normal faults may correspond to the Mesozoic North Provence edge of Dardeau (1988) and they were presumably inverted duirng later Alpine shortening. Note that the north-eastern and southern segment of the section is not shown on Fig. 4.26. 148

Fig. 4.30 Detailed geological map of the Castillon anticline, N of the village of la Cité and E of the Lac de Castillon. Note local unconformities at the base of the Bajocian (j1S) and Bajocian-Callovian (j2-3) formations in the hanging wall of the overriding Lambruisse-Lauppe thrust. See Fig. 4.24 for location. Note that the nortern part of the detailed map is not shown on Fig. 4.24. See Fig. 4.26 for key. 152

Fig. 4.31 Cross section (S11-S11') from the Provençal platform to the basinal Lambruisse-Lauppe thrust sheet, crossing the slope palaeogeogrpahic domain and the la Blache-Castellane thrust sheet. See Fig. 4.24 and Fig. 4.25 for cross section location. 154

Fig. 4.32 Diagrams shoving possible Early Jurassic-Early Cretaceous evolution of the salt diapirs and walls, and the intervening minibasins now located in the Teillon thrust sheet (not to scale) from the Liassic (a) to the Valanginian (c). The salt structures and the minibasins

formed in the slope palaeogeographic domain. (d) Zoom of the top of the Teillon diapir. The roof of the diapir was dismembered by extensional faults, presumably during Berriasian-Valanginian. 158

Fig. 4.33 Simplified map view of the eastern part of the southern structural domain. The map is not restored and only showing the approximate palisnpastic position of the minibasins and their bounding salt structures. Dashed lines show assumed salt structures. Fig. 4.23 was slightly modified based on the position of salt structures and minibasins to the ESE. Note that the complex network of salt walls, diapirs and primary minibasins was located between the Provencal platform and the pelagic domain. In the eastern part of Dauphinois and Vocontian basins only an elongated salt wall and the small Castillon pillow formed. Fig. 4.23 is modified and newly identified salt structures and bounding minibasins are shown here. 159

Fig. 4.34 Simplified geological map of the western part of the southern structural domain. Redrawn after Kerckhove & Roux (1976a) and Kerckhove & Roux (1978a). 166

Fig. 4.35 Structural map of the western part of the southern structural domain, showing synclines, their bounding Alpine structures or pre-Alpine salt structures and their Mesozoic palaeogeographic position. Data from Kerckhove & Roux (1976a) and Kerckhove & Roux (1978a). 167

Fig. 4.36 Detailed geological map of the Petit Mourre diapir and the surrounding synclines. See Fig. 4.34 for location and Fig. 4.35 for structural explanation. 170

Fig. 4.37 Uninterpreted (a) and interpreted (b) photo panorama of the Petit Mourre diapir and the adjacent Blieux syncline, looking to SE. Black epsilons indicate younging direction. See Fig. 4.36 for key and viewpoint location. 174

Fig. 4.38 Regional cross section (S8-S8') from the Valensole foreland basin to the Senez syncline. See Fig. 4.35 for cross section location. The section is intersecting the platform, slope and basin palaeogeogrpahic domains. Note the abrupt thickness changes of the Jurassic section between the la Gondole, Grande Plaine and Blieux synclines. 175

Fig. 4.39 Transects showing thickness variations of the basinal Jurassic sections and different stratal geometries, between the le Chiran and the Blieux synclines (a), and betwen the Grande Plaine and the Bliuex synclines (b). The smaller le Chiran and Grande Plaine synclines are separated from the large Bliuex syncline by the Petit Mourre diapir and its along-strike equvalent, the Petit Mourre-le Poil weld. All of these depocenters and the salt structures are located in the hanging wall of the Berbené thrust fault and its along-strike equivalent, the le Poil thrust. Measured sections are shown by logs and litholigies. Note that thicknesses are inferred in the core of the Blieux sycnline. For log location and geological key see Fig. 4.36. 177

Fig. 4.40 (a) Interpreted photo panorama of the core of the Petit Mourre diapir, looking to the SE The photo shows the exposed core of the diapir with the arched roof which is partly collapsed. White epsilons indicate younging direction. (b) Cross section of Grand Mourre diapir, redrawn after Roux (1972). Note the large scale slumping and the S-folds verging to the WSW in the Middle-Upper Jurassic section on the WSW flank of the diapir. White epsilons indicate younging direction. See Fig. 4.36 for key and Fig. 4.37 for viewpoint location. 179

Fig. 4.41 Uninterpreted (a) and interpreted (b) photo panorama of the NE flank of the Blieux syncline at Ravin de Riu section, NW of the village of Bliuex, looking to NE. Black epsilons indicate younging direction. See Fig. 4.36 for key and viewpoint location. 182

Fig. 4.42 Sequential evolution of the le Chiran and Blieux minibasins and their bounding salt structures, the Prau salt wall, the Petit Mourre diapir and the Montagne de Vibres salt swell from the Middle Jurassic (a) to the Middle-Late Cretaceous (c)..... 185

Fig. 4.43 (a) Interpreted photo panorama of the core of the Petit Mourre diapir, looking to the SE The photo shows the exposed core of the diapir, its arched roof and the topographic scarp formed on the south-western diapir margin. Black epsilons indicate younging direction. (b) Topographically arched roof of an active diapir. Extensional faulting and slumping occur over the top of the diapir while a thrust fault develops at the toe of the topographic scarp. Redrawn after Jackson & Hudec (2017). (c) Schematic section showing the imbrication of the Kimmeridgian-Tithonian limestone at the toe of the topographic scarp. 191

Fig. 4.44 Simplified map view of the western part of the southern structural domain during the Jurassic and Early Cretaceous. The dashed lines show assumed salt structures. The map is not restored and showing the approximate palinspastic position of the minibasins and their bounding salt structures. The minibasins, salt walls and diapirs were located along the edge of the Provençal platform on the slope and also in the basin palaeogeogrpahic domain. Additional salt structures and minibasins along the Provençal platform to the E are not shown here. 193

Fig. 4.45 Map-view schematic model of the southern structural domain during the Jurassic and Cretaceous time. Dashed lines show assumed salt structures. The early pre-Alpine salt structures and adjacent primary minibasins formed a complex network N and NE of the Provençal platform. The facies boundaries were defined by elongated salt walls, presumably developed over the footwall of Tethyan extensional faults. The map is not restored and only showing the approximate palinspastic position of the minibasins, diapirs and salt walls. 197

Fig. 4.46 Simplified geological map of the northern structural domain, between the villages of Boades and Lambruisse. Redrawn after Kerckhove & Roux (1976a), Kerckhove & Roux (1978a) and De Graciansky et al. (1981). See Fig. 4.47 for the structural explanation..... 200

Fig. 4.47 Structural map of the northern structural domain, showing synclines, their bounding Alpine structures or pre-Alpine salt structures of the southern part of the Digne arc and their Mesozoic palaeogeographic position. Data from Kerckhove & Roux (1976a), Kerckhove & Roux (1978a) and De Graciansky et al. (1981)..... 201

Fig. 4.48 Detailed geological map of the Gévaudan diapir and its surroundings. See Fig. 4.47 for structural explanation. 203

Fig. 4.49 Uninterpreted (a) and interpreted (b) photo panorama of the Clavoune section and the Gévaudan diapir, looking to the NNE. Black epsilons indicate younging direction. See Fig. 4.48 for key and viewpoint location. Photo taken by Célini, N. 204

Fig. 4.50 Cross section (S5-S5') from the Digne thrust sheet to the Lambruisse-Lauppe thrust sheet, crossing the Clavoune section and the Gévaudan diapir. See Fig. 4.46 for cross section location. 205

Fig. 4.51 Diagrams showing the possible evolution of the Gévaudan diapir from the Liassic (a) until the Barremian (c). The red dashed line on (a) showing an alternative interpretation for the top of the pre-salt basement and the possible position of a Tethyan extensional fault which formed during the rifting phase and initiated the diapirism. The Jurassic-Lower Cretaceous sections which are exposed now in the Digne nappe and the la Blache-Castellane thrust sheet are thinning towards the diapir and showing wedging geometries. Not to scale. 209

Fig. 4.52 Map-view schematic model of the study area during the Jurassic and Early Cretaceous times. Dashed lines represent assumed salt structures. The pre-Alpine salt structures and adjacent primary minibasins formed a complex network N and NE of the Provençal platform. Isolated diapirs such as the Gévaudan diapir also formed in the basin facies zone. The Gévaudan diapir was probably connected to the St-Vincent and Castellane diapirs through a N-S trending deeply buried salt wall. The Lambruisse-Lauppe salt wall was presumably connected to the la Cine salt wall. The map is not restored and only showing the approximate palinspastic position of the minibasins, diapirs and salt walls. 211

Chapter 5

Figure 1 (a) Tectonic map of the south-western part of the Western Alps. Modified after Schmid et al. (2004). (b) Regional geology map of the Southern Subalpine chains after Rouire et al. (1979) and Kerckhove et al. (1980) showing examples of known salt structures and salt-related structures: Barles flap (B) (Graham et al., 2012), Chasteuil salt structure (C) (Csicsek et al., 2019), Daluis diapir (D) (Mascle et al., 1988; Dardeau & De Graciansky, 1990; Brooke-Barnett et al., 2023), Gévaudan diapir (G) (Emre, 1977; Lickorish & Ford, 1998), La Robine minibasin (L) (Célini et al., 2020), Puget-Théniers diapir (P) (Dardeau & De Graciansky, 1990), Rouaine-Daluis fault system (R) (reactivated salt wall) (Brooke-Barnett et al., 2023), Vélodrome secondary minibasin (V) (Célini et al., 2022). Abbreviation: L-L thrust s. = Lambruisse-Lauppe thrust sheet. (c) Regional cross-section from the Valensole basin through the Digne nappe system. (d) Jurassic and Cretaceous facies distribution maps of the Southern Subalpine chains. Data from Cotillon (1968); Kerckhove & Roux (1976a); Kerckhove & Roux (1978a); De Graciansky et al. (1981); Cotillon (2010); Grosheny et al. (2017); Brooke-Barnett

(2022). Note that the maps are not restored palinspastically. Abbreviations: EU nappes = Embrunais-Ubaye nappes; lBC = la Blache-Castellane thrust sheet; TS = Taulanne syncline. 221

Figure 2 Lithostratigraphic column of the Southern Subalpine chains and the regional tectonic events in the Western Alps. Modified after Kerckhove & Roux (1976a) and Kerckhove & Roux (1978a), Campredon et al. (1980b) and De Graciansky et al. (1981)..... 222

Figure 3 Geological map of the Southern Subalpine chains based on the Entrevaux, Moustiers-Sainte-Marie, Castellane and Digne 1:50000 scale map sheets (Kerckhove & Roux, 1976a; Kerckhove & Roux, 1978a; Campredon et al., 1980b; De Graciansky et al., 1981). For Jurassic and Cretaceous facies distribution see Figure 1 and Figure 9. Abbreviations: Br = Brayal weld; Bo = Bourbonne syncline; Boad = Boades zone; BL = Bois de Lieye section; Ca = Castellane diapir; Cla = Clavoune roof strata section; FC = Font Chaude roof strata section; FS = Fontaine Salée flap; Gé = Gévaudan diapir; HS = Haute Sionne syncline; LC = le Clap syncline; LG = le Gion weld; LGa = La Grau anticline; Mo = Mouchon weld; Ro =Rouviére weld; SBs = Serre Blanchard syncline; SL = St-Lions weld; Th = Thon weld. 225

Figure 4 Detailed geological map of the vicinity of the Gévaudan diapir, between the village of Barrême and the hamlet of Gévaudan based on the Entrevaux and Digne 1:50000 scale map sheets (Campredon et al., 1980b; De Graciansky et al., 1981). For location see Figure 3. For Jurassic and Cretaceous facies distribution see Figure 1d. Abbreviations: Cla = Clavoune roof strata section; FC = Font Chaude roof strata section; FS = Fontaine Salée flap; SBs = Serre Blanchard syncline. 226

Figure 5 (a) Interpreted photo panorama of the Gévaudan diapir and the flanking vertical or slightly overturned Clavoune section and the completely overturned Fontaine Salée flap.

Black epsilons indicate younging direction. See Figure 4 for key and viewpoint location. (b) Cross section (S1-S1') from the Digne nappe to the Lambruisse-Lauppe thrust sheet, crossing the Gévaudan diapir, its flanking strata and the adjacent synclines (secondary minibasins) which developed on the top of the Albian-Cenomanian allochthonous salt. See Figure 3 and Figure 4 for cross section location. 227

Figure 6 Detailed geological map of the vicinity of the Castellane diapir and the la Grau anticline, between the town of Castellane and the village of Blieux based on the Castellane and Moustiers-Sainte-Maire 1:50000 scale map sheets (Kerckhove & Roux, 1976a; Kerckhove & Roux, 1978a). 230

Figure 7 (a) Interpreted photo panorama of the Haute Sionne syncline and the underlying allochthonous salt sheet looking to northwest. See Figure 6 for key and viewpoint location. In the foreground the allochthonous salt lies above the Albian-Cenomanian black shales. Above the allochthonous salt, note the large, olistoliths surrounded by Albian-Cenomanian black shales exposed in the Haute Sionne syncline. (b) Cross section (S2-S2') from the Provençal platform to the basinal Lambruisse-Lauppe thrust sheet, intersecting the Taulanne syncline of the Mesozoic slope facies zone and the Haute Sionne syncline and the la Blache-Castellane thrust sheet. Note the structural position of the Haute Sionne syncline above the Taulanne syncline and below the overriding thick, Mesozoic basinal succession of the la Blache-Castellane thrust sheet. The syncline lies structurally above the sheetlike Castellane diapir. For cross section location see Figure 3 and Figure 6. 232

Figure 8 Diagrams showing the possible evolution of the Gévaudan diapir from the Liassic-Middle Jurassic (a) until the Albian-Cenomanian (d). The red dashed line on (a) showing an alternative interpretation for the top of the pre-salt basement and the possible position of a

Tethyan extensional fault which formed during the rifting phase and initiated the diapirism. The Jurassic-Lower Cretaceous sections which are exposed now in the Digne nappe and the la Blache-Castellane thrust sheet are thinning towards the diapir and showing wedging geometries. 234

Figure 9 Structural map of the Southern Subalpine chains between the town of Castellane and the village of Clumanc. Data from Kerckhove & Roux (1976b), Kerckhove & Roux (1978a), Campredon et al. (1980b) and De Graciansky et al. (1981). Abbreviations: Br = Brayal weld; Bo = Bourbonne syncline; Cla = Clavoune roof strata section; FC = Font Chaude roof strata section; FS = Fontaine Salée flap; HS = Haute Sionne syncline; LG = le Gion weld; LGa = La Grau anticline; Mo = Mouchon weld; Ro =Rouviére weld; SL = St-Lions weld; Th = Thon weld. The transparent white polygon over the map indicates the possible extent of the Albian-Cenomanian salt canopy. White question marks indicate locations where the limit of the canopy is not known. Note that the map is not palinspatically restored. 237

Figure 10 (a) Local angular unconformity at the base of the Turonian limestone (c3) over the Cenomanian marl and marly limestone (c1-2), on the southwestern flank of the Douroulles syncline, east of the le Gion weld. (b) Interpreted photo of the eastern flank of the le Clap syncline, northwest of the subvertical Clavoune roof strata section. Note the angular unconformity at the base of the Cenomanian marly sediments (c1-2). A second angular unconformity was observed within the Cenomanian succession (c1-2). (c) Photo of the poorly sorted Coniacian-Santonian breccia east of the le Gion weld, on the southwestern flank of the Douroulles syncline and onlapping Poudingues d'Argens Formation. (d) Overturned beds of the Upper Cretaceous breccias on the eastern flank of the Barrême basin, adjacent to the Gévaudan diapir (the "Brèches anté-Argens" of Pairis (1971)). (e) and (f) Photos of the poorly

sorted Upper Cretaceous breccias exposed on the western flank of the Barrême basin. The breccias occur within coherent olistolith-olisthostrome units which intercalated in the Priabonian Nummulitic limestone and the Priabonian-Rupelian Globigerina marls (Elliott et al., 1985; De Graciansky et al., 1981; De Graciansky et al., 1982; Evans & Elliott, 1999). (g) Photo of poorly sorted Cenomanian-Coniacian breccias on the southwestern flank of the Haute Sionne syncline, exposed below the overriding la Blache-Castellane thrust sheet. See Figure 4 for viewpoint locations. 238

Figure 11 Diagram showing the possible configuration of secondary minibasins above the allochthonous salt around the feeder Gévaudan diapir during the Late Cretaceous. The model is also showing schematic stratal and structural geometries in the secondary minibasins and around the salt structures..... 242

Figure 12 Map-view schematic model of the Southern Subalpine chains during the Late Cretaceous showing the possible original location of salt structures in the platform-slope-basin palaeogeographic configuration. The yellow dotted line shows the possible extent of the salt canopy. White question marks indicate locations where the limit of the canopy is not known. Note that the shape and the position of salt structures and minibasins are not known for certain and this rough reconstruction, based on the restoration of a regional cross section shown in Figure 1c, showing their approximate palinspastic position. Abbreviations: Cla = Clavoune roof strata section; FC = Font Chaude roof strata section; FS = Fontaine Salée flap; MB = minibasin. 245

Figure 13 Diagrammatic sections showing possible Alpine evolution of the Gévaudan diapir and the adjacent primary minibasins below the salt canopy and the evolution of the second-generation salt structures and secondary minibasins above the canopy during the Alpine

compressional phase, from the Paleocene (a) until the Miocene-Pliocene (c) (not to scale). Abbreviations: Cla = Clavoune roof strata section; FS = Fontaine Salée flap; LG = le Gion salt structure and weld; Mo = Mouchon salt structure and weld; SL = St-Lions salt structure and weld. The section showing the different evolutionary stages along the S1-S1' cross section. For S1-S1' section line location, see Figure 3 and Figure 4. 248

Figure 14 Interpreted photo of overturned Upper Cretaceous breccias and the overlying Poudingues d'Argens conglomerates on the eastern flank of the Barrême basin. The Bois de Lieye section represents the rotated Paleocene core of the secondary minibasin. (b) Interpreted photo panorama of the western flank of the Barrême basin and the rotated minibasin fill exposed at the Bois de Lieye section. Image courtesy of Communauté de Communes Alpes Provence Verdon. See Figure 4 for viewpoint locations. 251

Figure 15 Cross section (S3-S3') from the Digne thrust sheet to the la Lambruisse-Lauppe thrust sheet, showing the position of the Barrême secondary minibasin above the welded allochthonous salt canopy and the resultant structural style of the latest stages of regional compression. Note the counterclockwise rotation of the Barrême primary minibasin and the position of the displaced lateral equivalent of the Clavoune roof strata section below the Barrême secondary minibasin. For cross section location and geological map see Figure 3 and Figure 4. 254

Figure 16 (a) 2D conceptual model showing the key elements and structural styles of the northern part of the pre-shortening salt tectonic system around the Gévaudan diapir, with examples of salt structures and salt withdrawal minibasins. The model is also showing schematic stratal and structural geometries in the minibasins and around the salt structures. (b) 2D schematic model synthesizing the key elements and structural style of the Alpine salt

tectonic system around the Gévaudan diapir and the incorporation of the Albian-Cenomanian salt canopy and associated secondary minibasins into the fold and thrust belt. The section line A-A' showing the modified state of the pre-Alpine salt tectonic system shown in Figure 16a and showing a salt tectonic model of the fold and thrust belt shown in Figure 16 (c). The model is also showing schematic stratal and structural geometries in the minibasins and around the salt structures and the compressional structures which developed during the regional Alpine shortening. Abbreviation: SM = secondary minibasin. (c) Regional cross-section from the Valensole basin through the Digne nappe system (also shown in Figure 1(c)). See Figure 1 (b) for key. Note that the sections are not restored. 256

Chapter 1: General introduction

1.1. Aim of the work

In the last couple of decades, our knowledge about salt tectonics has widened due to the improvements in seismic technologies, analogue modelling, and hydrocarbon exploration in offshore basins like the Gulf of Mexico. Salt tectonics attracts attention because many of the major hydrocarbon provinces can be found in salt basins (e.g., the Gulf of Mexico, the Lower Congo Basin, the North Sea and the Precaspian Basin) (Rowan, 2002; Jackson et al., 2008; Jackson et al., 2010; Jackson et al., 2020). In addition, many of the fold and thrust belts worldwide contain mobile evaporites, exposed diapiric structures, salt canopies and adjacent salt-withdrawal depocenters (e.g., the Zagros Mountains, the Pyrenees, the Northern Calcareous Alps and the Betics) (Callot et al., 2012; Lopez-Mir et al., 2015; Granado et al., 2019; Flinch & Soto, 2022). The structural style and evolution of these fold and thrust belts were highly influenced by the presence of the weak evaporites.

The Southern Subalpine chains of Haute-Provence represents one of these salt-influenced fold and thrust belts and it contains a well-documented succession of Upper Triassic rocks that include evaporite bodies associated with many of the Alpine structures. The Southern Subalpine chains have been studied over 100 years, therefore the stratigraphy and structural evolution of the area during Tethyan rifting and passive margin phases and also the subsequent Alpine compressional phase is well understood (Zurcher, 1895; Boussac, 1912; Goguel, 1939; Guérin-Desjardins, 1956; Cotillon, 1968; Roux, 1972; Lemoine et al., 1986; Dardeau, 1988; De Graciansky & Lemoine, 1988; Fry, 1989; Gidon & Pairis, 1992; De Graciansky et al., 1993; Lickorish & Ford, 1998; Evans & Elliott, 1999; Ford & Lickorish, 2004; Schwartz et al., 2017; Grosjean et al., 2017). The Upper Triassic evaporites were considered as a major décollement level for the thin-skinned Alpine fold and thrust belt (Goguel, 1963; Lickorish & Ford, 1998; Ford & Lickorish, 2004). Moreover, pre-Alpine diapiric structures were also identified in the last couple of decades (Mascle et al., 1988; Dardeau & De Graciansky, 1990). Some of the salt structures thought to have been developed during Tethyan rifting and passive margin phases of the Dauphinois and Vocontian basins, or later during the subsequent Alpine compressional phase (Mascle et al., 1988; Dardeau & De Graciansky, 1990; Gidon, 1997). However, most of the previous research carried out in the Southern Subalpine chains underestimated the importance of salt tectonic activity during the rifting, the subsequent passive margin phase, and the influence of precursor halokinetic structures in the Alpine evolution of the fold and thrust belt.

The Subalpine chains have been revisited in the last couple of years and research has revealed the significant influence of salt tectonics on the Mesozoic stratigraphy and passive margin evolution. In addition, the effects of the salt tectonic activity in the evolution of the fold and thrust belt have also been clarified (Graham et al., 2012; Brooke-Barnett et al., 2019; Graham et al., 2019; Célini et al., 2020; Célini, 2020; Csicsek et al., 2021; Brooke-Barnett, 2022; Célini et al., 2022; Brooke-Barnett et al., 2023).

The mountain belt of the Subalpine chains provides a natural laboratory for the investigation and better understanding of salt related structures, including those developed before the onset of the Alpine shortening.

The aim of this thesis is to investigate and describe the influence of salt tectonics in the evolution of the fold and thrust belt of the Subalpine chains, which have developed on a passive margin with a pre-Alpine, Jurassic-Cretaceous salt tectonic system, with a focus on an allochthonous salt canopy and associated secondary minibasins.

1.2 Organization of the thesis

The chapters of the thesis are organised as the following and their content is outlined below:

Chapter 1 is a general introduction to the subject of salt tectonics.

Chapter 2 is an introduction based on a literature review to the geological and tectonic setting and stratigraphy of the Southern Subalpine chains of Haute Provence, from the Early- and Middle Jurassic rifting of the Tethyan margin through the subsequent passive margin phase to Alpine shortening.

Chapter 3 describes salt tectonics and a few examples of known salt structures of the Southern Subalpine chains from northwest to southeast.

Chapter 4 provides a detailed description of Jurassic-Cretaceous primary minibasins subsided into autochthonous Triassic evaporite layer and bounding salt structures such as salt swells, pillows, salt stocks, diapirs and walls in the Southern Subalpine chains from south to north, between the town of Castellane and the village of Barrême.

Chapter 5 focuses on the formation and evolution of several Albian-Cenomanian allochthonous salt sheets which coalesced to form an extensive salt canopy which hosted several secondary minibasins during the Late Cretaceous. The configuration of the secondary

minibasins above the allochthonous salt and the characteristics of the Albian-Cenomanian and Upper Cretaceous sedimentation in the secondary minibasins are also described in this chapter.

This chapter also provides a detailed description of the evolution of the pre-existing salt structures of the autochthonous and allochthonous salt and the adjacent primary and secondary minibasins during the Alpine compressional phase. The influence of salt tectonics and salt related structures in the Late Cretaceous-Pliocene structural evolution of the fold and thrust belt in a regional context is also described in this chapter.

Chapter 6 presents the key conclusions and suggests possible options for future work.

1.3 Introduction to salt tectonics

1.3.1 'Salt, the viscous rock'

The concept of salt tectonics is defined loosely as any deformation involving evaporites or bodies of salt (Hudec & Jackson, 2007; Jackson & Hudec, 2017). Salt structures have been identified in syn-rift salt basins, passive margin salt basins, and also in major collisional belts.

The term 'salt' is used in this thesis, and more widely in tectonic literature to describe rocks composed of evaporites such as halite, gypsum and anhydrite together with non-evaporitic rocks or inclusions originally interbedded with the evaporites (Hudec & Jackson, 2007; Warren, 2016; Jackson & Hudec, 2017). Evaporites are incompressible and are significant tectonically because of their ability to flow and form diapiric structures in response to stress gradients created by gravity, burial or tectonic compression and extension. The sequence of creep mobility of evaporites is the following: anhydrite, gypsum, halite and bittern salts, but creep may be impeded by the competent carbonate and interbedded siliciclastic layers (Hudec & Jackson, 2007). On a geological timescale, evaporites are the weakest rocks in a deforming section.

Because of its physical properties (Fig. 1.1), salt can act as a viscous medium at the subsurface and emplaced into higher stratigraphic levels through its overburden, which deforms as a result (Hudec & Jackson, 2007). Evaporites are not usually in mechanical

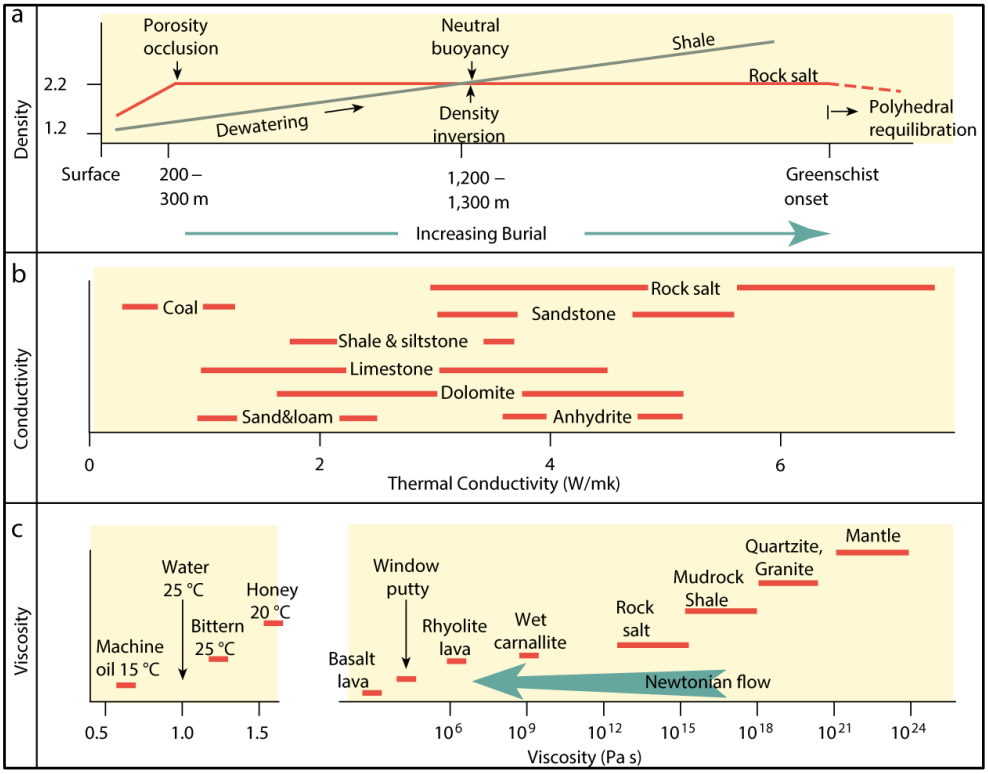


Fig. 1.1 Physical properties of salt compared to other lithologies (Warren, 2016).

equilibrium with their surrounding environment (Warren, 2016) and thus, salt flow and associated deformation may occur in many subsurface situations.

The density of rock salt is about 2200 kg/m^3 which means that it is less dense than common carbonates and compacted siliciclastic rocks (Hudec & Jackson, 2007). This means that salt can theoretically reach the surface solely by the difference in buoyancy (Hudec & Jackson, 2007).

Buoyancy used to be considered as the major driving force of salt movements, but nowadays it is widely recognised that differential loading is vastly more important. The term 'salt tectonics' describes and explains the temporal and spatial evolution of any deformation which is associated with the flow of evaporites. The term 'halokinesis' is sometimes used for the same process, though Hudec & Jackson (2007) and Jackson & Hudec (2017) suggest that the term should be restricted to deformation triggered only by gravity.

1.3.2 Processes of salt movement and diapir growth. Salt structures

Our understanding of salt tectonics has been enormously enhanced by analogue 'sand box' modelling. The description of the range of salt related structures presented in this chapter leans heavily on this experimental work and its iteration with modern seismic imaging from salt

provinces like the Gulf of Mexico. Much of this work has been summarised by Hudec et al. (2011) and Jackson & Hudec (2017). The range of possible salt geometries is shown in Fig. 1.2.

In the following chapters, I refer the term 'salt structure' as it was defined by Jackson & Hudec (2017): a 'map-scale body of salt that has changed shape by salt flow from its depositional configuration', including salt diapirs, salt pillows, salt anticlines, etc. I also use the term 'diapir' as a synonym of the 'salt structure'. Salt structures usually develop from low-amplitude, concordant structures like salt pillows and salt anticlines and evolve into discordant, high-amplitude structures like salt stocks and salt walls (Jackson & Talbot, 1986).

Autochthonous salt lies in its depositional position above the basement or pre-salt strata and is commonly referred to as the 'mother salt' (Jackson & Hudec, 2017). 'Allochthonous' salt means that evaporites which has been emplaced into a higher stratigraphic level than the source layer and overlies younger sediments (Hudec et al., 2011; Jackson & Hudec, 2017). Allochthonous salt bodies are 'sub-horizontal' or moderately dipping, sheetlike salt diapirs emplaced at stratigraphic levels above the autochthonous source layer (Hudec et al., 2011). Allochthonous salt emplacement may be occurred beneath a thin overburden or at the surface (Rowan, 2017). Allochthonous salt bodies may be connected to the autochthonous or source layer by a feeder or could be entirely detached from it when the feeder is welded out (Fig. 1.2).

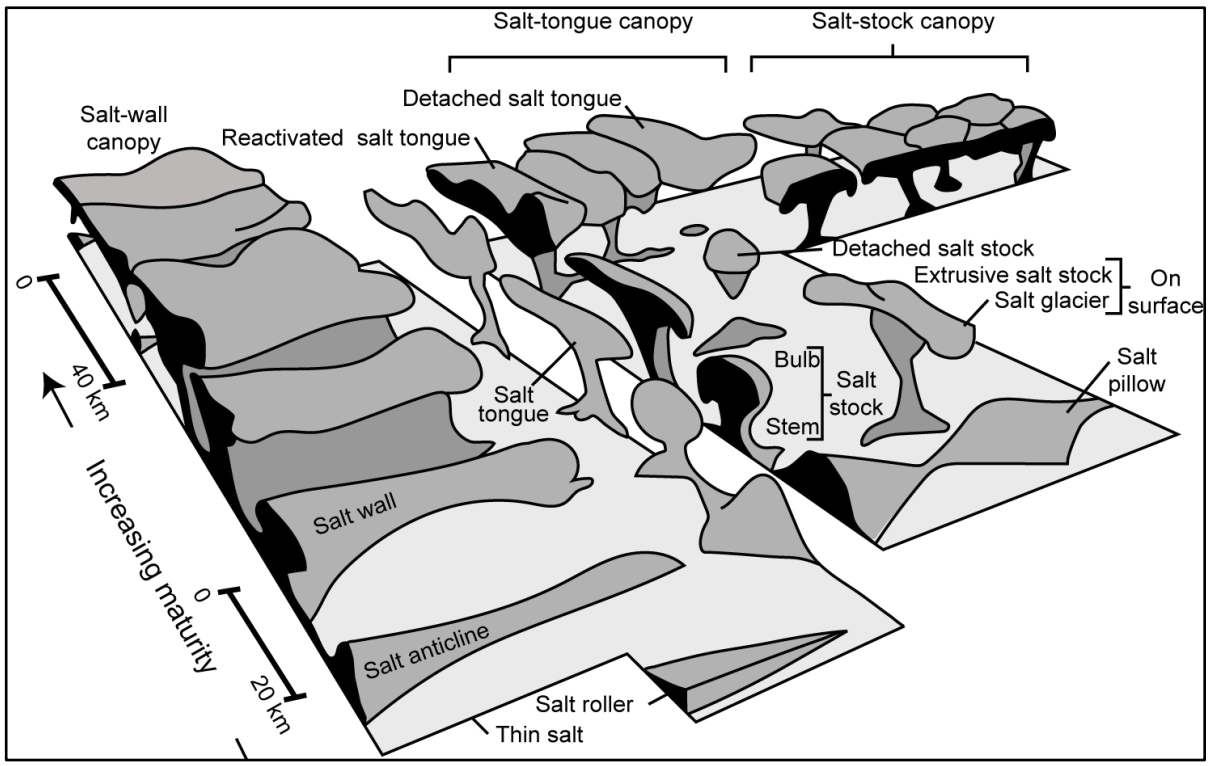


Fig. 1.2 Schematic shapes of salt structures in cross-section view and map view. Redrawn and modified after Jackson & Talbot (1991) and Jackson & Hudec (2017).

The movement of the salt can be triggered by extension, compression or the erosion of the overburden (Hudec & Jackson, 2012). The characteristics of the resulting salt structures and the salt system vary depending on tectonic environment and the structural maturity of the salt system. Reactive diapirs form during rifting when the overburden is thinned by regional extension (Vendeville & Jackson, 1992b; Jackson & Vendeville, 1994) creating space to allow the salt to flow into the overburden. Active diapirism is triggered by sedimentary load on the autochthonous salt layer and results the uplift and, potentially, piercement of the diapir roof (Fig. 1.3b). Compressional active diapirism results from regional shortening forcing the salt to rise and arch its roof coeval with squeezing of the diapir (Nelson, 1989; Schultz-Ela et al., 1993; Jackson & Hudec, 2017). 'Thrust piercement' is the term used when salt is carried in the hanging wall of a thrust fault (Fig. 1.3c).

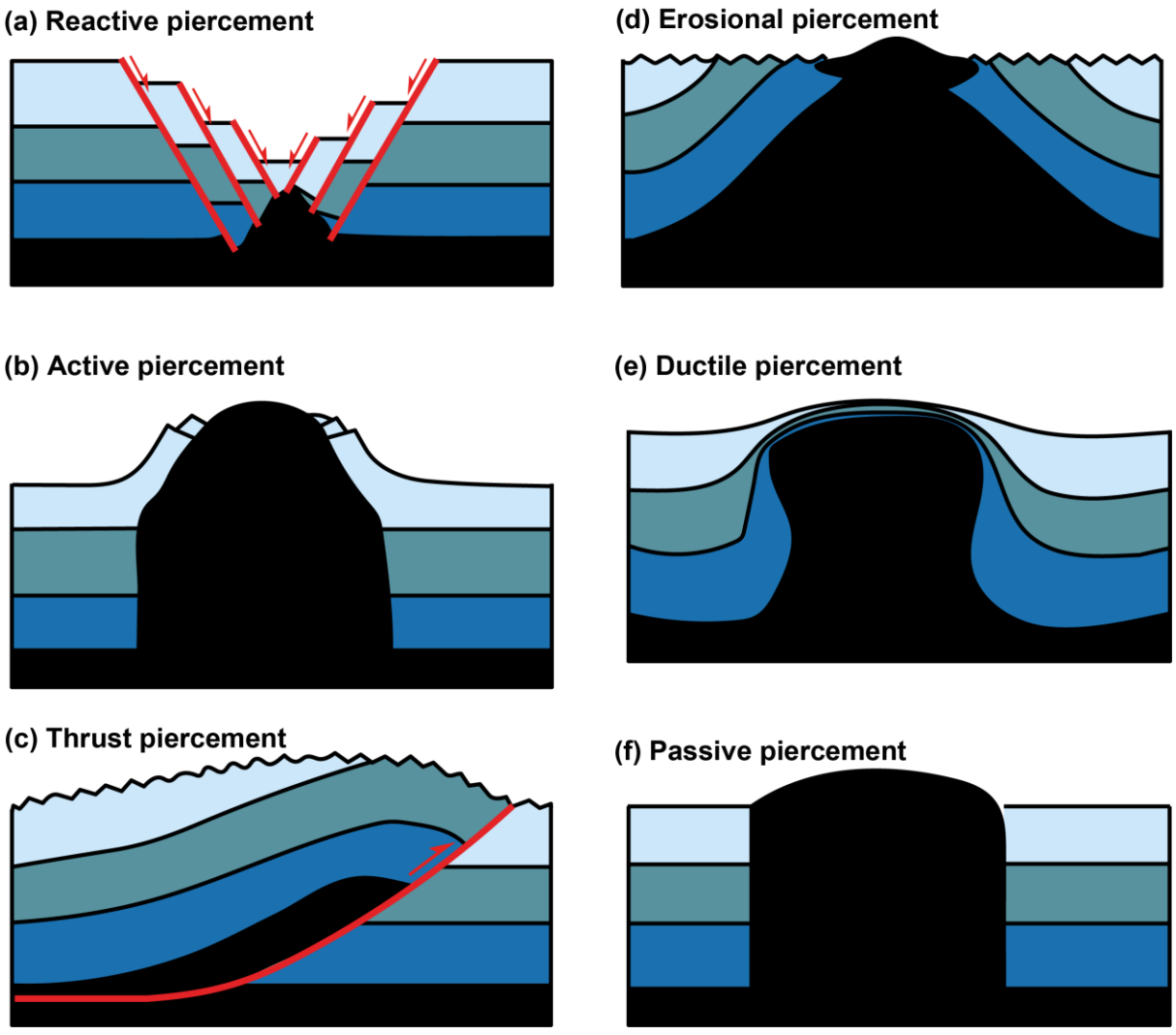


Fig. 1.3 Different modes of diapir piercement of the overburden (Hudec & Jackson (2007), colours changed).

Apparent piercement can occur when a diapir roof is eroded and the salt spreads over the eroded surface (unconformity) as in Fig. 1.3d (Jackson & Hudec, 2017). Ductile piercement is a rare mode of diapiric rise of salt through weak overburden. It means apparent 'piercement' as a diapir with a thin and weak overburden thin its roof during diapiric rise and later active piercement may occurs (Fig. 1.3e) (Jackson & Hudec, 2017).

Once a salt body breaks through its roof, it grows as a passive diapir (Fig. 1.3f). Passive diapirs rise while sediments are accumulating (Vendeville & Jackson, 1992b; Jackson & Hudec, 2017; Rowan & Giles, 2021), a process also called 'downbuilding' resulting in the apparent piercement of the thin roof of the diapir. Passive diapirism occurs near-surface, commonly beneath a thin roof of sediment (Rowan & Giles, 2021) and therefore does not necessarily indicate salt extrusion to the surface. Rowan & Giles (2021) called such structures passive diapirs (sensu lato). Downbuilding played a major role in the salt tectonics of the Tethyan margin during the Mesozoic (see Chapter 4 and Chapter 5).

1.3.3 Minibasins: Depocenters subsiding into salt

Diapir growth requires salt withdrawal, commonly with the associated formation of so-called 'minibasins' i.e. depocenters which subside into autochthonous or allochthonous salt and which can become surrounded partly or completely by a network of welds when the salt is expelled (Worrall & Snelson, 1989; Jackson & Talbot, 1991; Hudec et al., 2009). Rowan & Giles (2021)'s definition of the term 'minibasin' is a depocenter adjacent to a salt diapir or diapirs where accommodation space has been generated by the subsidence of the depocenter into the salt. The term 'salt weld' is used to describe the contact or tectonic discordance which represents a partly or completely vanished salt body (Jackson & Cramez, 1989; Jackson & Hudec, 2017) (see Chapter 1, § 1.3.4). Minibasins have been described globally in geological settings such as the Gulf of Mexico, South Atlantic salt basins, Paradox basin, Precaspian basin, Sivas basin, Sverdrup basin, Flinders Ranges, Moroccan salt basin and Zechstein salt basin (Tari et al., 2003; Jackson & Harrison, 2006; Rowan & Vendeville, 2006; Trudgill, 2011; Callot et al., 2014; Duffy et al., 2017; Legeay et al., 2020a). The width of salt withdrawal minibasins varies from less than ten to a few tens of kilometres (Hudec et al., 2009; Jackson & Hudec, 2017). The original salt thickness influences the shape and size of minibasins and diapirs. A relatively thin autochthonous salt layer might be the source of isolated salt stocks and interconnecting salt anticlines or ridges forming a polygonal network around the minibasins

(Rowan & Vendeville, 2006; Jackson & Hudec, 2017). Thicker salt gives rise to a series of connected salt walls which bound isolated minibasins.

Two fundamental types of minibasins can be distinguished: primary minibasins which rest on autochthonous evaporites and secondary minibasins which develop on allochthonous salt bodies (Fig. 1.4, Fig. 1.5) (Pilcher et al., 2011; Jackson & Hudec, 2017). In the Subalpine chains, both primary and secondary minibasins are exposed (see Chapter 4 and Chapter 5).

Two types of secondary minibasins have been recognised: bucket minibasins subside directly into the feeder of an allochthonous salt body (salt stock-canopy) and their base is relatively close to the autochthonous salt layer (Fig. 1.4). Bowl minibasins partially subside into individual diapiric structures and force out the salt (Fig. 1.4) (Pilcher et al., 2011; Jackson & Hudec, 2017).

The mechanism of minibasin subsidence is density driven subsidence which produces vertically stacked depocenters with raised rims and the deepest part of the minibasin over the thickest and most-compacted sediments (Fig. 1.6a) (Jackson & Hudec, 2017). Density driven subsidence is characteristic of mature minibasins. Once the infill of the minibasin is well-compacted, the depocenter subsides by sinking under its own weight (Jackson & Hudec, 2017). Hudec et al. (2009) described five alternative mechanisms other than density inversion, which could explain the subsidence of minibasins when their sedimentary fill is less dense than the salt. These are diapir shortening (Fig. 1.6b), extensional diapir fall (Fig. 1.6c), decay of salt topography (Fig. 1.6d), sedimentary topographic load (Fig. 1.6e), and sub-salt deformation (Fig. 1.6f). All of these can potentially trigger and maintain minibasin subsidence and the subsidence mechanism can change over time during different stages of minibasin evolution. Diapir shortening occurs during the early stages of regional shortening and the deformation is

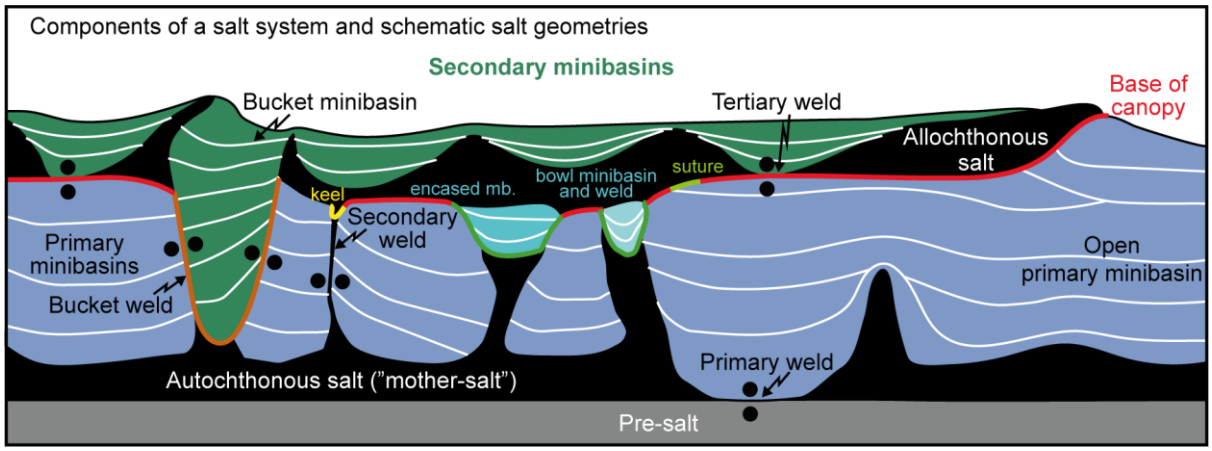


Fig. 1.4 Schematic salt geometries, minibasin types and types of structures in the Gulf of Mexico. Redrawn and modified after Pilcher et al. (2011).

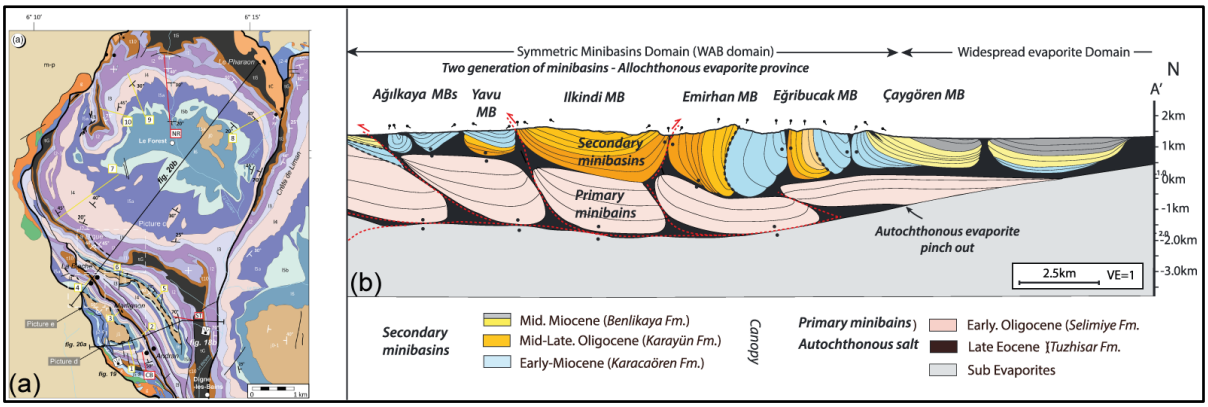


Fig. 1.5 (a) Map view of primary minibasins from the Southern Subalpine Chains, France. The La Robine unit consists of three Liassic depocenters separated by salt walls (Célini et al., 2020). (b) Example of primary and secondary minibasins from the Sivas basin, Turkey. The two generations of minibasins are separated by an allochthonous salt canopy (Kergaravat et al., 2016).

mainly accommodated by the salt. Depocenters are generated by rise and uplift of the intervening salt structures rather than the subsidence of the individual minibasins (Rowan, 2002). The interaction of shortening and minibasin subsidence produces asymmetric synclines, as abrupt lateral shifts occur in depocenters (Fig. 1.6b).

During regional extension, larger diapirs can fall as the salt structures widen and insufficient salt moves from the source layer into the diapir (Fig. 1.6c) (Vendeville & Jackson, 1992a; Jackson & Hudec, 2017). Subsidence occurs on the top of former bathymetric highs due to fall of a diapir and a minibasin can form over a structural low in base of salt (Hudec et al., 2009).

Minibasin subsidence over depleting diapiric feeders can be maintained by decay of salt topography (Fig. 1.6d). Once the salt layer cannot feed the diapir or is completely depleted, topographic relaxation occurs and the sediments accumulate in the newly formed minibasin (Hudec et al., 2009; Jackson & Hudec, 2017). These minibasins are generally bowl-shaped depressions and located on bathymetric slope.

Salt can be differentially loaded by accumulating sediments and this load can also trigger and drive minibasin subsidence (Fig. 1.6e). Sedimentary load at the up-dip end of a salt layer can drive basinward salt expulsion (Jackson & Hudec, 2017) and create minibasins located on bathymetric slopes which may migrate basinward (Hudec et al., 2009).

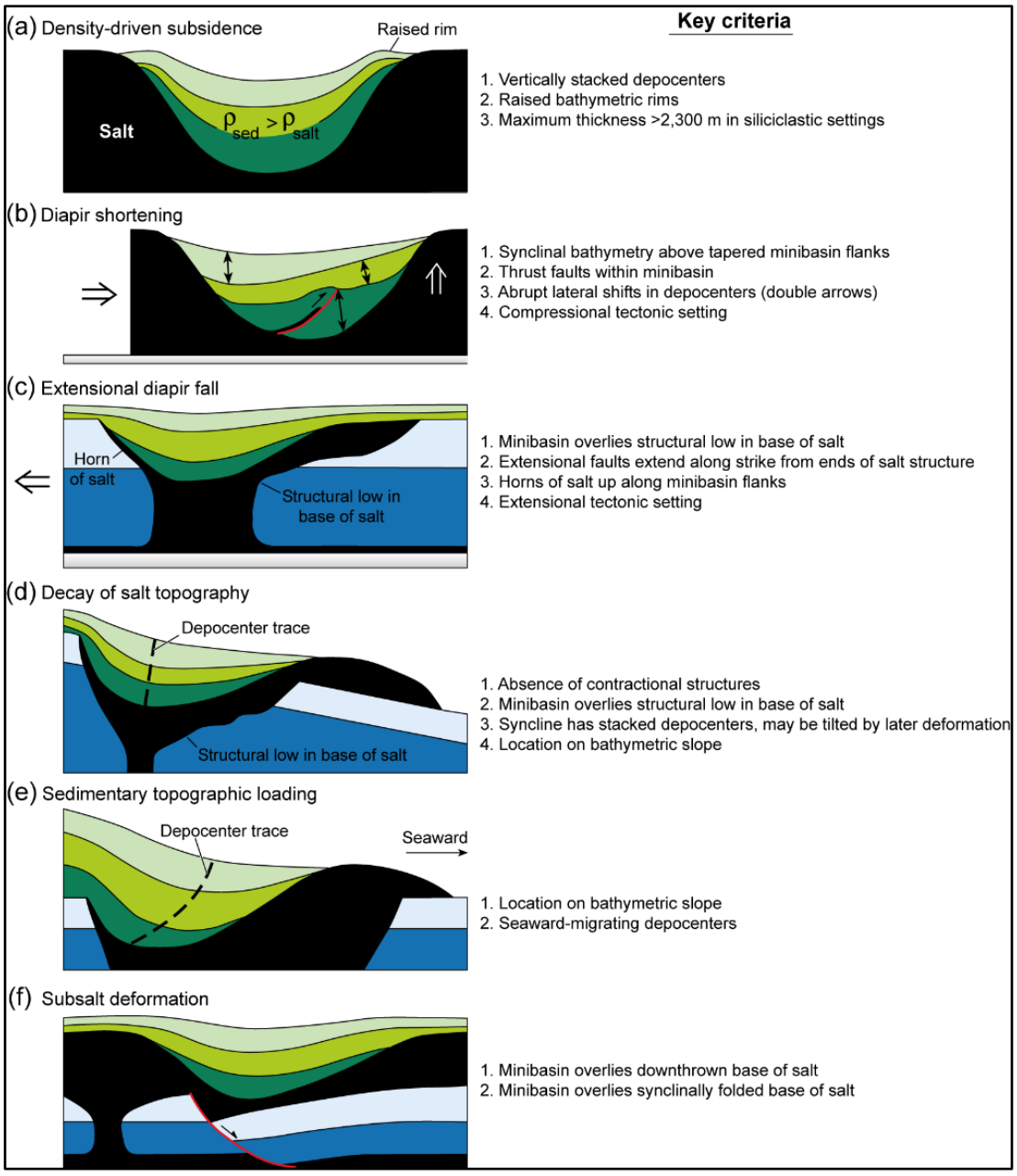


Fig. 1.6 Mechanisms of minibasin subsidence and key criteria to describe them (Hudec et al., 2009), (colours changed).

Thin-skinned extension (i.e., extension above a detachment surface) can also drive minibasin subsidence because extensional faults can deform the top of the salt body and produce a local depocenter which overlies the synclinally folded base of salt (Fig. 1.6f) (Hudec et al., 2009). Thick-skinned extension leads to subsalt deformation and reactive diapirism when the salt migrates into diapirs developed in the footwall of basement-faults (Fig. 1.7) (Dooley et al., 2005).

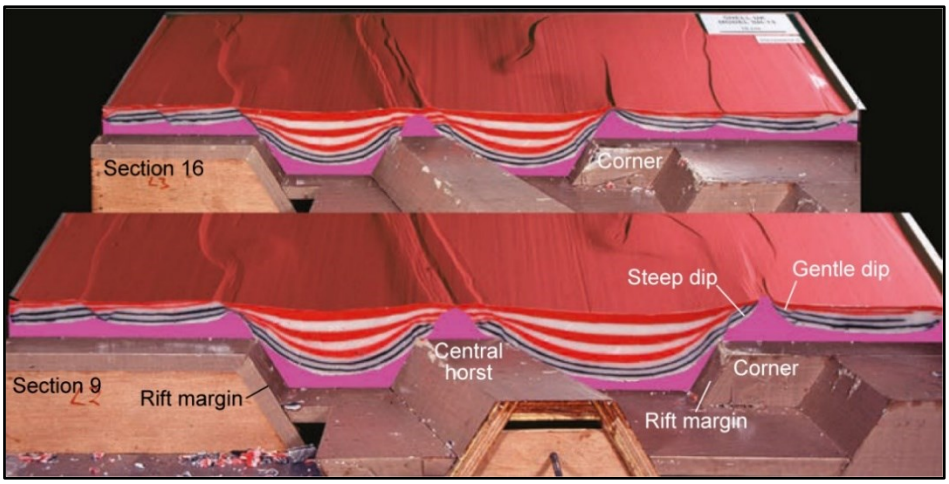


Fig. 1.7 Three-dimensional physical model shows reactive diapirs developed above footwall of basement faults during thick-skinned extension. Minibasins are located between emerging diapirs (Dooley et al., 2005).

1.3.4 Internal deformation within minibasins and salt-sediment interactions

In salt-withdrawal minibasins, a wide variety of stratal and structural features observed at different scales provide a lot of information about the growth of salt structures and the evolution of the salt system. The most prominent features along minibasin-edges are the so-called megaflaps. A megaflap is a kilometre-scale, steeply dipping, vertical or totally overturned wedge of sediments against a salt diapir or an equivalent weld (Fig. 1.8a and Fig. 1.8b) (Graham et al., 2012; Rowan et al., 2014; Callot et al., 2016; Rowan et al., 2016). Megaflaps have been identified in rift basins, passive margins, foreland basins and fold-and-thrust belts. Well known examples include the Willouran Ranges of South Australia (Hearon IV et al., 2015), the Gulf of Mexico (Rowan & Ratliff, 2012; Rowan et al., 2016; Ferrer et al., 2017), the Paradox Basin (Jobe et al., 2020), the Southern Pyrenees (Gannaway Dalton et al., 2022) and the Subalpine chains of Provence (Graham et al., 2012). An overturned megaflap which once represented the thin roof of a salt diapir is also exposed in the study area (see Chapter 4 and Chapter 5).

Megaflaps comprise the deepest minibasin strata and, in most of the cases, they are structurally concordant and stratigraphically conformable with the underlying salt (Hearon IV et al., 2015; Rowan et al., 2016). Megaflaps develop over long time scales (5 Myr to more than 100 Myr) (Rowan et al., 2016) and may be progressively folded by rising salt where the sediment-salt contact is gently dipping (Jackson & Hudec, 2017). They can form in primary or secondary minibasins over the autochthonous or the allochthonous salt levels due to drape folding during passive diapirism or contraction (Fig. 1.8 and Fig. 1.9) (Rowan et al., 2016). Megaflaps formed in secondary minibasins are usually thinner than flaps formed adjacent to diapirs developed on the autochthonous salt layer. Megaflap formation involves kink-band

migration and limb rotation similar to detachment folds (Suppe et al., 1997; Callot et al., 2016; Rowan et al., 2016; Rowan & Giles, 2021).

According to Rowan et al. (2016) the formation of megaflaps is not necessarily related to the emplacement of allochthonous salt but Callot et al. (2016) performed analogue experiments and observed that extrusion of allochthonous salt along the minibasin edges led to the formation of megaflaps. Smaller scale salt-sediment interactions and halokinetic deformation also occur

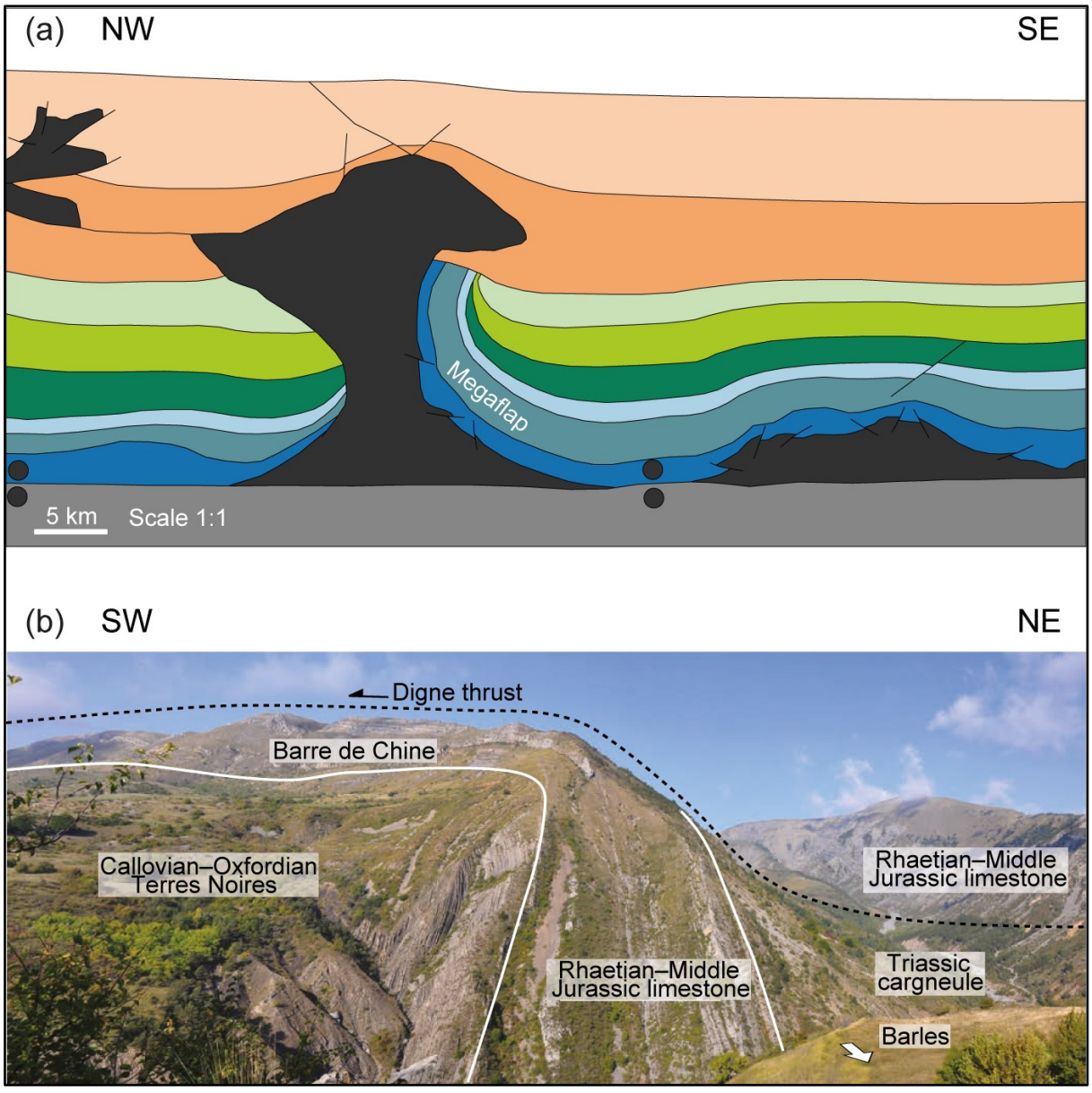


Fig. 1.8 Two examples of megaflaps. (a) A megaflap adjacent to Diapir C in the Atwater Foldbelt, northern Gulf of Mexico. The megaflap formed on the basinward side of the diapir due to contraction during the gravity spreading of the margin. The vertical relief of the megaflap is more than 5 km. (Rowan et al. (2016), colours changed). (b) Overturned flap of the Barre de Chine, Southern Subalpine Chains, France. The flap comprises a condensed and overturned section of Lower and Middle Jurassic rocks originally forming the flank of the Barles diapir. The overturning of the megaflap is related to the emplacement of an allochthonous salt sheet during the deposition the Callovian-Oxfordian Terres Noires formation. The allochthonous salt reached the surface and extruded as a salt nappe to the seabed. After Graham et al. (2012).

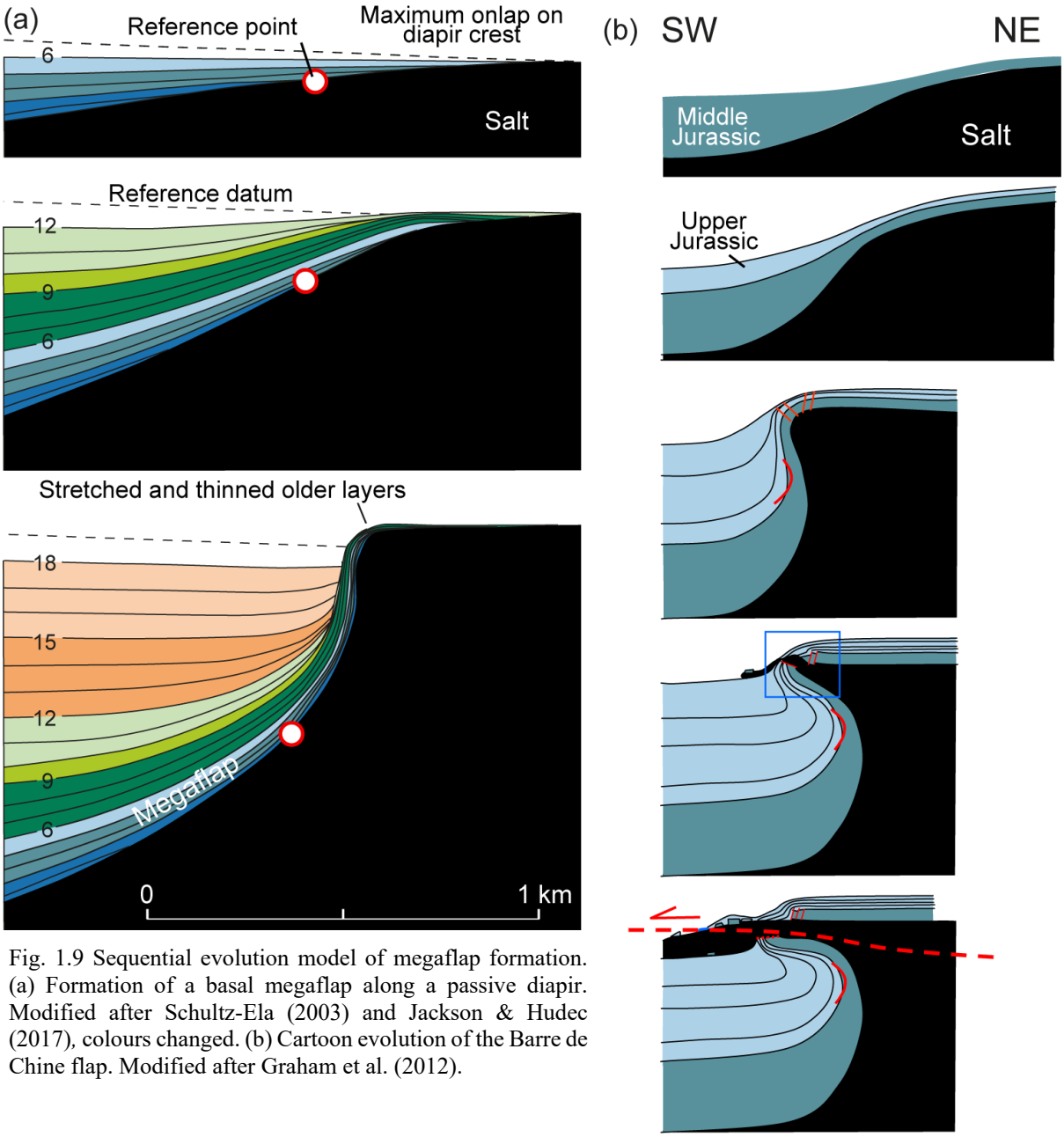


Fig. 1.9 Sequential evolution model of megaflap formation. (a) Formation of a basal megaflap along a passive diapir. Modified after Schultz-Ela (2003) and Jackson & Hudec (2017), colours changed. (b) Cartoon evolution of the Barre de Chine flap. Modified after Graham et al. (2012).

along the flanks of mature diapirs. Halokinetic sequences (HS) form along passive diapirs as the thin roof folds during salt rise over the timescale of several hundred thousand years to several million years (Giles & Rowan, 2012). Halokinetic sequences are successions of growth strata influenced by near surface or extrusive salt movement (Fig. 1.10). Halokinetic sequences have been described in shallow marine settings, deep-marine slope and basinal settings, and also sub-aerial depositional environments (Giles & Lawton, 2002; Rowan et al., 2003; Ringenbach et al., 2013; Hearon et al., 2014; Kergaravat et al., 2017). The sequences are bounded at their base and top by local angular unconformities (Giles & Lawton, 2002), though strata became conformable with distance from the diapir (Fig. 1.10a and b). The style of drape

folding and type of halokinetic sequence are influenced by the rate of sedimentation versus the rate of salt rise (Giles & Rowan, 2012). Rapid sedimentation can cover the diapir with thicker roof strata forming wedge-shaped halokinetic sequences (Fig. 1.10b). Drape folding generally occurs within 1 km of a diapir, and angular unconformities are usually less than 30º. Facies changes are gradational and mass-waste deposits are not particularly common. The topographic relief is negligible as sediments progressively fill up minibasins adjacent to rising diapirs. Stacked wedge halokinetic sequences with convergent base and top boundaries form tapered composite halokinetic sequences (CHS) (Fig. 1.10d). In the Southern Subalpine chains, halokinetic sequences present in the Liassic succession adjacent to the Astoin diapir (Célini et al., 2020).

Hook halokinetic sequences form when sediment accumulation cannot keep up with diapiric rise (Fig. 1.10a). In hook halokinetic sequences, drape folding occurs closer to the diapir than

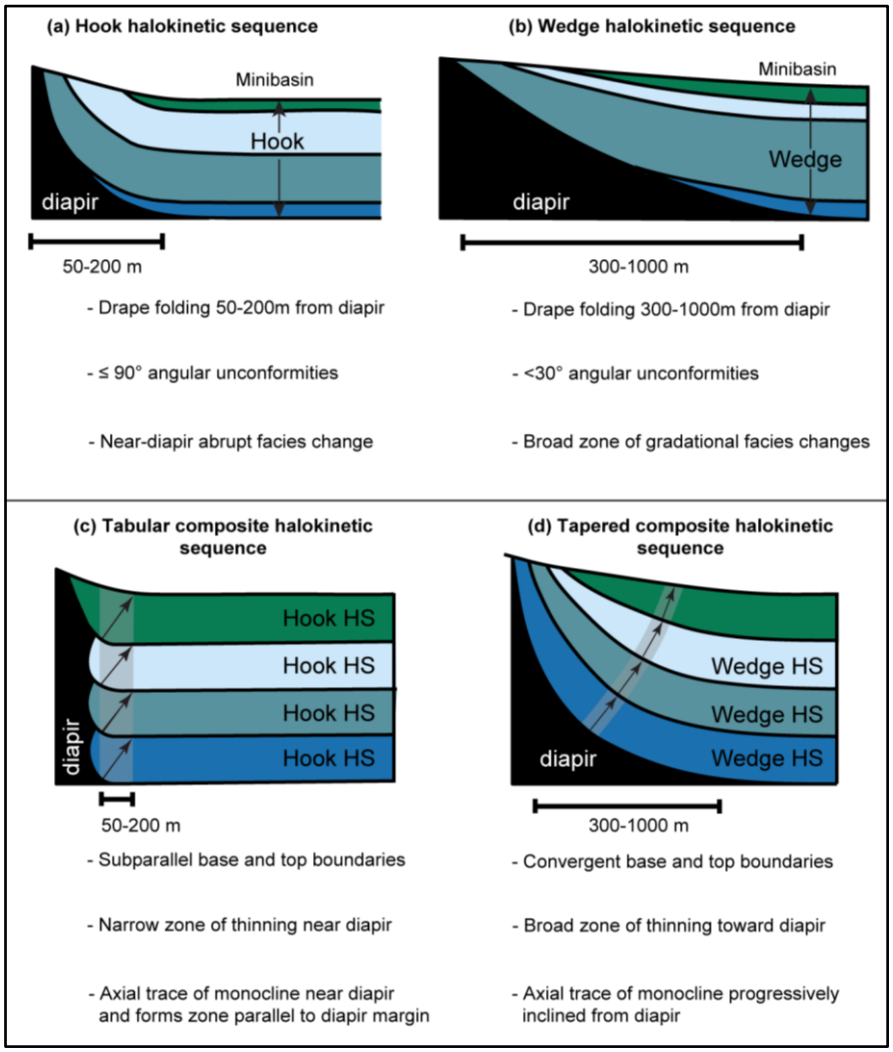


Fig. 1.10 Schematic sections showing halokinetic sequences (HS) and composite halokinetic sequences (CHS) forming adjacent to passive diapirs. (a) Hook halokinetic sequence. (b) Wedge halokinetic sequence. (c) Tabular composite halokinetic sequence. (d) Tapered composite halokinetic sequence. Modified after Giles & Rowan (2012).

in wedge halokinetic sequences (within 50-200 m) and the degree of local angular unconformities is much higher (up to 90º). Local facies variations and mass-waste deposits are common in hook halokinetic sequences. Tabular composite halokinetic sequence (CHS) form when the sediment-accumulation rate is less than the salt-rise rate and the hook halokinetic sequences are stacked together (Fig. 1.10c).

Hook and wedge halokinetic sequences are end-member styles and they can change over time as the diapir-rise rate or sedimentation rate changes (Fig. 1.10) (Giles & Lawton, 2002; Giles & Rowan, 2012). Transition or alternation between tapered and tabular composite halokinetic sequences (CHS) is also possible.

Post-depositional halokinetic deformation can also occur along diapirs. This is demonstrated by an isopachous stratal package on the eastern side of the Emirhan minibasin (Sivas basin, Turkey) (Fig. 1.11), where Unit 4 was folded during the deposition of Unit 5 (Ribes et al., 2015).

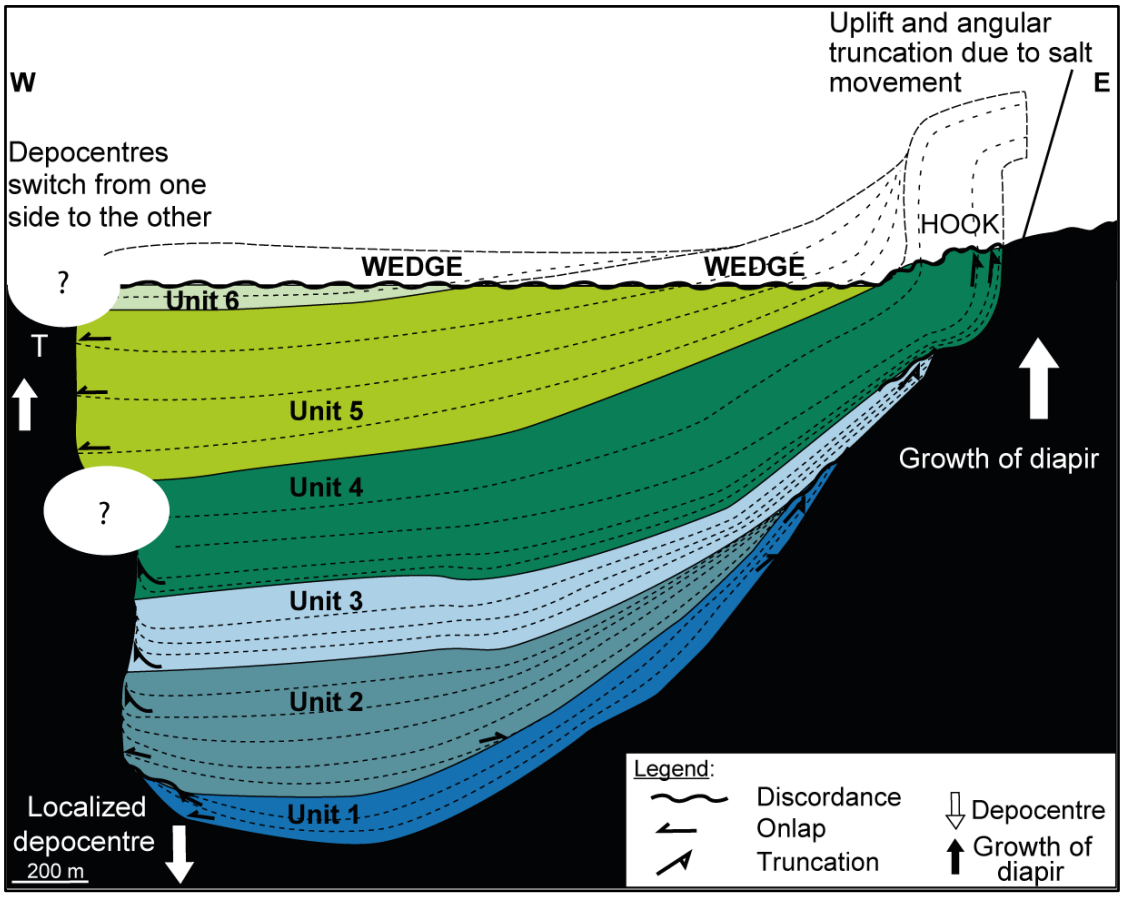


Fig. 1.11 Hook and wedge halokinetic sequences in the Sivas basin, Turkey (Ribes et al. (2015), colours changed).

1.3.5 Welds: structures marking vanished salt bodies

A salt weld is a tectonic discordance which marks a partly or completely depleted salt body which resulted from loss of original salt volume by creep or dissolution (Jackson & Cramez, 1989; Jackson & Hudec, 2017). Flanking strata can be concordant or discordant to the weld surface. It is possible to classify welds based on their position in the salt system and their geometry (Jackson & Cramez, 1989). A primary weld represents a subhorizontal or moderately dipping weld formed at the level of autochthonous salt (Fig. 1.4). Nearly vertical secondary welds are forming during the depletion of diapiric structures such as salt walls or salt stocks (Fig. 1.12). Tertiary welds are the lower contacts of allochthonous salt sheets (Fig. 1.4). Welds can form during all salt tectonic (halokinetic) processes, and during regional extension and also regional compression.

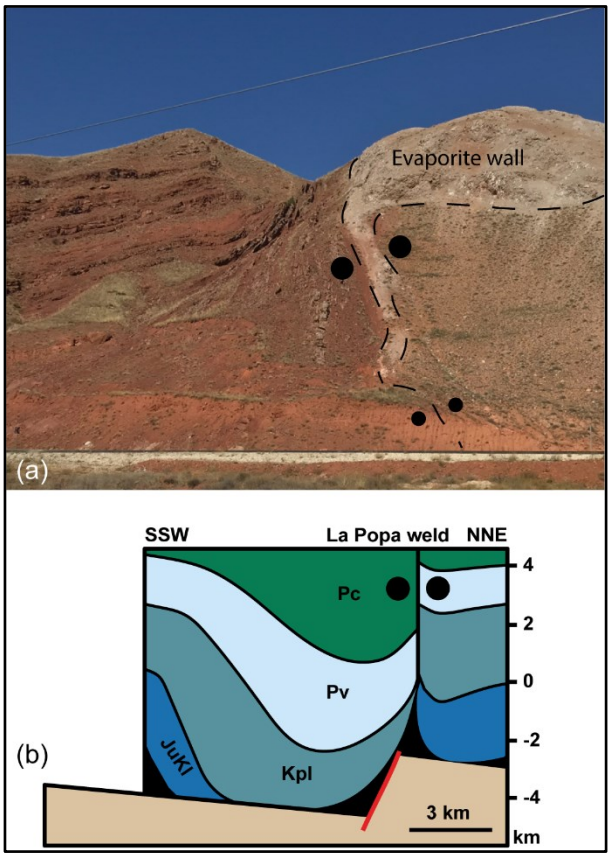


Fig. 1.12 (a) Outcrop example of a weld, SW of the Emirhan minibasin, Sivas basin, Turkey. The lower segment of the weld is completely welded. The upper segment of the weld is incomplete and contains a few meters of remnant gypsum (Jackson & Hudec, 2017; Kergaravat et al., 2017). Photo by Lajos Adam Csicsek. (b) Cross-section view of a subvertical secondary weld, La Popa basin, Mexico (Rowan et al. (2012), colours changed).

The identification of salt welds is commonly challenging in onshore shortened regions because displacement may occur along already partly or completely welded salt structures. Secondary welds formed during the early phases of regional shortening can be easily reactivated as thrust welds. Varying degrees of displacement can occur along salt walls perpendicular to the regional shortening direction (Duffy et al., 2018). After early welding, these welded walls can evolve into major thrust welds or thrust faults. Salt walls oriented obliquely to the regional shortening direction can form thrust welds with strike-slip component of movement (Jahani et al., 2017; Hassanpour et al., 2018; Duffy et al., 2021). Salt walls parallel to the shortening direction may become strike-slip faults and, during later stages of regional compression, become a fault-weld (Rowan & Vendeville, 2006; Brooke-Barnett, 2022; Brooke-Barnett et al., 2023).

Allochthonous salt sheets and canopies may be used as detachment surfaces during contractional deformation and become deflated to form tertiary welds. Regional and also local unconformities may represent welded extrusive salt sheets and canopies which once covered a considerable area (Graham and Csicsek 2020).

Welds are common features in the Southern Subalpine chains (see Chapter 3, § 3.4 and § 3.8) (Graham et al., 2019; Célini, 2020; Célini et al., 2020; Csicsek et al., 2021; Brooke-Barnett, 2022; Célini et al., 2022; Brooke-Barnett et al., 2023). In the study area, welds are also present in the Mesozoic and Tertiary successions (see Chapter 4 and Chapter 5).

1.3.6 Salt tectonics in compressional settings and folded belts

This thesis is concerned with salt tectonics in the fold and thrust belt of the SW Alps. Many of the Alpine mountain belts contain evaporitic successions and the structural style has been affected dramatically by salt tectonics (Davis & Engelder, 1985; Letouzey et al., 1995; Callot et al., 2007; Callot et al., 2012; Graham et al., 2012; Lopez-Mir et al., 2015; Jackson & Hudec, 2017; Soto et al., 2017; Granado et al., 2019; Callot et al., 2022; Flinch & Soto, 2022). Structural style depends on the thickness of the evaporite horizon, the nature of the overburden and the presence or absence of precursor salt structures (Fig. 1.13) (Hudec & Jackson, 2007; Jackson & Hudec, 2017). In thin-skinned (or detached) tectonic settings, a thin and continuous evaporite level with no precursor salt structures can act solely as a detachment surface for the advancing fold and thrust belt typically associated with thrust faults and narrow box-folds (Fig. 1.13a) (Hudec & Jackson, 2007). Where the pre-kinematic evaporite layer is thinner, salt-cored anticlines can form during regional contraction as salt flows into cores of the anticlines while the stronger overburden is folded (Jackson & Hudec, 2017). The structure of the fold and thrust belt is relatively simple, with little variation in structural style along-strike of the belt (Duffy et al., 2018).

Thick evaporitic levels may have been the source layer for precursor diapiric activity before the onset of regional shortening (Graham et al., 2012; Célini et al., 2020; Hudec et al., 2021; Strauss et al., 2021). Pre-orogenic salt structures deform early during regional shortening because they are mechanically weaker than their overburden. Diapirs are located closer to the hinterland will be deformed earlier and suffer more significant compressional deformation than the salt structures that are located closer to the foreland (Nilsen et al., 1995; Duffy et al., 2018). The structural style of mountain belts which contain preexisting salt structures is very different

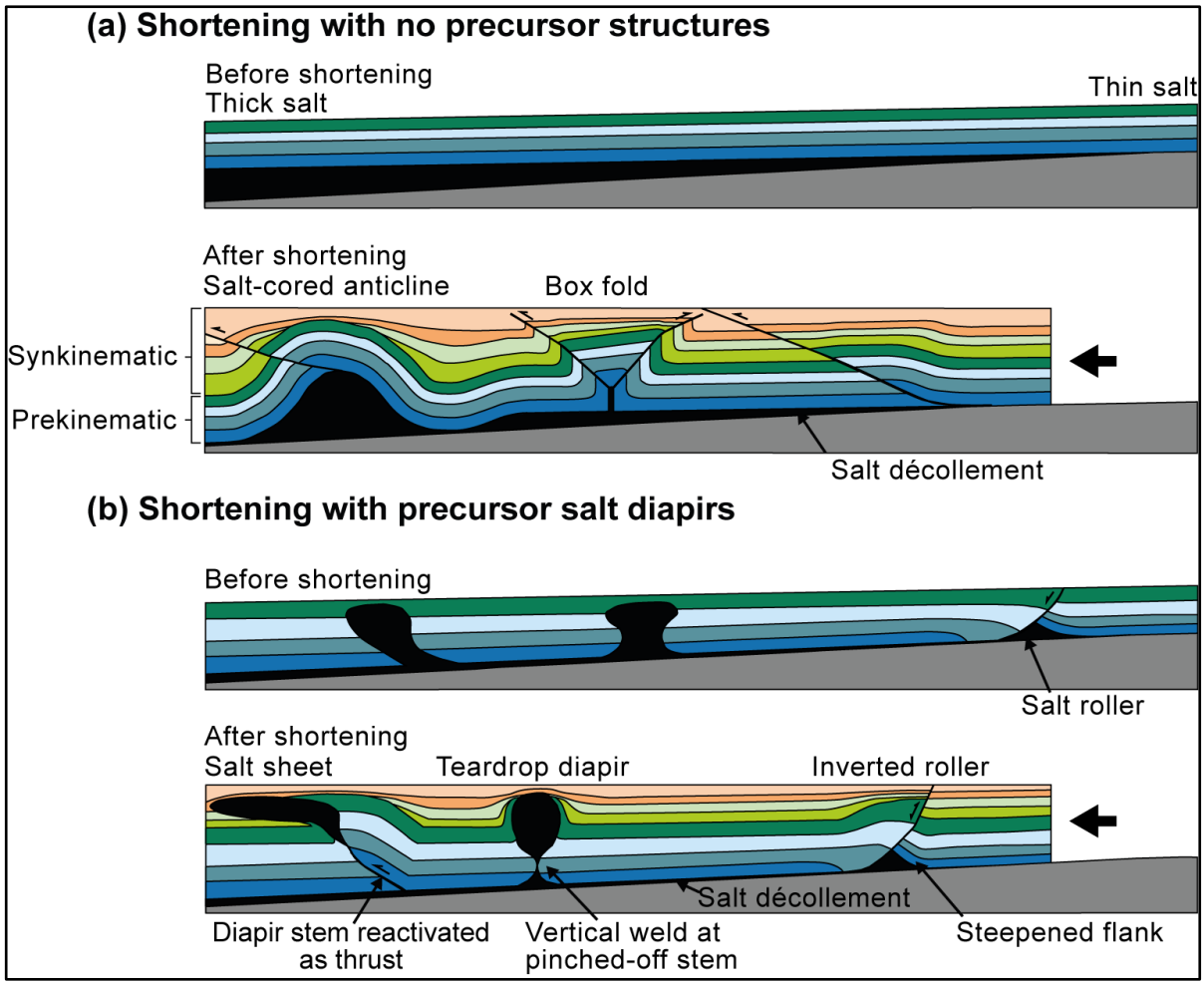


Fig. 1.13 Structural style in shortened regions which contain salt depends on the thickness of the evaporite level, its overburden, and the absence (a) or presence (b) of precursor salt structures (Hudec & Jackson (2007) and Jackson & Hudec (2017), colours changed).

from fold and thrust belts where the salt only provides a basal detachment surface for the folding and thrusting (Fig. 1.13a).

During diapir shortening, upward salt rise occurs and the roof of the diapir is arched. In some circumstances, salt also can intrude downward into the source layer and the base of the diapir (Dooley et al., 2009), but once the diapir stem is welded, the remnant bulb or teardrop diapir is not attached to the source layer anymore (Fig. 1.13b). However, diapiric rise of the remnant salt may well continue as the diapir flanks converge (Jackson & Hudec, 2017).

Earlier formed salt rollers (Bally, 1981) may be inverted during regional shortening (Fig. 1.13). Residual triangular salt pedestals commonly form at the base of the steeply dipping secondary welds and during regional shortening, these triangular pedestals may be used as ramps where thrust faults splay from the basal detachment surface (Fig. 1.14b). Secondary welds may be reactivated as thrust faults or shortcut thrusts may offset the vertical weld stems (Fig. 1.13b and Fig. 1.14b) (Hudec & Jackson, 2007; Duffy et al., 2018). Diapirs with low-

amplitude and gentle flanks preferentially act as ramps for the thrust faults, taller diapirs are likely to be detached from their pedestal by short cutting thrust faults (Callot et al., 2007; Jackson & Hudec, 2017). This phenomenon occurred also in the Southern Subalpine chains (see Chapter 5). Sedimentary rocks deposited around the salt structures remain relatively undeformed and mostly affected by folding and faulting (Callot et al., 2007; Duffy et al., 2018).

During the early stages of regional shortening, an isolated diapir can form a salient in a thrust front (Fig. 1.14b) (Dardeau & De Graciansky, 1990; Dooley et al., 2009; Duffy et al., 2018). During later stages of shortening, as diapirs become highly squeezed, the previously formed salients becomes reentrants in the thrust front and folds and thrusts are no longer continuous along-strike but connect pre-existing diapirs (Fig. 1.14) (Jackson & Hudec, 2017; Duffy et al., 2018).

Under a thick sedimentary cover, diapirs are narrowed but not necessarily welded. Diapiric salt is forced back to the source layer because the thick and strong cover impedes salt extrusion to surface (Fig. 1.14c). At low strain rates, gentle arching and crestal faulting occur above the shortened diapirs and individual diapirs are not connected by folds or thrusts. At higher strain

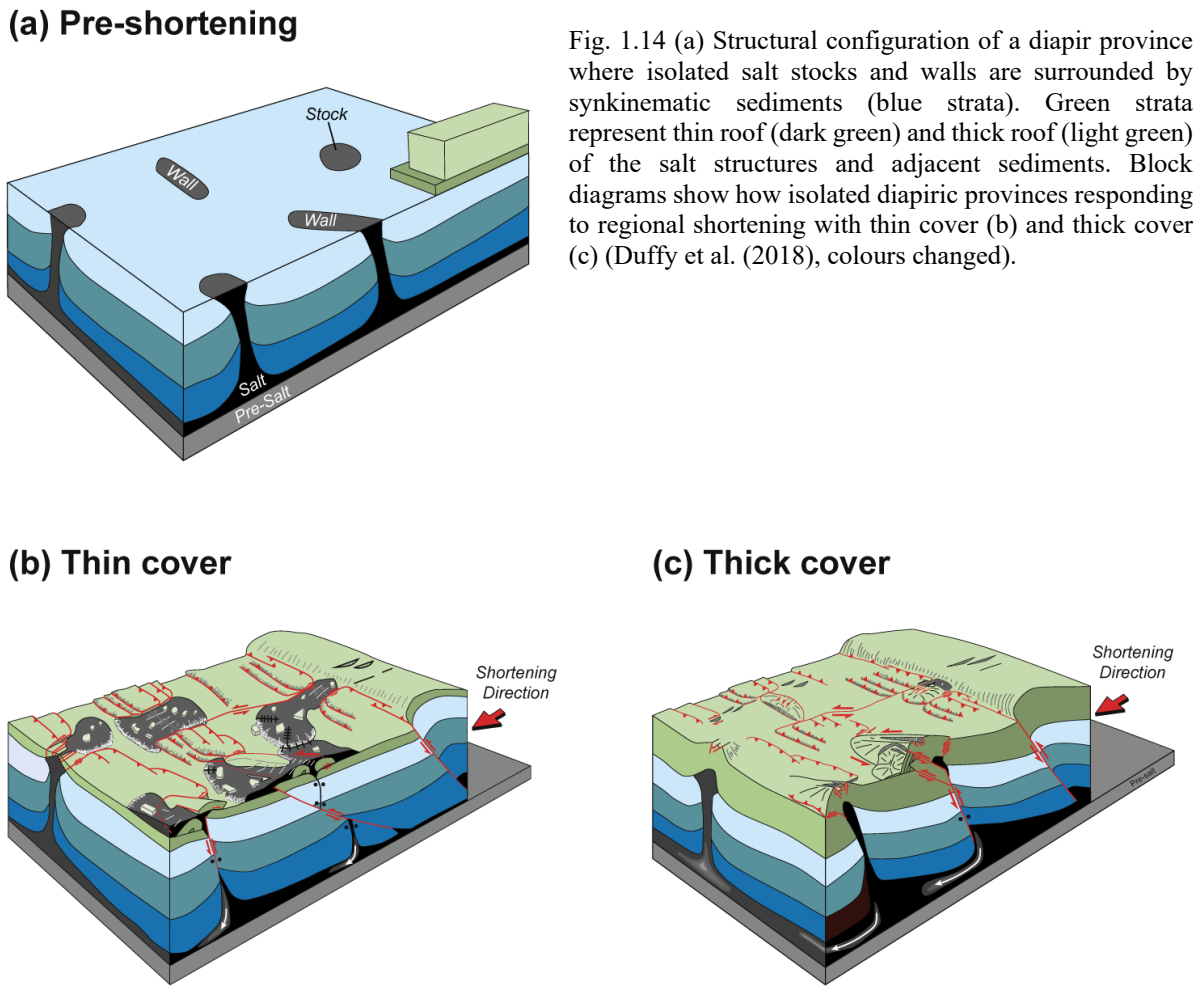


Fig. 1.14 (a) Structural configuration of a diapir province where isolated salt stocks and walls are surrounded by synkinematic sediments (blue strata). Green strata represent thin roof (dark green) and thick roof (light green) of the salt structures and adjacent sediments. Block diagrams show how isolated diapiric provinces responding to regional shortening with thin cover (b) and thick cover (c) (Duffy et al. (2018), colours changed).

rates, tear-faults can link diapirs across strike and minor salt extrusion may occur near the hinterland (Duffy et al., 2018).

Due to regional shortening, extrusive salt sheets are expelled to the surface through exposed diapirs (Fig. 1.14b). Extrusive salt sheets formed in the study area during the Alpine compressional phase (see Chapter 5). Salt stocks with thin and weak roofs can break apart their overburden, also leading to the extrusion of salt sheets (Fig. 1.14b). Dismembered blocks of a diapir roof (so-called rafts or carapace) float in the extrusive salt sheet (Fig. 1.14b) becoming grounded once the allochthonous salt body is welded out.

Hudec & Jackson (2006) suggested three different mechanisms of allochthonous salt sheet emplacement during regional shortening: plug-fed extrusion, plug-fed thrusting, and source-fed thrusting (Fig. 1.15). Plug-fed extrusion occurs when a salt sheet is emplaced from an exposed steep or vertical salt diapir (stock or wall). Plug-fed thrusts may form during regional shortening in orogenic belts or deep-water fold and thrust belts where a strong overburden impedes salt extrusion, the salt is expelled from a pre-existing diapir in the hanging wall of a thrust. Source-fed thrusts elevate salt in their hanging wall from the autochthonous evaporite layer during regional shortening. Hudec & Jackson (2006) have proposed that allochthonous

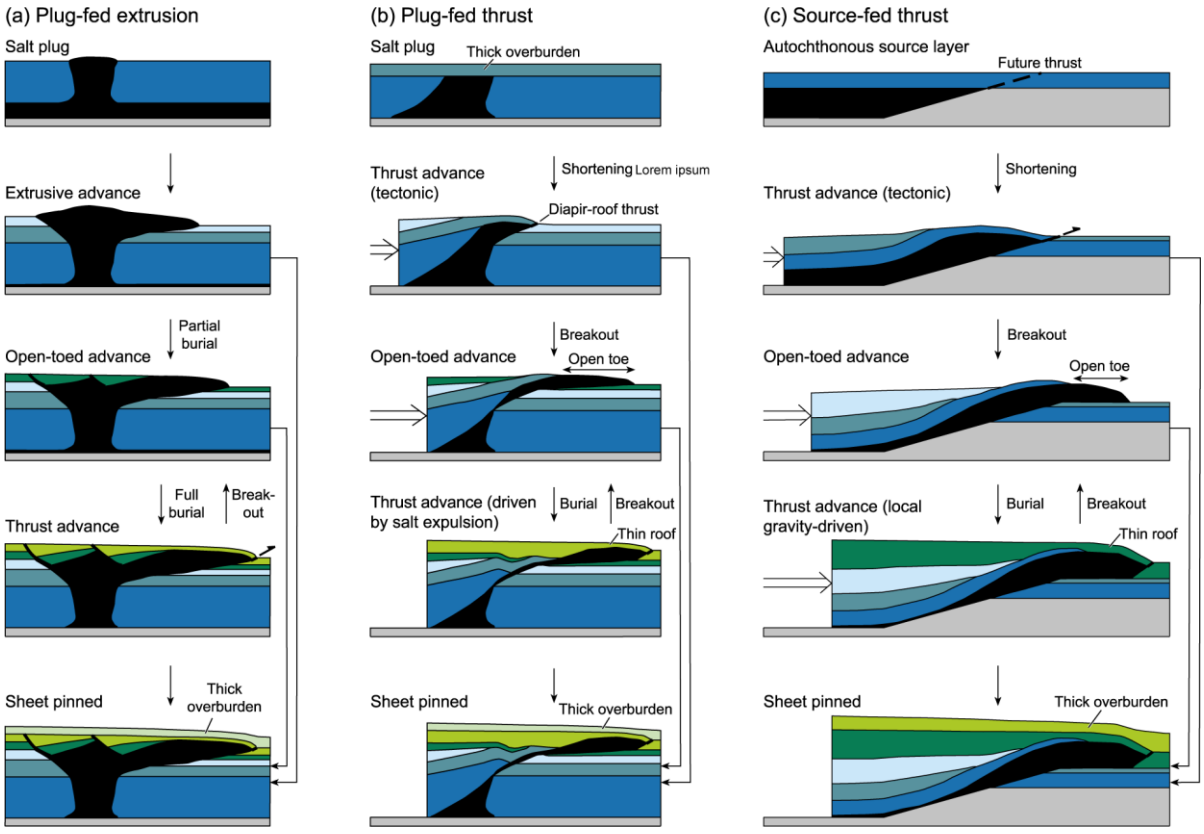


Fig. 1.15 Three mechanism of allochthonous salt sheet emplacement and evolutionary histories of the sheets (Hudec & Jackson (2006), colours changed).

salt sheets can advance with or without sedimentary overburden i.e., in an open-toe style or covered by an overburden which may either be thick or thin (Fig. 1.15). Salt sheets can merge together along sutures and form salt canopies (Fig. 1.4) which may be connected to the mother salt layer through vertical diapiric stems or totally detached from their original feeder diapirs (Jackson & Hudec, 2017). During the later stages of regional shortening, allochthonous salt bodies may be the source of a second generation of diapiric structures bounding secondary minibasins (Fig. 1.16).

Shortened salt basins which contain isolated minibasins floating in salt show a different structural style from basins containing only isolated diapiric structures. These regions are the so-called wall-and-basin structure regions (Harrison & Jackson, 2014; Kergaravat et al., 2016) or isolated-minibasin provinces (Duffy et al., 2021). The structural style of shortened regions is highly variable along strike because of the complex configuration of pre-existing diapirs and minibasins and their behaviours during regional shortening (Rowan & Vendeville, 2006; Ringenbach et al., 2013; Callot et al., 2014; Harrison & Jackson, 2014; Kergaravat et al., 2016; Duffy et al., 2017; Legeay et al., 2020b; Duffy et al., 2021).

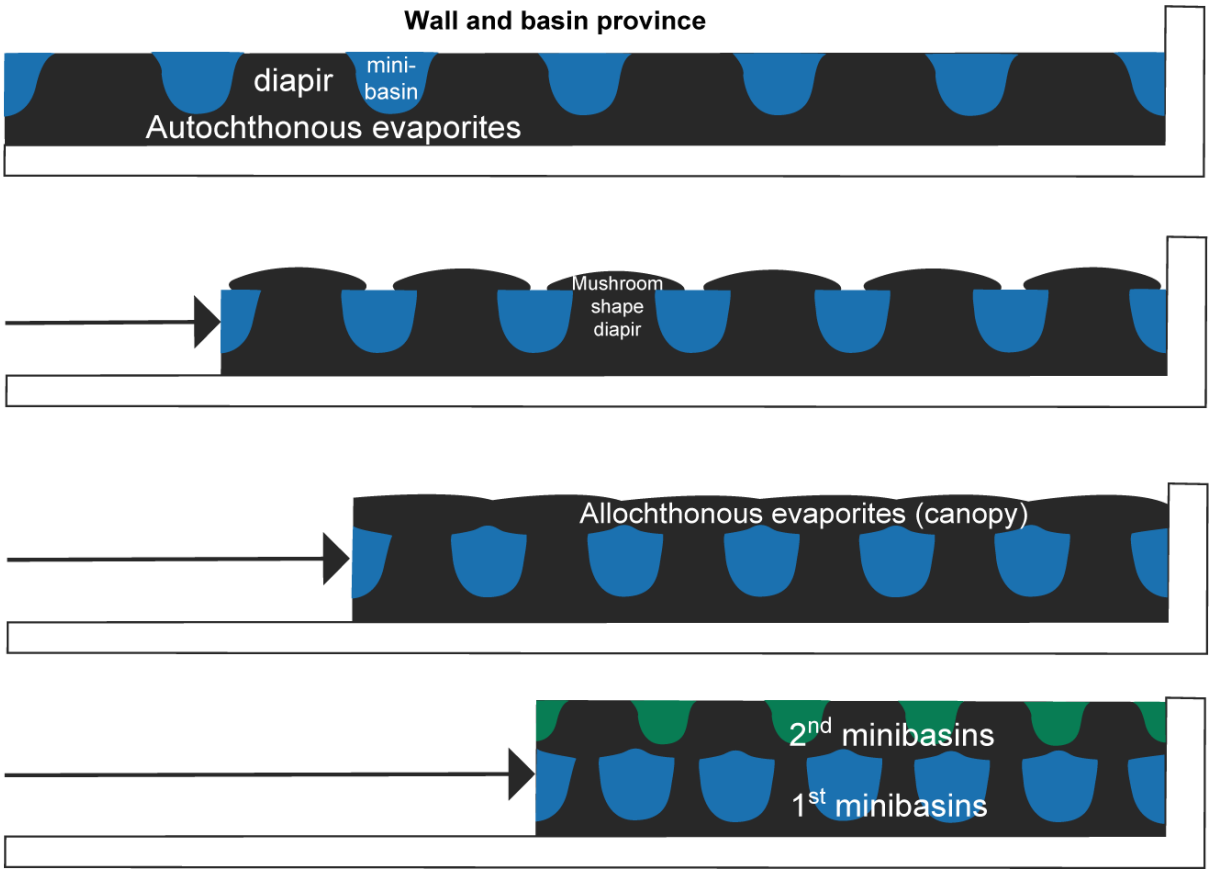


Fig. 1.16 Schematic evolution of two generations of minibasins below and above an allochthonous salt canopy in compressional setting. Salt sheets extruded over first generation of minibasins from mushroom shaped diapirs and amalgamated into an allochthonous evaporite canopy. Modified after Kergaravat et al. (2016).

At the onset of regional shortening, strain is localised in mechanically weak salt, and it starts to flow. At low strain rates minibasins remain predominantly undeformed, and although salt walls perpendicular to the regional shortening direction are usually shortened and welded (Fig. 1.17a), walls parallel to the shortening direction tend to stay open and allow salt to flow through (Fig. 1.17a) (Duffy et al., 2021). Minibasins surrounded by weak evaporites are translated, tilted and rotated during regional shortening as salt flows around them (Kergaravat et al., 2016; Duffy et al., 2021). Isolated minibasins can be tilted during regional shortening (Callot et al., 2016; Kergaravat et al., 2016; Ribes et al., 2017; Granado et al., 2019; Legeay et al., 2020b), or by asymmetric subsidence above an evaporite layer which is varied in thickness (Jackson et al., 2020) or in response to the shifting load of prograding sediments (Callot et al., 2016). The formation of rollovers may also lead to minibasin tilting (Jackson & Hudec, 2017). Rollovers represent stratal intervals which bend towards a normal fault or a diapir. Extensional rollovers form along listric faults during the displacement of hanging wall strata (Hamblin, 1965). Expulsion rollovers form during the expulsion of salt due to load of prograding sediments (Ge et al., 1997) Any syn-depostional tilting leads to the deposition of wedge-shaped sedimentary packages (Callot et al., 2016; Jackson et al., 2020).

In compressional settings, rotation around horizontal axes (i.e., tilting) is visible both in analogue models, on seismic and in nature in places like the Sivas basin and also here in Provence (see Chapter 5). Rotation around vertical axes has been demonstrated in analogue modelling in association with strike slip faulting or interaction with base-salt highs and irregularities (Fig. 1.17b) (Duffy et al., 2021). In the presence of a salt sheet or canopy, the depletion or pinch-out of the autochthonous salt level can itself cause the rotation of secondary minibasins (Kergaravat et al., 2016). In models (Callot et al., 2016), colliding minibasins were seen to rotate around lateral contacts with high degrees of rotation (up to 90^{o}) in some cases.

Modelling also suggests that the presence of intra-salt sediment bodies like rafts can change the lateral mobility of minibasins during regional shortening. In isolated-minibasin provinces intra-salt sediment packages can absorb shortening and buttress the minibasins so that intervening salt structures remain open and the minibasins remain widely spaced (Duffy et al., 2017).

In natural examples of shortened salt basins, we see isolated salt diapirs, primary minibasins and allochthonous salt levels (sheets and canopies) together with second generation diapirs and secondary minibasins, i.e., a wide variety of structural styles which vary temporally and spatially during their structural evolution.

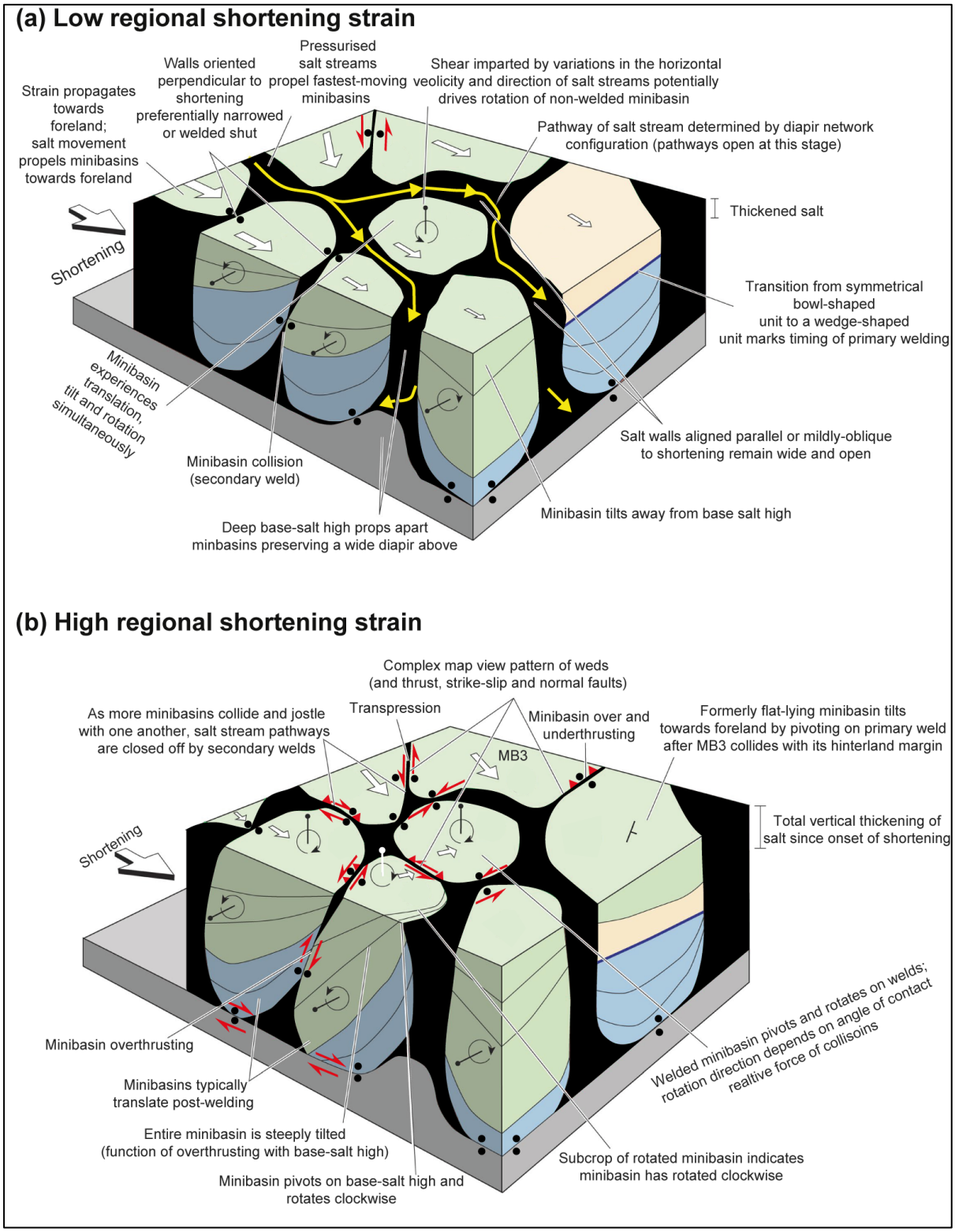


Fig. 1.17 Conceptual models showing structural styles and processes in shortened isolated minibasin provinces. Minibasins subsided into a single salt layer, and they were not welded at their base before the onset of the regional shortening. a) Low regional shortening strain. (b) High regional shortening strain (Duffy et al. (2021), colours changed).

1.4 Data/methodology/fieldwork

This work is based on geological mapping and structural analysis of the southwestern area of the Southern Subalpine chains. Geological maps (1:50 000 and 1:250 000 scale) and reports published by the BRGM (Bureau de Recherches Géologiques et Minières) (Kerckhove & Roux, 1976a; Kerckhove & Roux, 1976b; Kerckhove & Roux, 1978a; Rouire et al., 1979; Campredon et al., 1980a; Campredon et al., 1980b; Kerckhove et al., 1980; De Graciansky et al., 1981; De Graciansky et al., 1982) were an important resource and formed the basis for the mapping. IGN Topographic maps (1:25 000 and 1:50 000 scale) and aerial photographs of the study area were also essential parts of the dataset. The topographic and geological maps were integrated into ArcGIS and Midland Valley's Move software to be used as base maps for the detailed geological mapping. These maps were also used for section construction and structural analysis during two field seasons in 2018 and 2019. During fieldwork a tablet (iPad Pro) with Midland Valley's FieldMove software was used for digital geological mapping and recording structural data. Digital photographs were also taken. Oblique aerial images were acquired by drone in the Barrême, Blieux, Taulanne and Castellane areas (Fig. 2.1b). Cross-sections have been constructed using these data. Several cross-sections were drawn on paper and redrawn in Adobe Illustrator to help understand the structural and stratigraphic relationships of the area. Subsurface data including wells were provided by BRGM (Bureau de Recherches Géologiques et Minières) publicly available via the Infoterre and BSS (La Banque du sous-sol) websites.

Chapter 2: Geological setting and stratigraphy

The fold and thrust belt of the Subalpine chains of Provence in the southwest Alps encompasses the Provençal and Dauphiné paleogeographic zones of the external part of the deformed European margin of the Alpine orogen (Fig. 2.1a) (Lemoine et al., 1986; Schmid et al., 2004; Ford et al., 2006; Handy et al., 2010). During Jurassic and Cretaceous times, the area was part of the passive margin of Ligurian Tethys. The basement is made up of Variscan crystalline rocks overlain locally by Carboniferous mudstones and slates, Permian clastic sediments, Lower Triassic sandstones (Buntsandstein formation) and Middle Triassic limestone and dolomite (Muschelkalk). The Variscan basement is exposed northeast of the study area in the external massifs of Pelvoux and Argentera (Fig. 2.1a and Fig. 2.1b) while the Permian succession is at the surface in the Dôme de Barrôt (Lickorish & Ford, 1998; Sonnette et al., 2014) and on the southern and eastern flanks of the Argentera Massif (Fig. 2.1b). Autochthonous Triassic rocks are exposed around the Dôme de Barrôt (Fig. 2.1b) (Campredon et al., 1980a; Campredon et al., 1980b). Crystalline basement lies at the depth of 2-3 km beneath the most of the study area (Fig. 2.1c) (Ménard, 1979).

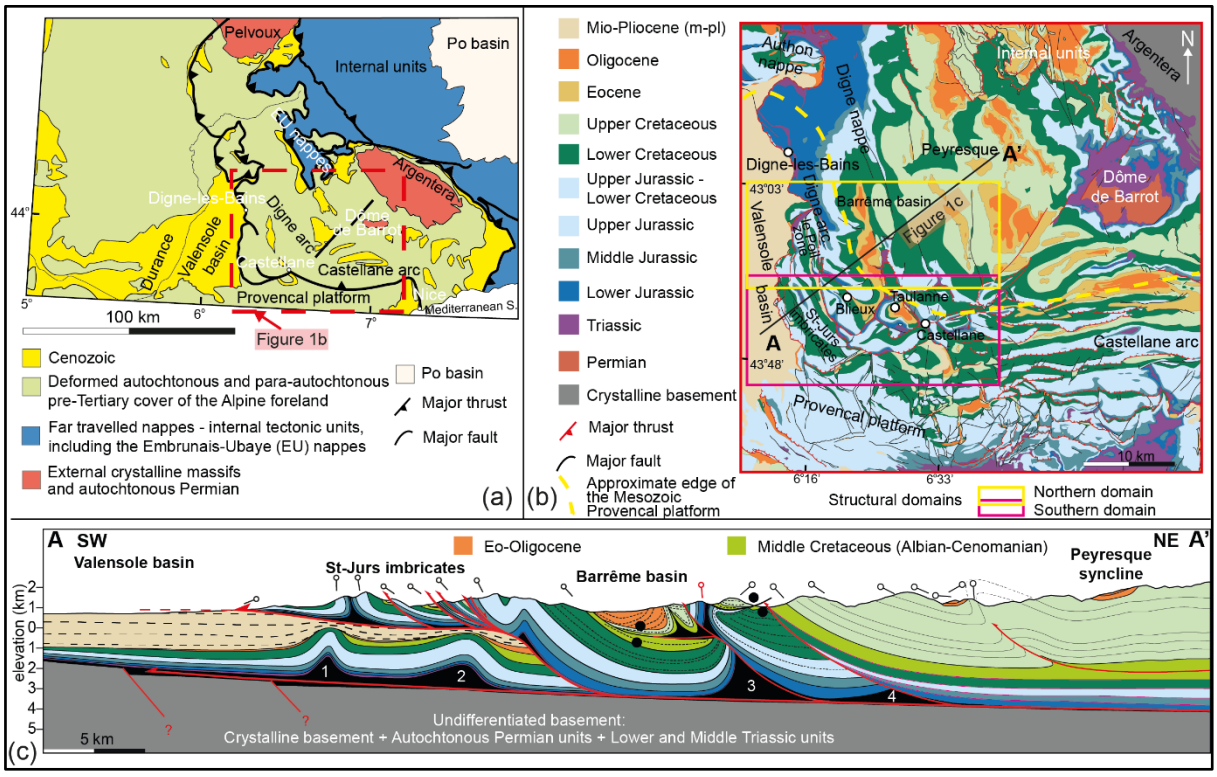


Fig. 2.1 Tectonic map of the Western Alps modified after Schmid et al. (2004). (b) Simplified geological map of Subalpine chains after Rouire et al. (1979) and Kerckhove et al. (1980). The study area subdivided into two structural domains, the northern domain and southern domain, respectively. (c) Regional cross-section of the study area. Numbers showing salt structures of the autochthonous salt layer. (1) 'the anticline at the lake', (2) Dôme de Châteauredon, (3) pedestal of the Gévaudan diapir, (4) pedestal of the la Cine salt wall.

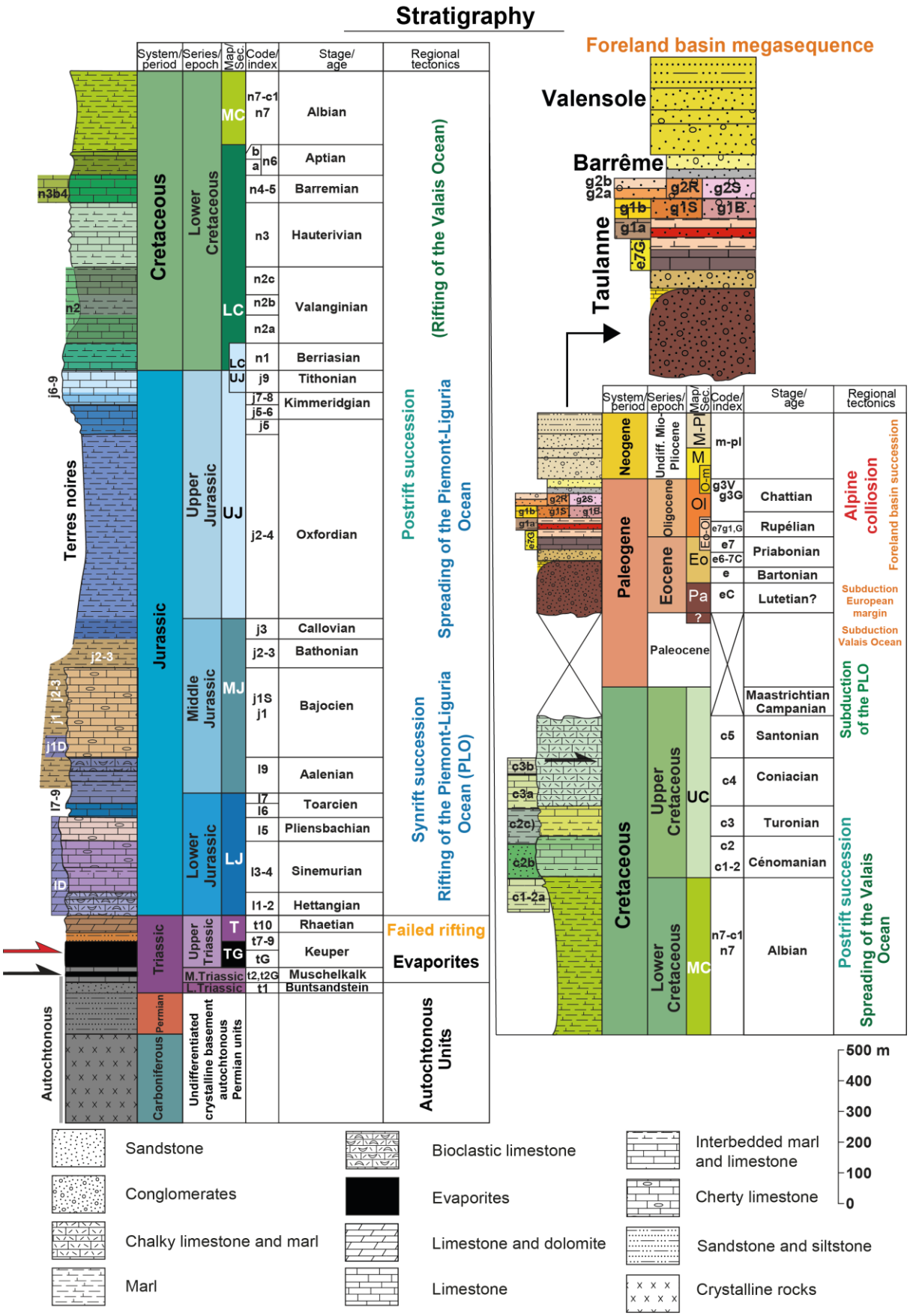


Fig. 2.2 Lithostratigraphic column of the study area and major tectonic events in the Western Alps. In the text, on maps and cross-sections I refer the lithostratigraphic units as they are shown in this column (Data from Kerckhove & Roux (1976a); Kerckhove & Roux (1978a); Campredon et al. (1980b); De Graciansky et al. (1981)).

Upper Triassic (Keuper) rocks present in outcrop include gypsum, dolomite, and mudstone, which may originally have been intercalated with other evaporites including halite, though these are now largely absent. In the northern part of the study area, near Tartonne and Moriez, springs where salt brine flows to the surface have been reported (Morin et al., 2004) suggesting the presence of halite in the subsurface. A salt spring also can be found to south, at Castellane (Roux, 1970; Kerckhove & Roux, 1976b; Bollinger et al., 2010). In the tectonically disturbed areas, the Keuper consists of a chaotic partly deformation-related breccia of carbonates and evaporites (the so called 'cargneule') (Fig. 2.3). Some authors have interpreted the cargneule as cap rock to sub-aerially exposed salt diapirs (Grandjacquet & Haccard, 1975; Graham et al., 2012). Cargneule breccia can also be formed by hydraulic fracturing and de-dolomitization (Warrak, 1974; Grandjacquet & Haccard, 1975) and the occurrence of cargneule breccia itself does not indicate diapiric activity. Determining both the original and recent thicknesses of the highly deformed Keuper succession in the Southern Subalpine chains is challenging. In surface exposures of the Triassic gypsum and cargneule breccia, the thickness varies between a few meters and several hundreds of meters. These Triassic evaporites form the main detachment surface on which thin-skinned Alpine folding and thrusting took place (Fig. 2.1c, Fig. 2.2) (Goguel, 1963; Lickorish & Ford, 1998; Ford & Lickorish, 2004) and also provided a source layer for diapirism (Mascle et al., 1988; Dardeau & De Graciansky, 1990). Evaporites are also present in the Middle Triassic Muschelkalk formation (the Lower Gypsum of Kerckhove & Roux (1976a)).



Fig. 2.3 Cargneule breccia from the Castellane diapir. Note the coin for scale.

The Early-Mid Jurassic rifting event, which eventually led to the opening of the Ligurian Tethys in the Late Jurassic was preceded by failed rifting in the Triassic (Fig. 2.2) (Lemoine et al., 1986; Dumont, 1988; Manatschal, 2004; Handy et al., 2010). There were several separate episodes of rifting during Early and Middle Jurassic times. The first is thought to have occurred in Late Hettangian–Early Sinemurian (Lemoine et al., 1986; Dumont, 1988) but the main rifting event in this part of Provence occurred in the mid Pliensbachian (Fig. 2.2) (Dardeau,

1988; Dumont, 1988; De Graciansky et al., 2010; Handy et al., 2010). The main extensional direction of the Liassic rifting was NW-SE (Fig. 2.4) which led to the formation of tilted fault blocks. A major fault which was active during the Tethyan rifting is the NE-SW trending Rouaine-Daluis fault (Fig. 2.4) situated NE of the study area and defining the northern boundary of the Castellane arc (Mascle et al., 1988; Dumont, 1988). North-west of this fault sedimentation was characterised by the deposition of limestone from the Hettangian to the early Pliensbachian while the Upper Pliensbachian, Toarcian and Aalenian successions are mainly

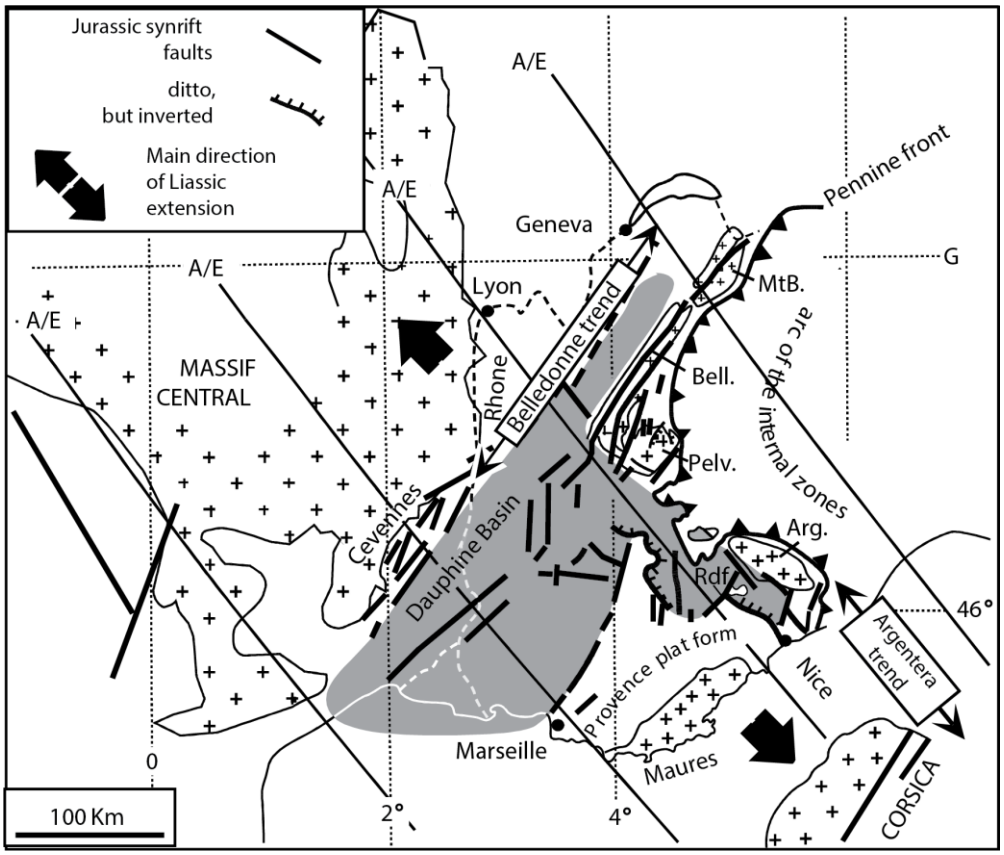


Fig. 2.4 Syn-rift tectonic framework of the Western Alps (De Graciansky et al., 2010). Two different trends of faults (NW-SE and NE-SW) developed during the rifting of the margin. D. = Daluis fault. External crystalline massifs: Arg. = Argentera, Bell. = Belledonne, MtB. = Mont blanc, Pelv. = Pelvoux, Rdf. = Rouaine-Daluis fault.

comprise of marly sediments (Fig. 2.2). Much of this area now comprises the Digne nappe with around 500 meters of syn-rift sediments in most places, reduced to 100-200 meters in the hemipelagic and platformal zones (De Graciansky et al., 1982). Reactive diapirism of the Triassic salt occurred during the rifting phases (Mascle et al., 1986; Mascle et al., 1988; Dardeau & De Graciansky, 1990; Célini et al., 2020). However, the presence of Tethyan extensional faults below the salt structures of the study area is only inferred because most of the diapirs in Southern Subalpine chains were detached from their original basement (Graham et al., 2012; Célini et al., 2020; Brooke-Barnett et al., 2020; Csicsek et al., 2021; Brooke-

Barnett et al., 2021; Célini et al., 2022; Brooke-Barnett, 2022). Passive diapirism occurred as early as the Hettangian and continued throughout the syn-rift phase of the margin in the Digne nappe area (Célini, 2020; Célini et al., 2020).

The passive margin phase, which followed the Jurassic rifting, was dominated by pelagic sedimentation in basinal areas and the development of carbonate platforms on the old rift margins (Lemoine et al., 1986; De Graciansky & Lemoine, 1988; Lickorish & Ford, 1998). Oceanic spreading started in the Bajocian and in the northern part of the Western Alps the oldest post-rift deposits are Bajocian-Bathonian pelagic sediments (Stampfli et al., 1998; Bill et al., 2001; Handy et al., 2010). In the Digne nappe area limestones and marls deposited during the Bajocian and Bathonian whereas in the Castellane-Taulanne area around the platform edge, the Bajocian is represented by dolomite and cherty limestone. In the basinal areas marly sedimentation continued during Bathonian-Callovian and Oxfordian times with the deposition of the Cancellophycus marly limestone and the Terres Noires black shale Formation. During the Kimmeridgian and Tithonian bioclastic and reefal limestones were deposited on the Provençal platform (Calcaires Blancs Formation) while partly resedimented and pelagic limestone was deposited in basinal areas (Digne Nappe and Vocontian Trough) (Beaudoin, 1977; Gray, 1990; Rameil, 2005). These massive limestone beds are forming prominent cliffs in the recent landscape of the Southern Subalpine Chains.

Salt movement also occurred during this post-rift phase of the structural evolution, with the formation of diapirs by sediment downbuilding (Célini, 2020; Célini et al., 2020). Associated minibasin formation started during the Liassic in the Digne nappe area and continued to develop on the thick autochthonous salt. Graham et al. (2012) and Célini et al. (2020) described a salt related flap at Barles (near Digne) where the condensed flank and roof section of a diapir now forms an overturned section of Lower and Middle Jurassic rocks at the margin of an Oxfordian minibasin (see Chapter 3, § 3.1). They argued that the overturning of Jurassic strata took place when salt reached the surface, extruded as a salt nappe at the seabed. Analogous structures have been described elsewhere in the basinal sequences of the Digne Nappe by Célini (2020), and Célini et al. (2020).

During the Latest Jurassic and Early Cretaceous an east-west trending depocentre known as the Vocontian Trough or Vocontian Basin formed in the northern part of Haute Provence.
De Graciansky & Lemoine (1988) and De Graciansky et al. (2010) argued that it was generated by rifting time-associated with the opening of the North-Atlantic. Shales and pelagic limestone deposition was dominant in the Vocontian Basin itself while carbonate platforms continuing to

develop along the basin margins. The Provençal platform and the Vercors can be regarded in this light (Arnaud, 1988; Lickorish & Ford, 1998).

Southwest of town of Castellane the Provençal carbonate platform drowned during the Late Berriasian–Early Valanginian something which Cotillon (1994) has argued that this event was a consequence of sea level rise and Vocontian rifting (Fig. 2.5). Similarly, in the Western part of the Castellane Arc, along the northern margin of the Provençal platform, Masse et al. (2009) documented a series tilted fault blocks covered unconformably by Valanginian sediments which were presumably active during the earliest Valanginian (Fig. 2.5). This extensional event may also be related to the Vocontian rifting, the opening of the Southern North Atlantic and rifting of the Valais Ocean (Handy et al., 2010; Tavani et al., 2018; Manatschal et al., 2006; Mohn et al., 2014).

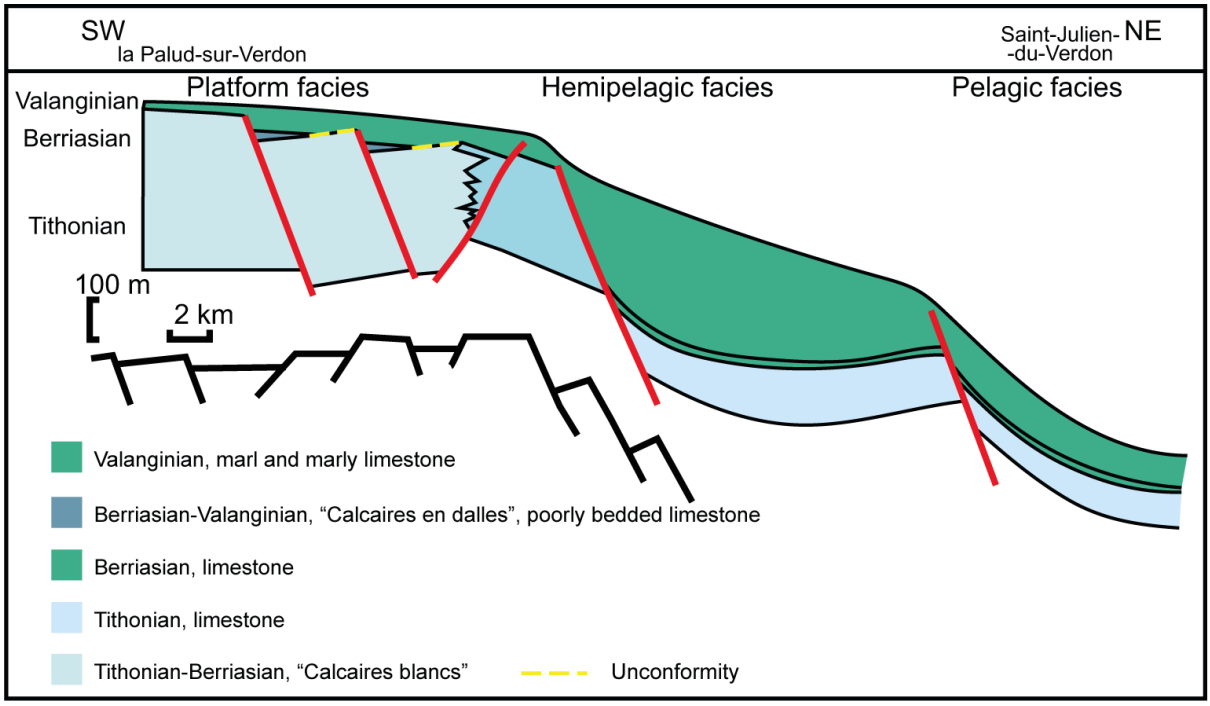


Fig. 2.5 Simplified section from the Provençale platform to the Dauphinois - Vocontian basin west of Castellane, highlighting facies variations in the Tithonian - Valanginian section. Modified after Cotillon (1994).

In the Vocontian basin sediments of Berriasian, Valanginian and Hauterivian age are dominated by alternating limestones and marls, though at the edge of the platform glauconitic limestone was deposited during the Barremian (Fig. 2.2).

Earlier formed salt structures kept growing during the Early Cretaceous. In the study area between Barrême and Castellane several elongated or sub-circular synclines bounded by salt walls or equivalent welds show local thickness changes and facies variations throughout the Middle and Upper Jurassic and also the Lower Cretaceous. The Taulanne syncline, the la Lagne

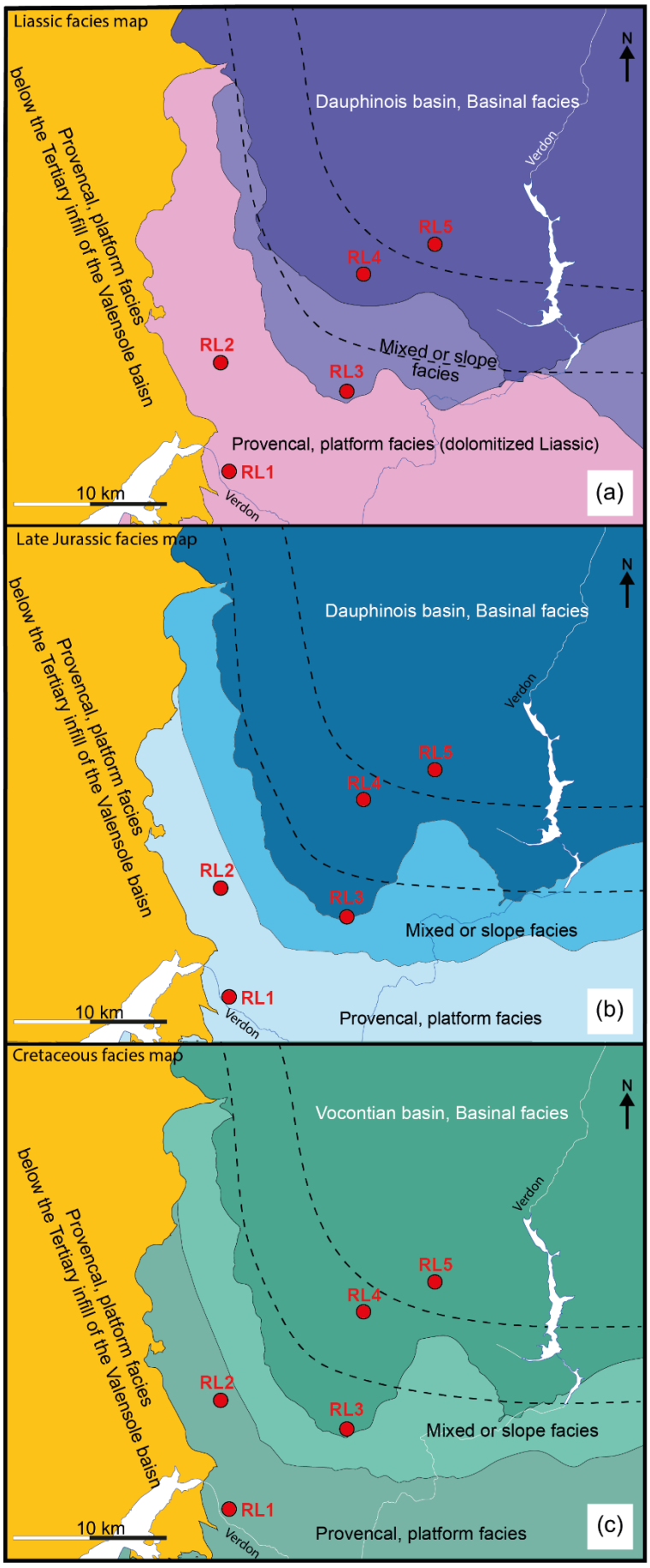
syncline, the Blieux syncline, the Porte de St-Jean syncline and the Taloire syncline in the southern structural domain and the Barrême syncline and the la Blache-Castellane thrust sheet in the northern structural domain all present features characteristic of primary minibasins subsiding into a relatively thick autochthonous salt layer (see Chapter 4). In Chapter 4, I describe the pre-compressional configuration of these primary minibasins and the salt structures which bound them.

During the middle of the Cretaceous (Aptian-Cenomanian) a thick succession of black shales (Marnes Bleues/Marnes Noires Formation) was deposited in basinal areas of Provence, as in most of the Alpine Tethyan region (De Graciansky et al., 1982). The overlying Upper Cretaceous is represented by the thick section of alternation of pelagic limestones and marls the youngest member of which being Turonian bioclastic limestones southwest of Castellane and Coniacian-Santonian white, chalky limestones east of Barrême (Kerckhove & Roux, 1976b; Kerckhove & Roux, 1978a; Campredon et al., 1980b; De Graciansky et al., 1981).

Salt tectonics continued throughout this time period and allochthonous salt sheets were emplaced during the Albian-Cenomanian high stand sourced from diapirs. Albian-Cenomanian salt breakout coincided with black shale deposition (see Chapter 5) and is seen around Castellane in the study area and also further east associated with the Daluis diapir on the flank of the Dôme de Barrôt (Graham et al., 2019; Graham & Csicsek, 2020; Brooke-Barnett, 2022). Minibasins started to form on the top of the allochthonous salt canopy from the mid-Cretaceous onwards. In Chapter 5, The possible pre-compressional extent of the Albian-Cenomanian allochthonous salt canopy and the potential primary feeders will be described. The nature of the preserved minibasin fill, the stratal and structural geometries of the secondary minibasins and the distribution of bounding salt structures developed on the allochthonous evaporite level are also discussed in Chapter 5.

The Alpine orogen started to form in the Late Cretaceous in response to the convergence of the African and European plates and the subduction of the Piemont-Ligurian Ocean. At this time the area of the Southern Subalpine chains became emergent, a series of early folds and thrusts formed, and a regional unconformity (the pre-Nummulitic unconformity) developed.

Basinal Upper Triassic, Jurassic, Cretaceous and Cenozoic rocks were thrust south westwards along the Keuper evaporite detachment in several phases of movement from the Late Cretaceous to the Mio-Pliocene (Lickorish & Ford, 1998; Schmid & Kissling, 2000; Ceriani et al., 2001; De Graciansky et al., 2010; Graham et al., 2012; Schwartz et al., 2017).



The palaeogeographic domains which had developed during Mesozoic became the distinctive tectonic units of the SW Alps. The Digne thrust translated the thick basinal succession of the Dauphiné and Vocontian basins onto the relatively thin carbonates of the Provençal platform (Gigot et al., 1974; Lickorish & Ford, 1998; Graham et al., 2012). The leading edge of the thrust system commonly comprises rocks which originally occupied the transitional domain between platform and basin (mixed or slope facies zone), characterized by reduced thicknesses of hemipelagic carbonates and alternations of carbonate and shale (Fig. 2.6, Fig. 2.7)

Fig. 2.6 Facies distribution maps of the Southern Subalpine chains during the Mesozoic. (a) Liassic facies distribution map. (b) Late Jurassic facies distribution map. (c) Cretaceous facies distribution map. The maps are not palinspastically restored. The northern and southern structural domains are shown together here. Locations of stratigraphic logs (RL1-5) shown on Fig. 2.7 are indicated by their code. Black dashed lines mark the approximate strike of the boundaries between the facies zones during the Mesozoic and define the edge of the Provençal platform. Modified from Ganeval (1973); Kerckhove & Roux (1976a); Kerckhove & Roux (1978a); De Graciansky et al. (1981); Dumont (1988) and Roux et al. (1988).

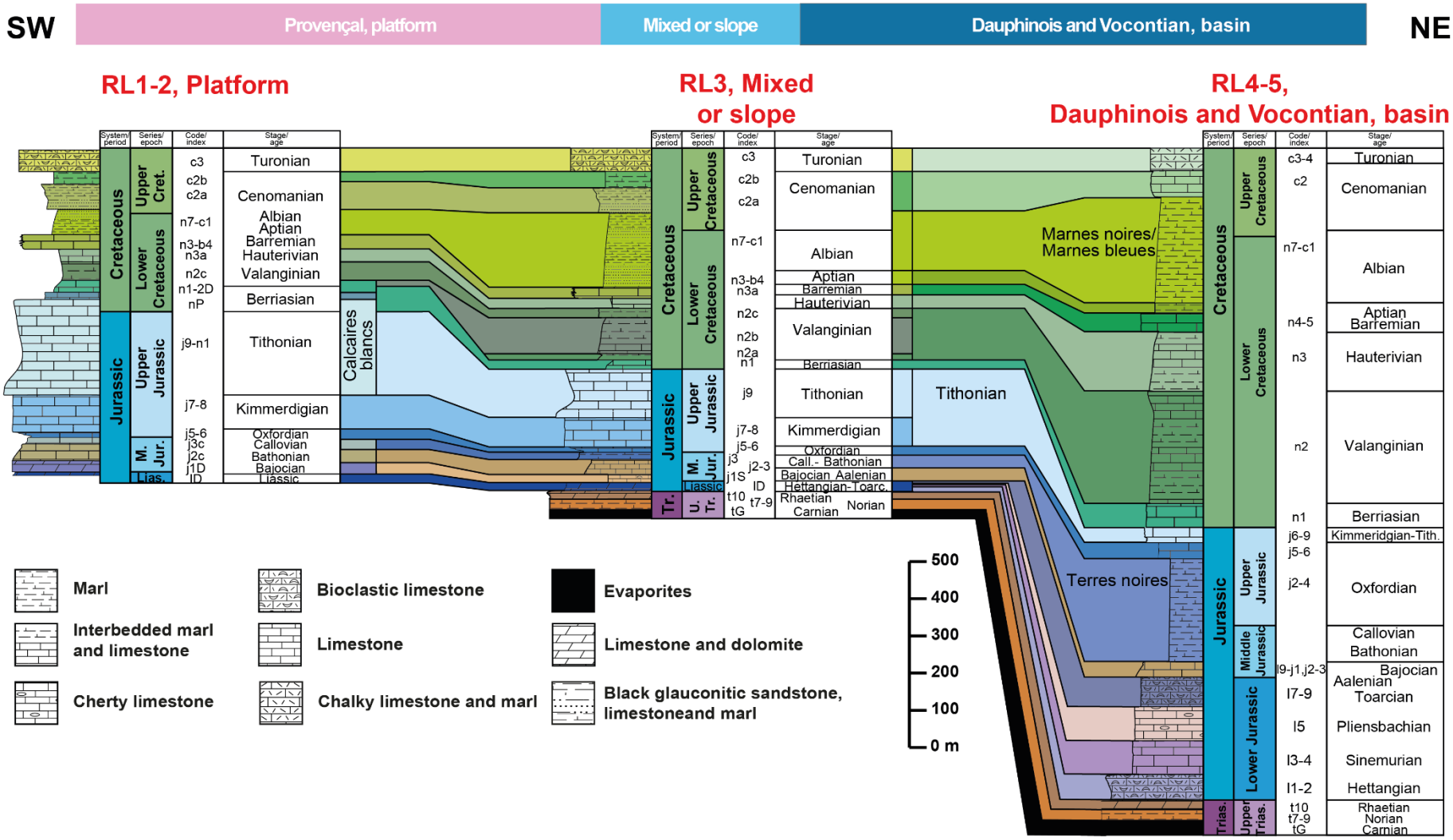


Fig. 2.7 Generalised stratigraphic sections from the Provençal platform to the Dauphinois and Vocontian basins intersecting the mixed or slope facies zone. Data from Kerckhove & Roux (1976a); Kerckhove & Roux (1978a); De Graciansky et al. (1981); Dumont (1988) and Roux et al. (1988). The sections illustrate facies and thickness variations of the Mesozoic stratigraphy. See Fig. 2.6 for location of the logs.

(Dumont, 1988; Roux et al., 1988). The structural trend of these palaeogeographic domains is likely to have been at least indirectly inherited from the rifting phase of the Ligurian Tethys (Fig. 2.4, Fig. 2.6). The Early-Middle Jurassic edge of the Provençal platform may be defined by an E-W trending normal fault system now located below the thrust related structures of the Castellane area (Fig. 2.4, Fig. 2.8) (Dardeau, 1988; De Graciansky et al., 2010; Graham et al., 2012). The presence of a similar but roughly N-S trending extensional fault system is might be postulated below the Digne arc and its lateral equivalent, St-Jurs imbricates (Fig. 2.1b and c) (Lickorish & Ford, 1998).

From Late Cretaceous to Mio-Pliocene a foreland basin formed in response to thrust sheet loading by the more internal Alpine thrust load (Ford et al., 1999; Gupta, 1999). The oldest member of the foreland basin megasequence is a locally restricted Palaeocene cobble, pebble and boulder conglomerate known as the Poudingues d'Argens which containing small amounts of sandstone, marl and palaeosol and sourced almost entirely from Upper Cretaceous pelagic limestones. It is overlain by the time-transgressive shallow water Lutetian - Priabonian Nummulitic limestone, the Upper Eocene – Lower Oligocene Globigerina Marls (Marnes Bleus) and the turbidites of the Grés d'Annot as the basin progressively deepened (Boussac, 1912; Pairis, 1971; Campredon, 1977; Sinclair et al., 1998).

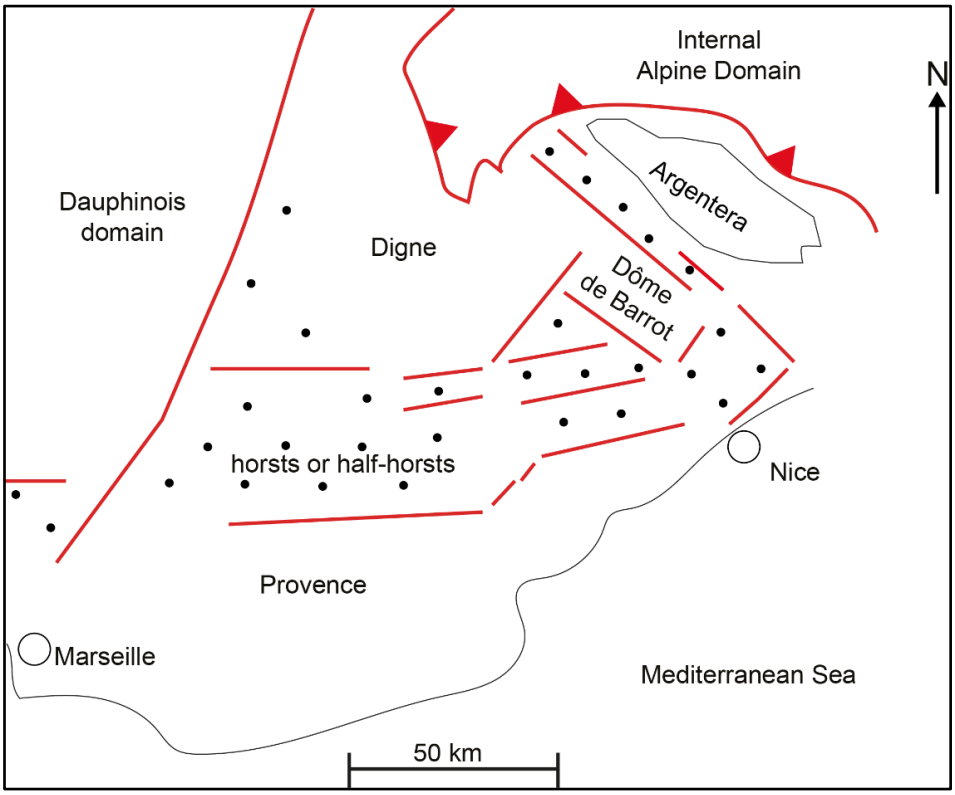


Fig. 2.8 Liassic and Middle Jurassic tectonic framework of the external Alpine domain (Kerckhove & Roux, 1978a; Dardeau, 1988). The solid red lines between Nice and the Dauphine domain represents a normal fault system which defined the northern edge of the Provençal platform. Black-dotted areas represent horts and half-horsts. Redrawn after Dardeau (1988).

Over large parts of the area, the Mesozoic succession is unconformably overlain by the Nummulitic Limestone. This early foreland basin megasequence preserved only in NW-SE oriented synclines (piggyback basins) in the hanging walls of Alpine thrust sheets (Ford et al., 1999; Joseph & Lomas, 2004; Grosjean et al., 2017). The western limit of the Nummulitic transgression was west of the village of Blieux and the Barrême basin (Fig. 2.1b) (Roux, 1972; Pairis, 1988).

The main collision phase is marked by the emplacement of the internal Embrunais-Ubaye nappes. These nappes which comprise internal Alpine units were emplaced towards to SW during the Late Eocene-Early Oligocene and caused significant deformation in their foreland (Kerckhove, 1969; Fry, 1989; Lickorish & Ford, 1998; Ford et al., 1999; Apps et al., 2004;

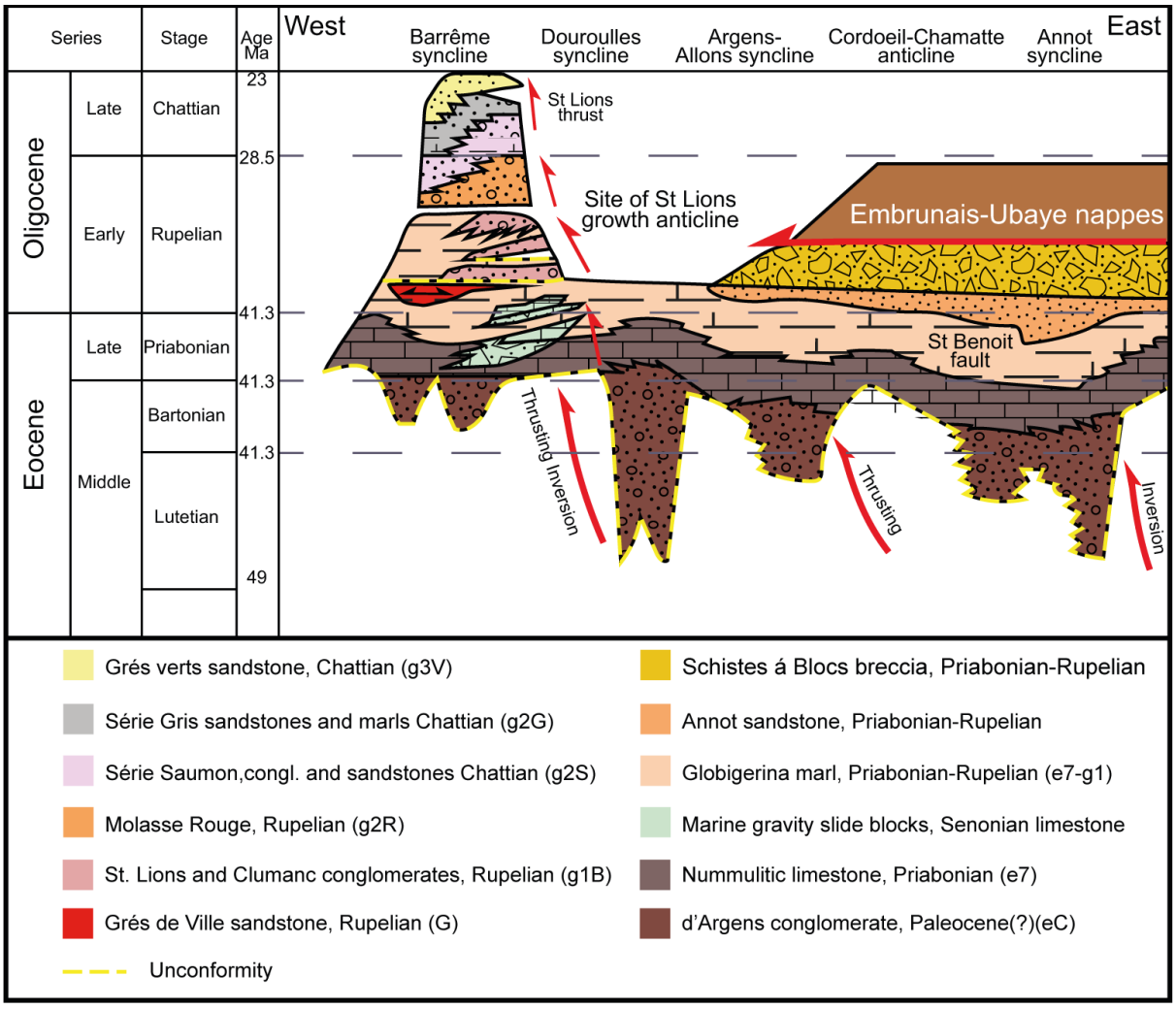


Fig. 2.9 Chronostratigraphic diagram of Eocene and Oligocene formations of the foreland basin system of Southern Subalpine chains (Evans et al. (2004), colours modified). Stratigraphic codes of the unites are (e.g, eC or e7 are used in figures, maps etc. in following chapters). For the location of the Barrême and Douroulles synclines see Fig. 2.1b. Note that the Argens-Allons syncline, the Cordoeil-Chamatte anticline and the Annot syncline are situated E of the study area. They are out of scope of the work presented here and not shown on Fig. 2.1b and c.

Ford et al., 2006). The western limit of the Embrunais-Ubaye nappes is situated east of Barrême and Peyresque synclines (Fig. 2.1b, Fig. 2.9) (Lickorish & Ford, 1998; Evans et al., 2004).

Foreland basin sedimentation became progressively terrestrial through Oligocene, Miocene and Pliocene time as Alpine loading continued and the depocentre migrated towards the continental terrestrial foreland (De Graciansky et al., 1989; Ford et al., 1999). In the Barrême basin the last marine influenced sediments were deposited during the Rupelian. The oldest Oligocene continental deposit is the so called Molasse Rouge (Red Molasse) consisting of red clays, sandstones and conglomerates and marking the transition from marine to terrestrial sedimentation (Evans & Elliott, 1999). Overlying this is the Série Grise (Grey Series) and the Série Saumon (Pink Series) which were deposited in a shallow lake. Fluvial sedimentation occurred again in the Barrême basin at the end of the Chattian (Green Sandstone formation, Grés Verts) (Fig. 2.9).

During the Oligocene compressional tectonics dominated but a series NNW-SSE trending extensional grabens developed in the Alpine foreland in response to E-W extension which may have been related to the formation of a graben system from the Gulf of Lion to the Rhine graben (Ford et al., 1999; Séranne, 1999).

From the Oligocene onwards, deformation followed the progressive loading and propagated into the foreland at least two distinct pulses. The mountain front reached the platform and its Mio-Pliocene 'molasse' cover in what is now the Valensole basin (Fig. 2.1) which was overridden by the SW directed Digne thrust sheet (Ford et al., 1999; Graham et al., 2012; Célini, 2020). The earliest Miocene was a time of uplift and erosion in the Southern Subalpine Chains and Aquitanian sediments are missing. Miocene sedimentation began with a marine transgression in the Burdigalian, and this marine deposition continued into the Serravallian.

From the Tortonian the Valensole basin was confined between the evolving fold and thrust belt to the east and the uplifting Vaucluse bloc to the west and filled with continental sediments (Ford et al., 1999) In the northern part of the Valensole basin the Mio - Pliocene element of the Digne thrust has a minimum displacement of 20 km. Southeast of Digne-les-Bains the tip folds of the Digne Thrust are unconformably overlain by the Nummulitic Limestone which implies that this segment of the Digne Thrust was active before the Priabonian. Oligocene and Mio-Pliocene displacement was transferred to the southern section of the mountain front along a lateral ramp (Lickorish & Ford, 1998). The displacement of the Digne Thrust is dispersed through a series of N-S trending faults of the Le Poil zone (Fig. 2.1b) which have dextral lateral component (De Graciansky et al., 1982; Lickorish & Ford, 1998). In the extreme southern part of the study area in the apex of the Castellane arc, the displacement along the mountain front

is decreased and the structural trend changes dramatically with the fold and thrust belt curving from N-S into the E-W trending section of the arc (Fig. 2.1a and Fig. 2.1b) where a series of south-verging thrust faults have formed during the Miocene (Ford & Lickorish, 2004). Around the Castellane Arc the strike of the Alpine structures is broadly parallel with the edge of the Mesozoic Provençal platform (Fig. 2.1b, Fig. 2.4), E-W trending in the southern wing of the arc, N-S trending south of Digne where the platform edge beneath the Valensole basin swings into this direction (Fig. 2.1b). Late in the deformation history, crystalline basement was elevated by thick-skinned thrusting which led to the elevation and exhumation of the external crystalline massifs (Ford et al., 1999; Van Der Beek et al., 2010; Graham et al., 2012; Schwartz et al., 2017).

Salt tectonics continued in the developing fold and thrust belt involving two evaporite levels. The Alpine compression modified the geometries of diapiric structures and shortened minibasins, squeezed diapirs and megaflaps (e.g. Teillon diapir, Chasteuil salt structure, Blieux basin, Taulanne basin etc.) (Graham et al., 2019) formed during Alpine compression while, at the same time, secondary minibasins developed on allochthonous salt (Célini et al., 2022).

Alpine contractional deformation from Late Cretaceous to the present also affected the Albian-Cenomanian allochthonous salt sheets and they became deflated and welded detachment surfaces (see Chapter 5).

In the Barrême and Castellane area deposition in the Alpine foreland basin was influenced by allochthonous evaporite sheets extruded during mid-Cretaceous and rapid changes in thickness and facies are present in the Eocene and Oligocene succession along salt structures or equivalent welds on the top of the allochthonous salt (Graham & Csicsek, 2020). Some of the secondary minibasins which formed on the allochthonous salt were emplaced as piggyback basins during Eocene-Oligocene times and basin depocenters migrated westwards possibly in response to progressive salt withdrawal in advance of thrust loading (see Chapter 5). Allochthonous evaporite emplacement and lateral salt migration during the Alpine orogeny is well documented elsewhere in the Digne nappe area and east of the study area (Graham et al., 2019; Brooke-Barnett et al., 2020; Graham & Csicsek, 2020; Brooke-Barnett, 2022; Célini et al., 2022).

In Chapter 5, the Alpine modification of the pre-existing primary salt structures of the Southern Subalpine chains and the syn-orogenic evolution of the Albian-Cenomanian allochthonous salt canopy and associated secondary minibasins will be described. Syn-orogenic sedimentation around and above the canopy and the final geometry of the allochthonous salt will also be discussed in this chapter.

In general, it is clear that pre-orogenic halokinetic deformation has a significant impact on the evolution of fold and thrust belts. The pre-Alpine salt tectonic system which developed during rifting and the passive margin phase and its impact on the regional tectonics will be discussed in Chapter 4 and Chapter 5. A conceptual model of the contractional salt tectonic system of the Southern Subalpine chains will be also presented in Chapter 5.

In Chapter 6, I summarise the key conclusions of this research and outline possible areas and aspects of future research.

Chapter 3: Previously recognised salt related structures and salt tectonics in the Subalpine Chains

The Southern Subalpine chains have been studied over more than 100 years, so the stratigraphy and structural evolution of the area during Tethyan rifting, the passive margin phase and the Alpine compressional phase are all well documented (Zurcher, 1895; Boussac, 1912; Goguel, 1939; Guérin-Desjardins, 1956; Cotillon, 1968; Roux, 1972; Lemoine et al., 1986; Dardeau, 1988; De Graciansky & Lemoine, 1988; Fry, 1989; Gidon & Pairis, 1992; De Graciansky et al., 1993; Lickorish & Ford, 1998; Evans & Elliott, 1999; Ford & Lickorish, 2004; Schwartz et al., 2017; Grosjean et al., 2017). Triassic evaporites are known to be the basal detachment surface for thin-skinned Alpine folding and thrusting (Goguel, 1963; Lickorish & Ford, 1998; Ford & Lickorish, 2004). In addition, diapiric structures have been identified in the last couple of decades (Mascle et al., 1988; Dardeau & De Graciansky, 1990). An aim of this thesis is to show that much of the previous research underestimated the importance of salt structures during Tethyan rifting, the passive margin phase and the

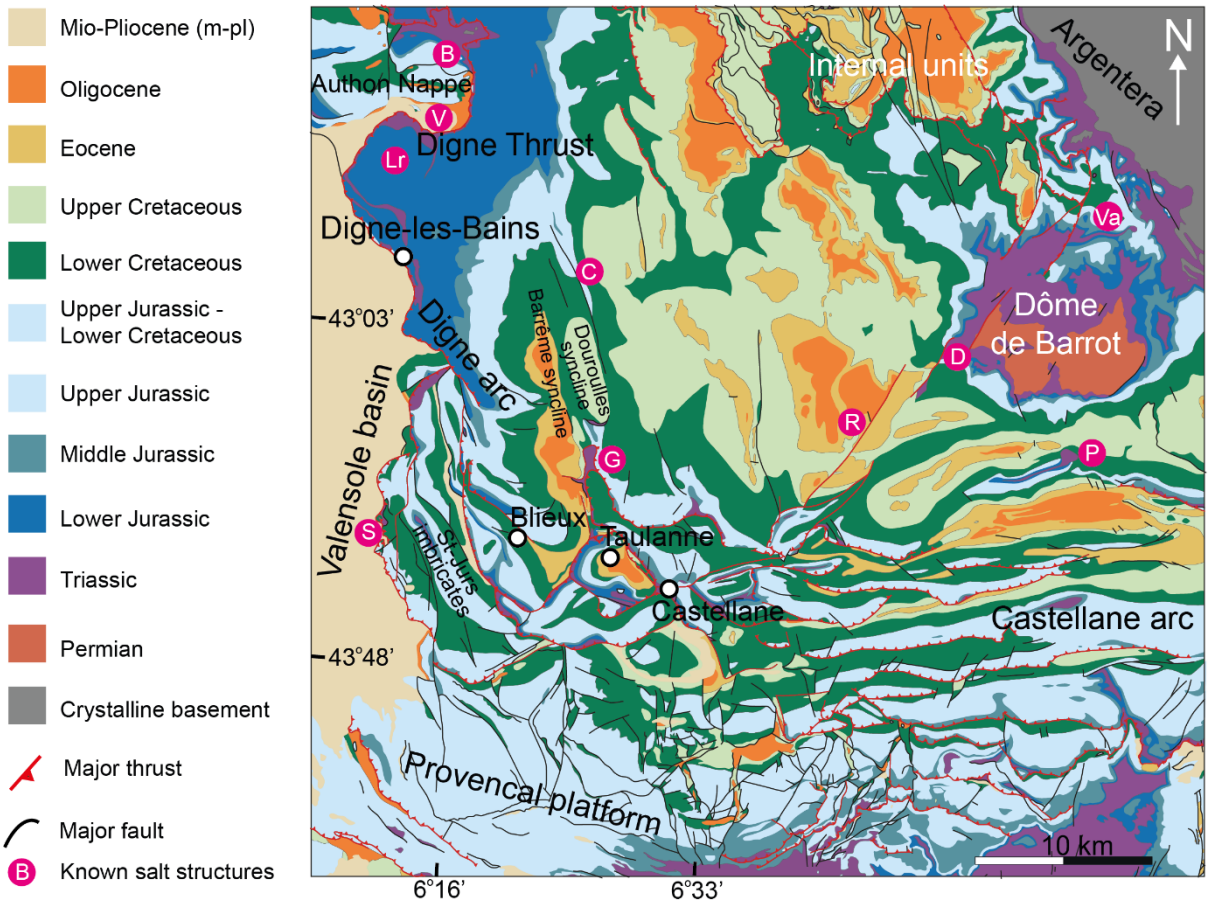


Fig. 3.1 Geological map of the Subalpine Chains showing examples of known salt structures: B = Barre de Chine flap, C = La Cine fault, D = Daluis diapir, G = Gévaudan diapir, Lr = La Robine unit, P = Puget-Théniers diapir, R = Rouaine-Daluis fault system, S = St-Jurs diapiric intrusion, V = Vélodrome minibasin, Va = Valberg-Beuil weld. Data from (Kerckhove & Roux, 1978a; Kerckhove & Roux, 1978b; Rouire et al., 1979; Kerckhove et al., 1980; Mascle et al., 1988; Dardeau & De Graciansky, 1990; Lickorish & Ford, 1998; Graham et al., 2012; Brooke-Barnett et al., 2019; Célini et al., 2020; Célini, 2020; Graham & Csicsek, 2020; Brooke-Barnett et al., 2021; Brooke-Barnett, 2022; Célini et al., 2022).

development of the fold and thrust belt. During the Mesozoic, sedimentation, facies belts and thickness variations of the Jurassic and Cretaceous of the Dauphinois and Vocontian basins have been affected by long-term salt activity.

Alpine shortening affected an already deformed succession, which contained a series of precursor salt structures and as in other shortened basins where earlier formed halokinetic structures are present, the weak salt bodies localised strain and the structural style of the Subalpine fold and thrust belt was strongly influenced by salt tectonics (Rowan & Vendeville, 2006; Callot et al., 2007; Graham et al., 2012; Duffy et al., 2018; Graham et al., 2019; Granado et al., 2019; Célini et al., 2020; Graham & Csicsek, 2020; Csicsek et al., 2021; Brooke-Barnett, 2022). Some of these salt structures now are located in the autochthonous foreland but they also can be found in the Digne Nappe, the Authon Nappe and the Castellane Arc (Fig. 3.1). In the following section, I briefly describe a few examples of known salt structures of the Southern Subalpine chains from northwest to southeast (Fig. 3.1).

3.1 Barles flap

The Barles flap (Graham et al., 2012) is located in the footwall of the Digne Thrust where it is exposed in the cliff of the Barre de Chine, north of the town of Digne-les-Bains (Fig. 3.1, Fig. 3.2). The completely overturned flap is formed of an anomalously thin section of Lower and Middle Jurassic limestone and shale, which does not show significant internal deformation. The overturned section is extremely reduced compared to the basinal section in the hanging wall of the Digne Thrust and contains hard-grounds, slumps and syn-sedimentary faults. Graham et al. (2012) argued that the condensed section of the Barre de Chine represents the

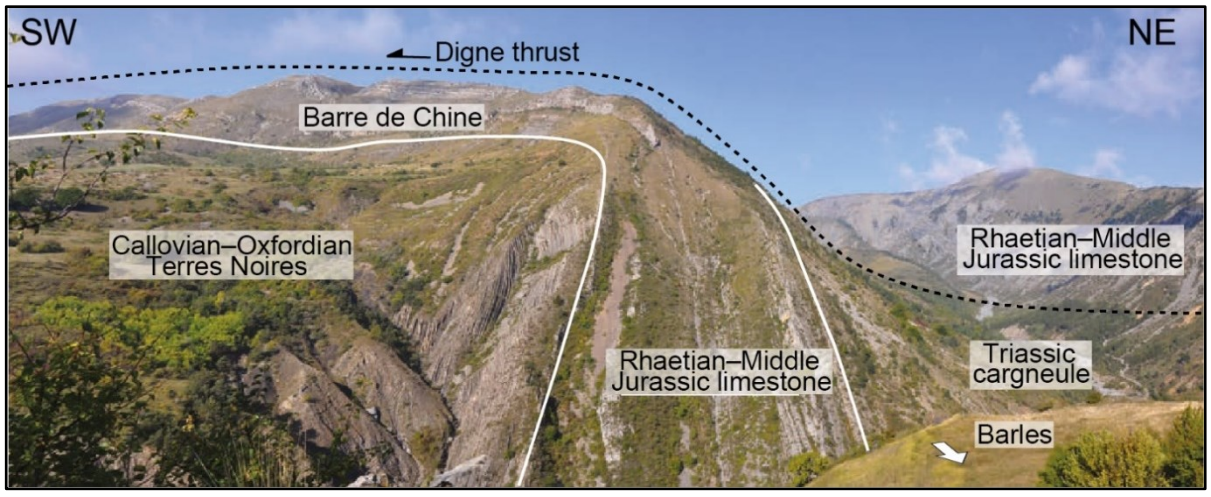


Fig. 3.2 The overturned flap of the Barre de Chine adjacent to the Barles diapir (shown here as Triassic cargneule) (Graham et al., 2012).

elevated roof of a Jurassic salt swell, it was overridden by an allochthonous salt-sheet during the deposition of the Callovian-Oxfordian Terres Noires Formation, and the overturned section was folded beneath it (Fig. 1.9b). Syn- sedimentary faulting and folding occurred before the overturning of the flap on the unstable flank of the Barles diapir. During subsequent Alpine deformation, the weak allochthonous salt level served as a detachment surface and the overturned section was overridden by the southwest verging Digne Nappe (Fig. 3.2).

3.2 La Robine unit

The La Robine unit lies near the front of the Digne Nappe (Fig. 3.1). The unit comprises the broad La Robine syncline and two tight synclines, the Courbons and Saint-Benoît synclines, previously interpreted as tip folds of the Digne Nappe (Gidon & Pairis, 1992) (Fig. 3.3).

The synclines deform the Triassic, Liassic and Middle Jurassic succession and are separated by salt cored anticlines. Abrupt thickness and facies variations are clear evidence of Jurassic salt tectonic activity. Between the synclines, onlaps, pinch-outs and local unconformities occur along the flanking salt bodies. Recent studies identified the La Robine syncline as a minibasin and the Courbons and Saint-Benoît synclines as smaller depocenters separated by salt walls and diapirs developed in the Dauphinois basin (Graham et al., 2012; Célini et al., 2020; Célini, 2020). Salt tectonic activity was initiated during the Liassic Tethyan rifting as reactive diapirs formed along normal faults. Diapirs continued to grow as passive diapirs due to sediment loading during the subsequent passive margin phase following rifting. Remnant gypsum

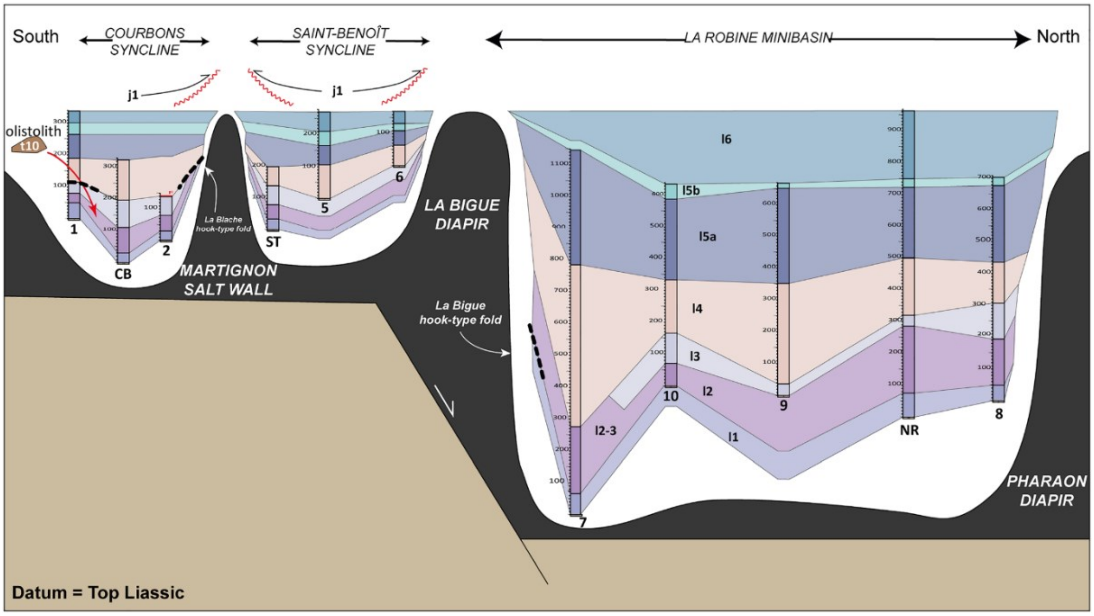


Fig. 3.3 Section showing abrupt thickness changes, unconformities in the Jurassic sections and bounding salt structures in the La Robine unit (Célini et al., 2020).

preserved along some of the bounding salt structures shows that the weak salt bodies were not welded out completely, suggesting, perhaps, that the diapirs and Jurassic depocenters were only slightly deformed by the Alpine compression as they were carried in the Digne Nappe and thrust over the Valensole basin (Fig. 3.1).

3.3 Vélodrome minibasin

The so-called Vélodrome is an Oligo-Pliocene depocentre located in the footwall of the Digne Thrust, north of the La Robine unit (Fig. 3.1). It was previously interpreted as a footwall syncline formed during the Mio-Pliocene emplacement of the Digne Nappe (Goguel, 1939; Gidon & Pairis, 1992), but recent studies have revealed the salt-related origin of the structure (Graham et al., 2012; Célini, 2020; Célini et al., 2022). The edges of the Vélodrome syncline are overturned in all directions and the entire syncline is closed and tilted toward the south (Fig. 3.4). On its northern flank, Oligocene molasse is in direct contact with the Jurassic-Cretaceous section of the Digne Nappe, along a folded unconformity. The Oligocene section is

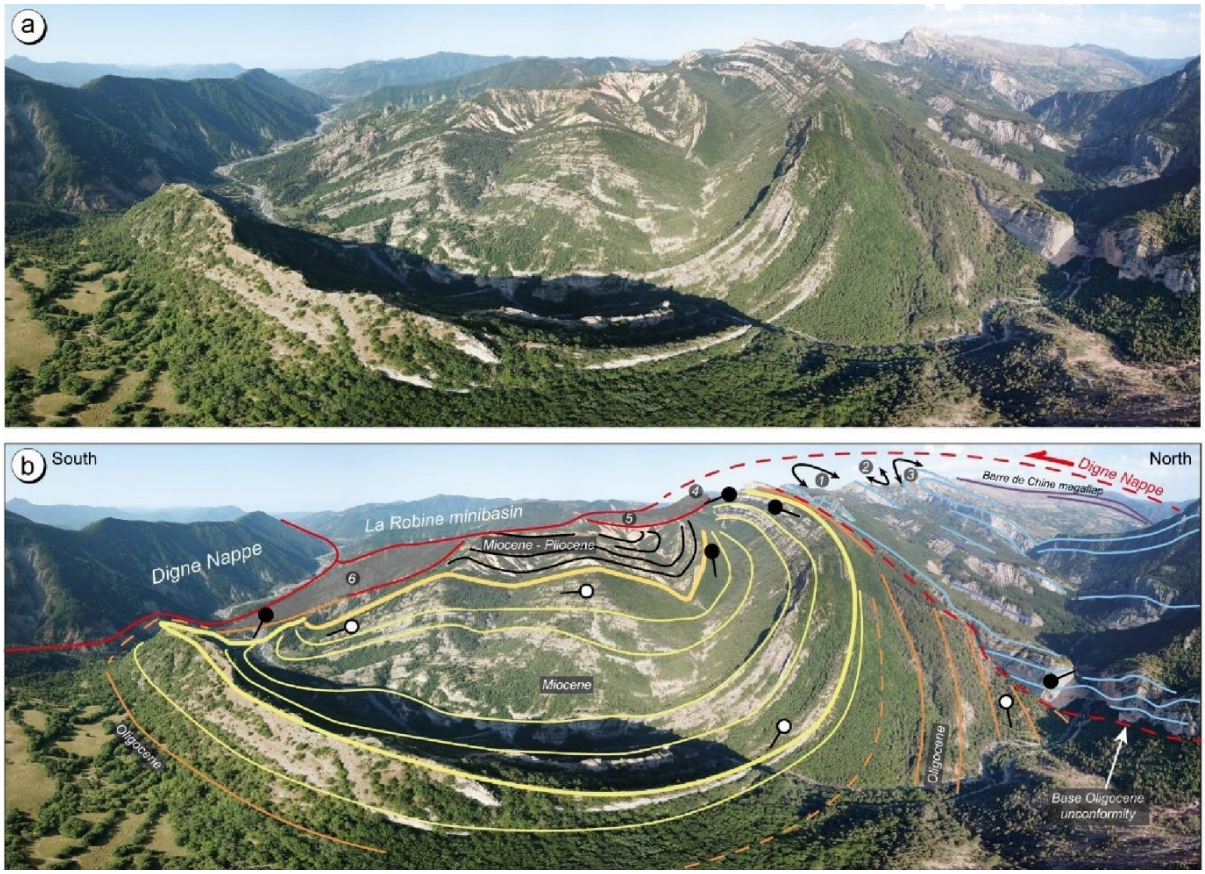


Fig. 3.4 Uninterpreted (a) and interpreted (b) photo panorama of the Vélodrome syncline (Célini, 2020; Célini et al., 2022) highlighting the overturned edges of the syncline. Angular unconformities and thickness changes occurred within the Oligocene and Mio-Pliocene fill of the secondary minibasin below the overriding Digne Nappe and La Robine unit.

unconformably overlain by Miocene marine sediments which are also overlain unconformably by Pliocene continental sediments. Within the Mio-Pliocene fill of the syncline, growth strata, abrupt thickness variations, onlaps, halokinetic sequences, olistoliths and successive unconformities were observed.

Célini et al. (2022) argued that the Vélodrome is a rotated and tightened secondary minibasin formed on the top of an extrusive salt sheet which extruded over as a salt-glacier on an Oligocene land surface at the front of the Authon Nappe. Source-fed thrust mechanism was responsible for the emplacement of large volume of allochthonous salt (Célini et al., 2022). The Late Miocene–Late Pliocene emplacement of the Digne Nappe, with simultaneous salt withdrawal, resulted in further folding of the northern edge of the secondary minibasin. The Vélodrome represents an example of a syn-orogenic secondary minibasin developed and translated at the front of the Subalpine fold and thrust belt and highlights the importance of salt tectonics during Alpine evolution of the fold and thrust belt.

3.4 La Cine fault

The la Cine fault (labelled as C in Fig. 3.1) is an NNW-SSE trending structure located in the hanging wall of the Digne Thrust, east of the town of Digne-les-Bains (Fig. 3.1). The fault is an apparent thrust fault running between the Gévaudan diapir (labelled as G in Fig. 3.1) and a structurally complex zone north of the Douroulles syncline (Fig. 3.1) (Beaudoin et al., 1983; Lickorish & Ford, 1998; Célini, 2020). To the north, it disappears (at the surface) within the Middle-Upper Jurassic section of the Digne Nappe. The fault bounds the Douroulles syncline and the Barrême syncline to the east and elevates a Lower Jurassic – Upper Cretaceous basinal section (Fig. 3.1). However, the Liassic section in the hanging wall of the fault is reduced, compared to the average thickness of the Liassic of the Digne Nappe and it contains local unconformities and olistoliths (Beaudoin et al., 1983; Célini, 2020). Beaudoin et al. (1983) observed abrupt thickness and facies changes of the Mesozoic section along the fault. They described the la Cine fault as a major structure which controlled facies and thickness of the Mesozoic succession, without further explanation. During Oligocene Alpine shortening, the la Cine fault was active as a thrust fault and dextral strike-slip movement occurred later, in the Mio-Pliocene (De Graciansky et al., 1981; De Graciansky et al., 1982; Beaudoin et al., 1983), According to Lickorish & Ford (1998) the la Cine fault is a Mesozoic normal fault which was reactivated during Alpine compression as a thrust fault.

Célini (2020) described Triassic gypsum in direct contact with Upper Pliensbachian strata of the reduced Liassic section and small blocks of Liassic along the fault between Upper Jurassic and Cretaceous rocks. Based on these stratigraphic and structural observations, Célini (2020) suggested that the La Cine fault is a NNW-SSE trending salt wall, which formed during the Liassic. The reduced Liassic section along the fault represents the thin roof of the diapiric structure. The La Cine salt wall remained active throughout the whole Mesozoic, and responsible for thickness and facies changes observed in the Jurassic-Cretaceous section along the structure. During the Alpine compressional phase, the pre-existing la Cine salt wall served as a ramp for Alpine thrusting in the Oligocene and Jurassic-Cretaceous basinal rocks are thrust over the Douroulles synclines. The salt wall subsequently became a weld (Fig. 3.5). Liassic rocks along the La Cine fault, between Upper Jurassic and Cretaceous sections, are representing the dismembered roof of the Mesozoic salt wall later incorporated into the weld (Fig. 3.5). As shortening continued, during the Mio-Pliocene, the la Cine weld was reactivated as a dextral strike-slip fault. This structure represents a long-lived salt structure which formed during the Tethyan rifting phase of the margin and remained active during the passive margin phase. During Alpine shortening, in the Oligocene and Mio-Pliocene, the precursor salt structure largely influenced the structural style of the folded belt in the region.

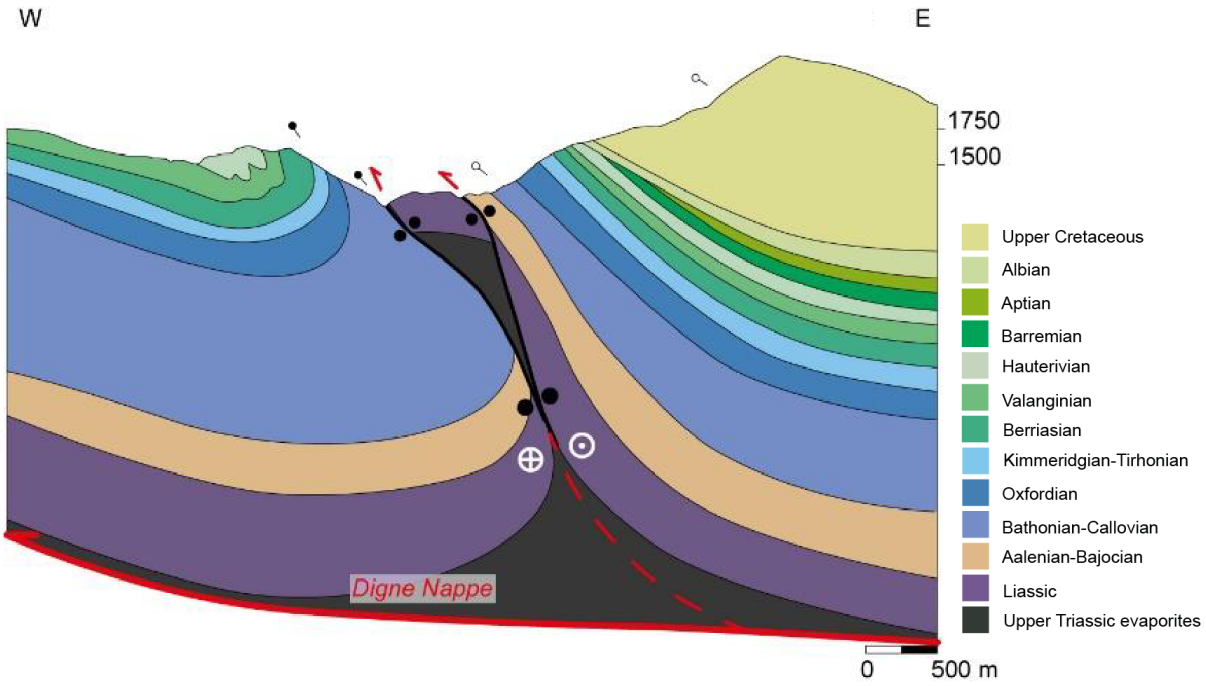


Fig. 3.5 Cross section across the la Cine weld, north of the Barrême syncline, showing thickness changes and unconformities in the Mesozoic section along the weld. The salt wall is completely welded in its central segment and remnant gypsum shown below a thin Liassic roof section in the upper part (Célini, 2020).

3.5 Gévaudan diapir

The Gévaudan diapir is situated in the transitional zone between the Digne Arc and the Castellane Arc, in the hanging wall of the Digne Thrust (Fig. 3.1). It consists of Upper Triassic gypsum and cargneule breccia and the surface exposure of the Keuper succession is around 2.5 – 3 sq. km. The extrusive character of the diapir was described by Emre (1977). Lickorish & Ford (1998) described the salt structure as diapiric intrusion and considered the age of the structure as Oligocene, which may be situated over a Mesozoic normal fault. The diapir was overridden on its basinward side by thick Jurassic-Cretaceous basinal succession. On its foreland flank, the diapir is connected to a thin salt sheet which may be related to Cretaceous extrusive salt-emplacement or to Oligocene over-thrusting (Jackson & Hudec, 2017) (Fig. 3.6).

However, recent fieldwork and structural investigation show the pre-orogenic salt tectonic origin of the Gévaudan diapir (see Chapter 4 and Chapter 5).

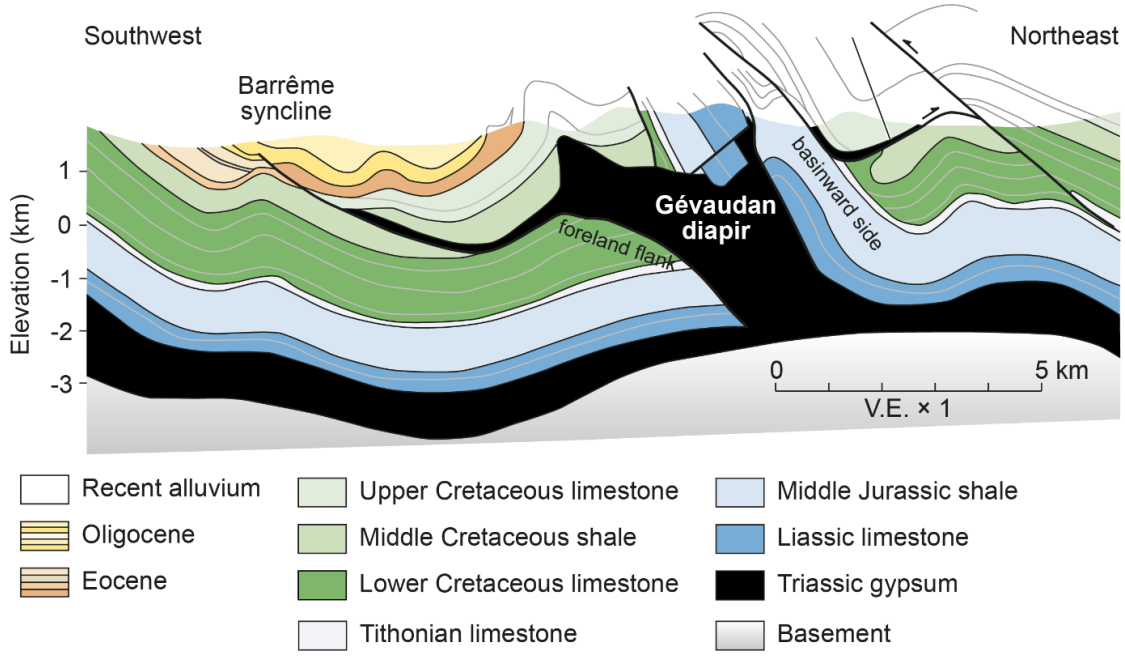


Fig. 3.6 Cross-section of Lickorish & Ford (1998) in Jackson & Hudec (2017).

3.6 St-Jurs 'diapiric intrusion'

Southwest of the Gévaudan diapir, along the frontal thrust of the fold and thrust belt, where the Valensole basin is overridden by the Mesozoic, a series of imbricate slices – the St Jurs Imbricates (Lickorish & Ford, 1998) (Fig. 3.1) – a gypsum body has been described by Kerckhove & Roux (1978b) as a diapiric structure which was injected along the frontal thrust

of the fold and thrust belt (Fig. 3.1) and they argued that the injection of gypsum occurred during the Pliocene because Oligo-Miocene rocks are strongly folded and locally overturned beneath the frontal thrust. South of St-Jurs these deformed beds are unconformably overlain by Upper Pliocene-Lower Pleistocene lacustrine limestone (Fig. 3.7) (Kerckhove & Roux, 1978a; Kerckhove & Roux, 1978b).

Along an NNW-SSE trending fault zone in this area Mio-Pliocene sediments and a section of relatively thin and folded Upper Jurassic and Lower Cretaceous rocks are in direct contact with Upper Triassic gypsum (Fig. 3.7). Upper Triassic Keuper typically forms the base of the hanging wall stratigraphy below Jurassic rocks because it acted as the basal detachment for thin-skinned Alpine deformation but the whole of the Liassic - Middle Jurassic section is missing at St-Jurs while 2.5 km northwest of the diapir within the St-Jurs Imbricates, the Liassic-Middle Jurassic section is 200 m thick. The upper part of the Keuper succession and the overlying Rhaetian rocks are also absent at the surface along the mountain front. The incomplete Jurassic section and thickness changes suggest that Triassic salt may have migrated into a local diapiric swell during Early and Middle Jurassic times and that Liassic and Dogger deposits were unable to completely cover the salt structure.

In the westernmost exposure of Triassic gypsum at St-Jurs, the Triassic evaporites are almost entirely surrounded by Berriasian limestone and massive, glauconitic limestone of Barremian age (shown in Fig. 3.7 as n1 and n3b4, respectively.). The anomalous contact of the



Fig. 3.7 Geological map showing the diapiric intrusion at the village of St-Jurs (Kerckhove & Roux, 1978a). Triassic gypsum is shown as tG. Upper Jurassic-Lower Cretaceous succession of the St-Jurs imbricates is shown in blue and green colours. Mio-Pliocene sediments of the Valensole basin and Quaternary cover are shown in pale brown colours.

evaporites and the Lower Cretaceous deposits suggests an extrusion of the salt over the Mesozoic section, sourced from a diapir formed during Jurassic time rather than an intrusion of the weak evaporites into the competent Upper Jurassic – Lower Cretaceous limestone succession, something proposed by Kerckhove & Roux (1978b). The extrusion may be a consequence of Alpine compression and related to squeezing of the earlier formed diapir during the Pliocene emplacement of the St-Jurs imbricates over the Valensole basin, but more work is required to confirm this interpretation.

3.7 Rouaine-Daluis fault system and the Daluis diapir

The Rouaine – Daluis fault system is an important NE-SW striking fault zone which runs from the Dôme de Barrôt and links into Alpine thrust faults around Castellane (Fig. 3.1). The fault system shows net sinistral offset. It is a long-lived salt structure which formed during regional extension and later was influenced by strike-slip and compressional tectonics (Brooke-Barnett et al., 2019; Brooke-Barnett et al., 2020; Brooke-Barnett et al., 2021; Brooke-Barnett, 2022; Brooke-Barnett et al., 2023) The fault system reactivated a long-lived salt wall which initiated during the Tethyan rifting in the footwall of a basement involved extensional fault (Brooke-Barnett, 2022; Brooke-Barnett et al., 2023). The extensional fault formed as a northwest-dipping normal fault, bounding a Jurassic tilted block (Lemoine et al., 1986; Mascle et al., 1988; Dardeau & De Graciansky, 1990; Brooke-Barnett, 2022). A major salt stock, the Daluis diapir formed along this Mesozoic salt wall. The diapir is located on the western flank of the Dôme de Barrôt, at the northern end of the Rouaine-Daluis fault system and it is recognised as a diapir formed during the Early-Middle Jurassic (Goguel, 1937; Bordet, 1950; Mascle et al., 1988; Dardeau & De Graciansky, 1990) (Fig. 3.1). Along the south-east bounding fault of the Rouaine-Daluis fault system, Triassic evaporites are in direct contact with a Jurassic-Lower Cretaceous section. Onlap of the Lower and Middle Jurassic sediments over the Triassic gypsum, thinning of the section against the diapir, a series of normal faults, olistolith deposition and slumping on the flank of the diapir indicate salt tectonic activity during Early and Middle Jurassic time (Mascle et al., 1988; Dardeau & De Graciansky, 1990) (Fig. 3.8). Abrupt thickness changes of the Upper Jurassic and Lower Cretaceous section, erosion surfaces, slumping and large scale folding due to gravity gliding on the flank of the Daluis diapir indicate that salt activity continued during the post-rift phase. Recent studies show that the diapir and the connecting salt wall continued to grow through the Late Jurassic and Early Cretaceous times as passive salt rise occurred due to sediment loading (Brooke-Barnett et al.,

2019; Brooke-Barnett et al., 2020; Brooke-Barnett et al., 2021; Brooke-Barnett, 2022; Brooke-Barnett et al., 2023). Minor Early Cretaceous reactivation of the extensional fault below the salt wall and the Daluis diapir may have occurred due to the Vocontian rifting and possibly triggered reactive salt rise once again (Dardeau, 1988; De Graciansky & Lemoine, 1988). The mature Daluis diapir sourced a thick allochthonous salt sheet during the Middle of the Cretaceous (possibly during the Aptian-Albian) (Brooke-Barnett et al., 2019; Brooke-Barnett et al., 2020; Brooke-Barnett et al., 2021; Brooke-Barnett, 2022; Brooke-Barnett et al., 2023) direct evidence of which can be seen south-west of the diapir, where bedding-parallel Triassic gypsum and caprock are intercalated within the Aptian-Albian black shales (Fig. 3.9). The thickness of the allochthonous gypsum (over 100 m further south) suggests that a considerable amount of evaporite was involved in allochthonous salt extrusion during the deposition of the

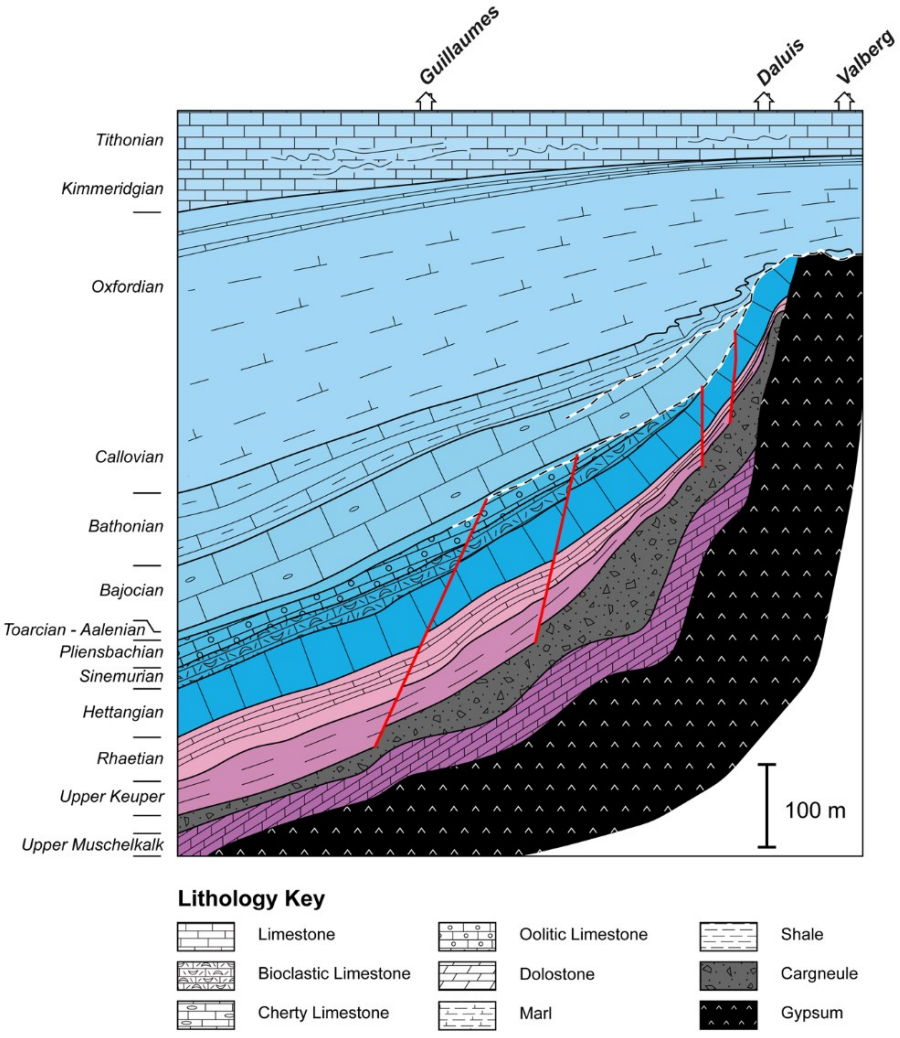


Fig. 3.8 Composite section showing the Daluis diapir during the deposition of the Tithonian limestone (Mascle et al., 1988; Brooke-Barnett, 2022). Thinning of the Jurassic section, slumping, local unconformities and syn-sedimetary faults occurred on the flank of the diapir.

black marls. During the Late Cretaceous, a thick section of Cenomanian-Turonian limestones and marls were deposited directly on the top of the salt sheet. Brooke-Barnett (2022) described slumps and low-angle normal faults in the Upper Cretaceous section south-west of the Daluis diapir sealed by Turonian sediments. The normal faults detaching on a surface within the Aptian-Albian black marls at the same stratigraphic level where the allochthonous salt was observed next to the Daluis diapir. These observations suggest that the allochthonous salt sheet was squeezed out due to the loading of Cenomanian-Turonian sediments and welded simultaneously with syn-sedimentary faulting and collapse of the overburden before the end of the Turonian.

From the Late Cretaceous onwards, the onset of the SW directed Alpine shortening triggered salt rise again and the Daluis diapir became shortened and squeezed. Thin-skinned sinistral tear faulting occurred along the Rouaine-Daluis fault system and the pre-existing salt wall. Due to the movement along the fault zone, the Aptian-Albian salt sheet was forced back towards the pre-existing salt wall and the Daluis diapir. Along the wall, and through the diapir, the Triassic salt extruded to the surface during the Eocene. Because of the evacuation of the salt into the Daluis diapir and the pre-existing salt wall, the sedimentary cover of the extrusive salt sheet collapsed along a Roho-like system (Brooke-Barnett, 2022; Brooke-Barnett et al., 2023) and

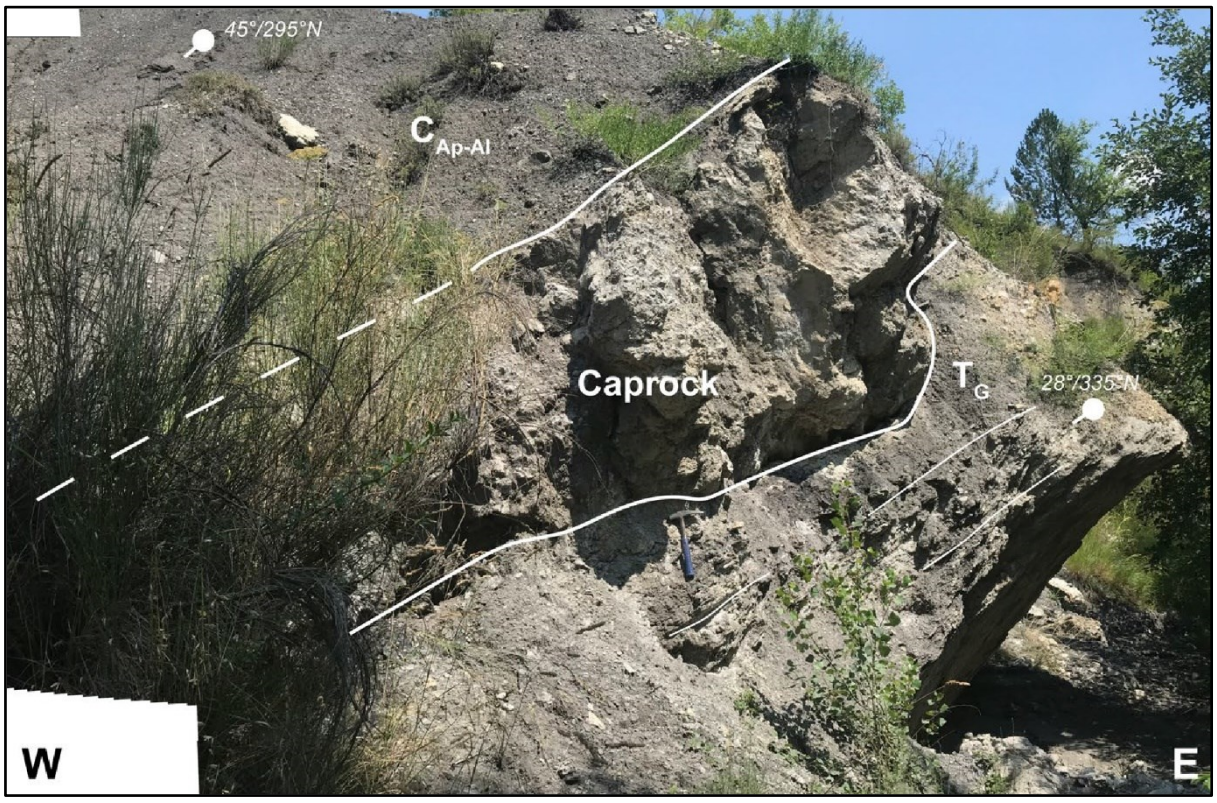


Fig. 3.9 Bedding parallel Triassic gypsum (T_G) and mineralised caprock within the Aptian-Albian black marls, observed south-west of the Daluis diapir (Brooke-Barnett, 2022).

the salt withdrawal basin was filled with Eocene and Oligocene sediments. During later phases of Alpine evolution of the area, due to continued SW directed compression, more than 5 kilometres of sinistral offset occurred along the Rouaine-Daluis fault system and dismembered the long-lived and once continuous salt-system (Brooke-Barnett et al., 2019; Brooke-Barnett et al., 2020; Brooke-Barnett et al., 2021; Brooke-Barnett, 2022; Brooke-Barnett et al., 2023).

3.8 Valberg-Beuil weld

The ENE-WSW trending Valberg-Beuil weld is situated on the northern flank of the Dôme de Barrôt and it is composed of Middle and Upper Triassic cargneule breccia of the Muschelkalk and Keuper formations (Fig. 3.1). The structure links two diapirs (Brooke-Barnett, 2022), between which some remnant gypsum is observable along the weld, while west of the western diapir the welding was complete (Fig. 3.10). The weld separates mostly steeply dipping to overturned Triassic-Upper Jurassic sections, which flatten out into the core of synclinal depressions north and south of the weld. South of the weld, along its strike, Lower-Middle Jurassic section thins and pinches out and the Terres Noires Formation rests on the top of the Triassic evaporites. On the southern side of the weld, overturned Lower and Middle Jurassic sections are affected by syn-sedimentary normal faulting (Fig. 3.10). These

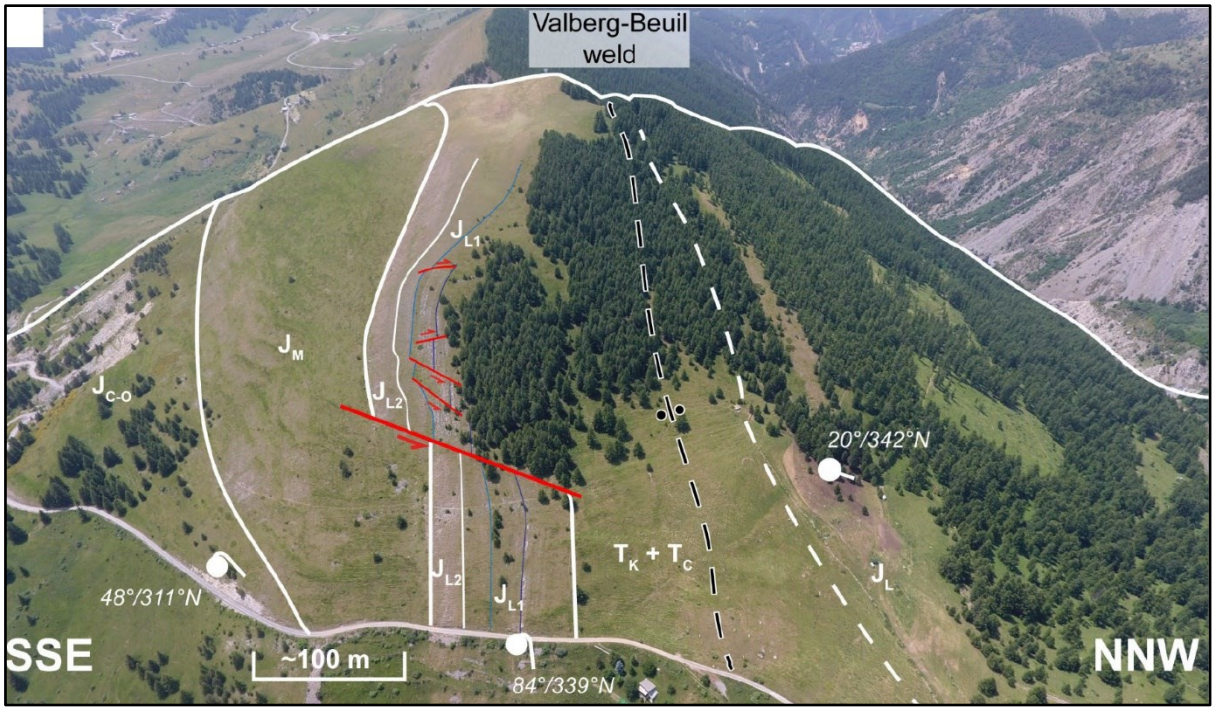


Fig. 3.10 Interpreted photo panorama of the western segment of the Valberg-Beuil weld (Brooke-Barnett, 2022). Syn-sedmientary normal faults crosscut the Liassic-Middle Jurassic section south of the weld and sealed here by Middle Jurassic sediments. Geological key: $T_K + T_C$ = Triassic Keuper and cargneule breccia; $J_{L1} + J_{L2} + J_L$ = Lower Jurassic; J_M = Bajocian-Bathonian; J_{C-O}= Callovian-Oxfordian. The weld is indicated by a dashed line and a pair of black dots.

extensional faults are sealed by Liassic or Middle Jurassic sediments whose thickness changes can be related to syn-sedimentary normal faulting. In the Kimmeridgian-Tithonian section, breccia levels were observed with proximity to the weld and the adjoining diapirs suggesting the presence of a nearby topographic high during Late Jurassic. North of the weld, E-W trending normal faults crosscut the Callovian-Lower Cretaceous section.

Based on these structural and stratigraphic observations, Brooke-Barnett (2022) argued that the welded salt structure has a similar history to the Daluis diapir and it was initiated as a reactive salt wall during the Early and Middle Jurassic associated with extension related to the Tethyan rifting. Later, and coeval with the subsidence of the passive margin, the diapir continued to rise as a passive diapir in response to sediment loading, at least until Callovian-Oxfordian times, when the salt reached the surface during the deposition of the Terres Noires Formation. Previous research suggested that diapirism was ceased at the time of the deposition of the Terres Noires (Dardeau & De Graciansky, 1990; Mascle et al., 1988). However, based on stratigraphical and structural observations like gradual thickness changes of the Kimmeridgian-Tithonian section and normal fault activity along the weld, Brooke-Barnett (2022) argued that the salt tectonic activity may have continued during the Early Cretaceous. The E-W trending normal faults north of the weld formed after the Early Cretaceous and they may have related to the collapse of the overburden north of the Valberg-Beuil salt wall.

3.9 Puget-Théniers diapir

The Puget-Théniers diapir is located south of the Dôme de Barrôt, in the eastern segment of the Castellane Arc (Fig. 3.1). The diapir developed over a basement involved Tethyan normal fault, during the Early and Middle Jurassic (Dardeau & De Graciansky, 1990). At its southwestern end the diapiric gypsum body links into the NE-SW trending Gourdon salt-cored anticline (Brooke-Barnett, 2022). Strata along the northern flank of the diapir are overturned to NNE (Fig. 3.11a). On the southeastern side of the diapir, a thin Liassic-Lower Cretaceous section abuts against Triassic gypsum (Campredon et al., 1980b). Here, all the Liassic, Middle Jurassic, Upper Jurassic and Lower Cretaceous formations pinch out locally. The Lower Cretaceous succession is onlapped by Turonian-Campanian sediments. The diapir was exposed during the Aptian, Albian and Cenomanian times and covered by Upper Cretaceous sediments

(Fig. 3.11b). Later, Alpine compression shortened and squeezed the diapir, but complete welding of the structure did not occur (Fig. 3.11a).

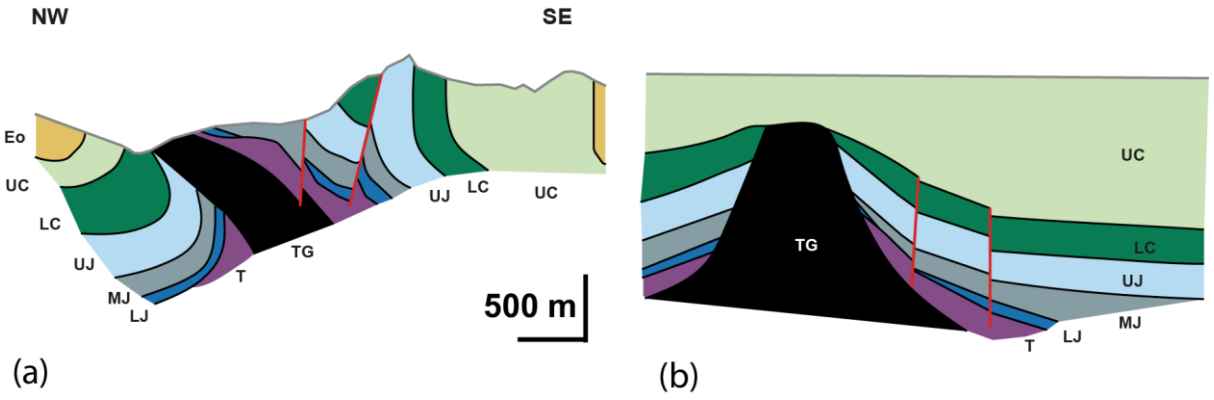


Fig. 3.11 (a). Section crossing the Puget-Théniers diapir. (b). Late Cretaceous restoration of the diapir and surrounding sediments. Redrawn after Dardeau & De Graciansky (1990). Note the thickness changes of the Jurassic-Cretaceous section, local unconformities and normal faults sealed by the Upper Cretaceous sediments on the flank of the salt body. See Fig. 2.2b for geological key.

3.10 Conclusion

In summary, diapirs formed during the Early and Middle Jurassic rifting of the margin (e.g., the Puget-Théniers diapir and the Daluis diapir) (Mascle et al., 1988; Dardeau & De Graciansky, 1990; Brooke-Barnett, 2022) continued to develop during the post-rift episode of Tethyan evolution and continued to develop or were profoundly modified during the Alpine contractional deformation (Kerckhove & Roux, 1978b; Lickorish & Ford, 1998). Many salt related structures were previously thought to have been formed as Alpine structures and their tectonic origin were emphasized. These include the Vélodrome syncline, the folds in the La Robine unit at the tip of the Digne nappe and the overturned section of the Barre de Chine at Barles (Goguel, 1939; Gidon & Pairis, 1992; Gidon, 1997). However, more recent studies show that many apparently Alpine structures have salt tectonic origin, and their evolution started during the Mesozoic (Graham et al., 2012; Graham et al., 2019; Brooke-Barnett et al., 2019; Célini et al., 2020; Graham & Csicsek, 2020; Brooke-Barnett et al., 2020; Brooke-Barnett et al., 2021; Csicsek et al., 2021; Brooke-Barnett, 2022; Célini et al., 2022). Abrupt thickness and facies changes, deposition of extremely reduced sections on the crest of the diapirs, anomalous contact of sediments with Triassic gypsum and cargneule (‘piercement of the overburden’), local unconformities and halokinetic sequences, syn-sedimentary normal faulting around salt bodies, slumps, deposition of olistoliths and breccia levels in flanking strata all provide

evidence of pre-Alpine salt tectonic activity during the syn-rift phase and post-rift phase of the evolution of the Tethyan margin in the Haute Provence area.

Anomalous contacts of the Triassic gypsum and cargneule with Jurassic-Cretaceous and Tertiary sediments, enigmatic structures, young on older contacts on thrusts and abrupt thickness and facies changes also occur in my study area around the Barrême basin, the town of Castellane and the village of Blieux (for location, see Fig. 3.1). Comparison of the well-known salt related structures of the Subalpine chains and analogues in other salt basins with structures observed in the study area may reveal their salt related origin. In the following chapters, I am going to demonstrate examples of salt tectonic activity throughout the Mesozoic and Tertiary evolution of this part of the Southern Subalpine chains. The following chapter (Chapter 4) shows examples of salt stocks, diapirs, walls and surrounding salt-withdrawal depocenters (i.e., primary minibasins) formed during the Tethyan rifting and the passive margin phase on the top of the autochthonous salt level (i.e., the mother salt layer). The subsequent chapter (Chapter 5) demonstrates evidence for allochthonous salt emplacement into higher stratigraphic levels during the passive margin phase and describes the effects of salt tectonics on the sedimentation above and around the allochthonous salt. Chapter 5 will also describe the incorporation and Alpine modification of the precursor salt related structures into the developing fold and thrust belt and document how they influenced the structural style of the Subalpine chains and syn-orogenic sedimentation from Late Cretaceous to Pliocene.

Chapter 4: Jurassic-Early Cretaceous minibasin formation above the autochthonous evaporite level

The aim of this chapter is to describe those salt withdrawal basins of the Southern Subalpine Chains which rest on the autochthonous Triassic evaporite together with their bounding salt structures such as salt swells, pillows, salt stocks, diapirs and walls. The description proceeds from south to north through the area of study. Structural descriptions are based on my observations, newly constructed geological and structural maps, series of cross sections and also previously published geological maps (1:50 000 and 1:250 000 scale) and reports (Kerckhove & Roux, 1976a; Kerckhove & Roux, 1976b; Kerckhove & Roux, 1978a; Kerckhove & Roux, 1978b; Campredon et al., 1980a; Campredon et al., 1980b; Kerckhove et al., 1980; De Graciansky et al., 1981; De Graciansky et al., 1982) (e.g. Fig. 4.1, Fig. 4.2, Fig. 4.5, Fig. 4.24, Fig. 4.25, Fig. 4.29). The study area is subdivided into two structural domains, the southern and northern domains, respectively. In the following chapters, I refer to these domains as they are shown in Fig. 2.1b. The southern structural domain comprises the eastern part of the Valensole basin, the southern part of the St-Jurs Imbricates from the Valensole basin to the Castellane arc, the northern part of the Mesozoic Provençal platform, and the western part of the Castellane arc (Fig. 2.1b). The northern structural domain comprises the eastern part of the Valensole basin S of the town of Digne-les-Bains, the northern part of the St-Jurs Imbricates, the southern part of the Digne arc and the Barrême basin (Fig. 2.1b).

Previous authors have recognised and described the pre-Alpine palaeogeographic position of different domains in the Tethyan platform-slope-basin context. The southern structural domain roughly represents the northern part of the Mesozoic Provençal platform and the slope of the Dauphinois and Vocontian basins (Fig. 4.2). The northern structural domain mostly comprises the predominantly pelagic domain of the Dauphinois and Vocontian basins (Fig. 4.47).

The structural style and position of the different palaeogeographic areas within the fold and thrust belt have been well documented in the literature (Kerckhove & Roux, 1976a; Kerckhove & Roux, 1978a; De Graciansky et al., 1981) though in some cases, previous structural subdivisions seem to be rather confusing. In their structural schemes, previous authors subdivided areas which share many tectono-stratigraphic characteristics. Many of the Alpine compressional structures which bound synclinal depocenters or indicate facies boundaries are anomalous contacts previously identified as Oligocene strike-slip faults or thrust faults, which taken together would require multidirectional thrusting during the Alpine compressional phases. In the following chapters, I refer to the palaeogeographic position and facies of the sub-areas of the study area as they were represented by Kerckhove & Roux (1976a); Kerckhove & Roux (1978a) and De Graciansky et al. (1981) in their structural schemes but present what I

consider to be a more precise tectono-stratigraphic subdivision of the area with a reinterpretation of salt cored anticlines, anomalous contacts, strike-slip faults, and their intervening synclines.

4.1 Jurassic-Early Cretaceous salt tectonics in the southern structural domain, around Blieux and Castellane. Observations, structural and stratal geometries

Jurassic-Early Cretaceous salt withdrawal basins (primary minibasins), resting on the autochthonous Triassic evaporites, exist around the villages of Blieux, Chasteuil, La Garde and the town of Castellane in the southern domain of the study area (Fig. 4.1, Fig. 4.2). The term 'salt structure' will be used as it was defined by Jackson & Hudec (2017): a 'map-scale body of salt that has changed shape by salt flow from its depositional configuration', a definition which encompasses salt diapirs, salt pillows and salt anticlines. The term 'diapir' is used as a synonym of the 'salt structure' in maps, cross sections, and annotated photo panoramas.

The eastern part of the southern structural domain is characterised by a series of synclines separated by anomalous contacts, salt cored anticlines or Alpine thrust faults. The structural style and trend of these structures are distinct from the western part of the southern domain and from the northern structural domain. The folds between the synclines have relatively short wavelengths and between the town of Castellane and the village of Blieux a series of structures both oblique and parallel to the Alpine trends of the Castellane arc and Digne arcs are present (Fig. 4.1, Fig. 4.2). Salt-related features like megaflaps, pinch-outs, local unconformities, minibasin scale wedge geometries and thickness changes affect the Jurassic-Early Cretaceous succession and show clear evidence of salt tectonic activity initiated as early as the Liassic which continued through the Jurassic and Early Cretaceous. Large-scale slump folds and breccia levels also occur on the flanks of salt structures. The southern structural domain was situated close to the Provençal platform edge during the Mesozoic and represents the slope and basin palaeogeographic domains of the Dauphinois and Vocontian basins. Most of the salt related structures of the southern structural domain occur along the edge of the Mesozoic Provençal platform (Fig. 4.2 and Fig. 4.35).

4.1.1. The Taloire syncline, the Porte de St-Jean syncline and the Taulanne syncline: depocenters and their bounding salt structures of the southern structural domain

The Taloire syncline, the Porte de St-Jean syncline and the Taulanne syncline are located in the eastern part of the southern structural domain on the slope between the Provençal platform and the Dauphinois and Vocontian basins (Fig. 4.2). The synclines are well known and have been considered for decades as Alpine structures (Kerckhove & Roux, 1976a; Kerckhove & Roux, 1978a; Grosjean et al., 2017) in spite of the fact that abrupt thickness and facies changes of the Jurassic-Cretaceous section were documented in the Taulanne syncline. These anomalous structural and stratigraphic relationships were considered to be associated with the presence of normal faults inherited from the Tethyan rifting (Cotillon, 1968; Beaudoin, 1969). The southern flank of the Taulanne syncline (Cadiéres de Brandis area, Fig. 4.2) and its bounding structures has been studied between Castellane and the village of Chasteuil by Roux (1968) and the Tertiary stratigraphy of the Taulanne basin was described by Guérin-Desjardins (1956) and Roux (1970). The structural framework of the Castellane-Blieux area was described by Roux (1972).

The Taloire syncline is carried in the hanging wall of the south verging Robion thrust fault, which overrides the edge of the Mesozoic Provençal platform (Fig. 2.6, Fig. 4.1, Fig. 4.2,). The Taloire syncline is a large, elongated, roughly ENE-WSW trending syncline, south of which is an ENE-WSW trending anticline, the Montagne de Robion (Fig. 4.1, Fig. 4.2). The Taloire syncline is bounded to the north by a curved Alpine thrust fault, the so-called 'Brans fault' which separates it from the small, E-W striking Porte de St-Jean syncline (Fig. 4.2). The Porte de St-Jean syncline is situated south of the Chasteuil salt structure (Fig. 4.2) which separates it from the much larger Taulanne syncline (Fig. 4.2). The Taulanne syncline is also bounded to the north by a major salt structure the St-Vincent diapir (Fig. 4.2) which lies to the south of a structurally complex zone, the Boades zone (see § 4.1.1.1). To the east the Taulanne syncline is overridden by the la Blache-Castellane thrust sheet (Fig. 4.1, Fig. 4.2).

The western border of the Taulanne and Taloire synclines is defined by the NE-SW trending Berbené fault (Roux, 1972; Brooke-Barnett, 2022), an apparent thrust fault which runs from the Alpine Robion thrust to the NE to merge with the la Blache-Castellane thrust immediately N of the village of Boades (Fig. 4.2). Along this fault, the Taulanne syncline and the Taloire syncline are in direct contact with the Blieux syncline and the Bourbonne syncline, which

belong to the basin palaeogeographic domain of the Dauphinois and Vocontian basins (Fig. 4.2). Further to the SW, in the hanging wall of the Robion thrust, along the Berbené fault, the Taloire syncline is in contact with the la Gondole syncline which is part of the palaeogeographic slope domain (Fig. 4.1, Fig. 4.2). The eastern part of the Taloire syncline is bounded to N by the basinal Haute Sionne syncline and the la Blache-Castellane thrust sheet which carries the Castellane diapir (Fig. 4.2). The NE boundary of the Taloire syncline is defined by the NW-SE trending Destourbes thrust (Fig. 4.2), a SW verging thrust which carries a complete Triassic-Upper Cretaceous section which was originally deposited in the slope palaeogeographic domain of the Dauphinois and Vocontian basins (Kerckhove & Roux, 1978a).

In the following section, the individual salt structures and adjacent depocenters are described from north to south.

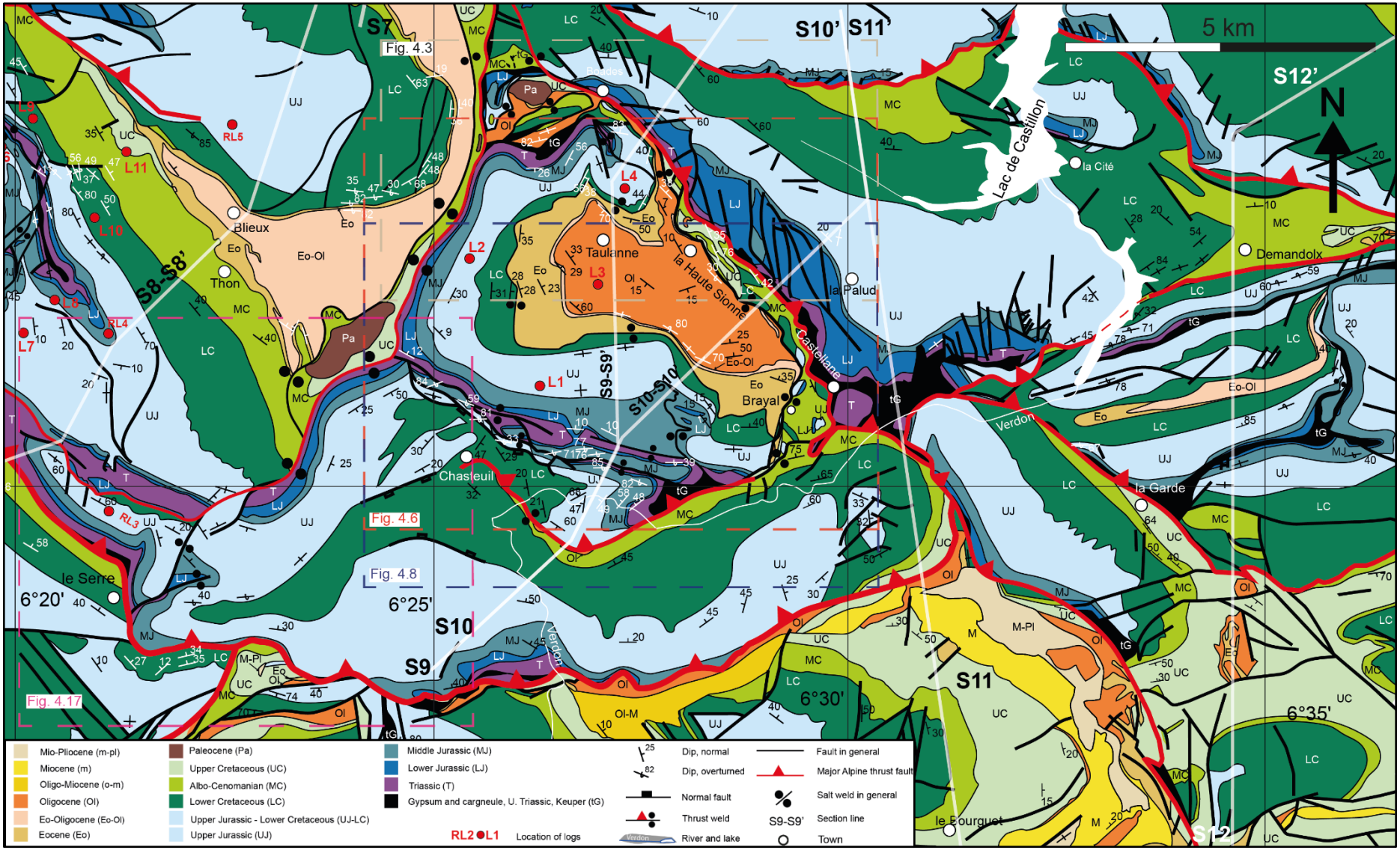


Fig. 4.1 Simplified geological map of eastern part of the southern structural domain, in the vicinity of Blieux and Castellane. Redrawn after Kerckhove & Roux (1976a) and Kerckhove & Roux (1978a). See Fig. 4.2 for the structural explanation.

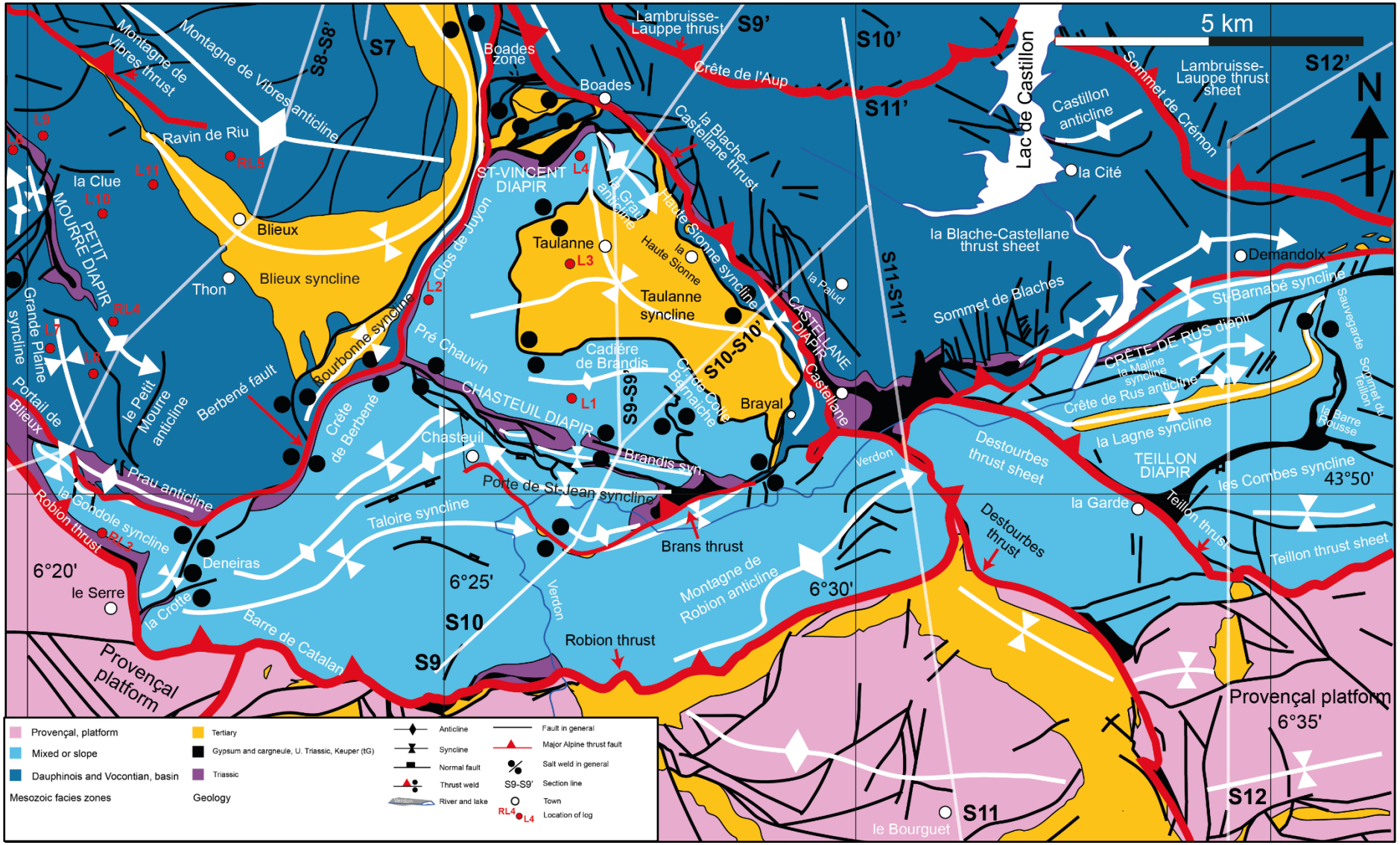


Fig. 4.2 Structural map of the eastern part of the southern structural domain showing synclines, their bounding Alpine structures or pre-Alpine salt structures and their Mesozoic palaeogeographic position. Data from Kerckhove & Roux (1976a) and Kerckhove & Roux (1978a). For geological map see Fig. 4.1.

4.1.1.1. The St Vincent diapir and the la Grau anticline. Structural and stratigraphic observations

The St-Vincent diapir is situated N of the Taulanne syncline and S of the village of Boades (Fig. 4.1, Fig. 4.2, Fig. 4.3). The outcrop width of the Triassic gypsum varies between 50 m

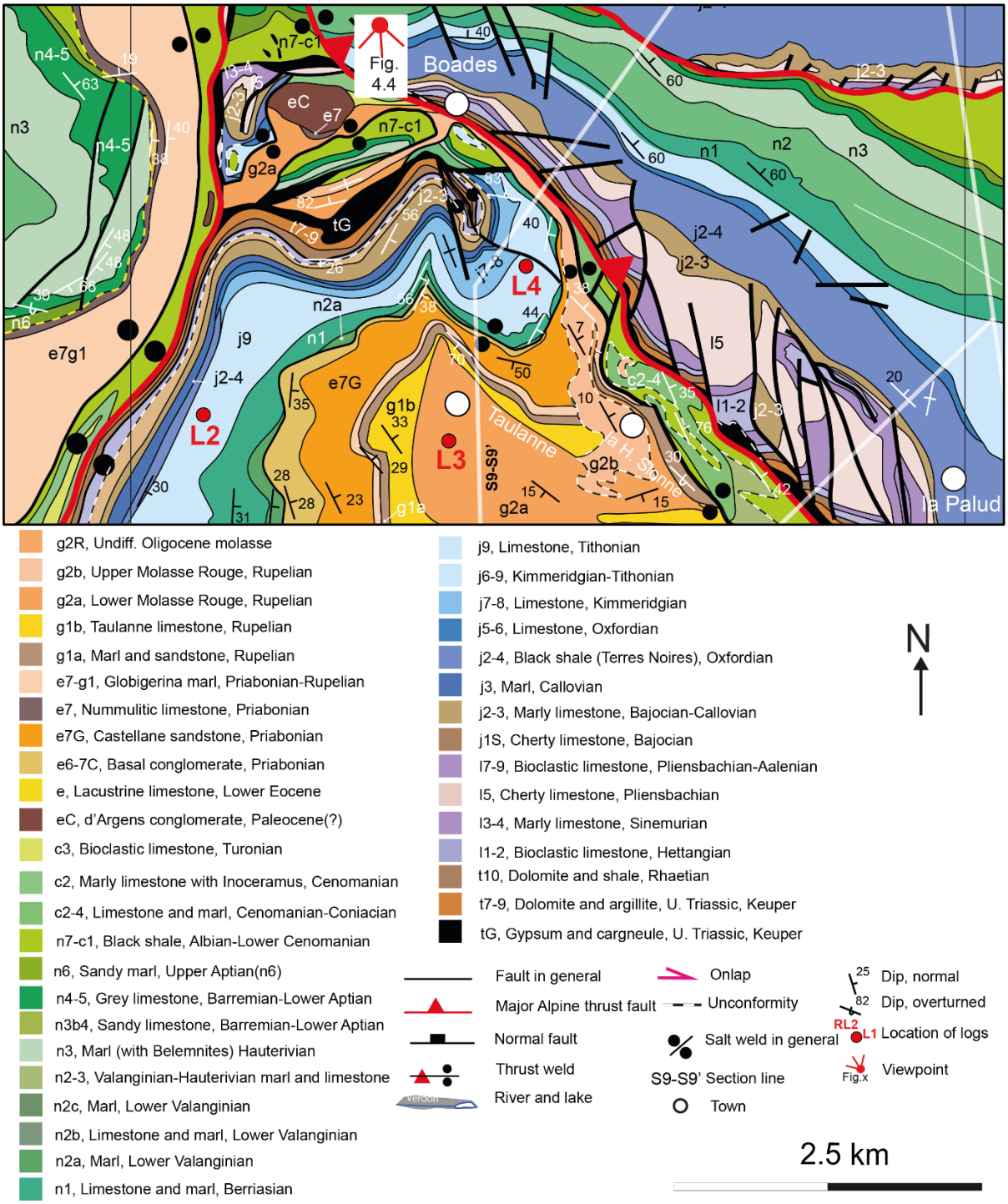


Fig. 4.3 Detailed geological map of the St-Vincent diapir and the northern part of the Taulanne syncline. See Fig. 4.1 for location. See Fig. 4.2 for structural map and explanation of the area.

and 100 m. According to Kerckhove & Roux (1978b), on the westernmost extent of the diapir, a large block of Lower Triassic Buntsandstein sandstone (around 10 by 50 m) is incorporated into the Upper Triassic Keuper gypsum (it is not shown on maps due to its size and unknown location). The presence of Lower Triassic rocks at the surface was attributed to basement involved faulting by Kerckhove & Roux (1978b).

To the W, the St-Vincent diapir is bounded by the Blieux syncline and the Bourbonne syncline (Fig. 4.2, Fig. 4.4). The diapir is separated from these synclines by the Berbené fault. To the N, the St-Vincent diapir is flanked by the highly deformed and complex Boades zone. On the northern side of the structure, the Keuper is in direct contact with an incomplete Cretaceous (Valanginian-Cenomanian, n2 – n7-c1) section and vertical beds of Rupelian 'Upper Molasse Rouge' (g2b). In its eastern segment, the Triassic gypsum body joins into the core of a tight, NW-SE trending and SE plunging anticline, the la Grau anticline (Fig. 4.2, Fig. 4.3, Fig. 4.4). Although the Keuper gypsum is not present at the surface in the core of this anticline, the Triassic-Lower Cretaceous section (Norian-Valanginian, t7-9 to n2a) folded around it is very reduced suggesting that it is a squeezed salt structure. The facies of the Jurassic is more like the Jurassic of the Cadiéres de Brandis area, i.e. the southern flank of the Taulanne syncline (see § 4.1.1 and § 4.1.1.2) rather than the basinal succession of the adjacent la Blache-

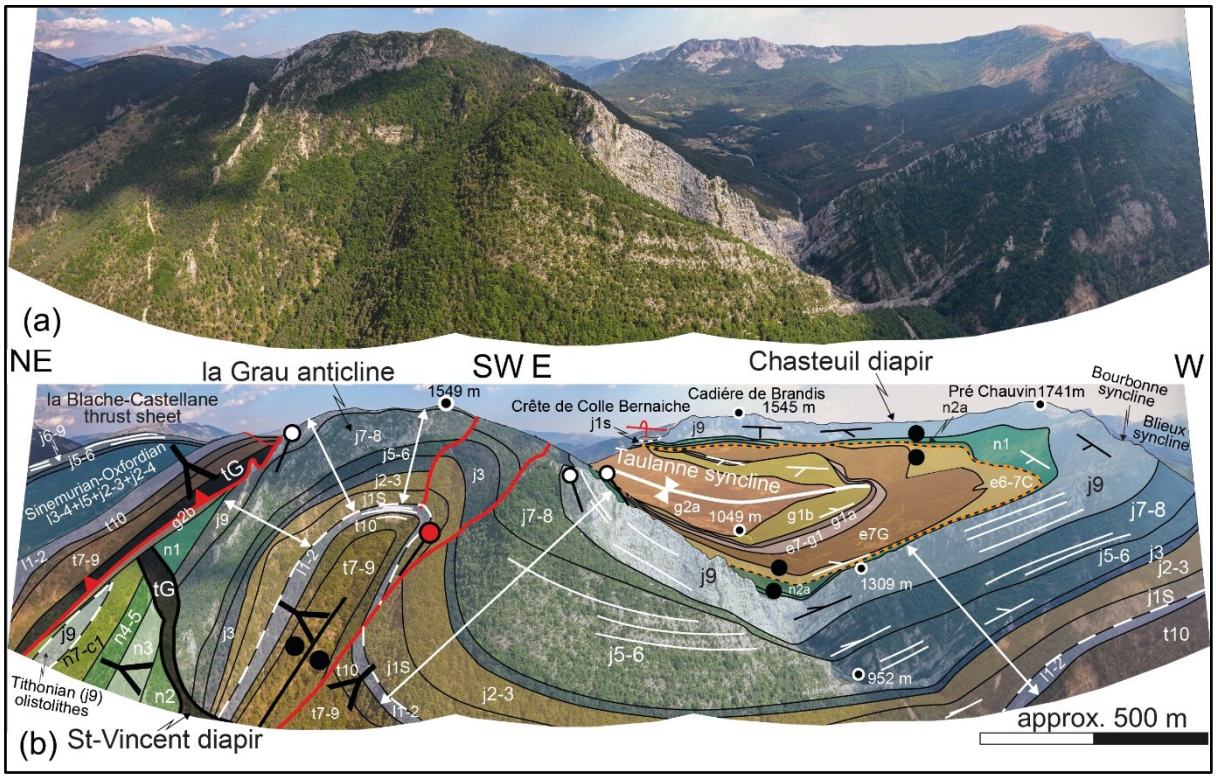


Fig. 4.4 Photo panorama of St-Vincent diapir, the la Grau anticline and the bounding Taulanne syncline, looking to SSE. See Fig. 4.3 for key and viewpoint location.

Castellane thrust sheet (Roux, 1970). The north-eastern limb of the anticline is nearly vertical, while its south-western limb is overturned to SW (Fig. 4.4). Here, a local unconformity is visible at the base of the Oxfordian limestone (j5-6) and the Callovian grey marl (j3) is missing between the Aalenian-Callovian (j2-3) and the Oxfordian (Fig. 4.3). The eastern part of the la Grau anticline is unconformably overlain the Upper Molasse Rouge (g2b) (Fig. 4.3, Fig. 4.4). On the southern limb of the la Grau anticline, Tithonian and Berriasian strata are unconformably overlain by the Priabonian Basal conglomerates (e6-7C) and the Castellane sandstone (e7G) which was deposited in the Taulanne syncline (Fig. 4.3).

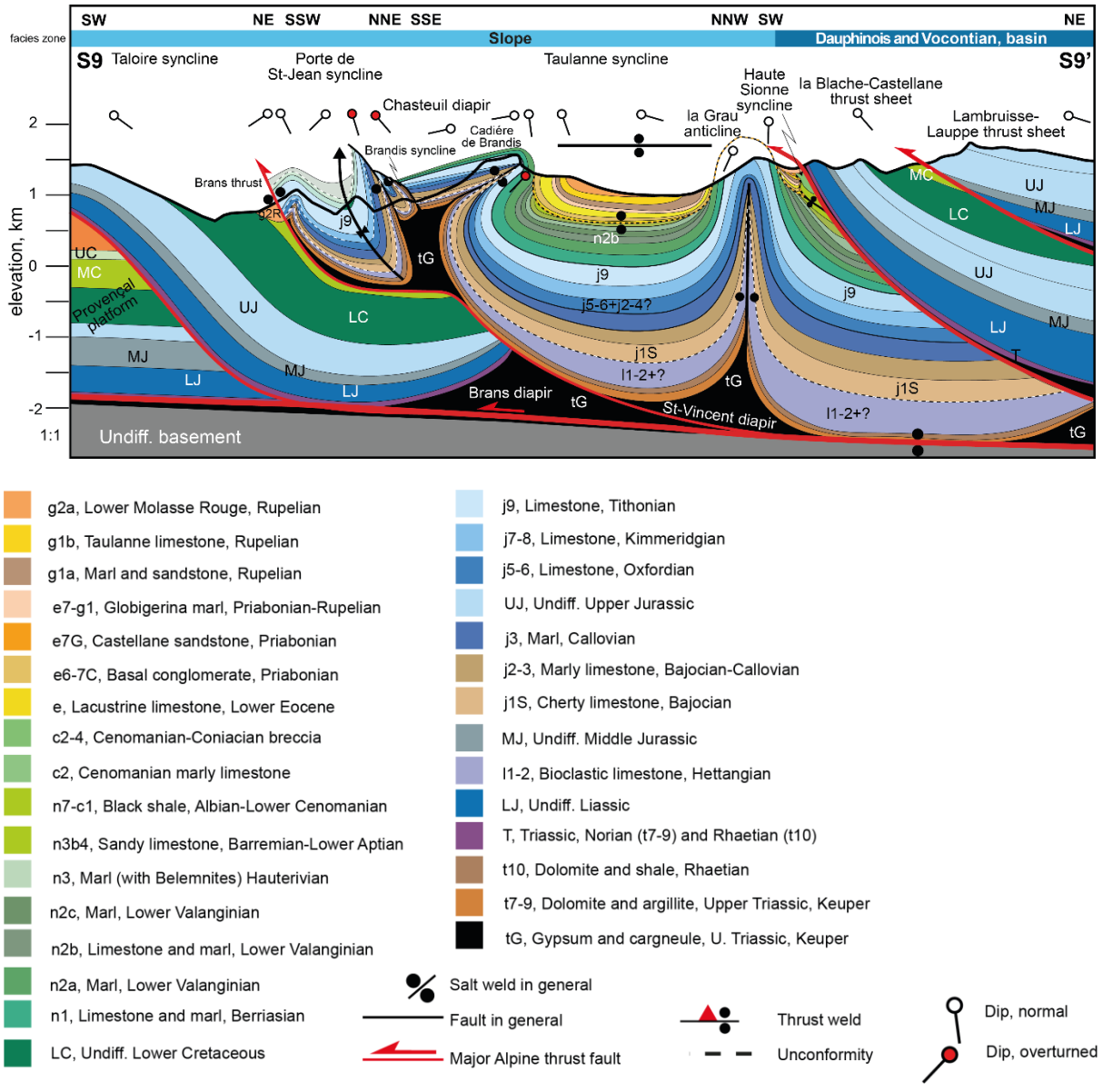


Fig. 4.5 Cross section (S9-S9') from the Provençal Platform to the basinal Lambruisse-Lauppe thrust sheet, intersecting Taloire syncline, the Porte de St-Jean syncline and the Taulanne syncline of the Mesozoic slope facies zone and the Haute Sionne syncline and the la Blache-Castellane thrust sheet. See Fig. 4.1 for cross section location. Note that the northern segment of the section is not shown on Fig. 4.1.

In the SW segment of the St-Vincent diapir, the Keuper gypsum is flanked by the Mesozoic infill of the Taulanne syncline. South of the salt body, a complete Triassic-Lower Cretaceous section dips away from the gypsum whereas the northern termination of the Taulanne basin forms a tight syncline between the St-Vincent diapir and the adjoining la Grau anticline (Fig. 4.2, Fig. 4.3, Fig. 4.4). Here, the Triassic-Lower Cretaceous section is unconformably overlain by the Priabonian basal conglomerates. The thickness of the Jurassic section (Hettangian to Tithonian, l1-2 to j9) shows lateral variations: it is reduced (approximately 250 m) at the crest of the la Grau anticline but 500 m to the SW at the northern termination of the Taulanne syncline. Further to the SW, the thickness is 400 m but thickens once again in the western limb of the Taulanne syncline (Fig. 4.1, Fig. 4.3). Significant thickening of the Oxfordian (j5-6) was observed at the northern termination of the Taulanne syncline, SW of the la Grau anticline (Fig. 4.4).

The most important structural observations around the St-Vincent diapir are the anomalous contact relations against the E-W trending Upper Triassic gypsum body. The Triassic gypsum separates the reduced, steeply dipping Norian-Berriasian (t7-9 to n1) section exposed on the eastern limb of the la Grau anticline from the incomplete Lower Cretaceous (Valanginian-Cenomanian, n2 – n7-c1) section which lies north of the Triassic gypsum. Outcrop conditions are poor south of the village of Boades, between the la Grau anticline and the la Blache-Castellane thrust sheet (Fig. 4.4), but the incomplete Lower Cretaceous section is considered being part of the Boades zone. In the upper part of this section, within the Albian-Lower Cenomanian black marls, a large block of Tithonian limestone (j9) can be seen in the immediate footwall of the overriding la Blache-Castellane thrust fault (Fig. 4.3, Fig. 4.4). The Tithonian block is surrounded entirely by Albian-Cenomanian black marls. Both sections flank the salt structure and the eastern termination of the gypsum body is covered by eastward dipping Oligocene Upper Molasse Rouge (g2b), immediately below the overriding la Blache-Castellane thrust sheet (Fig. 4.3, Fig. 4.4, Fig. 4.5).

4.1.1.2. The Taulanne syncline. Structural and stratigraphic observations

The Taulanne syncline is a 5-6 km (ca. 18 km^2) wide sub-circular basin with a 2-2.5 km thick Mesozoic fill in the core of the syncline, ranging from Upper Triassic (Norian, t7-9) to Lower Cretaceous (Valanginian, n2c) in age (Fig. 4.1, Fig. 4.2). Hauterivian, Barremian, Albian-Cenomanian and Turonian-Coniacian sediments may have also been deposited in the core of the syncline but they are eroded now or covered by Eocene and Oligocene sediments

(Fig. 4.6, Fig. 4.7). The presence of the Tertiary cover complicates the description of the composition, thickness, and facies of the Mesozoic succession in the core of the Taulanne syncline.

Topographically, the Taulanne syncline is open to the SE but surrounded by the ridges of Liassic limestone to the east and Tithonian limestone in all other directions. The syncline is bounded to the S and N by two salt structures: the Chasteuil salt structure and the St-Vincent diapir (Fig. 4.1, Fig. 4.2, Fig. 4.6). To the W, the syncline is bounded by the Blieux syncline and the Bourbonne syncline (Fig. 4.1, Fig. 4.2) separated from each other by the NE-SW trending the Berbené fault - an apparent thrust fault (Roux, 1972; Brooke-Barnett, 2022). Along this structure, the Taulanne syncline overrides the Blieux and Bourbonne synclines (Fig. 4.1, Fig. 4.2). In the western limb of the syncline (the Clos de Juyon section, Fig. 4.2), Carnian-Norian (Keuper, tG, t7-9) to Valanginian (n2a) section is exposed with dips around 30º to the ESE (Fig. 4.1, Fig. 4.6). NW of the Pré Chauvin peak, Keuper gypsum is exposed along the Berbené fault (Fig. 4.2 and Fig. 4.6).

In the western limb of the Taulanne syncline the thickness of the Norian-Valanginian section is around 750 m gradually thinning towards the St-Vincent diapir, the la Grau anticline and the Cadiéres de Brandis section (Fig. 4.6, Fig. 4.7). The Triassic-Lower Cretaceous succession in the western limb of the Taulanne syncline is unconformably overlain by basal Eocene conglomerates (e6-7C) (Fig. 4.1, Fig. 4.6). The Mesozoic sections of the eastern and south-eastern flanks of the Taulanne syncline are not exposed, but in the east an anomalous contact separates it from the Haute Sionne syncline (Fig. 4.2), which is a tight, NW-SE trending structure situated between the St-Vincent diapir and the town of Castellane (Fig. 4.1, Fig. 4.2 and Fig. 4.6). Further to the NW, the Taulanne syncline is overridden by the SW verging, NW-SE trending la Blache-Castellane Alpine thrust fault (Fig. 4.1, Fig. 4.2). This thrust carries in its hanging wall a thick and slightly folded Upper Triassic-Upper Cretaceous section (from Norian to Cenomanian), which dips around 20-30º to the NE (Fig. 4.1, Fig. 4.2, Fig. 4.5 and Fig. 4.6). The Jurassic-Cretaceous section deposited in the basin facies zone of the Dauphinois and Vocontian basins. The la Blache-Castellane thrust also carries a salt structure: the Castellane diapir (see § 4.1.2.3).

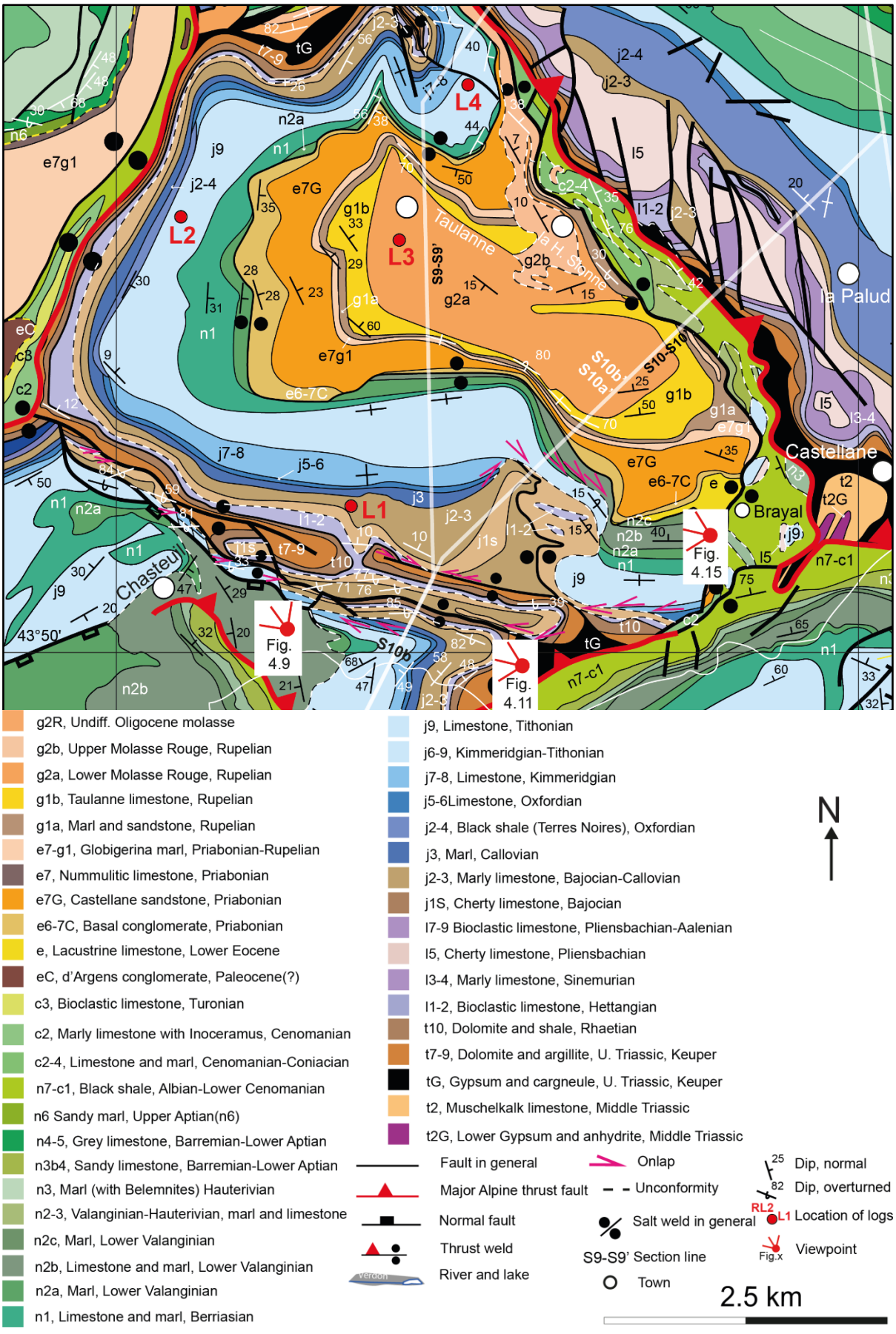


Fig. 4.6 Detailed geological map of the Taulanne syncline. See Fig. 4.1 for location. See Fig. 4.2 for structural map and explanation of the area.

The complete section of the Mesozoic fill of the Taulanne syncline is well exposed in the Cadiéres de Brandis section, in the western limb and also around the St-Vincent structure (Roux, 1968; Kerckhove & Roux, 1978a) (Fig. 4.1, Fig. 4.2, Fig. 4.3, Fig. 4.6). The Triassic succession is represented by the Keuper gypsum and cargneule breccia (tG), Norian dolomite and argillite (t7-9) and Rhaetian dolomite, shale, and sandstone (t10). On the flanks of the syncline the Liassic section is incomplete and represented only by Hettangian bioclastic

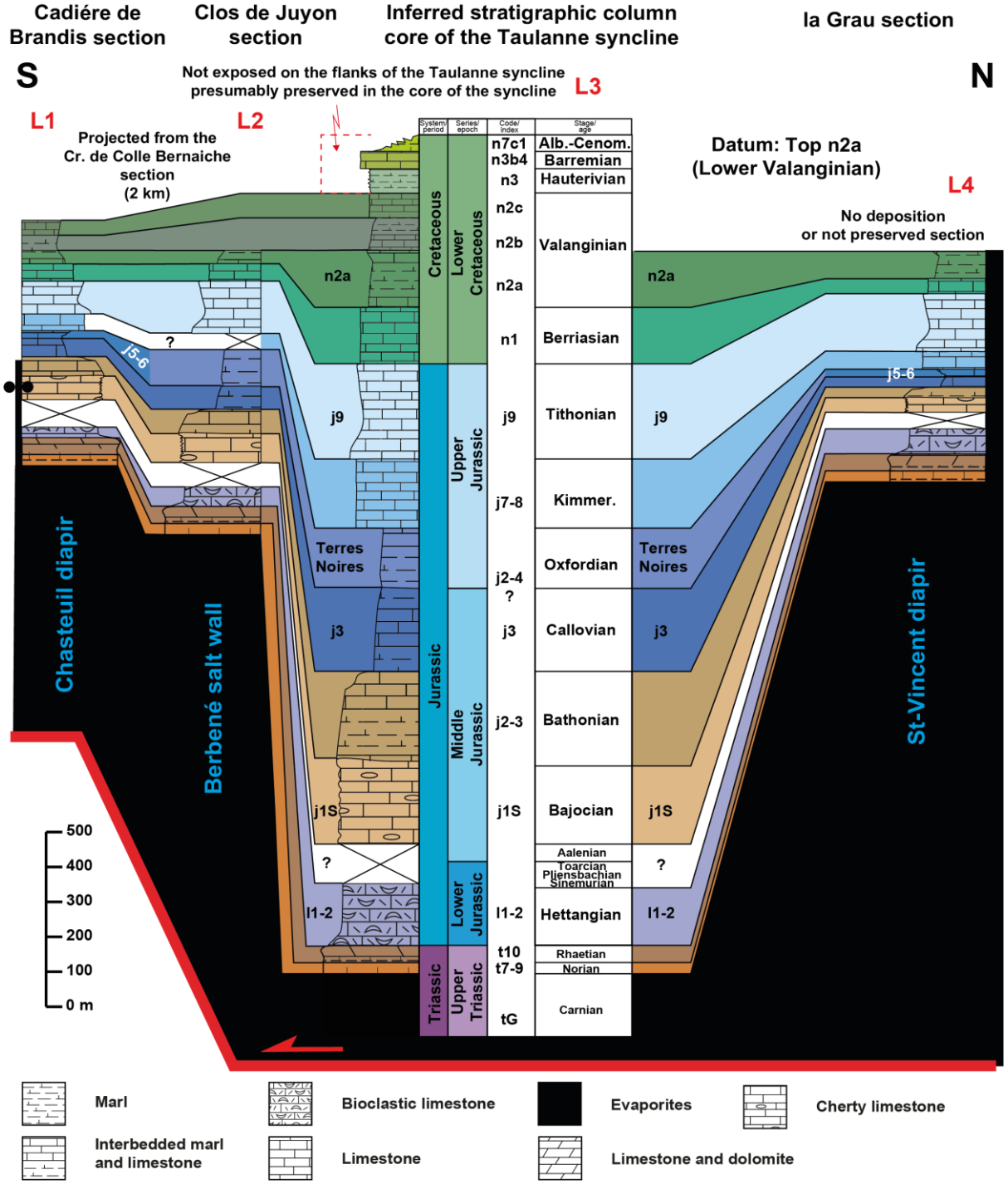


Fig. 4.7 Transect showing thickness variations between the core of the Taulanne syncline and the flanking Cadiéres de Brandis and la Grau sections. Note that thicknesses are inferred in the core of the Taulenne sycnline. See Fig. 4.2 location of the logs and Fig. 4.6 for geological key.

limestone (l1-2) characteristic of the slope facies zone along the Provençal platform edge (Kerckhove & Roux, 1978a), though according to Roux (1968) the Middle-and Upper Liassic may be present at the Cadières de Brandis section. The Liassic bioclastic limestone is unconformably overlain by Bajocian cherty limestone (j1S), a local unconformity which can be seen around the margins of the Taulanne syncline, around the flanks of the St-Vincent diapir, in the western limb, and N and E of the Cadiéres de Brandis section, around the village of Brayal (Fig. 4.1, Fig. 4.2, Fig. 4.3, Fig. 4.6). The Bajocian (j1S) passes into Bajocian-Callovian marly limestone (j2-3, Cancellophycus marly limestone Formation) and grey marl of Callovian age (j3). The Callovian grey marl is the lateral equivalent of the lower part of the Terres Noires Formation (j2-4). The Middle Jurassic succession shows affinities to the typical slope facies of the Dauphinois basin (Kerckhove & Roux, 1978a). On the southern flank of the Taulanne basin, in the Cadiéres de Brandis section, the Oxfordian (j5-6) is reduced and rich in ammonites. An identical formation is exposed on the northern flank of the Taulanne syncline around the St-Vincent diapir (j5-6). However, north of the Pré Chauvin peak (Fig. 4.2), between the Cadiéres de Brandis section and the St-Vincent diapir, in the western limb of the Taulanne syncline, the Oxfordian is represented by the black shales of the Terres Noires Formation (j2-4) (Fig. 4.6, Fig. 4.7). Oxfordian is overlain by Kimmeridgian (j7-8) which passes up into Tithonian limestone (j9). The Kimmeridgian-Tithonian section is exposed SW of the St Vincent diapir in the western limb and also in the Cadiéres de Brandis section (Fig. 4.2, Fig. 4.2and Fig. 4.6). According to Rameil (2005) the Kimmeridgian-Tithonian sediments exposed SW of the St-Vincent diapir are debris deposited in the toe of slope area. In the western limb of the Taulanne syncline, the Kimmeridgian limestone (j7-8) is missing between the Terres Noires Formation (j2-4) and the Tithonian limestone (j9) (Fig. 4.6) (Kerckhove & Roux, 1978a).

The Lower Cretaceous fill of the Taulanne syncline is exposed around its flanks, e.g., around the St-Vincent diapir, the western limb, the Cadiéres de Brandis section and also around the village of Brayal (Fig. 4.1, Fig. 4.2, Fig. 4.3, Fig. 4.6). It is composed of Berriasian (n1), Lower Valanginian (n2a, n2b) and Upper Valanginian (n2c) alternating limestone and marl beds which were deposited in the slope palaeogeographic domain. The Lower Cretaceous section is unconformably overlain all around the syncline by Eocene, Eocene-Oligocene and Oligocene sediments (Fig. 4.1, Fig. 4.2, Fig. 4.3, Fig. 4.6).

4.1.1.3. The Chasteuil salt structure

The WNW-ESE striking Chasteuil salt structure is situated between the village of Brayal and the Pré Chauvin peak (Fig. 4.1, Fig. 4.2, Fig. 4.8). It can be traced for ~ 5km along the southern margin of the Taulanne basin. The western and central part of the structure is mostly welded and Triassic Keuper evaporites are missing at the surface (Fig. 4.1, Fig. 4.2, Fig. 4.8). On its eastern end, the salt structure widens into a single Upper Triassic diapir. Keuper gypsum is exposed here over an area of ~ 0.5 km^2. The Chasteuil salt structure is bounded to the south by the Taloire syncline and the Porte de St-Jean syncline, to the west by the Blieux syncline and the Bourbonne syncline and to the north and north-east by the Taulanne syncline (Fig. 4.1, Fig. 4.2). The eastern termination of the salt structure is partly covered by Quaternary scree.

N of the Chasteuil salt structure, between the Pré Chauvin peak and the Cadiéres de Brandis mountain (Fig. 4.1, Fig. 4.2, Fig. 4.8), Norian-Tithonian (from t7-9 to j9) strata are right way up and dip gently to NNE and NE (Fig. 4.9, Fig. 4.10, Fig. 4.11 and Fig. 4.12). The dips become more gentle through the Cadiéres de Brandis section (Fig. 4.8, Fig. 4.9) which represents the reduced and incomplete section of the southern flank of the Taulanne syncline. Immediately N of the Cadiéres de Brandis Mountain, the upper part of the section, i.e., Tithonian-Valanginian strata (j9, n1, n2a, n2b) turns into vertical (Fig. 4.4, Fig. 4.8) and forming an anticline. To the W, beds curve around into the western limb of the Taulanne syncline where gentle dips were observed (around 30º to ENE) (Fig. 4.4, Fig. 4.8). N of the salt structure, the Tithonian-Valanginian section is unconformably overlain by steeply dipping or vertical Priabonian basal conglomerate and Castellane sandstone (e6-7C, e7G) (Fig. 4.4, Fig. 4.8).

South of the Cadiéres de Brandis peak, the lower part of the incomplete and horizontal section, i.e., Liassic (Hettangian, l1-2), Bajocian (j1S) and Bajocian-Callovian (j2-3) rocks are right way up. The Hettangian-Callovian section abuts against overturned Norian (t7-9) along an anomalous contact (Fig. 4.8). This WNW-ESE trending contact links to the large gypsum body of the Chasteuil diapir and separates the horizontal Cadiéres de Brandis section from a small and narrow syncline, (the Brandis syncline) formed of Triassic (t7-9, t10) and Liassic-Middle Jurassic rocks (Hettangian, Bajocian and Bajocian-Callovian, l1-2, j1S, j2-3).(Fig. 4.2, Fig. 4.8). The northern limb of this Brandis syncline is overturned to the S (Fig. 4.9, Fig. 4.10, Fig. 4.11 and Fig. 4.12). Along strike, the Brandis syncline can be traced for 3 km.

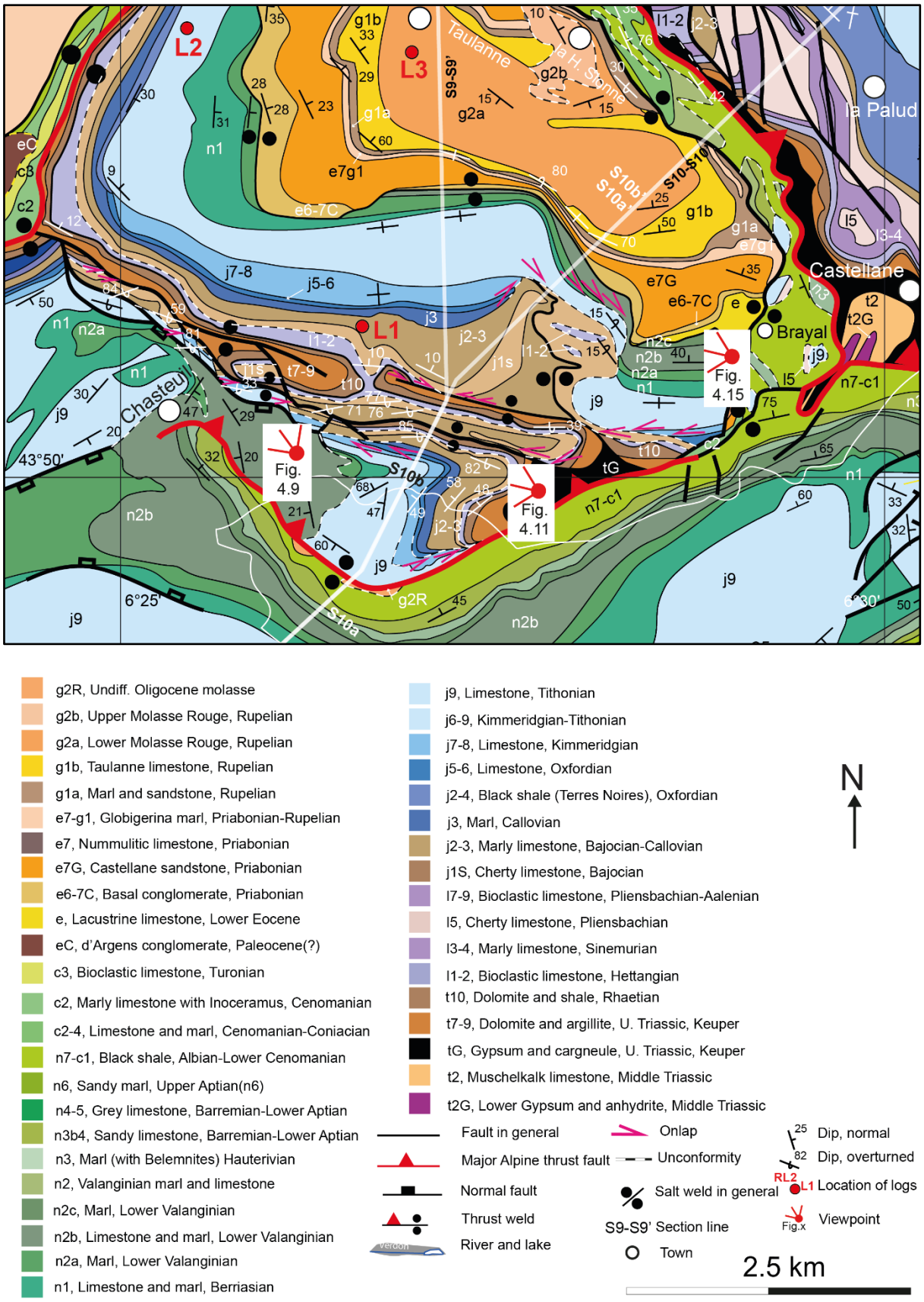


Fig. 4.8 Detailed geological map of the Chasteuil salt structure, the southern part of the Taulanne syncline, the Porte de St-Jean syncline and the northern part of the Taloire syncline. See Fig. 4.1 for location. See Fig. 4.2 for structural map and explanation of the area.

The eastern and western parts of the syncline are separated by an N-S trending anticline. In the core of this small anticline, Hettangian limestone is exposed (l1-2) (Fig. 4.8, Fig. 4.9). At the easternmost extent, on the southern limb of the Brandis syncline, Rhaetian dolomite (t10), Hettangian bioclastic limestone (l1-2) and Bajocian cherty limestone are in direct contact with the Keuper gypsum body of the Chasteuil salt structure (Fig. 4.8).

The Brandis syncline is bounded to the south by an apparently faulted contact where overturned Bajocian (j1S) and Aalenian-Callovian (j2-3) are in direct contact with Triassic (t7-9, t10), Liassic (l1-2) and Middle Jurassic (j1S) rocks which are also overturned to the S (Fig. 4.8). This section represents the northern flank of the Porte de St-Jean syncline (Fig. 4.2, Fig. 4.8) (see § 4.1.1.4).

Along strike to the west, Triassic (t7-9, t10), Hettangian (l1-2) and Bajocian (j1S) rocks in the limbs of the Brandis syncline are right way up (Fig. 4.8, Fig. 4.9, Fig. 4.10). Triassic evaporites are absent around the Brandis syncline S of the Pré Chauvin and Cadiéres de Brandis mountains (Fig. 4.1, Fig. 4.2, Fig. 4.9 and Fig. 4.10). Between the Crête de Berbené mountain and the Pré Chauvin peak (Fig. 4.1, Fig. 4.2), the syncline disappears, and the overturned northern limb of the Porte de St-Jean syncline is in tectonic contact with the gently dipping section of the SW limb of the Taulanne syncline (Fig. 4.1, Fig. 4.2, Fig. 4.8, Fig. 4.10, Fig. 4.11).

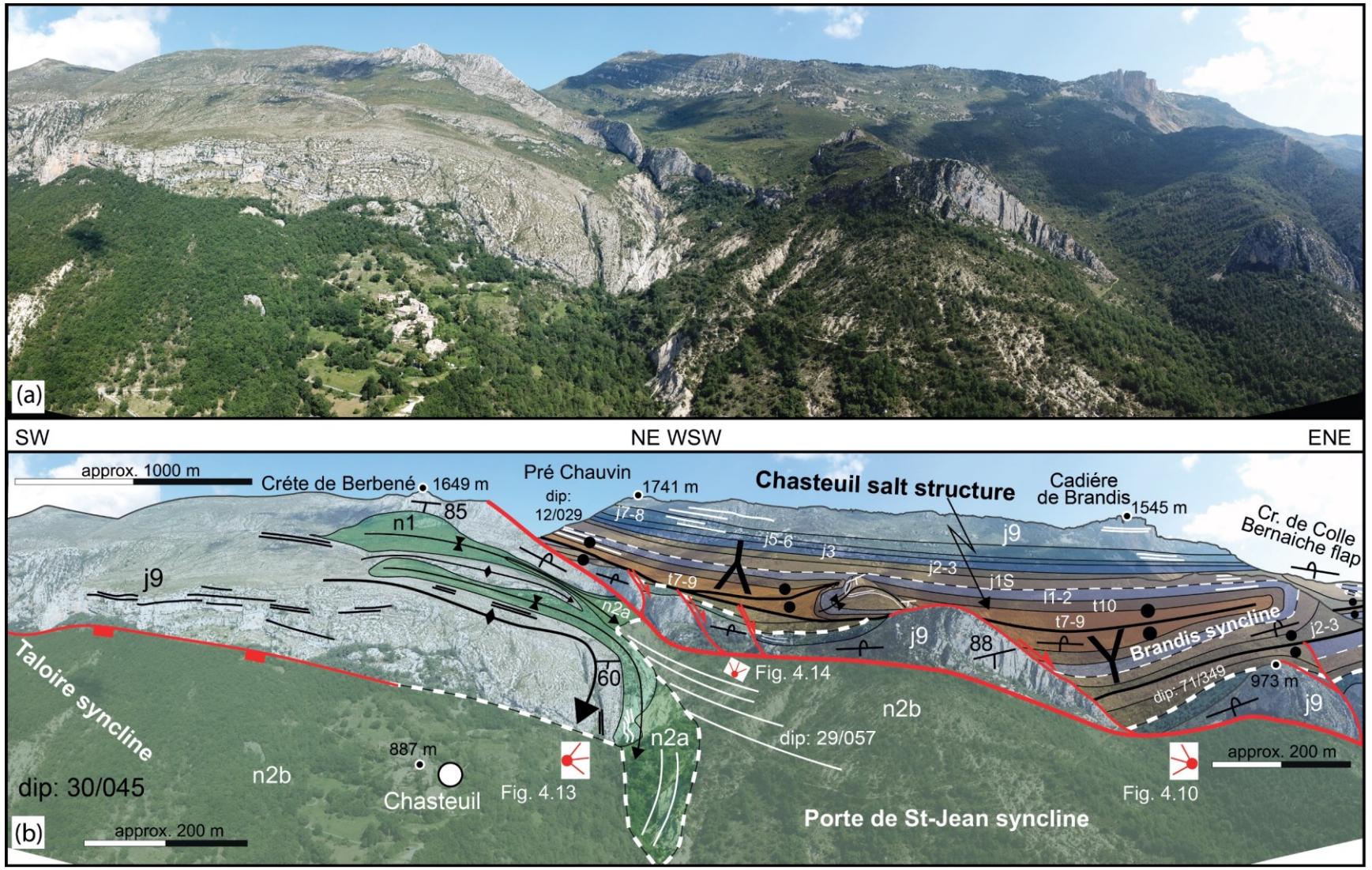


Fig. 4.9 Uninterpreted (a) and interpreted (b) photo panorama of the western sector of the Brandis syncline and the Chasteuil salt structure, the Porte de St-Jean syncline and the merging Taloire syncline in the background, in the vicinity of the village of Chasteuil. The photo presents an oblique cross section view of the welded Chasteuil salt structure. Black epsilons indicate younging direction. See Fig. 4.8 for geological key and viewpoint location.

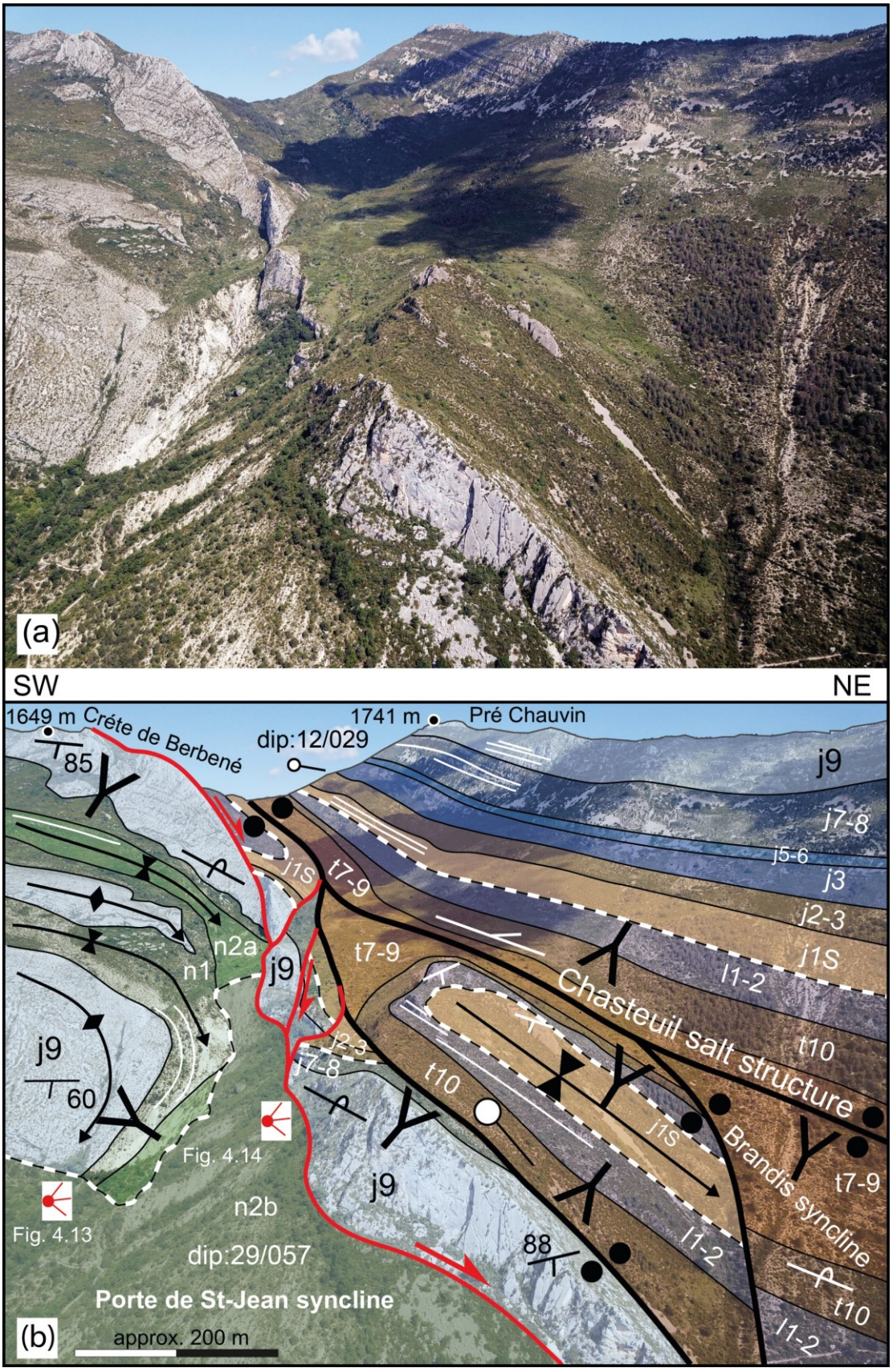


Fig. 4.10 Uninterpreted (a) and interpreted (b) photo panorama of the western sector of the Brandis syncline and the Chasteuil salt structure, the Porte de St-Jean syncline and the merging Taloire syncline, N of the village of Chasteuil, looking to NW. Black epsilons indicate younging direction. See Fig. 4.8 for geological key and Fig. 4.9 viewpoint location.

4.1.1.4. The Port de St-Jean syncline

The E-W striking Porte de St-Jean syncline is only c. 1.5 km wide and consists of Triassic (t7-9, t10), Jurassic (l1-2, j1S, j2-3, j3, j5-6, j7-8, j9) and Lower Cretaceous (n1, n2a, n2b) rocks folded into tight, west-plunging syncline with a steeply dipping to overturned northern limb (Fig. 4.2, Fig. 4.8, Fig. 4.11). To the S, the Porte de St-Jean syncline is bounded by a curved Alpine thrust fault, the Brans thrust (Fig. 4.1, Fig. 4.2), which runs between the western termination of the Haute Sionne syncline at the village of Brayal, towards the village of Chasteuil (Fig. 4.1, Fig. 4.2, Fig. 4.8, Fig. 4.11). Along this structure, the Porte de St-Jean syncline is thrust over the Taloire syncline. In the Taloire syncline, the Mesozoic succession is unconformably overlain by Oligocene red molasse (g2R) which is overturned beneath the Brans thrust (Fig. 4.1, Fig. 4.2, Fig. 4.8, Fig. 4.11). On the southern limb of the Porte de St-

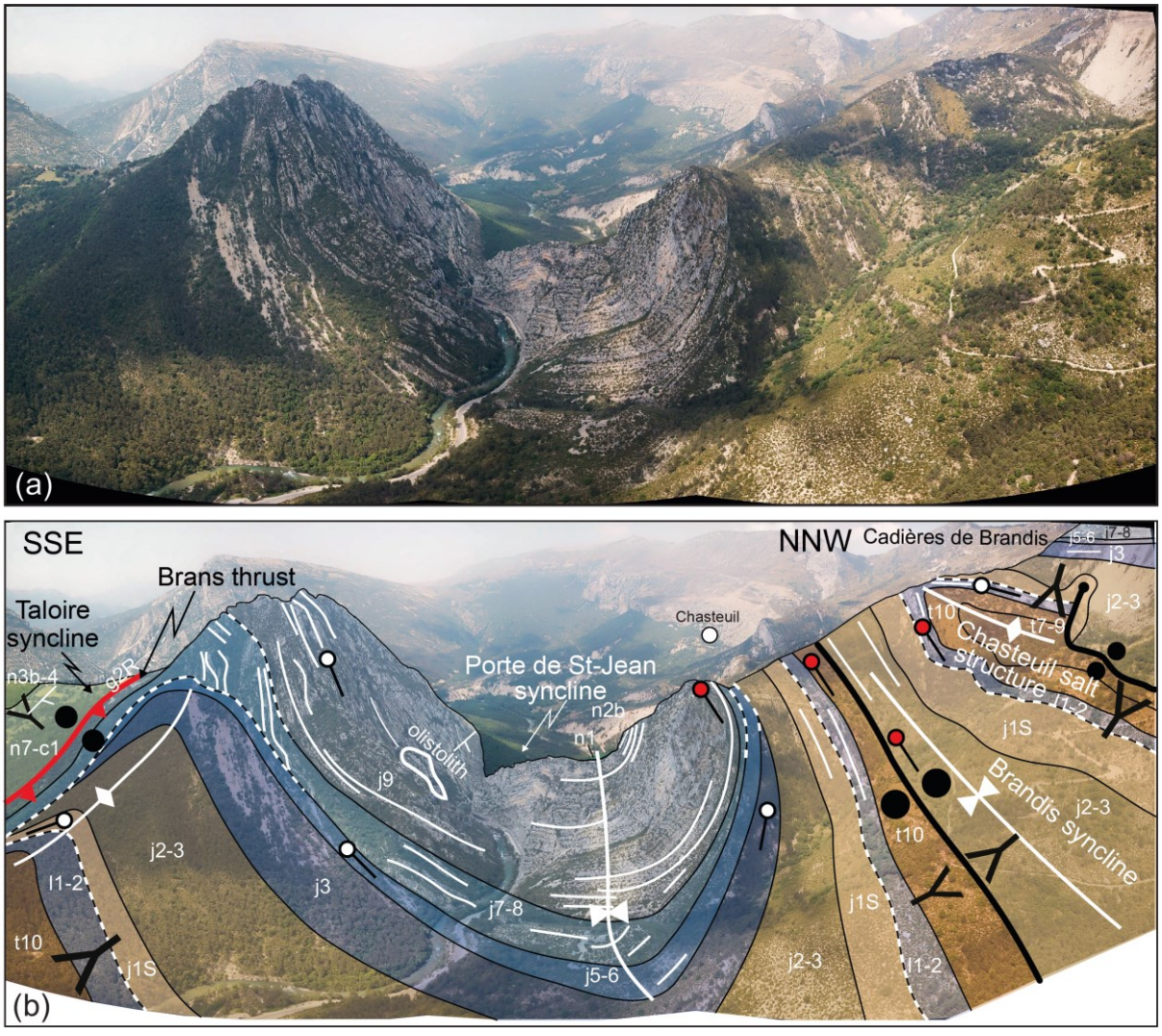


Fig. 4.11 Uninterpreted (a) and interpreted (b) photo panorama of eastern sector the the Porte de St-Jean syncline and the bounding Brans thrust and the Chasteuil salt structure. The black epsilons indicate younging direction. See Fig. 4.8 for geological key and viewpoint location.

Jean syncline, the Jurassic section gradually thins towards the Brans fault and forms an anticline in the hanging wall of the thrust (Fig. 4.8, Fig. 4.11, Fig. 4.12). Along the frontal limb the of this anticline, the 1:50000 geological map (Kerckhove & Roux, 1978a) shows Oxfordian limestone (j5-6), Callovian marl (j3), the Bajocian-Callovian (j2-3) and Bajocian cherty limestone (j1S) unconformably overlain by the Kimmeridgian limestone (j7-8). On the southern flank of the Porte de St-Jean syncline, an angular unconformity is also locally developed at the base of the Tithonian (j9) limestone (Fig. 4.11) Between these local unconformities, downlaps or rotated onlaps can be seen in the Kimmeridgian limestone (Fig. 4.11). A large intra-formational block of Tithonian limestone (j9) was observed in the core of the syncline. The block is surrounded by steeply dipping Tithonian limestone (j9) (Fig. 4.11)

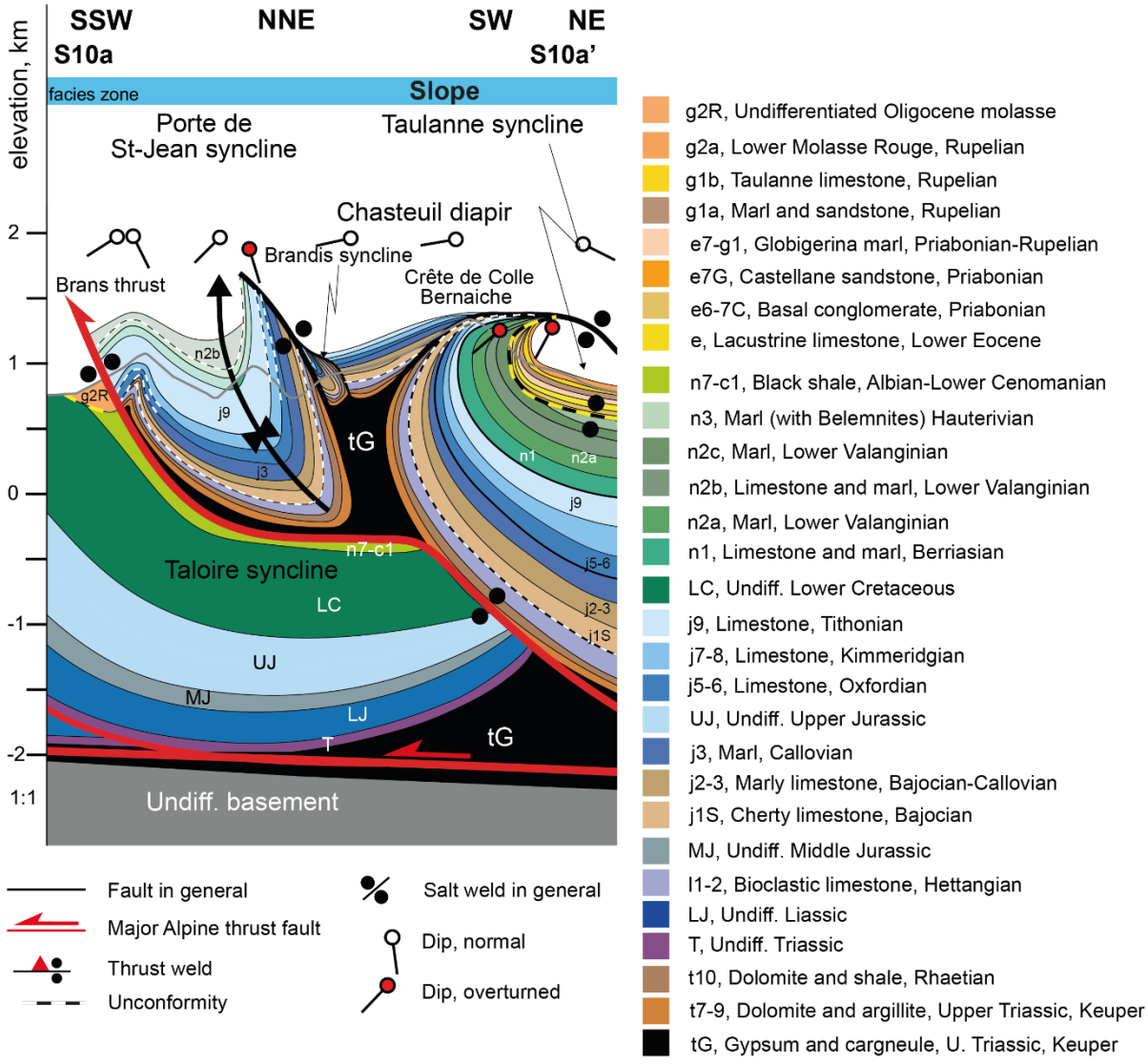


Fig. 4.12 Zoom of the S10 cross section (S10a – S10a') through the Taloire syncline, the Chasteuil salt structure and the bounding Porte de St-Jean syncline and the Taulanne syncline, illustrating gradual thickness changes, local unconformities and multidirectional tilting of independent depocenters. See Fig. 4.8 for cross section location.

(Kerckhove & Roux, 1978a). Roux (1968) described several breccia levels within the massive Tithonian limestone and brecciated limestone was also observed within the Bajocian cherty limestone of the Porte de St-Jean syncline.

The northern flank the Porte de St-Jean syncline is overturned to the SSW, and it is separated from the Brandis syncline by an anomalous contact which runs between the large gypsum body of the Chasteuil salt structure to the E and the Berbené fault to the W (Fig. 4.1, Fig. 4.2, Fig. 4.8). Along this contact, overturned Rhaetian, (t10), Hettangian (l1-2), Bajocian (j1S) and Aalenian-Callovian (j2-3) strata of the Porte de St-Jean syncline are in direct contact with Triassic (t7-9, t10), Liassic (l1-2) and Middle Jurassic (j1S) rocks which are also overturned to the S (Fig. 4.8).

On the northern flank of the Porte de St-Jean syncline, gradual thinning of the Jurassic section and local unconformities were observed (Fig. 4.8, Fig. 4.11). In some places, the Callovian grey marl (j3) locally pinches out between the Aalenian-Callovian marly limestone (j2-3) and the Oxfordian limestone (j5-6) (Fig. 4.8, Fig. 4.11). An angular unconformity also developed here at the base of the Kimmeridgian (j7-8) limestone over the Oxfordian limestone (Fig. 4.8). The map relationships and the view of the Porte de St-Jean syncline clearly display stratal thickening, from Hettangian to Lower Cretaceous (n1, n2a) in its core (Fig. 4.8, Fig. 4.11, Fig. 4.12).

In the western sector of the Porte de St-Jean syncline, the structural and stratal geometries are more complex than in the eastern domain. The axis of the Porte de St-Jean syncline plunges to the west; and to the S of the village of Chasteuil, the basin merges with the Taloire syncline (Fig. 4.1, Fig. 4.2, Fig. 4.8). The Porte de St-Jean syncline tightens, and the northern limb is overturned (Fig. 4.1, Fig. 4.2, Fig. 4.8). In the overturned section an unconformity at the base of the Kimmeridgian (j7-8) limestone is visible and Callovian grey marl (j3) and Oxfordian limestone are missing between the Aalenian-Callovian (j2-3) and the Kimmeridgian (Fig. 4.10). NW of the village of Chasteuil SW-NE trending synclines and anticlines can be seen in the Tithonian (j9) - Lower Valanginian (n2a) sections (Fig. 4.9, Fig. 4.10).

In the north-western part of the Porte de St-Jean syncline, Berriasian limestone (n1) and Lower Valanginian limestone and marl (n2a, n2b) are preserved and extend into the hinge of the syncline. Large scale slump folds can be seen north of the village of Chasteuil, in the Berriasian-Lower Valanginian succession (n1-n2a) (Fig. 4.13). The axial planes of the folds

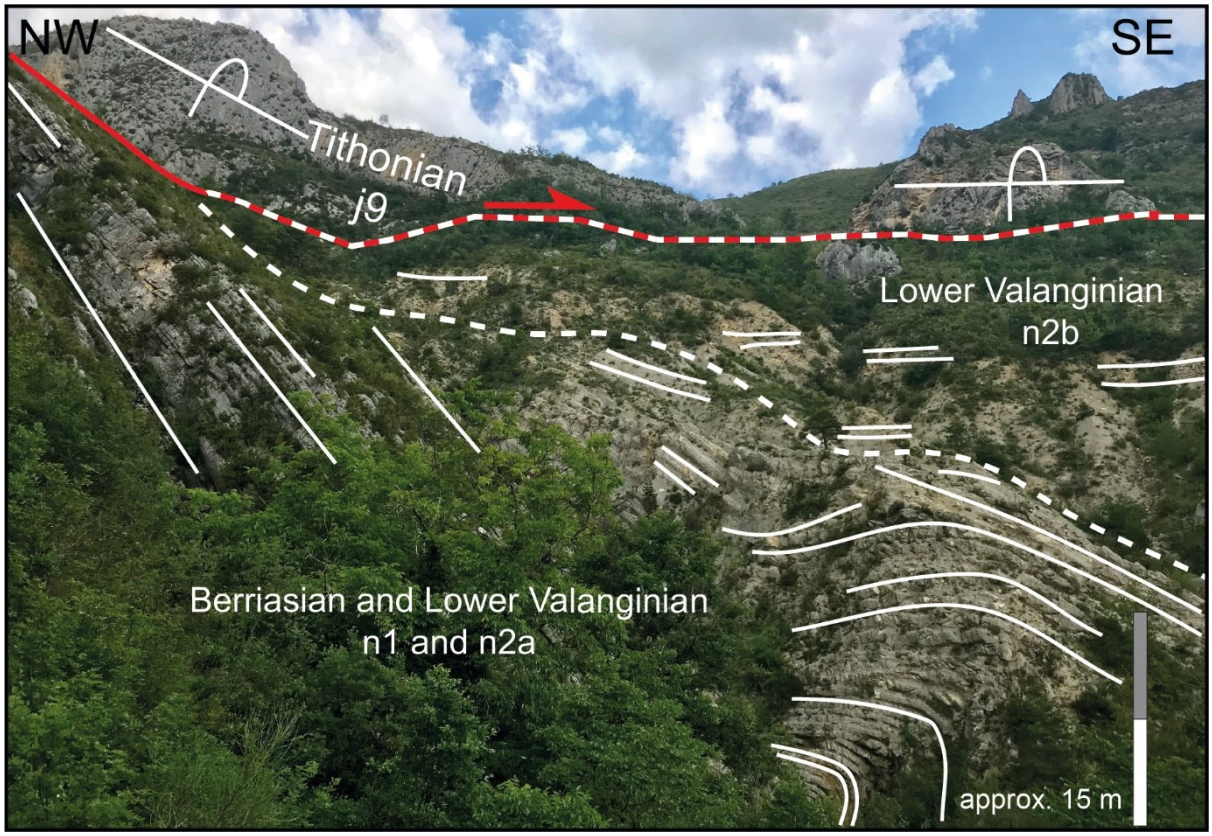


Fig. 4.13 Large-scale slump fold in the Berriasian-Lower Valanginian (n1 and n2a) section of the Porte de St-Jean syncline, at the village of Chasteuil. The orientaion of the slump fold suggests transport towards to SE. White dashed line marks the unconformity at the base of the Lover Valanginian marl and limestone formation (n2b). See Fig. 4.9 and Fig. 4.10 for viewpoint location.

dip towards to NW, suggesting SW transport direction, towards the core of the Porte de St-Jean syncline. In the vicinity of Chasteuil, the folding and overturning have affected the Triassic-Jurassic section and also the Berriasian (n1) and Lower Valanginian (n2a) strata, but the deformed section is covered by the upper part of the Lower Valanginian (n2b formation) dipping moderately to NE (Fig. 4.9, Fig. 4.13).

The basin is bounded to the north by a NW-SE trending fault zone (Fig. 4.8, Fig. 4.9, Fig. 4.10) and along the northern flank of the Porte de St-Jean syncline, faults cut through the overturned limb to detach on the top of the Lower Valanginian marl (n2b) which is highly deformed and boudinaged (Fig. 4.9, Fig. 4.10, Fig. 4.11 and Fig. 4.14). Structural elements indicate top-to-the southeast structural transport. The faults have a normal sense of motion, and they are connected to the anomalous contact between the Porte de St-Jean syncline and the Brandis syncline (Fig. 4.9, Fig. 4.10). NNE-SSW trending, low angle normal faults were measured here in the lower part of the overturned Upper Jurassic section, within the Kimmeridgian (j7-8) limestone where Roux (1968) described the sliding and collapse of the synclinal flank towards a pre-existing topographic depression. The Lower Valanginian n2b

formation is thickening dramatically from E to W, as the Porte de St-jean syncline plunges (Roux, 1968). S of the village of Chasteuil it reaches thicknesses at least 150 m. Large-scale slump folds were observed here, in the upper part of the Lower Valanginian (n2b) section (Fig. 4.13).

The Lower Valanginian succession (n2b) is folded around the tip of the Brans thrust fault and merges with the Lower Cretaceous infill of the Taloire syncline where the Lower Valanginian n2b formation dips around 30º towards the W (Fig. 4.1, Fig. 4.2, Fig. 4.8). S of the village of Chasteuil, where the Porte de St-Jean merge together with the Taloire syncline, a NE-SW trending fault is visible offsetting Lower Valanginian (n2b) rocks against Tithonian limestone (j9) (Fig. 4.9). The SE dipping structure defines the SSW boundary of the Porte de St-Jean and Taloire synclines (Fig. 4.1, Fig. 4.2, Fig. 4.8, Fig. 4.9).

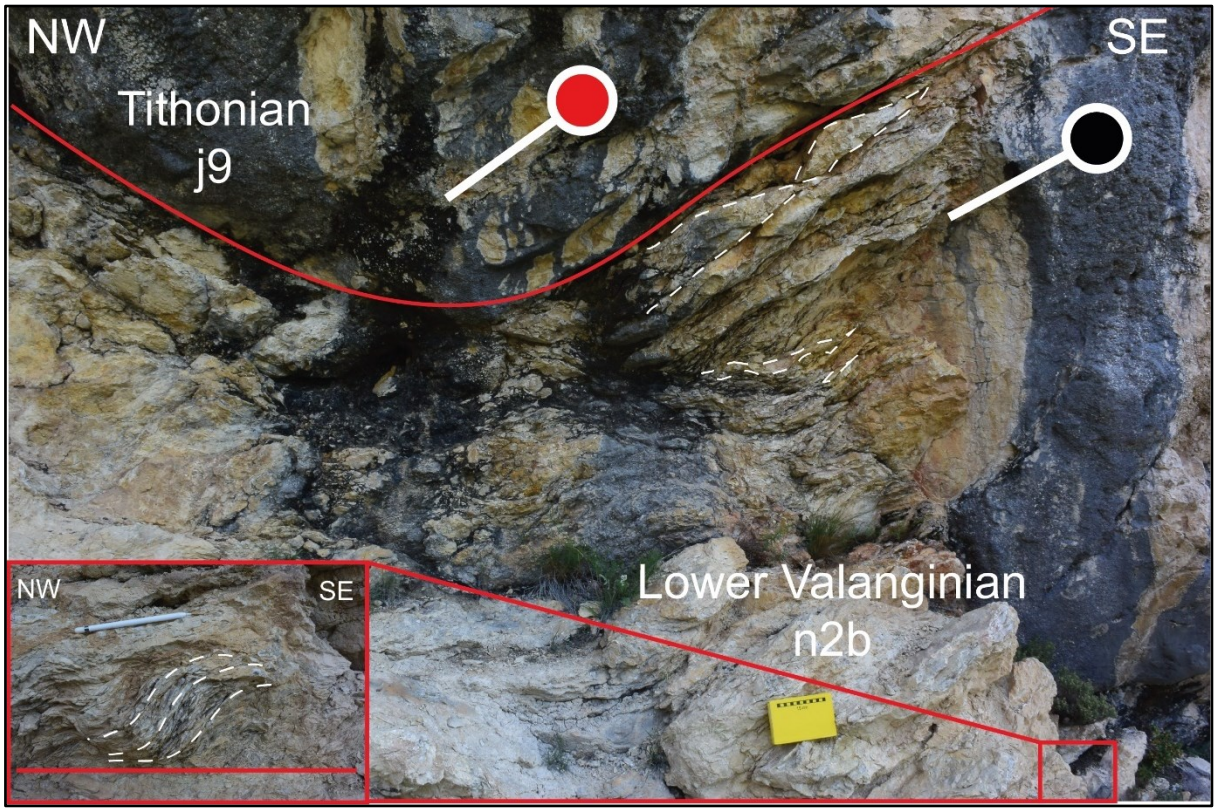


Fig. 4.14 The contact of the Tithonian limestone and the Lower Valanginian marl on the northern flank of the Port de St-Jean syncline, NE of the village of Chasteuil. The Lower Valanginian marl is right way up and the Tithonian limestone is overturned to SW. Note boudins and sheared layers in the Lower Valanginian marl. Note the field notebook for the scale. See Fig. 4.9 and Fig. 4.10 for viewpoint location.

4.1.1.5. An overturned flap at Brayal, the Crête de Colle Bernaiche section

Just as in the northern flank of the Porte de St-Jean syncline, overturning of the Jurassic-Lower Cretaceous section occurred elsewhere around the Chasteuil salt structure. In the Crête de Colle Bernaiche section, between the village of Brayal and the Cadiéres de Brandis cliff (Fig. 4.1, Fig. 4.2, Fig. 4.8), an incomplete, reduced, and overturned Hettangian (l1-2) to Lower Valanginian (n2c) section is exposed and shows successive unconformities (Fig. 4.2, Fig. 4.8, Fig. 4.15). The Crête de Colle Bernaiche section represents the south-western flank of the Taulanne syncline overturned toward the NE. Along strike, to NW and SE the section become steeply dipping or nearly vertical. The thickness of the incomplete Jurassic section is around 500 m. North of the large gypsum body of the Chasteuil salt structure, in the hanging wall of the Brans thrust, the lower part of the Crête de Colle Bernaiche section is exposed (Fig. 4.1,

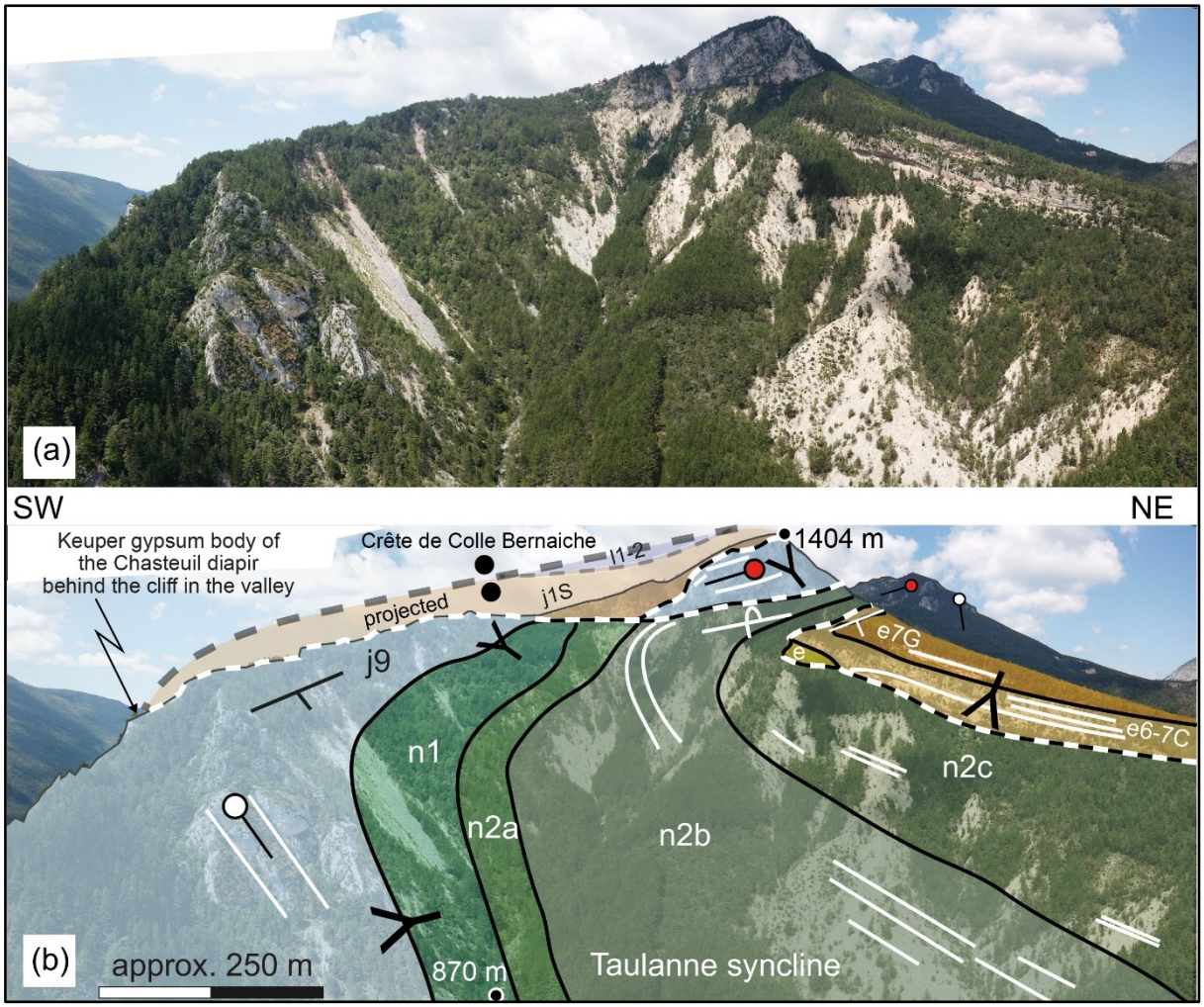


Fig. 4.15 Uninterpreted (a) and interpreted (b) photo panorama of the overturned section at the Crête de Colle Bernaiche, E of the Chasteuil salt structure, on SW flank of the Taulanne syncline. Black epsilons indicate younging direction. See Fig. 4.8 for geological key and viewpoint location.

Fig. 4.2, Fig. 4.8). It is composed of a Triassic-Lower Cretaceous succession (Fig. 4.8) with Keuper gypsum in direct contact with steeply dipping Norian (t7-9), Rhaetian (t10) and Bajocian (j1S) rocks in the SW flank of the Taulanne syncline (Fig. 4.1, Fig. 4.2, Fig. 4.8). Within the steeply dipping section, Rhaetian dolomite (t10) is unconformably overlain by Bajocian cherty limestone (j1S) and the Hettangian bioclastic limestone (l1-2) pinches out. A local unconformity also defined the top of the Bajocian: Oxfordian (j5-6), Kimmeridgian (j7-8) and Tithonian strata thin against the Bajocian and onlap it (Fig. 4.8). The Aalenian-Callovian (j2-3) marly limestone and the Callovian grey marl are missing between the Bajocian (j1S) and the Oxfordian (j5-6) and the Tithonian passes into a marly Lower Cretaceous succession (Berriasian-Valanginian, n1, n2a, n2b and n2c) dipping 40º toward to the N (Fig. 4.15, Fig. 4.16). The Berriasian-Lower Valanginian section thins against the overturned Jurassic section (Fig. 4.15).

The Mesozoic section of the Crête de Colle Bernaiche is unconformably overlain by Eocene sediments dipping 35 degrees toward the NNE at Brayal and is nearly vertical E of the Cadiéres de Brandis section (Fig. 4.8, Fig. 4.15). The N dipping Mesozoic succession of the Crête de Colle Bernaiche section together with the Tertiary infill of the Taulanne syncline is bounded to the E by an anomalous contact which separates the Taulanne and Haute Sionne synclines (Fig. 4.1, Fig. 4.2, Fig. 4.8).

Further to north-west, in the overturned segment of the Crête de Colle Bernaiche section, the Berriasian and Lower Valanginian (n1, n2a and n2b) succession is structurally overlain by Bajocian cherty limestone (j1S) and Tithonian limestone (j9) (Fig. 4.1, Fig. 4.2, Fig. 4.8, Fig. 4.15, Fig. 4.16). According to Roux (1968), Jurassic and Cretaceous strata are undeformed along the contact, for example in the steeply dipping lower part of the Crête de Colle Bernaiche section, in its overturned segment, Bajocian cherty limestone is bounded by unconformities and Bajocian-Callovian to Kimmeridgian (j2-3 to j7-8) strata pinch out against this local unconformity (Fig. 4.15, Fig. 4.16). To the west, the overturned Bajocian limestone (j1S) is in direct contact with gently dipping Bajocian-Callovian (j2-3) marly limestone of the Cadiéres de Brandis section (Fig. 4.2, Fig. 4.8). The anomalous contact between the overturned Crête de Colle Bernaiche section and the gently dipping Cadiéres de Brandis section is approximately NNW-SSE trending. It can be traced between the large gypsum body of the Chasteuil salt diapir and an unconformity at the base of the Middle-Upper Jurassic section of the Cadiéres de Brandis section (Fig. 4.8). Along this unconformity, the Callovian (j3) marl, the reduced Oxfordian (j5-6) and the Kimmeridgian limestone (j7-8) pinches out between the Aalenian-Callovian (j2-3) and the Tithonian (j9) (Fig. 4.1, Fig. 4.2, Fig. 4.8). This contact joins into the

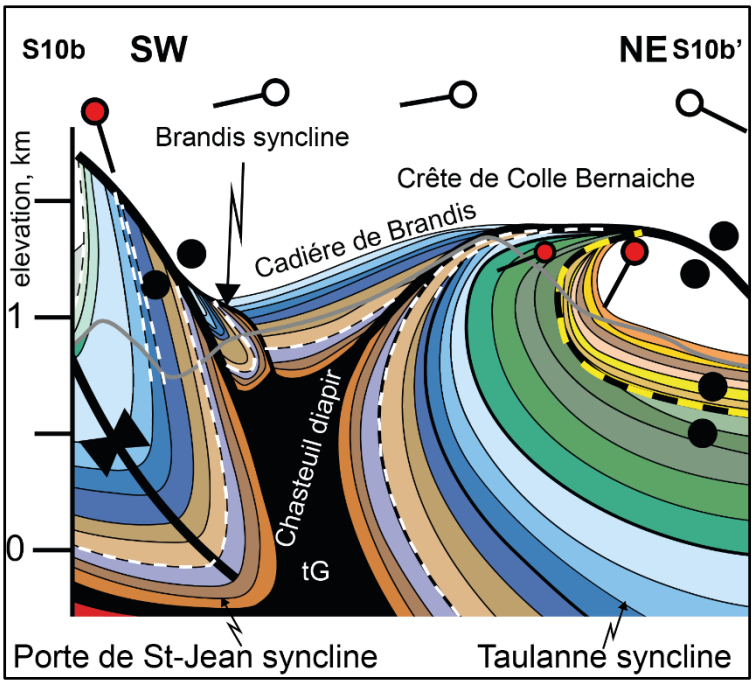


Fig. 4.16 Zoom of the S10 cross section (S10b-S10b') showing the Chasteuil salt structure and the overturned section of the Crête de Colle Bernaiche. See Fig. 4.8 for cross section location and Fig. 4.12 for key.

anomalous contact between the Brandis syncline and the Cadières de Brandis section, is considered as the same structure (Fig. 4.8). It separates the lower part of the Crête de Colle Bernaiche section (Norian, Rhaetian, Liassic and Bajocian) from the eastern part of the Brandis syncline and also the gently dipping section of the Cadières de Brandis Mountain (Fig. 4.1, Fig. 4.2, Fig. 4.8).

West of the anomalous contact which separates the Cadières de Brandis section and the overturned Crête de Colle Bernaiche section, Zurcher (1895) and Roux (1968) described large blocks and 'chaotic masses' ('masses chaotiques') of Tithonian limestone (j9) apparently resting on the top of Aalenian-Callovian marly limestone (j2-3). The blocks are surrounded by coarse breccia. Previous authors have suggested that these competent limestone blocks accumulated on the top of the Aalenian-Callovian marly limestone or slid off the flank of the Cadières de Brandis anticline.

4.1.1.6. The Taloire syncline and the la Crotte-Deneiras area

The stratigraphy and structural style of the southern Taloire syncline is far simpler than the Taulanne syncline and Porte de St-Jean synclines. The Mesozoic section of the Taloire syncline is composed of Upper Triassic to Upper Cretaceous slope facies (Fig. 4.1, Fig. 4.2, Fig. 4.17) (Kerckhove & Roux, 1976a). The Taloire syncline is an elongated, roughly ENE-WSW trending syncline (Fig. 4.2). South-west of the village of Chasteuil, the syncline is SW-NE trending, but its westernmost termination between the la Crotte area and Barre de Catalan trends ENE-WSW (Fig. 4.2).

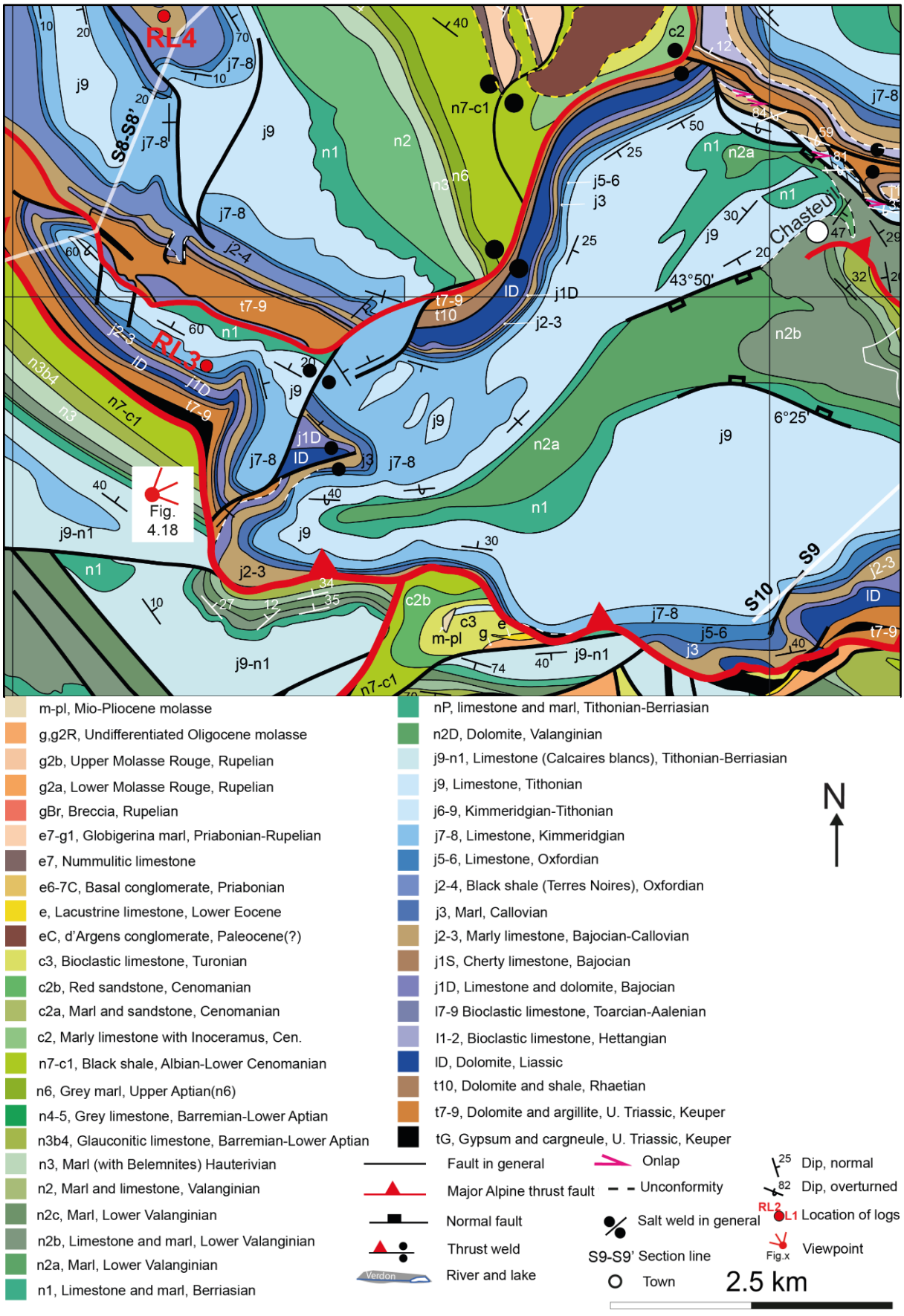


Fig. 4.17 Detailed geological map of the western part of the Taloire syncline, the la Gondole syncline and the esatern part of the Blieux syncline. See Fig. 4.2 for structural map and explanation of the area.

The thickness of the Mesozoic infill of the Taloire syncline is around 1.7 km in its core (Fig. 4.5, Fig. 4.12). The Upper Triassic-Lower Cretaceous section of the syncline is well exposed in the hanging wall of the Robion thrust between the Barre de Catalan cliff and the Montagne de Robion mountain, in the incised valley of the Verdon River (Fig. 4.1, Fig. 4.2). Upper Cretaceous rocks only preserved SW of the village of Chasteuil, in the core of the Taloire syncline and further to the E, on the eastern flank of the Montagne de Robion anticline (Fig. 4.1). On the southern flank of the Taloire syncline, E of the Barre de Catalan cliff, the Upper Triassic-Lower Cretaceous section dips around 40-45º to the north (Fig. 4.1, Fig. 4.2, Fig. 4.17). The Triassic is composed of Keuper gypsum (tG), Norian dolomite and argillite (t7-9), and Rhaetian dolomite (t10) (Fig. 4.17). The Liassic section is reduced (around 30 m) and composed of dolomite (lD) which passes up into Bajocian dolomite and limestone (j1D). Between the Liassic and the Bajocian, the Aalenian is represented by a hardground (Kerckhove & Roux, 1978b). The Liassic and Bajocian formations show similarities to the Liassic and Bajocian succession of the Provençal platform, rather than the adjacent Porte de St-Jean syncline and Taulanne synclines (Fig. 4.6, Fig. 4.8). The Upper Bajocian, Bathonian and Callovian is represented by a marly succession (j2-3 and j3) which is also exposed around the Chasteuil salt structure, on the flanks of the Porte de St-Jean and the Taulanne synclines (Fig. 4.8, Fig. 4.17). The Oxfordian, Kimmeridgian, and Tithonian formations (j5-6, j7-8 also j9) show close similarity to the Upper Jurassic of the Cadiéres de Brandis section of the southern flank of the Taulanne syncline, but on the SE flank of the Montagne de Robion anticline, Roux (1968) documented the occurrence of reefal limestone in the Tithonian succession implying that the southern part of the Taloire syncline was situated relatively close to the outer platform (Rameil, 2005). According to Roux (1968), the thickness of the Tithonian limestone decreases from S to N towards the Chasteuil salt structure. The only anomalous contact in the southern flank of the Taloire syncline was observed at the Barre de Catalan cliff, in the hanging wall of the Robion thrust where Keuper gypsum is in direct contact with the Kimmeridgian (j7-8) limestone (Fig. 4.1, Fig. 4.2, Fig. 4.17).

The Cretaceous of the Taloire syncline is much thicker and complete than the Cretaceous of the Taulanne and the Porte de St-Jean synclines (Fig. 4.8, Fig. 4.17). The Berriasian (n1) is made up of alternating limestones and marls, while the Valanginian (n2a, n2b, n2c) and Hauterivian (n3) are mainly composed of marls. In the Berriasian succession, on the NE flank of the Montagne de Robion anticline, I observed a channel filled with brecciated limestone (palaeocurrent data display WSW-ENE oriented transport).

The Upper Hauterivian and the Barremian (n3b4) are composed of glauconitic limestone, which is capped by a hardground containing phosphatic nodules (Kerckhove & Roux, 1978b). This hardground represents the Upper Barremian and the Lower Aptian.

The Barremian is overlain by Albian-Cenomanian glauconitic sandstone and black marls (n7-c1) and Cenomanian marl (c2b) is also preserved on the eastern flank of the Montagne de Robion anticline (Fig. 4.17). The Lower and Upper Cretaceous succession of the Taloire syncline represents the palaeogeographic slope of the Vocontian basin. The thickness of the Berriasian-Cenomanian section is around 750 m in the core of the Taloire syncline (Fig. 4.12).

Eocene strata are missing in the Taloire syncline and the Tertiary is represented only by Oligocene red molasse (g2R), which overlies Albian-Cenomanian black shales in the core of the Taloire syncline, in the immediate footwall of the Brans thrust (Fig. 4.8, Fig. 4.11).

The most intriguing stratal and structural geometries were observed in the western limb of the Taloire syncline, between the la Crotte area and the Crête de Berbené cliff (Fig. 4.2, Fig. 4.17). The la Crotte area is located in the immediate hanging wall of the Robion thrust (Fig. 4.2) and bounded to the NW by an anomalous contact which links the Berbené fault with the Robion thrust (the Berbené salt wall in Fig. 4.18). The NNE-SSW trending anomalous contact separates the la Crotte section of the Taloire syncline from the Triassic to Lower Cretaceous section of the la Gondole syncline which is also carried by the Robion thrust (Fig. 4.1, Fig. 4.2, Fig. 4.17, Fig. 4.18). Along the NNE-SSW trending anomalous contact, Liassic-Upper Jurassic section of SW flank of the la Gondole syncline is right way up and dipping towards NE (around 20-25^{o}) but steeper dips were observed in the Kimmeridgian limestone (j7-8) (Fig. 4.18).

On the south-western margin of the Taloire syncline, a relatively thin, vertical or locally overturned Triassic-Lower Cretaceous (Norian, t7-9 to Valanginian, n2a) section is exposed (Fig. 4.17, Fig. 4.18). Successive unconformities, pinch outs and a large Bajocian dolomite block within the Callovian were observed here (Fig. 4.18). Abrupt thickness changes were also observed (Fig. 4.18). On the south-western flank of the Taloire syncline, vertical Norian (t7-9) beds are unconformably overlain by Bajocian dolomite. The Bajocian succession dips around 60^{o} to the SE, creating a 30^{o} angular unconformity (Fig. 4.18). Rhaetian (t10) and Liassic (lD) rocks are missing between the Norian and the Bajocian. The Bajocian dolomite passes up to

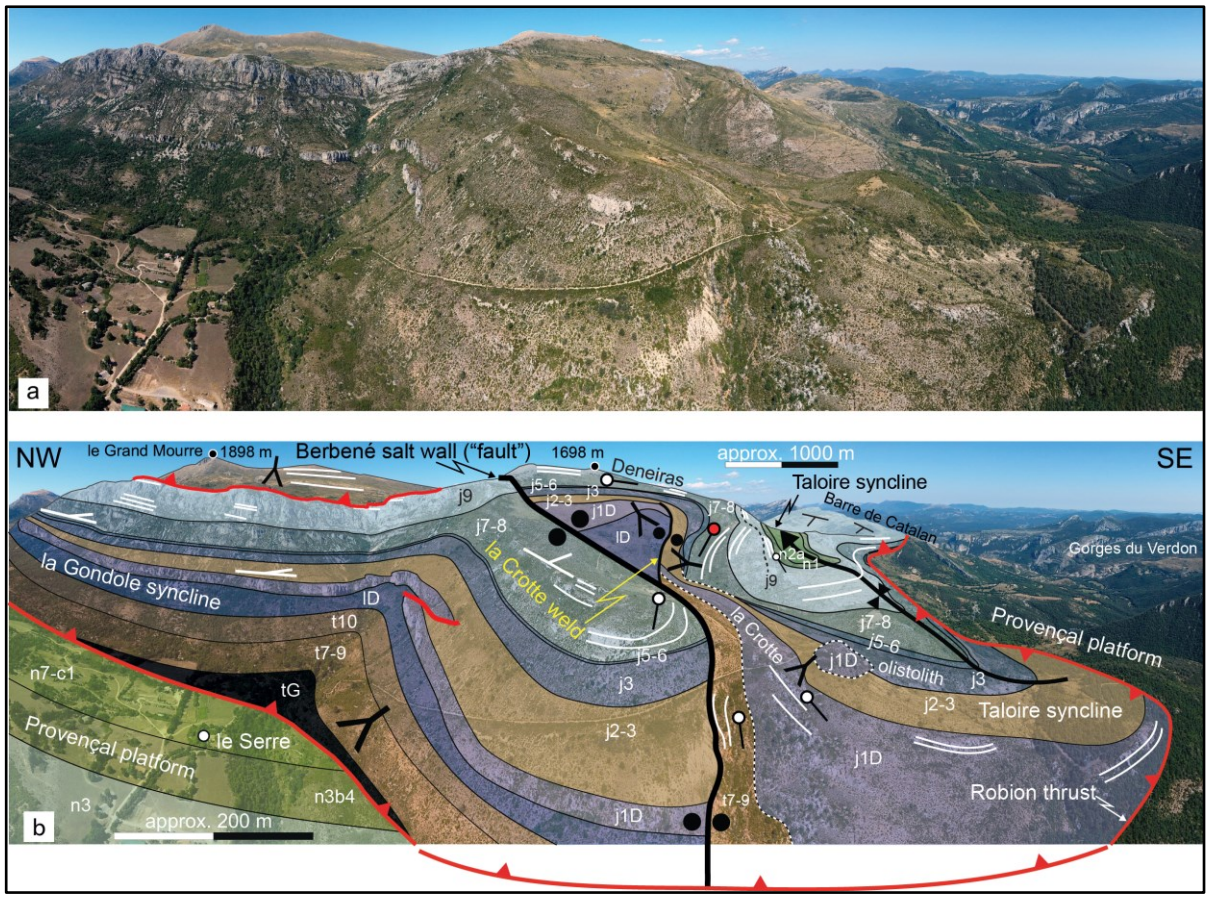


Fig. 4.18 Interpreted (a) and uninterpreted (b) photo panorama of the la Crotte area and Deneiras section of the Taloire syncline and the eastern termintaion of the la Gondole syncline. Black epsilons indicate younging direction. See Fig. 4.2 for structural explanation. See Fig. 4.17 for geological key and viewpoint location.

Upper Bajocian-Callovian marly limestone (j2-3) and along the contact a large block of Bajocian dolomite (j1D) approximately 100 m in diameter has been observed. It was also documented by Kerckhove & Roux (1978a) on their 1:50000 geological map.

Further to the N, along the la Crotte anomalous contact (shown as the la Crotte weld in Fig. 4.18 and see § 4.1.1.7), the Norian (t7-9), Bajocian (j1S) and overlying Upper Bajocian-Callovian (j2-3) strata are slightly overturned to SE. An unconformity developed at the top of the overturned Upper Bajocian-Callovian marly limestone (j2-3) and the Callovian (j3) and Oxfordian (j5-6) section thins and locally pinches out between the Bajocian-Callovian marly limestone and the also overturned Kimmeridgian (j7-8) limestone (Fig. 4.17, Fig. 4.18). The overturned Norian-Callovian (t7-9 to j2-3) section abuts against the NE-SW trending anomalous contact (labelled as la Crotte weld in Fig. 4.18) which links the Berbené fault with the Robion thrust (Fig. 4.1, Fig. 4.2, Fig. 4.17, the Berbené salt wall in Fig. 4.18, see § 4.1.1.7) and separates the overturned section from a reduced Liassic (lD) – Tithonian (j9) section which remains in normal position dipping 15° toward the NNE. The la Crotte weld possibly represents a vanishes salt body (see § 4.1.1.7). The gently dipping normal section is called the Deneiras

section (Fig. 4.2), forming the Deneiras cliff (Fig. 4.18). The thickness of the Liassic-Tithonian section is around 450-500 m in the southern face of the Deneiras mountain. In the hanging wall of the Robion thrust, E of the Barre de Catalan cliff, only a few kilometres away to the E, the thickness of the Liassic-Tithonian section is around 800 m (Fig. 4.2, Fig. 4.17).

A few hundreds of meters to the NE, the overturned section is complete again and the overturned Bajocian-Callovian-Kimmeridgian (from j2-3 to j7-8) section is folded over the anomalous contact of the la Crotte weld (Fig. 4.18), and forms an anticline (Fig. 4.18). The anomalous contact, which separates the overturned Norian-Callovian (t7-9 to j2-3) section from the gently dipping Liassic (lD) – Tithonian (j9) of the Deneiras section, apparently forms the core of this anticline but angular unconformities occur within the upper part of the Tithonian limestone in the overturned section. In contrast, the gently dipping Liassic-Tithonian section of the Deneiras mountain, and the overlying Berriasian and Lower Valanginian (n1 and n2a) section preserved on the overturned north-western flank (and also in the core) of the Taloire syncline do not show any internal unconformities (Fig. 4.18).

NE of the la Crotte anomalous contact (shown as the la Crotte weld in Fig. 4.18) and Deneiras sections, at the junction of the Berbené fault and the la Crotte structure, the Kimmeridgian and Tithonian limestone of the Deneiras section are exposed in a NW-SE trending syncline (Fig. 4.1, Fig. 4.2, Fig. 4.17). Further to the NE, a Triassic-Lower Cretaceous section exposed in the Crête de Berbené mountain, in the western limb of the Taloire syncline dips around a 25º to the SE (Fig. 4.1, Fig. 4.2, Fig. 4.17). The small syncline is bounded to the W by the Berbené fault which separates the syncline from the northern flank of the la Gondole syncline and the SW flank of the Blieux syncline (Fig. 4.1, Fig. 4.2, Fig. 4.17). This syncline formed between the gently ESE dipping Triassic Upper Jurassic section of the Crête de Berbené mountain and the Deneiras section. The Norian-Kimmeridgian section of Crête de Berbené mountain is in direct contact with the Kimmeridgian limestone of the Deneiras section (Fig. 4.1, Fig. 4.2, Fig. 4.17). Due to the poor outcrop conditions, the nature of this contact is uncertain. The Norian-Kimmeridgian section of the Crête de Berbené mountain is considered as the continuation of the Norian-Tithonian section exposed in the Deneiras section, presumably displaced later by the Berbené fault.

Further to the NE, the Triassic-Lower Cretaceous section gentle dips were observed (to SE) and doesn't show any internal unconformities (Fig. 4.1, Fig. 4.2, Fig. 4.17). However, the Norian-Berriasian section thins towards the Berbené fault, and its thickness is reduced (around 400 m). In this area, the Taloire syncline is amalgamated to the adjoining Porte de St-Jean syncline, and bounded to the NE by the NW-SE trending fault zone which links the Berbené

fault and the gypsum of the Chasteuil salt structure (Fig. 4.1, Fig. 4.2, Fig. 4.8 Fig. 4.17). It also bounds the Port de St-Jean syncline to the N (Fig. 4.8, Fig. 4.9, Fig. 4.10). The lower part of the Triassic-Lower Cretaceous section of the Crête de Berbené, i.e., the Norian-Kimmeridgian section (t7-9 to j7-8) abuts against the NW-SE trending fault zone, while in the upper part of the section, i.e., the Tithonian and Berriasian limestones turn vertical or slightly overturned at the junction of the Chasteuil salt structure and the Berbené fault, S of the Pré Chauvin peak (Fig. 4.1, Fig. 4.2, Fig. 4.8, Fig. 4.9, Fig. 4.17). Along the fault zone, where the Taloire syncline merges with the Porte de St-Jean syncline, the Upper Jurassic-Lower Cretaceous section is slightly thinner than in the SE limb of the Taloire syncline.

SW of the village of Chasteuil, on the SSE flank of the Taloire syncline, a NE-SW trending fault offsets Berriasian (n1) and Lower Valanginian (n2b) strata against Tithonian limestone (j9) (Fig. 4.9, Fig. 4.17). The SE dipping fault has a similar trace and offset to the NE-SW trending fault, which is bounding the Porte de St-Jean the WSW (Fig. 4.9,).

4.1.1.7. Newly identified minibasins and salt structures: Interpretation of the Taulanne syncline, the Porte de St-Jean syncline and Taloire syncline and their bounding salt structures

Stratal and structural geometries observed in the Taloire, Porte de St-Jean and Taulanne synclines and around their bounding structures are comparable with known salt related structures of the Southern Subalpine chains, other Alpine folded belts and other salt basins worldwide (Rowan & Vendeville, 2006; Pilcher et al., 2011; Graham et al., 2012; Callot et al., 2014; Lopez-Mir et al., 2015; Rowan et al., 2016; Saura et al., 2016; Kergaravat et al., 2017; Ringenbach et al., 2017; Soto et al., 2017; Teixell et al., 2017; Graham et al., 2019; Granado et al., 2019; Célini et al., 2020; Célini, 2020; Brooke-Barnett, 2022; Brooke-Barnett et al., 2023). Many of the observed structural elements in the area around the Taloire, Taulanne and Porte de St-Jean structures including thrusts which juxtapose young rocks on top of old and reduced and overturned sections cannot be explained solely by deformation related to the Alpine compression. Anomalous stratigraphic relationships within the Jurassic-Lower Cretaceous section, the occurrence of breccia levels, early syn-sedimentary folding, and abrupt thickness and facies changes in the Jurassic-Lower Cretaceous section all indicate pre-Alpine diapiric activity.

A reinterpretation of the structures observed in the Taloire, Porte de St-Jean and Taulanne synclines and around their bounding structures is presented here and a new salt tectonic model is proposed. Probably most of the above-described synclines are primary minibasins, and their bounding structures are interpreted as diapirs and elongated salt walls. The primary minibasins subsided into the autochthonous Upper Triassic evaporites during the Jurassic and Early Cretaceous as Triassic salt migrated from the deflating autochthonous salt layer into the bounding diapiric structures. Some of the bounding salt structures are completely squeezed, strongly modified, completely welded, or reactivated as Alpine compressional structures from the Late Cretaceous onwards, something which obviously complicates their identification and structural description.

The St-Vincent diapir bounded the Taulanne minibasin to the N while the Chasteuil salt structure separated it from the Porte de St-Jean minibasin. The SE plunging la Grau anticline divided the Taulanne minibasin into two large depocenters: the Taulanne minibasin sensu stricto and a NW-SE oriented minibasin, located below the Haute Sionne syncline and the la Blache-Castellane thrust sheet (Fig. 4.5 and see Chapter 5, § 3.1.2.1). The Porte de St-Jean and the Taloire minibasins now are separated by a weld inferred to have been a diapir, the Brans diapir (described later). The Porte de St-Jean minibasin was bounded to the E and N by the Chasteuil salt structure.

The Norian and Rhaetian strata (t7-9, t10) exposed along the flanks of the Taloire, Porte de St-Jean and Taulanne basins can be considered as a pre-kinematic layer because these formations did not show any thickness changes or facies variations. (Fig. 4.1, Fig. 4.3, Fig. 4.5, Fig. 4.7, Fig. 4.11).

Incomplete sections, facies variations and thickness changes of the Liassic succession across the minibasins all suggest that salt structures started to grow in the Early Jurassic, (Fig. 4.6, Fig. 4.8, Fig. 4.17). Sinemurian, Pliensbachian, and Toarcian sediments were probably deposited in the basins and also on the flanks of the early diapiric structures, but they have been truncated by the basal Bajocian unconformity and are now overlain by younger formations. However, the presence of the Sinemurian-Toarcian sediments at the core of the primary minibasins is not proven (Fig. 4.7).

Regional considerations suggest that the initiation of salt tectonic activity was triggered by the Early-Middle Jurassic Tethyan rifting, and therefore can be considered as reactive diapirism most probably developed over the footwall of extensional faults. This is well documented elsewhere in the Southern Subalpine chains (Mascle et al., 1988; Dardeau & De Graciansky, 1990; Graham et al., 2012; Graham et al., 2019; Célini et al., 2020; Célini, 2020; Brooke-

Barnett, 2022; Brooke-Barnett et al., 2023), but we cannot be completely certain because the pre-salt basement is not exposed in the southern structural domain around the village of Blieux and the town of Castellane. Outcrops of the Lower Triassic sandstone (Buntsandstein) and Middle Triassic Muschelkalk (t2, t2G) are locally present in the middle of diapiric structures as blocks incorporated into the diapiric material (Fig. 4.8). The large block of the Lower Triassic sandstone (Buntsandstein), which is embedded into the western part of the St-Vincent diapir may represent a large inclusion which was lifted from the fault scarp of an underlying Tethyan extensional fault, at the original location of the diapir. The ability of the salt to lift large inclusions from the edges of subsalt faults has been described by many authors in many salt provinces, e.g. in the Pyrenees by Canérot et al. (2005). Most of the diapirs in Southern Subalpine chains have been detached from their original basement. (Graham et al., 2012; Célini et al., 2020; Brooke-Barnett et al., 2020; Csicsek et al., 2021; Brooke-Barnett et al., 2021; Célini et al., 2022; Brooke-Barnett, 2022) so the presence of Tethyan extensional faults below the salt structures at their original location and the influence of these normal faults on triggering salt tectonic activity can only be inferred.

Continued Middle Jurassic diapiric activity is recorded by the local unconformity at the base of the Bajocian on the southern and northern flanks of the Porte de St-Jean syncline. This unconformity is also developed around the flanks of the Taulanne minibasin and on the SW flank of the Taloire syncline (Fig. 4.6). The lack of crestal grabens and inward-dipping normal faults around the diapiric structures and the presence of successive unconformities in the flanking strata around the Chasteuil salt structure suggest that the driving force may have been the differential loading of the overburden above the autochthonous salt layer. Passive diapirism which followed the reactive growth of the salt structures has been documented elsewhere in the Southern Subalpine chains through the later stages of the Tethyan rifting period and the subsequent passive margin phase (Célini et al., 2020; Célini, 2020; Brooke-Barnett, 2022)

A period of rapid growth of the Chasteuil salt structure occurred between the Bajocian and the Lower Valanginian (Fig. 4.19) and can be seen along the flanks of the Porte de St-Jean minibasin and the Taulanne minibasin. The overturned section at the Crête de Colle Bernaiche cliff displays clear evidence for this diapiric growth (Fig. 4.15, Fig. 4.16, Fig. 4.19).

The lower interval of the overturned section at Crête de Colle Bernaiche section on the SW flank of the Taulanne minibasin is interpreted as a kilometre-scale megaflap structure, where deep minibasin strata, i.e., Norian (t7-9), Rhaetian (t10), Hettangian (l1-2) and Bajocian (j1S) forming a steeply dipping or completely overturned stratal panel along the flank of the

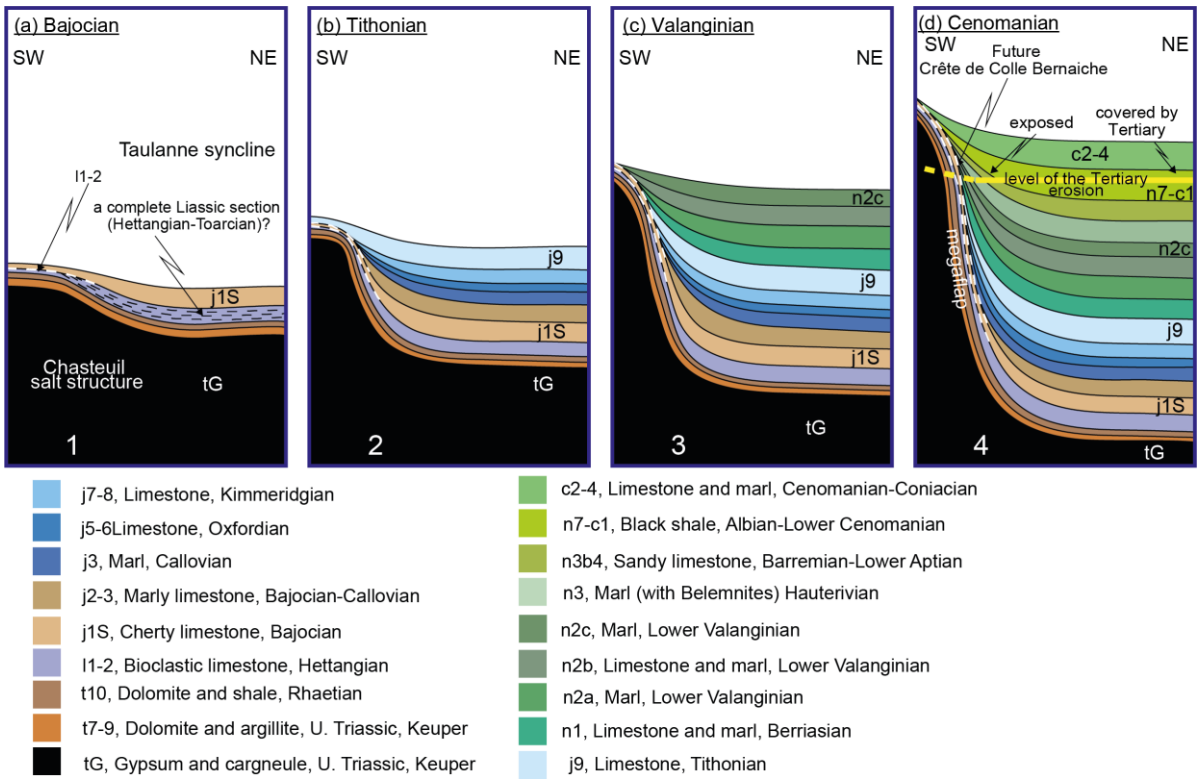


Fig. 4.19 Sequential evolution of the south-western limb of the Taulanne syncline (Crête de Colle Bernaiche section), from Bajocian (a) to Cenomanian (d) (not to scale). Note that sediments younger than Valanginian are not preserved on the flanks of the Taulanne syncline. Stratal and structural geometries of Hauterivian-Cenomanian formations shown here are highly speculative.

Chasteuil salt structure (Fig. 4.1, Fig. 4.2, Fig. 4.8, Fig. 4.19). The megaflap represents the thin roof of the early Chasteuil salt structure. The roof strata later reached a vertical attitude along the rising salt body during halokinetic drape folding (Fig. 4.19). In the overturned section at Crête de Colle Bernaiche section, the base of the flanking strata is structurally concordant with the welded feeder of the Chasteuil salt structure (Fig. 4.2, Fig. 4.8, Fig. 4.16). This weld is expressed in the NNW-SSE trending anomalous contact between the overturned Crête de Colle Bernaiche section and the gently dipping overlying Cadiéres de Brandis section (Fig. 4.1, Fig. 4.2, Fig. 4.8, Fig. 4.16).

This overlying Upper Bajocian-Valanginian section thins towards the megaflap and showing wedge geometries (Fig. 4.16, Fig. 4.19). Bajocian-Callovian (j2-3), Callovian (j3), Oxfordian (j5-6) and Kimmeridgian (j7-8) formations all pinch out between the Bajocian and the Tithonian limestone here (Fig. 4.8, Fig. 4.16, Fig. 4.19). In the overturned Crête de Colle Bernaiche section the Bajocian is unconformably overlain by Tithonian (j9), Berriasian (n1) and Lower Valanginian sediments (n2a) (Fig. 4.15, Fig. 4.16 Fig. 4.19). I assume that the unconformities at the base of the Tithonian, Berriasian and the Valanginian in the overturned Crête de Colle Bernaiche section represent a prominent onlap surface. The Bajocian-Callovian

(j2-3), Callovian (j3), Oxfordian (j5-6) and Kimmeridgian (j7-8) formations also onlap this unconformity in the subsurface, a few hundred of meters below the overturned Crête de Colle Bernaiche section (Fig. 4.16). The thinning of the Upper Bajocian-Valanginian section, the local unconformities and onlaps record the continued growth of the eastern part of the Chasteuil salt structure until the Valanginian (Fig. 4.19). The Jurassic-Lower Cretaceous infill of the Taulanne minibasin display clear minibasin scale wedging geometries (Fig. 4.5, Fig. 4.16) (Rowan & Giles, 2023). Sediments younger than Valanginian have been removed by Tertiary erosion on the flanks of the Taulanne syncline (Fig. 4.5). Therefore, the post-Valanginian (post n2c) stratal and structural geometries shown in Fig. 4.19d are highly speculative.

The megaflap likely reached a sub-vertical attitude around the Jurassic-Cretaceous boundary (Fig. 4.19b and c) but the overturning may have occurred later, during the Tertiary because the direct contact of the overturned megaflap and the overlying Eocene and Oligocene sediments is eroded in the Crête de Colle Bernaiche area. The vertical and slightly overturned Eocene and Oligocene strata which overlie the Lower Valanginian (n2b) N of the Crête de Colle Bernaiche section (Fig. 4.1, Fig. 4.2, Fig. 4.8) suggests that the almost complete overturning of the megaflap and folding of the Eocene and Oligocene sediments occurred later, during the Tertiary. The overturned megaflap structure may have been continuous to SE of the Crête de Colle Bernaiche because on the north side of the Chasteuil salt structure, where similar onlaps and pinch-outs are preserved in the steeply dipping Triassic-Jurassic section, more gentle dips were measured in the Berriasian section but the overturned section, if it existed, has been eroded away (Fig. 4.1, Fig. 4.2, Fig. 4.8).

Presumably, the St-Vincent diapir on the northern flank of the Taulanne minibasin has a similar growth history to the Chasteuil salt structure. The presence of a reduced Triassic-Lower Cretaceous section (Norian-Valanginian, t7-9 to n2a) near the diapir and in the core of the la Grau anticline along with the similarity of the facies of the Jurassic with that of the Jurassic of the Cadiéres de Brandis and the Crête de Colle Bernaiche and the lateral thickness variations between the la Grau anticline and the northern termination of the Taulanne syncline all suggest that the St-Vincent area also formed a topographic high during the rifting period and remained high during the post rift phase, at least until the Valanginian. Minor local unconformities also developed around the la Grau anticline (Fig. 4.3). The significant thickening of the Oxfordian (j5-6), SW of the la Grau anticline near the northern termination of the Taulanne syncline is interpreted as growth adjacent to the St-Vincent diapir (Fig. 4.4). The direct contact of the reduced Triassic-Lower Cretaceous section (Norian-Valanginian, t7-9 to n2a) with the Triassic gypsum of the St-Vincent diapir maybe represents the flanking strata of the diapir, although

the stratal and structural geometries are not clear due to the poor outcrop conditions along the Triassic salt body (Fig. 4.4). The la Grau anticline may have formed the easternmost extent of the St-Vincent diapir and was compressed into a tight anticline with an overturned forelimb during the Alpine compression (see Chapter 5, § 3.1.2.1).

The Taulanne primary minibasin is subcircular in plan view, suggesting that it may have been surrounded entirely by salt structures. The Berbené fault (Fig. 4.1, Fig. 4.2,) - an Oligo-Miocene strike-slip fault defining the western margin of the Taulanne and Taloire minibasins and limiting the St-Vincent and Chasteuil salt structures to the W has been interpreted by Brooke-Barnett (2022) as a NE-SW trending reactivated Mesozoic salt wall. I assume that the Berbené structure originally connected the Chasteuil salt structure to the St-Vincent diapir (Fig. 4.23) and was reactivated as a strike-slip fault during Alpine compression because its orientation was favourable to reactivation as a strike-slip fault (Fig. 4.1, Fig. 4.2). This model and the presence of an early formed salt structure are supported by observations and the structural reinterpretation of the Taulanne minibasin.

The thickness of the Norian-Valanginian section is around 750 m in the western limb of the Taulanne basin, SE of the Berbené fault (Clos de Juyon section, Fig. 4.2) and presumably the section thickens towards the centre of the minibasin (Fig. 4.7). Gradual thinning can be seen along strike towards the St-Vincent diapir and the Chasteuil salt structure (Cadiéres de Brandis section) but successive unconformities or pinch-outs were not observed here although the base-Bajocian unconformity, which is locally developed on the flanks of the Taloire and Porte de St-Jean minibasins and along the Chasteuil salt structure and St-Vincent diapir is also present SW of the Berbené fault, in the western limb of the Taulanne minibasin (Clos de Juyon section) (Fig. 4.2, Fig. 4.8).

Facies variations in the Upper Jurassic section are visible along the Berbené Fault. The Oxfordian is represented in the western limb of the Taulanne minibasin by thin black shales of the Terres Noires Formation (j2-4) while highly condensed limestone (j5-6) deposited around and above the Chasteuil salt structure, the St-Vincent diapir and the la Grau anticline. A minor angular unconformity at the base of the Tertiary reveals that the western limb of the Taulanne minibasin (Clos de Juyon section, Fig. 4.2) was slightly elevated before the deposition of the basal Eocene conglomerates (e6-7C) (Fig. 4.6). These observations suggest that the Berbené salt wall existed during the Mesozoic and formed a topographic high which bounded the Taulanne basin to the W and maybe linked the Chasteuil salt structure and St-Vincent diapir (Fig. 4.23). The salt wall may have formed simultaneously with the Chasteuil salt structure and St-Vincent diapir, during Tethyan rifting in Early to Middle Jurassic time. The absence of

successive unconformities, breccia levels, slumped intervals and the gradational Oxfordian facies variations show that the linking Berbené wall represented lower topography than the Chasteuil salt structure or the St-Vincent diapir. After the Bajocian, Jurassic and Berriasian-Lower Valanginian sediments were able to cover the top of the salt wall.

The Mesozoic section of the eastern flank of the Taulanne minibasin is not exposed (Fig. 4.2, Fig. 4.6), but it may well have been a salt wall which was similar to the Berbené wall.

S of the Chasteuil salt structure, the tight, west-plunging Porte de St-Jean minibasin also displays evidence for continuous Early Jurassic-Early Cretaceous salt tectonic activity. The map relationships and the view of the Porte de St-Jean syncline clearly display stratal thickening, from Hettangian to the Berriasian-Valanginian (n1, n2a) in its core (Fig. 4.11, Fig. 4.12, Fig. 4.20). The gradual thinning of the Hettangian-Valanginian section toward the northern and southern flanks of the basin are interpreted as growth strata. The thickness changes, absence of Sinemurian, Pliensbachian, and Toarcian sediments and the local unconformities which developed in the Middle-and Upper Jurassic succession (Fig. 4.8, Fig. 4.11, Fig. 4.12), suggest that Porte de St-Jean minibasin subsided into the deflating mother - salt layer during the rifting and passive margin phases, from the Hettangian to the Valanginian (Fig. 4.20). The Porte de St-Jean minibasin was bounded to the N by the Chasteuil salt structure but the identification of its southern bounding salt structure is less straightforward (Fig. 4.1, Fig. 4.2).

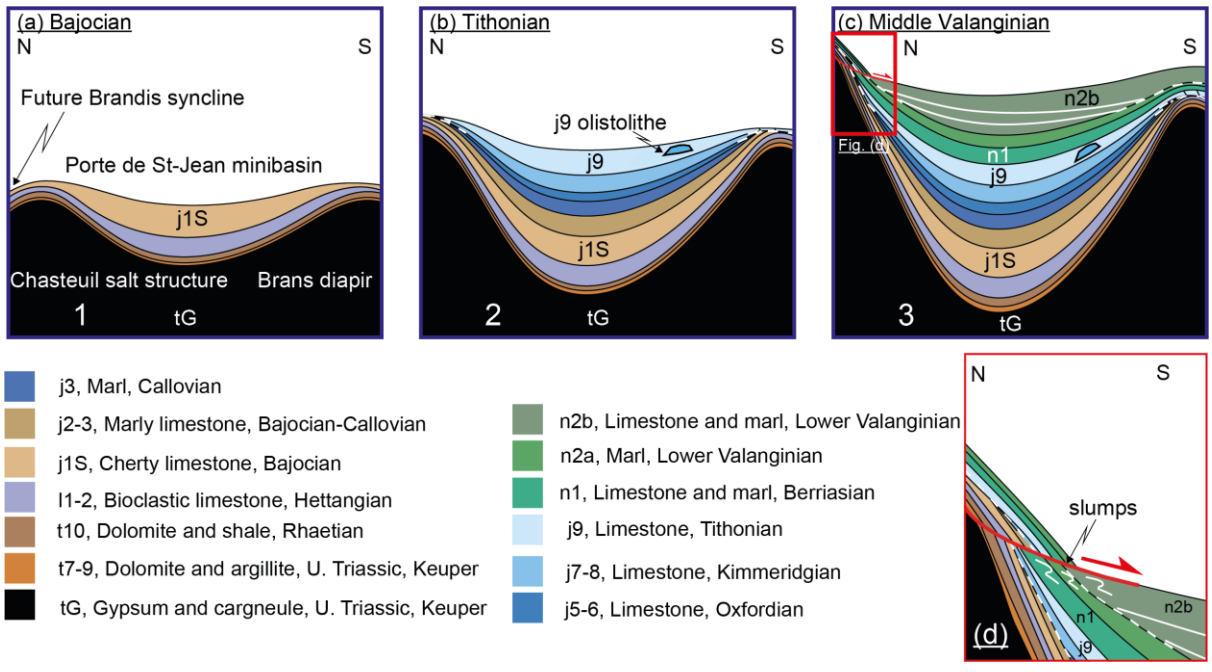


Fig. 4.20 Sequential evolution of the Porte de St-Jean minbasin and its bounding salt salt structures, the Chasteuil salt structure and the Brans diapir, from Bajocian (a) to Valanginian (c) (not to scale). (d). Zoom of the northern flank of the Porte de St-Jean minibasin. Note that the pedestal of Brans diapir possibly located in the subsurface, below the Cadières de Brandis section, along the Alpine basal detachment at the depth of 3 km.

The gradual thinning of the Jurassic section towards the Brans fault (Fig. 4.1, Fig. 4.2), with unconformities at the base of the Kimmeridgian (j7-8) and Tithonian (j9) limestones and the occurrence of apparent downlaps (rotated onlaps?) in the Kimmeridgian limestone on the southern flank of the Porte de St-Jean minibasin (Fig. 4.11) suggest that the Porte de St-Jean minibasin and the Taloire minibasin may have been separated during the Jurassic by a salt structure, the Brans diapir (Fig. 4.5, Fig. 4.20). The pedestal of this diapir must be located in the subsurface, below the Cadiéres de Brandis section, along the Alpine basal detachment at the depth of 3 km (Fig. 4.5). The Brans diapir was decapitated during the Alpine compressional phase and its northern limb served as a ramp for the Brans thrust, which overrides Oligocene molasse (g2R) in the Taloire syncline and carries the Porte de St-Jean minibasin, the Chasteuil salt structure and the Taulanne minibasin in its hanging wall (Fig. 4.5). The curved map-view pattern of the Brans thrust maybe reflects to the original map-view geometry of the Brans diapir (Fig. 4.1, Fig. 4.2, Fig. 4.8). The fact that the Brans thrust is connected to the large gypsum body of the Chasteuil salt structure (i.e., the Chasteuil diapir) suggests that the undeformed Brans diapir may have been connected to the Chasteuil salt structure and the two salt bodies enclosed the Porte de St-Jean minibasin (Fig. 4.23). The minibasin was open further to the W and may also have been linked to the Taloire syncline (Fig. 4.1, Fig. 4.2, Fig. 4.23).

A large Tithonian block in the Porte de St-Jean minibasin (Fig. 4.11) is interpreted as an olistolith. The presence of such an intra-formational olistolith within the Tithonian limestone (j9) (Fig. 4.20) together with the occurrence of breccia levels within both the Tithonian and the Bajocian (j1S) also suggests that the minibasin was bounded by local topographic highs during Middle and Upper Jurassic time. Angular unconformities along the flanks of the Porte de St-Jean minibasin, beneath the Oxfordian (j5-6), Kimmeridgian (j7-8) and Tithonian (j9) formations (Fig. 4.8, Fig. 4.9 Fig. 4.10, Fig. 4.11, Fig. 4.12, Fig. 4.20) suggest that salt tectonic activity culminated during the Late Jurassic.

The most unambiguous salt related structures which display evidence for Early Cretaceous salt tectonic activity are exposed in the western sector of the Porte de St-Jean minibasin, where Berriasian limestone (n1) and Lower Valanginian limestone and marl (n2a, n2b) are preserved.

NW of the village of Chasteuil SW-NE trending synclines and anticlines are seen in the Tithonian (j9) - Lower Valanginian (n2a) section. The axes of the folds are NE-SW trending and parallel with the Alpine compressional direction. The folding and overturning have affected the Triassic-Jurassic section and the Berriasian (n1) and the Lower Valanginian (n2a) formations but this deformed section is unconformably overlain by the Lower Valanginian n2b unit, dipping moderately to NE (Fig. 4.8, Fig. 4.9, Fig. 4.10), so the folds cannot be Alpine.

Syn-sedimentary slumping observed in the Berriasian-Lower Valanginian section displays further salt movement and instability along the flank of the diapir and the orientation of the observed slump folds suggests transport to the SE, towards the centre of the minibasin (Fig. 4.13).

Based on the map-view pattern of the Jurassic-Cretaceous formations and the observed structural geometries, the eroded Chasteuil salt structure is interpreted as a mushroom-shaped squeezed diapir (Fig. 4.1, Fig. 4.2, Fig. 4.5, Fig. 4.8). The anomalous contacts which run between the large remnant gypsum body eastwards to the Berbené fault and westwards to the Cadiéres de Brandis anticline, the Brandis syncline, and the Porte de St-Jean minibasin, are interpreted as welds (Fig. 4.1, Fig. 4.2, Fig. 4.8, Fig. 4.9, Fig. 4.10, Fig. 4.11). The reduced sections of the Cadiéres de Brandis and Brandis syncline represent the elevated former roof of the mushroom shaped Chasteuil salt structure. The Jurassic sections of the Cadiéres de Brandis and the Brandis syncline are almost complete compared to the flanks of the primary minibasins. Only the base-Bajocian unconformity formed on the crest of the diapir in the Brandis syncline and in the Cadiéres de Brandis anticline (Fig. 4.2, Fig. 4.8, Fig. 4.12), whereas the younger Middle-and Upper Jurassic sediments were able to cover the salt structure. The most significant stratigraphic gap between the Bajocian cherty limestone (j1S) and the Lower Valanginian marl (n2a) developed along the eastern flank of the Chasteuil salt structure, W of the village of Brayal. The remnant gypsum body of the Chasteuil structure is also located at the easternmost extent of the salt structure. The large blocks and 'chaotic masses' ('masses chaotiques') of Tithonian (j9) limestone, which apparently rest on the top of Aalenian-Callovian marly limestone (j2-3) are interpreted as downslided blocks, originated from the dismembered roof of the salt structure. These blocks are also located at the easternmost extent of the gently dipping section of the Cadiéres de Brandis anticline, close to the overturned Crête de Colle Bernaiche section, suggesting the eastern part of the salt structure formed the highest point during the Jurassic and Cretaceous. The 'salt-cored' anticline (i.e., the Chasteuil salt structure or Chasteuil diapir) may have been plunged to the W and linked to the Berbené salt wall (Fig. 4.23).

The overturning of the northern flank of the Porte de St-Jean minibasin and the Brandis syncline may have been occurred simultaneously with the overturning of the Crête de Colle Bernaiche section and the squeezing and partial welding of the Chasteuil salt structure, during the Tertiary.

The normal faults which cut through the overturned limb of the Porte de St-Jean minibasin and detach on the top of the Lower Valanginian marl (n2b) may have been formed prior to the

overturning of the northern flank of the minibasin (Fig. 4.9, Fig. 4.10, Fig. 4.20). The sliding and collapse of the flank of the Porte de St-Jean minibasin ('syncline') towards a pre-existing topographic depression, described by Roux (1968) may have been resulted from the over-steepening of the northern flank of the minibasin (Fig. 4.20).

The Taloire minibasin is only partially exposed, but the visible part displays less evidence of Jurassic-Cretaceous salt tectonic activity than either the Porte de St-Jean or Taulanne minibasins. The interpretation presented in Fig 4.5 is that the Brans diapir and its flanking strata were overridden by the Brans thrust after the deposition of the Lower Oligocene red molasse (g2R) and they are not exposed (Fig. 4.5). The Jurassic-Cretaceous sediments of the Taloire minibasin might be expected to show gradual thinning towards the pedestal of the Brans diapir (Fig. 4.5) but more precise description is not possible. The identification of the southern bounding salt structure of the Taloire minibasin is also problematic.

The Montagne de Robion anticline plunges to ENE and its axial trace is parallel to the axial trace of the Taloire syncline. It is the best candidate as the possible southern bounding salt body of the minibasin (Fig. 4.1, Fig. 4.2). According Roux (1968) the Montagne de Robion anticline formed before the Eocene (Priabonian). The area which is now forming the Montagne de Robion anticline was situated in the upper part of the palaeogeographic slope domain of the Dauphinois and Vocontian basins (Kerckhove & Roux, 1978a). However, the presence of the Tithonian reefal limestone on the SE flank of the anticline and palaeocurrent data (flow parallel to the axial trend of the Taloire minibasin and the Montagne de Robion anticline) suggest that area may have formed a palaeotopographic high during the Late Jurassic. I assume that the Montagne de Robion anticline formed as a wide salt swell with low relief along the edge of the Provençal platform during the Jurassic and was later tightened by Alpine shortening.

Although this interpretation is speculative, other well exposed salt related structures which do display clear evidence of salt tectonic activity during Jurassic and Early Cretaceous time were observed in the western part of the Taloire minibasin and suggest that like the other minibasins described here, the evolution of the Taloire syncline was highly affected by salt tectonic processes.

The reduced, vertical or locally overturned Triassic-Lower Cretaceous (Norian, t7-9 to Valanginian, n2a) section, which is exposed in the la Crotte area (Fig. 4.1, Fig. 4.2, Fig. 4.18), is interpreted as the flanking strata of an early salt structure (Fig. 4.23). Successive unconformities, pinch-outs, abrupt thickness changes of the Jurassic section all can be related to the growth of this salt structure.

The anomalous contact which separates the la Gondole syncline and the Taloire minibasin is interpreted as a weld which is presumably the continuation of the NE-SW trending Berbené salt wall (Fig. 4.1, Fig. 4.2, Fig. 4.18). The anomalous contact which separates the overturned la Crotte section and the gently dipping section of the Deneiras cliff and links into the weld representing the Berbené salt wall (Fig. 4.1, Fig. 4.2, Fig. 4.17), is also interpreted as a weld. This weld is the la Crotte weld (Fig. 4.18).

The growth of the SW segment of the Berbené salt wall is well documented by stratal geometries exposed along its flank, in the Taloire minibasin. The growth of the diapir may have been started as early as the Liassic, and the initiation of salt tectonics related to the Tethyan rifting. The salt wall presumably formed as a reactive diapir, similarly to the Chasteuil salt structure, the St-Vincent diapir and other salt diapirs which started to grow during the Liassic (Célini et al., 2020; Célini, 2020; Brooke-Barnett, 2022). However, it is unclear whether or not Early-Middle Jurassic extensional faults played a part in the early evolution of the Berbené salt wall.

The absence of the Rhaetian dolomite (t10) and Liassic dolomite (lD) between the Norian and the Bajocian sediments, and the presence of the angular unconformity at the base of the Bajocian in the la Crotte area can be taken as evidence of the early growth of the Berbené salt wall (Fig. 4.18, Fig. 4.21) and that during the deposition of the Bajocian dolomite, the Norian-Liassic section was upturned and eroded along the flank of the minibasin (Fig. 4.21).

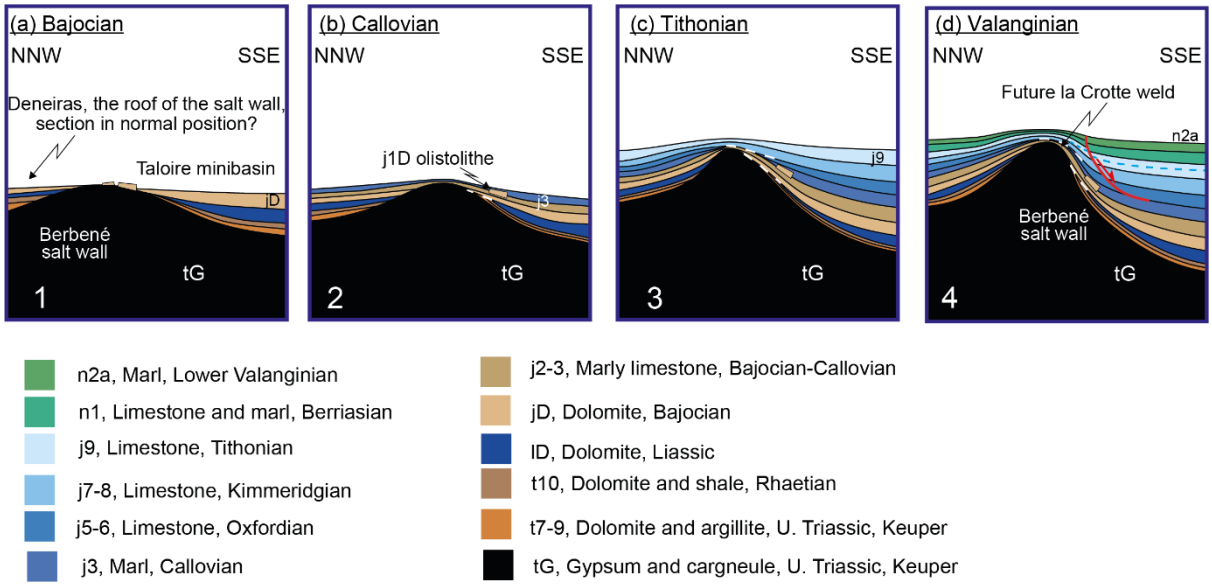


Fig. 4.21 Sequential evolution of the SW flank of the Taloire minibasin and its bounding structure, the Berbené salt wall, at the la Crotte section, from the Bajocian to the Valanginian. The absence of sediments younger than Lower Valanginian in the la Crotte section of the Taloire minibasin mean that the complete Early Cretaceous and Late Cretaceous history of the basin cannot be ascertained. Not to scale.

The large block of Bajocian dolomite observed along the flank of the Taloire minibasin is interpreted as an olistolith, which once represented the thin roof of the Berbené wall (Fig. 4.21). The olistolith slid off the flank of the growing Berbené salt wall as a dismembered roof fragment during the deposition of the Bajocian-Callovian marls (j2-3 and j3) (Fig. 4.21, Fig. 4.22). During the Bajocian, the salt may have been exposed on the seafloor for a short period, but during Late Bajocian times, sedimentation was able to cover the diapir again because the thin Bajocian-Callovian marly limestone (j2-3) does not abut against the la Crotte weld, but is folded over the structure (Fig. 4.17, Fig. 4.18, Fig. 4.21). It therefore must have formed thin roof over the diapiric salt.

The Bajocian-Oxfordian section exposed in the la Crotte overturned section thins towards the la Crotte weld and represents a minibasin-scale wedge geometry (Fig. 4.21). The Bajocian-Oxfordian strata show a broad zone of halokinetic drape folding along the growing diapir (Fig. 4.21c). As with the Chasteuil salt structure, the absence of a crestal graben, the lack of inward-dipping syn-sedimentary normal faults around the salt wall and the presence of the Bajocian-Oxfordian large scale wedge suggest that the Berbené salt wall continued to growth during the post-rift phase as a passive diapir under a thin roof which was bounded by drape folds (Rowan & Giles, 2021). The diapiric growth was presumably maintained by sediment loading on the autochthonous salt layer. Passive diapirism continued during the Kimmeridgian and Tithonian, which is suggested by the gradual thinning of the Kimmeridgian and Tithonian limestone towards the diapiric structure and the occurrence of intraformational unconformities within the Tithonian limestone (Fig. 4.18, Fig. 4.21). On a large scale, the Jurassic section of the Taloire minibasin is showing thinning wedge geometries (Rowan & Giles, 2023) towards the Berbené salt wall.

The facies associations of the Bajocian-Callovian (j2-3 and j3) and the Oxfordian-Tithonian (j5-6, j7-8 and j9) of the la Crotte and Deneiras sections (Fig. 4.2, Fig. 4.18, Fig. 4.21) are almost identical to the sections exposed around the Chasteuil salt structure, on the flanks of the Porte de St-Jean and the Taulanne minibasins (Fig. 4.8, Fig. 4.17). This also suggests that the Taloire minibasin was bounded to the SW by a salt structure similar to the Chasteuil salt structure. The reduced and gently dipping Deneiras section represents a complete Triassic-Upper Jurassic section, the roof of the Berbené salt wall (Fig. 4.21).

In the la Crotte area, Berriasian (n1) and Valanginian (n2a) sediments are preserved in the core and on the flank of the Taloire minibasin (Fig. 4.1, Fig. 4.2, Fig. 4.17, Fig. 4.18). Lower Cretaceous strata are overturned together with the underlying Norian-Tithonian section suggesting that Berriasian and Valanginian sediments may have been onlapping the Jurassic

flanking strata or able to cover the Upper Jurassic section over the top of the Berbené salt wall (Fig. 4.21).

Further to the NE along the welded Berbené salt wall, between the Deneiras area and the western limb of the Taulanne minibasin (Clos de Juyon section, Fig. 4.2) the Triassic-Lower Cretaceous section of the western limb of the Taloire minibasin, i.e. the Crête de Berbené area (Fig. 4.2) dips gently to the SE and doesn't show any internal unconformities (Fig. 4.1, Fig. 4.17). The exposed Liassic-Tithonian section is thin (approximately 400 m) as in the Deneiras section to the SW (Fig. 4.1, Fig. 4.2) and it is more reduced than the Liassic-Tithonian section of the western limb of the Taulanne minibasin, N of the Chasteuil salt structure (Fig. 4.1, Fig. 4.2). Near the village of Chasteuil, where the Taloire minibasins is amalgamated with the adjoining Porte de St-Jean syncline (Fig. 4.2), the Norian-Kimmeridgian section (t7-9 to j7-8) of the Crête de Berbené is abuts against the weld which represents the western termination of the Chasteuil salt structure (Fig. 4.8, Fig. 4.9, Fig. 4.10), while the overturned, relatively thin Tithonian-Berriasian section is crosscut by the NW-SE trending faults which also crosscut the overturned flank of the Porte de St-Jean minibasin (Fig. 4.1, Fig. 4.2, Fig. 4.8, Fig. 4.9, Fig. 4.17).

I assume that the Crête de Berbené area (Fig. 4.2), i.e. the western limb of the Taloire minibasin represents the flanking strata of the Berbené salt wall and the junction of the Chasteuil salt structure and salt wall (Fig. 4.23). The direct contact of the Norian-Kimmeridgian section (t7-9 to j7-8) with the welded Chasteuil salt structure and the overturning of the thin Tithonian-Berriasian (j9-n1) section which joins the northern flank of the Porte de St-Jean minibasin suggest that the joint Taloire and Porte de St-Jean minibasins were bounded and enclosed here by the diapiric structures, at the junction of the Berbené salt wall and the Chasteuil salt structure (Fig. 4.23). I assume that the formation of the NE-SW trending folds observed in the Tithonian-Berriasian section near Chasteuil may be also related to salt tectonics. The axial trace of these folds is

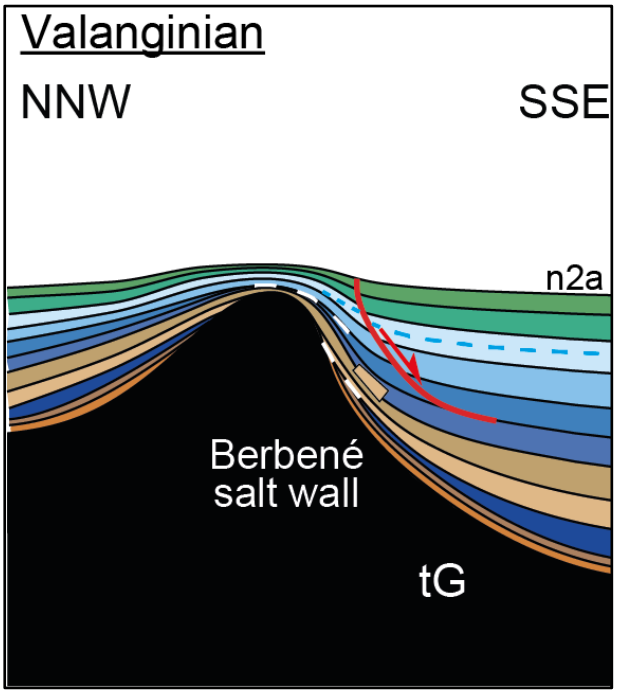


Fig. 4.22 Normal faulting occured along the SE flank of the Berbené salt wall, during the Early Valanginian, and led to the failure of the flanking strata. See Fig. 4.21 for key. Not to scale.

parallel to the Berbené salt wall and also the Alpine compressional direction and they may have been formed during the Valanginian, due to instability along the topographically arched roof of the Berbené salt wall.

I suppose that the two NE-SW trending faults observed SW of Chasteuil (Fig. 4.17) are normal faults and their formation related to salt tectonic processes. The faults are roughly parallel with the welded Berbené salt wall and the axial trend of the Taloire minibasin and may have been formed as crestal structures over the bounding salt structures of the minibasin (i.e., the Berbené salt wall to the NW and the Robion anticline to the SW) (Fig. 4.23).

The normal faults probably formed due to salt withdrawal from below the minibasin and the steepening and failure of the flank of the growing Berbené salt wall during the Valanginian (Fig. 4.22). An alternative interpretation is that these faults are actually unconformities at the base of the Berriasian (n1) and Lower Valanginian (n2a and n2b) formations which overlie the Tithonian limestone (j9) on the flanks of the Taloire minibasin.

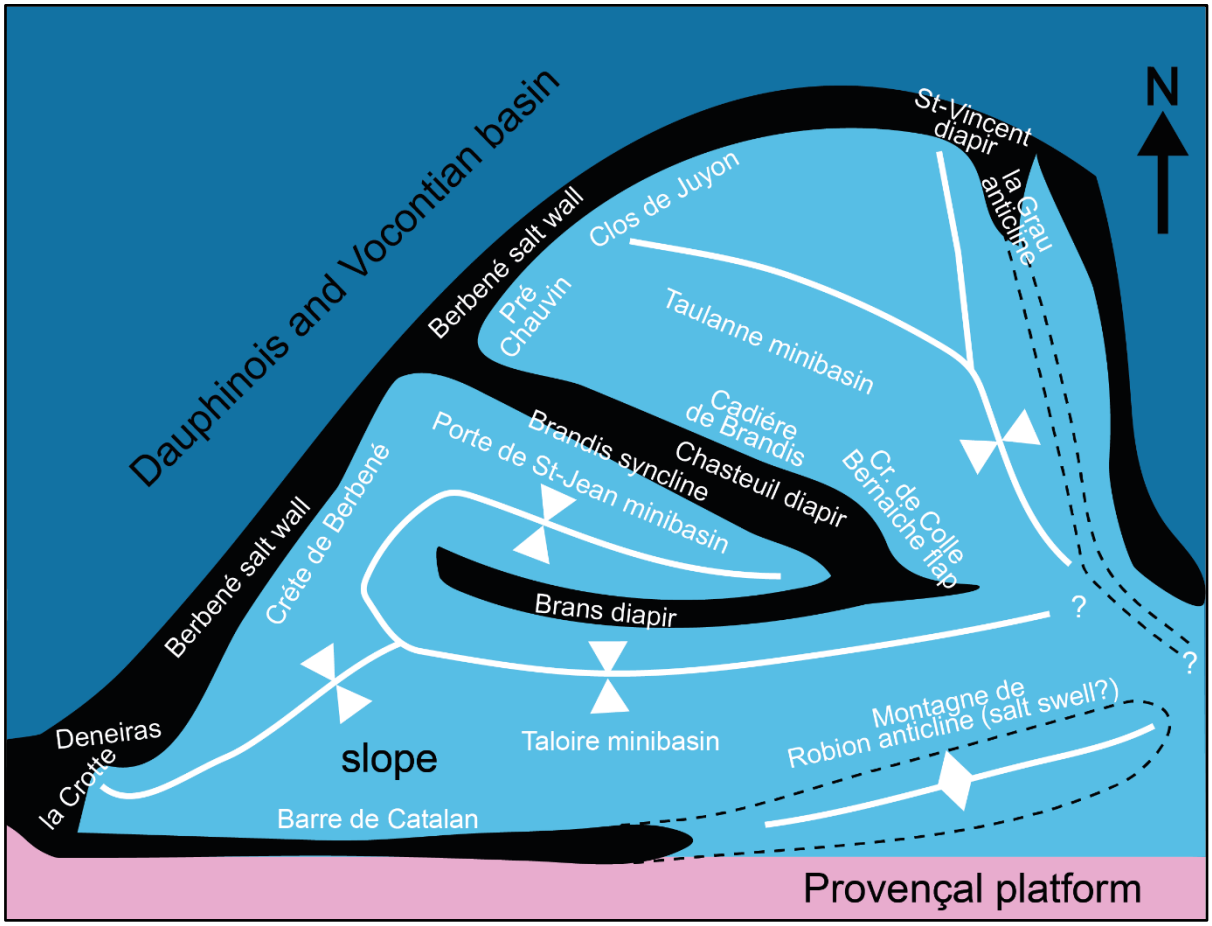


Fig. 4.23 Simplified map view of the Taloire minibasin, the Porte de St-Jean minibasin, the Taulanne minibasin and the salt structures which bounded these depocenters. The map is not restored and only showing the approximate palinspastic position of the minibasins and their bounding salt structures. Note that all the minibasins were located between the Provençal platform and the pelagic domain of the Dauphinois and Vocontian basins. Additional salt structures and minibasins to the WNW and ESE along the Provençal platform are not shown here.

Based on the observed structural and stratal geometries and also the reinterpretation of synclines, salt cored anticlines and Alpine structures, I conclude that the eastern part of the southern structural domain contains a system of primary minibasins and the network of bounding salt structures, like diapirs and elongated salt walls (Fig. 4.23), all formed prior to the Alpine shortening. Some of the salt structures are squeezed, strongly modified, or completely welded, and sometimes reactivated as Alpine compressional structures whereas intervening the minibasins remained relatively undeformed.

The Taloire minibasin, the Porte de St-Jean minibasins and the Taulanne minibasin subsided simultaneously into the autochthonous Upper Triassic evaporites during the rifting period and the passive margin phase. The initiation of salt tectonics may have been related to the Early-Middle Jurassic rifting, which led to the formation of reactive diapirs, presumably over the footwall of Tethyan extensional faults. Later, during the passive margin phase, the diapirs continued to grow due to sediment loading on the autochthonous salt layer as passive diapirs, at least until the deposition of the Lower Valanginian sediments. The thickness and facies of the Jurassic and the Early Cretaceous sediments were highly influenced by the presence of the elongated or subcircular depocenters and the topography expressed by the emerged salt bodies. The primary minibasins (Taloire minibasins, the Porte de St-Jean minibasin and the Taulanne minibasin) and also the diapiric structures (the St-Vincent diapir and la Grau anticline, the Chasteuil salt structure, the Brans diapir and also the Berbené salt wall) formed along the edge of the Provençal platform, in the slope palaeogeographic domain of the Dauphinois and Vocontian basins (Fig. 4.23).

Further to the E along the edge of the Provençal platform, similar stratal and structural geometries, and structural style were observed (Fig. 4.1, Fig. 4.2), in the Destourbes thrust sheet, the Teillon thrust sheet and the southern part of the la Blache-Castellane thrust sheet. I am going to describe my observations, analyse and interpret the salt related structures of these area in the following section.

4.1.2. The Destourbes thrust sheet, the Teillon thrust sheet and the southern part of the la Blache-Castellane thrust sheet. The eastern part of the southern structural domain

Rapid thickness and facies changes, anomalous contacts of the Triassic salt with reduced and overturned Jurassic-Lower Cretaceous sections can also be seen east and south-east of the salt structures and minibasins of the previously described Taulanne and Chasteuil areas (see § 4.1.1). They exist in three different thrust sheets: the Destourbes, Teillon and la Blache-Castellane thrust sheets (Fig. 4.25) and evidence for early salt tectonic activity was observed in all of them.

The Destourbes and Teillon thrust sheets are situated SE of the Chasteuil salt structure, E of the Taloire minibasin (Fig. 4.24, Fig. 4.25) and define the westernmost portion of the E-W trending part of the Castellane Arc (Fig. 2.1) They represent the slope palaeogeographic domain of the Dauphinois and Vocontian basins (Kerckhove & Roux, 1976a; Kerckhove & Roux, 1978a). The Destourbes thrust sheet displays less evidence of Jurassic and Early Cretaceous salt tectonic activity than the others, but the Teillon thrust sheet contains some of the most spectacular salt structures of the southern structural domain. The la Blache-Castellane thrust sheet comprises a thick Upper Triassic-Upper Cretaceous section and a large accumulation of Triassic gypsum, the Castellane diapir. The Jurassic and Cretaceous formations are basinal and are thrust over the Destourbes and Teillon sheets of the palaeogeographic slope domain (Fig. 4.25).

The detailed stratigraphic and structural description of the Teillon thrust sheet has been described by Jacqmin (1950) who depicted rapid thickness changes in the Upper Jurassic-Lower Cretaceous section and syn-sedimentary folding around Keuper gypsum bodies. The Lower Cretaceous stratigraphy of the area was studied by Cotillon (1968) who recorded current marks on an Early Aptian unconformity surface and documented hemipelagic submarine topography. Cotillon (1985) and Cotillon (2010) described E-W trending palaeotopographic highs in the transition zone between the Vocontian basin and the Provençal platform, i.e. on the palaeogeographic slope. Cotillon et al. (2000) and Cotillon (2010) proposed a tectonic origin for the palaeorelief.

The following description of the structures which indicate salt tectonic activity proceeds from west to east with the Destourbes and Teillon thrust sheets first, then the overriding basinal la Blache-Castellane thrust sheet (Fig. 4.25).

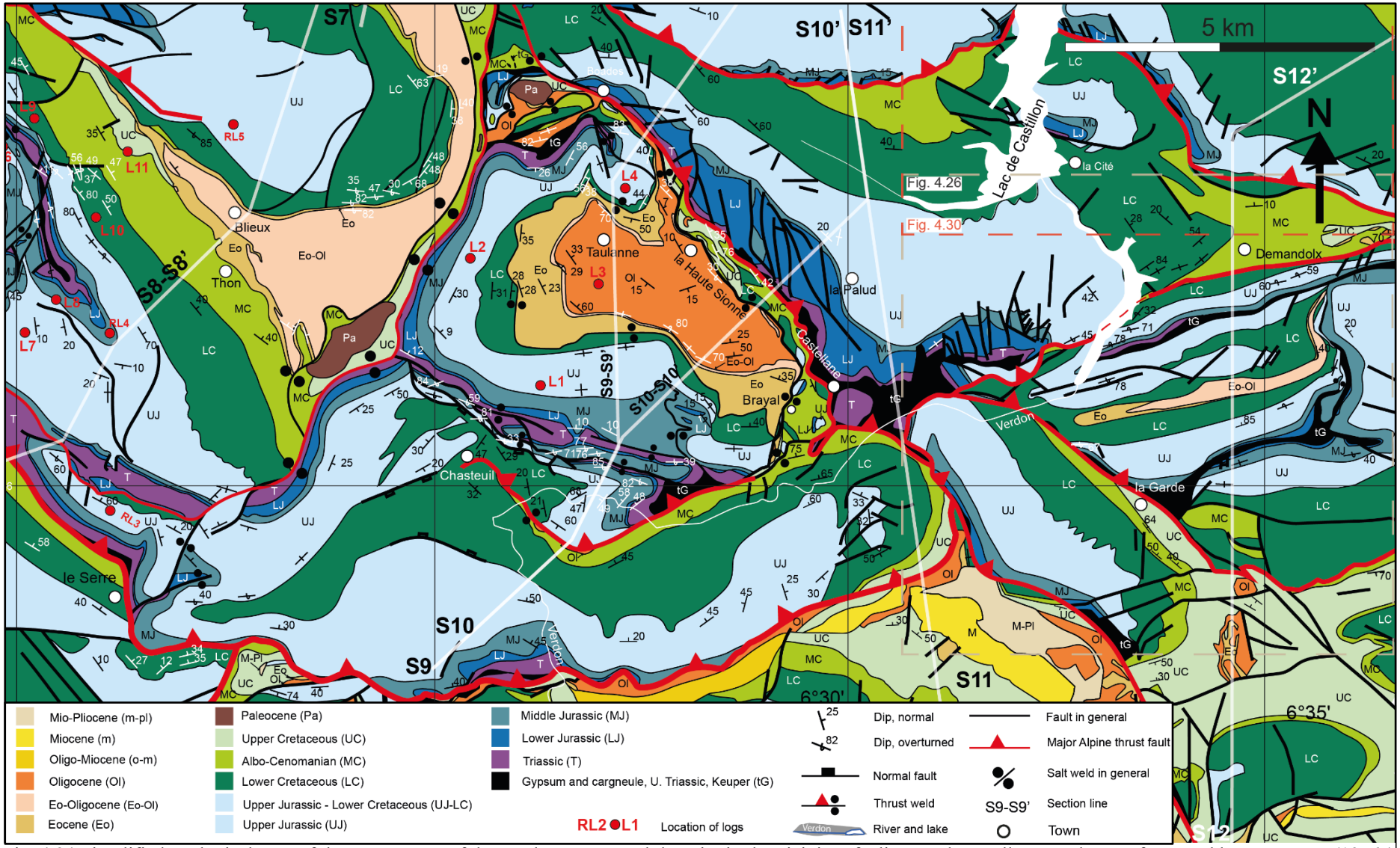


Fig. 4.24 Simplified geological map of the eastern part of the southern structural domain, in the vicinity of Blieux and Castellane. Redrawn after Kerckhove & Roux (1976a) and Kerckhove & Roux (1978a). See Fig. 4.25 for the structural explanation.

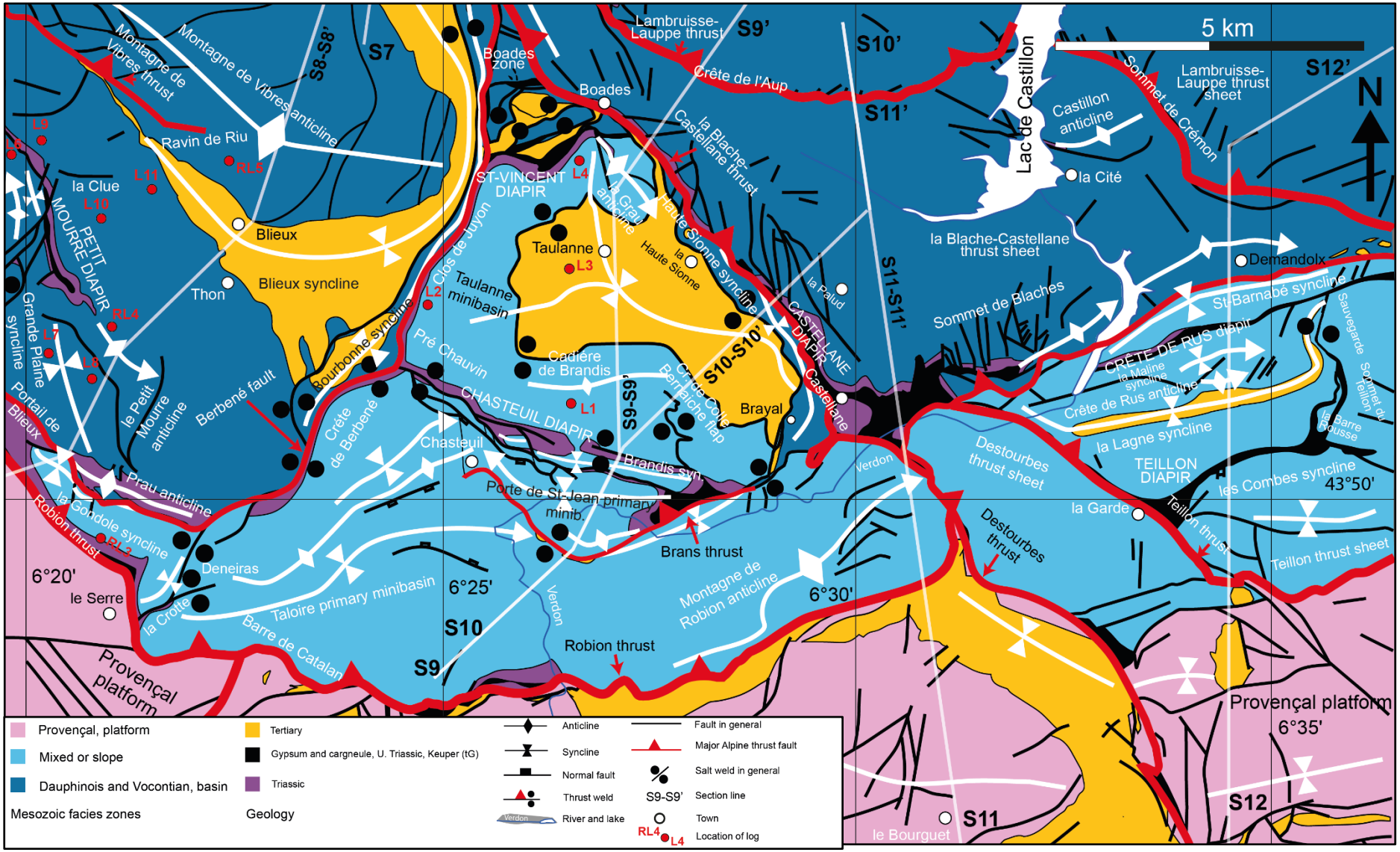


Fig. 4.25 Structural map of the eastern part of southern structural domain, showing synclines, their bounding Alpine structures or pre-Alpine salt structures and their Mesozoic palaeogeographic position. Data from Kerckhove & Roux (1976a) and Kerckhove & Roux (1978a).

4.1.2.1. The Destourbes thrust sheet. Stratal and structural observations

The Destourbes thrust sheet is situated SE of the town of Castellane (Fig. 4.25). The NW-SE trending, SW verging Destourbes thrust runs from the Castellane diapir towards the edge of the Provençal platform (Fig. 4.24 and Fig. 4.25). The thrust sheet overrode the Taloire primary minibasin, the Robion anticline, and the northern edge of the Provençal platform. To the N, the Destourbes thrust sheet is bounded by the la Blache-Castellane thrust sheet and the Castellane diapir in its hanging wall (Fig. 4.25). To the E and NE, it is bounded by the Teillon thrust fault (Fig. 4.24, Fig. 4.25). To the S, the Destourbes thrust sheet is separated from the Provençal platform by a roughly E-W trending fault (Fig. 4.24, Fig. 4.25).

The thrust sheet contains of a complete and relatively thick and undeformed Upper Triassic-Upper Cretaceous section of around 1000 m. (Fig. 4.24). The approximate thickness of both the Jurassic and Cretaceous sections are around 500 m. The Liassic is assumed to be complete and is represented by dolomite (lD). According to Kerckhove & Roux (1976a), the Liassic is overlain by Bajocian cherty limestone (j1S), and the Aalenian is missing. The Middle Jurassic section shows similarities to the Bajocian-Callovian succession of the Porte de St-Jean and Taulanne minibasins (Fig. 4.6) and is composed of marly limestone (j2-3). The Upper Jurassic section is represented by typical Oxfordian-Tithonian limestone in slope facies (j5-6, j7-8 and j9) whereas the Cretaceous succession shows affinities both to the platform and the slope facies zone, but the transition between the slope and the platform facies zones is somewhat ambiguous. The Lower and Upper Cretaceous is composed of a more sandy or glauconitic succession than the typical mixed succession of the slope palaeogeographic domain.

Anomalous stratigraphic relationships were observed NW and SW of the village of la Garde, in the immediate hanging wall of the Destourbes thrust (Fig. 4.24, Fig. 4.25 and Fig. 4.26) where a NW-SE trending doubly plunging anticline formed in the hanging wall of the Destourbes thrust (Fig. 4.24).

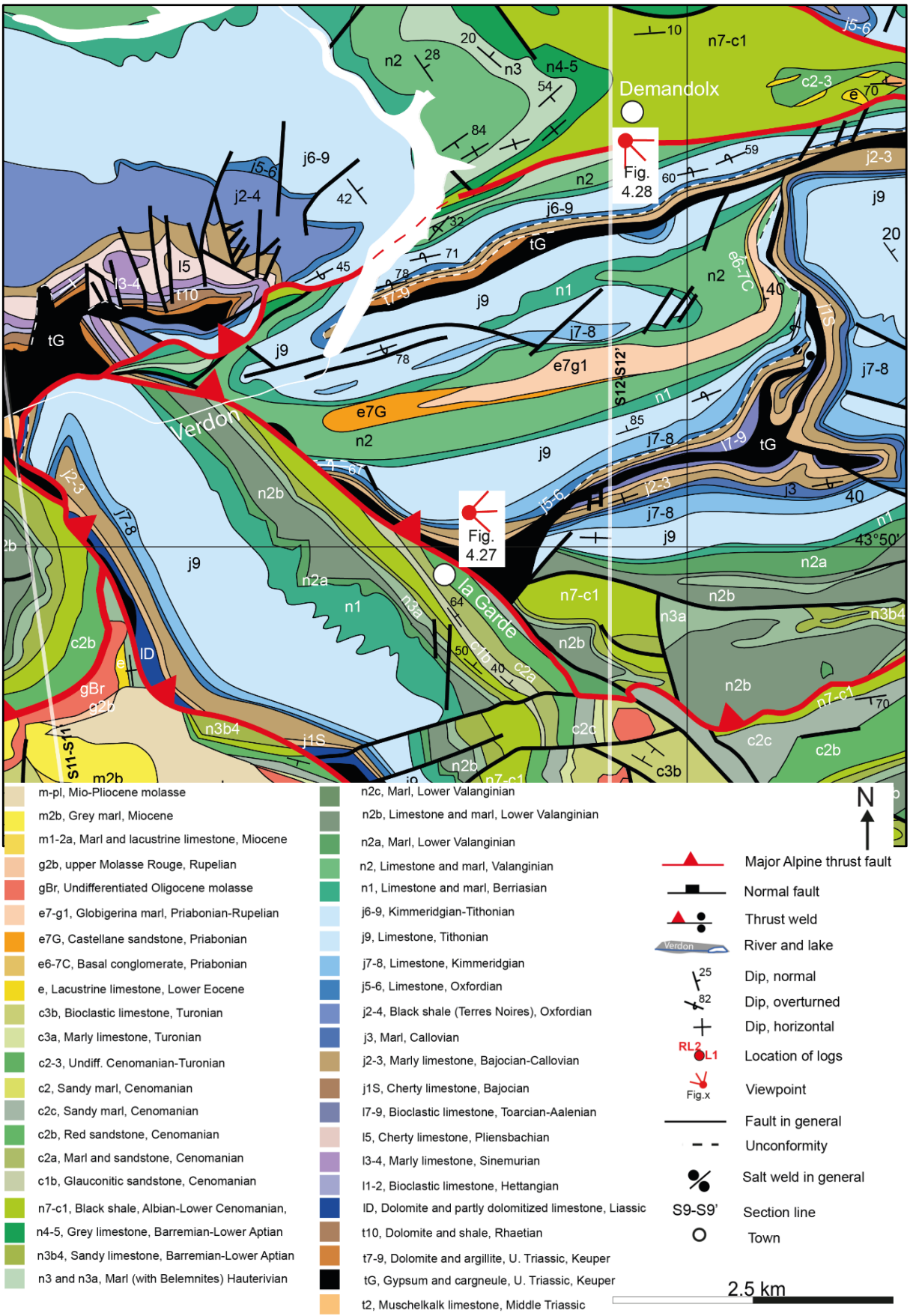


Fig. 4.26 Detailed geological map of the Destourbes and Teillon thrust sheets of the slope palaeogeographic domain. The thrust sheets overthrusted the edge of the Provençal platform and they are overriden by the basinal la Blache-Castellane thrust sheet (Fig. 4.25). See Fig. 4.24 for location and Fig. 4.25 for structural explanation.

At the transition between the platform and the slope facies zones, where the Destourbes thrust overthrusted the Upper Cretaceous and overlying Oligocene (gBr) of the Provençal platform, Upper Triassic gypsum (tG) in the hanging wall of the thrust is in direct contact with the Jurassic-Lower-Middle Cretaceous section (Fig. 4.24). Several WSW-ENE trending faults crosscutting the Jurassic-Cretaceous section and displaying dextral offset and the contact with the salt is apparently faulted. However, the Tithonian limestone and the Albian-Cenomanian black marls directly overlie the Keuper gypsum (Fig. 4.26).

A local unconformity was also observed further to the NW, in the Middle Jurassic section of the hanging wall of the Destourbes thrust just S of the Castellane diapir (Fig. 4.24, Fig. 4.25, Fig. 4.26). Here, Bajocian-Callovian marly limestone (j2-3) unconformably overlies Liassic dolomite (lD) and the Bajocian cherty limestone (j1S) is missing (Fig. 4.26).

4.1.2.2. The salt structures and intervening synclines of the Teillon thrust sheet. Stratigraphic and structural observations

The Teillon thrust sheet is situated E of the Destourbes thrust sheet, in the hanging wall of the NW-SE trending, SW verging Teillon thrust, which overrides the Upper Jurassic-Upper Cretaceous section of the Destourbes thrust sheet. SE of the village of la Garde, the NW-SE trending segment of the Teillon thrust curves to roughly WSW-ENE and is thrust over the Albian-Cenomanian (n7-c1) and Cenomanian (c2c) formations of the Provençal platform (Fig. 4.26). The area where the strike of the Teillon thrust changes dramatically corresponds to the transition from the slope to the platform facies zone in the footwall of the thrust (Fig. 4.25). Like the Destourbes thrust sheet, the Teillon thrust sheet is also bounded by the basinal Upper Triassic-Upper Jurassic section of the la Blache-Castellane thrust sheet (Fig. 4.24, Fig. 4.25, Fig. 4.26). In the Teillon thrust hanging wall there are a series of WSW-ENE trending synclines, the les Combes syncline, the la Lagne syncline, the la Maline syncline, and the northernmost St-Barnabé syncline (Fig. 4.24, Fig. 4.25, Fig. 4.29). The wavelengths are relatively short between the axes of these synclines, ranging from 1 to 2 km (Fig. 4.24, Fig. 4.25, Fig. 4.26). The synclines are separated by tight anticlines which were originally diapirs - the Teillon diapir, the Crête de Rus anticline and Crête de Rus diapir. The Teillon diapir separates the les Combes syncline from the la Lagne syncline, while the Crête de Rus anticline is situated between the la Lagne syncline and the small la Maline syncline. The Crête de Rus diapir separates the la Maline syncline from the larger St-Barnabé syncline (Fig. 4.25).

Most of these salt structures and anticlines are WSW-ENE trending, but the Upper Triassic gypsum body of the Teillon diapiric structure is actually composed of three elongated Keuper gypsum and cargneule breccia bodies (tG.). In the la Barre Rousse area (Fig. 4.25), the WSW-ENE trending diapir splits into two N-W trending salt bodies which join together again further to the N and link into the WSW-ENE oriented Crête de Rus diapir in the Sauvegarde area (Fig. 4.24, Fig. 4.25, Fig. 4.26, Fig. 4.27). Along these branches of Teillon diapir, Triassic gypsum is locally missing at the surface and represented by only an anomalous contact or apparent fault. The two N-S trending branches of the diapir separate the la Lagne syncline from an incomplete and reduced Liassic-Upper Jurassic (from l7-9 to j9) section which is gently dipping (around a 20^{o}) to the ENE and exposed at the Sommet du Teillon area (Fig. 4.24, Fig. 4.25, Fig. 4.26, Fig. 4.27). W of the N-S trending segment of the Teillon diapir, the axis of the la Lagne syncline also trends N-S parallel with the salt body (Fig. 4.25).

Within the Teillon thrust sheet, more complete Mesozoic stratigraphy is preserved in the northernmost St-Barnabé syncline and the southernmost les Combes syncline, where the youngest sediments are the Albian-Cenomanian black shales (n7-c1) (Fig. 4.24, Fig. 4.25, Fig. 4.26). In the la Lagne and the la Maline synclines the youngest preserved Mesozoic sediments are the Valanginian limestones and marls (n2). I assume that Jurassic and the lower part of the Lower Cretaceous section (i.e., the Berriasian and Valanginian) are similar in all of the synclines (Fig. 4.29).

The Norian (7-9) Keuper argillite is exposed N of the Crête de Rus diapir where it is unconformably overlain by Middle Jurassic (Bajocian, j1S) sediments (Fig. 4.26). In the Teillon thrust sheet, as in the Taulanne minibasin, the Norian is considered as a pre-kinematic layer which shows no facies or thickness changes and is lumped together with the Keuper gypsum in cross sections and evolutionary diagrams. The Rhaetian dolomite (t10) is missing in the Teillon thrust sheet. Presumably, Rhaetian sediments have been truncated by local unconformities (described later).

Liassic strata are exposed around the Teillon diapir, in the la Lagne and the les Combes syncline and also in the gently dipping section of the Sommet du Teillon area (Fig. 4.26). The Liassic is incomplete and represented by only the Toarcian-Aalenian bioclastic limestone (l7-9) which directly overlies the Upper Triassic Keuper gypsum (tG) (Fig. 4.26). The Norian (t7-9), Rhaetian (t10), Hettangian, Sinemurian and Pliensbachian formations are absent on the flanks of the synclines and also in the gently dipping Sommet du Teillon section, E of the N-E trending segment of the Teillon diapir. The Toarcian-Aalenian bioclastic limestone is not present in the Destourbes thrust sheet (nor in the previously described Taulanne, Porte de St-

Jean and Taloire minibasins (Fig. 4.8)) where the Liassic is dolomitic (lD) or represented only by the Hettangian bioclastic limestone (l1-2) (Fig. 4.6, Fig. 4.17 and Fig. 4.26).

The facies of the Middle Jurassic is similar to that of the Destourbes thrust sheet and the Middle Jurassic section of the primary minibasins of the slope facies zone (Fig. 4.3, Fig. 4.6, Fig. 4.8, Fig. 4.17 and Fig. 4.24). The Middle Jurassic section is exposed around the Teillon diapir and on the southern flank of the St-Barnabé syncline (Fig. 4.26). The Bajocian (j1S) is represented by cherty limestone, and it passes into Bajocian-Callovian marly limestone (j2-3). The Upper Callovian is composed of grey marl (j3) which is exposed on the northern flank of the les Combes syncline and also in the Sommet du Teillon section. The Upper Jurassic section is identical to the Oxfordian-Tithonian succession of the primary minibasins west of the town of Castellane (j5-6, j7-8 and j9) and exposed on the southern flanks of the synclines and the gently dipping Sommet du Teillon section (Fig. 4.26).

The lower part of the Cretaceous section comprises Berriasian (n1) and Valanginian (n2, n2a, n2b) limestones and marls present in all of the synclines (Fig. 4.26). The Hauterivian-Cenomanian (from n3 to n7-c1) which is preserved in the southernmost les Combes and the northernmost St-Barnabé synclines comprises Hauterivian marl (n3, n3a), Barremian-Lower Aptian sandy limestone (n3b4) and Albian-Cenomanian (n7-c1) black shales (Fig. 4.26).

Tertiary sediments are only preserved in the core of the la Lagne syncline where they overly Lower Cretaceous strata (Fig. 4.26). The Eocene is represented by a Priabonian basal conglomerate (e6-7C) and the so-called ‘Castellane sandstone’ (e7G) with the conglomerate only preserved in the eastern part of the syncline. The Castellane sandstone is overlain by Priabonian-Rupelian Globigerina marl (e7-g1) and therefore comparable with the Tertiary succession of the Taulanne minibasin (Fig. 4.6 and Fig. 4.26) except that in the la Lagne syncline, younger Rupelian and Chattian sediments are not preserved or not deposited.

Like the Mesozoic stratigraphy of these synclines, the observed structural styles are also comparable in the les Combes, la Lagne, la Maline and St-Barnabé synclines. Local thickness changes, pinch-outs and anomalous contacts were observed in the Jurassic-Cretaceous on the limbs of the diapiric structures and anticlines which separate the individual synclines. The Mesozoic strata around the salt structures are usually vertical or overturned and abrupt thickness changes in the Jurassic and Lower Cretaceous section between the limbs and the cores of the synclines were also shown by cross section construction (S12-S12’ section, Fig. 4.29). The S12-S12’ cross section traverses the Mesozoic platform, slope, and basin from the footwall of the Teillon thrust to the overriding basinal la Blache-Castellane thrust sheet. It shows the structural style of the Teillon thrust sheet in detail and contrasts it with the relatively

simple structural style of both the Provençal platform and the Lambruisse-Lauppe thrust sheet which overthrusted the la Blache-Castellane thrust sheet N and NE of the village of Demandolx (Fig. 4.24, Fig. 4.25, Fig. 4.26). Stratal and structural geometries and thickness changes of the Jurassic-Cretaceous section of the Teillon thrust sheet are described here from south to north, crossing the individual synclines and their bounding structures.

On the southern flank of the les Combes syncline, in the hanging wall of the WNW-ENE trending segment of the Teillon thrust, Lower Cretaceous formations (n2b, n3a and n3b4) are highly folded, generally gently dipping to the N and overthrusting the Middle-Upper Cretaceous (n7-c1 and c2c) formations of the Provençal platform (Fig. 4.26). The thickness of the Lower-Middle Cretaceous is approximately 400 m in the hanging wall of the Teillon thrust but Triassic and Jurassic rocks are not exposed in the hanging wall of the thrust fault.

In the core of the les Combes syncline, along a roughly E-W trending fault, the Valanginian marl (n2b) is apparently thrust over Hauterivian-Cenomanian (n3a, n3b4 and n7-c1) formations (Fig. 4.26). Although no dips were measured here the Lower Cretaceous section is assumed to be steeply dipping or vertical on both sides of the fault. The E-W trending apparent thrust fault joins into a large gypsum body at the western termination of the Teillon diapir, in the immediate hanging wall of the Teillon thrust. Lower and Middle-Upper Cretaceous rocks situated in the core and the SW flank of the les Combes syncline abut against this salt body (Fig. 4.25, Fig. 4.26).

Further to the N, on the northern flank of the les Combes syncline, a Toarcian-Aalenian-Lower Valanginian section is exposed (Fig. 4.26). The Toarcian-Aalenian–Lower Valanginian section (l7-9 to n2a) turns vertical or slightly overturned along the WSW-ENE oriented gypsum body of the Teillon diapir exposed in the Ravin de Graviéres valley (Fig. 4.29), Fig. 4.27). The width of the Triassic gypsum body is approximately 100 m and the Keuper is overlain unconformably by the thin Toarcian-Aalenian bioclastic limestone (around 40 m) and Norian (t7-9) with Rhaetian (t10) and Hettangian-Pliensbachian formations missing (Fig. 4.26, Fig. 4.27). In the upper part of the flanking section, i.e., the Bajocian-Cenomanian (j1S to n7-c1) section is continuous and local unconformities were not observed although the thickness of the Middle-and Upper Jurassic section on the northern flank of the les Combes syncline is reduced. The Bajocian-Callovian section is only 40 m here, whereas the thickness of the overlying Callovian grey marl is approximately 50 m. The thickness of the Upper Jurassic section (j5-6, j7-8, j9) is around 330 m (Fig. 4.26) and the total thickness of the Jurassic (Toarcian -Tithonian, l7-9 to j9) section is around 450-500 m (Fig. 4.26, Fig. 4.27). The Lower-Middle Cretaceous section (n1 to n7-c1) is also reduced (around 200 m) but based on the observed thicknesses and

dips at the surface, the Jurassic-Cretaceous section seems to thicken towards the core of the les Combes syncline. The thickness of the Jurassic-Upper Cretaceous section (l7-9 to n7-c1) in the core of the les Combes syncline is around 1250 m. I assume that the Jurassic-Cretaceous section thins against the Teillon thrust as shown on the S12-S12' cross section (Fig. 4.29). However, the pre-Valanginian section is not exposed on the southern flank of the syncline, hence the pre-Valanginian stratal and structural geometries shown in Fig. 4.29 are highly speculative.

Further to the W, along the strike of the northern limb of the les Combes syncline (Fig. 4.26), as the vertical and thin Jurassic section (Toarcian-Aalenian, l7-9 to Tithonian, j9) abuts against the westernmost extent of the Teillon diapir which is widens into a large salt body at the village of la Garde, in the immediate hanging wall of the Teillon thrust (Fig. 4.24, Fig. 4.25 and Fig. 4.26).

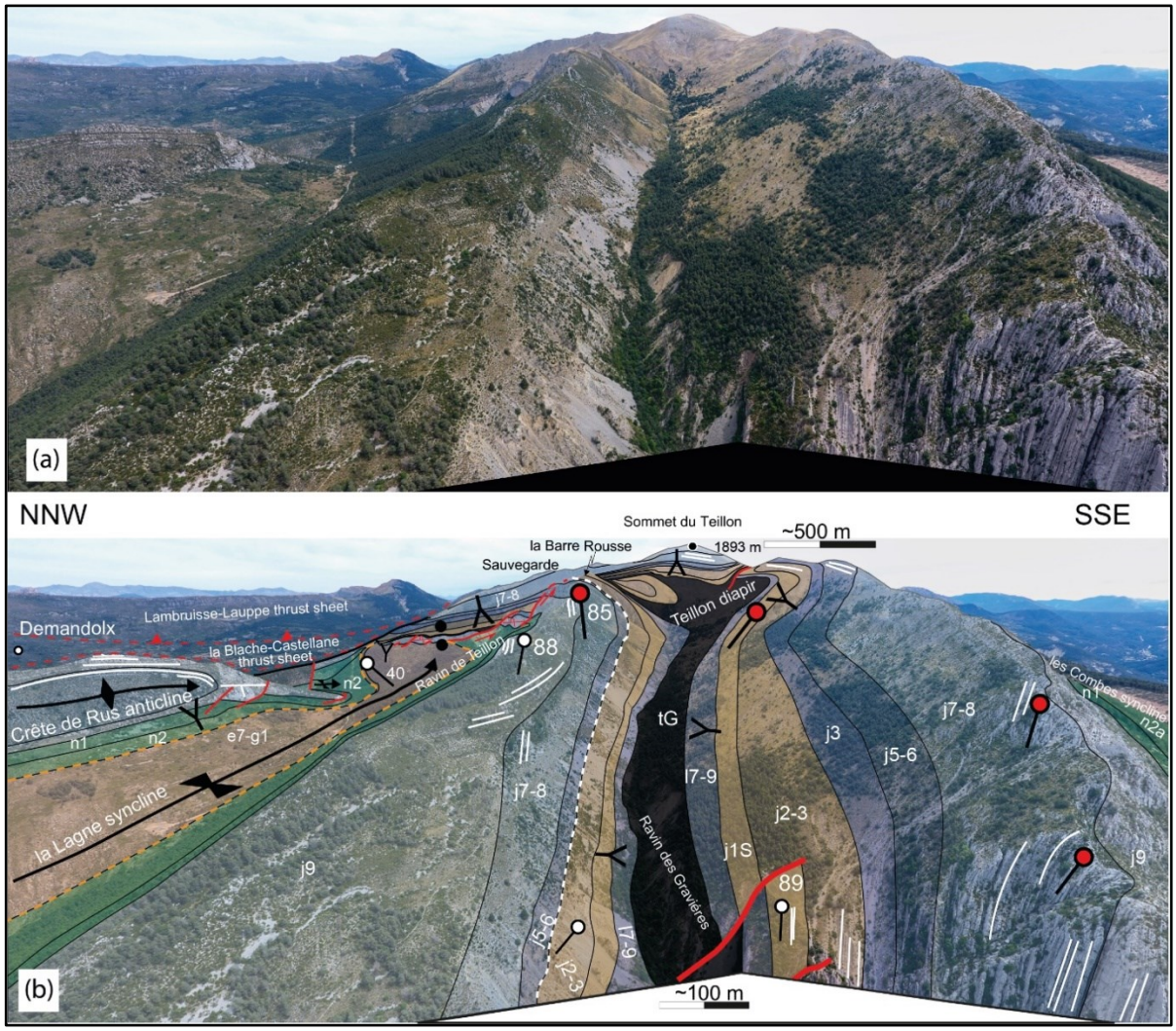


Fig. 4.27 Uninterpreted (a) and interpreted (b) photo panorama of the Teillon diapir and the Crête de Rus anticline with the bounding la Lagne and les Combes synclines, looking to E. See Fig. 4.26 for key and viewpoint location.

The vertical Jurassic-Cretaceous section is continuous further to the E and becomes almost completely overturned to the S (dips around 40° overturned to N), S of the la Barre Rousse section, at the triple junction of the Keuper evaporite bodies of the Teillon salt structure (Fig. 4.25, Fig. 4.26, Fig. 4.27). The WSW-ENE trending segment of the diapiric salt separates the overturned flank of the les Combes syncline from the gently dipping strata of the Sommet du Teillon section (Fig. 4.27). At the Sommet du Teillon section, the thickness of the incomplete and reduced Liassic-Upper Jurassic (from l7-9 to j9) section is only 400 m (Fig. 4.27, Fig. 4.28, Fig. 4.29).

In the overturned section, the Toarcian-Aalenian (l7-9) and Bajocian (j1S) cherty limestone abut against the Keuper gypsum, whereas on the top of the mountain, in the gently dipping section, the salt is unconformably overlain by the Liassic and also the Bajocian (Fig. 4.26, Fig. 4.27).

N of the WSW-ENE trending segment of the Teillon diapir, on the southern flank of the la Lagne syncline, similar structural style and stratal geometries were observed. The Teillon diapir is bounded by a steeply dipping or vertical Toarcian-Aalenian-Valanginian section (l7-9 to n2) (Fig. 4.26, Fig. 4.27, Fig. 4.28, Fig. 4.29). The Upper Triassic gypsum is unconformably overlain by thin Toarcian-Aalenian bioclastic limestone only around 25 m thick. The Middle Jurassic is composed of the Bajocian cherty limestone (j1S, around 30 m) and the Bajocian-Callovian marly limestone (j2-3, around 30 m) but the Callovian grey marl is missing, and the Bajocian-Callovian marly limestone (j2-3) is unconformably overlain by the Oxfordian limestone (j5-6, approximately 25 m thick). The Kimmeridgian-Tithonian section (j7-8 and j9) is approximately 320 m thick and the complete thickness of the Jurassic (Toarcian -Tithonian, l7-9 to j9) section is only 430 m in the southern limb of the la Lagne syncline while in the centre of the syncline the Liassic-Lower Cretaceous section reaches a thickness of 1100 m (Fig. 4.29).

To the W, the incomplete Liassic-Middle Jurassic section is overturned to the N and abuts against the Keuper gypsum which is in also direct contact with the Oxfordian (j5-6) limestone (Fig. 4.26). NE of the village of la Garde, the salt is overlain by the Bajocian cherty limestone (j1S) (Fig. 4.26).

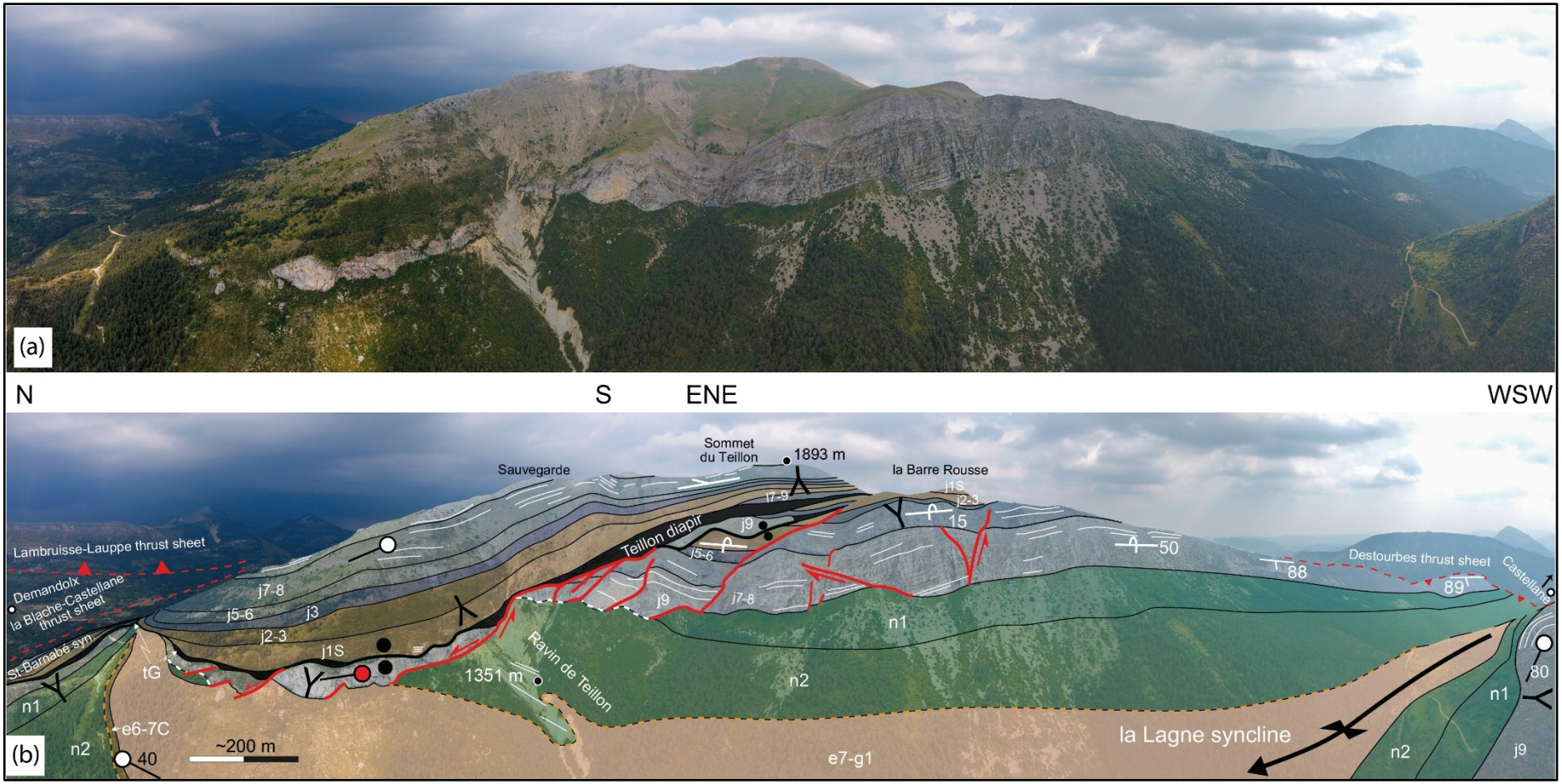


Fig. 4.28 Uninterpreted (a) and interpreted photo panorama of the Teillon diapir and the la Lagne syncline, looking to SE and showing the overtunred flank of the syncline and the gently dipping top of the mushroom shaped diapir. Black epsilons indicate younging direction. See Fig. 4.26 for key and viewpoint location.

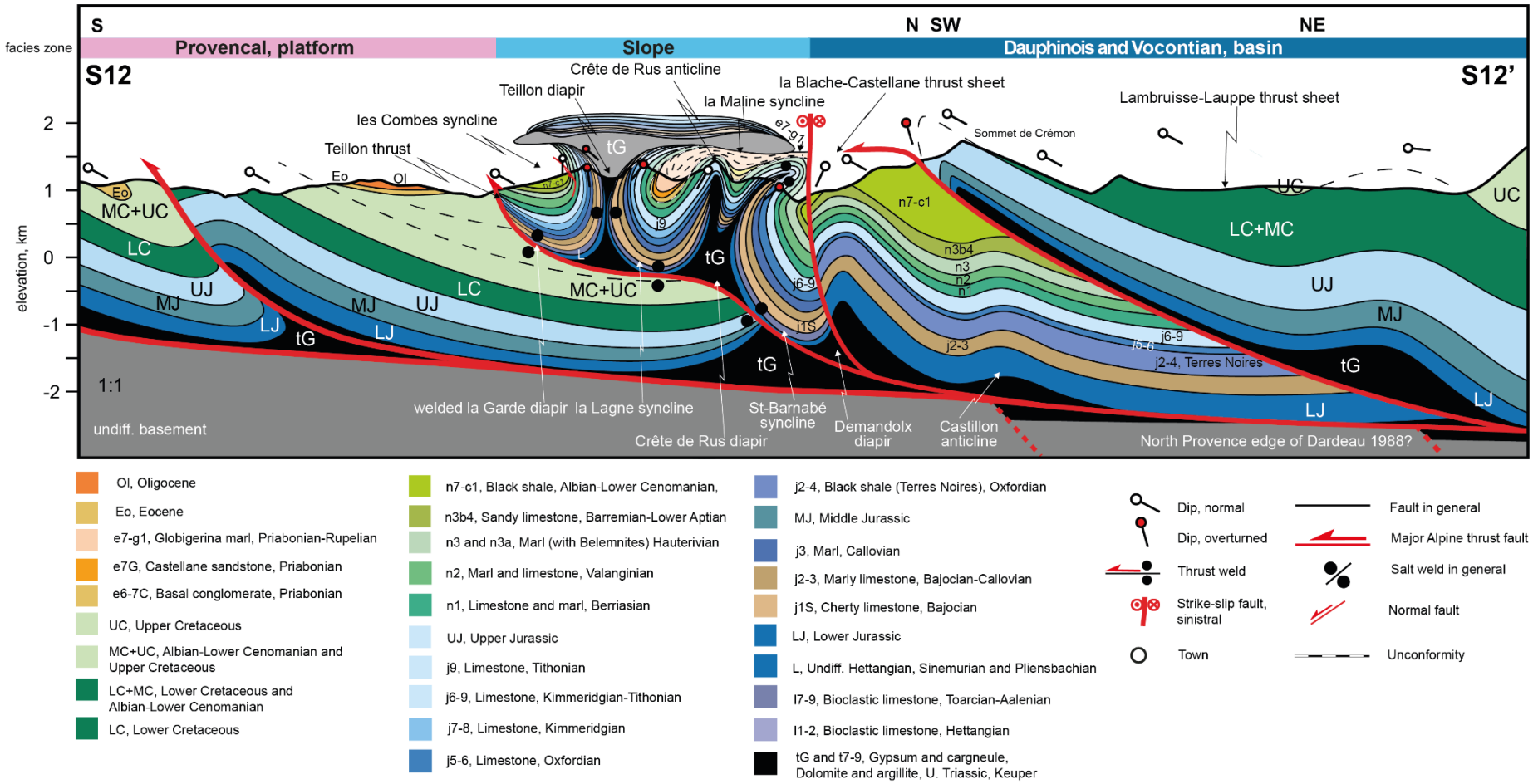


Fig. 4.29 Regional cross section (S12-S12') from the Provençal platform to the basinal Lambruisse-Lauppe thrust sheet through the Teillon thrust sheet which represents the Mesozoic slope palaeogeographic domain. See Fig. 4.24, Fig. 4.25 and Fig. 4.26 for cross section location. The location of basement involved extensional faults is highly specualtive. These normal faults may correspond to the Mesozoic North Provence edge of Dardeau (1988) and they were presumably inverted duirng later Alpine shortening. Note that the north-eastern and southern segment of the section is not shown on Fig. 4.26.

A minor local unconformity was observed in the overturned section, at the base of the Berriasian (n1) which overlies the Kimmeridgian limestone (j7-8) (Fig. 4.26). In the hanging wall of the Teillon thrust, between the village of la Garde and the Verdon River, a large block of gypsum is bounded to the W by the thrust and surrounded by Valanginian sediments in all other directions (Fig. 4.24, Fig. 4.25, Fig. 4.26). E of the S12-12' section line, the Jurassic-Lower Cretaceous section of the southern flank of the la Lagne syncline thins towards to the E and becomes completely overturned 2 km to the E of the S12-S12' section line, at the triple junction of the elongated salt bodies of the Teillon diapir (la Barre Rousse section, Fig. 4.25 Fig. 4.26, Fig. 4.27, Fig. 4.28). The overturned section is separated from the gently dipping Sommet du Teillon and Sauvegarde sections by the N-S oriented segment of the Teillon diapir (Fig. 4.27). The thickness of the salt between the normal and overturned section is a few meters or locally negligible.

At the triple junction of the three 'arms' of the Teillon diapir, NW of the Sommet du Teillon area there is a small and narrow syncline in Bajocian (j1S), Bajocian-Callovian (j2-3) and Callovian (j3) rocks. The syncline is entirely surrounded by the Keuper gypsum, and its eastern flank is apparently overturned. Further to the N, the Callovian grey marl (j3) which is preserved in the core of the syncline is in direct contact with a large block of Tithonian limestone (j9) This Tithonian block is separated from the gently dipping section of the Sommet du Teillon section by the Keuper gypsum of the N-S trending 'arm' of the Teillon diapir and from the overturned section of the eastern flank of the la Lagne syncline by an anomalous contact (Fig. 4.26, Fig. 4.28).

The observed structural and stratal geometries are complex along the N-S trending branch of the Teillon diapir, in the overturned section of the eastern flank of the la Lagne syncline. The Middle Jurassic-Upper Jurassic section is completely overturned below the Triassic gypsum and thinning towards the N-S trending segment of the diapir. The Bajocian-Oxfordian section (j1S, j2-3 and j2-4) abuts against the anomalous contact along the large Tithonian block. The Middle-Upper Jurassic section is reduced, and several normal faults crosscut the overturned limb of the syncline (Fig. 4.28). Some of these faults crosscut only the Upper Jurassic section, while other faults also offset the Middle Jurassic section. The larger extensional faults are apparently detached on the top of the Keuper gypsum of the diapir (Fig. 4.28) These normal faults are apparently overturned and sealed by the Berriasian (n1) or Valanginian (n2) sediments. In the overturned section, a minor unconformity developed locally at the base of the Valanginian (n2) which overlies the Tithonian (j9) limestone. In the Ravin de Teillon section (Fig. 4.28), the salt is overlain by the Tithonian limestone, and both are in direct

contact with the Valanginian sediments (n2) along one of the normal faults. Normal fault development may have been responsible for the extensional thinning of the Kimmeridgian-Tithonian (j7-8 and j9) section. N of the Ravin de Teillon section, the thickness of the Tithonian limestone is only a few meters (Fig. 4.28). Further to the N, the overturned section is overlain by Tertiary sediments.

The structural style is far simpler on the northern flank of the la Lagne syncline where the exposed Kimmeridgian-Valanginian section dips gently to the SSE. The Berriasian (n1) and Valanginian (n2) are unconformably overlain by Tertiary sediments. The la Lagne syncline is separated from the small la Maline syncline by the Crête du Rus anticline. Kimmeridgian limestone is exposed in the core of this anticline (Fig. 4.27).

To the NNE, on the southern flank of the la Maline syncline, the Kimmeridgian-Valanginian section dips steeply to the NNW. Berriasian and Valanginian sediments are exposed in the core of the syncline. On northern flank of the la Maline syncline Oxfordian-Tithonian section is exposed which is in direct contact with the salt and steeply dipping to the SSE or locally overturned to the N along the WSW-ENE oriented Crête de Rus diapir (Fig. 4.26). A Liassic-Middle Jurassic section is presumably present below the Oxfordian-Valanginian section in the la Maline syncline (Fig. 4.29). The thickness of the Liassic-Lower Cretaceous section is around 400 m on the flanks la Maline syncline and presumably thickens towards its core (around 800 m) (Fig. 4.29).

The WSW-ENE oriented Crête de Rus diapir and the Crête de Rus anticline separate the la Maline syncline and la Lagne synclines from the St-Barnabé syncline (Fig. 4.25, Fig. 4.26). However, E of the town of Castellane, Valanginian strata (n2) are folded over the crest of the W-plunging anticline and diapir and the la Lagne and St-Barnabé synclines merge together (Fig. 4.25, Fig. 4.26).

N of the Crête de Rus diapir, on the southern flank of the St-Barnabé syncline, a Triassic-Upper Cretaceous section is exposed which is overturned to the N. Around the western extent of the diapir, the Norian argillite (t7-9) is exposed and it is overlain unconformably by the Bajocian cherty limestone (j1S) (Fig. 4.26, the Norian argillite and the unconformity at the base of the Bajocian limestone are not shown on Fig. 4.29). The Bajocian is overlain by the Bajocian-Callovian marly limestone (j2-3). ESE of the village of Demandolx, the salt is overlain directly by the Bajocian-Callovian marly limestone (j2-3) which is unconformably overlain along the Crête de Rus diapir by the Oxfordian limestone (j5-6) (Fig. 4.26). Like on the southern flank of the la Lagne syncline, the Callovian grey marl (j3) is missing between the Bajocian-Callovian marly limestone and the Oxfordian limestone. Both the Middle- and Upper

Jurassic sections are reduced. The thickness of the Middle Jurassic section is around 100 m. The Kimmeridgian-Tithonian section is approximately 200 m thick. The Cretaceous section is composed of the same succession as the les Combes syncline (Fig. 4.26, Fig. 4.29). The Cretaceous section is slightly thicker than on the southern flank of the les Combes syncline (approximately 480 m). In addition, the Jurassic and Cretaceous sections thicken towards to N. In the core of the syncline the complete thickness of the Mesozoic section is around 1500-1600 m which is much thicker than in the core of the les Combes syncline and similar to the thickness of the fill of the Taloire minibasin of the Mesozoic slope minibasin domain (see Chapter 4, § 4.1.1.6). The lower part of the section, i.e., the Middle and Upper Jurassic dip steeply (around 60-70º) to SSE whereas more gentle dips were measured in the Lower Cretaceous section, which dips around 30º to SSE. To the N, the St-Barnabé syncline is bounded presumably by a steep, roughly E-W trending fault (Fig. 4.24, Fig. 4.25, Fig. 4.26). Along this major fault, the Valanginian-Cenomanian (n2 to n7-c1) section of the syncline is in direct contact with the Triassic-Upper Cretaceous (tG to n7-c1) section and overlying Eocene sediments (e) of the la Blache-Castellane thrust sheet (Fig. 4.24 Fig. 4.25).

4.1.2.3 The southern part of the la Blache-Castellane thrust sheet

The la Blache-Castellane thrust sheet carries a thick, relatively undeformed Triassic-Upper Cretaceous section (Fig. 4.24 and Fig. 4.26). The Jurassic-Cretaceous section was deposited in the basin palaeogeographic zone of the Dauphinois and Vocontian basins (Fig. 4.25). The thrust sheet is structurally less complex than the Teillon thrust sheet. However, the La Blache-Castellane thrust also carries salt structures like the Castellane diapir which is exposed around the town of Castellane and the salt-cored Castillon anticline, E of the Lac de Castillon lake (Picard, 1965). The la Blache-Castellane thrust sheet is overridden by the Lambruisse-Lauppe thrust sheet which also carries a thick basinal Jurassic-Cretaceous section.

The Castillon anticline is a tight salt cored anticline, and it is situated N of the village of la Cité (Fig. 4.30). The anticline is roughly WNW-ESE oriented and formed in the hanging wall of a WNW-ESE trending fault (Fig. 4.24, Fig. 4.25 and Fig. 4.30). Along this fault, Triassic gypsum, Rhaetian dolomite (t10) and a Liassic-Lower Cretaceous section (from l1-2 to n2) possibly overthrusted a Tithonian-Valanginian (from j9 to n2) section (Fig. 4.30). The frontal

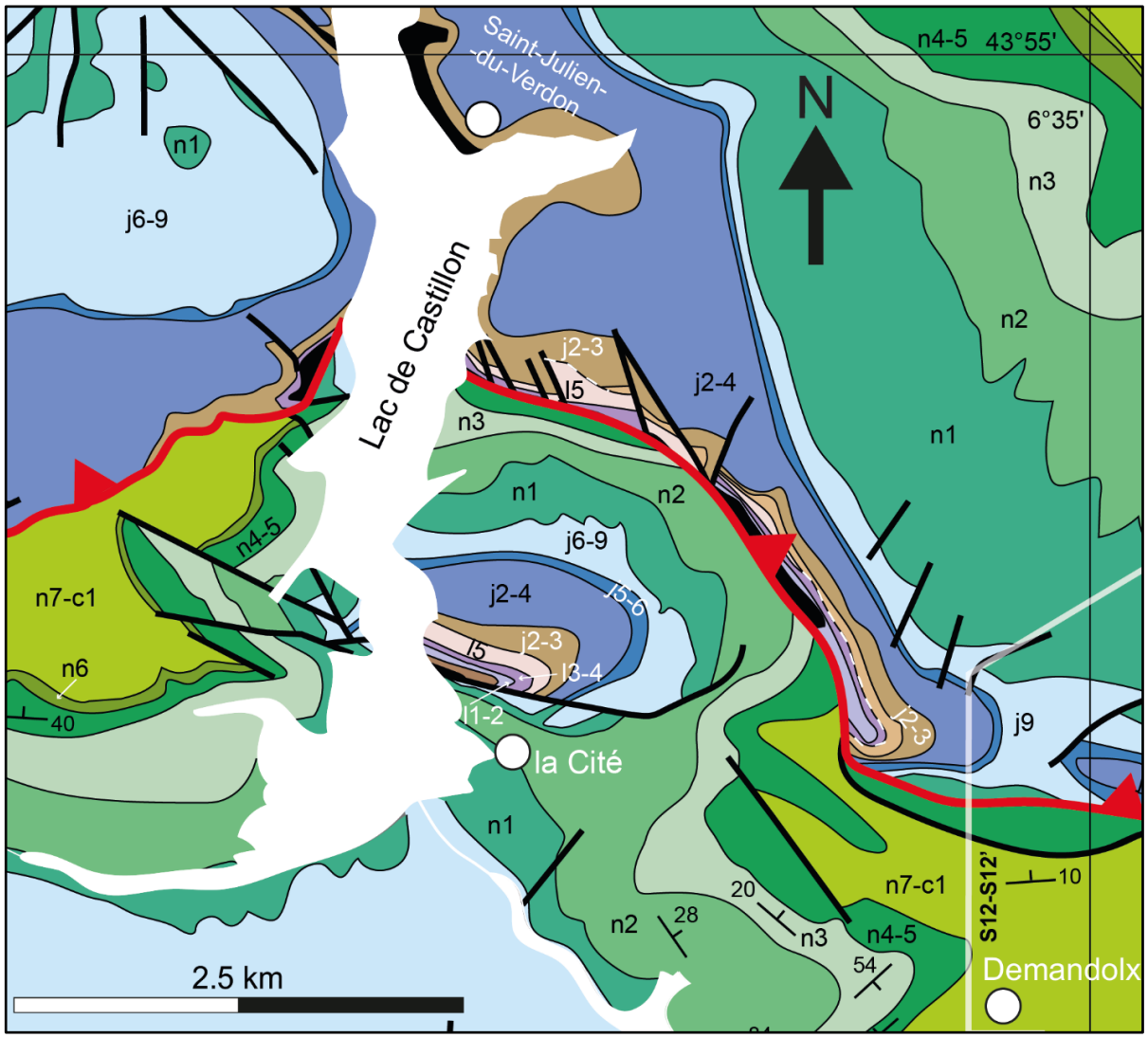


Fig. 4.30 Detailed geological map of the Castillon anticline, N of the village of la Cité and E of the Lac de Castillon. Note local unconformities at the base of the Bajocian (j1S) and Bajocian-Callovian (j2-3) formations in the hanging wall of the overriding Lambruisse-Lauppe thrust. See Fig. 4.24 for location. Note that the nortern part of the detailed map is not shown on Fig. 4.24. See Fig. 4.26 for key.

limb of the anticline is overturned to the S while its backlimb dips towards to NNE around 50º. Local unconformities, pinch-outs or young-on-older contacts were not observed in the Jurassic-Cretaceous section. Minor unconformities only formed locally at the base of the Bajocian (j1S) and the Bajocian-Callovian (j2-3) in the hanging wall of the overriding Lambruisse-Lauppe thrust. However, the thickness of the basinal Jurassic and Cretaceous sections of the Castillon anticline are reduced, compared to the average thickness of the basinal section of the Dauphinois and Vocontian basins (Fig. 2.7). The thickness of the Jurassic section (from l1-2 to j6-9) is around 450 m and the Lower Cretaceous section (Berriasian to Barremian, from n1 to n4-5) is only 200 m. In contrast, the thickness of the Jurassic section in the overriding Lambruisse-Lauppe unit is around 750 m and the Berriasian-Barremian section of the la

Blache-Castellane thrust sheet is around 500 thick, NW of the village Demandolx, only 2-3 km to the SE from the Castillon anticline.

The Castellane diapir is situated SW of the Castillon anticline. N of the E-W oriented fault, which is bounding the St-Barnabé syncline and the Mesozoic slope palaeogeographic domain from the north, a thick Triassic-Upper Cretaceous basinal section forms an eastward plunging anticline (Fig. 4.26). E of the village of Demandolx, between the axis of the anticline and the presumably steep, roughly E-W trending fault, Upper Cretaceous sediments (c2-3) strata folded into a syncline and overlain by Eocene and Oligocene sediments (e and Ol). The frontal limb of the anticline is vertical or overturned to the S (Fig. 4.24, Fig. 4.25, Fig. 4.26).

The Castellane diapir is apparently represents the core of this anticline and it comprises three elongated Keuper gypsum and cargneule breccia bodies (tG) (Fig. 4.24, Fig. 4.25, Fig. 4.26). The diapir also exposes hundred metres scale blocks and slivers of gypsum (Lower Gypsum, t2G) and limestone of the Middle Triassic Muschelkalk Formation (t2) (Fig. 4.6 and Fig. 4.26). Surface exposure of the Triassic gypsum and cargneule breccia is approximately 2.3 km^2. The core of the diapir lies in the centre of the town of Castellane. The E-W trending segment of the la Blache-Castellane thrust fault curves into an NW-SE trending segment at the junction where the three gypsum bodies merge and form the Castellane diapir (Fig. 4.25). Along its E-W trending segment, the la Blache-Castellane thrust fault overrides the slope palaeogeographic domain, i.e. the St-Barnabé syncline and the merged la Lagne syncline of the Teillon thrust sheet and the Taloire minibasin (Fig. 4.1, Fig. 4.2, Fig. 4.31). Along its NW-SE trending segment, the thrust overrides the Haute Sionne syncline and the Taulanne minibasin (Fig. 4.2, Fig. 4.6, Fig. 4.24, Fig. 4.31). The hanging wall stratigraphy of the la Blache-Castellane thrust shows affinities to the typical basin facies of the Dauphinois and Vocontian basins (Fig. 2.7). The Liassic is composed of Hettangian bioclastic limestone (l1-2), Sinemurian marly limestone (l3-4) and Pliensbachian cherty limestone (l5). However, the Upper Liassic (i.e. the Toarcian) and also the Aalenian is reduced or locally missing in the la Blache-Castellane thrust and in the Lambruisse-Lauppe sheet (Fig. 4.6, Fig. 4.26) (Kerckhove & Roux, 1976a; Kerckhove & Roux, 1976b; Kerckhove & Roux, 1978a; Kerckhove & Roux, 1978b). The thickness of the Liassic section is around 200-250 m.

The Middle Jurassic is represented by Bajocian-Callovian marly limestone (j2-3) which gradually passes up into the Callovian-Oxfordian Terres Noires Formation (j2-4) (Fig. 4.6, Fig. 4.26). The thickness of the Bajocian-Callovian section is approximately 100-120 m. The Terres Noires is 300-350 m thick (Kerckhove & Roux, 1978b)

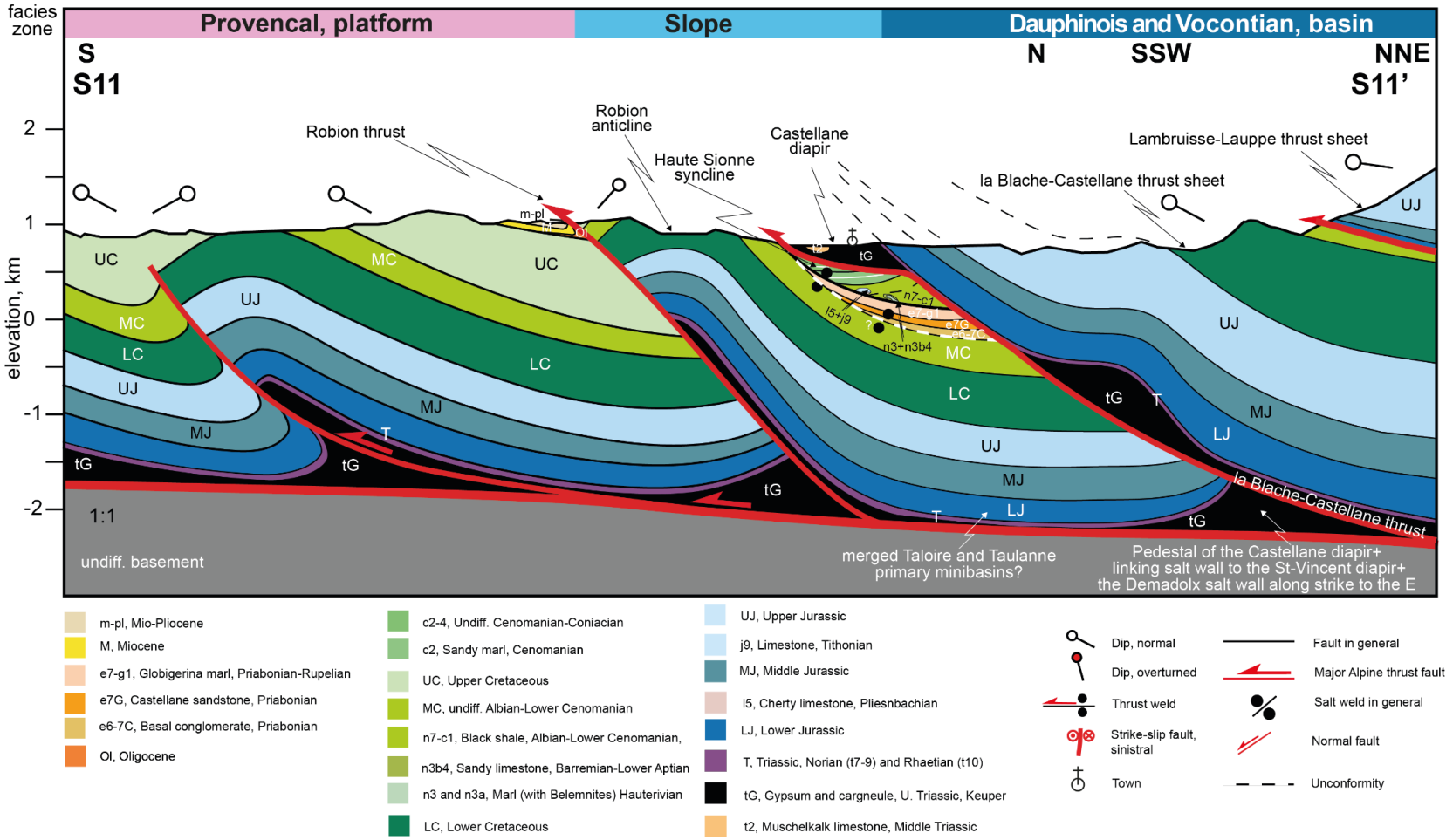


Fig. 4.31 Cross section (S11-S11') from the Provençal platform to the basinal Lambruisse-Lauppe thrust sheet, crossing the slope palaeogeogrpahic domain and the la Blache-Castellane thrust sheet. See Fig. 4.24 and Fig. 4.25 for cross section location.

The Terres Noires is overlain by the Oxfordian limestone which is overlain by the limestone dominated Kimmeridgian-Tithonian section (j6-9) (Fig. 4.6, Fig. 4.26). The thickness of the Upper Jurassic limestone dominated succession is around 150 m. The thickness of the Lower Cretaceous section is around 750 m (Fig. 4.31).Cross-section construction revealed that the Jurassic-Cretaceous sections of the la Blache-Castellane thrust sheet thicken toward to NE and NNE (Fig. 4.31). Thickening of the Mesozoic section from the platform edge towards the NE through the slope facies zone was also described by Kerckhove & Roux (1976a); Kerckhove & Roux (1976b); Kerckhove & Roux (1978a); Kerckhove & Roux (1978b). Along strike of the la Blache-Castellane thrust to the NW, abrupt thickness changes were also observed: at the village of Boades, in the hanging wall of the thrust the thickness of the Liassic is less than 200 m, the Middle Jurassic (j2-3) is around 100 m. The Upper Jurassic section is approximately 500 m, similar to the thickness of the Upper Jurassic NE of the Castellane diapir (Fig. 4.31). The Lower Cretaceous is slightly thinner NE of the village of Boades, approximately 600 m (Fig. 4.24).

Anomalous stratigraphic relationships were only observed locally, around the town of Castellane. Along the NW-SE trending segment of the la Blache-Castellane thrust sheet the complete Liassic section abuts against the Upper Triassic evaporites (Fig. 4.8). N of the Verdon River, on the backlimb of the anticline which formed along the E-W trending segment of the thrust, the Liassic abuts against the salt. In addition, the salt is in direct contact with the Bajocian-Callovian (j2-3) marly limestone (Fig. 4.26).

4.1.2.4 Interpretation of the Destourbes thrust sheet, the Teillon thrust sheet and the southern part of the la Blache-Castellane thrust sheet

Based on the observed stratal and structural geometries, thickness changes of the Jurassic-Upper Cretaceous section and the reinterpretation of anomalous contacts and Alpine compressional structures within the Destourbes and Teillon thrust sheets, I suggest that salt tectonic activity was more widespread spatially along the northern edge of the Mesozoic platform during Jurassic and Lower Cretaceous times. Diapirs and intervening minibasins are exposed in the slope palaeogeographic domain E of the Chasteuil area. The described primary minibasins, small, elongated depocenters subsided into the autochthonous Keuper evaporites during the Jurassic, Early Cretaceous and also the Albian-Cenomanian, simultaneously with salt-withdrawal from below the minibasins and the migration of salt into the bounding salt structures, e.g., the Teillon or Crête de Rus diapirs (Fig. 4.32).

The Destourbes thrust sheet display less evidence of salt tectonics. However, the anomalous stratigraphic relationships in the hanging wall of the thrust may indicate early salt tectonic activity. The observed local unconformities like the unconformity at the base of Bajocian-Callovian marly limestone (Fig. 4.26) may have been developed on the flank of an early diapiric structure, the Destourbes salt structures (Fig. 4.33). According to Kerckhove & Roux (1976a), the Aalenian is missing in the hanging wall of the Destourbes thrust, which indicates the presence of a palaeotopographic high during the late stages of the Tethyan rifting. The direct contact of the Tithonian limestone and the Albian-Cenomanian sediments with the Keuper gypsum (Fig. 4.26) may recorded the local exposure of the diapiric salt during Late Jurassic and Albian-Cenomanian times. The orientation of the NW-SE trending salt structure may have been oblique to the northern edge of the Mesozoic Provençal platform (Fig. 4.33). The Destourbes salt wall was situated between the Taloire minibasin and the Destourbes area. However, this interpretation is highly speculative.

The Teillon thrust sheet displays more clear evidence of early diapiric activity. Local thickness changes between the cores and flanks of the synclines, pinch-outs, the presence of incomplete sections and anomalous contacts in the Jurassic-Cretaceous section around the diapiric structures and anticlines suggest that the WSW-ENE trending synclines carried by the Teillon thrust are primary minibasins. These minibasins were bounded by approximately WSW-ENE trending elongated salt structures (Fig. 4.32 and Fig. 4.33). Most of the salt structures were relatively broad and parallel to the northern edge of the Mesozoic platform (Fig. 4.32 and Fig. 4.33).

However, some of the salt bodies, like other salt structures of the slope facies zone were oblique to the structural trend of the platform edge and some of these oblique structures may have been linked into WSW-ENE trending salt structures (Fig. 4.33). This may have led to the formation of a polygonal network of salt structures around isolated depocenters, similarly to the Northern Gulf of Mexico where minibasins are separated by a network of salt ridges (Rowan & Vendeville, 2006) (see § 4.3).

Occurrence of thin and incomplete Liassic sections on the flanks of the Teillon diapir suggests that the salt structures started to grow as early as the Liassic like other salt structures of the slope facies, e.g., the Chasteuil salt structure (see § 4.1.1.7). The initiation of salt tectonics may have been related to the Liassic-Middle Jurassic rifting of the margin. I assume that salt walls and diapirs of the Teillon thrust sheet were also initiated as reactive diapirs during the Liassic. However, the effects of regional extension in the initiation of salt tectonics in the Teillon area is only inferred because the salt structures were detached from their original

basement (Graham et al., 2012; Célini et al., 2020; Brooke-Barnett et al., 2020; Csicsek et al., 2021; Brooke-Barnett et al., 2021; Brooke-Barnett, 2022; Célini et al., 2022).

The Teillon diapir separated the les Combes minibasin from the la Lagne minibasin (Fig. 4.32, Fig. 4.33). The Crête de Rus diapir and the Crête de Rus anticline presumably formed two topographic highs over the wide Crête de Rus diapir (Fig. 4.32). The smaller la Maline minibasin was bounded to the N and to the S by these topographic highs during the Jurassic and Early Cretaceous (Fig. 4.32). Alternatively, the la Maline depocenter maybe started to form later, over the exposed Crête de Rus diapir during the Late Jurassic. The minibasin is narrow and older rocks than the Oxfordian limestone (j5-6) are not exposed in the la Maline minibasin. If that is the case, the la Maline minibasin formed as a bowl minibasin, which subsided into the previously formed allochthonous salt body of the Crête de Rus diapir. Thus, it is considered as a special type of secondary minibasin because it rests on allochthonous salt (Fig. 1.4) (Jackson & Hudec, 2017; Granado et al., 2019).

The Crête de Rus diapir separated the St-Barnabé and the la Maline minibasins (Fig. 4.32, Fig. 4.33). The Teillon diapir linked into the Crête de Rus diapir at the junction of the la Lagne and la Maline minibasins (Fig. 4.33). The Crête de Rus diapir may have been linked into the St-Vincent diapir through a curved and deeply buried salt wall. I assume that this deeply buried salt structure corresponds to the SE plunging la Grau anticline which divided the Taulanne minibasin into two large depocenters (Fig. 4.33). This salt wall was located on the basinward side of the slope palaeogeographic domain (shown by a dashed line between the St-Vincent diapir and the Crête de Rus diapir on Fig. 4.33). Hence, the St-Barnabé minibasin was also continuous to the WNW and NW and it corresponds to the primary minibasin NE of the la Grau anticline diapir which is located now below the Haute-Sionne syncline and the la Blache-Castellane thrust sheet (Fig. 4.5, Fig. 4.33).

Two inferred diapiric structures separated the slope from the platform and basin palaeogeographic domains: the la Garde salt wall and the Demandolx salt wall (Fig. 4.32 and Fig. 4.33). The thinning of the Lower Cretaceous section of southernmost les Combes minibasin towards the E-W trending segment of the Teillon thrust fault suggest that this depocenter may have been bounded to the S by an inferred salt structure, the la Garde wall which separated the platform from the slope facies zone (Fig. 4.32 and Fig. 4.33) but more precise description is not possible.

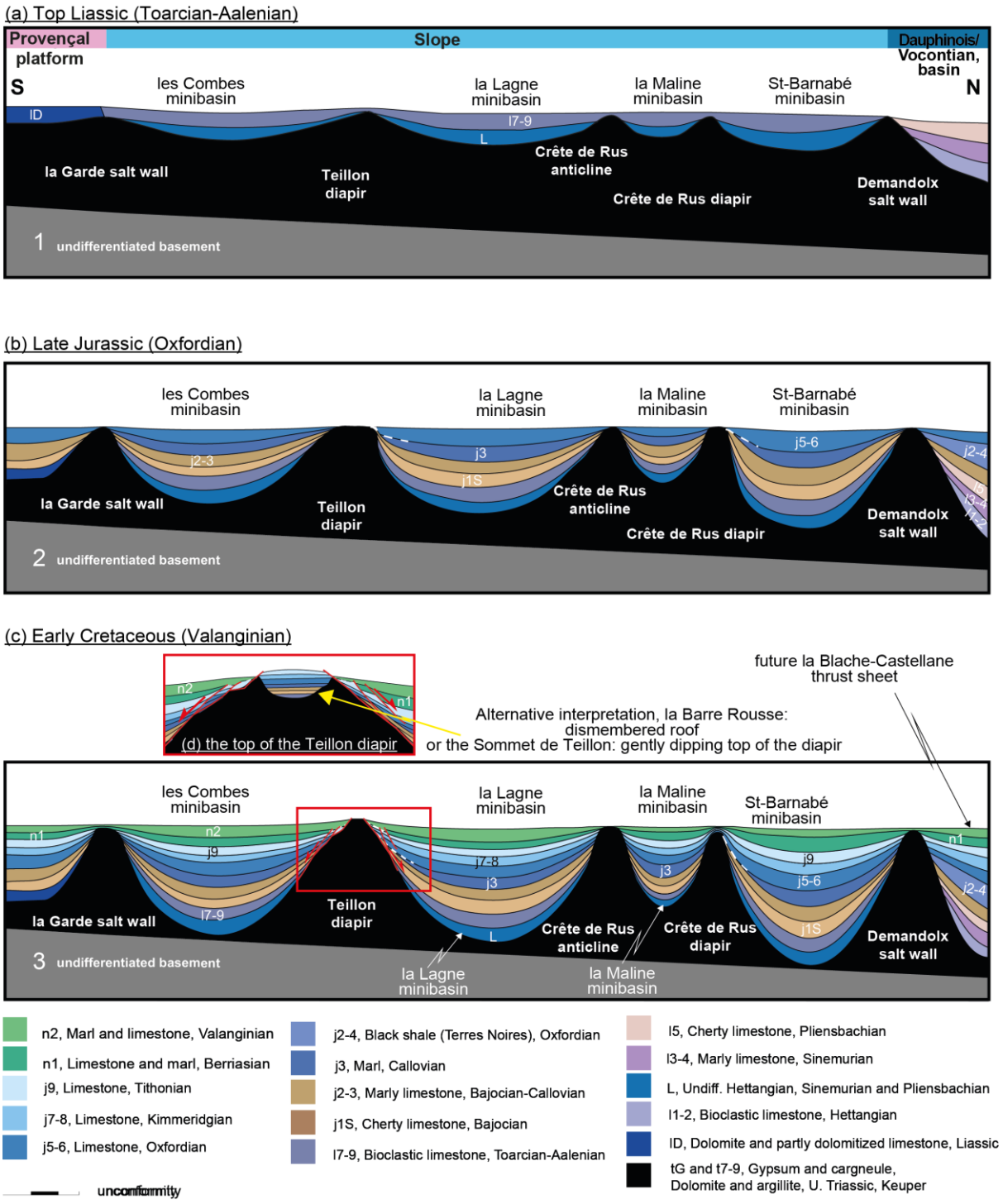


Fig. 4.32 Diagrams shoving possible Early Jurassic-Early Cretaceous evolution of the salt diapirs and walls, and the intervening minibasins now located in the Teillon thrust sheet (not to scale) from the Liassic (a) to the Valanginian (c). The salt structures and the minibasins formed in the slope palaeogeographic domain. (d) Zoom of the top of the Teillon diapir. The roof of the diapir was dismembered by extensional faults, presumably during Berriasian-Valanginian.

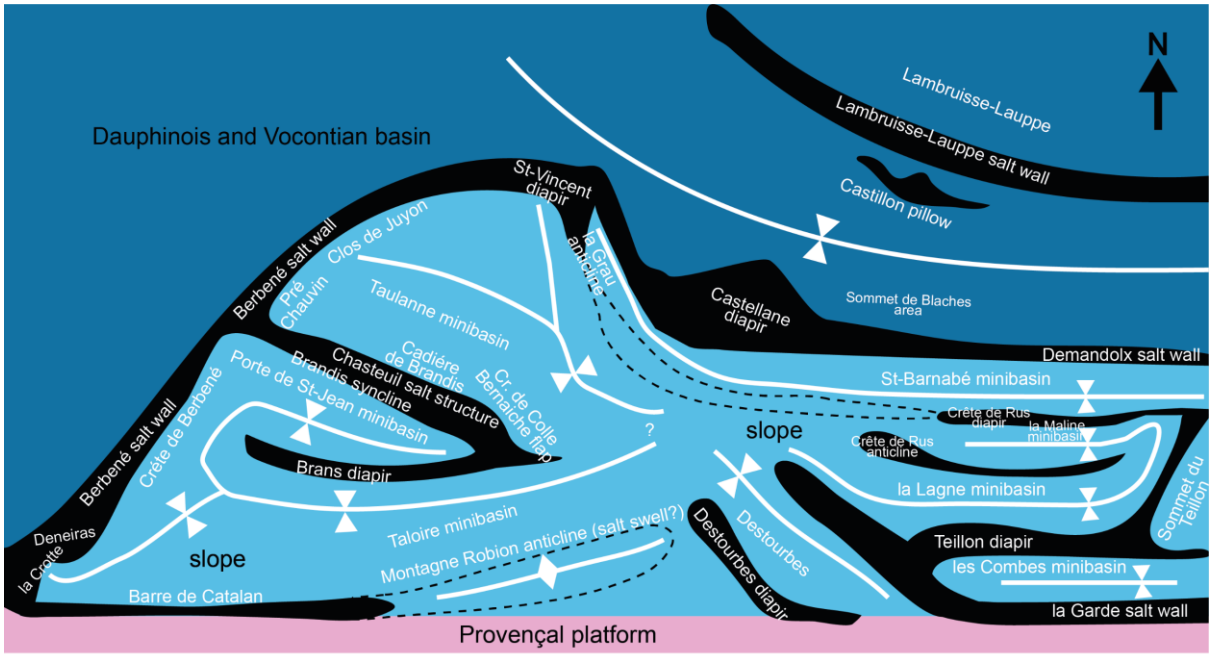


Fig. 4.33 Simplified map view of the eastern part of the southern structural domain. The map is not restored and only showing the approximate palisnpastic position of the minibasins and their bounding salt structures. Dashed lines show assumed salt structures. Fig. 4.23 was slightly modified based on the position of salt structures and minibasins to the ESE. Note that the complex network of salt walls, diapirs and primary minibasins was located between the Provencal platform and the pelagic domain. In the eastern part of Dauphinois and Vocontian basins only an elongated salt wall and the small Castillon pillow formed. Fig. 4.23 is modified and newly identified salt structures and bounding minibasins are shown here.

The la Garde salt wall presumably bounded the les Combes minibasin to S and merged with the westernmost extent of the Teillon diapir to form a NW-SE trending salt wall (Fig. 4.33).

The vertical and thin Jurassic section on the northern flank of the les Combes minibasin (Toarcian-Aalenian, l7-9 to Tithonian, j9) abut against the remnant of this salt body This wall bounded the les Combes and also la Lagne minibasins to the W (Fig. 4.33).

The overturned and incomplete Liassic-Middle Jurassic section of the southern flank of the la Lagne minibasin also abut against the Keuper gypsum of the merged la Garde-Teillon salt structure. NE of the village of la Garde, the salt is overlain by the Bajocian cherty limestone (j1S) and the Keuper is also in direct contact with the Oxfordian (j5-6) limestone (Fig. 4.26). This suggests that the merged Teillon-la Garde salt structure was active and exposed throughout the Middle- and Late Jurassic.

The northernmost St-Barnabé minibasin and the slope facies zone was bounded to the N by the inferred Demandolx salt wall which is not exposed at the surface (Fig. 4.29). The pedestal of this salt wall is possibly situated now at the depth of 2.5 km, below the la Blache-Castellane thrust sheet (Fig. 4.31). The Demandolx salt wall was reactivated during the Alpine compressional phase as a steep, sinistral strike-slip fault which is forming the E-W trending segment of the la Blache-Castellane Alpine fault, E of the town of Castellane.

The diapiric activity was continuous through the Middle and Late Jurassic in the northern part of the Teillon thrust sheet: evidence for this activity can be seen around the Crête de Rus diapir where the salt is overlain by overturned Bajocian (j1S) and Bajocian-Callovian (j2-3) strata. Salt tectonic activity occurred also during the Late Jurassic: it is recorded by the base-Oxfordian unconformity on the southern flanks of the St-Barnabé minibasin and the la Lagne minibasin.

Diapirism may have been maintained by differential loading over the autochthonous salt layer during the Middle and Late Jurassic and salt structures grew passively during the later stages of the rifting and the early stages of the passive margin phase (Fig. 4.32). The Demandolx and la Garde salt walls and the Crête de Rus diapir may have been exposed over short periods or covered by a thin roof (Fig. 4.32b). However, only minor local unconformities were observed and halokinetic sequences not developed along the diapirs. Instead, large, minibasin-scale wedges formed between the rising salt structures (Fig. 4.29, Fig. 4.32) (Rowan et al., 2016; Rowan & Giles, 2021; Rowan & Giles, 2023) which is indicated by stratal geometries, thinning, and folding of the Jurassic-Early Cretaceous section. The lack of slumps or breccia levels on the flanks of the gypsum bodies suggests that the salt structures were probably broad, and gentle salt structures such as anticlines, diapirs or walls (Fig. 4.32).

The Teillon diapir was partly buried under a relatively thin roof during the Middle- and Late Jurassic (Fig. 4.32a and b). The sedimentation was able to keep up with the growth of the diapiric structure in the eastern part of the diapir, at least until the Late Jurassic. I assume that the Sommet du Teillon and Sauvegarde areas are representing this roof (Fig. 4.28). The gently dipping and reduced Middle-Upper Jurassic section of the Sommet du Teillon area and the small and narrow syncline which is formed of Bajocian (j1S), Bajocian-Callovian (j2-3) and Callovian (j3) rocks may have been deposited on the top of the Teillon diapir (Fig. 4.32d). The large Tithonian limestone (j9) block of the la Barre Rousse area which is separated from the gently dipping section of the Sommet du Teillon section and the eastern flank of the la Lagne minibasin by the Keuper gypsum is also representing the dismembered roof of the diapir (Fig. 4.28). The diapir roof was dismembered presumably along the extensional faults exposed now in the overturned eastern flank of the la Lagne minibasin (Fig. 4.28 and Fig. 4.32). These normal faults are apparently overturned and sealed by the Berriasian (n1) or Valanginian (n2) sediments, which suggest diapirism has slowed down or ceased during the Berriasian-Valanginian. The unconformity at the base of the Valanginian also developed during this stage of the evolution of the Teillon diapir (Fig. 4.32c). The direct contact of the Tithonian limestone (j9) and the Valanginian (n2) sediments with the Keuper in the Ravin de Teillon section is

interpreted as the evidence for the exposure of the salt in the footwall of an extensional fault (Fig. 4.28 and Fig. 4.32d). I assume that the normal faults formed prior to the overturning of the northern flank of the la Lagne minibasin. Similar faults, which crosscut the Middle-Upper Jurassic and the Upper Jurassic section along the diapir may have been formed also on the northern flank of the les Combes minibasin, but they are not preserved. A local change in the aggradation rate around the Teillon diapir or the load of an overburden wedge (maybe the depositional load of the thick platformal limestone, the Calcaires blancs, see Chapter 2), may have triggered the halokinetic active rise of the diapir during the Late Jurassic. The actively rising diapir arched its roof, which was extensionally thinned along the normal faults which may have formed due to extensional unroofing of the diapir and gravitational instability along its flank (Fig. 4.32d). However, this interpretation is highly speculative.

Evidence of Cretaceous salt tectonic activity can be seen on the SW flank of the la Lagne minibasin where the Kimmeridgian (j7-8) limestone is overlain by Berriasian sediments (n1) (Fig. 4.26). This unconformity may have formed on the flank of the NW-SE trending segment of the la Garde-Teillon salt body. The presence of this local unconformity recorded Early Cretaceous rise of the diapiric salt. The direct contact of the Triassic gypsum with the Valanginian (n2) in the hanging wall of the Teillon thrust, NW of the village of la Garde is also indicating the local Early Cretaceous exposure of the salt of the la Garde and the Teillon diapir (Fig. 4.32c).

The salt structures presumably continued to grow from the Hauterivian to the Albian-Cenomanian. The thinning of the Hauterivian-Cenomanian section towards the Teillon and Crête de Rus diapirs maybe related to the continuous rise of the salt. The Aptian-Cenomanian E-W trending palaeotopographic highs of the Teillon area, described by Cotillon (1985) and Cotillon (2010), in the transitional zone between the Vocontian basin and the Provençal platform presumably correspond to the earlier formed, E-W oriented salt walls and diapirs inherited from the Jurassic and Early Cretaceous. The approximately E-W trending fault in the core of the les Combes syncline is interpreted as a normal fault, which formed on the steep southern flank of the tall Teillon diapir during the Late Cretaceous and became vertical as the squeezing of the diapir occurred simultaneously with the overturning of the flanking strata. Alternatively, it may have been formed during the overturning of the flanks of the diapir, during the development of the fold and thrust belt.

During the Alpine compressional phase, the salt structures were squeezed, partly or completely welded and in some cases possibly reactivated as thrust faults or strike-slip faults (Fig. 4.29). Most of the salt cored anticlines and thrust faults in the Teillon thrust sheet, which

were previously interpreted as Alpine structures (Jacqmin, 1950; Kerckhove & Roux, 1976b), presumably formed prior to the onset of regional Alpine compression. The overturned section of the eastern flank of the la Lagne minibasin is interpreted as an overturned flap (Graham et al., 2019; Graham, 2022). Direct evidence for Mesozoic salt extrusion was not observed in the Teillon thrust sheet. Overturning of the flanking strata around the mushroom shaped Teillon and Crête de Rus diapirs possibly occurred later, during the Oligocene.

I assume that N of the Teillon and Destourbes thrust sheets, in the basinal la Blache-Castellane thrust sheet stratal geometries, anomalous contacts and thickness changes of the Jurassic-Cretaceous section, display simultaneous salt tectonic activity N of the slope facies zone, in a more basinward position.

The tight salt cored Castillon anticline is interpreted as a salt structure with a long growth history. The salt structure originally formed as a WNW-ESE trending salt pillow or anticline which developed in the Mesozoic basin palaeogeographic domain (Fig. 4.24 and Fig. 4.25). The Rhaetian (t10) dolomite, similarly to other locations of the southern structural domain, is considered as a pre-kinematic interval over the salt structure. The initiation of the growth of the Castillon salt pillow is unclear. The thickness of the Jurassic and also the Cretaceous section is reduced which displays a long growth history of the salt pillow. Local unconformities, pinch-outs or young-on-older contacts are absent. This suggests that the salt pillow was growing slowly from the Liassic onward, presumably due to halokinesis (Jackson & Hudec, 2017). The growth of the structure may have been maintained by lateral variations of the thickness or density of the overburden, which caused differential loading over the mother-salt layer and led to the growth of the pillow. The salt pillow was later highly modified by Alpine shortening.

The Castellane diapir shows more complex structural style and salt-related geometries than the Castillon anticline. The large exposure of the Triassic salt which exposes the hundred metres scale blocks and slivers of the Lower Gypsum (t2G) and the Middle Triassic Muschelkalk Formation (t2) (Fig. 4.6 and Fig. 4.26) is interpreted as a remnant of an early formed diapiric structure which was displaced by the la Blache-Castellane thrust and highly modified by Alpine compression (see Chapter 5, § 3.2). The salt structure possibly formed as a WNW-ESE trending salt diapir (Fig. 4.33). I assume that the diapir, similarly to the St-Vincent diapir which is also including large blocks of the pre-salt basement (i.e., the Lower Triassic Buntsandstein formation) developed over the footwall of a Tethyan extensional fault and the blocks of the pre-salt succession are inclusions lifted by the diapir from the fault scarp. The pedestal of the diapir is situated at the depth of 2.5-3 km, below the footwall ramp of the la Blache-Castellane thrust fault (Fig. 4.31) but more precise description is not possible.

The thinning of the Jurassic-Cretaceous basinal section in the hanging wall of the la Blache-Castellane thrust sheet, towards the Castellane diapir and the direct contact of the Liassic-Middle Jurassic section with the Upper Triassic Keuper indicate that the salt body was emergent during the Liassic and the transition from the rifting to passive margin phase.

The diapir may have been connected to the Demandolx salt wall during the Mesozoic (Fig. 4.33). The large, eastward plunging anticline which is situated N of the E-W trending segment of the la Blache-Castellane thrust is formed of the relatively thin Jurassic-Cretaceous section, deposited on the on the northern flank of the Demandolx diapir (Fig. 4.33). NW of the Castellane diapir and E of the village of Boades the Jurassic-Cretaceous basinal section is also relatively thin. This suggests that a continuous, presumably NW-SE trending salt structure was situated NW of the Castellane diapir. Because the slope palaeogeographic domain was limited to the N and NE by the St-Vincent diapir, I assume that the Castellane diapir may have been connected to the St-Vincent diapir by a deeply buried salt wall, similarly to the connection of the Crête de Rus diapir to the St-Vincent diapir (Fig. 4.33). Hence, the NW-SE trending segment of the St-Barnabé minibasin was bounded to the SW by the linking salt wall of the St-Vincent diapir and the Crête de Rus diapir, i.e., the la Grau anticline. To the NE, the minibasin was bounded and separated from the basin palaeogeographic domain by the linking salt wall of the Castellane diapir and the St-Vincent diapir (Fig. 4.33). The pedestal of this linking salt wall is presumably situated NE of the St-Vincent diapir, at the depth of 2.5-3 km below the la Blache-Castellane thrust sheet (Fig. 4.5). The St-Vincent diapir, the Castellane diapir and the Demandolx diapir represented the facies boundary between the basin and slope domains during Jurassic-Cretaceous times. Alternatively, the pedestal of the Castellane diapir may have been separated from the St-Vincent and the Demandolx salt structures and the diapir was later displaced by the la Blache-Castellane thrust.

In the same way as the Castellane diapir and the Crête de Rus diapir linked at depth to the St-Vincent diapir, I suppose that the St-Vincent salt structure was also connected to the Chasteuil salt structure by the Berbené salt wall (see §, 4.1.1.7). Hence, the Castellane and St-Vincent diapir developed as isolated diapirs and formed at the junctions of the of salt walls or ridges (Rowan & Vendeville, 2006). I assume that these ridges may have been parallel to Tethyan extensional faults at their original location, e.g., the NW-SE trending ridge between the Castellane and the St-Vincent diapirs because the ridge has an elongated shape, and it connects diapirs which comprise blocks of the pre-salt basement.

N of the Castellane diapir and the Castillon salt pillow, the minor local unconformities in the Lambruisse-Lauppe thrust sheet at the base of the Bajocian (j1S) and the Bajocian-

Callovian sediments (Fig. 4.30) may have been associated with pre-Alpine salt tectonic activity and possibly formed on the NE flank of an elongated salt wall, the Lambruisse-Lauppe salt wall (Fig. 4.33). This salt wall was maybe parallel with the linked salt body of the Demandolx salt wall and the linking wall between the Castellane diapir and the St-Vincent diapir (Fig. 4.33).

The reinterpretation of the Destourbes thrust sheet, the salt structures and the intervening synclines of the Teillon thrust sheet led to the following conclusion: the eastern part of the southern structural domain, E of the Chasteuil area, contain a well-developed minibasin and salt-ridge system which started from as early as the Liassic (Fig. 4.32 and Fig. 4.33). The minibasins and salt-ridge system represents the eastern continuation of the system of primary minibasins and their bounding salt structures of the Chasteuil area which developed between the Provençal platform and Dauphinois and Vocontian basins (Fig. 4.33). The anomalous contacts of the Cretaceous section with the Triassic salt and thickness changes of the post-Valanginian succession in the les Combes and St-Barnabé minibasins indicate that the salt tectonic activity continued during the later stages of the passive margin phase, beyond the Valanginian, at least until the Albian-Cenomanian.

The reinterpretation of the Castillon anticline and the Castellane diapir of the la Blache-Castellane thrust sheet indicates that salt tectonics was not restricted to the slope facies zone in the eastern part of the southern structural domain. In the basin facies zone, salt pillows, diapirs and salt walls also formed: the Castillon salt pillow, the Castellane diapir and the Lambruisse-Lauppe salt wall. The thickness changes of the Cretaceous section in the basin domain display that salt tectonics also continued in the la Blache-Castellane thrust sheet. The three large facies zones were separated during the Jurassic and Early-Middle Cretaceous by elongated and deeply buried salt ridges. At the junction of these ridges, isolated diapiric structures formed, e.g., the Castellane diapir. The salt tectonic activity was probably initiated by the Tethyan regional extension. The salt structures continued to grow as passive diapirs due to differential loading. However, the Teillon diapir may be experienced a short period of halokinetic active rise during the Jurassic-Cretaceous transition. Halokinesis may have been responsible for the long growth of the Castillon salt pillow from the Liassic until the Middle of the Cretaceous.

Further to the W and NW of the previously described Chasteuil area, the observed structural style, stratal geometries, facies, and thickness changes in the Jurassic-Middle- and Upper Cretaceous sections of the slope and basin palaeogeographic domain are comparable to the observed geometries in the eastern part of the southern structural domain. In the following

section, I describe and interpret the salt related structures of the slope and basin facies zone W of the Chasteuil area.

4.1.3 The Petit Mourre diapir and the adjacent synclines of the southern structural domain

The NW-SE trending Petit Mourre diapir or salt cored anticline and NW-SE trending synclines adjacent to the diapiric structure (the la Gondole, the Blieux, the le Chiran and the Grande Plaine synclines) are situated W of the previously described Chasteuil salt structure and the surrounding minibasins (see §, 4.1.1.7), in the western part of the southern structural domain (Fig. 2.1b, Fig. 4.34, Fig. 4.35). The Petit Mourre diapiric structure together with the adjacent synclines are bounded to the SE by the Berbené fault, whereas the la Gondole syncline is overridden by the Berbené fault and separated from the Taloire minibasin by the welded segment of the Berbené salt wall (Fig. 4.34, Fig. 4.35) (see §, 4.1.1.7). To the E, the Blieux syncline is in direct contact with the Bourbonne syncline along an anomalous contact (see Chapter 5, § 4) and separated from the Chasteuil salt structure, the Taulanne minibasin and the Boades zone by the NW-SE trending Berbené fault (Fig. 4.35). The Blieux syncline is bounded to the NE by the Montagne de Vibres thrust and the tip fold of the thrust, the Montagne de Vibres anticline (Fig. 4.35). The Petit Mourre anticline and the adjacent synclines have been considered as Alpine structures (Roux, 1972; Kerckhove & Roux, 1976a; Kerckhove & Roux, 1978a). However, anomalous contacts, local unconformities, young-on-older structures, rapid thickness and facies changes of the Jurassic-Cretaceous succession were observed in the Blieux syncline and around the Petit Mourre anticline (Cotillon, 1968; Beaudoin, 1969; Roux, 1972). The thickness and facies variations were considered being related to the normal faults inherited from the Tethyan rifting. During the rifting period and the subsequent passive margin phase, the la Gondole syncline was closer to the edge of the Provençal platform, next to the Taloire minibasin while the Petit Mourre diapiric structure and le Chiran, Grande Plaine and Blieux synclines were situated in the basinal palaeogeographic domain of the Dauphinois and Vocontian basins (Fig. 4.35) and overthrusted the slope palaeogeographic domain (Fig. 4.35). The Blieux syncline and the surrounding area had been studied by Roux (1972), who described the Petit Mourre anticline as a diapiric fold. In the following section, I am going to describe the la Gondole syncline, the overriding Petit Mourre diapiric structure and the observed structural and stratal geometries and salt related structures in the adjacent synclines: the le Chiran syncline, the Grande Plaine syncline and the Blieux syncline (Fig. 4.34, Fig. 4.35).

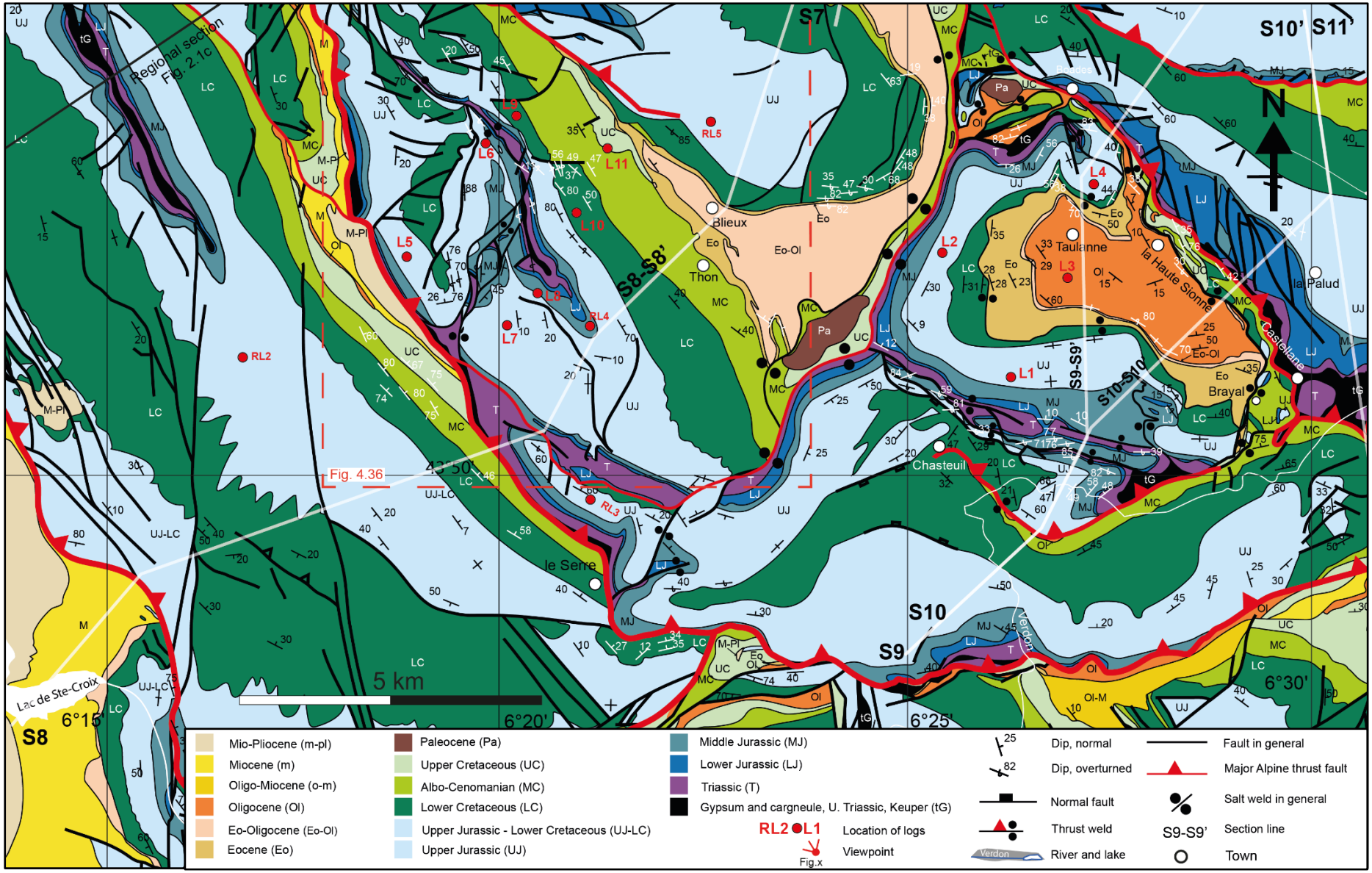


Fig. 4.34 Simplified geological map of the western part of the southern structural domain. Redrawn after Kerckhove & Roux (1976a) and Kerckhove & Roux (1978a).

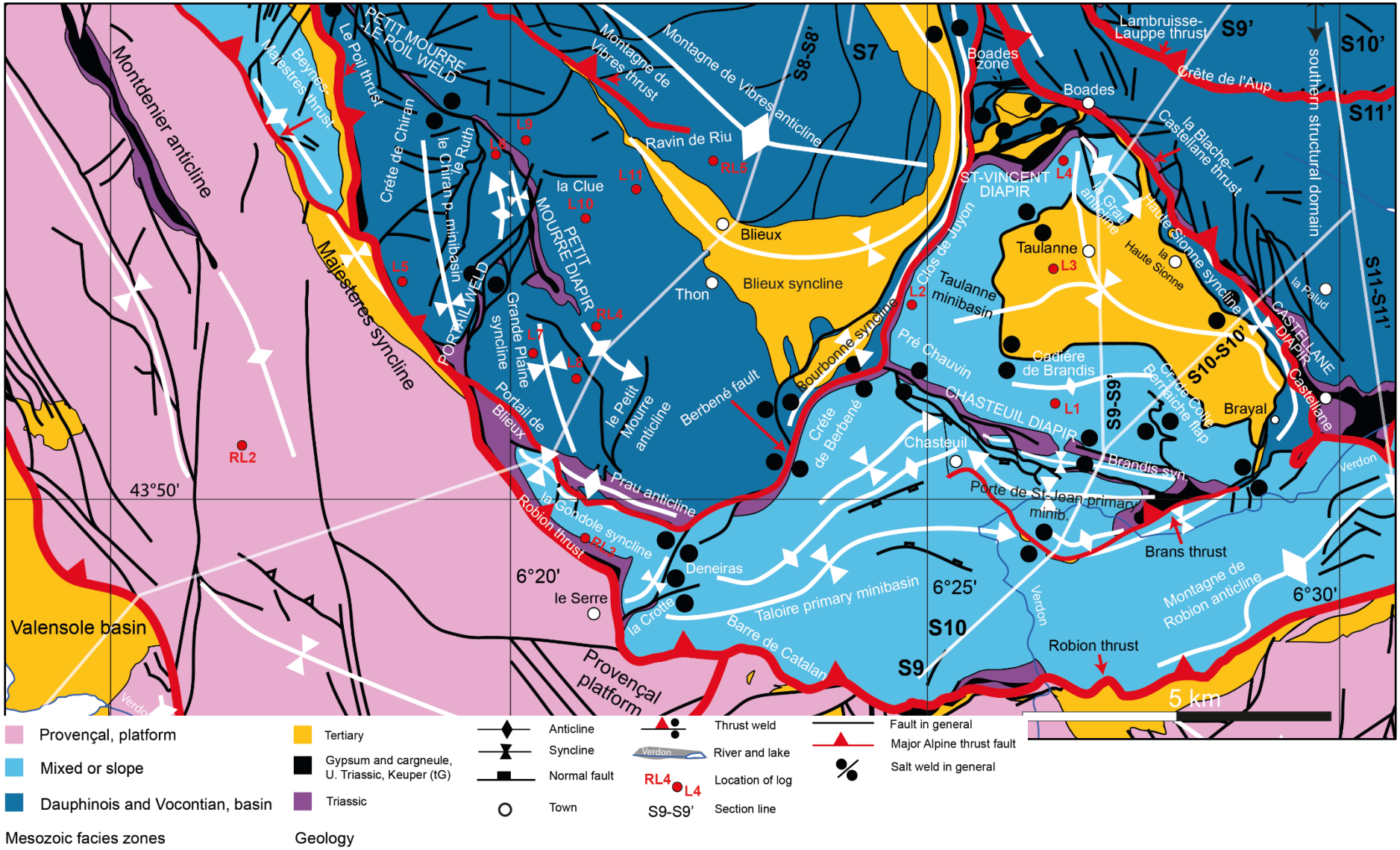


Fig. 4.35 Structural map of the western part of the southern structural domain, showing synclines, their bounding Alpine structures or pre-Alpine salt structures and their Mesozoic palaeogeographic position. Data from Kerckhove & Roux (1976a) and Kerckhove & Roux (1978a).

4.1.3.1 The la Gondole syncline. Structural and stratigraphic observations

The la Gondole syncline is situated west of the Taloire minibasin and southwest of the Porte de St-Jean minibasin and the Chasteuil salt structure (Fig. 4.35). Like the Taloire minibasin, the la Gondole syncline is also carried by the Robion thrust in its hanging wall. At the junction of the welded Berbené salt wall and the Robion thrust, E of the village of le Serre, the approximately E-W trending and S verging segment of the Robion thrust which carries the Taloire minibasin, curves into a NW-SE trending, SW verging thrust fault which carries the la Gondole syncline (Fig. 4.34, Fig. 4.35). The NW-SE trending segment of the Robion thrust overrides the Triassic-Upper Cretaceous section of the Provençal platform and also the Miocene (m) and Mio-Pliocene (m-pl) sediments deposited in the Majestres syncline which is a small piggyback-basin (Lickorish & Ford, 1998) (Fig. 4.34, Fig. 4.35, Fig. 4.39). Further to the northwest, the continuation of the Robion thrust is the SW verging Beynes-Majestres thrust (Fig. 4.35).

The la Gondole syncline is separated from the Taloire minibasin by the welded Berbené salt wall (Fig. 4.18). Along the weld, gently dipping (to the northeast) Norian-Tithonian section (t7-9 to j9) of the la Gondole syncline is in direct contact with the steeply dipping Norian dolomite and argillite (t7-9), the SE flanking strata of the welded Berbené salt wall (see § 4.1.1.6). Steeper dips were observed in the Kimmeridgian limestone (j7-8) along the weld (Fig. 4.18).

The upper part of the Kimmeridgian (j7-8) and also the Tithonian and Berriasian rocks of the la Gondole syncline (j9-n1) are in direct contact along the welded Berbené wall with the NE dipping, Liassic-Kimmeridgian section of the Deneiras cliff (see § 4.1.1.6 and § 4.1.1.7) (Fig. 4.17, Fig. 4.18, Fig. 4.34).

The La Gondole syncline is composed of a thin section of Triassic, Jurassic and Lower Cretaceous rocks folded into a tight, NW-SE trending syncline. The thickness of the Jurassic section is around 450 m. From the southeast to northwest, dips become overturned from normal on the northern limb of the syncline (Fig. 4.17, Fig. 4.34, Fig. 4.39). In the western part of the syncline, its northern limb is overturned to the SW and the thickness of the Jurassic section is reduced, approximately 270 m (Fig. 4.17). Here, between the NW-SE trending thrust segment of the Berbené fault and the Robion thrust, a large exposure of Keuper (argillite and dolomite, t7-9) is exposed (Fig. 4.36).

The succession of the la Gondole syncline deposited around the margin of the Provencal platform, at the upper part of the slope palaeogeographic domain of the Dauphinois and Vocontian basins (Fig. 4.35) (Kerckhove & Roux, 1978a). The Liassic (lD) and also the Bajocian (j1D) are represented by dolomite, similar to the section at the Créte de Berbené and the Montagne de Robion sections on the western limb of the Taloire minibasin (see §, 4.1.1.6) (Fig. 4.17). The Middle-Upper Jurassic section exhibit similar characteristics to the Middle- and Upper Jurassic section of the Taulanne minibasin, the Porte de St-Jean minibasin, and the Taloire minibasin (Fig. 4.6, Fig. 4.8, Fig. 4.17). The Lower Cretaceous is represented only by Berriasian limestone (n1) which is also identical to the Berriasian succession of the Taulanne, the Porte de St-Jean and the Taloire minibasins (Fig. 4.6, Fig. 4.8, Fig. 4.17). Angular unconformities, pinch-outs, slumps, or breccia levels are absent in the reduced section of the la Gondole syncline.

To the N, the syncline is bounded by a NW-SE trending thrust fault, which links into the NE-SW trending Berbené fault and represents its SW verging thrust segment (Fig. 4.34, Fig. 4.35). At the NW termination of the la Gondole syncline, the Robion thrust is apparently overridden by the NW-SE trending thrust segment of the Berbené fault, which carries basinal rocks in its hanging wall. The along-strike continuation of the Berbené fault is the Le Poil thrust (Fig. 4.34, Fig. 4.35) which overthrusted the Beynes-Majestres thrust sheet. The succession of the Beynes-Majestres thrust sheet represents the slope palaeogeographic domain (Fig. 4.35).

4.1.3.2 The Petit Mourre diapiric structure and adjacent synclines: the le Chiran, Grande Plaine and Blieux synclines

The NW-SE trending Petit Mourre diapir is situated N of the la Gondole syncline, in the hanging wall of the NW-SE trending thrust segment of the Berbené fault and its western continuation, the le Poil thrust (Fig. 4.34, Fig. 4.35, Fig. 4.36). The SW verging thrust segment of the Berbené fault and the le Poil thrust overthrusted the la Gondole syncline and also the Triassic-Upper Cretaceous section of the Provençal platform and the Majestres syncline (Fig. 4.34, Fig. 4.35, Fig. 4.38). Further to the NW, the le Poil thrust is overriding the Beynes-Majestres thrust sheet which represents the slope palaeogeographic domain (Fig. 4.35).

The Petit Mourre diapir is forming a tight salt cored anticline with steeply dipping or slightly overturned north-eastern and south-western flanks (Fig. 4.36, Fig. 4.37). Between the le Portail de Blieux area and the la Clue section, the Keuper gypsum is exposed over an area of ~ 0.2 sq.

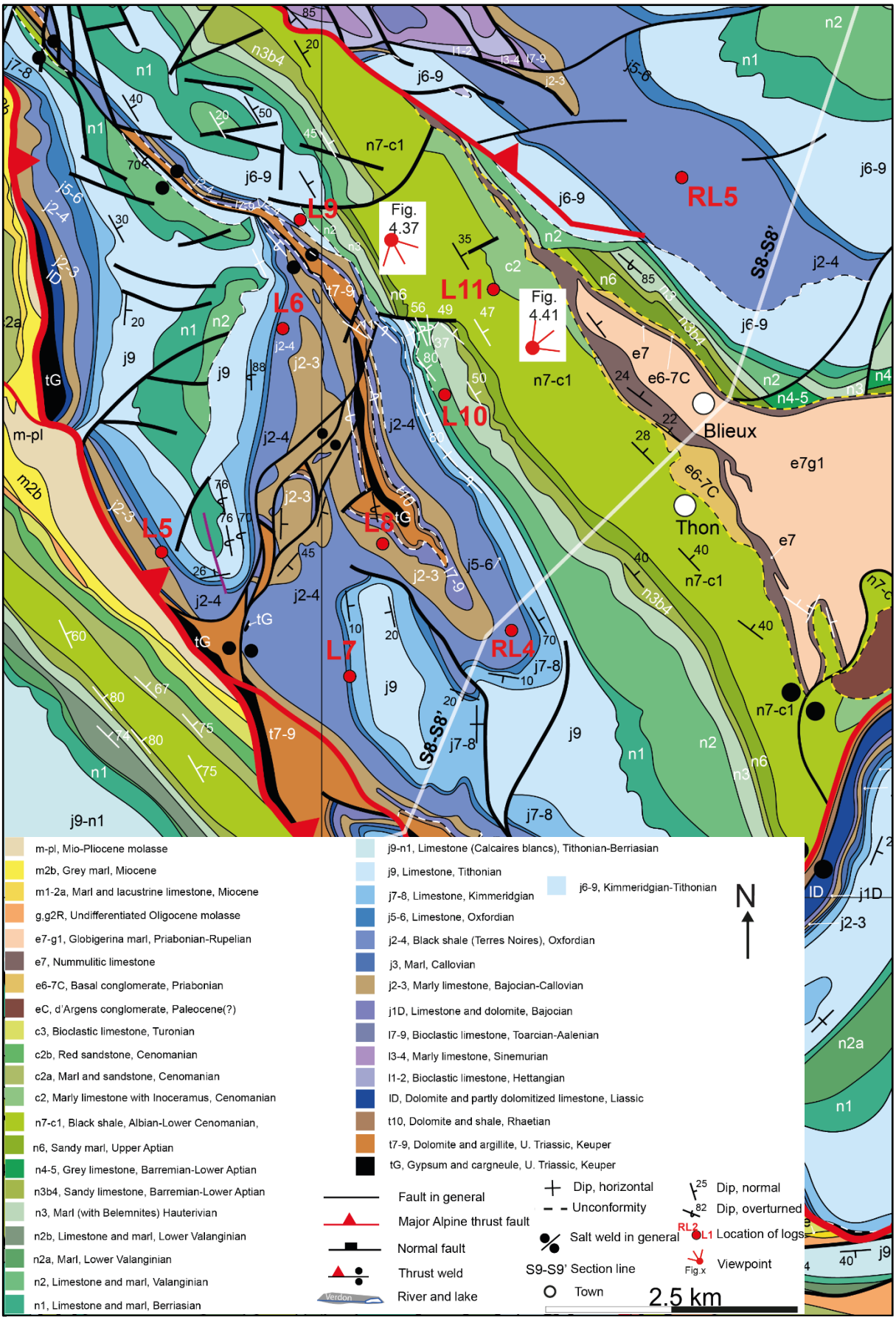


Fig. 4.36 Detailed geological map of the Petit Mourre diapir and the surrounding synclines. See Fig. 4.34 for location and Fig. 4.35 for structural explanation.

km (Fig. 4.34, Fig. 4.35, Fig. 4.36) Further to the SE, the diapir is linked into the Petit Mourre anticline (Fig. 4.35). The Petit Mourre anticline is plunging to the SE. To the NW, the diapiric gypsum is missing at the surface (Fig. 4.36) and only the overlying Norian argillite (t7-9) exposed in the core of the anticline (shown as Petit Mourre-le Poil weld on Fig. 4.35).

The Petit Mourre diapir is linked into a large exposure of Keuper gypsum and argillite (tG and t7-9) in the immediate hanging wall of the Berbené thrust by an NNE-SSW trending fault zone and a series of anomalous contacts (shown as Portail weld on Fig. 4.35).

The Petit Mourre diapir is flanked to the WSW by two small, roughly NNW-SSE trending synclines which are situated in the hanging wall of the thrust segment of the Berbené fault and its western continuation, the le Poil thrust. The diapir and the Petit Mourre anticline are bounded to the NE by a large and elongated syncline, the Blieux syncline (described later) (Fig. 4.34, Fig. 4.35, Fig. 4.36). Fold wavelengths are relatively short between the axes of the synclines and ranging between 1.5-3.5 km (Fig. 4.34, Fig. 4.35, Fig. 4.36).

The two roughly NNW-SSE trending synclines SW of the Petit Mourre diapir are the le Chiran and the Grande Plaine synclines (Fig. 4.34, Fig. 4.35, Fig. 4.36). The le Chiran syncline is composed of a thin and incomplete Liassic-Upper Cretaceous section (Fig. 4.34, Fig. 4.35). The thickness of the Jurassic section (Liassic to Tithonian, lD and l7-9 to j9) is around 500-600 m in the le Chiran syncline (Fig. 4.36 and Fig. 4.39, L5 measured sections) and thinning towards to the NE (Fig. 4.36 and Fig. 4.39, L6 measured section). On the SW flank of the syncline, the Liassic is reduced (around 50-70 m) and composed of partly dolomitized limestone (lD). On the contrary, along the Petit Mourre diapir, on the eastern flank of the le Chiran syncline, the Liassic is represented only by the Toarcian-Aalenian bioclastic limestone which unconformably overlies the Norian and Rhaetian sediments and also the Keuper gypsum (Fig. 4.36). Locally, a breccia level occurs at the base of the bioclastic limestone. The thickness of the Toarcian-Aalenian limestone is around 55 m on the eastern flank of the le Chiran syncline (Fig. 4.39). The Toarcian-Aalenian bioclastic limestone passes up into a more marly Bajocian-Oxfordian succession which is composed of the Bajocian-Callovian marly limestone with Cancellophycus trace fossils (j2-3) and the Bathonian-Oxfordian Terres Noires Formation (j2-4). The Upper Oxfordian-Tithonian section (j5-6, j7-8 and j9) is represented by massive limestone beds, forming the highest peaks in the area. The Lower Cretaceous sediments preserved in the core of the le Chiran syncline are Berriasian limestone (n1) and Valanginian marl (n2). At the northernmost extent of the syncline, the Valanginian marl is unconformably overlain by Albian-Cenomanian sediments (Fig. 4.36).

The smaller Grande Plaine syncline is composed of a very similar succession to the le Chiran syncline (Fig. 4.39). However, its Liassic is not dolomitic and only represented by the Toarcian-Aalenian bioclastic limestone on both flanks of the syncline (Fig. 4.36 and Fig. 4.39, L7 and L8 measured sections). In addition, on the SW flank of the syncline, the stratigraphy is incomplete: the oldest preserved strata in the hanging wall of the thrust segment of the Berbené fault are the Toarcian-Aalenian bioclastic limestone and the Bajocian-Callovian marly limestone with Cancellophycus trace fossils (j2-3) which overthrusted the la Gondole syncline (Fig. 4.36).

Cretaceous strata are not preserved in the core of the Grande Plaine syncline and the upper part of the Upper Jurassic section is presumably eroded (Fig. 4.34, Fig. 4.35, Fig. 4.36, Fig. 4.39). The thickness of the Jurassic section (Liassic to Tithonian, l7-9 - j9) is around 500 m in the westernmost extent of the Grande Plaine syncline (Fig. 4.36, L7 measured section). The syncline is plunging towards to SE and the Jurassic presumably thickens in the core of the syncline and could reach the thickness of 600-800 m SW of the village of Thon (Fig. 4.38 and Fig. 4.39). The Jurassic and Lower Cretaceous successions of the le Chiran and the Grande Plaine synclines were deposited in the basinal facies zone of the Dauphinois basin (Kerckhove & Roux, 1978a; De Graciansky et al., 1981). However, the thickness of the Jurassic section which deposited in these synclines is reduced, compared to the average thickness of the Jurassic succession in the basin palaeogeographic domain (Fig. 2.7 and Fig. 4.39). For example, the thickness of the Jurassic section which is exposed in the core of the Montagne de Vibres anticline, only 5 km to the NE from the le Chiran and Grande Plaine syncline, reaches the thicknesses of 800-1000 m (Fig. 4.34, Fig. 4.35, Fig. 4.36 and Fig. 4.38).

Just like the stratigraphy, the observed structural styles are also similar in the Chiran and the Grande Plaine synclines. The western flank of the le Chiran syncline dips around a 20-30º to the E or ENE (Fig. 4.36). However, around the SE termination of the syncline, NE dipping Liassic (lD) and Middle Jurassic (j2-3) strata abut against the Keuper (Norian argillite, t7-9) in the hanging wall of the Berbené thrust (Fig. 4.34, Fig. 4.36).

N of the Portail de Blieux area, the Upper Jurassic-Lower Cretaceous section (j2-4 to n1) on the eastern flank of the syncline is overturned to the WSW along the NNE-SSW trending fault zone and anomalous contacts (shown as Portail weld on Fig. 4.35). The poorly exposed fault zone and the anomalous contacts are separating the le Chiran syncline from the Grande Plaine syncline (Fig. 4.34, Fig. 4.35, Fig. 4.36). Within the fault zone Triassic (t7-9 and t10), the incomplete Liassic (l7-9) and Middle-Upper Jurassic rocks (j2-3, j2-4) are folded into tight

synclines and anticlines (Fig. 4.36). The fold axes are roughly parallel with the NNE-SSW trending fault zone.

Further to the N, the lower part of the section in the le Chiran syncline, i.e. the Middle Jurassic (j2-3) and the Liassic bioclastic limestone (l7-9) are overturned to the WSW and abut against the NNE-SSW trending fault zone and anomalous contacts (the Portail weld) (Fig. 4.35, Fig. 4.36). On the NE flank of the le Chiran syncline, the Triassic (Norian and Rhaetian, t7-9 and t10) is also overturned to the SW. The overturned Toarcian-Aalenian bioclastic limestone (l7-9) is in direct contact with the Triassic gypsum (tG) and the overlying Norian argillite (t7-9) and the Rhaetian dolomite (t10). I assume that the Triassic is unconformably overlain by the Liassic sediments here (Fig. 4.36).

Further to the NW, in the le Ruth area (Fig. 4.35), where Norian argillite (t7-9) is exposed in the core of the Petit Mourre diapir, an anomalous contact (shown as Petit Mourre-le Poil weld on Fig. 4.35) separates the Blieux syncline from the le Chiran syncline. Along this NW-SE trending contact, on the overturned NE flank of the le Chiran syncline, the Middle Jurassic (j2-3) and the Terres Noires Formation thins and onlaps onto the Toarcian-Aalenian (l7-9) bioclastic limestone (Fig. 4.36). The overturned Upper Oxfordian limestone (j5-6) and the massive Kimmeridgian-Tithonian limestone and the Lower Cretaceous (Berriasian and Valanginian, n1 and n2) section abut against the anomalous contact which separates the le Chiran and Blieux synclines (Fig. 4.34, Fig. 4.35, Fig. 4.36). Along the NE flank of the le Chiran syncline the Valanginian (n2) is structurally overlain by the Tithonian (j9) limestone (Fig. 4.36). Further to the NW, the Lower Cretaceous (Valanginian, n2) is unconformably overlain by Albian-Cenomanian sediments (n7-c1) which also abut against the NW-SE trending anomalous contact (Fig. 4.36). Hauterivian (n3), Barremian (n3b4) and Aptian (n6) strata are pinching out between Valanginian and the Albian-Cenomanian here.

A very similar structural style was observed along the flanks of the Grande Plaine syncline. The south-western flank of the syncline dips gently (around a 10^{o}) to the ENE (Fig. 4.36) but steeper dips (around a 45^{o}) were measured in the Portail de Blieux area, along the NNE-SSW trending anomalous contacts and faults (the Portail weld) (Fig. 4.35, Fig. 4.36). On the NE flank of the Grande Plaine syncline, the Norian (t7-9) and Rhaetian (t10) rocks are overturned to the WSW and unconformably overlain by the Toarcian-Aalenian (l7-9) bioclastic limestone (Fig. 4.35, Fig. 4.36). The Upper Jurassic section is crosscut by an approximately NNW-SSE trending fault. The Upper Jurassic (j2-4 to j9) section is gently dipping to the SW along the fault, but further to the SE, vertical dips were also observed in the Kimmeridgian (j7-8) limestone (Fig. 4.36). NW of the thrust segment of the Berbené fault, at the lateral termination

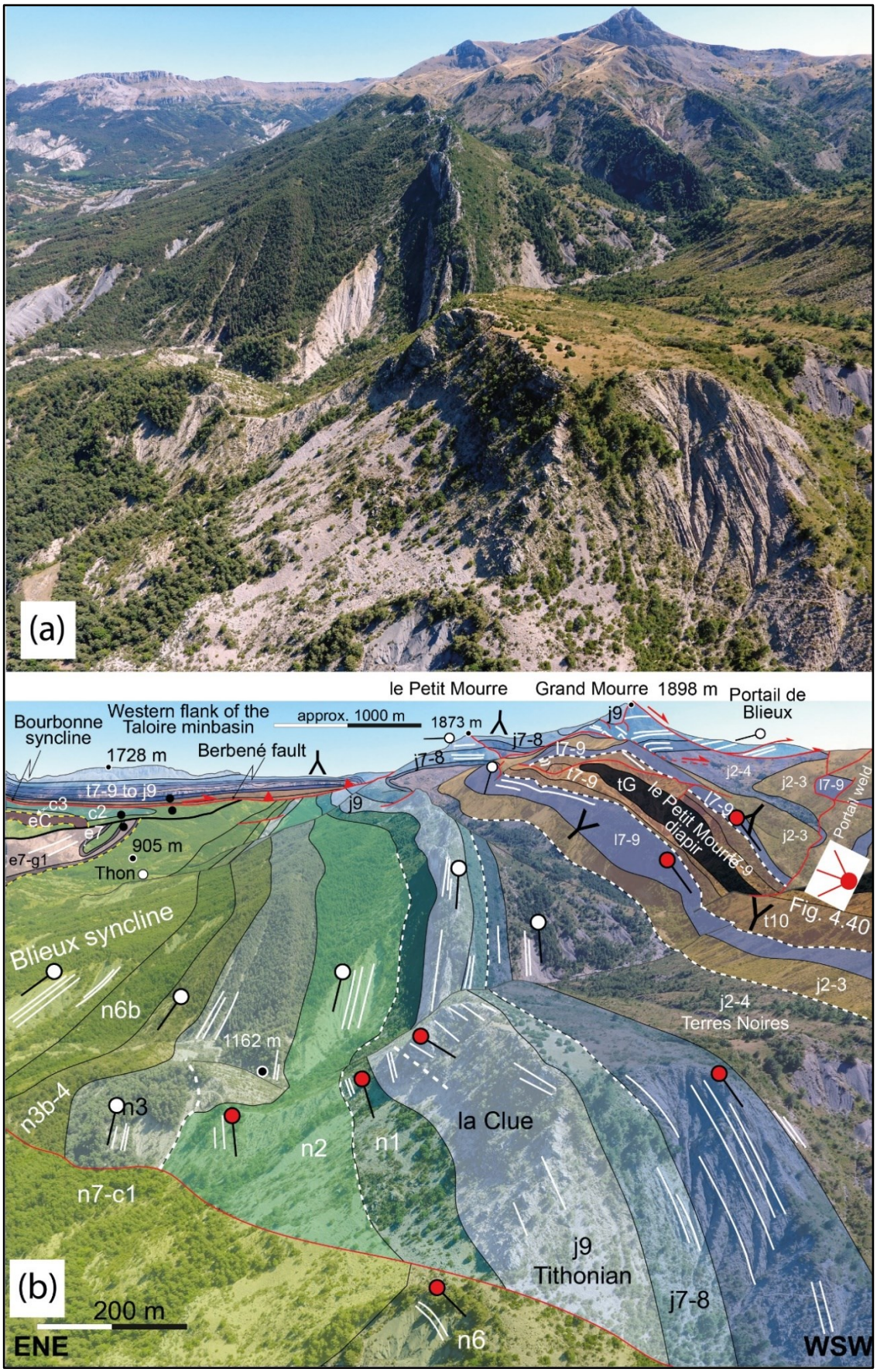


Fig. 4.37 Uninterpreted (a) and interpreted (b) photo panorama of the Petit Mourre diapir and the adjacent Blieux syncline, looking to SE. Black epsilons indicate younging direction. See Fig. 4.36 for key and viewpoint location.

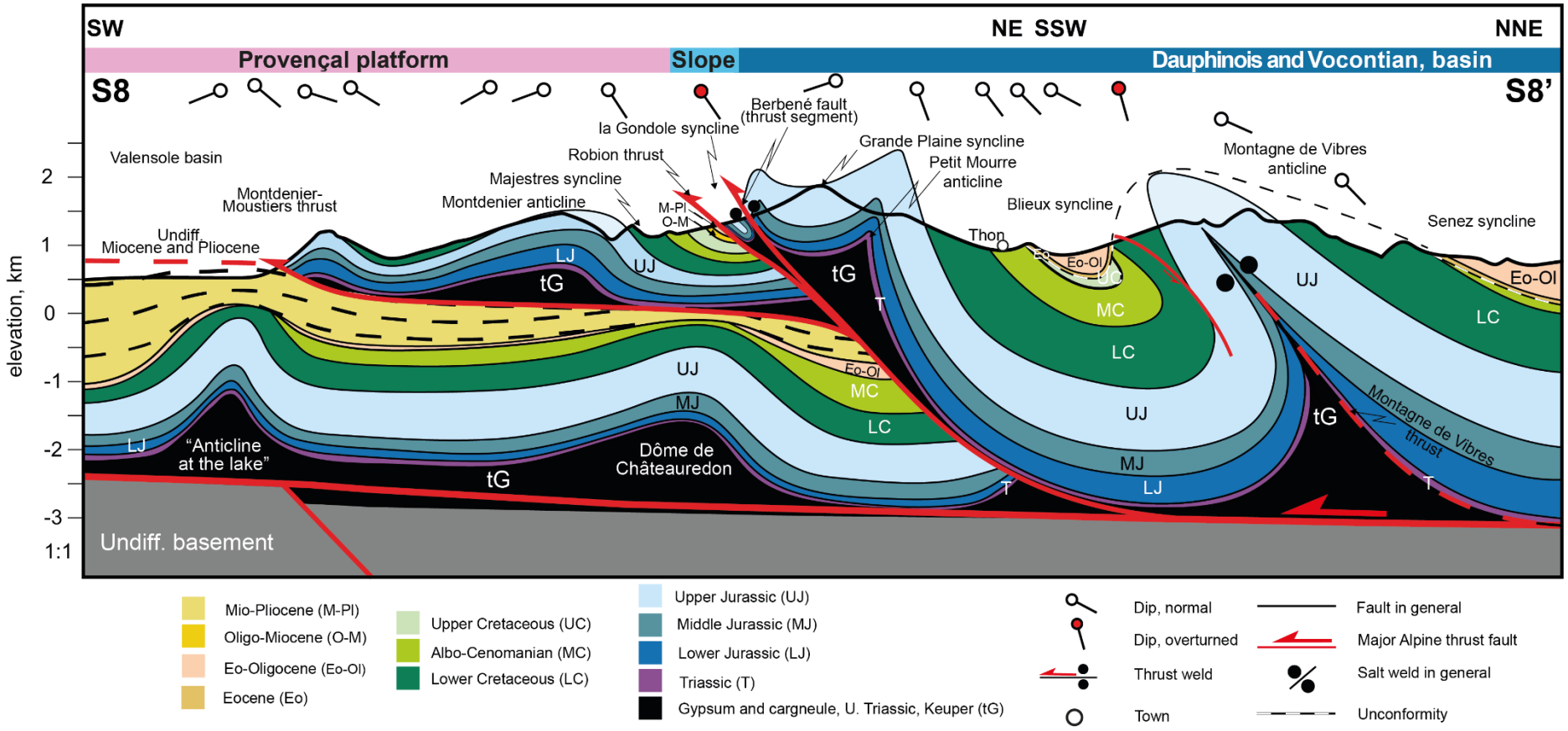


Fig. 4.38 Regional cross section (S8-S8') from the Valensole foreland basin to the Senez syncline. See Fig. 4.35 for cross section location. The section is intersecting the platform, slope and basin palaeogeogrpahic domains. Note the abrupt thickness changes of the Jurassic section between the la Gondole, Grande Plaine and Blieux synclines.

of the Petit Mourre anticline, beds are folded over the crest of the Petit Mourre anticline and the Grande Plaine syncline is amalgamated with the Blieux syncline (Fig. 4.34, Fig. 4.35, Fig. 4.36). In the hanging wall of the thrust segment of the Berbené fault, a NW-SE trending anticline formed, and this anticline bounds the Grande Plaine syncline to SW. Norian argillite (t7-9) is exposed in the core of the anticline what I have called the Prau anticline (Fig. 4.35, Fig. 4.36).

The unconformity at the base of the Toarcian-Aalenian (l7-9) bioclastic limestone was also observed here. Norian (t7-9) and Rhaetian (t10) strata are overlain by thin bioclastic limestone (l7-9) on the flanks of this anticline (Fig. 4.36). In addition, the Middle Jurassic (j2-3) is also in direct contact with the Norian argillite (Fig. 4.36). Two roughly N-S trending faults which display sinistral offset the NE flank of the anticline (Fig. 4.36).

The two faults offset the incomplete Norian-Bajocian-Callovian (t7-9 to j2-3) section and the faults die out at the base of the Terres Noires (j2-4) Formation. Between the faults, Rhaetian (t10) and Toarcian-Aalenian (l7-9) strata are unconformably overlain by the Terres Noires.

On the SW flank of the large Blieux syncline, which is bounding the Petit Mourre diapir to the NE, a thin Triassic-Lower-Middle Cretaceous section is exposed (Fig. 4.34, Fig. 4.35, Fig. 4.36, Fig. 4.37, Fig. 4.38). The Jurassic section is similar to Jurassic section of the le Chiran and the Grande Plaine synclines (from Toarcian-Aalenian (l7-9) to Tithonian (j9)) (Fig. 4.36, Fig. 4.38, Fig. 4.39).

In the la Clue section, the thickness of the reduced Jurassic section (Toarcian-Aalenian to Tithonian, l7-9-j9) is approximately 600-650 m (Fig. 4.36, Fig. 4.37, Fig. 4.39). However, cross section construction based on surface data has revealed that the complete thickness of the Jurassic section in the core of the Blieux syncline is around 1.5 km (Fig. 4.38, Fig. 4.39).

The Lower Cretaceous is composed of Berriasian (n1), Valanginian (n2) which are also exposed in the le Chiran syncline but missing in the Grande Plaine syncline. Hauterivian marl (n3), Berriasian limestone, Albian marl and limestone (n6) and the Albian-Cenomanian black shales (n7-c1) are also exposed on the SE flank of the Blieux syncline. Upper Cretaceous rocks (Cenomanian marl and marly limestone, c2) are preserved only in the core of the Blieux syncline, NW of the village of Thon (Fig. 4.36, Fig. 4.38).

On the SW flank of the Blieux syncline, W of the village of Thon, the Triassic (t7-9, t10) is overturned to the NE and unconformably overlain by the overturned Toarcian-Aalenian (l7-9) bioclastic limestone (Fig. 4.36, Fig. 4.37). Hettangian, Sinemurian and Pliensbachian sediments are not represented in the Liassic section. The thickness of the Liassic section is around 90 m (Fig. 4.39).

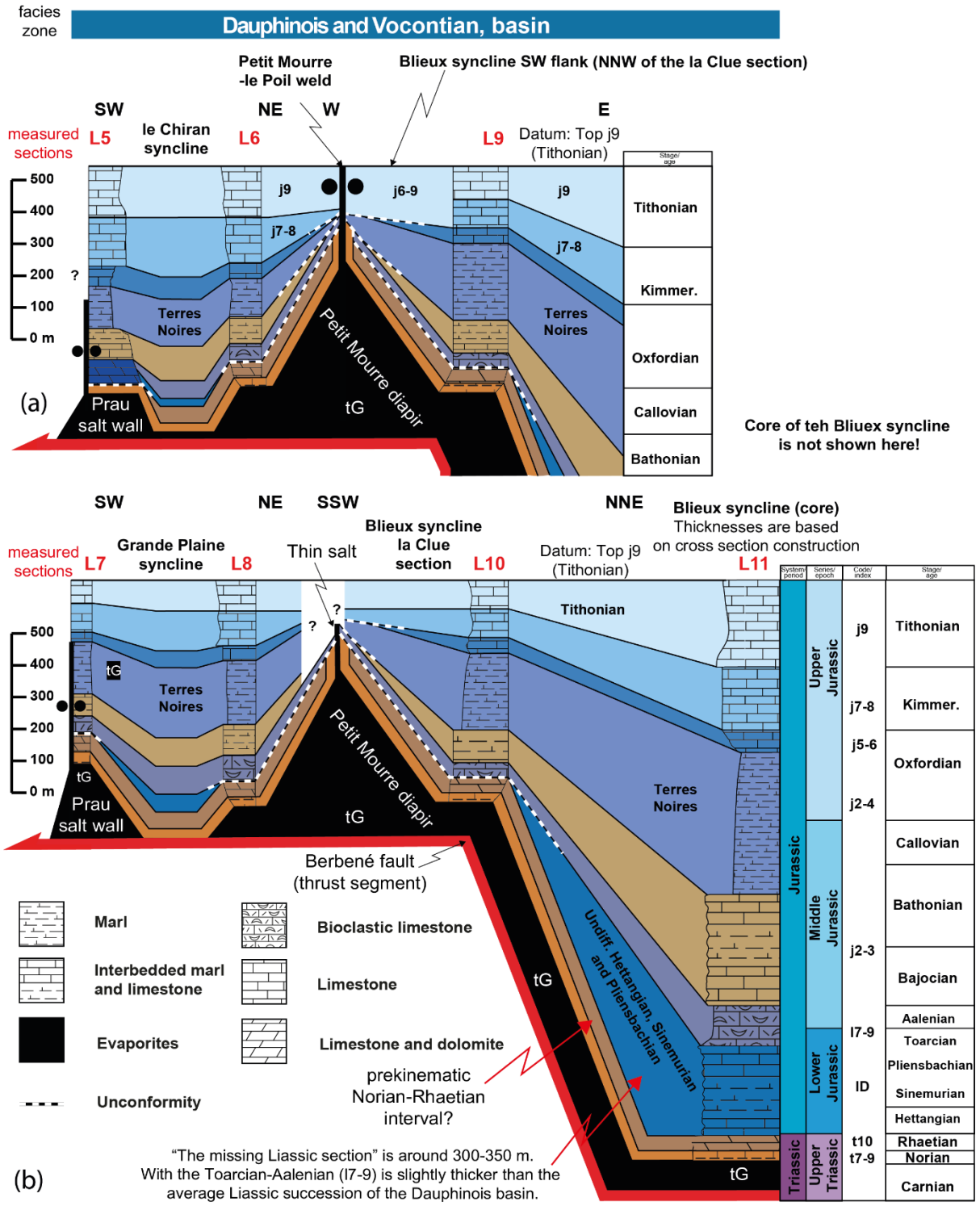


Fig. 4.39 Transects showing thickness variations of the basinal Jurassic sections and different stratal geometries, between the le Chiran and the Blieux synclines (a), and betwen the Grande Plaine and the Bliuex synclines (b). The smaller le Chiran and Grande Plaine synclines are separated from the large Bliuex syncline by the Petit Mourre diapir and its along-strike equvalent, the Petit Mourre-le Poil weld. All of these depocenters and the salt structures are located in the hanging wall of the Berbené thrust fault and its along-strike equivalent, the le Poil thrust. Measured sections are shown by logs and litholigies. Note that thicknesses are inferred in the core of the Blieux sycnline. For log location and geological key see Fig. 4.36.

The overlying Middle Jurassic marly limestone is thin (around 85 m) and slightly overturned to the NE and capped by the vertical and thin section of the Terres Noires (j2-4, around 250 m). The overlying Oxfordian limestone (j5-6, around 40 m) is also vertical. The Kimmeridgian (j7-8), Tithonian (j9), Berriasian (n1) strata steeply dip to the NE (around 80-85°). This suggests the presence of an angular unconformity between the vertical Bathonian-Oxfordian (j2-4 and j5-6) section and the overlying Kimmeridgian-Berriasian section (Fig. 4.37). The Kimmeridgian-Tithonian section (j7-8 and j9) is reduced (approximately 200 m) (Fig. 4.39).

In the Hauterivian-Cenomanian (n3 to n7-c1) section, more gentle dips were observed (Fig. 4.37). The Hauterivian (n3) and the Barremian (n3b4) strata dip around 55° to the NE and the Albian-Cenomanian black shale is dipping around 40° to the NE (Fig. 4.36, Fig. 4.37). The thickness of the Berriasian-Barremian section is reduced (approximately 400-450 m), the thickness of the Albian-Cenomanian section (n6, n7-c1, c2) is around 500-550 m.

The complete thickness of the Cretaceous deposits on the SW flank of the Blieux syncline is around 900-1000 m. However, in the core of the Blieux syncline, the total thickness of the Cretaceous section is almost doubled (around 1800 m) (Fig. 4.38).

The observed dips in the Triassic-Lower-Middle Cretaceous section along the Petit Mourre salt cored anticline show sedimentary wedging and thinning for the whole Jurassic and Lower-Middle Cretaceous section towards the Petit Mourre anticline and the diapiric gypsum (Fig. 4.36, Fig. 4.37.)

Further to the NW, W of the village of Blieux, more complex geometries were observed in the flanking strata of the Petit Mourre diapir. In the la Clue area, E of the diapir, not just the Liassic-Middle Jurassic, but also the Upper Jurassic and the Berriasian-Valanginian (from n1 to n2) strata are overturned around 40-50° to NE and local unconformities were observed in the overturned section (Fig. 4.36, Fig. 4.37). An angular unconformity can be seen in the upper section of the Tithonian limestone (j9), between the overturned Berriasian (n1) and the Valanginian (n2), which is also truncated by a local unconformity at the base of the Hauterivian marl (n3) (Fig. 4.37). The overturned section is bounded to the N by a roughly E-W trending fault. The length of the fault is around 1.5 km. This fault offsets the Upper Jurassic-Upper Cretaceous section (j2-4 to n7-c1) and dies out in the Albian-Cenomanian black shales (n7-c1). Strata are also overturned on the northern side of the E-W trending fault (Fig. 4.37). Further to the NW, along the SW flank of the Blieux syncline, at least two other faults with similar trend, offset and length were observed (Fig. 4.34, Fig. 4.35, Fig. 4.36).

N of the E-W trending fault, in a structurally complex zone, several local unconformities can be seen: the Kimmeridgian-Tithonian limestone (mapped together and labelled here as j6-

9), the Terres Noires Formation (j2-4) and also the Bajocian-Callovian marly limestone with Cancellophycus trace fossils (j2-3) are unconformably overlain by the Valanginian marl (n2) (Fig. 4.36). Further to the NW, a local unconformity developed at the base of the Kimmeridgian-Tithonian (j6-9) and the Terres Noires (j2-4) and Oxfordian limestone (j5-6) pinch out between the Kimmeridgian-Tithonian and the Bajocian-Callovian (Fig. 4.36). Minor local unconformities were also observed: the Norian argillite (t7-9) is unconformably overlain by the Terres Noires or elsewhere a steeply dipping Bajocian-Oxfordian section (j2-3, j2-4 and j5-6) onlap onto the Toarcian-Aalenian (l7-9) bioclastic limestone (Fig. 4.36).

The la Clue area also provides some of the best viewpoints to the exposed core of the Petit Mourre diapir, and the most intriguing structural features were observed here (Fig. 4.37, Fig. 4.40a and b). The salt cored anticline was also described from this viewpoint by Zurcher (1895) and Roux (1972) (Fig. 4.38b, Fig. 4.40). Oblique aerial images were acquired along the flank of the Blieux syncline and around the core of the diapir, which largely helped with the description of the diapir and its flanking strata (Fig. 4.37). The diapiric salt is exposed in the core of the Petit Mourre anticline and flanking Liassic and Middle Jurassic strata of the Blieux,

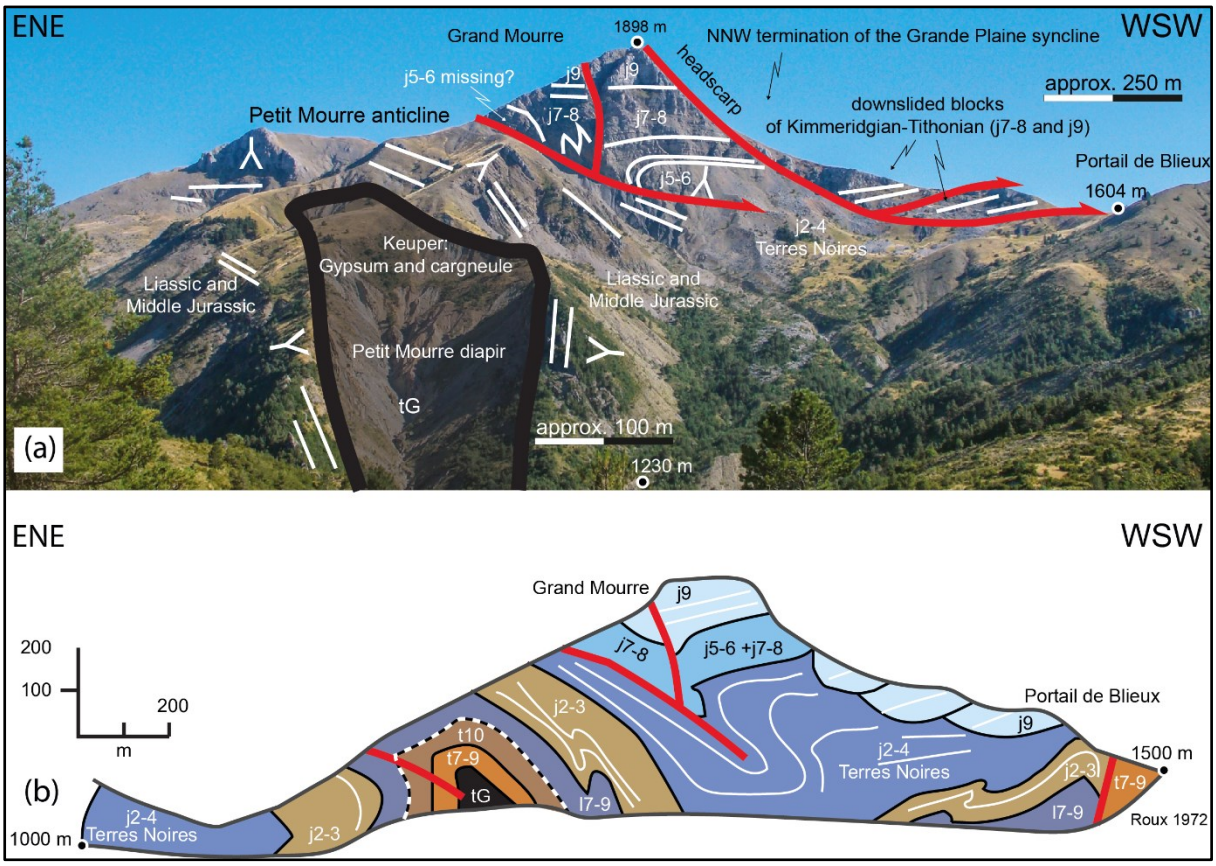


Fig. 4.40 (a) Interpreted photo panorama of the core of the Petit Mourre diapir, looking to the SE The photo shows the exposed core of the diapir with the arched roof which is partly collapsed. White epsilons indicate younging direction. (b) Cross section of Grand Mourre diapir, redrawn after Roux (1972). Note the large scale slumping and the S-folds verging to the WSW in the Middle-Upper Jurassic section on the WSW flank of the diapir. White epsilons indicate younging direction. See Fig. 4.36 for key and Fig. 4.37 for viewpoint location.

and the Grande Plaine synclines are vertical or slightly overturned to the NE and to the SW (Fig. 4.40a). In the background, the Grand Mourre and the Petit Mourre mountains expose gently dipping Upper Jurassic limestones (j5-6, j7-8 and j9) (Fig. 4.40). The Petit Mourre Mountain represents the crest of the Petit Mourre diapir while the Grande Mourre corresponds to the Grande Plaine syncline.

Below the top of the Grand Mourre mountain, within the Oxfordian (j5-6) and the Kimmeridgian limestone (j7-8) several folds were observed. Folding did not affect the beds of the overlying Tithonian limestone (j9). On the NE face of the mountain, the Oxfordian limestone is absent between the Terres Noires and the Kimmeridgian limestone (Fig. 4.36, Fig. 4.40a). Several normal faults offset the competent Kimmeridgian and Tithonian limestone and detach on the top of the black shales of the Terres Noires (Fig. 4.40a and b). Folding of the Oxfordian and Kimmeridgian beds also occurred in the hanging wall of these normal faults. Downslided blocks of the Tithonian limestone (j9) apparently rest on the detachment surface. According to Kerckhove & Roux (1978a) these blocks are Quaternary scree deposits and they formed due to the collapse of the Grande Mourre cliff. However, further to the SE, where similar cliffs are forming NW-SE oriented ridges and similar topography (e.g., the Petit Mourre cliff), these blocks were not observed. They occur only on the SW flank of the syncline, within a few hundreds of meters from the core of the Petit Mourre diapir. Further to the WSW, around the Portail de Blieux area, some of the downslided limestone blocks are apparently imbricated (Fig. 4.40a). According to Roux (1972), the Tithonian limestone (j9) directly rests on the top of the Terres Noires Formation (Fig. 4.40b). The folding also affected the Middle Jurassic marly limestone (j2-3) and the underlying Toarcian-Aalenian (l7-9) bioclastic limestone and some minor S-folds occur here (Fig. 4.40b).

In the Portail de Blieux area, the Liassic-Oxfordian section (l7-9 to j2-4) is in direct contact with the Keuper (Norian argillite, t7-9) along the NNE-SSW trending anomalous contacts and faults which separates the le Chiran and the Grande Plaine synclines (the Portail weld), which represents the top of the Keuper gypsum (Fig. 4.40b).

In addition, in the Portail de Blieux area, on the SW flank of the Grande Plaine syncline, along the NNE-SSW trending fault zone (shown as Portail weld on Fig. 4.35), a large block of Upper Triassic Keuper gypsum exposed within the Terres Noires Formation (j2-4) (Fig. 4.36). The size of the block is approximately 20 by 80 m, and it is entirely surrounded by the black shales of the Terres Noires.

Further to NE of the Petit Mourre diapir and the la Clue section, on the NE flank of the Blieux syncline, the Albian-Cenomanian formations (n7-c1 and c2) are unconformably

overlain by Eocene sediments: the Priabonian basal conglomerate (e6-7C) and the Nummulitic limestone (e7) dip towards to NE around 25º. The youngest preserved Tertiary sediment in the Blieux syncline is the Priabonian-Rupelian Globigerina marl (shown as e7-g1 on Fig. 4.36 and Eo-Ol on Fig. 4.38).

The Blieux syncline is bounded the NE by the Montagne de Vibres thrust and the tip fold of this Alpine structure, the SE plunging Montagne de Vibres anticline (Fig. 4.35). The thrust is overriding the Lower and Upper Cretaceous rocks and the Eocene sediments in the Blieux syncline (Fig. 4.34, Fig. 4.35, Fig. 4.36).

N of the village of Blieux, the frontal limb of the Montagne de Vibres anticline is slightly overturned to the SW and composed of an Upper Jurassic-Lower-Middle Cretaceous section (Fig. 4.34, Fig. 4.35, Fig. 4.36, Fig. 4.38). Further to the NW, in the hanging wall of the Montagne de Vibres thrust, Liassic and Middle Jurassic rocks are exposed in the core of the hanging wall anticline (Fig. 4.34, Fig. 4.36). The Jurassic and Cretaceous section of the Montagne de Vibres thrust represents a thicker, more basinal and complete section compared to the SW flank of the Blieux syncline and the succession exposed in the le Chiran and Grande Plaine synclines around the Petit Mourre diapir (Fig. 4.35, Fig. 4.36). The facies and thickness of the Jurassic and Cretaceous section is similar to the basinal succession of the la Blache-Castellane thrust sheet, which is overriding the NE flank of the Taulanne minibasin, the St-Vincent diapir and the la Grau anticline (Fig. 4.1, Fig. 4.2, Fig. 4.5, Fig. 4.6). The Jurassic section is relatively thick in the hanging wall of the Montagne de Vibres thrust: in the core of the Montagne de Vibres anticline is around 800-1000 m and thickening towards to NE (towards the Senez syncline) and can reach the thicknesses of 1000-1200 m in the back limb of the anticline (Fig. 4.38). The thickness of the Lower and Upper Cretaceous section is thinner than on the SW flank of the Blieux syncline (around 750-800 m). NE of the core of the Montagne the Vibres anticline, the Upper Cretaceous is eroded along the S8-S8' section line. However, like the Jurassic section, the Lower-Middle Cretaceous section also thickens towards to NE and reaches the thicknesses of 1000 m (Fig. 4.38). SE of the tip point of the Montagne de Vibres anticline, the Upper Jurassic-Upper Cretaceous section (UJ, LC and UC on Fig. 4.34) is offset by multiple, roughly NNE-SSW trending normal faults. However, these faults did not offset the Tertiary unconformity and the overlying Eocene rocks (Fig. 4.1, Fig. 4.3, Fig. 4.34, Fig. 4.36).

On the overturned NE flank of the Blieux syncline (i.e., the overturned frontal limb of the Montagne de Vibres anticline), E of the village of Blieux, the Jurassic-Cretaceous section is overturned together with overlying Tertiary sediments (Fig. 4.34). However, a significant

angular unconformity was observed: the Lower Cretaceous dips around 40º overturned to SSW below the vertical or slightly overturned Nummulitic limestone (Fig. 4.34, Fig. 4.36).

NW of the village of Blieux, this angular unconformity can be seen at the base of the Eocene sediments, but with more complex geometries present in the Mesozoic section (Fig. 4.41).

Observed stratal and structural geometries in the Upper Jurassic and Lower Cretaceous section are similar to the geometries which were described on the SW flank of the Blieux syncline, NW of the la Clue section (Fig. 4.36). At the tip point of the Montagne de Vibres thrust, in the Ravin de Riu section (Fig. 4.35, Fig. 4.36, Fig. 4.41), the Terres Noires Formation

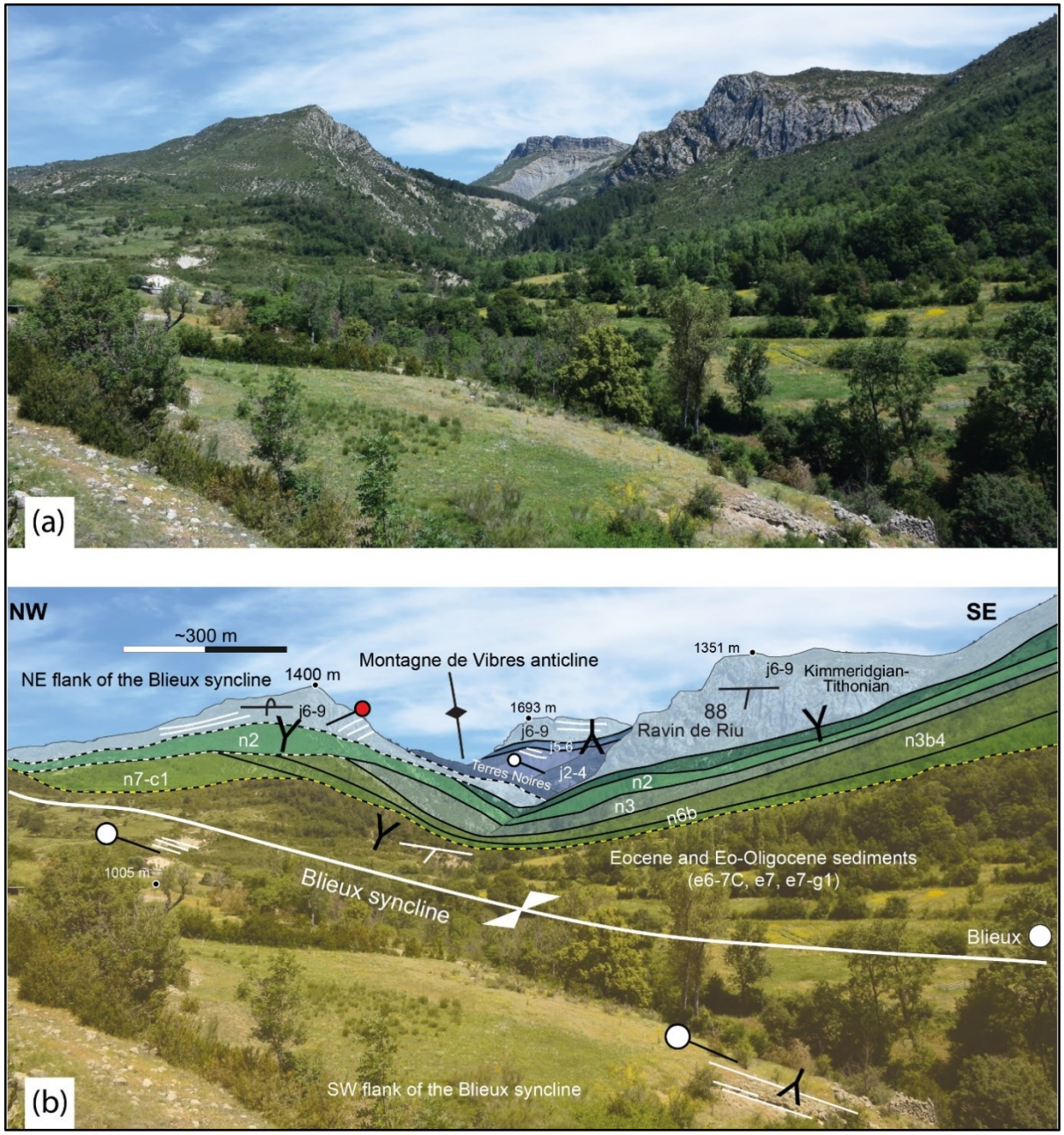


Fig. 4.41 Uninterpreted (a) and interpreted (b) photo panorama of the NE flank of the Blieux syncline at Ravin de Riu section, NW of the village of Bliuex, looking to NE. Black epsilons indicate younging direction. See Fig. 4.36 for key and viewpoint location.

is unconformably overlain by the Kimmeridgian-Tithonian limestone (j6-9) and the Upper Oxfordian limestone (j5-6) pinches out (Fig. 4.36). Only a 1.5 km to the NE, on the NE flank of the Montagne de Vibres anticline, the Upper Oxfordian limestone is exposed between the Terres Noires (j2-4) and the Kimmeridgian-Tithonian limestone (j6-9) (Fig. 4.41).

On the NE flank of the Blieux syncline, the Kimmeridgian-Tithonian limestone (j6-9) is unconformably overlain by the Valanginian marl (n2) (Fig. 4.35, Fig. 4.36, Fig. 4.41), and the Berriasian limestone (n1) is pinching out between the massive Upper Jurassic limestone and the Valanginian marl (Fig. 4.36, Fig. 4.41). In addition, the Hauterivian-Cenomanian (from n3 to n7-c1) section is structurally overlain here by the overturned and incomplete Tithonian-Valanginian section (Fig. 4.41). The overturned Jurassic-Upper Cretaceous section is unconformably overlain by the Eocene sediments dipping to the SW (Fig. 4.36, Fig. 4.41).

4.1.3.3 Interpretation of the la Gondole, le Chiran, the Grande Plaine synclines, the Blieux syncline and their bounding structures

Based on the observed stratal and structural geometries, thickness changes of the Jurassic-Upper Cretaceous section and the reinterpretation of anomalous contacts and Alpine compressional structures around the Petit Mourre diapir, I assume that similarly to the eastern part of the southern structural domain, the well-developed minibasin and salt-ridge system is continuous to the WNW, in the hanging wall of the Robion thrust and along-strike, in the Beynes-Majestres thrust sheet and also in the overriding thrust sheet which comprise basinal successions (Fig. 4.35).

The minibasins like the Taulanne, Porte de St-Jean, la Lagne and les Combes minibasins and their bounding salt structures were situated in the slope palaeogeographic domain during the Mesozoic, along the northern edge of the Provençal platform (Fig. 4.23, Fig. 4.35). The la Gondole syncline, which is also representing the slope facies zone, is composed of an anomalously thin section of Triassic, Jurassic, and Lower Cretaceous rocks, and separated from the Taloire minibasin by the NE-SW trending welded Berbené salt wall. However, the la Gondole area may have been bounded by a NW-SE trending salt structure to the SW, which is eroded now in the hanging wall of the Robion thrust (Fig. 4.34, Fig. 4.35, Fig. 4.36, Fig. 4.38). To the NW, the syncline is bounded by the large exposure of Keuper rocks (gypsum, tG and dolomite and argillite, t7-9) which suggest that the NW-SE trending la Gondole area may have been bounded by salt structures at least in three directions (to the SE, SW, and NW, respectively). The la Gondole syncline is interpreted as an identical section to the Deneiras

section (Fig. 4.18, Fig. 4.21) and corresponds to the thin roof of the SW termination of the Berbené salt wall or maybe a larger salt body which was located at the triple junction of the Berbené salt wall and two adjoining salt bodies, now eroded on the leading edge of the Robion thrust (Fig. 4.34, Fig. 4.35, Fig. 4.36, Fig. 4.44). The lack of abrupt facies and thickness changes towards the core of the syncline and the absence of angular unconformities, pinch-outs, slumps, or breccia levels also suggests that the thin section of the la Gondole syncline may have been represented the elevated roof of a large salt body during the Jurassic and Early Cretaceous time instead of the WNW flanking strata of the Berbené salt wall.

The overturning of the NE flank of the la Gondole syncline may have been related to the overthrusting of the NW-SE trending segment of the Berbené fault during the Alpine compressional phase. The la Gondole syncline was carried together in the hanging wall of the Robion thrust with the Taloire minibasin and the bounding Berbené salt wall and overthrusted the edge of the Mesozoic Provençal platform during the Mio-Pliocene (Fig. 4.34, Fig. 4.35, Fig. 4.36, Fig. 4.38).

Reduced, incomplete and overturned sections, young-on-older contacts, anomalous stratigraphic relationships, abrupt facies and thickness changes were also observed in the basinal Jurassic, Lower and also the Middle-Upper Cretaceous succession in the hanging wall of the thrust segment of the Berbené fault and its lateral equivalent, the le Poil thrust which overridden the slope palaeogeographic zone and the NW-SE trending edge of the Provençal platform (Fig. 4.34, Fig. 4.35, Fig. 4.36). This implies that, similarly to the eastern part of the southern structural domain, the salt tectonics was not restricted to the slope palaeogeographic domain in the western part of the southern structural domain and salt tectonic activity continued during the later stages of the passive margin phase, beyond the Valanginian, at least until the Albian-Cenomanian.

I assume that similarly to the slope and basin palaeogeographic domain to the E, primary minibasins formed in the basinal palaeogeographic domain in the western part of the southern structural domain and these depocenters subsided into the autochthonous Upper Triassic evaporite layer during the Jurassic, Early Cretaceous and Middle-Upper Cretaceous, simultaneously with the migration of the salt from the mother salt layer into bounding diapiric structures. The le Chiran, Grande Plaine and Blieux synclines are primary minibasins, which were separated by elongated salt structures, presumably salt walls (Fig. 4.42, Fig. 4.44). Most of these salt walls may have been parallel to the edge of the NW-SE trending edge of the Provençal platform (Fig. 4.44). Due to their favourable orientation, from the Late Cretaceous onward, during the Alpine compressional phase, most of the salt walls were squeezed, partly

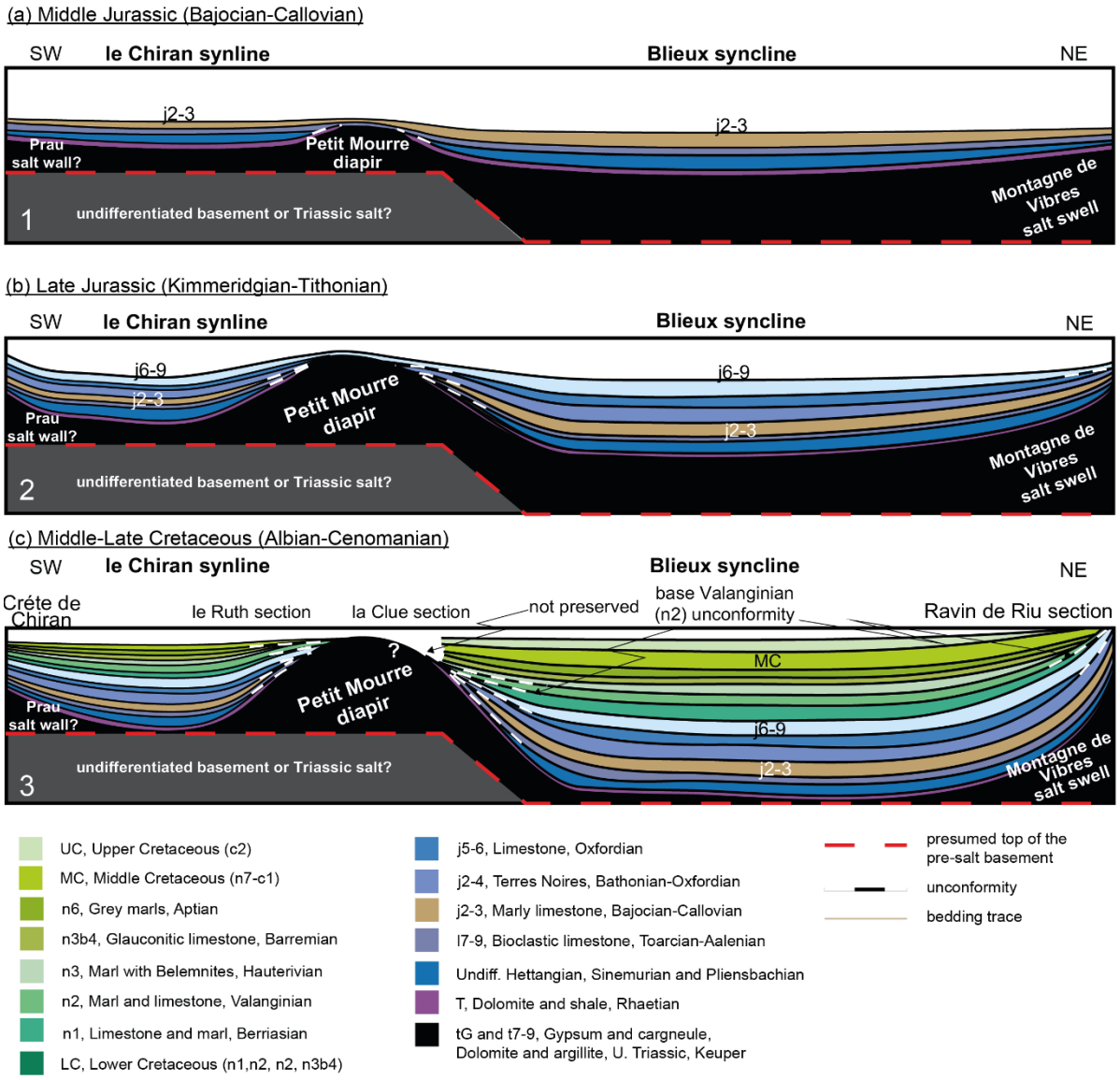


Fig. 4.42 Sequential evolution of the le Chiran and Blieux minibasins and their bounding salt structures, the Prau salt wall, the Petit Mourre diapir and the Montagne de Vibres salt swell from the Middle Jurassic (a) to the Middle-Late Cretaceous (c).

or completely welded, possibly reactivated as thrust faults or incorporated into structurally complex fault zones, thus they were interpreted previously as Alpine compressional structures (Roux, 1972). Some of these bounding salt bodies are eroded or completely welded now in the hanging wall of SW verging Alpine thrust faults, which complicates the accurate identification of these early formed salt structures.

In the hanging wall of the NW-SE trending segment of the Berbené fault and its lateral equivalent, the le Poil thrust (Fig. 4.35), the local unconformities, pinch-outs and onlaps around the Petit Mourre anticline suggest that the NW-SE trending, SE plunging anticline formed as an early diapiric structure, presumably an elongated salt wall. I assume that the Petit Mourre diapir formed the highest point of this salt structure. To the NW, the diapir is completely welded

and represented only by the Norian argillite (t7-9) (Fig. 4.35) at the surface. This weld is the Petit Mourre-le Poil weld (Fig. 4.34 Fig. 4.35 Fig. 4.36).

The abrupt facies and thickness variations of the Jurassic and Cretaceous section to the NE and SW of the Petit Mourre diapir suggest that the smaller le Chiran and Grande Plaine minibasins were separated from the large and elongated Blieux minibasin by the Petit Mourre diapiric structure (Fig. 4.34, Fig. 4.35, Fig. 4.36, Fig. 4.37, Fig. 4.39). The smaller minibasins were separated by a proposed salt structure, the NNW-SSE oriented Portail salt structure, which is now welded (shown as the Portail weld on Fig. 4.35) and forming a complex fault zone between the large exposure of Keuper gypsum and Norian argillite (tG and t7-9) in the immediate hanging wall of the Berbené thrust and the Petit Mourre diapir (Fig. 4.34, Fig. 4.35, Fig. 4.36).

The anomalous contacts of the Liassic, Middle Jurassic and the Terres Noires on the SW flank of the le Chiran minibasin and the incomplete section preserved on the SW flank of the Grande Plaine minibasins suggest that these depocenters were also bounded to the SW by a salt structure which is now eroded in the hanging wall of the Berbené and le Poil thrusts (Fig. 4.34, Fig. 4.35, Fig. 4.36, Fig. 4.42). The large exposure of Keuper in the immediate hanging wall of the Berbené thrust, at the SSW termination of the Portail weld and the NW-SE trending Prau anticline which is bounding the Grande Plaine minibasin to the SW maybe represent the remnant of this salt body (Fig. 4.35, Fig. 4.36). I have called this eroded salt structure the Prau salt wall (Fig. 4.42,Fig. 4.44). I assume that the Prau salt structure separated la Gondole syncline from the Grande Plaine minibasin (Fig. 4.44).

The Blieux minibasin was bounded to the SW by the Petit Mourre diapir and by the Montagne de Vibres salt swell to the NE (described later). The minibasin and salt-ridge system may have been bounded to the SE by the NE-SW trending Berbené salt wall during the Jurassic and Lower Cretaceous which represents a facies boundary between the slope and basin domains (Fig. 4.44).

Similarly, to the minibasins to the E (e.g., the Taulanne minibasin), the Norian -Rhaetian section exposed along the flanks of the le Chiran, Grande Plaine and Blieux minibasins interpreted as a prekinematic interval.

The occurrence of thin and incomplete Liassic sections on the flanks of the le Chiran, Grande Plaine and Blieux synclines suggests that the salt structures started to form as early as the Liassic (Fig. 4.42a). A complete Lower Jurassic section (lD, Liassic dolomite) is only preserved on the SW flank of the le Chiran syncline (Fig. 4.36). However, the Hettangian, Sinemurian and Pliensbachian strata are absent on the NE flank of the le Chiran minibasin, on

the SW and NE flanks of the Grande Plaine minibasin and on the SW flank of the Blieux minibasin (Fig. 4.36, Fig. 4.37, Fig. 4.39, Fig. 4.42). The Hettangian, Sinemurian and Pliensbachian sediments probably deposited in the minibasins, and also on the flanks of the early diapiric structures, but they have been eroded by the basal Toarcian unconformity (Fig. 4.35, Fig. 4.36, Fig. 4.37,Fig. 4.39, Fig. 4.42). However, the presence of Hettangian, Sinemurian and Pliensbachian strata in the centre of the le Chiran, Grande Plaine and Blieux minibasins is uncertain.

I assume that the initiation of salt tectonic activity may have been related to the Early-Middle Jurassic regional extension and rifting of the margin. Similarly to other locations around the Southern Subalpine chains, reactive diapirs and salt walls developed along Tethyan extensional faults and depocenters started to form around them (Mascle et al., 1988; Dardeau & De Graciansky, 1990; Graham et al., 2012; Graham et al., 2019; Célini et al., 2020; Célini, 2020; Brooke-Barnett, 2022). However, most of the diapirs and minibasins in Southern Subalpine chains were detached from their original basement (Graham et al., 2012; Célini et al., 2020; Brooke-Barnett et al., 2020; Csicsek et al., 2021; Brooke-Barnett et al., 2021; Brooke-Barnett, 2022; Célini et al., 2022), hence the effects of the Tethyan normal faulting on the initiation of the salt tectonic activity in the Blieux area, similarly to the Chasteuil area is only inferred.

However, the presence of Tethyan normal faults below the Petit Mourre diapir and the le Chiran, Grande Plaine and Blieux minibasins at their original location can explain the observed thickness changes and variations of the sizes of the minibasins (Fig. 4.36, Fig. 4.38, Fig. 4.42). The smaller and shallower le Chiran and Grande Plaine minibasins may have been located over the footwall of an inferred basement involved normal fault, while the Blieux minibasin may have been located in the hanging wall of this extensional fault. Fist the Petit Mourre diapir was fed from both the hanging wall and footwall of the extensional fault. The deformation presumably has been partly decoupled between the basement and the overburden of the Triassic evaporites. The salt flowed laterally from the footwall to the hanging wall across the fault plane, filled the relief which was created by the extensional faulting and became thinner in the footwall and resulted in the formation of smaller minibasins over the high block. This phenomenon is well known in other salt basins and reproduced by analogue modelling (Jackson & Vendeville, 1994; Ge & Vendeville, 1997; Jackson & Hudec, 2017). Thickness changes can also be explained by the increased differential loading caused by syn-kinematic sedimentation in the hanging wall of the extensional fault or the original thickness of the salt underlying the minibasins over the footwall and the hanging wall of the extensional fault (Ge & Vendeville, 1997; Dooley et al., 2005).

Salt tectonic activity continued through the later stages of the Tethyan rifting and also the transition to the passive margin phase, during the Late Liassic and Middle Jurassic (Fig. 4.42). The rifting ceased by the Bathonian-Callovian (Mascle et al., 1988; Handy et al., 2010). The earlier formed reactive diapirs, similarly to other reactive diapirs described elsewhere in the Subalpine chains, continued to emerge as passive diapiric structures during the passive margin phase due to differential loading above the autochthonous evaporite layer (Célini et al., 2020; Célini, 2020; Brooke-Barnett, 2022). However, successive unconformities and sedimentary wedging of the Liassic-and Middle Jurassic section along the Petit Mourre diapir display the clear evidence for passive diapirism which suggests that passive diapiric activity may have been started earlier, during the Toarcian (Fig. 4.42a). The deformation may have been completely decoupled by the time of the deposition of the Toarcian-Aalenian bioclastic limestone (l7-9) and differential loading was responsible for the growth of the diapiric structures. Wedge geometries also occur in the incomplete Middle Jurassic-Middle-Upper Cretaceous section on the NE flank of the le Chiran minibasin and on the SW flank of the Blieux minibasin. On the overturned NE flank of the Blieux minibasin, the lower part of the Jurassic section, i.e. the Liassic-Middle Jurassic section, is not exposed and thinning and wedging was only observed in the Upper Jurassic-Lower Cretaceous section flanking the Montagne de Vibres salt swell (Fig. 4.36, Fig. 4.41, Fig. 4.42). I assume that the Prau salt wall and the Portail wall which linked the Prau wall to the Petit Mourre diapir may have been grown passively during this period.

Within the minibasin scale wedge of the Liassic-Lower-Middle Cretaceous section on the flanks of the Petit Mourre diapir, several low angle unconformities were observed along the diapir margins (Fig. 4.42). The large scale wedge geometry and the local unconformities developed along the growing Petit Mourre passive diapir as the thin roof strata were drape folding over the edge of the diapir (Giles & Rowan, 2012; Rowan & Giles, 2021) (Fig. 4.42). The salt may have been exposed occasionally but the sedimentation rate was generally higher than the salt-rise rate and Jurassic sediments were able to cover the diapir and formed a relatively thick roof over the salt structure (Fig. 4.42). Direct contact of the onlapping Berriasian (n1), Valanginian (n2) and Albian-Cenomanian (n7-c1) sediments onto the Petit Mourre diapir and Petit Mourre-le Poil weld only preserved in the le Chiran minibasin on the SW diapir flank (Fig. 4.35, Fig. 4.36), hence their relationship to the salt interface is not clear on the NE flank of the diapir, in the Blieux basin (Fig. 4.36, Fig. 4.42). The observed S-folds and slumping in the Grande Plaine minibasin, on the SW flank of the Petit Mourre diapir in the Toarcian-Aalenian (l7-9) bioclastic limestone, the Bajocian-Callovian marly limestone (j2-3)

and Bathonian-Oxfordian Terres Noires (j2-4) all display the presence of the local topographic high. However, the lack of reworked sediments, debris flows, and breccia levels suggest that the passively growing Petit Mourre diapir had relatively low and gentle relief (Fig. 4.42)

The wedging and the presence of the unconformity at the base of the Toarcian-Aalenian (l7-9) bioclastic limestone on the SW and NE flank of the Petit Mourre diapir marks the passive growth of the Petit Mourre diapir (Fig. 4.39a, Fig. 4.42c). The Bajocian-Callovian marly limestone (j2-3) also displays wedging geometries. A local unconformity also developed at the base of the Terres Noires formation both on the SW and NE flank of the Petit Mourre diapir, in the le Chiran and the Blieux minibasin which show the continued growth of the salt structure (Fig. 4.36, Fig. 4.37, Fig. 4.39, Fig. 4.42).

Along the Prau salt wall, the SW bounding structure of the le Chiran and Grande Plaine syncline and the Portail wall which separated the smaller synclines, thinning of the Liassic and Middle-Jurassic section and locally the base-Toarcian (l7-9) unconformity were observed on the flanks of the Grande Plaine minibasin (Fig. 4.36). However, the local unconformity at the base of the Terres Noires did not occur here or not preserved (Fig. 4.36).

The Terres Noires formation (j2-4) and the Upper Oxfordian limestone (j5-6) on the NE flank of the diapir also display large scale wedging (Fig. 4.39, Fig. 4.42). The Oxfordian succession is partly removed by the local unconformity which developed at the base of the Kimmeridgian-Tithonian (j7-8, j9 and also mapped together as j6-9) limestone (Fig. 4.36, Fig. 4.37, Fig. 4.42). This unconformity is truncated progressively older rocks from NW to SE on the SW flank of the Blieux minibasin: N of the la Clue section the Kimmeridgian-Tithonian limestone is in direct contact with the Bajocian-Callovian marly limestone (j2-3) while to the NW it overlies the Terres Noires (j2-4) (Fig. 4.36). This suggests that the flanking strata of the Petit Mourre diapir was tilted towards to the NNW.

The thinning and wedging of the Kimmeridgian-Tithonian section were also observed on the overturned NE flank of the le Chiran syncline. However, in the le Ruth section, the structural geometries are more complicated: the Tithonian (j9) limestone abuts against the Petit Mourre – le Poil weld here (Fig. 4.35, Fig. 4.36), which is interpreted as successive onlap onto the now welded Petit Mourre diapir. The Terres Noires (j2-4), the Upper Oxfordian (j5-6) and Kimmeridgian (j7-8) formations are pinching out between the salt and the Tithonian limestone (Fig. 4.36, Fig. 4.39, Fig. 4.42).

The subsequent growth of Petit Mourre diapir and the Montagne de Vibres salt structure are shown by the large scale thinning and wedging of the Kimmeridgian-Tithonian (j6-9) limestone and the Berriasian sediments (n1) in the le Chiran minibasin, on the SW flank of the Petit

Mourre diapir, and also on the SW and NE flank of the Blieux primary minibasin, (Fig. 4.36, Fig. 4.37, Fig. 4.41, Fig. 4.42). The direct contact of the Kimmeridgian-Tithonian (j6-9) limestone and the Valanginian (n2) marl, interpreted as an angular unconformity (Fig. 4.36, Fig. 4.41 Fig. 4.42) also clearly display of the continuous salt tectonic activity in the area.

Some of the passively growing diapiric structures locally reached the surface and became exposed, at least during the Late Jurassic, simultaneously with the deposition of the Terres Noires Formation: direct evidence can be seen at the Portail the Blieux area where the large block of Upper Triassic Keuper gypsum is emplaced into the Terres Noires (j2-4), deposited in the Grande Plaine primary minibasin. The source of the extruded allochthonous salt may have been the Portail wall or the Petit Mourre diapir (Fig. 4.35, Fig. 4.36). The extent of the allochthonous salt is not known, maybe the gypsum block represents the remnant of a small extrusive sheet.

During the Jurassic and the Berriasian, the development of minibasin-scale wedge geometries occurred simultaneously with the passive growth of the Petit Mourre diapir and the Montagne de Vibres salt swell. However, some of the observed structural geometries on the crest of the Petit Mourre diapir suggest that the diapir may have shifted to a different mode of diapirism for a short period and the Petit Mourre diapir may have been undergone a stage of halokinetic active rise during the Late Jurassic. Maybe a local change in the aggradation rate around the diapir during the deposition of the Upper Jurassic limestone beds led to the burial of the diapir under a thicker roof. Halokinetic active diapirism occurred, and the diapir continued its growth as an active diapir which arched its roof. Evidence for the Late Jurassic active rise of the Petit Mourre diapir can be seen SE of the exposed core of the Petit Mourre diapir, where the Petit Mourre Mountain represents the crest of the diapir (Fig. 4.40a and b, Fig. 4.43a).

The observed normal faults on the SW face of the mountain, which offset the Kimmeridgian and Tithonian limestone and detaching on the top or the upper part of the Terres Noires (Fig. 4.40a and b) are interpreted as the normal faults which formed due to the uplift and arching of the roof of the Petit Mourre diapir which became an active diapir during the Late Jurassic (Fig. 4.43b). The extension may have thinned the roof of the diapir. The Grande Mourre Mountain forms the arched roof of the active diapir, and its SW face represents a topographic scarp (Fig. 4.43a). The imbrication of the Kimmeridgian-Tithonian limestone blocks occurred shortly after their deposition at the toe of the topographic scarp (Fig. 4.43c). As the extensional unroofing of the diapir occurred, the salt became exposed again and after the short period of active diapirism, the Petit Mourre structure continued to grow as a passive diapir. However, the

occurrence of wedge stratal geometries in the Lower Cretaceous section records the burial of the Petit Mourre salt structure under a thicker roof during the Early Cretaceous (described later).

The Prau anticline which is the assumed south-western bounding salt structure of the Grande Plaine and the le Chiran minibasins, also show indirect evidence for active diapirism: the two approximately NNE-SSW trending faults which offset the incomplete Norian-Bajocian-Callovian (t7-9 to j2-3) section and die out at the base of the Terres Noires (j2-4) Formation (Fig. 4.36) are interpreted as normal faults which developed over the arched roof of the active Prau salt wall during the Late Jurassic. A graben may have been formed between these radial faults, where the Rhaetian (t10) and Toarcian-Aalenian (l7-9) strata are unconformably overlain by the Terres Noires Formation, deposited during the post-rift phase (Fig. 4.36). However, the orientation of these normal faults and the graben is almost perpendicular to the strike of the NW-SE trending salt wall, which suggests that the formation of these faults may

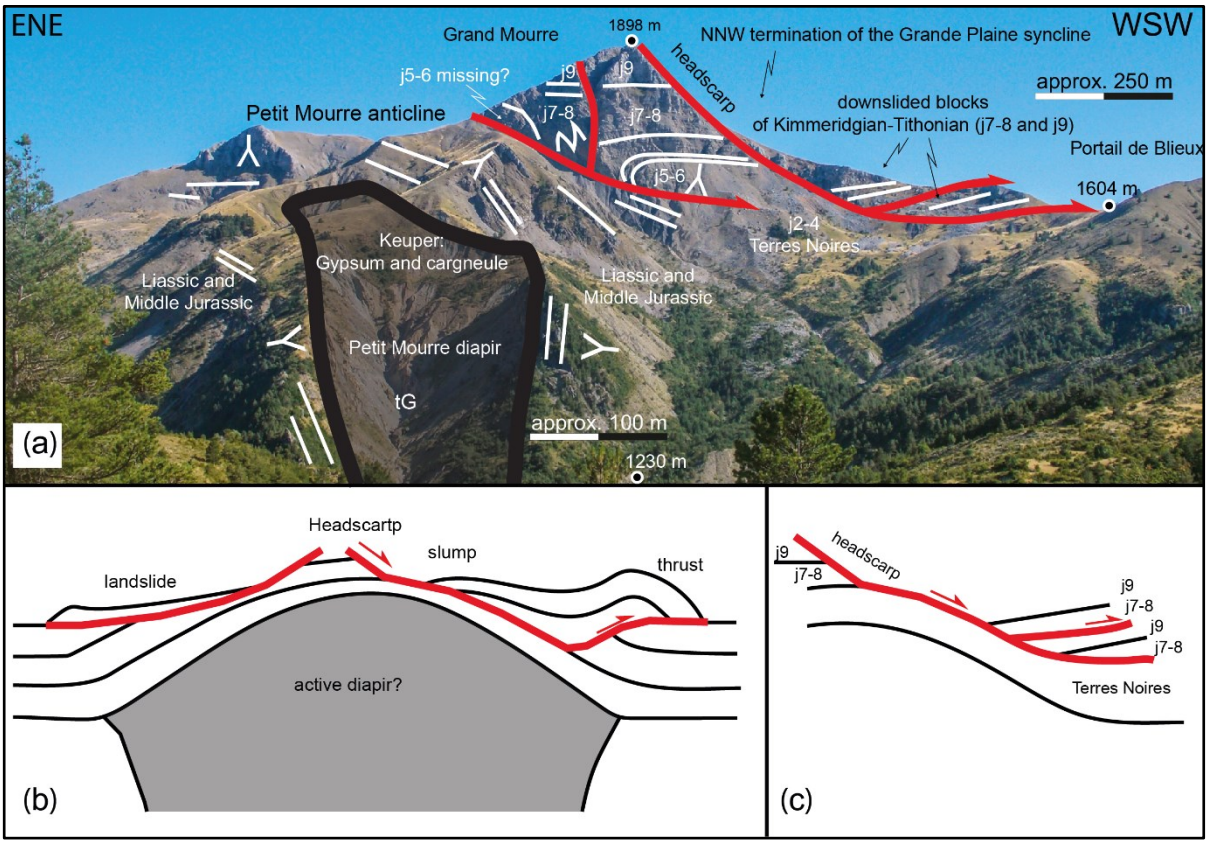


Fig. 4.43 (a) Interpreted photo panorama of the core of the Petit Mourre diapir, looking to the SE The photo shows the exposed core of the diapir, its arched roof and the topographic scarp formed on the south-western diapir margin. Black epsilons indicate younging direction. (b) Topographically arched roof of an active diapir. Extensional faulting and slumping occur over the top of the diapir while a thrust fault develops at the toe of the topographic scarp. Redrawn after Jackson & Hudec (2017). (c) Schematic section showing the imbrication of the Kimmeridgian-Tithonian limestone at the toe of the topographic scarp.

have been related to the compressional active rise of the salt structure (Jackson & Hudec, 2017) which occurred during the Alpine compressional phase. It is possible that the extensional structures at the Petit Mourre diapir are also related to compressional active diapirism and are much younger than the Late Jurassic.

The continuation of the passive diapirism resulted in the minibasin scale wedging of the Lower Cretaceous sections and stratal thinning towards the salt structures (Fig. 4.42). Stratal wedging of the Valanginian marl (n2) (Fig. 4.42c) occurred along the Petit Mourre diapir in the Blieux minibasin. The Valanginian marl is truncated by a local low-angle angular unconformity at the base Hauterivian marl (n3), observed in the la Clue section (Fig. 4.36, Fig. 4.37, Fig. 4.42). Wedge geometries observed on the SW flank of the Petit Mourre diapir, in the le Chiran minibasin (Fig. 4.36, Fig. 4.42) also display the continuous passive growth of the salt structure. The Hauterivian (n3) and also the Valanginian (n2) strata are also truncated by the low-angle unconformity at the base of the Albian-Cenomanian (n7-c1) black marls, in the northwestern termination of the le Chiran minibasin (Fig. 4.36, Fig. 4.42). This local unconformity marks the continuous diapiric rise of the salt through the later stages of the passive margin phase.

Along the Montagne de Vibres salt swell, on the NE flank of the Blieux minibasin, an onlap surface developed at the top of the overturned Valanginian marly succession (n2) in the Ravin de Riu section (Fig. 4.36, Fig. 4.41, Fig. 4.42). The Hauterivian (n3), Berriasian (n3b4), Aptian (n6) and the Albian-Cenomanian sediments are onlapping to the Valanginian (n2) limestone and marl here which suggests that the growth of the Montagne de Vibres salt swell was coeval with the rise of the Petit Mourre diapir (Fig. 4.42).

The post-Cenomanian evolution of the bounding salt structures of the Blieux, le Chiran and Grande Plaine minibasins is unclear because most of the Upper Cretaceous sediments are removed by the Tertiary erosion (Fig. 4.36).

The Jurassic-Cretaceous minibasin-scale wedge geometries are characterised by convergent boundaries and broad zone of thinning towards the diapir (Rowan & Giles, 2023).

The reinterpretation of the la Gondole, le Chiran, Grand Plaine and Blieux synclines and the adjacent salt cored anticlines and Alpine structures led to the following conclusion: the western part of the southern structural domain contain a well-developed minibasin and salt-ridge system which formed prior to the Alpine shortening (Fig. 4.44). The minibasins and salt-ridge system was situated NW of the Mesozoic Berbené salt wall (Fig. 4.44). This system represents the western continuation of the system of primary minibasins and their bounding salt structures which developed along the edge of the Provençal platform (Fig. 4.44).

The la Gondole syncline was bounded by salt structures at least in three directions (to the SE, SW, and NW, respectively) and represents the thin roof of the Berbené salt wall or a large salt body which was located at the triple junction of the Berbené salt wall and two adjoining salt bodies (the la Crotte area), at the upper part of the slope, immediately at the edge of the Provençal platform (Fig. 4.44).

However, NE of the la Gondole area, the NW-SE trending Prau salt wall, the Petit Mourre diapir, the Montagne de Vibres salt swell and the NNW-SSE oriented Portail salt wall were all situated in the basinal palaeogeographic domain of the Dauphinois and Vocontian basins (Fig. 4.35, Fig. 4.44).

The initiation of salt tectonics was coeval with the Tethyan rifting and regional extension. The elongated salt walls and salt swells together with the Petit Mourre diapir all started to emerge from the autochthonous salt layer during the Liassic as reactive diapirs. Diapiric structures presumably developed over the footwall of NW-SE trending Tethyan extensional faults, which were parallel with edge of the Provençal platform. Salt walls and diapirs bounded a series of elongated, NW-SE trending minibasins, which subsided into the autochthonous Keuper evaporites during the rifting period and the subsequent passive margin phase. The presence of basement-involved extensional faults below salt structures and the minibasins may

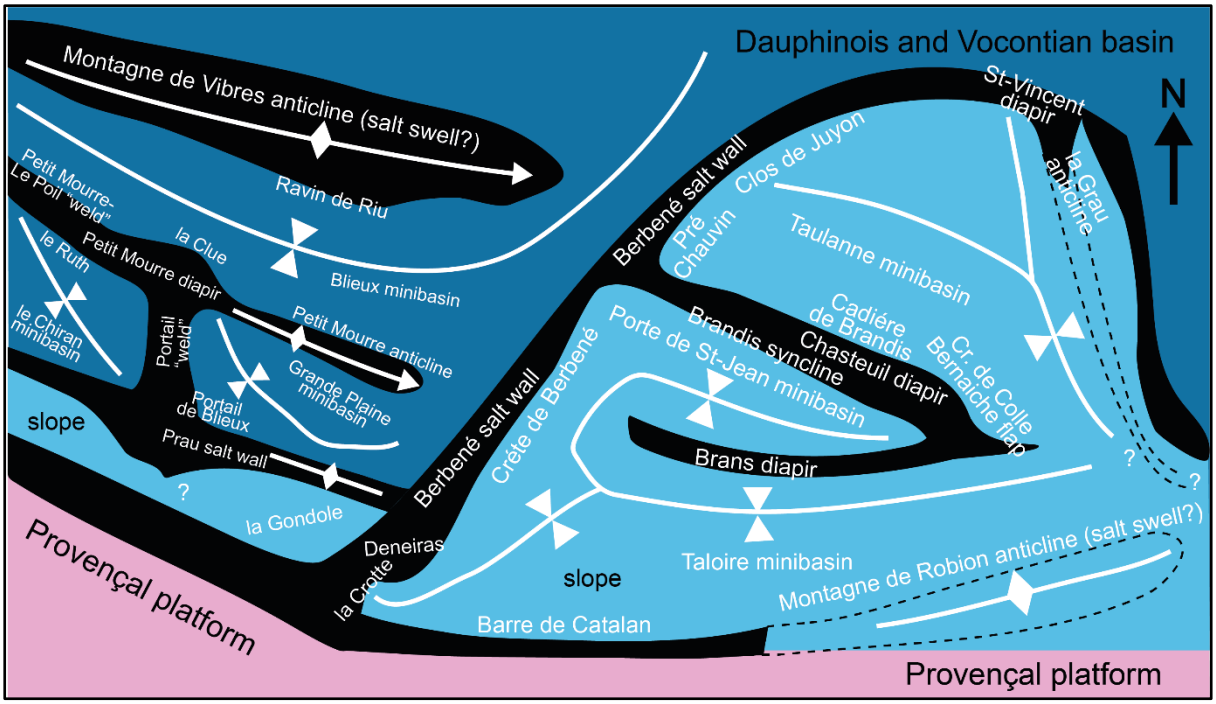


Fig. 4.44 Simplified map view of the western part of the southern structural domain during the Jurassic and Early Cretaceous. The dashed lines show assumed salt structures. The map is not restored and showing the approximate palinspastic position of the minibasins and their bounding salt structures. The minibasins, salt walls and diapirs were located along the edge of the Provençal platform on the slope and also in the basin palaeogeogrpahic domain. Additional salt structures and minibasins along the Provençal platform to the E are not shown here.

have been responsible for the observed thickness changes and variations of the sizes of the minibasins (Fig. 4.36, Fig. 4.38, Fig. 4.42). The smaller and shallower le Chiran and Grande Plaine minibasins were separated by the Portail wall and situated closer to the slope palaeogeographic domain. I assume that these smaller depocenters were located over the footwall of an inferred basement involved normal fault, while the deeper and larger Blieux minibasin may have been located in the hanging wall of this NW-SE trending extensional fault.

Passive diapirism followed the reactive rise of the salt structures and occurred already during the rifting period, as early as the Toarcian. This early transition may have been related to the complete decoupling of deformation by the time of the deposition of the Toarcian-Aalenian bioclastic limestone and differential loading was responsible for the continued growth of the diapiric structures from the Toarcian onward.

The sedimentation rate was presumably higher than the salt-rise rate and growth of the salt structures was accompanied by the formation of local unconformities and minibasin-scale thinning wedges along the Petit Mourre diapir and the Montagne de Vibres salt swell from the Toarcian to the Albian-Cenomanian. The wedging sedimentary packages developed along the growing passive diapirs as their thin roof folded over the edge of the salt structures (Rowan & Giles, 2021). The passively growing diapiric structures locally reached the seafloor, became exposed and minor salt extrusion occurred at least during the deposition of the Bathonian-Oxfordian Terres Noires Formation.

However, some of the salt structures like the Petit Mourre diapir and the Prau salt wall may have seen a stage of halokinetic active rise during Kimmeridgian-Tithonian. During halokinetic active diapirism the roofs of the diapirs were uplifted and arched (Fig. 4.40a and b, Fig. 4.43a). The extension may have thinned the roof of the diapirs. The extensional unroofing of the diapirs led to salt exposure again and a new stage of passive diapirism started. However, the salt structures presumably became buried again. The occurrence of large-scale wedge geometries in the Lower-Middle Cretaceous section records this renewed burial of the Petit Mourre diapir under a thick roof. The Jurassic-Cretaceous infill of the minibasins display clearly minibasin scale, thinning-wedge geometries (Rowan & Giles, 2023).

The presence of the well-developed system of primary minibasins and salt ridges in the basin palaeogeographic domain during the Jurassic, Lower and also the Middle-Upper Cretaceous indicates that the salt tectonics was not restricted to the slope facies zone to the N and NE of the Provençal platform. On the contrary, salt tectonic activity was spatially more widespread and continued during the later stages of the passive margin phase, beyond the Valanginian, at least until the Albian-Cenomanian.

Most of the salt structures of the basin palaeogeographic domain were strongly modified, squeezed, or completely welded and detached from their original basement and were carried in the hanging wall of the NW-SE trending thrust segment of the Berbené fault and the Le Poil thrust during the Alpine compressional phase and overthrusted the slope facies zone and also the edge of the Provençal platform.

4.1.4 Interpretation of the Jurassic-Early Cretaceous salt related structures of the southern structural domain

Many of the observed structural elements and the structural style of the southern structural domain cannot be explained by deformation related to the Alpine compression alone. Anomalous stratigraphic relationships, occurrence of breccia levels, early syn-sedimentary folding, abrupt thickness, and facies changes of the Jurassic, Lower Cretaceous and also the Albian-Cenomanian sections clearly indicate pre-Alpine diapiric activity in the slope and basin facies zones of the southern structural domain (Fig. 4.45).

The southern structural domain provides a good example of a well-developed system of primary minibasins and bounding salt structures with isolated diapirs at the junction of salt ridges. This system started to form along the edge of the Mesozoic Provençal platform as early as the Liassic. The salt walls and diapirs presumably formed over the footwall of basement involved Tethyan extensional faults as reactive diapirs. The structural trend of the palaeogeographic domains was likely to have been inherited from the configuration of Tethyan extensional structures and salt structures which were superimposed over these normal faults, and they defined the Mesozoic facies boundaries (Fig. 4.33). In some cases, the irregular topography of the pre-salt basement which formed during the rifting phase led to the formation of shallower and deeper primary minibasins. The original thickness of evaporites in the autochthonous salt layer is not known. However, the thickness of the Jurassic-Cretaceous of the deeper minibasins suggests that a significant amount of Keuper evaporites were involved in salt tectonic processes. A polygonal network of salt diapirs and walls formed in the Chasteuil and Teillon area. To the NE, more isolated salt structures developed in the basin facies zone. In contrast, W of the Teillon and Chasteuil areas, this network of the slope palaeogeographic domain is less developed and the basin facies zone is characterised by the complex system of elongated primary minibasins and salt diapirs, ridges and walls (Fig. 4.45). However, this structural configuration is presumably apparent and related to the Alpine modification of the minibasin and ridge province. The salt tectonic activity in the southern structural domain

continued after the end of the rifting phase, during the passive margin phase, at least until the Albian-Cenomanian. The salt structures grew as passive diapirs due to differential loading, but some of the diapirs went through a short period of halokinetic reactive rise while others were growing for a long period from Liassic until the Late Cretaceous due to halokinesis.

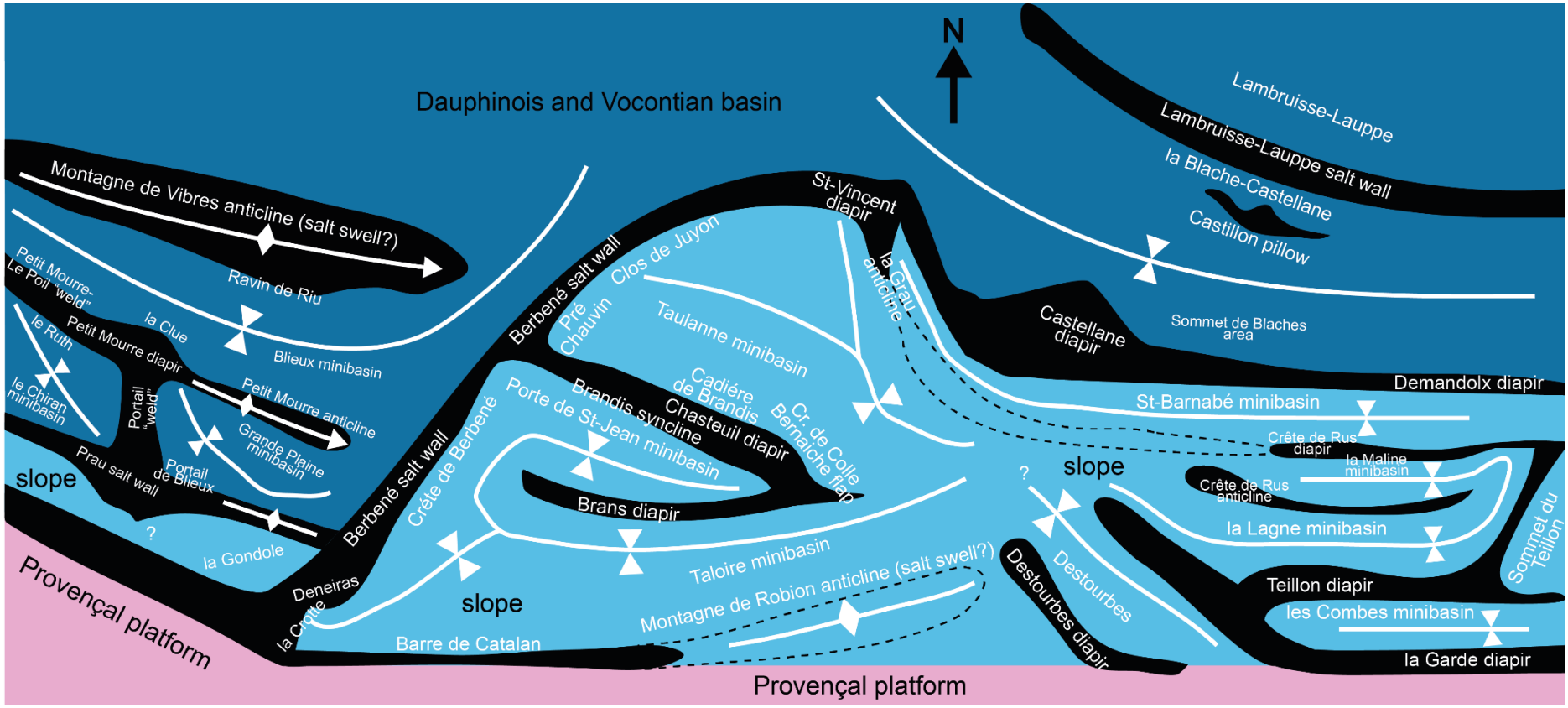


Fig. 4.45 Map-view schematic model of the southern structural domain during the Jurassic and Cretaceous time. Dashed lines show assumed salt structures. The early pre-Alpine salt structures and adjacent primary minibasins formed a complex network N and NE of the Provençal platform. The facies boundaries were defined by elongated salt walls, presumably developed over the footwall of Tethyan extensional faults. The map is not restored and only showing the approximate palinspastic position of the minibasins, diapirs and salt walls.

4.2 Jurassic-Early Cretaceous salt tectonics in the northern structural domain around Barrême. Observations, structural and stratal geometries

The aim of the following sub-chapter is to provide evidence for early salt tectonic activity N of the southern structural domain, in the vicinity of the villages of Barrême and Gévaudan (Fig. 4.46, Fig. 4.47). The northern structural domain comprises the eastern part of the Valensole basin S of the town of Digne-les-Bains, the northern part of the St-Jurs imbricates, the southern part of the Digne arc and the Barrême basin (Fig. 2.1b). However, in the following section, observations are focussed on the eastern part of the northern structural domain and on a narrow, approximately N-S trending zone where the Upper Triassic evaporites are exposed along a series of anomalous contacts and Alpine structures, between the village of le Gion and the village of Boades (Fig. 4.46 and Fig. 4.47). The northern structural domain of the study area is composed of a series of Alpine thrust sheets, which comprise thick basinal Jurassic-Cretaceous sections and overlying Tertiary sediments. The Alpine thrust faults of the northern structural domain are roughly NW-SE and NNW-SSE trending, which is the typical structural trend of the southern part of the Digne arc but distinct from the southern structural domain (Fig. 4.25). However, a series of E and SE trending folds are also present to the NW, W and SW of the village of Barrême. These folds are the lateral tip folds of a splay of the Digne thrust (Graham et al., 2012) (Fig. 4.46 and Fig. 4.47). To the NW and W of the northern structural domain, in the northern part of the Valensole basin (Fig. 2.1), the Mio-Pliocene element of the Digne thrust has a minimum displacement of 20 km. However, the tip folds at Barrême are unconformably overlain by the Nummulitic Limestone, which implies that this segment of the Digne Thrust was active before the Priabonian. The western part of the northern domain is situated in the hanging wall of the Digne thrust and the Montagne de Vibres thrust (Fig. 4.47). Further to the NW, the Digne thrust is overriding the Mesozoic slope and platform facies zones while the Montagne de Vibres structure over-thrusted the le Poil zone and the Blieux minibasin (Fig. 2.1 and Fig. 4.35). The Digne and Montagne de Vibres thrusts carry NNW-SSE oriented synclines filled with Tertiary sediments (piggyback basins), the Barrême and Senez synclines. The Barrême and Senez synclines are connected to the NW-SE trending Blieux minibasin.

The eastern part of the northern structural domain comprises the northern part of the la Blache-Castellane thrust sheet and the overriding Lambruisse-Lauppe thrust sheet which also carry thick sections deposited in the basin facies zone during the Jurassic and Cretaceous (Fig. 4.46 and Fig. 4.47). N of the village of Gévaudan, the NNW-SSE trending Lambruisse-Lauppe

thrust fault is linked into the La Cine fault through a NE-SW trending fault (Fig. 4.47) (see Chapter 3, § 3.4). Between the eastern and western part of the northern structural domain, i.e., the hanging wall of the Digne and Montagne de Vibres thrust faults and E of the Tertiary piggyback basins and in the footwall of the la Blache-Castellane and Lambruisse-Lauppe thrust sheets, a structurally complex zone is exposed. This zone is connected to the large outcrops of Keuper gypsum: the St-Vincent diapir, the la Grau anticline and the adjoining Boades zone to the S (see § 4.1.1.1) and to the Gévaudan diapir to the N (Fig. 4.46, Fig. 4.47). In the following section, I am going to describe the observed structural and stratal geometries and salt related structures of the Jurassic-Early Cretaceous section of the northern structural domain between the Gévaudan diapir and the St-Vincent diapir (Fig. 4.47).

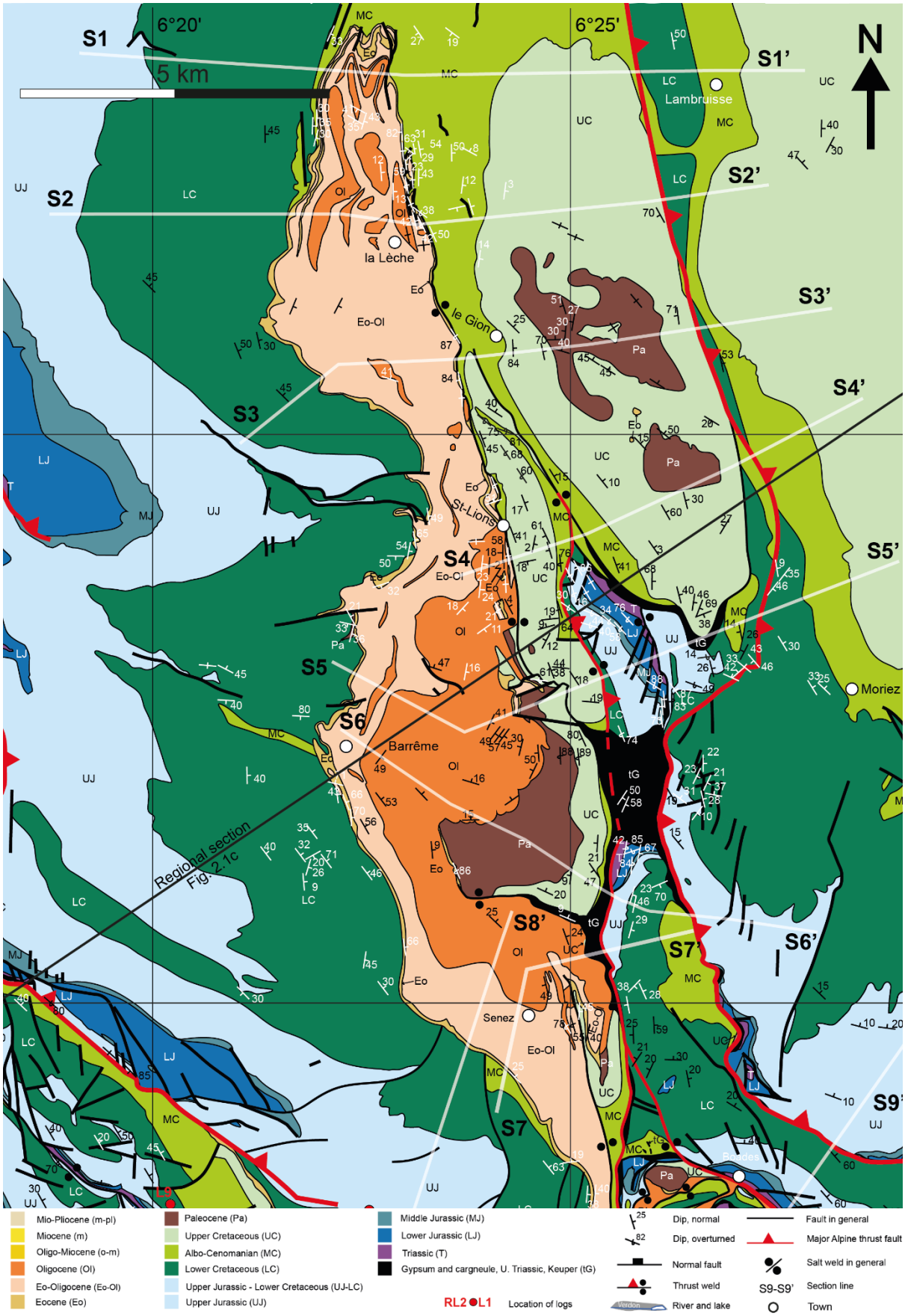


Fig. 4.46 Simplified geological map of the northern structural domain, between the villages of Boades and Lambruisse. Redrawn after Kerckhove & Roux (1976a), Kerckhove & Roux (1978a) and De Graciansky et al. (1981). See Fig. 4.47 for the structural explanation.

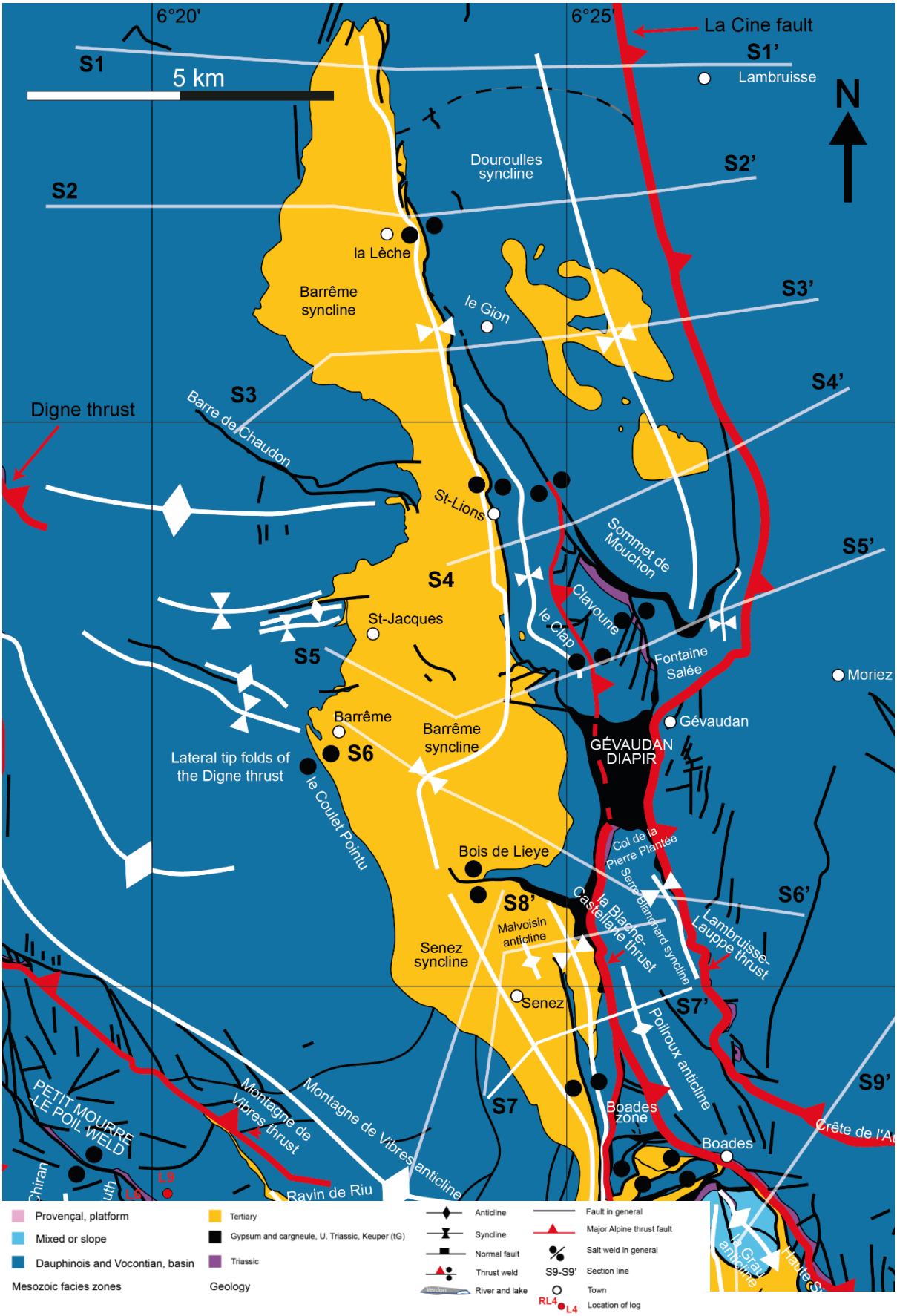


Fig. 4.47 Structural map of the northern structural domain, showing synclines, their bounding Alpine structures or pre-Alpine salt structures of the southern part of the Digne arc and their Mesozoic palaeogeographic position. Data from Kerckhove & Roux (1976a), Kerckhove & Roux (1978a) and De Graciansky et al. (1981).

4.2.1 The Gévaudan diapir and its flanking strata: the Clavoune and the Col de la Pierre Plantée sections

Evidence for pre-Alpine salt tectonic activity can be seen in the northern structural domain, in the vicinity of the villages of Barrême and Gévaudan, around the Gévaudan diapir. The diapir is situated in the northern part of the la Blache-Castellane thrust sheet, at the junction of the la Blache-Castellane and the Lambruisse-Lauppe thrust faults (Fig. 4.47). The salt structure is a well-known: Emre (1977) described the salt body as diapiric while Lickorish & Ford (1998) identified the diapir as an early formed structure which developed along a major extensional fault during the Mesozoic and later became strongly shortened during the Alpine compressional phase. Like the Castellane diapir (see § 4.1.2.3), the Gévaudan diapir comprises several elongated Keuper gypsum and cargneule breccia bodies (tG) which amalgamated into a single diapiric structure (Fig. 4.24, Fig. 4.25, Fig. 4.26). The diapir also exposes large blocks of the Norian (7-9) argillite (it is shown together with the Keuper gypsum as tG on Fig. 4.46). The surface exposure of the Triassic gypsum and cargneule breccia is approximately 3 km^2 (Fig. 4.46). Hence, the Gévaudan diapir is the largest 'accumulation' of diapiric salt in the study area.

The diapir is bounded to the W by Upper Cretaceous sediments and the Tertiary infill of the Barrême and Senez piggyback basins (Fig. 4.46, Fig. 4.47). To the E, the Triassic salt is overridden by the Upper Jurassic-Lower Cretaceous basinal section of the Lambruisse-Lauppe thrust sheet, which is gently dipping to the E (Fig. 4.46).

At the Clavoune mountain, N of the diapir, a subvertical or locally overturned and extremely reduced Triassic-Lower Cretaceous section (from Norian to Barremian, t7-9 to n4-5) is exposed which is overthrusted a syncline formed of Middle-and Upper Cretaceous sediments (Fig. 4.46, Fig. 4.49 and Fig. 4.50). The Norian (t7-9) and Rhaetian (t10) strata are overturned to SW and separated from a complex and highly deformed zone of Upper Jurassic and Cretaceous rocks of the Fontaine Salée section by an anomalous contact (Fig. 4.46 and Fig. 4.47, Fig. 4.49, described later). This anomalous contact is linking the Gévaudan diapir with an approximately NW-SE trending salt body which is separating the Middle-Upper Cretaceous section of the Douroulles syncline from the Clavoune and the Fontaine Salée sections (see Chapter 5. § 3.1 and § 3.2) (Fig. 4.46, Fig. 4.47, Fig. 4.48, Fig. 4.49, Fig. 4.50). The Liassic section of the Clavoune mountain contains several unconformities and sedimentary gaps.

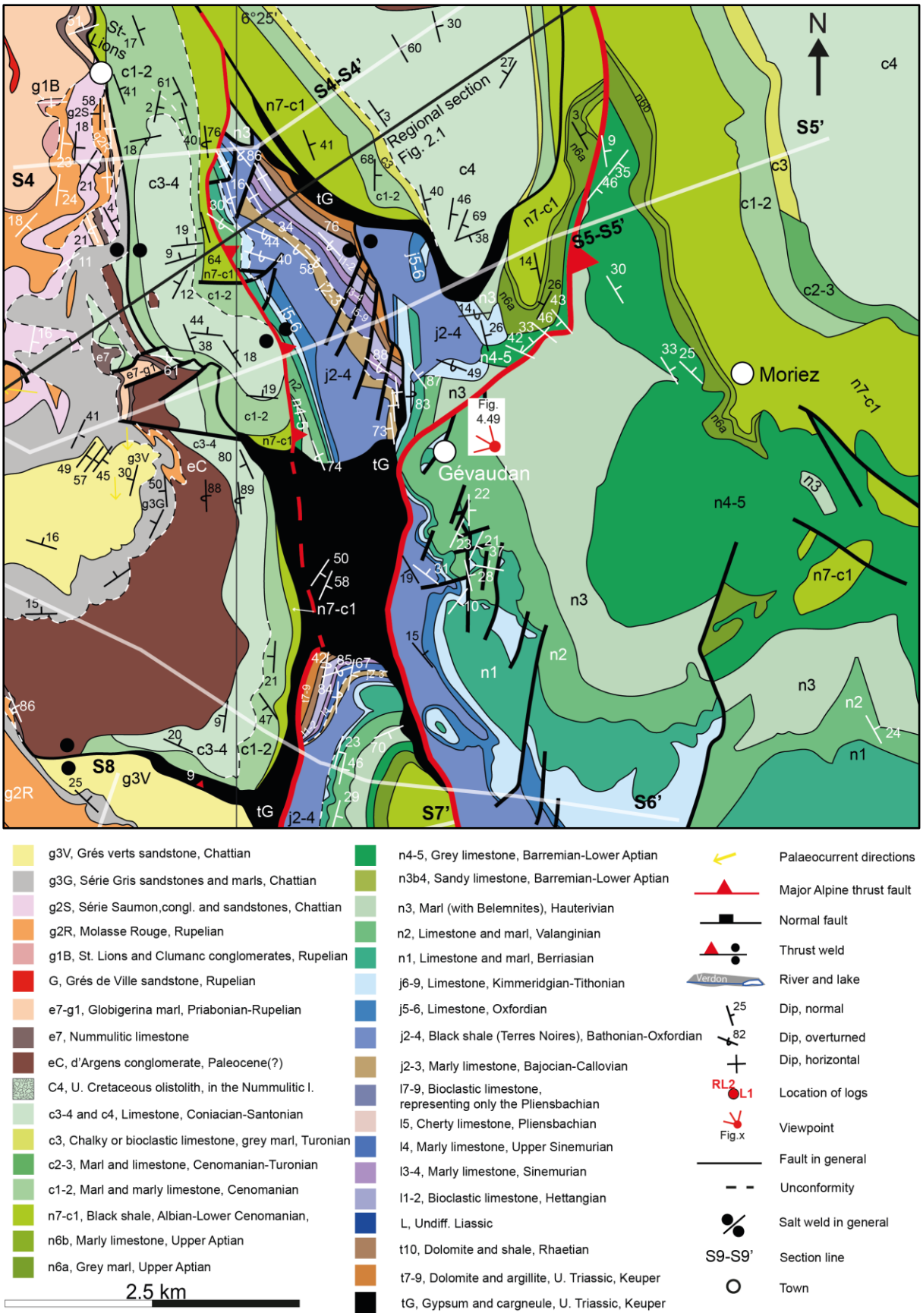


Fig. 4.48 Detailed geological map of the Gévaudan diapir and its surroundings. See Fig. 4.47 for structural explanation.

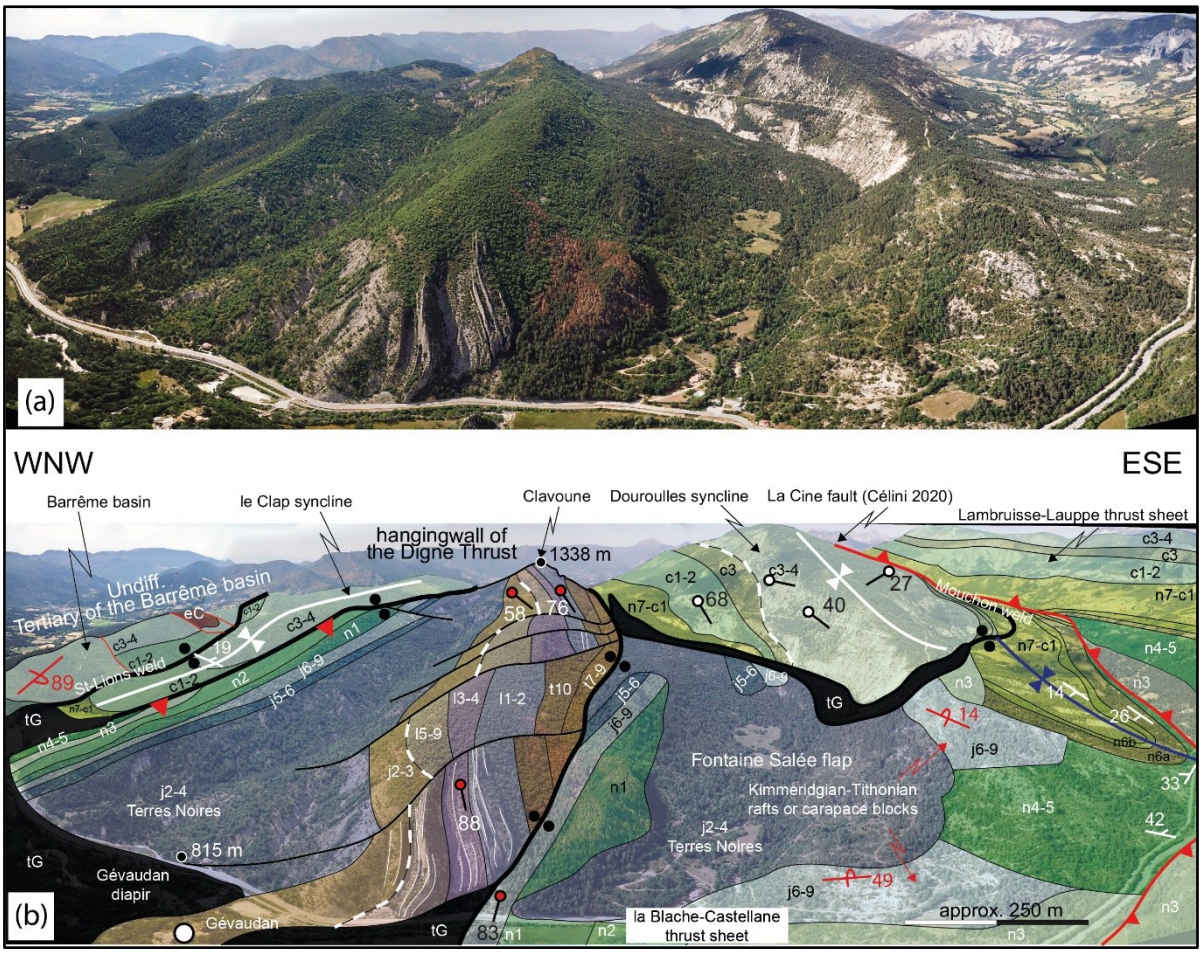


Fig. 4.49 Uninterpreted (a) and interpreted (b) photo panorama of the Clavoune section and the Gévaudan diapir, looking to the NNE. Black epsilons indicate younging direction. See Fig. 4.48 for key and viewpoint location. Photo taken by Célini, N.

De Graciansky et al. (1982) referred to this thin and incomplete Liassic section as 'Gévaudan type Liassic' and noted that the unique Liassic facies of the basin palaeogeographic domain is similar to the Liassic sections which deposited along the edge of the Provençal platform. The 'Gévaudan-type' Liassic section at the Clavoune is only 150 m thick. A few kilometres to the NW, in the Digne nappe, the Liassic can reach a thickness of 1500 meters NNW of the village of Barrême. The Early Jurassic section in the Clavoune section is consists of Hettangian bioclastic limestone (l1-2), Sinemurian bioclastic limestone (l3-4) and Pliensbachian cherty and bioclastic limestones (l5-9). The Sinemurian bioclastic limestone contains oyster (Gryphaea) fossils in 'life position' (De Graciansky et al., 1982). The upper part of the Liassic section is incomplete as almost the entire Toarcian section is missing. The Liassic section is unconformably overlain by an incomplete Middle Jurassic section where the Lower Aalenian is missing. The Cancellophycus marly limestone (j2-3) formation is slightly older in the Clavoune section than in the southern structural domain, around Castellane, as it was deposited in the Bajocian. The base of the formation is represented by an erosional unconformity.

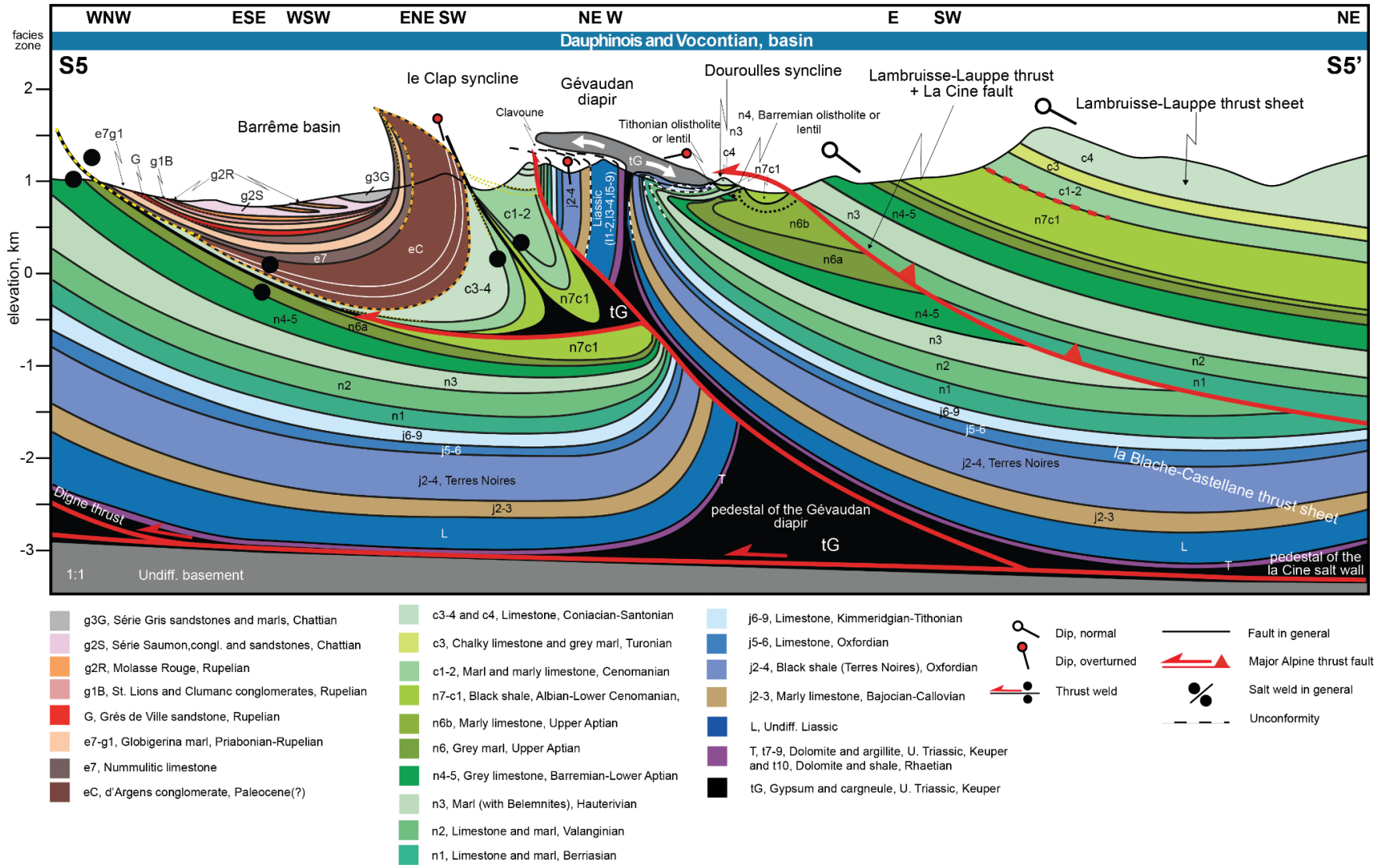


Fig. 4.50 Cross section (S5-S5') from the Digne thrust sheet to the Lambruisse-Lauppe thrust sheet, crossing the Clavoune section and the Gévaudan diapir. See Fig. 4.46 for cross section location.

The Bajocian Cancellophycus marly limestone is overlain by the Terres Noires (Bathonian-Oxfordian), which is reduced, only 100-150 m. Several NE-SW trending faults crosscut the Liassic and Middle Jurassic section and offset the base-Bajocian unconformity. These faults linked into the anomalous contact which is bounding the Clavoune section to the E, and they are apparently sealed by the Terres Noires (Fig. 4.48). The Terres Noires passes into the Upper Oxfordian limestone (j5-6) which is overlain by a reduced Kimmeridgian-Tithonian (j6-9) limestone dominated section. The Upper Jurassic section is in vertical position or slightly overturned to the SW (Fig. 4.48, Fig. 4.49, Fig. 4.50). The Lower Cretaceous section is also vertical, and it is composed of Berriasian (n1), Valanginian (n2), Hauterivian (n3) and Barremian-Lower Aptian sediments (n4-5). The thickness of the Lower Cretaceous section is reduced (around 200 m). The vertical Liassic-Lower Aptian (l1-2 to n4-5) section of the Clavoune mountain is abuts against the Gévaudan diapir to the S and bounded by an Alpine thrust fault to the W (Fig. 4.46, Fig. 4.47, Fig. 4.48). Along this thrust, the Liassic-Lower Aptian section of the Clavoune mountain is overriding the le Clap syncline (Fig. 4.47), which is composed of Middle-and Upper Cretaceous rocks and separated from the Barrême syncline by an anomalous contact (see Chapter 5, § 3.1.1).

To the E, the Clavoune section is bounded by the Fontaine Salée section which is representing the northernmost extent of the basinal section of the la Blache-Castellane thrust sheet (Fig. 4.47, Fig. 4.48 and Fig. 4.49). The Fontaine Salée section is structurally complex or „chaotic' and it is composed of Upper Jurassic-Upper Cretaceous succession, which is similar to the upper part of the Clavoune section. Liassic and Middle Jurassic rocks are not exposed to E of the diapir. Springs where salt brine flows to the surface are located here, E of the Clavoune mountain (Morin et al., 2004). The lower part of the Fontaine Salée section is composed of vertical beds of the Terres Noires (j2-4) which is overlain by thin Kimmeridgian-Tithonian (j6-9) limestone, which passes into a reduced Lower Cretaceous section (n1, n2, n3 and n4-5). Albian and Albian-Cenomanian (n6a, n6b and n7-c1) formations preserved in the core of a roughly N-S trending syncline, in the footwall of the Lambruisse-Lauppe thrust (Fig. 4.47, Fig. 4.48,Fig. 4.49). The vertical Cretaceous section of the Fontaine Salée area is structurally overlain by overturned Upper Jurassic (j2-4, j5-6 and j6-9) strata. The overturned Terres Noires (j2-4) is in direct contact with Berriasian (n1), Valanginian (n2), Hauterivian (n3) and Barremian (n4-5) rocks. Along the anomalous contact, which is bounding the Fontaine Salée section to the W, the deeper part of the section, i.e., the vertical Oxfordian-Berriasian (j2-4 to n1) is apparently exposed in a window below the overturned Terres Noires. The overturned Kimmeridgian-Tithonian section is composed of large blocks which are approximately 400-

500 m in diameter (Fig. 4.49). A large block of Hauterivian (n3) was also observed which is in direct contact with Tithonian, Albian-Cenomanian rocks (n6a, n6b and n7-c1) and the Triassic gypsum. The Fontaine Salée section is separated from the Douroulles syncline by a large, NW-SE trending gypsum body (see Chapter 5, § 3.1.1).

To the S and SW, the Gévaudan diapir is bounded by the Triassic-Middle Cretaceous section (t7-9 to n7-c1) of the la Blache-Castellane thrust sheet. SSE of the diapir, a NNW-SSE trending anticline and a NNW-SSE oriented syncline formed in the hanging wall of the thrust, the Poilroux anticline and the Serre Blanchard syncline, respectively (Fig. 4.47). On the northern flank of the Serre Blanchard syncline, the complete Jurassic-Middle Cretaceous section is in direct contact with the Keuper gypsum. Further to the SE, Upper Cretaceous (UC) sediments are also exposed in the core of the Serre Blanchard syncline, in the immediate footwall of the Lambruisse-Lauppe thrust sheet (Fig. 4.46). The northern flank of the Serre Blanchard syncline (Col de la Pierre Plantée section) exposes a reduced and overturned 'Gévaudan type Liassic' section along the Keuper gypsum. The base of the Col de la Pierre Plantée section is composed of Norian and Rhaetian (t7-9 and t10) rocks which are overlain by the reduced Liassic section (around 100 m). The Liassic section is slightly different from the Clavoune section, and it is composed of Hettangian (l1-2), Sinemurian (l3 and l4) cherty and marly limestone formations. The Pliensbachian, Toarcian and Aalenian sediments are missing and the Liassic is section is unconformably overlain by the Bajocian marly limestone (Cancellophycus marly limestone formation, j2-3). The Liassic section and the lower part of the Bajocian marly limestone are overturned to the E and SE. However, locally more gentle dips were measured in the upper part of the Bajocian section, dipping around 70º to the ESE, creating a 20º angular unconformity. Similarly, to the Clavoune section, the Middle Jurassic is overlain by the Terres Noires, which is also really thin (around 100-150 m). The Terres Noires can reach the thickness of 600-700 m further to the NW in the hanging wall of the Digne thrust (De Graciansky et al., 1982). The Terres Noires is overlain unconformably by thin Kimmeridgian-Tithonian (j6-9) limestone and the Upper Oxfordian limestone (j5-6) is missing here. The Upper Jurassic section is dipping towards the ESE. The Terres Noires is also overlain unconformably by the Berriasian (n1) on the eastern flank of the Gévaudan diapir. The Kimmeridgian-Tithonian is dismembered into large blocks along this local unconformity. The limestone blocks are approximately 100-150 m in diameter. Further to the S, these unconformities can be seen in the hanging wall of the la Blache-Castellane thrust sheet approximately 2 km of the diapir. The Berriasian-Hauterivian section is dipping around 30-40º to the SE, also creating an angular unconformity. The Barremian, Aptian, Albian-Cenomanian and Cenomanian sediments (n4-5, n6a, n7-c1 and c1-

2) are preserved in the core of the Serre Blanchard syncline which is bounding the diapir to the SE (Fig. 4.47 and Fig. 4.48). A local unconformity also developed on the western flank of this syncline, at the base of the Albian-Cenomanian (n7-c1) black shales which overlies the Barremian limestone (n4-5) E of the village of Senez, where the la Blache-Castellane thrust sheet is overriding the Boades zone, in the hanging wall of the thrust, Lower Cretaceous rocks are exposed in the core of the Poilroux anticline.

4.2.2 Interpretation of the Gévaudan diapir and its flanking sections

Based on the observed stratal and structural geometries around the Gévaudan diapir, I interpret the Gévaudan salt structure as an early formed, relatively isolated, and roughly N-S trending salt diapir which developed in the basinal facies zone of the Dauphinois basin. Similarly, to the southern structural domain, the Norian-Rhaetian section (t7-9 and t10) is considered as a pre-kinematic interval. The Gévaudan diapir started to grow during the Liassic (Fig. 4.51), simultaneously with the rifting of the margin. This growth is indicated by the occurrence of incomplete sections, facies variations and thickness changes of the Liassic succession around the diapir. Lickorish & Ford (1998) suggested that the Gévaudan diapir was formed along a Mesozoic extensional fault. I assume that the diapiric growth was initiated by regional extension and the salt structure started to grow in the footwall of this Tethyan normal fault as a reactive diapir. However, similarly to the southern structural domain of the study area, the pre-salt basement is not exposed around the village of Barrême and the Gévaudan diapir. Hence, the presence of an extensional fault below the diapir (or at the original location of the diapir) is not proven. The diapir was bounded to the E and W by depocenters which were subsided into the autochthonous salt layer simultaneously with the growth of the diapir, i.e., primary minibasins. The diapir was bounded to the W by the basinal succession, which is exposed now in the hanging wall of the Digne thrust and the Montagne de Vibres thrust fault (Fig. 4.47). This depocenter is the Barrême minibasin (primary minibasin) (Fig. 4.52). To the E, the diapir was presumably flanked by the Serre Blanchard syncline which is interpreted as a primary minibasin (Serre Blanchard minibasin) (Fig. 4.52). The reduced and incomplete Liassic sections of the Clavoune mountain, N of the diapir and the Col de la Pierre Plantée area, S of the diapir, are representing the oldest roof strata of the Gévaudan salt structure. The Clavoune section was situated SW of the diapir while the Col de la Pierre Plantée section represents the NE flanking strata of the diapir (Fig. 4.51).

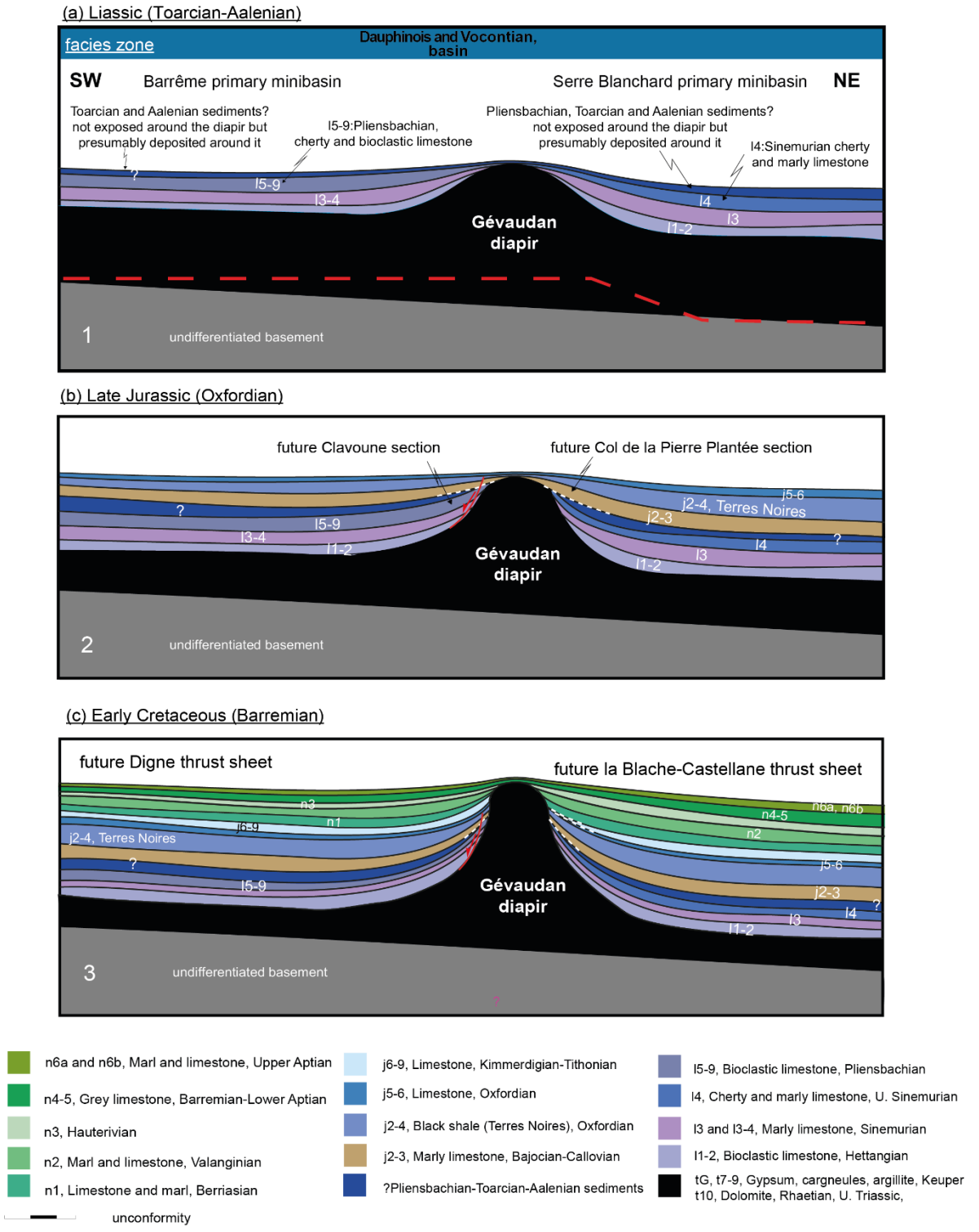


Fig. 4.51 Diagrams showing the possible evolution of the Gévaudan diapir from the Liassic (a) until the Barremian (c). The red dashed line on (a) showing an alternative interpretation for the top of the pre-salt basement and the possible position of a Tethyan extensional fault which formed during the rifting phase and initiated the diapirism. The Jurassic-Lower Cretaceous sections which are exposed now in the Digne nappe and the la Blache-Castellane thrust sheet are thinning towards the diapir and showing wedging geometries. Not to scale.

However, this Mesozoic configuration was highly modified by the Alpine compression (see Chapter 5, § 5). The Jurassic-Cretaceous section of the Fontaine Salée section (Fig. 4.49, Fig. 4.50) is also interpreted as the eastern flanking strata of the diapir. The presence of the thin, incomplete Liassic sections and oyster fossils (Gryphaea) in life position in the Sinemurian succession of the Clavoune section suggest that the salt stock formed a considerable palaeotopographic high as early as the Liassic in the basinal facies zone (Fig. 4.51, Fig. 4.52). The pedestal of the early formed diapir is now located along the basal detachment surface, in the footwall of the la Blache-Castellane thrust fault, at the depth of 2.5-3 km (Fig. 4.50). The width of the pedestal is around 2.5 km. The anomalous contact which is separating the Clavoune section from the Jurassic-Cretaceous section of the Fontaine Salée section area (Fig. 4.49, Fig. 4.50) is interpreted as the partly welded remnant of the stem of the original Gévaudan diapir which is highly modified by Alpine compression. Sediment accumulation around the diapir was simultaneous with salt withdrawal from the autochthonous salt layer into the diapir.

A period of rapid growth of the Gévaudan diapir occurred during the Bajocian, which is recorded by the base-Bajocian unconformity on both flanks of the diapir (Fig. 4.51). Cross-section construction revealed that the Middle-, Upper Jurassic and also the Lower Cretaceous sections, which are exposed now in the Clavoune section and the la-Blache-Castellane thrust sheet, are thinning and wedging toward the Gévaudan diapir and forming a thinning wedge minibasin tectonostratigraphic succession (Fig. 4.50) (Rowan & Giles, 2023). I assume that during the late stages of the rifting and the early stages of the passive margin phase, the salt structure was growing as a passive diapir. The salt tectonic activity may have been maintained by differential loading of the sediments over the autochthonous salt layer. Within the large-scale wedge of the Middle Jurassic Lower Cretaceous section on the NE flank of the Gévaudan diapir, several low angle unconformities were observed (Fig. 4.51). The diapir was presumably covered by a thin roof during most of the Jurassic and Early Cretaceous.

The Jurassic-Cretaceous section of the Fontaine Salée section (Fig. 4.49, Fig. 4.50) is also representing the roof strata of the diapir. The overturned Jurassic section is interpreted as a flap, which I have called the Fontaine Salée flap (Fig. 4.49, Fig. 4.50).

The formation of the overturned flap may have been related to the extrusion of salt from the Gévaudan diapir which occurred during the middle of the Cretaceous (see Chapter 5, § 3.2) or occurred later, during the Alpine compressional phase. The large blocks of the Kimmeridgian-Tithonian (j6-9) are interpreted as rafts which may have been dismembered during the overturning of the flap.

The small syncline, which is situated E of the Fontaine Salée flap, at the footwall of the Lambruisse-Lauppe thrust sheet, may have been corresponded to the Serre Blanchard syncline and it formed its north-eastern continuation during the Jurassic and the Cretaceous (Fig. 4.52).

This syncline maybe was continuous towards to SE and corresponds to the same syncline, which bounded the Castellane and St-Vincent diapirs to the NE (Fig. 4.45 and Fig. 4.52). The eastern flank of this syncline (i.e. the eastern segment of the la Blache-Castellane thrust sheet) is not exposed in the footwall of the overriding Lambruisse Lauppe thrust sheet (Fig. 4.25 and Fig. 4.47). However, I suggest that this syncline was bounded to the NE by the Lambruisse-Lauppe salt wall (Fig. 4.52). According to Célini (2020), the la Cine salt wall, now represented

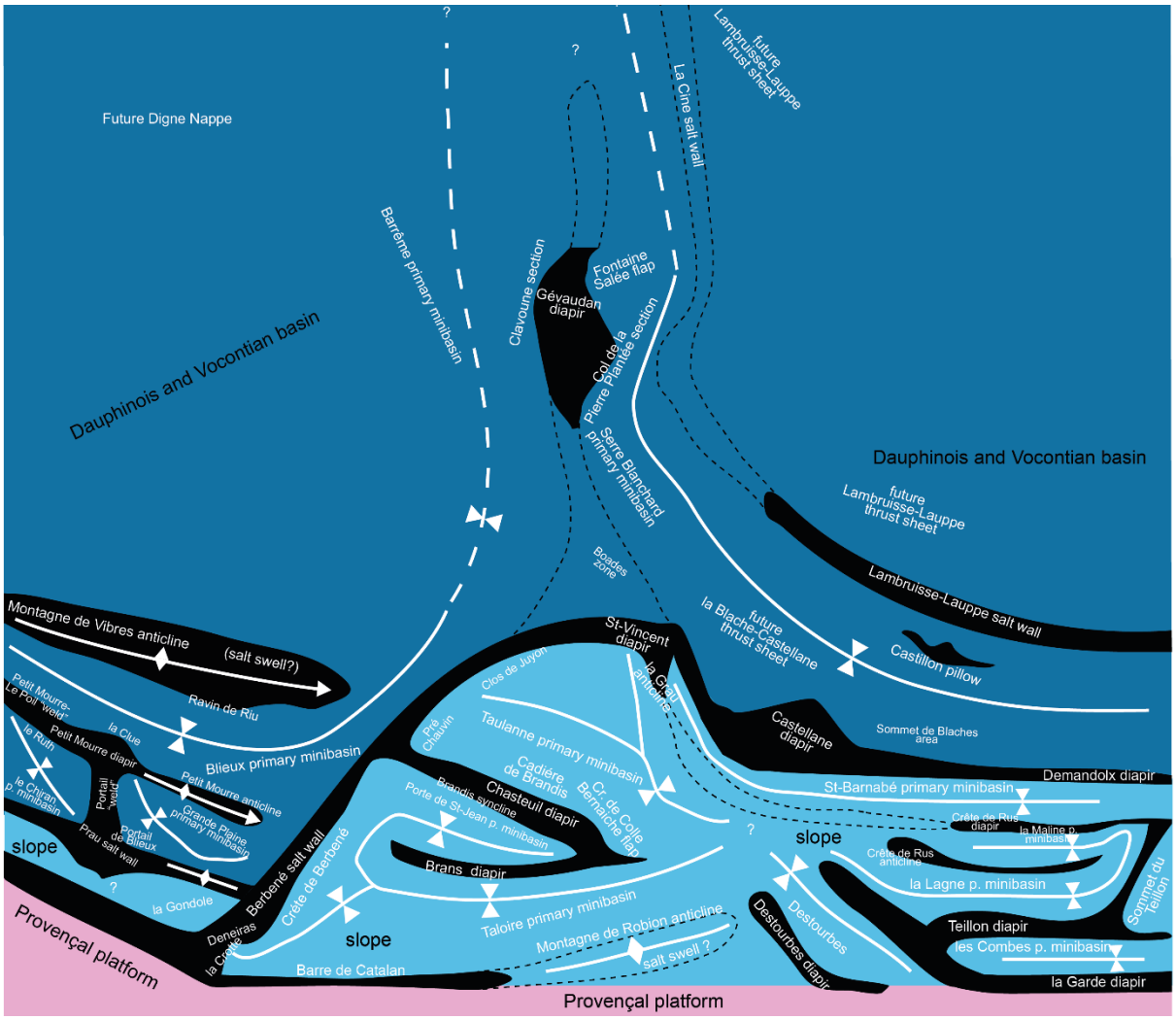


Fig. 4.52 Map-view schematic model of the study area during the Jurassic and Early Cretaceous times. Dashed lines represent assumed salt structures. The pre-Alpine salt structures and adjacent primary minibasins formed a complex network N and NE of the Provençal platform. Isolated diapirs such as the Gévaudan diapir also formed in the basin facies zone. The Gévaudan diapir was probably connected to the St-Vincent and Castellane diapirs through a N-S trending deeply buried salt wall. The Lambruisse-Lauppe salt wall was presumably connected to the la Cine salt wall. The map is not restored and only showing the approximate palinspastic position of the minibasins, diapirs and salt walls.

by the La Cine fault, which is connected to the Lambruisse-Lauppe thrust, remained active throughout the whole Mesozoic. During the Alpine compressional phase, the La Cine wall may have served as a ramp for an advancing Alpine thrust fault in the Oligocene and the Jurassic-Cretaceous basinal rocks over-thrusted the Barrême and Douroulles synclines (see Chapter 5, § 5). The basinal Jurassic-Cretaceous section of the Lambruisse-Lauppe thrust is also overriding the Douroulles syncline and forms the southern continuation of the la Cine fault. This suggests that the Lambruisse-Lauppe salt wall may have been connected to the La Cine wall, presumably E of the Gévaudan diapir and corresponding to the same elongated salt structure, i.e., a pre-Alpine salt wall, which may have been bounded the Serre Blanchard primary minibasin to the E and NE (Fig. 4.52).

I also suggest the Gévaudan diapir was linked to the St-Vincent diapir of the southern structural domain through an approximately N-S trending, deeply buried salt wall, which represented the NW continuation of the salt wall which linked the St-Vincent diapir and the Castellane diapir. This salt structure may have been bounded the Serre Blanchard syncline to the W (Fig. 4.52). However, this interpretation is highly speculative due to poor outcrop conditions between the Gévaudan diapir and the St-Vincent diapir.

I conclude that the northern structural domain containing a network of pre-Alpine salt diapirs and salt walls. The presence of these diapirs and salt ridges in the basin palaeogeographic domain during the Jurassic, Lower and Middle Cretaceous indicates that the salt tectonic activity was not restricted to the slope facies zone and to the southern part of the basin facies zone. On the contrary, salt tectonic tectonics was widespread in the northern, more basinal part of the basin palaeogeographic domain and highly influenced the sedimentation, facies, and thickness of the Jurassic and also the Lower Cretaceous successions of the Dauphinois and Vocontian basins.

4.3 Conclusion of the chapter

In this chapter, I described and analysed several Jurassic-Early Cretaceous salt withdrawal basins, i.e., primary minibasins, resting on the autochthonous Triassic salt layer and their bounding salt structures such as salt swells, salt stocks, diapirs and walls in the Southern Subalpine Chains from south to north, around Blieux, Chasteuil, Castellane, la Garde and Barrême. The study of the southern and northern structural domains of the study area reveals that several pre-Alpine diapiric structures were formed during the Jurassic and Cretaceous. Similarly, to other well-known structures of the Subalpine chains, these salt structures started

to grow as reactive diapirs during the rifting of the margin. Passive diapirism occurred as early as the Liassic, simultaneously with the rifting, and continued through the passive margin phase, at least until the Cenomanian. A salt tectonic model was introduced in this chapter, which described the formation and evolution of a well-developed minibasin and salt-ridge system. This complex system was situated during the Jurassic and Cretaceous time to the N and NE of the Provencal platform. The original thickness and distribution of the Keuper evaporites which were involved in the salt tectonic processes is not known. However, the number and the size of the primary minibasins and the pre-contractional distribution of these depocenters all suggest that the autochthonous salt layer may have been the thickest in the southern structural domain, adjacent to the northern edge of the Provençal platform. Most of the mature salt structures were situated in the slope palaeogeographic domain of the Dauphinois and Vocontian basins and highly affected the sedimentation and facies distribution in the Dauphinois and Vocontian basins. The salt structures which formed in the slope facies zone of the southern structural domain were mostly parallel to the edge of the Mesozoic platform, but some of the structures were obliquely oriented to the platform edge and linked the platform-parallel diapiric structures. Platform-parallel diapiric structures and adjacent minibasins were also identified in the basin facies zone of the southern structural domain around Blieux. The basin palaeogeographic domain was separated from the slope facies zone by elongated salt walls and isolated diapiric structures, which formed at the junction of these walls. However, a complex zone of pre-Alpine salt structures was almost perpendicular to the edge of the platform, at the apex of the future Castellane arc. This roughly N-S trending salt structure, presumably a wall, linked the isolated Gévaudan diapir of the basinal palaeogeographic domain to the bounding and most basinward diapiric structure of the slope domain, the St-Vincent diapir. In the following chapter, I am going to present new evidence for continuous salt tectonic activity after the Early Cretaceous, which is ended up in the extrusion of the Keuper salt to the seafloor during the deposition of the Albian-Cenomanian black shales. Salt tectonics climaxed in the formation of salt sheets which may have been amalgamated and formed a large salt canopy above the system of primary minibasins, diapirs and salt walls of the slope and basin palaeogeographic domains. This allochthonous salt body hosted a complex network of secondary minibasins and their bounding salt structures from the Albian-Cenomanian onward.

Chapter 5. An Albian-Cenomanian salt canopy and secondary minibasins in the sub-Alpine fold and thrust belt of Haute Provence, France

The following chapter will be submitted for publication as a paper entitled ‘An Albian-Cenomanian salt canopy and secondary minibasins in the sub-Alpine fold-and-thrust belt of Haute Provence, France’ to a peer reviewed journal, e.g., Tectonics (Authors: Csicsek, L.A., Graham, R. and Lonergan, L.). The grammar and graphic styles of this chapter follow the AGU Publications manuscript style guidelines. There is some repetition of the content from previous chapters in the introduction, geological setting and data and observations sections of this chapter. Please note that in some cases, names of geographical locations and geological structures were changed in order to simplify descriptive and interpretative sections.

An Albian-Cenomanian salt canopy and secondary minibasins in the sub-Alpine fold and thrust belt of Haute Provence, France.

Lajos Adam Csicsek[1], Rodney Graham[1], and Lidia Lonergan[1]

[1]Department of Earth Science and Engineering, Imperial College London, London, UK

Corresponding author: Lajos Adam Csicsek (l.csicsek17@imperial.ac.uk, adamcsicsek@gmail.com)

Key Points

- Jurassic-Cretaceous salt tectonics on the Tethyan margin culminated in the extrusion of evaporites onto the seafloor during the Albian-Cenomanian.
- Salt sheets coalesced to form a canopy. Second generation salt structures and secondary minibasins developed above the canopy during the Late Cretaceous.
- Secondary minibasins were carried as piggyback basins during Alpine shortening. Interaction of salt tectonics and thrusting resulted in formation of hybrid basins.

Abstract

Allochthonous salt is common in deep-water areas of salt-bearing passive margins and present in onshore fold and thrust belts. However, only a few examples of salt canopies and associated secondary minibasins are known in onshore areas. The Subalpine chains of Haute Provence have been studied for over 100 years and containing Upper Triassic evaporites. However, the importance of salt tectonics during the Tethyan rifting and subsequent passive margin subsidence and the influence of pre-existing salt structures in the evolution of the fold and thrust belt have been underestimated. This work describes a pre-Alpine salt canopy and associated secondary minibasins and their incorporation into the fold and thrust belt. Salt structures started to develop during the Early-Middle Jurassic rifting and continuous salt tectonic activity resulted in the emplacement of Upper Triassic evaporites onto the Albian-Cenomanian seafloor. Salt extrusion coincided with global sea level high stand and deposition of black shales. Allochthonous salt was emplaced from mature diapirs, and salt sheets coalesced to form a canopy. During the Late Cretaceous, second-generation salt structures developed above the canopy and bounded secondary minibasins. Late Cretaceous-Pliocene Alpine compression led to the squeezing of salt structures and depletion of the canopy. Secondary minibasins were carried as piggyback basins during Alpine shortening. The interaction of salt tectonics and thrusting resulted in the formation of asymmetric hybrid basins such as the Barrême basin. The almost completely welded salt canopy and the secondary minibasins could be considered as one of the few onshore examples of canopies and secondary minibasins.

1. Introduction

Our knowledge of salt tectonics has increased greatly since 1995 and 1996, the publication of AAPG Bulletin and Geological Society Special Publication on salt tectonics (Jackson et al., 1995; Alsop et al., 1996) largely because of the high quality seismic data shot during hydrocarbon exploration in offshore salt basins like the Gulf of Mexico (Rowan et al., 1999; Pilcher et al., 2011) and the South Atlantic (Jackson et al., 2000; Marton et al., 2000). Minibasins are present in almost all salt basins due to the generation of accommodation space by the subsidence of depocenters into the salt (Tari et al., 2003; Stewart, 2007; Trudgill, 2011). A distinction is made between primary minibasins which have subsided into autochthonous salt and secondary minibasins which have developed on allochthonous salt emplaced at stratigraphic levels above the autochthonous source layer (Hudec et al., 2011; Pilcher et al., 2011).

Allochthonous salt is found in compressional settings such as the Zagros Mountains in Iran (Jahani et al., 2009) as well as in deep-water areas of salt-bearing passive margins such as the Gulf of Mexico (Hudec & Jackson, 2009). Secondary minibasins have also been described onshore in the Sverdrup basin in Canada (Jackson & Harrison, 2006; Harrison & Jackson, 2014), the Flinders and Willouran Ranges in Australia (Hearon IV et al., 2015; Rowan et al., 2020), the Sivas basin in Turkey (Ringenbach et al., 2013; Callot et al., 2014; Kergaravat et al., 2016; Kergaravat et al., 2017; Ribes et al., 2017) and the Betics in Southern Spain (Flinch & Soto, 2017; Pedrera et al., 2020; Flinch & Soto, 2022).

The Southern Subalpine chains of Haute-Provence are a salt-influenced fold and thrust belt containing a well-documented succession of Upper Triassic (Keuper) rocks that include evaporites. The Southern Subalpine chains are well-studied (Zurcher, 1895; Boussac, 1912; Goguel, 1939; Guérin-Desjardins, 1956; Cotillon, 1968; Roux, 1972; De Graciansky et al., 1981; Lemoine et al., 1986; Dardeau, 1988; De Graciansky & Lemoine, 1988; Fry, 1989; Gidon & Pairis, 1992; De Graciansky et al., 1993; Lickorish & Ford, 1998; Evans & Elliott, 1999; Ford & Lickorish, 2004; Grosjean et al., 2017; Schwartz et al., 2017). The Keuper evaporites have long been known as the basal detachment surface on which thin-skinned Alpine folding and thrusting took place, and diapiric structures were also identified. Many of these diapirs were thought to have been formed during regional Alpine compression (Goguel, 1939; Kerckhove & Roux, 1978b; Gidon & Pairis, 1992; Gidon, 1997; Lickorish & Ford, 1998), though some were identified as pre-Alpine structures which developed along extensional faults during the Early-Middle Jurassic rifting of the European margin. (Kerckhove & Roux, 1976b; Arnaud et al., 1977; Emre, 1977; Kerckhove & Roux, 1978b; Mascle et al., 1986; Mascle

et al., 1988; Dardeau & De Graciansky, 1990). Notwithstanding this work, however, the importance of salt tectonics during Tethyan rifting and the passive margin subsidence which followed it, and the influence of precursor salt structures in the evolution of the Alpine fold and thrust belt have been underestimated, and pre-Alpine allochthonous salt was not recognised.

Recent work has identified salt-withdrawal depocenters adjacent to diapirs as well as salt-related structures (Figure 1b) such as overturned megaflaps and allochthonous salt sheets. It has become clear that Upper Triassic evaporites extruded to the surface during periods of black shale deposition in the Jurassic (Bathonian-Callovian) (Graham et al., 2012; Célini et al., 2020) and Cretaceous (Aptian-Albian) (Brooke-Barnett et al., 2023) and also became emplaced in a compressional setting during the Paleogene (Célini et al., 2022). The presence of these salt sheets locally influenced sedimentation on both the passive margin and also during the deposition of the foreland basin megasequence (Célini et al., 2020; Célini et al., 2022; Brooke-Barnett et al., 2023).

Syn-orogenic sediments representing a foreland basin succession are preserved in well-known northwest-southeast trending synclines such as the Annot basin and the Barrême basin (Artoni & Meckel, 1998; Evans & Elliott, 1999; Ford et al., 1999; Joseph & Lomas, 2004). These basins have been described in detail from both structural and sedimentological points of view and are usually considered to be piggyback or thrust-sheet-top basins. Here we present that some of these basins are primarily secondary minibasins developed on a Late Cretaceous extrusive salt canopy before being incorporated into the Tertiary fold and thrust belt.

2. Geological setting of the Southern Subalpine chains of Haute Provence

The Southern Subalpine fold and thrust belt of the Western Alps (Figure 1a) represents the external part of the deformed European margin of the Alpine orogen (Lemoine et al., 1986; Schmid et al., 2004; Ford et al., 2006; Handy et al., 2010). During the Jurassic and Cretaceous the area was part of the proximal margin of the Piemont-Ligurian branch of the Alpine Tethys (Lemoine et al., 1986; Lemoine & Trümpy, 1987; Manatschal & Müntener, 2009; De Graciansky et al., 2010; Handy et al., 2010; Mohn et al., 2010; Manatschal & Chenin, 2023). Late Triassic (Keuper) evaporites (Figure 2) composed of gypsum, mudstone, dolomite and de-dolomitized carbonate ‘cargneule’ breccia visible in outcrop at the present day may have been intercalated originally with other evaporites such as halite (Grandjacquet & Haccard, 1975; Kerckhove & Roux, 1978a; Kerckhove & Roux, 1978b; De Graciansky et al., 1981; De Graciansky et al., 1982). Halite is now absent at the surface (Mennessier, 1959; Roux, 1970; Lemoine et al., 1986) but several salt springs and an important Neolithic site of salt

mining are known in the Southern Subalpine chains suggest the presence of halite at depth (Roux, 1970; Kerckhove & Roux, 1976b; Morin et al., 2004; Bollinger et al., 2010).

The Early-Middle Jurassic rifting which led to the opening of the Ligurian Tethys was preceded by failed rifting during the Late Triassic, but the main rifting event in this part of the Western Alps occurred during the Pliensbachian (Lemoine et al., 1986; Dardeau, 1988; Dumont, 1988; De Graciansky et al., 2010; Handy et al., 2010). The complex network of Tethyan extensional faults defined a platform-slope-basin palaeogeographic configuration (Figure 1d) (Kerckhove & Roux, 1976a; Kerckhove & Roux, 1978a; De Graciansky et al., 1981).

The basinal domain (part of the Dauphinois Basin of the Western Alps) was bounded to the south and west by the Provençal carbonate platform (Lemoine et al., 1986; Dardeau, 1988; De Graciansky et al., 2010). Hemipelagic sedimentation occurred in the transitional slope domain between the platform and the basin (Kerckhove & Roux, 1976a; Kerckhove & Roux, 1978a; De Graciansky et al., 1981; Gidon, 1997; Graham et al., 2012). The passive subsidence which followed the Early-Middle Jurassic rifting was dominated by continuous pelagic sedimentation in basinal areas and the development of carbonate platforms on the rift margins (Lemoine et al., 1986; De Graciansky & Lemoine, 1988; Lickorish & Ford, 1998).

A second phase of rifting associated either with the opening of the more northerly Valais branch of Alpine Tethys (Figure 2) or the opening of the Bay of Biscay-Pyrenean rift system occurred during the Early Cretaceous and led to the formation of the approximately east-west trending Vocontian basin (Manatschal et al., 2006; Handy et al., 2010; Mohn et al., 2014; Tavani et al., 2018). Lower Cretaceous shale and pelagic limestone deposition was dominant in the Vocontian Basin itself while carbonate platforms continued developing along the basin margins (Arnaud, 1988; Lickorish & Ford, 1998; Cotillon, 2010; De Graciansky et al., 2010). A thick succession of Aptian-Cenomanian black shales (Marnes Bleues Formation) followed in the basin (de Boer, 1983; Bréhéret, 1988; Bréhéret & Brumsack, 2000; De Graciansky et al., 2010) while the overlying Upper Cretaceous consists of thick section of alternating pelagic limestones and marls (Figure 2).

The thin-skinned fold and thrust belt of the Southern Subalpine chains developed from the pelagic, slope and platformal palaeogeographic domains of the Jurassic Dauphinois and Cretaceous Vocontian basins from Late Cretaceous until the Pliocene (Figure 1) as basinal Upper Triassic, Jurassic, Cretaceous rocks and overlying Cenozoic sediments were thrust south-westwards along the basal evaporite detachment (Lickorish & Ford, 1998; Schmid & Kissling, 2000; Ceriani et al., 2001; De Graciansky et al., 2010; Graham et al., 2012; Schwartz et al., 2017).

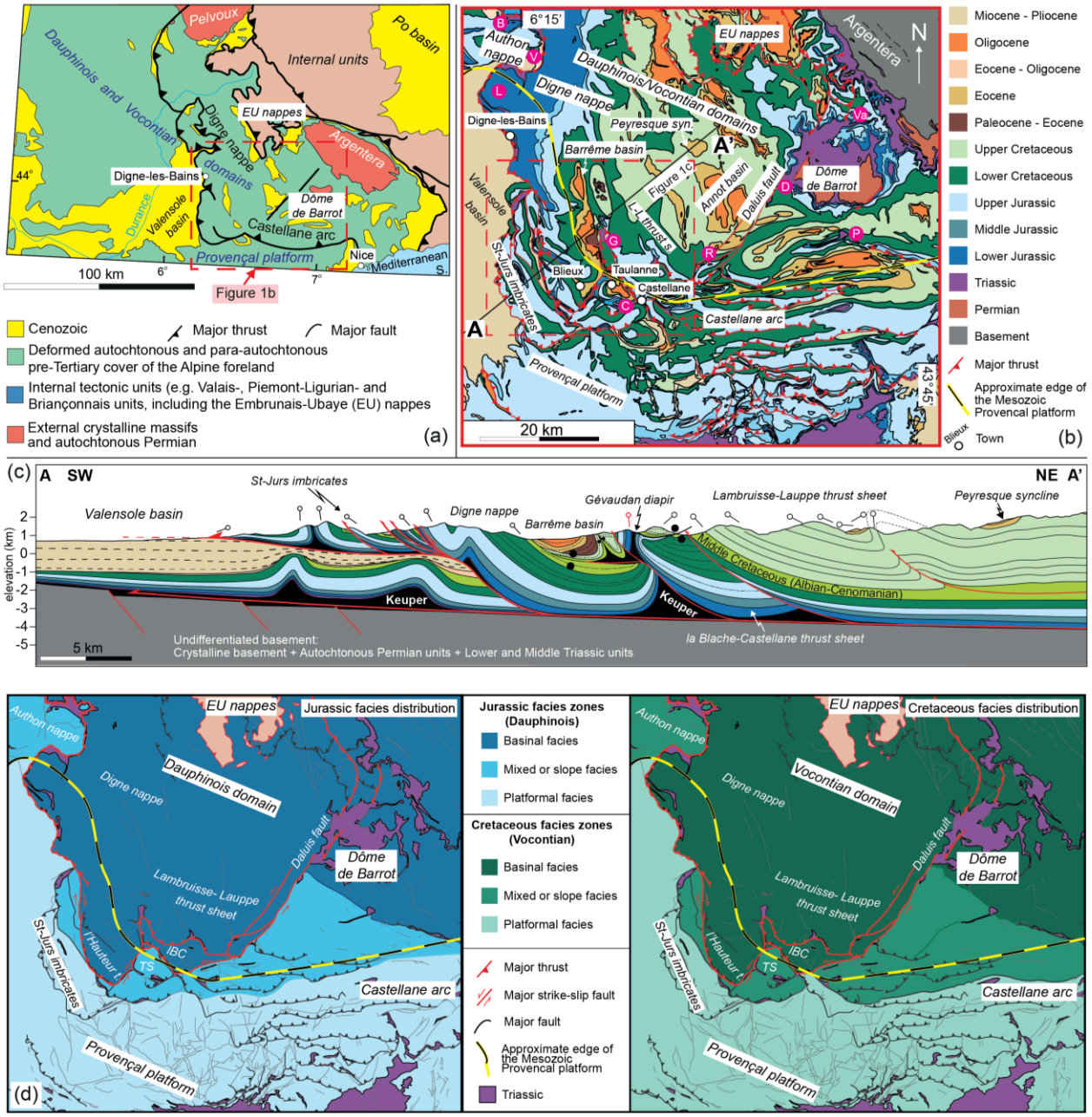


Figure 1 (a) Tectonic map of the south-western part of the Western Alps. Modified after Schmid et al. (2004). (b) Regional geology map of the Southern Subalpine chains after Rouire et al. (1979) and Kerckhove et al. (1980) showing examples of known salt structures and salt-related structures: Barles flap (B) (Graham et al., 2012), Chasteuil salt structure (C) (Csicsek et al., 2019), Daluis diapir (D) (Mascle et al., 1988; Dardeau & De Graciansky, 1990; Brooke-Barnett et al., 2023), Gévaudan diapir (G) (Emre, 1977; Lickorish & Ford, 1998), La Robine minibasin (L) (Célini et al., 2020), Puget-Théniers diapir (P) (Dardeau & De Graciansky, 1990), Rouaine-Daluis fault system (R) (reactivated salt wall) (Brooke-Barnett et al., 2023), Vélodrome secondary minibasin (V) (Célini et al., 2022). Abbreviation: L-L thrust s. = Lambruisse-Lauppe thrust sheet. (c) Regional cross-section from the Valensole basin through the Digne nappe system. (d) Jurassic and Cretaceous facies distribution maps of the Southern Subalpine chains. Data from Cotillon (1968); Kerckhove & Roux (1976a); Kerckhove & Roux (1978a); De Graciansky et al. (1981); Cotillon (2010); Grosheny et al. (2017); Brooke-Barnett (2022). Note that the maps are not restored palinspastically. Abbreviations: EU nappes = Embrunais-Ubaye nappes; lBC = la Blache-Castellane thrust sheet; TS = Taulanne syncline.

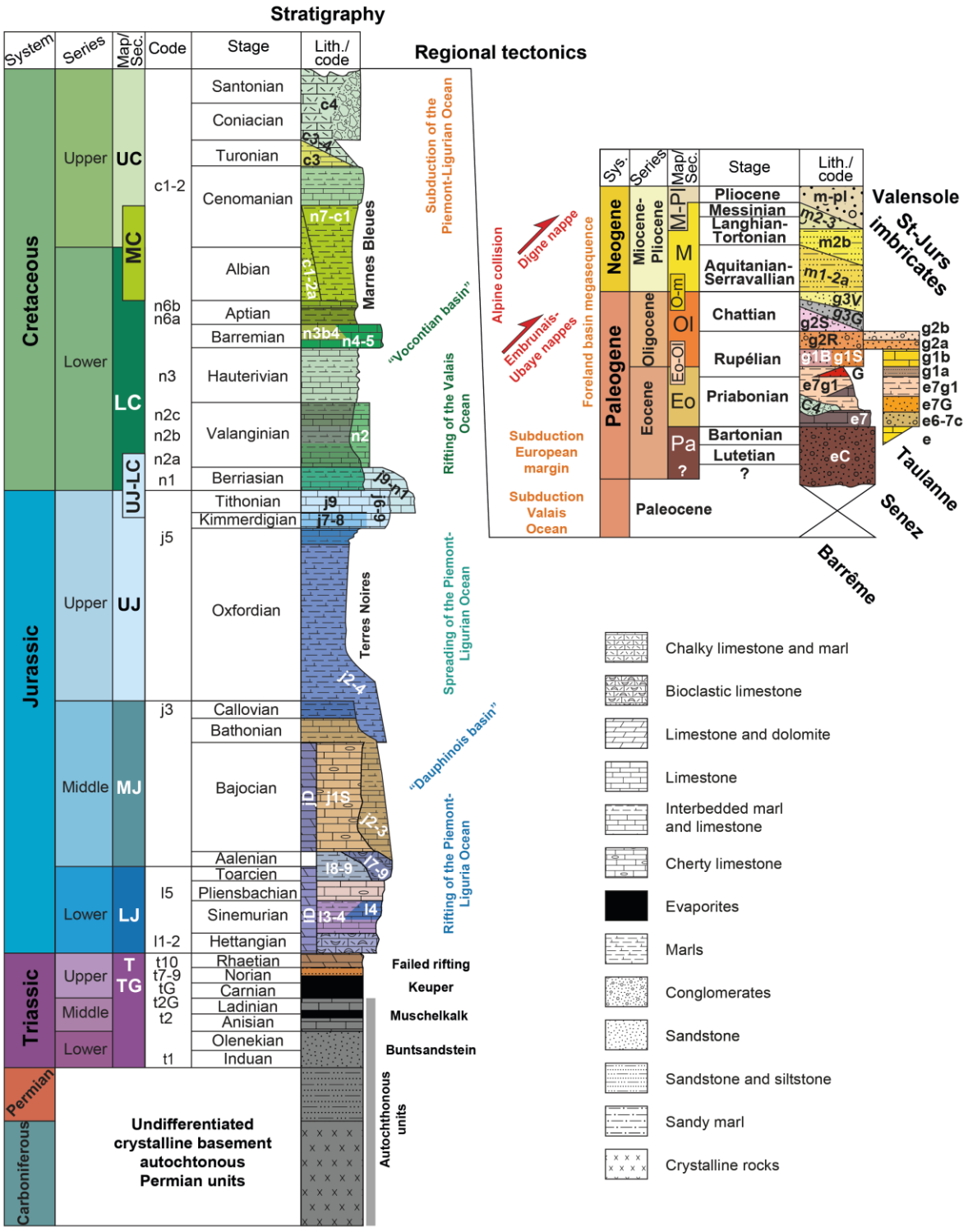


Figure 2 Lithostratigraphic column of the Southern Subalpine chains and the regional tectonic events in the Western Alps. Modified after Kerckhove & Roux (1976a) and Kerckhove & Roux (1978a), Campredon et al. (1980b) and De Graciansky et al. (1981).

A foreland basin developed in the area from Late Cretaceous to Mio-Pliocene in response to internal Alpine thrust load (Ford et al., 1999; Gupta, 1999). The fill of this flexural basin is preserved in a series of small, approximately northwest-southeast trending thrust-top basins such as Barrême and Annot (Figure 1b) (Evans & Elliott, 1999; Ford et al., 1999; Joseph & Lomas, 2004). The oldest unit of the foreland basin megasequence is the non-marine cobble, pebble and boulder conglomerate known as the Poudingues d'Argens Formation sourced almost entirely from Cretaceous pelagic limestones (Apps, 1987; Evans & Mange-Rajetzky, 1991; Evans & Elliott, 1999; Apps et al., 2004).

The Poudingues d'Argens Formation is overlain by the time-transgressive foreland basin megasequence of the Lutetian-Priabonian Nummulitic Limestone, the Priabonian-Rupelian Globigerina Marls and the turbidites of the Grés d'Annot Formation as the basin progressively developed, migrated and filled (Boussac, 1912; Pairis, 1971; Campredon, 1977; Sinclair et al., 1998; Sztrákos & du Fornel, 2003).

The main collision phase in the Alps occurred during the Late-Eocene — Early Oligocene. At that time internal Alpine units known as the Embrunais-Ubaye nappes were emplaced towards to southwest over the Dauphinois-Vocontian domain and the foreland basin (Figure 1a, b and d) (Kerckhove, 1969; Fry, 1989; Lickorish & Ford, 1998; Ford et al., 1999; Apps et al., 2004; Ford et al., 2006), probably adding significantly to the load driving the crustal subsidence. The Digne nappe was initiated at this time emplacing a thick Jurassic-Cretaceous Dauphinois-Vocontian basinal succession over the slope sequences and the relatively thin carbonates of the Provençal platform.

During Oligocene, Miocene, and Pliocene times the depocentre migrated towards the continental foreland (De Graciansky et al., 1989; Ford et al., 1999) and sedimentation in the flexural basin became progressively terrestrial. Molasse deposition continued southwest of the Barrême area during the Miocene-Pliocene, in the thrust-top basins of the St-Jurs imbricates and also in the Valensole foreland basin (Figure 1b, c and Figure 2).

During the Miocene and Pliocene, a minimum of 20 km displacement occurred along the Digne thrust system. However, lateral tip folds of a splay of the Digne thrust at village of Barrême are unconformably overlain by the Nummulitic Limestone Formation, which indicates that the southern segment of the Digne thrust was active before the Priabonian (Graham et al., 2012).

3. Evidence for allochthonous salt emplacement into higher stratigraphic levels during the Albian-Cenomanian

Direct evidence for pre-Alpine salt tectonic activity and allochthonous salt emplacement can be seen at several localities between Castellane and Barrême. Several large Upper Triassic diapiric structures are exposed north of the Provençal platform, within the southwest and south verging thrust sheets which transport the slope and basinal succession (Figure 1b and d). Some of these evaporite occurrences are bounded by reduced, subvertical and overturned Jurassic-Lower Cretaceous sections, and the observed stratal and structural geometries record the pre-Alpine emplacement of the Upper Triassic evaporites at the seafloor on the Tethyan passive margin. In the following section direct evidence for allochthonous salt emplacement will be presented and a number of salt structures are described in detail.

3.1 Data and observations

3.1.1 Stratigraphic and structural relationships around Gévaudan diapir (northern region)

With a surface exposure of approximately 3 sq. km, the Gévaudan diapir (Emre, 1977; Lickorish & Ford, 1998; Jackson & Hudec, 2017), is the largest salt structure of the study area. It is located between the village of Barrême and the hamlet of Gévaudan, on the eastern flank of the Barrême thrust-sheet-top basin (Figure 1b, Figure 3, Figure 4).

The diapir contains Upper Triassic gypsum, mudstone and cargneule breccia. The eastern side of it is overridden by the Lambruisse-Lauppe thrust sheet – a thick section of Jurassic-Cretaceous sediments in basinal facies (Figure 1, Figure 3 and Figure 4). To the west and southwest, the diapir is bounded by Upper Cretaceous rocks and the Cenozoic molasse of the Barrême basin and its southern continuation, the Senez syncline (Figure 3 and Figure 4). These asymmetric synclines with subvertical or locally overturned eastern flanks have been considered for decades as thrust-sheet-top fragments of the foreland basin (Elliott et al., 1985; Artoni & Meckel, 1998; Lickorish & Ford, 1998; Evans & Elliott, 1999; Evans et al., 2004; Schwartz et al., 2012).

To the north, northeast and south the Gévaudan diapir is flanked by subvertical or locally overturned, reduced Triassic-Lower Cretaceous sections (Figure 3 and Figure 4).

3.1.1.1 Flanking strata of the Gévaudan diapir: the Clavoune, Fontaine Salée and Font Chaude sections

North of the diapir, at Clavoune (shown as 'Cla' in Figure 3 and Figure 4), a subvertical to overturned Triassic-Lower Cretaceous section is exposed (Figure 3, Figure 4, Figure 5a and b). Upper

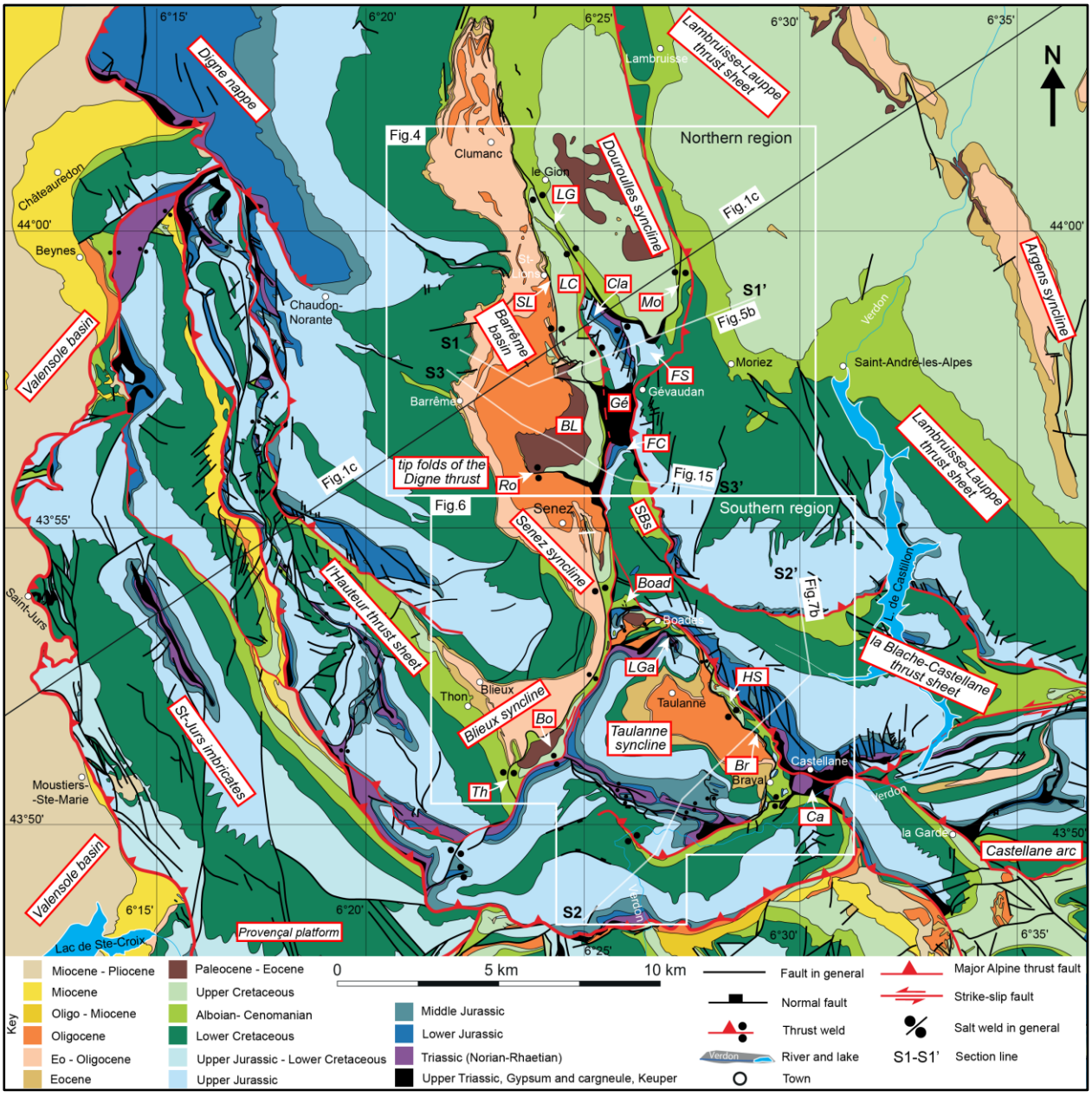


Figure 3 Geological map of the Southern Subalpine chains based on the Entrevaux, Moustiers-Sainte-Marie, Castellane and Digne 1:50000 scale map sheets (Kerckhove & Roux, 1976a; Kerckhove & Roux, 1978a; Campredon et al., 1980b; De Graciansky et al., 1981). For Jurassic and Cretaceous facies distribution see Figure 1 and Figure 9. Abbreviations: Br = Brayal weld; Bo = Bourbonne syncline; Boad = Boades zone; BL = Bois de Lieye section; Ca = Castellane diapir; Cla = Clavoune roof strata section; FC = Font Chaude roof strata section; FS = Fontaine Salée flap; Gé = Gévaudan diapir; HS = Haute Sionne syncline; LC = le Clap syncline; LG = le Gion weld; LGa = La Grau anticline; Mo = Mouchon weld; Ro =Rouviére weld; SBs = Serre Blanchard syncline; SL = St-Lions weld; Th = Thon weld.

Triassic rocks are overturned to southwest and overlain by a uniquely thin, Lower Jurassic section comparable with the Liassic sections of the slope facies zone and containing several unconformities

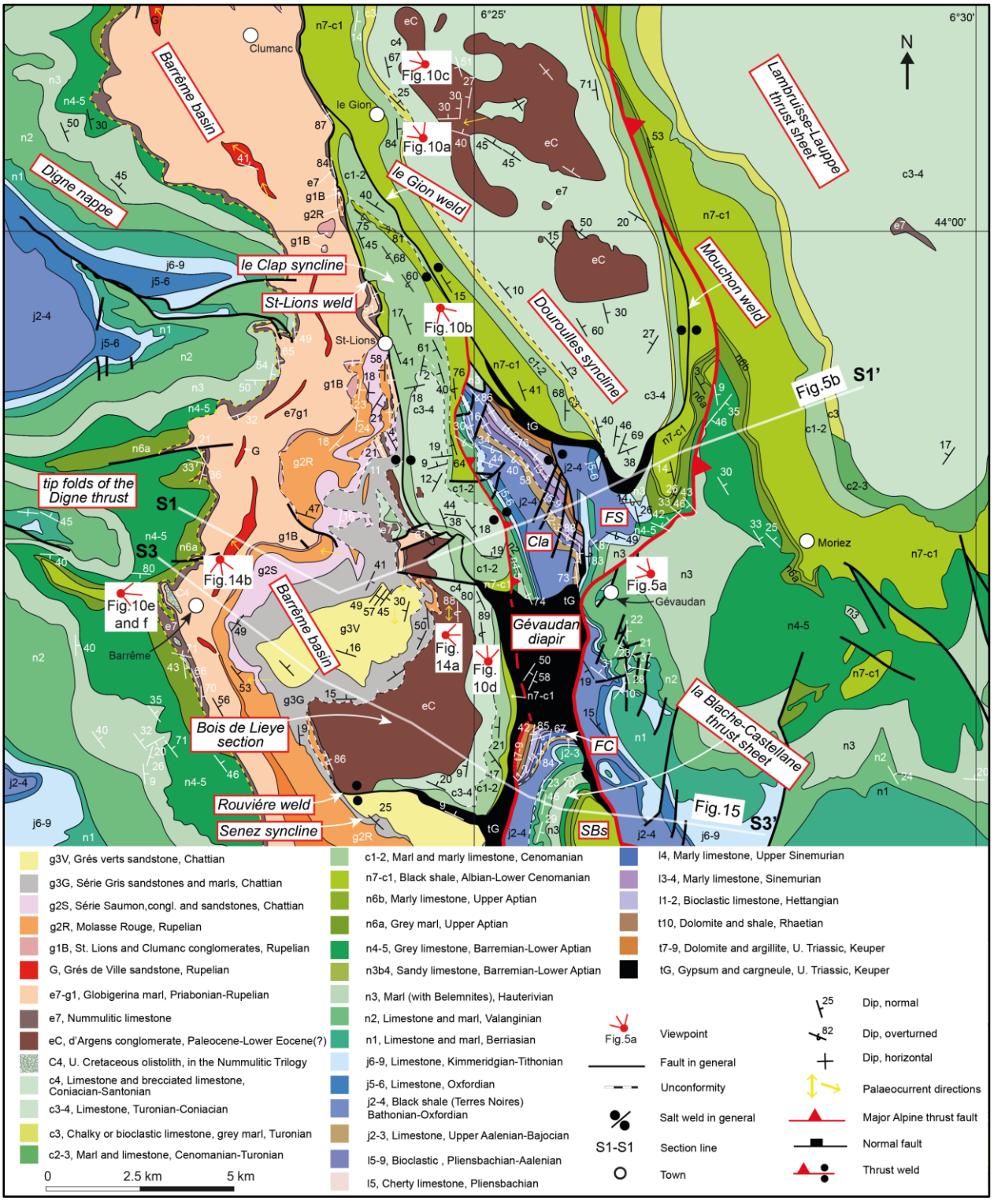


Figure 4 Detailed geological map of the vicinity of the Gévaudan diapir, between the village of Barrême and the hamlet of Gévaudan based on the Entrevaux and Digne 1:50000 scale map sheets (Campredon et al., 1980b; De Graciansky et al., 1981). For location see Figure 3. For Jurassic and Cretaceous facies distribution see Figure 1d. Abbreviations: Cla = Clavoune roof strata section; FC = Font Chaude roof strata section; FS = Fontaine Salée flap; SBs = Serre Blanchard syncline.

and sedimentary gaps (De Graciansky et al., 1982). The Liassic succession is unconformably overlain by an incomplete Middle Jurassic section which passes up into the reduced section of Bathonian-Oxfordian black shales (Terres Noires Formation) (Figure 3, Figure 4, Figure 5a and b). This is in turn overlain by a reduced, limestone dominated Oxfordian-Tithonian section (j5-6 and j6-9). The Middle-Upper Jurassic section is also subvertical or slightly overturned to the southwest (Figure 4, Figure 5)

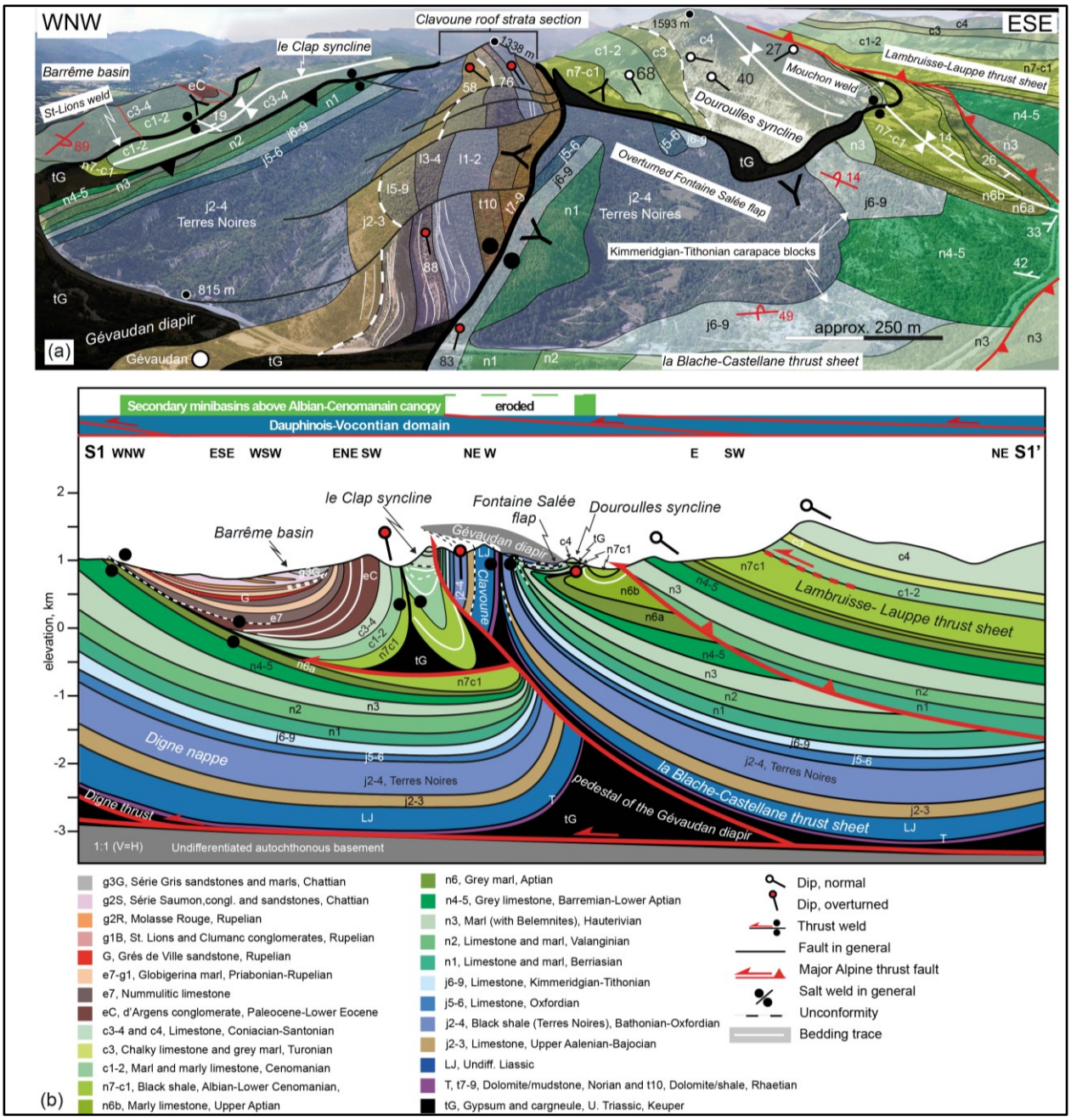


Figure 5 (a) Interpreted photo panorama of the Gévaudan diapir and the flanking vertical or slightly overturned Clavoune section and the completely overturned Fontaine Salée flap. Black epsilons indicate younging direction. See Figure 4 for key and viewpoint location. (b) Cross section (S1-S1') from the Digne nappe to the Lambruisse-Lauppe thrust sheet, crossing the Gévaudan diapir, its flanking strata and the adjacent synclines (secondary minibasins) which developed on the top of the Albian-Cenomanian allochthonous salt. See Figure 3 and Figure 4 for cross section location.

and overlain by a thin and vertical Berriasian-Lower Aptian section (from n1 to n4-5) (Figure 4, Figure 5a and Figure 5b).

The reduced Jurassic-Early Cretaceous Clavoune section abuts against the Gévaudan diapir to the south and is bounded to the west and north-west by an Alpine thrust fault (Figure 4, Figure 5). Along strike it is overthrusted Albo-Cenomanian (n7-c1) and Upper Cretaceous rocks (c1-2 and c3-4) and Poudingues d'Argens conglomerates of the le Clap syncline (Figure 3 and Figure 5). Further west, the le Clap syncline is bounded by the Tertiary molasse section of the Barrême syncline (Figure 3, Figure 4). The synclines are separated by a north-south trending discordant surface (previously interpreted as a fault) which links into the Gévaudan diapir at the southwestern termination of the Clavoune (Figure 3, Figure 4 and Figure 5) (De Graciansky et al., 1981).

Several northeast-southwest trending faults crosscut the subvertical Liassic-Middle Jurassic section of the Clavoune mountain (Figure 4, Figure 5a). These faults are sealed by the Terres Noires Formation and link into a north-south trending, discordant contact (Figure 4, Figure 5a) which separates the subvertical Clavoune Triassic-Lower Cretaceous section from a zone of highly deformed Jurassic and Cretaceous rocks of the Fontaine Salée (shown as 'FS' in Figure 3 and Figure 4) section to the east (Figure 5a).

Bathonian-Upper Cretaceous rocks are seen in outcrop here (Figure 4, Figure 5a). Triassic and older Jurassic rocks are not exposed (Figure 4) but are probably present in the subsurface (Figure 5b). The lower part of the section, the Bathonian-Oxfordian Terres Noires Formation is slightly overturned to the east-southeast (j2-4) and passes up into a thin, limestone dominated Oxfordian-Tithonian section (j5-6 and j6-9). The Upper Jurassic rocks are overlain by a reduced and vertical Lower Cretaceous section (from Berriasian, n1 to Lower Aptian, n4-5) and further to the east-southeast Upper Aptian (n6a and n6b) sediments and black shales of the Albian-Cenomanian Marnes Bleues Formation (n7-c1) are exposed in the footwall of the Lambruisse-Lauppe thrust sheet, in the core of a small, roughly north-south trending syncline (Figure 4, Figure 5a).

The vertical Cretaceous section is structurally overlain by overturned Jurassic strata and overturned Terres Noires are in direct contact with Lower Cretaceous strata (Figure 4, Figure 5b). Along the discordant surface bounding the Fontaine Salée section on the west the structurally deeper part of the section (Oxfordian-Berriasian, j5-6 to n1), is exposed in a small window below overturned Terres Noires (Figure 4 and Figure 5a). The overlying, overturned Kimmeridgian-Tithonian (j6-9) is composed of large blocks which are approximately 400-500 m in diameter exposed between the overturned Terres Noires and the eastward dipping Lower Cretaceous (Figure 4, Figure 5a and Figure

5b) A large block of Hauterivian (n3) is also exposed in direct contact with a Tithonian block (Figure 5a).

Springs bringing salt brines to surface and an important Neolithic site of salt mining are located in this area (Morin et al., 2004) inferring the presence of halite within the original Keuper section. Northeast of the diapir the overturned Fontaine Salée section is overlain structurally by a large accumulation of Keuper evaporites (Figure 4, Figure 5a and Figure 5b). This evaporite body is connected to the Gévaudan diapir through the discordant surface which separates the subvertical Clavoune section from the overturned Fontaine Salée section (Figure 4, Figure 5a). The thickness and lateral extent of the Upper Triassic gypsum can only be inferred. We assume that the exposed Keuper gypsum is continuous along strike and the thickness of the present-day evaporites is around 50-100 m (Figure 4, Figure 5a). Further to the northwest, a 50 m thick layer of Upper Triassic evaporites are embedded into Albian-Cenomanian black shales (Figure 4, Figure 5a).

South of the diapir, a reduced Jurassic-Cretaceous succession (the Font Chaude section, shown as 'FC' in Figure 3 and Figure 4) is exposed on the northern flank of the Serre Blachard syncline (shown as SBs in Figure 3 and Figure 4). The Triassic-Jurassic section here is almost identical to the Triassic-Jurassic section of Clavoune, also contains several sedimentary gaps and angular unconformities (Figure 4) and is unconformably overlain by Berriasian- and Albian-Cenomanian (from n2 to, n7-c1) (Figure 4). It is structurally overlain by Upper Triassic evaporites (Figure 4) which rests on the top of Albian-Cenomanian black shales in the core of the Serre Blanchard syncline (Figure 3, Figure 4).

3.1.2 Stratigraphic and structural relationships around the la Grau anticline and Castellane diapir (southern region)

Reduced and subvertical sections, atypical stratigraphic relationships, abrupt facies and thickness changes of the Mesozoic succession around large exposures of Upper Triassic evaporites also occur south of the Gévaudan diapir, between Barrême and Castellane (Figure 3 and Figure 6).

3.1.2.1 The la Grau salt-cored anticline

South-west of the village of Boades, on the northern flank of the Taulanne syncline (Figure 3 and Figure 6), the core of the la Grau anticline (Figure 6) (Roux, 1970) exposes Upper Triassic gypsum. Kerckhove & Roux (1978b) reported a large block of Lower Triassic Buntsandstein sandstone (around 10 by 50 m) incorporated into the evaporite. The earlier authors attributed the presence of Lower

Triassic rocks at the surface to basement involved faulting. On the northern flank of the Taulanne syncline Keuper evaporites are flanked by a thin Jurassic-Lower Cretaceous section in the slope facies

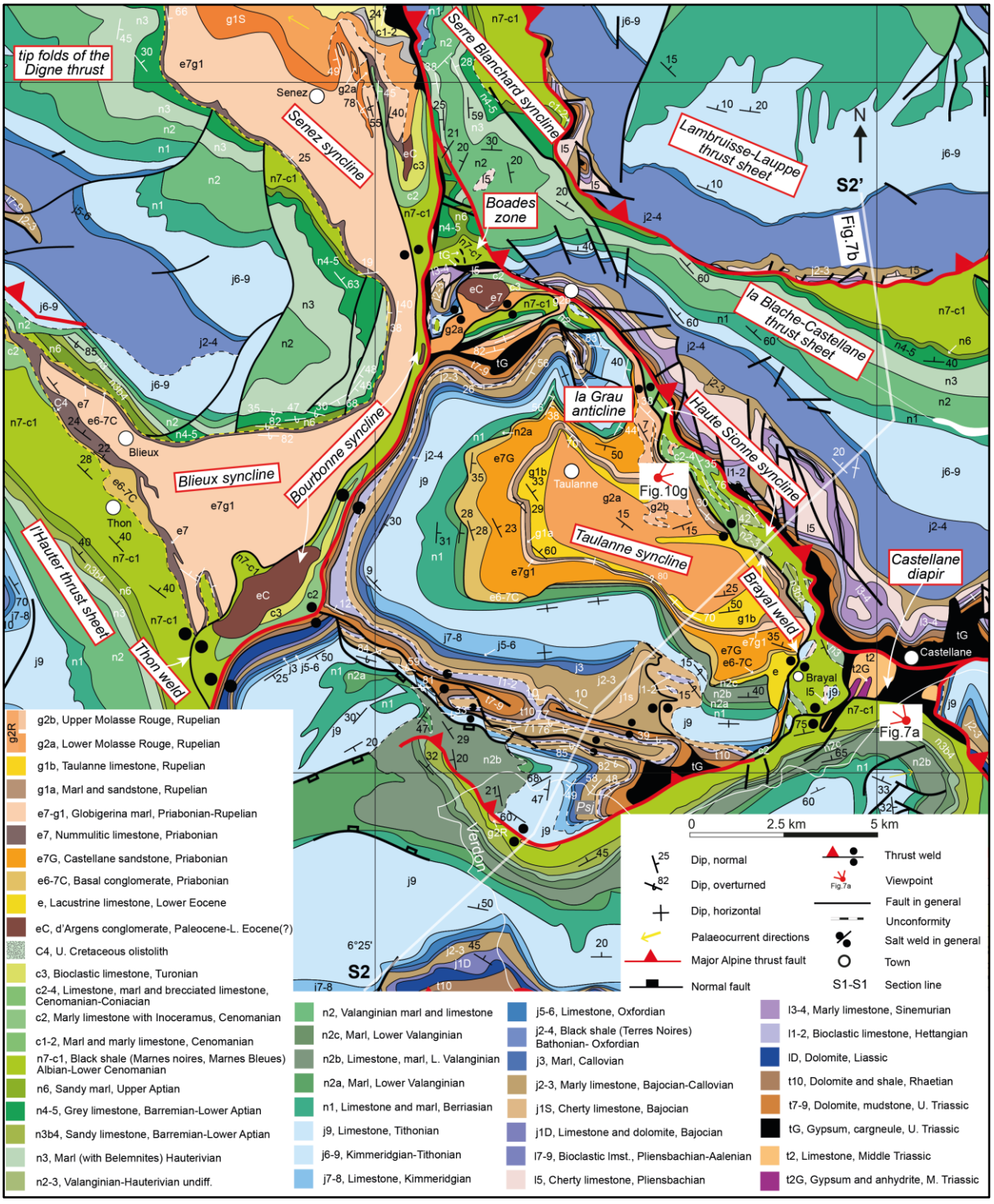


Figure 6 Detailed geological map of the vicinity of the Castellane diapir and the la Grau anticline, between the town of Castellane and the village of Blieux based on the Castellane and Moustiers-Sainte-Maire 1:50000 scale map sheets (Kerckhove & Roux, 1976a; Kerckhove & Roux, 1978a).

(Kerckhove & Roux, 1978a) (Figure 1d). The Mesozoic succession is unconformably overlain by Eocene and Oligocene syn-orogenic sediments of the Taulanne syncline (Kerckhove & Roux, 1978a). North of the syncline, the evaporite is flanked by a thin, highly deformed and incomplete basinal Jurassic-Cretaceous section (De Graciansky et al., 1981) now exposed beneath the la Blache-Castellane thrust sheet (Figure 1d, Figure 3 and Figure 6). Here the Mesozoic rocks are unconformably overlain by Paleocene, Eocene and Oligocene syn-orogenic sediments (Figure 6). De Graciansky et al. (1981) and Kerckhove & Roux (1978a) referred to this structurally complex area as the Boades zone (Figure 3 and Figure 6) where several anomalous contacts against elongated evaporite bodies which link through discordant contacts (previously interpreted as faults) in the core of the la Grau anticline (Figure 3 and Figure 6) (Kerckhove & Roux, 1978a; De Graciansky et al., 1981). These evaporite bodies are flanked by highly folded Jurassic- and Cretaceous sediments and by subvertical syn-orogenic Rupelian molasse. Large blocks of basinal Liassic cherty limestone (l5) are incorporated into the evaporites (Figure 6).

In the footwall of the la Blache-Castellane thrust sheet (Figure 3 and Figure 6), along an east-west trending evaporite body, three blocks of the Upper Triassic gypsum (tG) approximately 100 m in diameter are exposed within the Albian-Cenomanian black shales (n7-c1) (Figure 6). A large block of resistant Tithonian limestone (j9) also crops out within these shales.

3.1.2.2 The Castellane diapir

Further to the SE along the la Blache-Castellane thrust sheet, south-west of Castellane (Figure 3), a sheet-like diapir of Keuper gypsum containing slivers of Muschelkalk is exposed within Albian-Cenomanian (n7-c1) black shales (Figure 6, Figure 7a). Surface exposure of the Triassic gypsum is approximately 2.3 sq. km, and it is made up of four elongated Keuper gypsum bodies which have amalgamated to form the Castellane diapir (Figure 6).

Large olistoliths of resistant Pliensbachian (l5) and Tithonian (j9) limestone (Figure 7a) together with Valanginian-Hauterivian (n2-3), Hauterivian (n3) and Barremian-Lower Aptian (n3b4) blocks are also exposed within Albian-Cenomanian black shales (Figure 6). These blocks are adjacent to the sheet-like evaporites within the black shales (Figure 6) and one of them display an unconformity where Pliensbachian limestone is in direct contact with Tithonian limestone (Figure 6, Figure 7a).

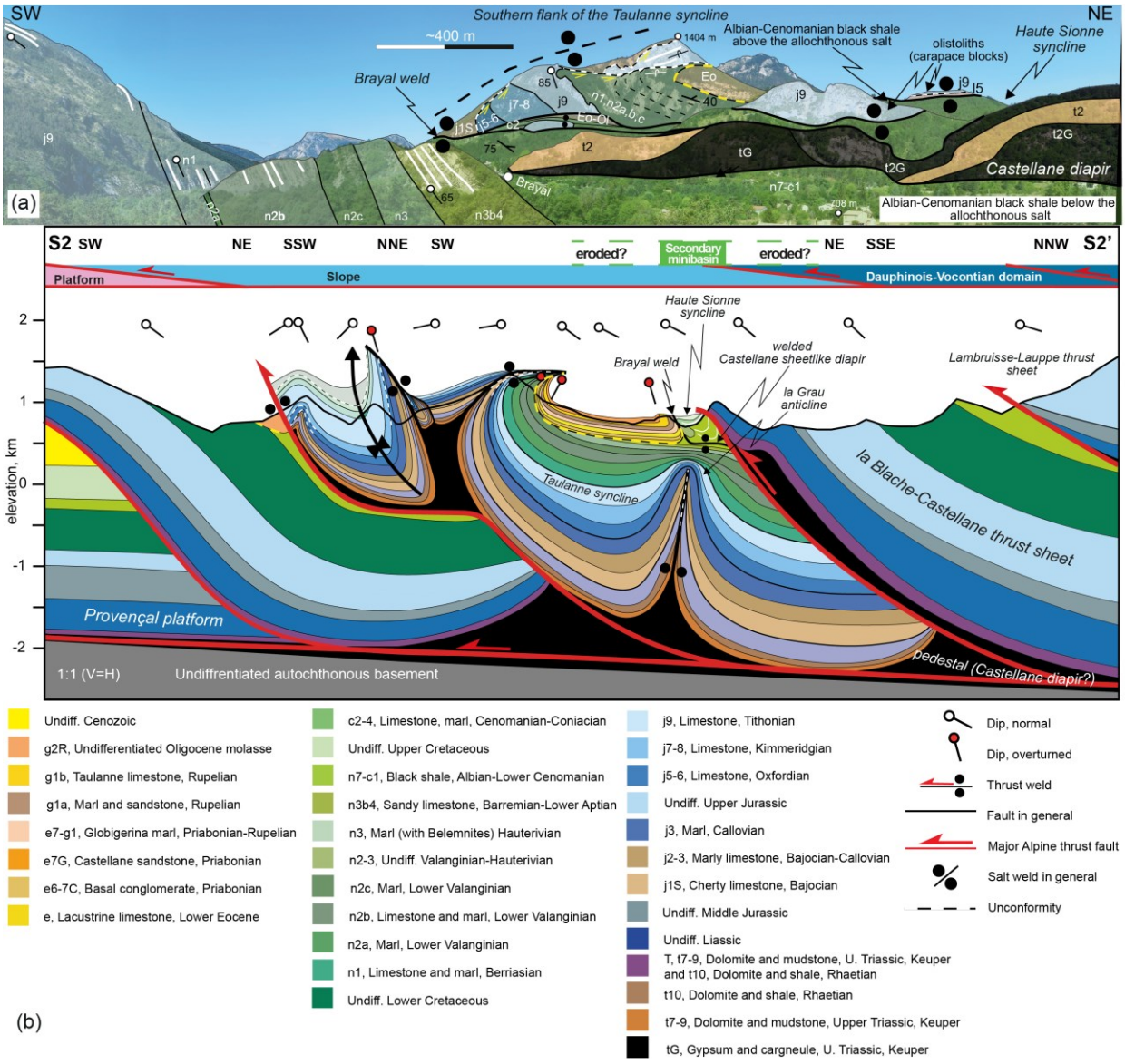


Figure 7 (a) Interpreted photo panorama of the Haute Sionne syncline and the underlying allochthonous salt sheet looking to northwest. See Figure 6 for key and viewpoint location. In the foreground the allochthonous salt lies above the Albian-Cenomanian black shales. Above the allochthonous salt, note the large, olistoliths surrounded by Albian-Cenomanian black shales exposed in the Haute Sionne syncline. (b) Cross section (S2-S2') from the Provençal platform to the basinal Lambruisse-Lauppe thrust sheet, intersecting the Taulanne syncline of the Mesozoic slope facies zone and the Haute Sionne syncline and the la Blache-Castellane thrust sheet. Note the structural position of the Haute Sionne syncline above the Taulanne syncline and below the overriding thick, Mesozoic basinal succession of the la Blache-Castellane thrust sheet. The syncline lies structurally above the sheetlike Castellane diapir. For cross section location see Figure 3 and Figure 6.

3.2 Interpretation

Based on the stratigraphic and structural observations described above salt structures started to develop from the Early Jurassic and continued to grow during the Middle and Late Jurassic and Early Cretaceous. During the deposition of the Albian-Cenomanian black shales, continuous salt tectonic activity became more rapid than sedimentation and resulted in the sheet-like emplacement of the Keuper evaporites, onto Albo-Cenomanian topographic surfaces.

Anomalously thin stratigraphic thicknesses in basinal facies, local unconformities, and structural discontinuities in the Jurassic and Lower Cretaceous section around the Gévaudan diapir indicate diapiric growth during the Tethyan rifting and the subsequent passive margin subsidence. We interpret the reduced, subvertical and overturned Clavoune, Fontaine Salée and Font Chaude Jurassic-Cretaceous sections (Figure 3, Figure 4 and Figure 6) as condensed carapaces or roof strata of a salt structure which started to grow during the Liassic co-eval with the first rifting of the margin. This early growth is indicated by the occurrence of incomplete sections, facies variations and thickness changes of the Liassic succession around the diapir (Figure 8a). It can therefore be considered as reactive diapirism perhaps developed over the footwall of extensional faults, something documented elsewhere in the Southern Subalpine chains (Mascle et al., 1988; Dardeau & De Graciansky, 1990; Graham et al., 2012; Célini et al., 2020; Brooke-Barnett et al., 2023), but not demonstrable here because the pre-salt basement is not exposed and most of the diapirs have been detached from their roots (Graham et al., 2012; Célini et al., 2020; Célini et al., 2022). Lower and Middle Triassic rocks are only exposed as blocks incorporated into diapiric material (e.g. Buntsandstein at the la Grau anticline and Muschelkalk at the Castellane diapir) but are likely derived from the fault scarps of underlying Tethyan extensional faults. The ability of salt to lift large inclusions from the edges of subsalt faults has been described by many authors in many salt provinces, e.g. in the Pyrenees by Canérot et al. (2005). Lickorish & Ford (1998) suggested that the Gévaudan diapir was formed along a Mesozoic extensional fault growing in the footwall as a reactive diapir (Figure 8a).

The northeast-southwest trending faults which crosscut the subvertical Liassic-Middle Jurassic section at Clavoune mountain may have been formed above the crest of the reactive diapir (Figure 8b). They are sealed by the Terres Noires Formation which mark the early post rift subsidence of the basin. Continuous diapir growth, perhaps maintained by differential loading during the Mid-Late Jurassic and Early Cretaceous is recorded by the thin Middle Jurassic-Lower Cretaceous sections around the diapir (Figure 8b and c). The diapir was presumably bounded to the east and west by primary minibasins. The Serre Blanchard syncline south of the diapir and the small syncline which is exposed east of the

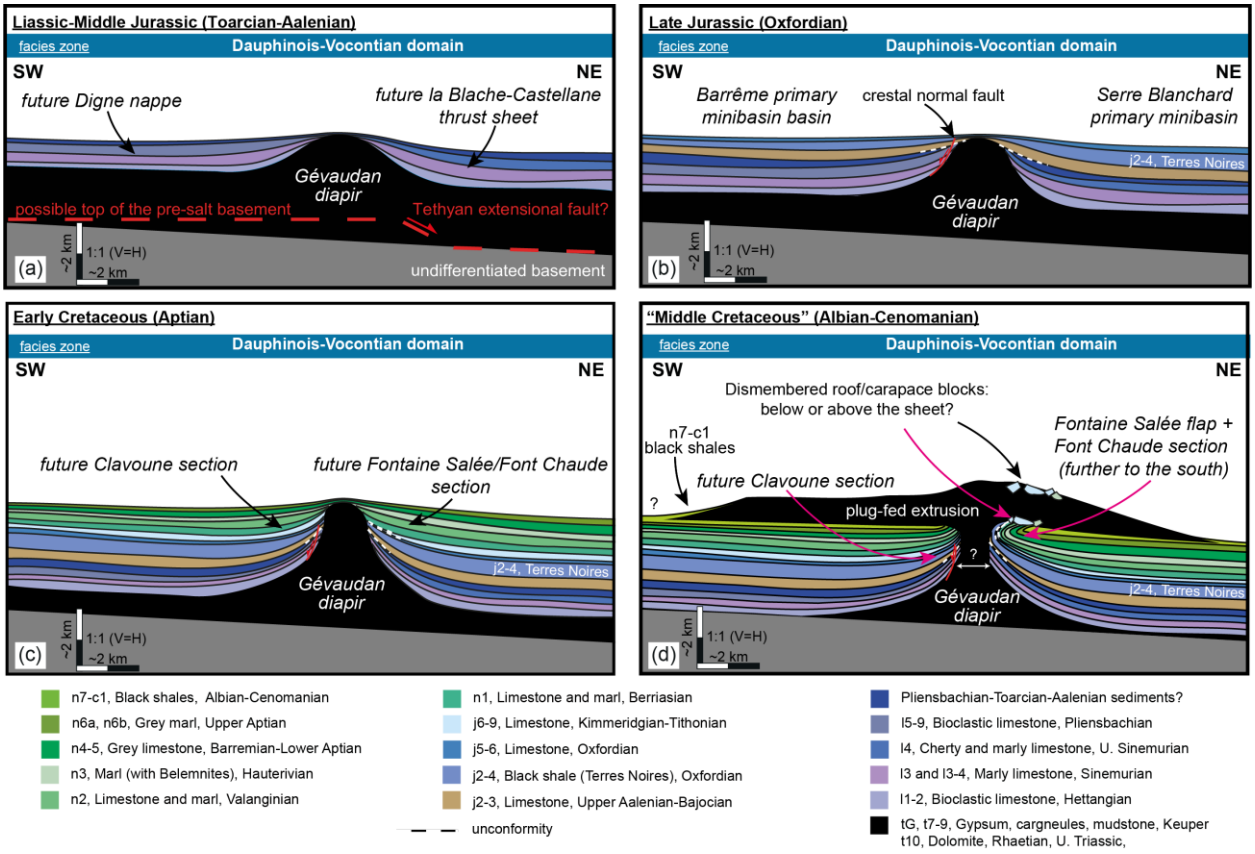


Figure 8 Diagrams showing the possible evolution of the Gévaudan diapir from the Liassic-Middle Jurassic (a) until the Albian-Cenomanian (d). The red dashed line on (a) showing an alternative interpretation for the top of the pre-salt basement and the possible position of a Tethyan extensional fault which formed during the rifting phase and initiated the diapirism. The Jurassic-Lower Cretaceous sections which are exposed now in the Digne nappe and the la Blache-Castellane thrust sheet are thinning towards the diapir and showing wedging geometries.

Fontaine Salée section may represent the depocentre on the east side of the Gévaudan diapir while on the west side it may the thick and complete Jurassic-Cretaceous section now exposed in the hanging wall of the Digne thrust is essentially the primary 'Barrême minibasin' (Figure 8b).

The la Grau anticline on the northern flank of the Taulanne syncline has a similar growth history to the Gévaudan diapir. The presence of a thin and incomplete Jurassic-Lower Cretaceous section suggests that the anticline was probably salt cored, formed a topographic high during the rifting and remained elevated during the passive margin phase. The northern limb of the anticline is a thin, incomplete, and highly folded Jurassic-Cretaceous section interpreted here as roof strata which may have been deposited on the basinward side of the salt structure.

It was noted above that Keuper gypsum bodies are present within the Albian-Cenomanian black shales around the Gévaudan diapir, north of the la Grau anticline and adjacent to the Castellane diapir are exposed as isolated blocks or large gypsum bodies floating within shales. The presence of these

allochthonous evaporites within the Albian-Cenomanian sediments is direct evidence for the local exposure of the salt to the seafloor during the middle of the Cretaceous.

Upper Triassic evaporites structurally overlying overturned sections represent the remnants of allochthonous salt extruded from the feeder of the Gévaudan diapir during the Albo-Cenomanian (Figure 8d). The thin roof sections of the diapir are overturned below the extruded salt, but the folding preceded the regional Alpine compression. The Fontaine Salée section is interpreted as a completely overturned flap which was folded beneath allochthonous salt (Figure 8d). The contact which separates the Clavoune and Fontaine Salée sections possibly represents the welded stem of the Gévaudan diapir which sourced the allochthonous evaporites. This means that Gévaudan diapir *sensu stricto* – the large accumulation of gypsum south-west of Gévaudan hamlet (Figure 3) is at least partly allochthonous and is not a salt stock.

The elongated evaporite bodies connected to the core of the la Grau anticline are also interpreted as remnants of an allochthonous sheet. Allochthonous salt may have been emplaced from the feeder of the la Grau anticline and evolved into a discordant, high-amplitude salt structure during the middle of the Cretaceous as salt extruded to the seafloor. The identification of the feeder of the allochthonous salt is difficult, however, because the la Grau salt structure is highly deformed and partly welded.

The origin of the Keuper evaporites exposed at Castellane is ambiguous, because along with their surrounding Albian-Cenomanian black shales, they are overridden by the la Blache-Castellane thrust sheet which is detached in thick Keuper evaporites (Figure 3, Figure 6, Figure 7a and Figure 7b). Assuming that the structural relationships here are analogous to those of the Upper Triassic evaporites within Albian-Cenomanian shales north-east of the Gévaudan diapir, we might interpret the Triassic gypsum and Muschelkalk to be a sheet-like diapir or allochthonous salt sheet, entirely encased in Albo-Cenomanian sediments and overridden by the la Blache-Castellane thrust sheet. The source of the allochthonous salt would presumably have been a salt diapir - the original Castellane diapir before its displacement by thrusting. The pedestal of this diapir would presumably be subsurface, 2-2.5 km below the la Blache-Castellane thrust sheet, along the Alpine basal detachment (Figure 7b).

Upper Jurassic (Kimmeridgian-Tithonian) and Lower Cretaceous (Hauterivian) olistoliths below the allochthonous salt at the Fontaine Salée section are interpreted as dismembered carapace blocks which were deposited on the flank of the Gévaudan diapir and were dismembered during the overturning of the flap (Figure 8d). Pliensbachian cherty limestone blocks incorporated into the allochthonous salt bodies and Tithonian limestone emplaced into the Albian-Cenomanian black shales are also interpreted as dismembered carapace. Large olistoliths of Pliensbachian and Tithonian limestone together with smaller blocks of Lower Cretaceous probably slid onto the Albian-

Cenomanian black shales during allochthonous salt emplacement (Figure 6). The local unconformity between Pliensbachian and Tithonian limestones seen in one of the olistoliths presumably formed on the elevated roof of the feeder diapir.

4 Indirect evidence for the existence of an Albian-Cenomanian salt canopy on the Tethyan margin

The original extent of the salt sheets described above is very difficult to ascertain because salt degrades easily by dissolution if it is exposed to the topographic surface (Warrak, 1974; Harrison & Jackson, 2014; Warren, 2016; Jackson & Hudec, 2017). However, the distribution of remnant evaporites interbedded within the Albian-Cenomanian black shales suggests that the sheets may have covered significant area of the Albian-Cenomanian seabed. Indirect evidence suggests that these allochthonous sheets may have advanced laterally and coalesced shortly after their emplacement to form a much larger salt canopy. In the following, we present indirect evidence for the presence of this extensive salt canopy and a second generation of salt-withdrawal basins which developed above the allochthonous salt.

4.1 Data and observations

Some salt sheet remnants are isolated and exposed within Albian-Cenomanian black shales but many of the allochthonous evaporite bodies are connected to their presumed feeder diapirs (or welds) or to each other by Alpine thrust and strike-slip faults or discordant surfaces which were previously interpreted as faults (De Graciansky et al., 1981) (indicated by pairs of black dots in Figure 3 and Figure 9). A network of these discordant surfaces and allochthonous salt bodies is exposed in a north-south trending, 3-5 km wide zone between the village of Clumanc and the town of Castellane (Figure 3, Figure 4, Figure 6, Figure 9).

In this zone, allochthonous salt bodies, linked by discordant surfaces and some Alpine structures and bound narrow, elongated synclines filled only with Albian-Cenomanian and younger Upper Cretaceous sediments overlain by Paleogene (Figure 3, Figure 4, Figure 6). The synclines are now part of the hanging wall of the Digne nappe, the la Blache-Castellane thrust sheet, the l'Hauter thrust sheet (along the eastern flank of the Blieux syncline) and the eastern flank of the Taulanne syncline. They include the Douroulles, le Clap, Barrême, Senez, Bourbonne and Haute Sionne synclines (Figure 3, Figure 4, Figure 5, Figure 6, Figure 7 and Figure 9).

Jurassic and Lower Cretaceous rocks exist in some of these synclines, but only as dismembered carapace blocks incorporated into allochthonous salt or redeposited into Albian-Cenomanian black shales. Their distribution is shown by yellow stars in Figure 9.

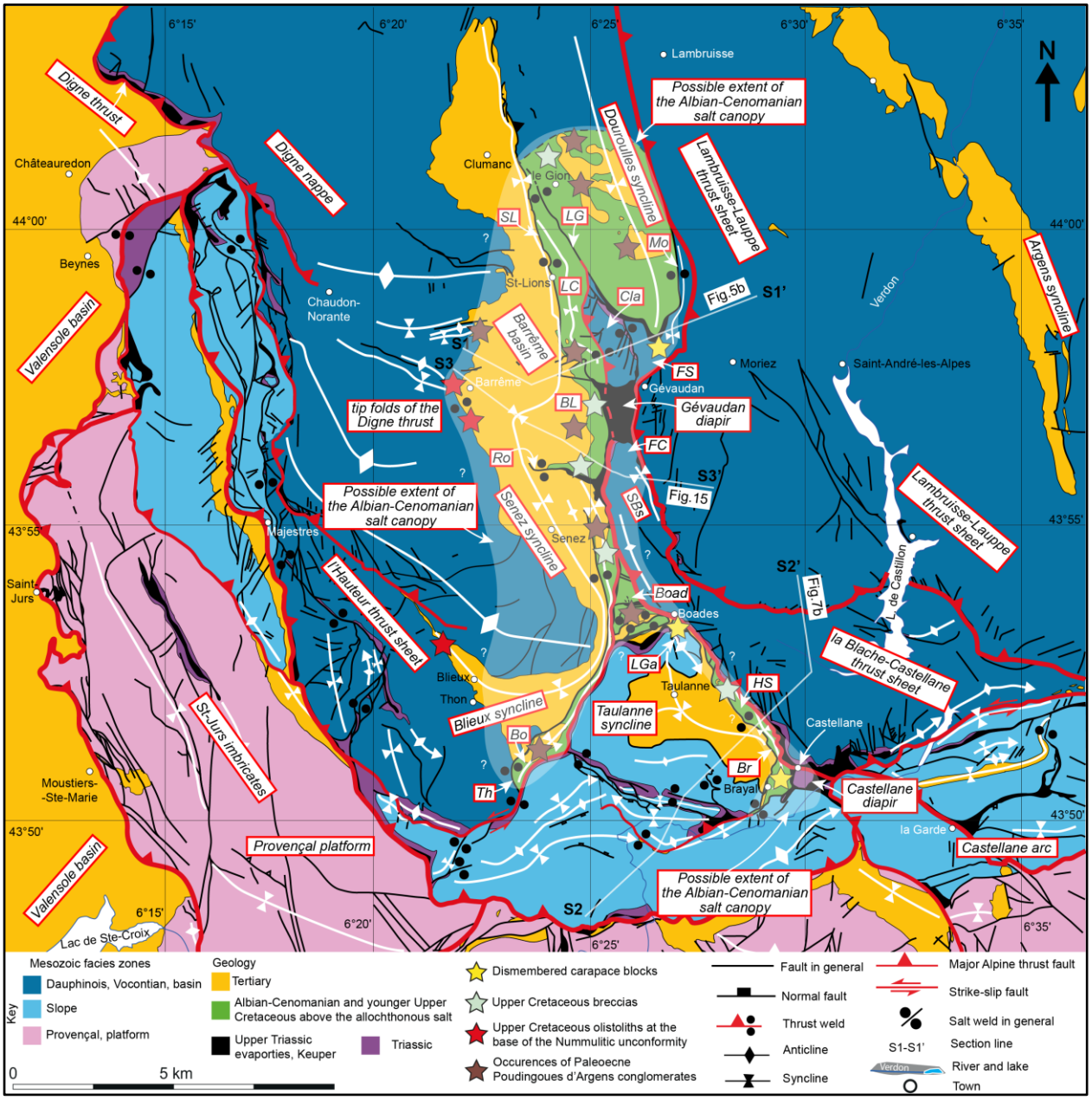


Figure 9 Structural map of the Southern Subalpine chains between the town of Castellane and the village of Clumanc. Data from Kerckhove & Roux (1976b), Kerckhove & Roux (1978a), Campredon et al. (1980b) and De Graciansky et al. (1981). Abbreviations: Br = Brayal weld; Bo = Bourbonne syncline; Cla = Clavoune roof strata section; FC = Font Chaude roof strata section; FS = Fontaine Salée flap; HS = Haute Sionne syncline; LG = le Gion weld; LGa = La Grau anticline; Mo = Mouchon weld; Ro =Rouviére weld; SL = St-Lions weld; Th = Thon weld. The transparent white polygon over the map indicates the possible extent of the Albian-Cenomanian salt canopy. White question marks indicate locations where the limit of the canopy is not known. Note that the map is not palinspatically restored.

Albian-Cenomanian and younger Upper Cretaceous sediments in the narrow synclines commonly onlap onto bounding allochthonous salt bodies or the linking discordant surfaces which link the salt bodies (Figure 4, Figure 5a, Figure 6 and Figure 7a). Thickness changes and local unconformities and pinch-outs are ubiquitous (Figure 4, Figure 5a and b, Figure 7b, Figure 10a and b). Sudden changes of fold wavelengths are common in the narrow, elongated synclines (Figure 3, Figure 4 and Figure 6).

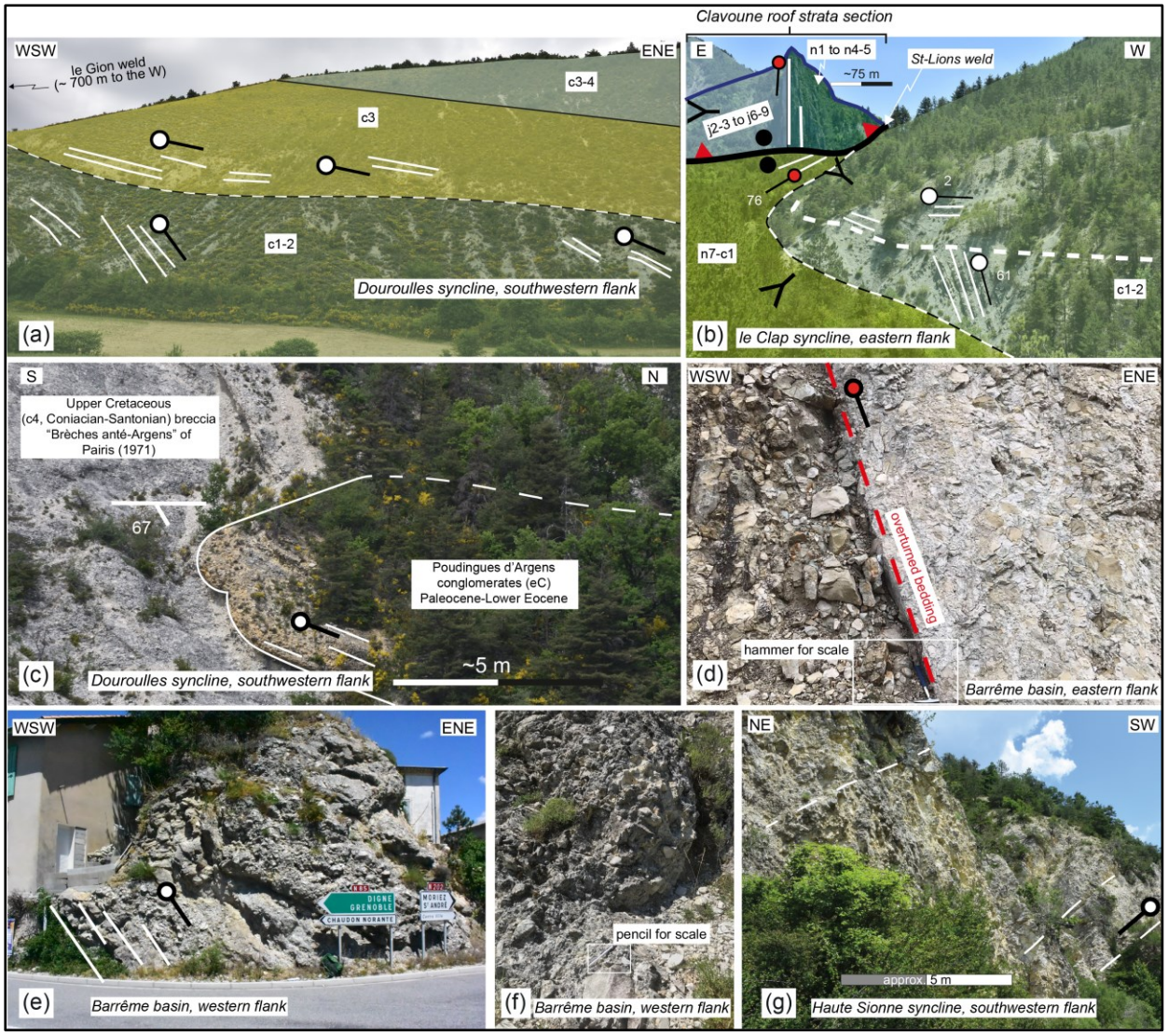


Figure 10 (a) Local angular unconformity at the base of the Turonian limestone (c3) over the Cenomanian marl and marly limestone (c1-2), on the southwestern flank of the Douroulles syncline, east of the le Gion weld. (b) Interpreted photo of the eastern flank of the le Clap syncline, northwest of the subvertical Clavoune roof strata section. Note the angular unconformity at the base of the Cenomanian marly sediments (c1-2). A second angular unconformity was observed within the Cenomanian succession (c1-2). (c) Photo of the poorly sorted Coniacian-Santonian breccia east of the le Gion weld, on the southwestern flank of the Douroulles syncline and onlapping Poudingues d'Argens Formation. (d) Overturned beds of the Upper Cretaceous breccias on the eastern flank of the Barrême basin, adjacent to the Gévaudan diapir (the "Brèches anté-Argens" of Pairis (1971)). (e) and (f) Photos of the poorly sorted Upper Cretaceous breccias exposed on the western flank of the Barrême basin. The breccias occur within coherent olistolith-olisthostrome units which intercalated in the Priabonian Nummulitic limestone and the Priabonian-Rupelian Globigerina marls (Elliott et al., 1985; De Graciansky et al., 1981; De Graciansky et al., 1982; Evans & Elliott, 1999). (g) Photo of poorly sorted Cenomanian-Coniacian breccias on the southwestern flank of the Haute Sionne syncline, exposed below the overriding la Blache-Castellane thrust sheet. See Figure 4 for viewpoint locations.

The Cretaceous fill of the synclines is mostly made up of Albian-Cenomanian black shales with overlying Upper Cretaceous pelagic sediments (Figure 4, Figure 6, Figure 10a and b). Locally, however, a unique sedimentary facies, is seen within these structures. This consists of poorly sorted, intraformational Upper Cretaceous breccias with erosive bases exposed on the flanks of the synclines adjacent to their bounding salt bodies and their linking with discordant surfaces (Kerckhove & Roux, 1978a; Pairis, 1971; De Graciansky et al., 1981) (Figure 9, Figure 10c, 10d, 10e, 10f and 10g). The occurrences of Upper Cretaceous breccias are shown by pale green stars in Figure 9. The breccias are usually overlain by the Paleocene-Lower Eocene Poudingues d'Argens Formation (eC) composed of pebble – to cobble-grade well rounded, clast-supported channelised conglomerates (Figure 10c) (Elliott et al., 1985; Evans & Elliott, 1999). Locally the base of the Poudingues d'Argens Formation is composed of the reworked angular clasts of the underlying Upper Cretaceous breccias (Figure 10c).

A thick accumulation of Upper Cretaceous breccias is also exposed in the upper part of the Cretaceous section in the eastern flank of the Barrême syncline (Barrême basin) (Figure 9, Figure 10d) and in the Bois de Lieye, west of the Gévaudan diapir (Figure 4, Figure 5, Figure 9) (Pairis, 1971). The overturned Middle-Upper Cretaceous section thins against the Keuper evaporites of the Gévaudan diapir (Figure 4) and the Albian- Cenomanian black shales (n7-c1) pinch out locally along the diapir, with gypsum in direct contact with the Cenomanian-Santonian beds. Jurassic and Lower Cretaceous rocks are absent (Figure 4, Figure 5). In the southern part of the Bois de Lieye section, local unconformities are developed in the Upper Cretaceous section adjacent to the Gévaudan diapir (Figure 4) and it is assumed that, below the regional unconformity, the overturned Cenomanian-Santonian section thickens at depth (Figure 5b).

At the Bois de Lieye, the subvertical Albian-Santonian is unconformably overlain by an extremely thick, vertical, or slightly overturned section of the Paleocene-Lower Eocene Poudingues d'Argens conglomerates (Figure 4). The thickness of the Poudingues d'Argens is around 500 m here whereas on the western flank of the Barrême syncline, it is only a few meters thick between underlying Lower Cretaceous rocks and overlying Nummulitic limestone (Figure 3, Figure 4).

West of the village of Barrême, in the western limb of the asymmetric Barrême syncline Upper Cretaceous sediments are missing and the Tertiary regional unconformity lies above Lower Cretaceous rocks forming the lateral tip folds of a splay from the Digne thrust (Figure 3, Figure 4). De Graciansky et al. (1981), Elliott et al. (1985) and Evans & Elliott (1999) describe 100m-scale olistoliths (Figure 4) composed of Upper Cretaceous breccias and lithified limestones (shown as C4 in Figure 4) resedimented during the Nummulitic deposition. The blocks are intercalated within the Priabonian Nummulitic limestone (e7) and overlying Priabonian-Rupelian Globigerina marls (e7g1) (Figure 4)

(Evans & Elliott, 1999). Eocene-Oligocene sediments dip uniformly towards to the east at 20-40º (Figure 4), although steeper dips (around 70º) occur around the olistoliths, immediately above the Nummulitic regional unconformity (Figure 4). Evans & Elliott (1999) suggested that the olistoliths were emplaced as gravity-driven submarine slides and blocks which originating from the eastern limb of the synclinal depocenter because Upper Cretaceous rocks do not occur west of the village of Barrême (Chauveau & Lemoine, 1961; Bodelle, 1971; Evans & Elliott, 1999).

Further south, on the southwestern flank of the Blieux syncline Grosjean et al. (2017) described similar, 100m-scale olistoliths composed of Upper Cretaceous breccias and limestones (C4) intercalated at the base of Nummulitic limestone (Figure 6). The distribution of the olistoliths is shown by red stars in Figure 9. Upper Cretaceous breccias are also present in Bourbonne syncline, in the l'Hauter thrust sheet and the Haute Sionne syncline, on the eastern flank of the Taulanne syncline (Figure 6, Figure 9 and Figure 10g). The narrow and elongated Bourbonne and Haute Sionne synclines are bounded by Alpine structures (Figure 3, Figure 6, Figure 9) and separated from the Jurassic-Lower Cretaceous and Eocene-Oligocene of the Blieux and Taulanne synclines by discordant surfaces which link Alpine faults and the remnants of allochthonous salt bodies (Figure 3, Figure 6 and Figure 9).

The fill of the Bourbonne and Haute Sionne synclines is similar to the Albian-Cenomanian and younger Upper Cretaceous succession of the Douroulles, le Clap and Barrême synclines (Figure 3, Figure 4, Figure 6 and Figure 9). Guérin-Desjardins (1956) described pre-Priabonian conglomerates correspond to the Paleocene Poudingues d'Argens conglomerates in the Haute Sionne syncline.

4.2 Interpretation

The discordant surfaces bounding the elongated synclines and connecting allochthonous salt bodies to their feeder diapirs or to each other are interpreted as welded salt structures. These salt structures, possibly originally elongated salt walls, are now squeezed, partly or completely welded, or reactivated as Alpine structures. We recognise the le Gion, Mouchon, St-Lions, Rouviére, Thon and Brayal welds (Figure 3 and Figure 9). Pinch-outs against allochthonous salt bodies and their linking welds, local unconformities along the bounding structures of the synclines and thickness and facies changes in the Albian-Cenomanian black shales and Upper Cretaceous pelagic sediments within the synclines all suggest Late Cretaceous sedimentation in minibasins. Given the lack of Jurassic and Lower Cretaceous strata, we conclude that the minibasins formed on allochthonous salt i.e., they are secondary minibasins.

According to Harrison & Jackson (2014), the oldest roof or onlapping strata along a diapir provide clues about its source layer. The oldest onlapping formation along the allochthonous salt bodies and welds here is the Albian-Cenomanian Marnes Bleues Formation. This suggests that the salt bodies are the remnants of the Albian-Cenomanian salt sheets or represent salt structures rooted in the allochthonous salt (Figure 8d and Figure 11).

The poorly sorted Upper Cretaceous breccias exposed in the Douroulles, Barrême, Bourbonne and Haute Sionne synclines are interpreted as debris flow deposits derived from the top of salt structures which developed from the allochthonous salt from the Albo-Cenomanian onwards. We assume that the intraformational breccias deposited in secondary minibasins are analogous with the 'pre-Argens' breccias described by Pairis (1971) on the overturned eastern flank of the Barrême basin below the regional Tertiary unconformity and adjacent to the Gévaudan diapir.

Giles & Lawton (2002) described similar debris-flow deposits composed of sediments which once onlapped the El Papalote diapir of the La Popa basin in Mexico. Harrison & Jackson (2014) documented sedimentary breccias associated to the growth of salt structures above a salt canopy in the 'wall and basin' province of the Sverdrup basin in Canada.

The occurrences of breccias along the flanks of secondary minibasins clearly indicates the presence of local topographic highs, what presumable use to be growing salt structures fed from the allochthonous salt (Figure 11). The allochthonous salt and overlying stratigraphy is deeply eroded now because of Alpine uplift and the Upper Cretaceous breccias are unconformably overlain by thick accumulation of the oldest member of the Alpine foreland basin megasequence, the Paleocene-Lower Eocene Poudingues d'Argens conglomerates. We suggest that the Poudingues d'Argens Formation formed by the reworking of underlying Upper Cretaceous breccias during the early phases of Alpine compression.

Northeast of Barrême, thin Poudingues d'Argens are preserved locally at the base of the foreland basin megasequence in synclines such as the Argens syncline (Figure 3) (De Graciansky et al., 1982; Apps, 1987; Apps et al., 2004) but in the Barrême area, thick accumulations of the Poudingues d'Argens Formation are only preserved in secondary minibasins (Figure 3, Figure 4, Figure 6 and Figure 9) and may have been deposited only there. Exposures of the Poudingues d'Argens conglomerates are shown by brown stars in Figure 9.

Sudden changes in fold wavelengths in the secondary minibasins and overriding thrust sheets also support the existence of the salt canopy. Jackson & Harrison (2006), Rowan & Vendeville (2006) and Kergaravat et al. (2016) all suggested that fold wavelengths tend to be shorter above shortened allochthonous salt canopies because the level of the detachment is shallower and there is a relatively

thin overburden. We suggest that the folding of the Upper Cretaceous secondary minibasin fill in the Haute Sionne syncline or the short wavelength folding of the supra-canopy Cretaceous and Poudingues d'Argens in the Douroulles secondary minibasin provide new field examples of this phenomenon.

The Albian-Santonian succession of the Barrême syncline is almost identical to the fill of the Douroulles and le Clap secondary minibasins and there is indirect evidence to suggest that it started to form during the Cretaceous as secondary minibasin above allochthonous salt. The stratal and structural geometries along the eastern flank of the minibasin, thickness changes, the local pinch-outs and direct contact of Albian-Cenomanian black shales and younger Upper Cretaceous sediments with the Keuper gypsum of the Gévaudan diapir, the presence of the thick Upper Cretaceous debris-flow deposits and the thick overlying Poudingues d'Argens conglomerates all suggest that the Upper Cretaceous section of the Barrême basin may itself represent a secondary minibasin, bounded to the east by allochthonous salt (Figure 11).

The indirect evidence that Upper Cretaceous debris flow deposits occur as olistoliths in the Priabonian-Rupelian sediments suggests that the basin may also have been bounded on its flank by an elongated salt structure, which may represent the western limit of the salt canopy (Figure 11). Chauveau & Lemoine (1961), Bodelle (1971) and Evans & Elliott (1999) all suggested that these

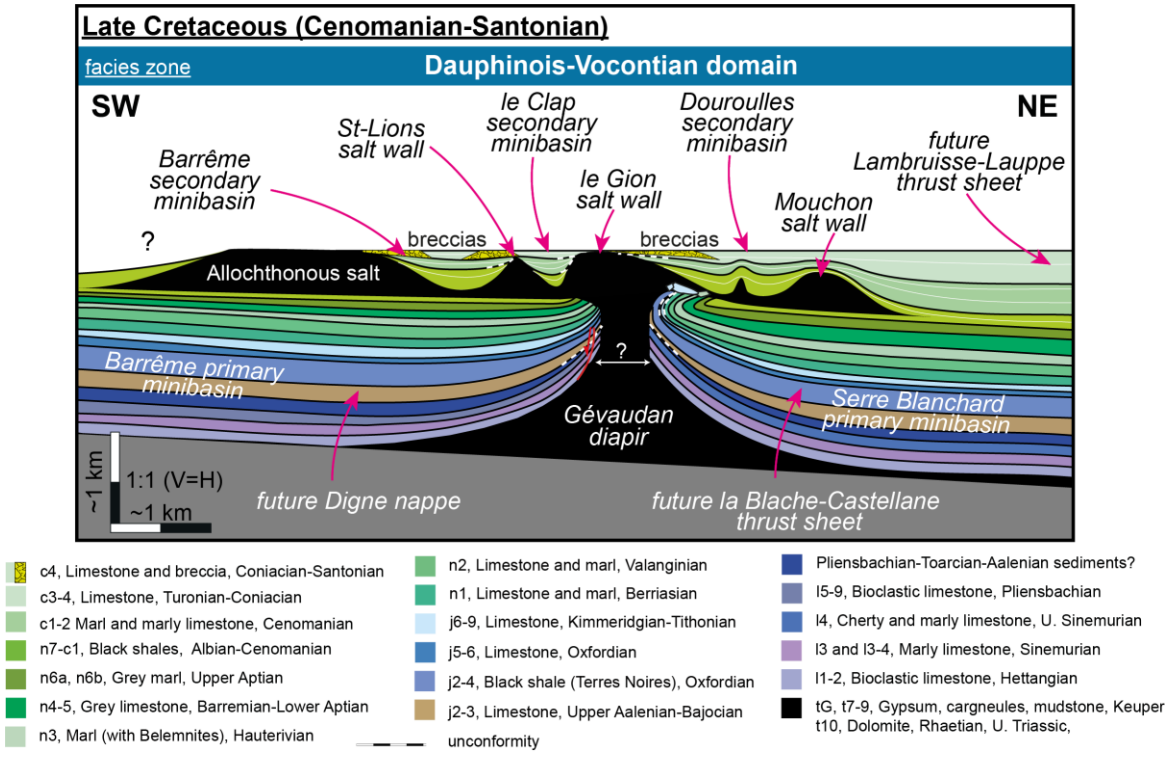


Figure 11 Diagram showing the possible configuration of secondary minibasins above the allochthonous salt around the feeder Gévaudan diapir during the Late Cretaceous. The model is also showing schematic stratal and structural geometries in the secondary minibasins and around the salt structures.

olistoliths are derived from the eastern flank of the Barrême syncline and their emplacement is related to thrusting along the eastern flank of the basin but we suggest the alternative interpretation that they were diapir-derived, having developed during the Late Cretaceous from the failure of the roof of a north-northwest – south-southeast trending salt structure. The width and the length of the salt structure is not known, although the large volume of debris-flow deposits suggests that it may have been a relatively large salt wall forming a significant topographic high (Figure 11). The northern limit of the salt body is not known (Figure 3, Figure 4 and Figure 9).

The presence of the allochthonous salt locally influenced the facies and the thickness of the Albian-Cenomanian and younger Upper Cretaceous succession. Cross-sections show that the thickness of the fill of the secondary minibasins decreased from north to south with supra-canopy sediments around 500 m around the town of Castellane (e.g., the Haute Sionne secondary minibasin, Figure 7b) and perhaps up to 1.5 km north of the Gévaudan diapir (e.g., le Clap secondary minibasin, Figure 5b).

5 Discussion

Our study gives a detailed description of an allochthonous salt canopy which developed on the Tethyan margin during the middle of the Cretaceous and hosted several secondary minibasins during the Late Cretaceous. The identification of large exposures of Upper Triassic evaporites in the Southern Subalpine chains as the remnants of an allochthonous salt canopy and the re-interpretation of some of the piggyback basins of the fold and thrust belt as secondary minibasins also call for new models to describe the structural evolution of the Subalpine chains between Clumanc and Castellane.

The canopy and the associated minibasins were incorporated into the developing fold and thrust belt from the Late Cretaceous onwards. We discuss below how allochthonous salt was emplaced into progressively higher stratigraphic levels, describe the possible Late Cretaceous and Alpine evolution of the canopy and its secondary minibasins and describe the influence of salt tectonics in the structural evolution of the fold and thrust belt and its syn-orogenic sedimentation.

5.1 Cretaceous structural evolution

5.1.1 Albian-Cenomanian emplacement of Keuper evaporites into higher stratigraphic levels: extrusion from feeder diapirs

Salt extrusion occurred during a period of tectonic quiescence. Three allochthonous salt sheets have been identified north of the Provençal platform and may have been formed as plug-fed extrusions emplaced from tall feeder diapirs (Figure 8d) (Hudec & Jackson, 2006; Jackson & Hudec, 2017). Salt extrusion coincided with the deposition of black shales during the Albian-Cenomanian and may have been triggered by decreased aggradation and sediment starvation. Brooke-Barnett (2022) and Brooke-Barnett et al. (2023) have also described 100m thick bedding parallel gypsum within Aptian-Albian black shales near the Daluis diapir and interpreted the allochthonous salt as a remnant of an Aptian-Albian extrusive sheet.

Older salt sheets have also been documented north of this Barrême area, where salt reached the surface during the deposition of the black shales of the Bathonian-Oxfordian Terres Noires Formation (Graham et al., 2012; Célini et al., 2020; Célini, 2020). According to Hallam (2001) and Haq (2018) the Bathonian-Callovian period was characterized by high global sea level. During the Aptian and the Early Albian, the global sea level was also relatively high and stable for a long period (Haq, 2014). This suggests that widespread allochthonous salt sheet initiation and emplacement during a long period of tectonic quiescence may have been related to global sea level high stands and regional sediment starvation.

5.1.2 The formation and possible extent of the Albian-Cenomanian salt canopy and secondary minibasin formation above the allochthonous salt

The extrusive salt sheets are likely to have coalesced to form an approximately north-south trending salt canopy (Figure 9 and Figure 12). The base-salt relief was presumably low because the sheets and canopy formed during a period characterised by low sedimentation rate (Figure 11). Above the canopy, elongated second generation salt structures and adjacent secondary minibasins developed during the Late Cretaceous. Approximately north-northwest – south-southeast trending salt walls developed above the canopy around the Gévaudan diapir and bounded elongated secondary minibasins.

What initiated secondary minibasin subsidence on the allochthonous salt is unclear. The onset of the diapiric activity is marked by thickness changes of Albian-Cenomanian black shales (Figure 5b and Figure 7b) suggesting that the individual secondary minibasins started to form as early as Albian-Cenomanian time, shortly after the extrusion of the salt and the coalescence of the canopy. Minibasin formation may have been triggered by irregularities in the surface of the allochthonous salt formed by dissolution of the evaporites (Jackson et al., 2010; Jackson & Hudec, 2017). Alternatively, the sheets may have coalesced along sutures with suture trenches (Dooley et al., 2012) along the contacts of amalgamating sheets.

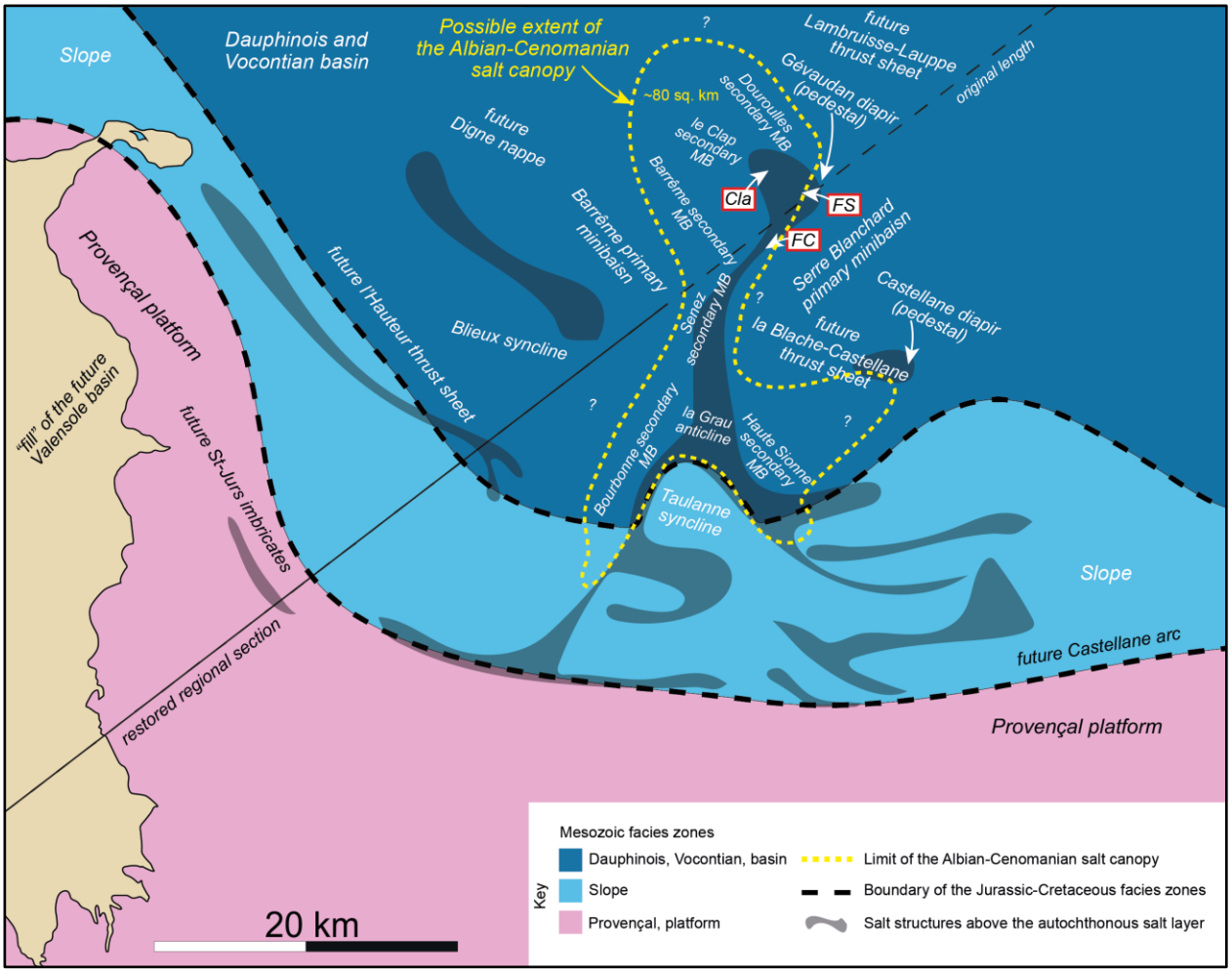


Figure 12 Map-view schematic model of the Southern Subalpine chains during the Late Cretaceous showing the possible original location of salt structures in the platform-slope-basin palaeogeographic configuration. The yellow dotted line shows the possible extent of the salt canopy. White question marks indicate locations where the limit of the canopy is not known. Note that the shape and the position of salt structures and minibasins are not known for certain and this rough reconstruction, based on the restoration of a regional cross section shown in Figure 1c, showing their approximate palinspastic position. Abbreviations: Cla = Clavoune roof strata section; FC = Font Chaude roof strata section; FS = Fontaine Salée flap; MB = minibasin.

In the Digne nappe and the l'Hauter thrust sheet, west of the zone where remnants of the canopy and the secondary minibasins are exposed, Upper Cretaceous sediments are thin and commonly reworked as olistoliths on the Tertiary unconformity. This is the case along the western flank of the Barrême basin (Figure 4, Figure 9) and along the south-western limb of the Blieux syncline (Figure 6, Figure 9) though in some places Upper Cretaceous rocks are absent altogether. In contrast, east of the remnants of the canopy, in the overriding Lambruisse-Lauppe thrust sheet, a thick succession of basinal Upper Cretaceous is present. We assume that where the canopy was present, Late Cretaceous sedimentation occurred in secondary minibasins which subsided relatively quickly into the allochthonous salt. Thin Upper Cretaceous sediments may have been deposited west of the canopy as peripheral sediments in primary minibasins (Figure 11) around its edges while at the same time thick pelagic sediments were deposited east of the canopy, in the Vocontian basin (Figure 11 and Figure 12).

The spatial distribution of secondary minibasins helps to define the limits of the allochthonous salt and the extent of the now mostly welded canopy (Figure 9), though clearly its pre-erosional extent and geometry has been modified and largely obscured by Alpine deformation and Tertiary syn-tectonic sedimentation. The Douroulles, le Clap, Barrême, Bourbonne and Haute Sionne synclines (Figure 3, Figure 4, Figure 6 and Figure 9) are all interpreted as shortened secondary minibasins. They are now exposed in thrust sheets which telescoped the basin to slope transition (Figure 9) but a basic restoration suggests that the allochthonous salt level spread over tens of kilometres and may have been up to 80 sq. km in extent stretching from the northern of the edge of the Provençal platform into the basin facies zone, around the Gévaudan diapir and beyond (Figure 12).

5.2 The Alpine modification of the salt tectonic system of the Subalpine chains. How the canopy and the secondary minibasins were incorporated into the fold and thrust belt

From the Late Cretaceous onwards, south-west directed Alpine shortening transformed the structural evolution of Haute Provence. The formation of the salt-detached, thin-skinned fold and thrust belt affected a basin already deformed by salt tectonics and which contained two levels of evaporites in many places. A series of evolutionary diagrams illustrate the detailed Alpine evolution of the compressional salt tectonic system around the Gévaudan diapir (Figure 13).

5.2.1 Pre-Priabonian (Pre-Nummulitic) structural evolution of the salt tectonic system

At the onset of Alpine shortening, the thick sedimentary pile of the basin began to detach from its basement along the Keuper evaporites (Figure 13a). The two levels of evaporites acted as décollement levels and the deformation decoupled below and above them. The displacement of two major Alpine thrust sheets – the Lambruisse-Lauppe thrust sheet and the Digne nappe – started east and west of the Gévaudan diapir (Figure 13a).

The Lambruisse-Lauppe thrust sheet carries a thick Upper Cretaceous basinal section over the eastern flank of the Douroulles secondary minibasin and the canopy (Figure 13a). Eroded debris was shed into the Douroulles secondary minibasin during the Paleocene resulting in the deposition of a thick succession of Poudingues d'Argens conglomerates. Simultaneously, underlying Upper Cretaceous breccias were reworked into Poudingues d'Argens conglomerates (Figure 10c and Figure 13a).

Short wavelength folding occurred above the shallow evaporite detachment in the Douroulles secondary minibasin, whereas long-wavelength, broad anticlines formed in the overriding Lambruisse-Lauppe thrust sheet. The relatively thin and weak supra-canopy succession of the Douroulles, le Clap and Barrême secondary minibasins were highly folded whereas the underlying Serre Blanchard and Barrême primary minibasins remained relatively undeformed suggesting that the deformation was decoupled by the canopy (Figure 13a).

Poudingues d'Argens was deposited further to the west-southwest, in the le Clap and the Barrême secondary minibasins with the thickest section deposited in the eastern part of the Barrême secondary minibasin (around 500-600 m in the Bois de Lieye section) (Figure 4, Figure 5b, Figure 13a). The rapid minibasin subsidence may have been triggered and maintained by sedimentary topographic loading or differential loading of the thick accumulation of the Poudingues d'Argens above the allochthonous salt (Figure 13a).

Sedimentary loading and Alpine compression likely triggered southwest – or west-southwest directed salt expulsion and open-toed advance of the allochthonous salt towards to the foreland (Figure 13a). North of the village of Barrême, on the western flank of the Barrême secondary minibasin the thickness of the Poudingues d'Argens Formation is only a few meters suggesting the presence of a local topographic high on the western margin of the secondary minibasin during the deposition of the conglomerates.

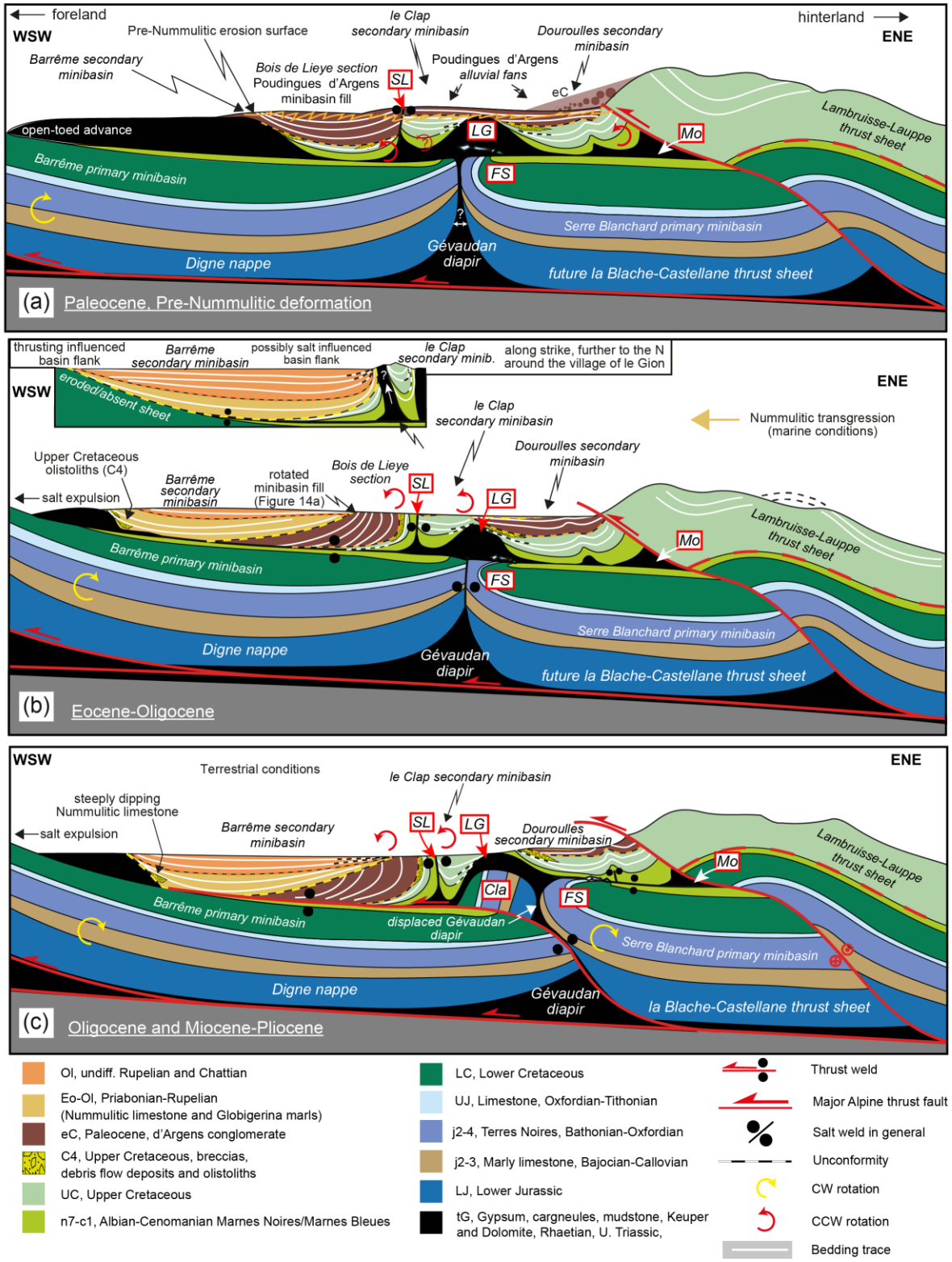


Figure 13 Diagrammatic sections showing possible Alpine evolution of the Gévaudan diapir and the adjacent primary minibasins below the salt canopy and the evolution of the second-generation salt structures and secondary minibasins above the canopy during the Alpine compressional phase, from the Paleocene (a) until the Miocene-Pliocene (c) (not to scale). Abbreviations: Cla = Clavoune roof strata section; FS = Fontaine Salée flap; LG = le Gion salt structure and weld; Mo = Mouchon salt structure and weld; SL = St-Lions salt structure and weld. The section showing the different evolutionary stages along the S1-S1' cross section. For S1-S1' section line location, see Figure 3 and Figure 4.

Although Evans & Elliott (1999) suggested that this topographic high it might be interpreted as one of the developing lateral tip folds of the Digne thrust, we propose that it is more likely to have been associated with the westward migration of allochthonous salt (Figure 13a).

The Barrême secondary minibasin seems to have been confined to the east and west by salt-related topography during the deposition of the Poudingues d'Argens (Figure 13a). Paleocurrent data measured on channel fills in the Bois de Lieye section (Figure 4, Figure 14a) suggest north-south flow, parallel with the bounding salt structures of the secondary minibasin (Figure 13a). The westward expulsion of the salt from the allochthonous canopy probably initiated the first phase of rotation of the secondary minibasins above the canopy (Figure 13a).

West of the salt canopy the Digne thrust started to emplace a thick basinal succession of the Jurassic and Cretaceous onto the thin carbonates of the slope and the Provençal platform (Figure 9) (Gigot et al., 1974; Lickorish & Ford, 1998; Graham et al., 2012). Northwest of the village of Barrême lateral tip folds of a splay of the Digne thrust are unconformably overlain by the Nummulitic limestone which implies movement along this segment of the thrust before Priabonian (Lickorish & Ford, 1998; Evans & Elliott, 1999; Graham et al., 2012). Minor clockwise rotation of the Barrême primary minibasin below the canopy might be associated with this movement (Figure 13a).

At the same time the original Gévaudan diapir below the canopy was shortened and squeezed. Squeezing of the diapir may have increased the flow of salt to the allochthonous level as the diapiric stem narrowed or closed. This in turn would have added to salt expulsion from the canopy towards to west–south-west (Figure 13a).

South of the Gévaudan area the canopy and secondary minibasins were deeply eroded before the deposition of the foreland basin succession and the Bourbonne and Haute Sionne secondary minibasins are overlain only by thin Paleocene Poudingues d'Argens (Figure 3, Figure 6).

5.2.2 The Eocene-Oligocene (Priabonian-Chattian) structural evolution of the salt tectonic system

Flexural subsidence and synchronous southwest directed Nummulitic transgression occurred during the Priabonian (Figure 13b). The counter-clockwise rotation of the Barrême primary minibasin in Digne nappe and the overthrusting of the Lambruisse-Lauppe thrust sheet continued. The collision of the relatively undeformed Barrême and Serre Blanchard primary minibasins presumably led to the closure of the stem of the Gévaudan by this time (Figure 13b).

An entirely different structural style developed above the canopy. Short wavelength folding continued in the Douroulles and in the le Clap secondary minibasins. Continuous salt expulsion along the western edge of the canopy and progressive salt withdrawal triggered a major phase of counterclockwise rotation in the Barrême secondary minibasin accompanied by an abrupt westward shift of the basin depocenter (Figure 13b). The steeper dips in the Nummulitic Limestone above the Lower Cretaceous section on the western flank of the Barrême secondary minibasin (Figure 14b) suggesting that the underlying Jurassic - Lower Cretaceous section was separated from the Priabonian-Rupelian sediments by a detachment – presumably the extruding allochthonous salt (Figure 13b). The canopy became almost completely welded below the eastern and central part of the Barrême secondary minibasin (Figure 13b). The salt was presumably squeezed out to the west creating the rotation recorded by the thick, subvertical section of the Poudingues d'Argens conglomerates on its eastern flank in the Bois de Lieye section (Figure 4, Figure 5b, Figure 13b, Figure 14a and b). Together with the underlying Albian-Cenomanian and Upper Cretaceous the overturned and subvertical section of the Poudingues d'Argens represents the highly rotated centre of the Barrême secondary minibasin (Figure 13b). The precursor Cretaceous secondary minibasin and its overlying Poudingues d'Argens now lies unconformably below the Eocene-Oligocene along the welded base of the canopy (Figure 4, Figure 5b, Figure 13b).

Structural geometries show clearly that the first phase of counter-clockwise rotation occurred before the deposition of the Nummulitic Limestone because the overturned Poudingues d'Argens Formation is unconformably overlain on the western side of the Bois de Lieye section, along the Rouviére weld by the steeply dipping Nummulitic limestone (Figure 14b) itself unconformably overlain by northward dipping Oligocene molasse (Figure 4, Figure 5b, Figure 14b) suggesting that the minibasin was rotated further during the Oligocene. Between the villages of le Gion and Senez (Figure 3 and Figure 4), local angular unconformities developed in the Oligocene succession along the eastern flank of the Barrême secondary minibasin due to the continuous counter-clockwise rotation of the depocenter (Figure 4, Figure 14b).

The depletion of the canopy and the major phase of rotation of the Barrême secondary minibasin occurring during the Late Eocene–Early Oligocene may possibly have been associated with the emplacement of the internal Embrunais-Ubaye nappes. The interaction of salt tectonics and thrusting resulted in the formation of what might be called an 'asymmetric hybrid basin'. Analogues of this have been reported in other fold and thrust belts. Kergaravat et al. (2017) documented minibasin rotation and associated depocenter migration within secondary minibasins in a contractional setting in the Sivas basin of central Anatolia. Santolaria et al. (2022) described analogue models of counter-clockwise

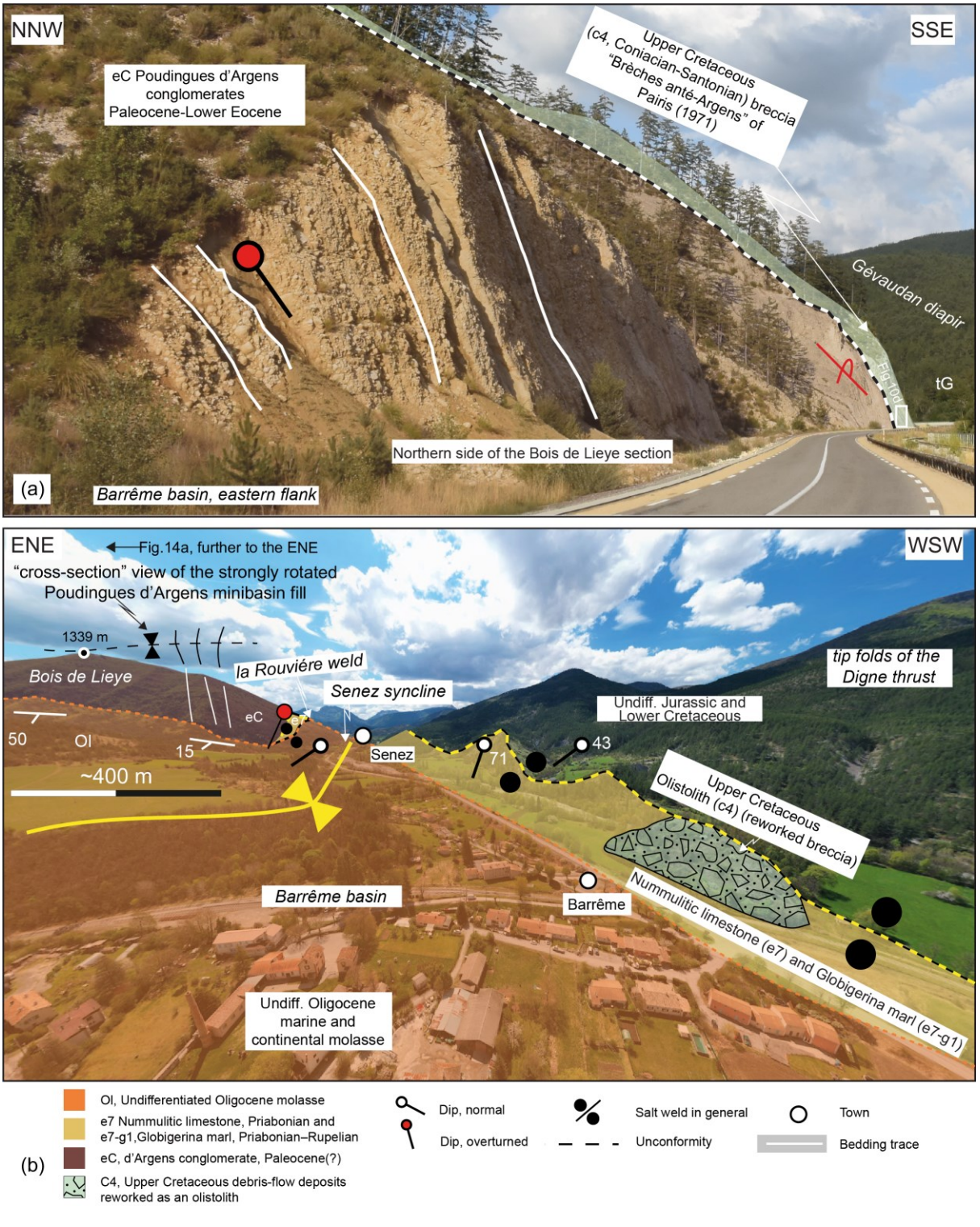


Figure 14 Interpreted photo of overturned Upper Cretaceous breccias and the overlying Poudingues d'Argens conglomerates on the eastern flank of the Barrême basin. The Bois de Lieye section represents the rotated Paleocene core of the secondary minibasin. (b) Interpreted photo panorama of the western flank of the Barrême basin and the rotated minibasin fill exposed at the Bois de Lieye section. Image courtesy of Communauté de Communes Alpes Provence Verdon. See Figure 4 for viewpoint locations.

rotation of a minibasin about a sub-horizontal axis simultaneous with the migration of a weld. The illustrated relationship between the rotated minibasin and the weld in their model is similar to that proposed here for the welded canopy and western flank of the Bois de Lieye rotated minibasin fill. We suggest that the Barrême secondary minibasin provides a new example of a highly rotated secondary minibasin developing in a fold and thrust belt and filled with synorogenic sediments.

Allochthonous salt emplacement also occurred during the later stages of regional Alpine compression. Salt was emplaced towards to south-west from the salt canopy, possibly below the supra-canopy Upper Cretaceous-Paleocene fill of the Barrême secondary minibasin during the Late Oligocene. It is recorded on the southern side of the Bois de Lieye section where northeast dipping Chattian alluvial sediments (Grés verts Formation, g3V) are structurally overlain by a thick and 1 km wide Keuper gypsum body which is linked to the allochthonous salt of the Gévaudan diapir (Figure 4). Allochthonous salt may have been emplaced over the Late Chattian land surface during the deposition of the Chattian molasse in the Senez syncline, i.e., the southern continuation of the Barrême secondary minibasin (Figure 3, Figure 4, Figure 9). The base salt geometry may have been similar to observed seismic analogues of advancing salt sheets of the deep-water Gulf of Mexico (Jackson & Hudec, 2017). However, exposure is extremely poor below the sheet margin and the relationship of the salt, and the underlying sediments is not known.

It has been mentioned above that the southern part of the region, where the salt canopy and the secondary minibasins were relatively thin, most of the allochthonous salt and the supra-canopy minibasins were largely removed by erosion by the Eocene (Figure 3, Figure 6). Around Castellane, along the northern edge of the Provençal platform the presence of a thinner canopy and its depletion or erosion resulted in the development of different structural style and minibasin rotation and salt expulsion have not occurred.

We suggest that in the southern region, structures like the la Grau salt cored anticline developed above the autochthonous salt and Alpine shortening was largely accommodated by the weak pre-existing salt structures which were squeezed and almost completely welded (Figure 7b). Syn-orogenic sedimentation was influenced by folding associated to the squeezing of salt structures surrounding the Taulanne and Blieux minibasins and relatively thick Eocene-Oligocene sequences were deposited in these synclines which had started life as primary Mesozoic minibasins.

The significant deformation and modification of the pre-existing salt related structures in the southern area coincided with the main collision phase. The emplacement of the internal Embrunais-Ubaye nappes may have been responsible for the complete welding of the allochthonous salt level and emplacement of the la Blache-Castellane thrust sheet. The last remnants of the allochthonous salt

canopy below the Bourbonne and Haute Sionne secondary minibasins were probably welded during the Oligocene when the Haute Sionne minibasin was pushed towards to southwest above the Eocene-Oligocene fill of the Taulanne syncline (Figure 3, Figure 6 and Figure 9).

The emplacement of the allochthonous Chattian salt sheet at Senez probably records the last episode of salt tectonic activity in the area. From the Miocene onwards, the salt tectonic system advanced into a thrust-dominated stage of its evolution.

5.2.3 The Miocene-Pliocene evolution of the salt tectonic system

After the Oligocene Alpine deformation propagated towards the foreland and the deformation front reached the Provençal platform and its Miocene-Pliocene molasse cover (Figure 1c, Figure 9 and Figure 16b). In the north the Barrême primary minibasin, the Gévaudan diapir and the remnants of the allochthonous salt canopy together with the secondary minibasins were carried passively in Alpine thrust sheets and the Barrême primary minibasin was probably subject to further clockwise rotation (Figure 13c). By the Miocene-Pliocene, regional compression became the dominant process because most of the allochthonous salt and the stem of the Gévaudan diapir became depleted and welded (Figure 13c). Regional compression resulted in the emplacement of the near-crest flank of the Gévaudan diapir which now forms the allochthonous structural horse of the Clavoune (Figure 5, Figure 13c and Figure 15). The out-of-sequence Alpine thrust fault which decapitated the Gévaudan diapir ramped up to the canopy on the basinward side of the triangular diapiric pedestal. The Clavoune section which represents the original southwestern flank and roof of the Gévaudan diapir overthrusted the le Clap secondary minibasin along a splay (Figure 3, Figure 4, Figure 5, Figure 13c and Figure 15). The almost completely welded salt canopy served as an upper detachment surface and the Barrême secondary minibasin was thrust westwards (Figure 13c and Figure 15), although displacement dies out westwards and the structure remains blind (Figure 13c and Figure 15).

Further to the south, along the S3-S3’ section line (Figure 3, Figure 15), the Alpine thrust fault presumably crosscut the Gévaudan diapir and elevated the eastern flank of the diapir so that the Font Chaude section and the adjacent Serre Blanchard primary minibasin are exposed now in the la Blache-Castellane thrust sheet (Figure 4, Figure 5, Figure 9, Figure 13c and Figure 15). The along-strike continuation of the Clavoune section lies beneath the remnants of the salt canopy and the rotated minibasin fill of the Barrême secondary minibasin, possibly below the Bois de Lieye section (Figure 15).

In the southern area salt structures continued to be squeezed and secondary minibasins shortened. North of the la Grau salt cored anticline, the Castellane sheet-like diapir and the Haute Sionne secondary minibasin together with Rupelian syn-orogenic sediments were overthrusted by the la Blache-Castellane thrust sheet (Figure 3, Figure 6 and Figure 9).

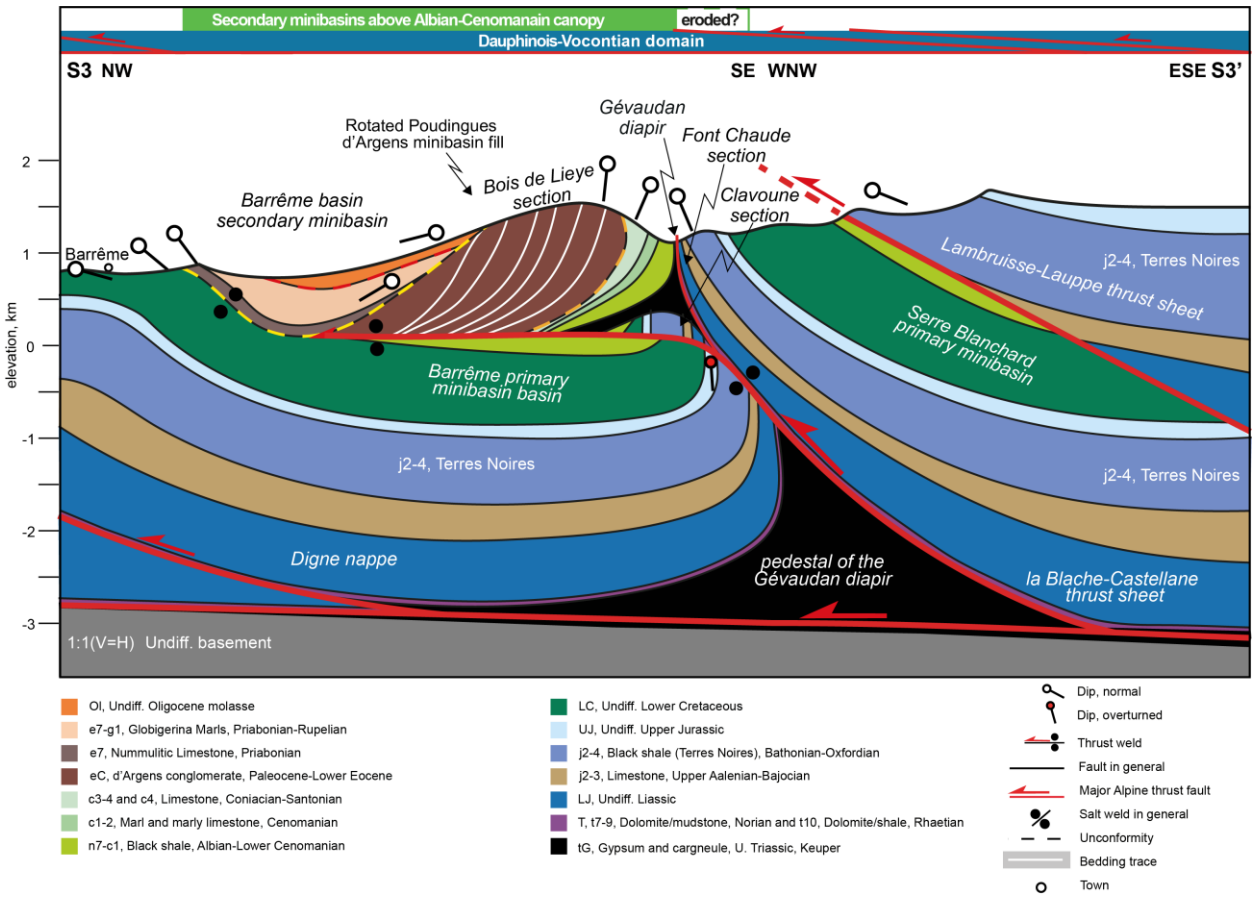


Figure 15 Cross section (S3-S3') from the Digne thrust sheet to the la Lambruisse-Lauppe thrust sheet, showing the position of the Barrême secondary minibasin above the welded allochthonous salt canopy and the resultant structural style of the latest stages of regional compression. Note the counterclockwise rotation of the Barrême primary minibasin and the position of the displaced lateral equivalent of the Clavoune roof strata section below the Barrême secondary minibasin. For cross section location and geological map see Figure 3 and Figure 4.

5.3 Salt canopy and associated secondary minibasins in fold and thrust belts

In the Digne nappe system a pre-existing salt canopy which formed during the middle of the Cretaceous and hosted several secondary minibasins (Figure 16a) is exposed beyond the orogenic front and was carried passively in the fold and thrust belt (Figure 16b). The structural style between the mountain front and the salt canopy is relatively simple with the Keuper evaporites providing the basal

detachment surface for folding and thrusting and associated with imbricate thrust faults and salt cored anticlines (Figure 16b).

However, the structural style of the Subalpine chains is very different where the pre-shortening salt tectonic system was well developed (Figure 9 and Figure 16b). The simplified cross sections shown in Figure 16b highlight the response of the two generations of salt structures and minibasins to the regional Alpine shortening and also help to visualise the different components of the compressional salt tectonic system of the Southern Subalpine chains.

The key structural elements and shortening styles of the compressional salt tectonic system of the Southern Subalpine chains are the following (Figure 16b and c):

- The autochthonous level served as a basal detachment for the Alpine thrusting and folding.
- Alpine shortening was accommodated mostly by weak pre-existing salt structures which were squeezed, welded, and completely shut before the development of Alpine thrust faults on their basinward flanks (e.g., the Gévaudan diapir).
- Primary minibasins filled with thick Jurassic-Lower Cretaceous succession remained relatively undeformed and some of these minibasins were rotated in the hanging wall of major Alpine thrust faults about horizontal axes.
- In the northern region the salt canopy was almost completely welded due to the westward migration and expulsion of the allochthonous salt.
- Progressive salt expulsion from the canopy and open-toed advance of the salt triggered counter-clockwise rotation of secondary minibasins about horizontal axes, which was accompanied by a westward shift in depocenter location (e.g., in the Barrême secondary minibasin)
- Sudden changes in fold wavelengths could occur above allochthonous salt, whereas long-wavelength, broad anticlines formed east and west of the canopy, in the hanging wall of major Alpine thrust faults which carries thick basinal succession.
- Secondary minibasins may have been carried as piggyback basins in actively deforming fold and thrust belts.

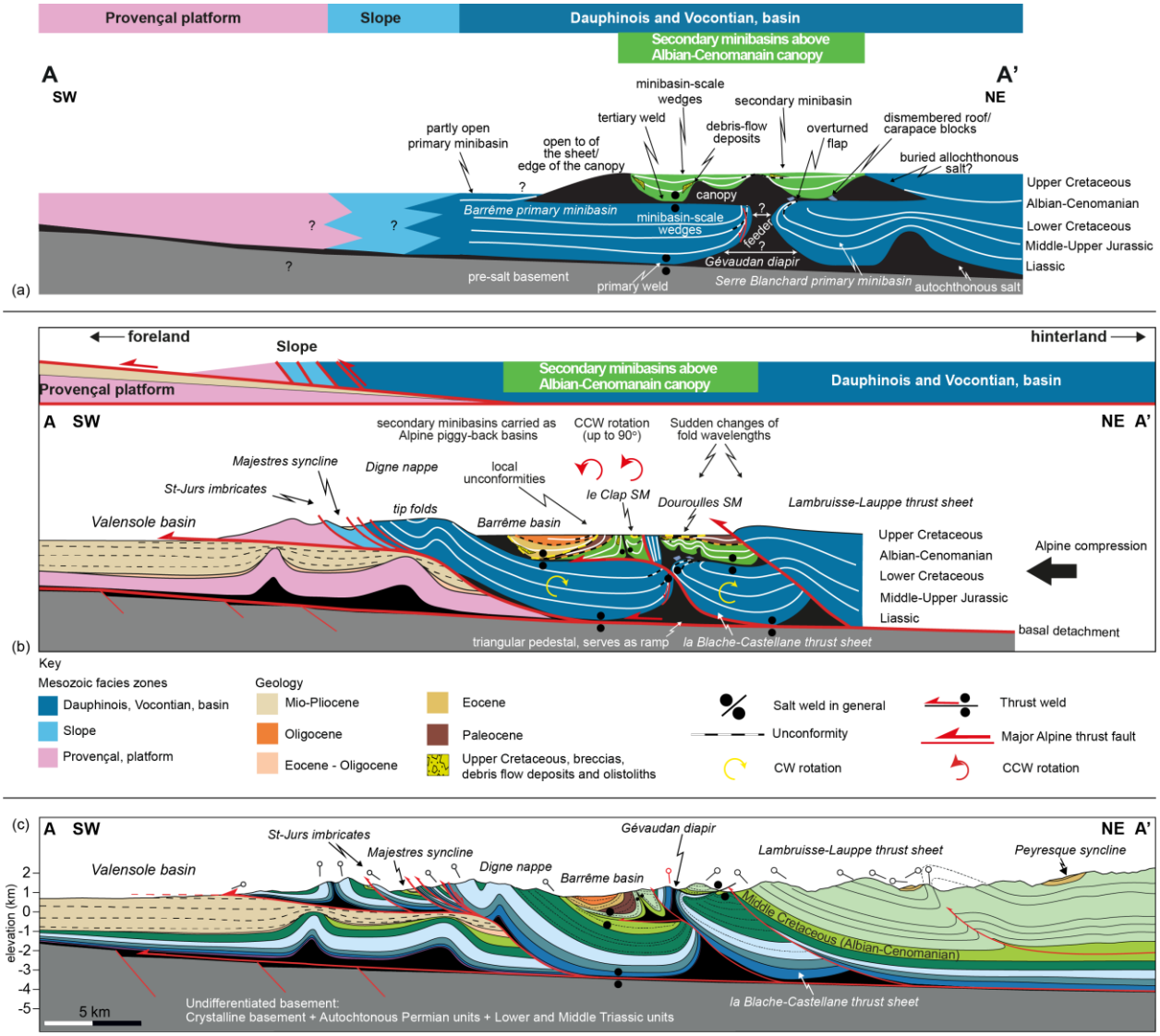


Figure 16 (a) 2D conceptual model showing the key elements and structural styles of the northern part of the pre-shortening salt tectonic system around the Gévaudan diapir, with examples of salt structures and salt withdrawal minibasins. The model is also showing schematic stratal and structural geometries in the minibasins and around the salt structures. (b) 2D schematic model synthesizing the key elements and structural style of the Alpine salt tectonic system around the Gévaudan diapir and the incorporation of the Albian-Cenomanian salt canopy and associated secondary minibasins into the fold and thrust belt. The section line A-A' showing the modified state of the pre-Alpine salt tectonic system shown in Figure 16a and showing a salt tectonic model of the fold and thrust belt shown in Figure 16 (c). The model is also showing schematic stratal and structural geometries in the minibasins and around the salt structures and the compressional structures which developed during the regional Alpine shortening. Abbreviation: SM = secondary minibasin. (c) Regional cross-section from the Valensole basin through the Digne nappe system (also shown in Figure 1(c)). See Figure 1 (b) for key. Note that the sections are not restored.

6 Conclusion

We have documented a salt tectonic system which contained two levels of evaporites with a second generation of minibasins above allochthonous salt. Our geological mapping and cross section construction has revealed the following:

Several salt structures and adjacent primary minibasins started to form as early as the Liassic triggered by the Tethyan rifting. The first-generation salt structures developed north of the Provençal carbonate platform above the autochthonous salt along the slope and further to the north, in the basin palaeogeographical domain of the Jurassic Dauphinois and the Cretaceous Vocontian basins.

Continuous salt tectonic activity led to the emplacement of Keuper evaporites onto the seafloor during the Albian-Cenomanian. Stratigraphic and structural relationships around the Gévaudan diapir and the la Grau salt-cored anticline show evidence of salt breakout from pre-existing diapirs which led locally to the overturning of the condensed roof strata. At Castellane Muschelkalk and Keuper gypsum and limestone form a sheet-like allochthonous diapir entirely surrounded by the Albian-Cenomanian sediments and overridden by the la Blache-Castellane thrust sheet. Salt sheets formed as plug-fed extrusions and their emplacement coincided with the deposition of black shales during the Albo-Cenomanian triggered by decreased aggradation and sediment starvation.

Extrusive sheets coalesced to form of a salt canopy which covered large areas of the Tethyan margin. The pre-erosional extent of the approximately north-south trending canopy may have been around 80 sq. km. A second generation of salt structures developed above the canopy, and bounded elongated secondary minibasins. Above the southern part of the canopy smaller and shallower secondary minibasins developed suggesting that the thickness of the allochthonous salt may have decreased towards the northern edge of the Provençale platform. The presence of the allochthonous canopy locally influenced the facies and the thickness of the Albian-Cenomanian and younger Upper Cretaceous sediments.

During regional Alpine compression, the vertical or steeply dipping Gévaudan diapir which had been connected to the autochthonous salt layer was squeezed to form a weld and was crosscut by and Alpine thrust fault during the later phases of shortening.

Sediments deposited in primary minibasins consist of thick, relatively competent Jurassic and Cretaceous carbonates and remained relatively undeformed. The Barrême and Serre Blanchard primary minibasins rotated about horizontal axes in the hanging wall of major Alpine thrust faults.

Where the Albian-Cenomanian canopy was originally thicker, the Alpine syn-kinematic sedimentation above the allochthonous salt was strongly affected by salt tectonic activity during the

Paleocene, Eocene, and Oligocene. Syn-orogenic sediments were deposited in thrust-sheet-top basins superimposed over the earlier formed secondary minibasins in the actively deforming fold and thrust belt. Progressive west directed salt expulsion from the canopy triggered counterclockwise rotation of the Barrême secondary minibasin, accompanied by a westward shift of the depocenter and almost complete welding of the allochthonous salt. The interaction of the Alpine compression and progressive salt withdrawal resulted in the formation of hybrid asymmetric basins influenced by both thrusting – and salt tectonics. The Barrême basin is the best example of this phenomenon.

The significant deformation and modification of the pre-existing salt tectonic system was associated with the main collision phase and the south-west directed thrusting in Provence which may in turn have been driven by the emplacement of the internal Embrunais-Ubaye nappes during the Late Eocene-Early Oligocene. Propagation of shortening from the hinterland towards the foreland resulted in the formation of Alpine thrust sheets which telescoped thick basinal successions above the Mesozoic slope and platform palaeogeographic domains and the allochthonous salt canopy with its associated secondary minibasins were carried passively in the hanging wall of major Alpine thrust faults. The eastern edge of the canopy was overthrusted by the thick Jurassic-Cretaceous sections exposed now in the Lambruisse-Lauppe and la Blache-Castellane thrust sheets.

The salt canopy and associated salt-withdrawal depocenters of the Southern Subalpine chains could be considered as one of the few onshore examples of well-exposed canopies and secondary minibasins, and as far as we are aware, is the first time that such a thing has been documented in the Alps. We hope that this new salt tectonic model synthesizes the key elements of the system and suggest that it may have implications for other salt influenced fold and thrust belts.

Chapter 6. Conclusions and future work

6.1 Key conclusions

The thesis is based on extensive fieldwork conducted in the Southern Subalpine chains in the vicinity of the town of Castellane and the village of Barrême and describes the evolution of a Mesozoic salt tectonic system which contained two levels of evaporites and two generations of minibasins which were incorporated into the developing fold and thrust belt of the Southern Subalpine chains during the Late Cretaceous-Pliocene Alpine shortening.

The key conclusions of the thesis are outlined below.

Several salt structures and adjacent primary minibasins started to form as early as the Liassic above the Upper Triassic Keuper evaporites during the Tethyan rifting north of the Provençal platform. The initiation of salt tectonic activity was possibly triggered by the Early-Middle Jurassic Tethyan rifting which led to the formation of reactive diapirs developed over the footwalls of extensional faults. The salt structures grew passively due to differential loading over the autochthonous salt layer during the late stages of rifting and the early stages of the subsequent passive margin phase.

Passive diapirism and extensive salt tectonic activity led to the formation of a well-developed minibasin and salt-ridge system above the autochthonous salt along the slope and further to the north, in the basin palaeogeographical domain of the Dauphinois and Vocontian basins. Jurassic-Lower Cretaceous facies boundaries associated with the platform-slope-basin palaeogeographic domains were defined more or less by elongated salt walls and isolated diapiric structures, which possibly formed at the junction of the buried salt walls. The salt diapirs and walls which developed above the autochthonous salt in the slope facies zone formed a polygonal network of salt structures around isolated depocenters, similarly to the Northern Gulf of Mexico where minibasins are separated by a network of salt ridges. In the basin, elongated primary minibasins were bounded by more linear salt structures.

Due to continuous salt tectonic activity, the salt tectonic system became more mature, resulting in the emplacement of Upper Triassic Keuper evaporites onto the seafloor during the Albian-Cenomanian. Stratigraphic and structural relationships around the Gévaudan, Castellane and St-Vincent diapirs and the la Grau anticline provide evidence of salt breakout from tall, pre-existing diapirs which led locally to the overturning of the condensed roof strata. Feeder diapirs were situated at the boundary of the slope and basin palaeogeographic domains and also further to the north, in the basin facies zone. Allochthonous salt sheets formed as plug-fed extrusions. Salt extrusion coincided with the deposition of black shales during the Albian-Cenomanian and may have been triggered by decreased aggradation and sediment starvation.

The extrusive salt sheets advanced from the feeder diapirs laterally and coalesced to form an approximately N-S trending salt canopy. The canopy spilled over the well-developed primary minibasin and salt-ridge system which formed during the rifting and the subsequent passive margin phase. The thickness of the allochthonous salt may have been decreased up to the slope, towards the northern edge of the Provençale platform. The canopy partly covered the primary minibasins and thin Upper Cretaceous sediments deposited as peripheral sediments around the edges of the canopy. The pre-erosional extent of the approximately N-S trending canopy may have been around 80 sq. km. This could be the first description of such canopy in the Western Alps.

From the Albian-Cenomanian onwards, the canopy sourced a second-generation of salt structures, presumably salt walls which bounded elongated, approximately N-S trending salt-withdrawal depocenters, e.g., the Barrême and Haute Sionne secondary minibasins. Secondary minibasin formation may have been triggered by irregularities in the surface of the allochthonous salt which formed due to dissolution of the evaporites or by the presence of local topographic lows which formed where the extrusive sheets coalesced. The presence of the allochthonous salt strongly influenced the thickness and facies of the supra-canopy Upper Cretaceous succession.

From Late Cretaceous onwards, the fold and thrust belt of the Southern Subalpine chains developed on the Tethyan passive margin and the Jurassic-Cretaceous salt tectonic system with its two levels of evaporites and two generations of minibasins was profoundly modified. Regional Alpine shortening was accommodated partly by thin skinned shortening along the basal detachment and preferentially affected the mechanically weak pre-existing salt structures. Elongated salt walls and diapirs localised the nucleation of major Alpine thrusts and, where appropriately oriented, served as ramps where the thrust faults splayed from the basal detachment surface.

The vertical or steeply dipping salt structures such as the Gévaduan diapir which were connected to the autochthonous salt layer were squeezed to form welds and were crosscut by thrust faults during the later phases of Alpine shortening.

Sediments deposited in primary minibasins consist of thick Jurassic-Cretaceous carbonate successions and remained relatively undeformed. Many of the primary minibasins (e.g., the Barrême and Serre Blanchard primary minibasins) rotated about horizontal axes in the hanging wall of major Alpine thrust faults.

Around Barrême, where the Albian-Cenomanian canopy was originally thicker, Alpine syn-kinematic sedimentation occurred above the allochthonous salt and was strongly affected by

salt tectonic activity during the Paleocene, Eocene, and Oligocene. Syn-orogenic sediments were deposited in piggyback basins superimposed over the earlier formed secondary minibasins in the actively deforming fold and thrust belt. These basins were confined by shortened, roughly N-S trending salt walls. Progressive west directed salt expulsion from the canopy triggered counter-clockwise rotation of the Barrême secondary minibasin, accompanied by a westward shift of the depocenter and almost complete welding of the allochthonous salt. The interaction of the Alpine compression and progressive salt withdrawal resulted in the formation of hybrid, thrusting– and salt tectonics–influenced asymmetric basins, e.g., the Barrême basin.

Around Castellane, where the Albian-Cenomanian allochthonous salt was originally thinner, the erosion and welding of the canopy occurred during the early phases of the regional compression. The depletion or erosion of the canopy resulted in the development of different structural style and minibasin rotation and salt expulsion have not occurred during the Eocene and Oligocene.

Siginificant deformation and modification of the pre-existing salt-related structures like squeezing of diapirs, depletion of the canopy, the major phase of rotation of the Barrême secondary minibasin and a renewed phase of salt sheet emplacement from the allochthonous salt were all associated with the main collision phase and the south-west directed emplacement of the internal Embrunais-Ubaye nappes during the Late Eocene-Early Oligocene.

Propagation of shortening from the hinterland towards the foreland resulted in the formation of major Alpine thrust faults which telescoped thick basinal successions above the primary minibasin and salt-ridge system of the slope palaeogeographic domain and the allochthonous salt canopy with its associated secondary minibasins.

The most important outcome of my new research is the identification of the almost completely welded Albian-Cenomanian salt canopy and the secondary minibasins which were incorporated into the fold and thrust belt, and strongly influenced sedimentation on both the passive margin and also during the deposition of the foreland basin megasequence. The salt canopy and associated secondary minibasins of the Southern Subalpine chains could be considered as one of the few onshore examples of well-exposed canopies and secondary minibasins.

6.2 Future work

The Southern Subalpine chains provides relatively good outcrop conditions to investigate salt related structures which developed on the Tethyan margin during the Mesozoic and later, during the subsequent Alpine compressional phase. This study focused on the salt structures and adjacent minibasins which developed on the slope and in the basin palaeogeographic domains of the Dauphinois and Vocontian basins above two levels of Triassic evaporites in the area around Castellane and Barrême.

However, the slope and basin palaeogeographic domains were continuous along the Provençal platform further to the northeast, to the west and northwest of the study area and salt diapirs, walls, minibasins and allochthonous salt sheets have been identified in thrust sheets which have emplaced rocks in slope and basin facies zones over the platform.

North of the study area and the town of Digne-les-Bains, Graham et al. (2012), Célini (2020), Célini et al. (2020) and Célini et al. (2022) described several pre-Alpine salt structures like overturned flaps, salt structures and adjacent minibasins which developed in the slope and basin palaeogeographic domain and were later displaced and highly modified by Alpine shortening.

Regional summary of the allochthonous salt bodies and minibasins in the fold and thrust belt of Haute-Provence was provided by Graham et al. (2019) and NE of the town of Castellane, Brooke-Barnett et al. (2021), Brooke-Barnett (2022) and Brooke-Barnett et al. (2023) described pre-Alpine salt structures and their effects in the evolution of the fold and thrust belt of the Subalpine Chains along the Rouaine-Daluis fault system and further to the NE around the Dome de Barrôt.

Although Brooke-Barnett (2022) described briefly the le Poil zone of the slope (see Chapter 2) where the displacement of the Digne Thrust is dispersed through a series of N-S trending faults which have dextral lateral component (De Graciansky et al., 1982; Lickorish & Ford, 1998), the slope facies zone between the Digne thrust sheet and the mountain front has not been properly studied recently.

The le Poil fault zone was active at least during the Oligocene and the Mio-Pliocene. Based on literature review, Brooke-Barnett (2022) suggested that the le Poil zone may have been formed as a salt wall during the Mesozoic and later, during the Alpine compressional phase it was optimally oriented for reactivation as a dextral strike-slip fault.

The le Poil zone is situated NW of my study area, and it is linked into the squeezed Petit Mourre diapir (see Chapter 4, § 4.1.3.2) which developed in the basin facies zone through the

Petit Mourre-le Poil weld. Local unconformities and pinch-outs in the Upper Jurassic section and onlapping Berriasian, Valanginian and Albian-Cenomanian sediments onto Petit Mourre diapir and the Petit Mourre-le Poil weld were described in the le Chiran minibasin (see Chapter 4, § 4.1.3.3). This suggests that the presumed le-Poil salt wall was active during the Late Jurassic and Cretaceous times.

I suggest that salt tectonic activity was spatially widespread NW of the study area in the transitional zone between the slope and basin palaeogeographic domains during the Mesozoic. It would be worthwhile to further investigate and describe the le Poil zone with our new understanding of the salt tectonics system of the Southern Subalpine chains.

Potential salt related structures are also located in the autochthonous Provençal platform area. Southwest of the town of Castellane, the Provençal carbonate platform drowned during the Late Berriasian – Early Valanginian and Cotillon (1994) has argued that this event was a consequence of sea level rise and Vocontian rifting (see Chapter 2). In the Western part of the Castellane Arc, along the northern margin of the Provençal platform, Masse et al. (2009) also documented a series of tilted fault blocks covered unconformably by Valanginian sediments. Maybe the extension in the platform domain has important regional implications.

Direct evidence of Berriasian – Early Valanginian regional extension was not observed in the slope or basin palaeogeographic domains in the study area. In contrast, the observed early Cretaceous normal faults in the southern structural domain around the Chasteuil salt structure in the Porte de St-Jean and Taloire primary minibasins recorded only local, salt related deformation (see Chapter 4, § 4.1.1.7). Extensive salt tectonic activity occurred in the upper part of the slope facies zone, around the Chasteuil salt structure during the Late Jurassic and the Early Cretaceous (see Chapter 4, § 4.1.1.7) whereas further to the north, in the basin facies zone, salt tectonics culminated in the extrusion of the salt to the seafloor during the Albian-Cenomanian (see Chapter 5). It is possible that the Mesozoic salt tectonic system had a regional, gravity driven thin-skinned deformation component. Analogues have been described on modern passive margins (Marton et al., 2000; Fort et al., 2004). The regional, gravity driven thin-skinned system may have been progressively redistributed the Upper Triassic salt basinward from the Late Jurassic to the Late Cretaceous. Local extension occurred during the passive margin evolution and normal faults developed in the platform domain which may have been represented the up-dip extensional domain of the gravitational salt tectonic system. The diapirs and salt walls of the slope facies zone may have corresponded to the diapir-pillow domain of the gravity driven salt tectonic system of recent passive margins. The tall diapirs of the basin facies zone may have been situated in the more basinward located, allochthonous salt

dominated domain of the salt tectonic system. The Late Jurassic–Early Cretaceous movement of the mobile evaporites may have been triggered by the load of the thick carbonate succession of the Provençal platform which deposited during the Tithonian-Berriasian (Kerckhove & Roux, 1978b) and may have been responsible for basinward salt movement along the mother salt layer, but further work is needed to confirm this hypothesis.

Salt tectonic activity may have been also occurred in Cenozoic times in the area of the Provençal platform. During the Oligocene compressional tectonics dominated but a series of NNW-SSE trending extensional grabens developed in the Alpine foreland in response to E-W extension which may have been related to the formation of the Rhone-Rhine graben system. N-S trending grabens may have formed in the Haute Provence platform in response to the regional extension (Ford et al., 1999; Séranne, 1999). Indeed, the Moustiers-Sainte-Marie 1:50000 map sheet of Kerckhove & Roux (1978a) suggests that the Upper Triassic salt may have been emplaced into some of the N-S trending grabens. East of the village of la Palud-sur-Verdon gypsum is in direct contact with steeply dipping Upper Jurassic and Cretaceous rocks in an approximately N-S trending fault zone (see Chapter 4, Fig. 4.34) which maybe corresponds to one of the Oligocene extensional structures. In addition, NE of the village of la Palud-sur-Verdon, in the footwall of the Robion thrust, Upper Triassic salt is in direct contact with Oligocene sediments (Fig. 4.1) which suggests that the salt was exposed to the surface in the foreland during the regional extension. The detailed analysis of the platform area could reveal that reactive salt rise may have been occurred in the foreland of the advancing fold and thrust belt.

A more detailed analysis of the salt influenced Eocene-Oligocene syn-kinematic sedimentation in the minibasins of the northern structural domain, e.g., the Barrême basin would make for an interesting study, but more important, future work would need to involve the restoration of regional cross sections across the Castellane arc and the Digne arc.

References

Alsop, G. I., Derek John Blundell & Davison, I. (eds.) (1996) *Salt Tectonics*. London, The Geological Society.

Apps, G. (1987) Evolution of the Grès d'Annot Basin, South West Alps. PhD Thesis, University of Liverpool, Liverpool.

Apps, G., Peel, F. & Elliott, T. (2004) The structural setting and palaeogeographical evolution of the Grès d'Annot basin. *Geological Society, London, Special Publications.* 221 (1), 65-96.

Arnaud, H. (1988) Subsidence in certain domains of southeastern France during the Ligurian Tethys opening and spreading stages. *Bulletin de la Société géologique de France.* 4 (5), 725-732.

Arnaud, H., Gidon, M. & Pairis, J.-L. (1977) Précisions sur la structure des chaînes subalpines méridionales dans la région de Faucon-Turriers-Clamensane (Alpes de Haute-Provence). *Geologie Alpine.* 53, 5-34.

Artoni, A. & Meckel, L. D. (1998) History and deformation rates of a thrust sheet top basin: the Barrême basin, western Alps, SE France. *Geological Society, London, Special Publications.* 134 (1), 213-237.

Bally, A. (1981) Thoughts on the tectonics of folded belts. *Geological Society, London, Special Publications.* 9 (1), 13-32.

Beaudoin, B. (1969) Esquisse paléogéographique du Jurassique supérieur-Crétacé, Esquisse inférieur subalpin dans les Basses-Alpes. *CR Acad. Sci. Fr.* 269, 1239-1242.

Beaudoin, B. (1977) Méthodes d'analyse sédimentaire et reconstitution du bassin: le Jurassique terminal-Berriasien des chaînes subalpines méridionales. Université de Caen.

Beaudoin, B., Renaud, P., Cojan, I. & Desmaison, Y. (1983) Mise en évidence du contrôle tectonique de la sédimentation: le jeu de l'accident du Col de la Cine au long du Mésozoïque (région de Digne, SE de la France). *Comptes rendus de l'Académie des sciences. Série 2, Mécanique, Physique, Chimie, Sciences de l'univers, Sciences de la Terre.* 303 (9), 857-862.

Bill, M., O'Dogherty, L., Guex, J., Baumgartner, P. O. & Masson, H. (2001) Radiolarite ages in Alpine-Mediterranean ophiolites: Constraints on the oceanic spreading and the Tethys-Atlantic connection. *GSA Bulletin.* 113 (1), 129-143.

Bodelle, J. (1971) Les formations nummulitiques de l'arc de Castellane. BRGM.

Bollinger, L., Nicolas, M. & Marin, S. (2010) Hydrological triggering of the seismicity around a salt diapir in Castellane, France. *Earth and Planetary Science Letters.* 290 (1-2), 20-29.

Bordet, P. (1950) Le dôme permien de Barrot (AM.) et son auréole de terrains secondaires-Alpes françaises du sud.

Boussac, J. (1912) Etudes stratigraphiques sur le Nummulitique alpin. Mémoires pour servir à l'explication de la carte géologique détaillée de la France, Imprimerie Nationale (Paris).

Bréhéret, J.-G. & Brumsack, H.-J. (2000) Barite concretions as evidence of pauses in sedimentation in the Marnes Bleues Formation of the Vocontian Basin (SE France). *Sedimentary Geology.* 130 (3-4), 205-228.

Bréhéret, J. G. (1988) Episodes de sédimentation riche en matière organique dans les marnes bleues d'âge aptien et albien de la partie pélagique du bassin vocontien. *Bulletin de la Société géologique de France.* 4 (2), 349-356.

Brooke-Barnett, S. (2022) The effects of salt tectonics in the evolution of a fold and thrust belt, south-west Alps. Doctor of Philosophy (PhD). Imperial College London.

Brooke-Barnett, S., Csicsek, L. A., Célini, N., Callot, J.-P., Graham, R., Lonergan, L. & Ringenbach, J.-C. (2021) Reconstructing the development of salt structures in the margin of a shortened carbonate rich basin; Subalpine chains of southeast France. *AAPG Europe Evaporite Processes and Systems, Online.*

Brooke-Barnett, S., Csicsek, L. A., Graham, R. & Lonergan, L. (2020) Salt tectonics in the Subalpine Chains of SE France, from rifting to Alpine shortening. *EGU General Assembly 2020, Online*.

Brooke-Barnett, S., Graham, R., Lonergan, L. & Csicsek, L. A. (2019) Influence of salt tectonics on the subalpine chains of SE France under extensional, strike-slip and compressional regimes. *Salt Tectonics: Understanding Rocks that Flow., London*.

Brooke-Barnett, S., Graham, R., Lonergan, L. & Csicsek, L. A. (2023) Salt tectonics along a strike-slip fault system in the sub-Alpine chains of southeastern France, from the Triassic to the Oligocene. *AAPG Bulletin.* 107 (1), 87-122.

Callot, J.-P., Célini, N., Jourdon, A., Legeay, E., Mouthereau, F., Le Pourhiet, L. & Ringenbach, J.-C. (2022) *The role of salt in mountain building, from minibasin formation to orogen dynamic*. EGU General Assembly 2022, Vienna, Austria, 23–27 May 2022.

Callot, J.-P., Ribes, C., Kergaravat, C., Bonnel, C., Temiz, H., Poisson, A., Vrielynck, B., Salel, J.-F. & Ringenbach, J.-C. (2014) Salt tectonics in the Sivas basin (Turkey): crossing salt walls and minibasins. *Bulletin de la Société géologique de France.* 185 (1), 33-42.

Callot, J.-P., Salel, J.-F., Letouzey, J., Daniel, J.-M. & Ringenbach, J.-C. (2016) Three-dimensional evolution of salt-controlled minibasins: Interactions, folding, and megaflap development. *AAPG Bulletin.* 100 (9), 1419-1442.

Callot, J.-P., Trocmé, V., Letouzey, J., Albouy, E., Jahani, S. & Sherkati, S. (2012) Pre-existing salt structures and the folding of the Zagros Mountains. *Geological Society, London, Special Publications.* 363 (1), 545-561.

Callot, J. P., Jahani, S. & Letouzey, J. (2007) The role of pre-existing diapirs in fold and thrust belt development. *Thrust belts and foreland basins*, Springer, pp. 309-325.

Campredon, R. (1977) Les formations paléogenes des Alpes Maritimes franco-italiennes. *Mémoire hors-série de la Société géologique de France.* 9, 199.

Campredon, R., Aicard, P., Bambier, A. & Durozoy, G. (1980a) Carte Geologique de la France a 1/50000, Notice explicative de la feuille d'Entrevaux. *Bur. Rech. Geol. Min. Orleans, France.*

Campredon, R., Bordet, P., Giannerini, G. & Manigault, B. (1980b) Carte Geologique de la France a 1/50000, Feuille d'Entrevaux. *Bur. Rech. Geol. Min. Orleans, France.*

Canérot, J., Hudec, M. R. & Rockenbauch, K. (2005) Mesozoic diapirism in the Pyrenean orogen: Salt tectonics on a transform plate boundary. *AAPG Bulletin.* 89 (2), 211-229.

Célini, N. (2020) Le rôle des évaporites dans l'évolution tectonique du front alpin: le cas de la nappe de Digne. Université de Pau et des Pays de l'Adour.

Célini, N., Callot, J.-P., Pichat, A., Legeay, E., Graham, R. & Ringenbach, J.-C. (2022) Secondary minibasins in orogens: Examples from the Sivas Basin (Turkey) and the sub-Alpine fold-and-thrust belt (France). *Journal of Structural Geology.* 156, 104555.

Célini, N., Callot, J. P., Ringenbach, J. C. & Graham, R. (2020) Jurassic salt tectonics in the SW sub-alpine fold-and-thrust belt. *Tectonics.* 39 (10), e2020TC006107.

Ceriani, S., Fügenschuh, B. & Schmid, S. M. (2001) Multi-stage thrusting at the" Penninic Front" in the Western Alps between Mont Blanc and Pelvoux massifs. *International Journal of Earth Sciences.* 90 (3), 685-702.

Chauveau, J.-C. & Lemoine, M. (1961) Contribution à l'étude géologique du synclinal du tertiaire de Barrême (moitié nord): Bulletin Service de la Carte Géologique de la France.

Cotillon, P. (1968) Le Crétacé inférieur de l'arc subalpin de Castellane entre l'Asse et le Var: stratigraphie et sédimentologie. Université de Lyon.

Cotillon, P. (1985) Hauts-fonds de la Marge Nord-Est Provencale au Cretace Inferieur. Un exemple de controles tectonique et bathymetrique. *Bulletin de la Section des Sciences.* 9, 25-38.

Cotillon, P. (1994) The platform of" Calcaires blancs de Provence" in the tectonic arc of Castellane (SE France). Evolution during the Early Cretaceous; importance in sedimentary and tectonic behavior of a margin. *Géologie Méditerranéenne.* 21 (3), 55-58.

Cotillon, P. (2010) Sea bottom current activity recorded on the southern margin of the Vocontian basin (southeastern France) during the lower Aptian. Evidence for a climatic signal. *Bulletin de la Société géologique de France.* 181 (1), 3-18.

Cotillon, P., Banvillet, M., Gaillard, C., Grosheny, D. & Olivero, D. (2000) Les surfaces à Rhizocorallium de l'Aptien inférieur sur la bordure méridionale du bassin Vocontien (France Sud-Est), marqueurs de dynamiques locales; leur relation avec un événement anoxique global. *Bulletin de la Société géologique de France.* 171 (2), 229-238.

Csicsek, L. A., Brooke-Barnett, S., Callot, J.-P., Célini, N., Graham, R., Lonergan, L. & Ringenbach, J.-C. (2021) Pre-orogenic diapirs and extrusive salt sheets. Southern Subalpine Chains, Haute Provence, France. Effects of precursor halokinetic structures in the evolution of a fold and thrust belt. *AAPG GTW Evaporites Processes and Systems, Salzburg*.

Csicsek, L. A., Brooke-Barnett, S., Graham, R. & Lonergan, L. (2019) The effects of salt tectonics in the evolution of a fold and thrust belt, Subalpine Chains, Western Alps. *Salt tectonics: Understanding rocks that flow: Meeting of The Geological Society, London, London* pp. 33-34.

Dardeau, G. (1988) Tethyan evolution and Alpine reactivation of Jurassic extensional structures in the French "Alpes Maritimes". *Bulletin de la Société géologique de France.* 4 (4), 651-657.

Dardeau, G. & De Graciansky, P. (1990) Halocinèse et rifting téthysien dans les Alpes-Maritimes (France). *Bulletin des centres de recherches exploration-Production Elf-Aquitaine.* 14 (2), 443-464.

Davis, D. M. & Engelder, T. (1985) The role of salt in fold-and-thrust belts. *Tectonophysics.* 119 (1-4), 67-88.

de Boer, P. L. (1983) Aspects of middle cretaceous pelagic sedimentation in Southern Europe: production and storage of organic matter, stable isotopes, and astronomical influences. Utrecht University.

De Graciansky, P.-C. & Lemoine, M. (1988) Early Cretaceous extensional tectonics in the southwestern French Alps; a consequence of North-Atlantic rifting during Tethyan spreading. *Bulletin de la Société géologique de France.* 4 (5), 733-737.

De Graciansky, P.-C., Roberts, D. G. & Tricart, P. (2010) The Western Alps, from rift to passive margin to orogenic belt: an integrated geoscience overview. Elsevier.

De Graciansky, P., Dardeau, G., Lemoine, M. & Tricart, P. (1989) The inverted margin of the French Alps and foreland basin inversion. *Geological Society, London, Special Publications.* 44 (1), 87-104.

De Graciansky, P. C., Dardeau, G., Dumont, T., Jacquin, T., Marchand, D., Mouterde, R. & Vail, P. (1993) Depositional sequence cycles, transgressive-regressive facies cycles, and extensional tectonics; example from the southern subalpine Jurassic basin, France. *Bulletin de la Société géologique de France.* 164 (5), 709-718.

De Graciansky, P. C., Durozoy, G., Ganeval, J. & Gigot, P. (1982) Carte Geologique de la France a 1/50000, Notice explicative de la feuille de Digne. *Bur. Rech. Geol. Min. Orleans, France.*

De Graciansky, P. C., Guillemot, J., Ganeval, J. & Gigot, P. (1981) Carte Geologique de la France a 1/50000, Feuille de Digne. *Bur. Rech. Geol. Min. Orleans, France.*

Dooley, T., McClay, K., Hempton, M. & Smit, D. (2005) *Salt tectonics above complex basement extensional fault systems: results from analogue modelling*, *Geological Society, London, Petroleum Geology Conference series*, Geological Society of London.

Dooley, T. P., Hudec, M. R. & Jackson, M. P. (2012) The structure and evolution of sutures in allochthonous salt. *AAPG Bulletin.* 96 (6), 1045-1070.

Dooley, T. P., Jackson, M. P. & Hudec, M. R. (2009) Inflation and deflation of deeply buried salt stocks during lateral shortening. *Journal of Structural Geology.* 31 (6), 582-600.

Duffy, O. B., Dooley, T. P., Hudec, M. R., Fernandez, N., Jackson, C. A. L. & Soto, J. I. (2021) Principles of shortening in salt basins containing isolated minibasins. *Basin research.* 33 (3), 2089-2117.

Duffy, O. B., Dooley, T. P., Hudec, M. R., Jackson, M. P., Fernandez, N., Jackson, C. A. & Soto, J. I. (2018) Structural evolution of salt-influenced fold-and-thrust belts: a synthesis and new insights from basins containing isolated salt diapirs. *Journal of Structural Geology.* 114, 206-221.

Duffy, O. B., Fernandez, N., Hudec, M. R., Jackson, M. P., Burg, G., Dooley, T. P. & Jackson, C. A.-L. (2017) Lateral mobility of minibasins during shortening: Insights from the SE Precaspian Basin, Kazakhstan. *Journal of Structural Geology.* 97, 257-276.

Dumont, T. (1988) Late Triassic-early Jurassic evolution of the western Alps and of their European foreland; initiation of the Tethyan rifting. *Bulletin de la Société géologique de France.* 4 (4), 601-611.

Elliott, T., Apps, G., Davies, H., Evans, M., Ghibaudo, G. & Graham, R. (1985) *A structural and sedimentological traverse through the Tertiary foreland basin of the external Alps of south-east France*, *International Symposium on Foreland Basins. International Association of Sedimentologists, Excursion guide book, Fribourg*

Emre, T. (1977) Contribution à l'étude de quelques diapirs du S.-E. de la France. Alpes françaises du sud.

Evans, M. J. & Elliott, T. (1999) Evolution of a thrust-sheet-top basin: The Tertiary Barreme basin, Alpes-de-Haute-Provence, France. *Geological society of America bulletin.* 111 (11), 1617-1643.

Evans, M. J., Elliott, T., Apps, G. M. & Mange-Rajetzky, M. A. (2004) The Tertiary Grés de Ville of the Barrême basin: Feather edge equivalent to the Grés d'Annot? *Geological Society, London, Special Publications.* 221 (1), 97-110.

Evans, M. J. & Mange-Rajetzky, M. A. (1991) The provenance of sediments in the Barrême thrust-top basin, Haute-Provence, France. *Geological Society, London, Special Publications.* 57 (1), 323-342.

Ferrer, O., Roca, E., Muñoz, J. A., Rowan, M. G., Carrera, N. & Giles, K. A. (2017) *3-D Experimental Modeling of Megaflaps Developed During Differential Loading: Application to the Gulf of Mexico*, *AAPG Annual Convention and Exhibition*

Flinch, J. F. & Soto, J. I. (2017) Allochthonous Triassic and salt tectonic processes in the Betic-Rif orogenic arc. *Permo-Triassic Salt Provinces of Europe, North Africa and the Atlantic Margins*, Elsevier, pp. 417-446.

Flinch, J. F. & Soto, J. I. (2022) Structure and Alpine tectonic evolution of salt canopy in the western Betic Cordillera (Spain). *Marine and petroleum geology.* 105782.

Ford, M., Duchêne, S., Gasquet, D. & Vanderhaeghe, O. (2006) Two-phase orogenic convergence in the external and internal SW Alps. *Journal of the Geological Society.* 163 (5), 815-826.

Ford, M., Lickorish, W. & Kusznir, N. (1999) Tertiary foreland sedimentation in the Southern Subalpine Chains, SE France: a geodynamic appraisal. *Basin research.* 11 (4), 315-336.

Ford, M. & Lickorish, W. H. (2004) Foreland basin evolution around the western Alpine Arc. *Geological Society, London, Special Publications.* 221 (1), 39-63.

Fort, X., Brun, J.-P. & Chauvel, F. (2004) Salt tectonics on the Angolan margin, synsedimentary deformation processes. *AAPG Bulletin.* 88 (11), 1523-1544.

Fry, N. (1989) Southwestward thrusting and tectonics of the western Alps. *Geological Society, London, Special Publications.* 45 (1), 83-109.

Ganeval, J. (1973) Paléogéographie et tectonique dans la zone de décrochement de Creisset-Le Poil (Branche nord-ouest de l'arc de Castellane, Alpes de Haute Provence)-Alpes françaises. Université Scientifique et Médicale de Grenoble.

Gannaway Dalton, C. E., Giles, K. A., Muñoz, J. A. & Rowan, M. G. (2022) Interpreting the nature of the Aulet and Adons diapirs from sedimentologic and stratigraphic analysis of flanking minibasin strata, Spanish Pyrenees, Catalunya, Spain. *Journal of Sedimentary Research.* 92 (3), 167-209.

Ge, H., Jackson, M. P. & Vendeville, B. C. (1997) Kinematics and dynamics of salt tectonics driven by progradation. *AAPG Bulletin.* 81 (3), 398-423.

Ge, H. & Vendeville, B. C. (1997) Influence of active subsalt normal faults on the growth and location of suprasalt structures.

Gidon, M. (1997) Les chaînons subalpins au nord-est de Sisteron et l'histoire tectonique de la nappe de Digne. *Geologie Alpine.* 73, 23-57.

Gidon, M. & Pairis, J. (1992) Relations entre le charriage de la Nappe de Digne et la structure de son autochtone dans la vallée du Bès (Alpes de Haute-Provence, France). *Eclogae Geologicae Helvetiae.* 85 (2), 327-359.

Gigot, P., Grandjacquet, C. & Haccard, D. (1974) Evolution tectono-sedimentaire de la bordure septentrionale du bassin tertiaire de Digne depuis l'Eocene. *Bulletin de la Société géologique de France.* 7 (2), 128-139.

Giles, K. A. & Lawton, T. F. (2002) Halokinetic sequence stratigraphy adjacent to the El Papalote diapir, northeastern Mexico. *AAPG Bulletin.* 86 (5), 823-840.

Giles, K. A. & Rowan, M. G. (2012) Concepts in halokinetic-sequence deformation and stratigraphy. *Geological Society, London, Special Publications.* 363 (1), 7-31.

Goguel, J. (1937) Description tectonique de la bordure des Alpes de la Bléone au Var. Université de Paris.

Goguel, J. (1939) Tectonique des chaînes subalpines entre la Bléone et la Durance. Librairie polytechnique Ch. Béranger.

Goguel, J. (1963) L'interpretation de l'arc des Alpes occidentales. *Bulletin de la Société géologique de France.* 7 (1), 20-33.

Graham, R. (2022) *Allochthonous salt sheets in the external SW Alps*. Copernicus Meetings.

Graham, R., Brooke-Barnett, S., Csicsek, A., Lonergan, L., Célini, N., Callot, J. & Ringenbach, J. (2019) *Allochthonous salt in the fold and thrust belt of Haute Provence, SW Alps*, *81st EAGE Conference and Exhibition 2019*, European Association of Geoscientists & Engineers.

Graham, R. & Csicsek, A. (2020) *The Barreme Basin and the Gevaudan diapir-an example of the interplay between compressional tectonics and salt diapirism*, Copernicus Meetings.

Graham, R., Jackson, M., Pilcher, R. & Kilsdonk, B. (2012) Allochthonous salt in the sub-Alpine fold–thrust belt of Haute Provence, France. *Geological Society, London, Special Publications.* 363 (1), 595-615.

Granado, P., Roca, E., Strauss, P., Pelz, K. & Muñoz, J. A. (2019) Structural styles in fold-and-thrust belts involving early salt structures: The Northern Calcareous Alps (Austria). *Geology.* 47 (1), 51-54.

Grandjacquet, C. & Haccard, D. (1975) Analyse des sediments polygeniques neogenes a facies de cargneules associes a des gypses dans les Alpes du Sud; extension de ces facies au pourtour de la Mediterranee occidentale. *Bulletin de la Société géologique de France.* 7 (2), 242-259.

Gray, A. F. (1990) Carbonate Platform Margin Evolution in Response to Sea Level Changes: The Deposition and Diagenesis of the Calcaires Blancs De Provence. The University of Manchester (United Kingdom).

Grosheny, D., Ferry, S., Lécuyer, C., Thomas, A. & Desmares, D. (2017) The Cenomanian–Turonian Boundary Event (CTBE) on the southern slope of the Subalpine Basin (SE France) and its bearing on a probable tectonic pulse on a larger scale. *Cretaceous Research.* 72, 39-65.

Grosjean, A. S., Pittet, B., Gardien, V., Leloup, P. H., Mahéo, G. & Barraza Garcia, J. (2017) Tectonic heritage in drainage pattern and dynamics: the case of the French South Alpine Foreland Basin (ca. 45–20 Ma). *Basin research.* 29, 26-50.

Guérin-Desjardins, B. (1956) Synclinal tertiaire de Castellane (Basses-Alpes). Dipl. Et. sup., . Grenoble.

Gupta, S. (1999) Controls on sedimentation in distal margin palaeovalleys in the Early Tertiary Alpine foreland basin, south-eastern France. *Sedimentology.* 46 (2), 357-384.

Hallam, A. (2001) A review of the broad pattern of Jurassic sea-level changes and their possible causes in the light of current knowledge. *Palaeogeography, Palaeoclimatology, Palaeoecology.* 167 (1-2), 23-37.

Hamblin, W. (1965) Origin of “reverse drag” on the downthrown side of normal faults. *Geological society of America bulletin.* 76 (10), 1145-1164.

Handy, M. R., Schmid, S. M., Bousquet, R., Kissling, E. & Bernoulli, D. (2010) Reconciling plate-tectonic reconstructions of Alpine Tethys with the geological–geophysical record of spreading and subduction in the Alps. *Earth-Science Reviews.* 102 (3-4), 121-158.

Haq, B. U. (2014) Cretaceous eustasy revisited. *Global and Planetary change.* 113, 44-58.

Haq, B. U. (2018) Jurassic sea-level variations: a reappraisal. *GSA today.* 28 (1), 4-10.

Harrison, J. & Jackson, M. (2014) Exposed evaporite diapirs and minibasins above a canopy in central Sverdrup Basin, Axel Heiberg Island, Arctic Canada. *Basin research.* 26 (4), 567-596.

Hassanpour, J., Jahani, S., Ghassemi, M. R., Alavi, S. A. & Zeinali, F. (2018) Evolution of the Karebas Fault System and adjacent folds, central Zagros fold-and-thrust belt, Iran: Role of pre-existing halokinesis (salt structures and minibasins) and detachment levels. *Journal of Asian Earth Sciences.* 164, 125-142.

Hearon IV, T. E., Rowan, M. G., Lawton, T. F., Hannah, P. T. & Giles, K. A. (2015) Geology and tectonics of Neoproterozoic salt diapirs and salt sheets in the eastern Willouran Ranges, South Australia. *Basin research.* 27 (2), 183-207.

Hearon, T. E., Rowan, M. G., Giles, K. A. & Hart, W. H. (2014) Halokinetic deformation adjacent to the deepwater Auger diapir, Garden Banks 470, northern Gulf of Mexico: Testing the applicability of an outcrop-based model using subsurface data. *Interpretation.* 2 (4), SM57-SM76.

Hudec, M. R., Dooley, T. P., Burrel, L., Teixell, A. & Fernandez, N. (2021) An alternative model for the role of salt depositional configuration and preexisting salt structures in the evolution of the Southern Pyrenees, Spain. *Journal of Structural Geology.* 146, 104325.

Hudec, M. R. & Jackson, M. P. (2006) Advance of allochthonous salt sheets in passive margins and orogens. *AAPG Bulletin.* 90 (10), 1535-1564.

Hudec, M. R. & Jackson, M. P. (2007) Terra infirma: Understanding salt tectonics. *Earth-Science Reviews.* 82 (1-2), 1-28.

Hudec, M. R. & Jackson, M. P. (2009) Interaction between spreading salt canopies and their peripheral thrust systems. *Journal of Structural Geology.* 31 (10), 1114-1129.

Hudec, M. R. & Jackson, M. P. (2012) De Re Salica: Fundamental principles of salt tectonics. *Regional Geology and Tectonics: Phanerozoic Passive Margins, Cratonic Basins and Global Tectonic Maps*, Elsevier, pp. 18-41.

Hudec, M. R., Jackson, M. P. & Schultz-Ela, D. D. (2009) The paradox of minibasin subsidence into salt: Clues to the evolution of crustal basins. *Geological society of America bulletin.* 121 (1-2), 201-221.

Hudec, M. R., Jackson, M. P., Vendeville, B. C., Schultz-Ela, D. D. & Dooley, T. P. (2011) The salt mine: A digital atlas of salt tectonics. Bureau of Economic Geology The University of Texas at Austin.

Jackson, C. A., Kane, K. E. & Larsen, E. (2010) Structural evolution of minibasins on the Utsira High, northern North Sea; implications for Jurassic sediment dispersal and reservoir distribution.

Jackson, C. A. L., Duffy, O. B., Fernandez, N., Dooley, T. P., Hudec, M. R., Jackson, M. P. & Burg, G. (2020) The stratigraphic record of minibasin subsidence, Precaspian Basin, Kazakhstan. *Basin research.* 32 (4), 739-763.

Jackson, M. & Harrison, J. (2006) An allochthonous salt canopy on Axel Heiberg Island, Sverdrup Basin, Arctic Canada. *Geology.* 34 (12), 1045-1048.

Jackson, M. & Talbot, C. J. (1991) A glossary of salt tectonics. Bureau of Economic Geology, University of Texas at Austin.

Jackson, M. & Vendeville, B. (1994) Regional extension as a geologic trigger for diapirism. *Geological society of America bulletin.* 106 (1), 57-73.

Jackson, M. P., Cramez, C. & Fonck, J.-M. (2000) Role of subaerial volcanic rocks and mantle plumes in creation of South Atlantic margins: implications for salt tectonics and source rocks. *Marine and petroleum geology.* 17 (4), 477-498.

Jackson, M. P. & Hudec, M. R. (2017) Salt tectonics: Principles and practice. Cambridge University Press.

Jackson, M. P., Hudec, M. R., Jennette, D. C. & Kilby, R. E. (2008) Evolution of the Cretaceous Astrid thrust belt in the ultradeep-water Lower Congo Basin, Gabon. *AAPG Bulletin.* 92 (4), 487-511.

Jackson, M. P. & Talbot, C. J. (1986) External shapes, strain rates, and dynamics of salt structures. *Geological society of America bulletin.* 97 (3), 305-323.

Jackson, M. P. A. & Cramez, C. (1989) Seismic recognition of salt welds in salt tectonics regimes. *Gulf of Mexico salt tectonics, associated processes and exploration potential: Society of Economic Paleontologists and Mineralogists Gulf Coast Section, 10th annual research conference program and abstracts.* 66–71.

Jackson, M. P. A., Roberts, D. G. & Snelson, S. (1995) Salt Tectonics: A Global Perspective. American Association of Petroleum Geologists.

Jacqmin, A. (1950) Étude géologique de la Montagne de Teillon, près Castellane (Basses-Alpes). Université de Grenoble.

Jahani, S., Callot, J. P., Letouzey, J. & Frizon de Lamotte, D. (2009) The eastern termination of the Zagros Fold-and-Thrust Belt, Iran: Structures, evolution, and relationships between salt plugs, folding, and faulting. *Tectonics.* 28 (6).

Jahani, S., Hassanpour, J., Mohammadi-Firouz, S., Letouzey, J., de Lamotte, D. F., Alavi, S. A. & Soleimany, B. (2017) Salt tectonics and tear faulting in the central part of the Zagros Fold-Thrust Belt, Iran. *Marine and petroleum geology.* 86, 426-446.

Jobe, J. A. T., Giles, K. A., Hearon, T. E., Rowan, M. G., Trudgill, B., Dalton, C. E. G. & Jobe, Z. R. (2020) Controls on the structural and stratigraphic evolution of the megaflap-bearing Sinbad Valley salt wall, NE Paradox Basin, SW Colorado. *Geosphere.* 16 (1), 297-328.

Joseph, P. & Lomas, S. A. (2004) Deep-water sedimentation in the Alpine foreland basin of SE France: New perspectives on the Grès d'Annot and related systems—An introduction. *Geological Society, London, Special Publications.* 221 (1), 1-16.

Kerckhove, C. (1969) La "zone du Flysch" dans les nappes de l'Embrunais-Ubaye (Alpes occidentales). *Geologie Alpine*. 45, 5-204.

Kerckhove, C., Barfety, J. C., Bogdanoff, S., Lemoine, M., Carraro, F., Jorda, M., Monjuvent, G., Gidon, M. & Malaroda, R. (1980) Carte Géologique de la France, Gap (1:250 000). *Ministère de l'industrie, Service géologique national.*

Kerckhove, C. & Roux, M. (1976a) Carte Géologique de la France a 1/50000, Feuille de Castellane. *Bur. Rech. Geol. Min. Orleans, France.*

Kerckhove, C. & Roux, M. (1976b) Carte Géologique de la France a 1/50000, Notice explicative de la feuille de Castellane. *Bur. Rech. Geol. Min. Orleans, France.*

Kerckhove, C. & Roux, M. (1978a) Carte Géologique de la France a 1/50000, Feuille de Moustiers-Ste-Marie. *Bur. Rech. Geol. Min. Orleans, France.*

Kerckhove, C. & Roux, M. (1978b) Carte Géologique de la France a 1/50000, Notice explicative de la feuille de Moustiers-Ste-Marie. *Bur. Rech. Geol. Min. Orleans, France.*

Kergaravat, C., Ribes, C., Callot, J.-P. & Ringenbach, J.-C. (2017) Tectono-stratigraphic evolution of salt-controlled minibasins in a fold and thrust belt, the Oligo-Miocene central Sivas Basin. *Journal of Structural Geology.* 102, 75-97.

Kergaravat, C., Ribes, C., Legeay, E., Callot, J. P., Kavak, K. S. & Ringenbach, J. C. (2016) Minibasins and salt canopy in foreland fold-and-thrust belts: The central Sivas Basin, Turkey. *Tectonics.* 35 (6), 1342-1366.

Legeay, E., Ringenbach, J.-C. & Callot, J.-P. (2020a) *Along-Strike Variation of Halokinesis and Structural Inheritance Along the West African Salt Basin, South Atlantic*, *EGU General Assembly Conference Abstracts*

Legeay, E., Ringenbach, J.-C., Kergaravat, C., Pichat, A., Mohn, G., Vergés, J., Kavak, K. S. & Callot, J.-P. (2020b) Structure and kinematics of the Central Sivas Basin (Turkey): salt deposition and tectonics in an evolving fold-and-thrust belt. *Geological Society, London, Special Publications.* 490 (1), 361-396.

Lemoine, M., Bas, T., Arnaud-Vanneau, A., Arnaud, H., Dumont, T., Gidon, M., Bourbon, M., de Graciansky, P.-C., Rudkiewicz, J.-L. & Megard-Galli, J. (1986) The continental margin of the Mesozoic Tethys in the Western Alps. *Marine and petroleum geology.* 3 (3), 179-199.

Lemoine, M. & Trümpy, R. (1987) Pre-oceanic rifting in the Alps. *Tectonophysics.* 133 (3-4), 305-320.

Letouzey, J., Colletta, B., Vially, R. a. & Chermette, J. (1995) Evolution of salt-related structures in compressional settings.

Lickorish, W. H. & Ford, M. (1998) Sequential restoration of the external Alpine Digne thrust system, SE France, constrained by kinematic data and synorogenic sediments. *Geological Society, London, Special Publications.* 134 (1), 189-211.

Lopez-Mir, B., Muñoz, J. A. & García-Senz, J. (2015) Extensional salt tectonics in the partially inverted Cotiella post-rift basin (south-central Pyrenees): structure and evolution. *International Journal of Earth Sciences.* 104 (2), 419-434.

Manatschal, G. (2004) New models for evolution of magma-poor rifted margins based on a review of data and concepts from West Iberia and the Alps. *International Journal of Earth Sciences.* 93 (3), 432-466.

Manatschal, G. & Chenin, P. (2023) Fossil rifted margins in the Alps. *Geological Field Trips and Maps. Journal of the Italian Geological Society and of the Geological Survey of Italy.* 15 (1.2), 1-207.

Manatschal, G., Engström, A., Desmurs, L., Schaltegger, U., Cosca, M., Müntener, O. & Bernoulli, D. (2006) What is the tectono-metamorphic evolution of continental break-up: the example of the Tasna Ocean–Continent Transition. *Journal of Structural Geology.* 28 (10), 1849-1869.

Manatschal, G. & Müntener, O. (2009) A type sequence across an ancient magma-poor ocean–continent transition: the example of the western Alpine Tethys ophiolites. *Tectonophysics.* 473 (1-2), 4-19.

Marton, L. G., Tari, G. C. & Lehmann, C. T. (2000) Evolution of the Angolan passive margin, West Africa, with emphasis on post-salt structural styles. *Geophysical Monograph-American Geophysical Union.* 115, 129-150.

Mascle, G., Arnaud, H., Dardeau, G., Debelmas, J., Delpech, P.-Y., Dubois, P., Gidon, M., de Graciansky, P.-C., Kerckhove, C. & Lemoine, M. (1988) Salt tectonics, Tethyan rifting and Alpine folding in the French Alps. *Bulletin de la Société géologique de France.* 4 (5), 747-758.

Mascle, G., Arnaud, H., Dardeau, G., Debelmas, J. & Dubois, P. (1986) Halocinèse précoce sur la marge téthysienne alpine: vers une réinterprétation des zones de gypse des Alpes. *Comptes rendus*

de l'Académie des sciences. Série 2, Mécanique, Physique, Chimie, Sciences de l'univers, Sciences de la Terre. 302 (15), 963-968.

Masse, J.-P., Villeneuve, M., Leonforte, E. & Nizou, J. (2009) Block tilting of the North Provence early Cretaceous carbonate margin: stratigraphic, sedimentologic and tectonic data. *Bulletin de la Société géologique de France.* 180 (2), 105-115.

Ménard, G. (1979) Relations entre structures profondes et structures superficielles dans le sud-est de la France. Essai d'utilisation de données géophysiques. PhD diss. Universite Scientifique et Medicale de Grenoble.

Mennessier, G. (1959) Étude tectonique des confins alpino-provençaux entre le Verdon et l'Argens. n° 87 edn. Bull. Soc. Géol. Fr, Société géologique de France.

Mohn, G., Manatschal, G., Beltrando, M. & Haupert, I. (2014) The role of rift-inherited hyper-extension in Alpine-type orogens. *Terra Nova.* 26 (5), 347-353.

Mohn, G., Manatschal, G., Müntener, O., Beltrando, M. & Masini, E. (2010) Unravelling the interaction between tectonic and sedimentary processes during lithospheric thinning in the Alpine Tethys margins. *International Journal of Earth Sciences.* 99, 75-101.

Morin, D., Catherine, L., Fontugne, M. & Guiomar, M. (2004) *Aux origines de l'extraction du sel en Europe (VIe millénaire av. JC), La source salée de Moriez-Alpes-de-Haute-Provence*, *XXVIe congrès préhistorique de France*, *Avignon*

Nelson, T. H. (1989) Style of salt diapirs as a function of the stage of evolution and the nature of the encasing sediments. *Society of Economic Paleontologists and Mineralogists Gulf Coast Section, 10th annual research conference program and abstracts.* 109-110.

Nilsen, K. T., Vendeville, B. C. & Johansen, J.-T. (1995) Influence of regional tectonics on halokinesis in the Nordkapp Basin, Barents Sea.

Pairis, J. (1971) Tectonique et sedimentation tertiaire sur la marge orientale du bassin de Barreme (Alpes de Haute-Provence). *Geologie Alpine.* 47 (2), 203-214.

Pairis, J. L. (1988) Paléogène marin et structuration des Alpes Occidentales françaises (domaine externe et confins sud-occidentaux du subbriançonnais). Université Joseph-Fourier-Grenoble I.

Pedrera, A., Ruiz-Constán, A., García-Senz, J., Azor, A., Marín-Lechado, C., Ayala, C., de Neira, J. A. D. & Rodríguez-Fernández, L. R. (2020) Evolution of the South-Iberian paleomargin: From hyperextension to continental subduction. *Journal of Structural Geology.* 138, 104122.

Picard, P. (1965) Contribution à l'étude géologique du chainon de la Bernarde au NE de Castellanne (Basses Alpes) _ feuilles au 1/20000° Castellanne 1-2. Université de Grenoble.

Pilcher, R. S., Kilsdonk, B. & Trude, J. (2011) Primary basins and their boundaries in the deep-water northern Gulf of Mexico: Origin, trap types, and petroleum system implications. *AAPG Bulletin.* 95 (2), 219-240.

Rameil, N. (2005) Carbonate sedimentology, sequence stratigraphy, and cyc-lostratigraphy of the Tithonian in the Swiss and French Jura Mountains: a high-resolution record of changes in sea level and climate. PhD. Université de Fribourg.

Ribes, C., Kergaravat, C., Bonnel, C., Crumeyrolle, P., Callot, J. P., Poisson, A., Temiz, H. & Ringenbach, J. C. (2015) Fluvial sedimentation in a salt-controlled mini-basin: stratal patterns and facies assemblages, Sivas Basin, Turkey. *Sedimentology.* 62 (6), 1513-1545.

Ribes, C., Kergaravat, C., Crumeyrolle, P., Lopez, M., Bonnel, C., Poisson, A., Kavak, K. S., Callot, J. P. & Ringenbach, J. C. (2017) Factors controlling stratal pattern and facies distribution of fluvio-lacustrine sedimentation in the Sivas mini-basins, Oligocene (Turkey). *Basin research.* 29, 596-621.

Ringenbach, J.-C., Kergaravat, C., Ribes, C., Pichat, A., Legeay, E., Salel, J. & Callot, J. (2017) *Salt Tectonics in the Sivas Basin (Turkey): Outstanding Seismic Analogues*, *AAPG/SEG International Conference & Exhibition*

Ringenbach, J.-C., Salel, J.-F., Kergaravat, C., Ribes, C., Bonnel, C. & Callot, J.-P. (2013) Salt tectonics in the Sivas Basin, Turkey: Outstanding seismic analogues from outcrops. *First Break.* 31 (6), 93-101.

Rouire, J., Bodelle, J., Bordet, P., Autran, A., Beaudoin, B., Gidot, P., Haccard, D., Lemoine, M., Gennesseaux, M., Blanc, J. & Bellaiche, G. (1979) Carte Géologique de la France, Nice (1:250 000). *Ministère de l'industrie, Service géologique national.*

Roux, M. (1968) Etude géologique du massif des Cadières de Brandis, à l'Ouest de Castellane. *Géologie Alpine, t.* 44, 339-352.

Roux, M. (1970) Le synclinal de Taulanne (Basses-Alpes) et les conséquences du chevauchement de Castellane sur sa bordure nord-est. *Geologie Alpine.* 46, 177-188.

Roux, M. (1972) Etude tectonique des chaînons subalpins entre Majastres et Castellane (Alpes-de-Haute-Provence). *Geologie Alpine.* 48, 187-199.

Roux, M., Bourseau, J.-P., Bas, T., Dumont, T., de Graciansky, P.-C., Lemoine, M. & Rudkiewicz, J.-L. (1988) Bathymetric evolution of the Tethyan margin in the Western Alps (data from stalked crinoids); a reappraisal of eustatism problems during the Jurassic. *Bulletin de la Société géologique de France.* 4 (4), 633-641.

Rowan, M., Hearon Iv, T., Kernen, R., Giles, K., Gannaway-Dalton, C., Williams, N., Fiduk, J., Lawton, T., Hannah, P. & Fischer, M. (2020) A review of allochthonous salt tectonics in the Flinders and Willouran ranges, South Australia. *Australian Journal of Earth Sciences.* 67 (6), 787-813.

Rowan, M. G. (2002) Salt-related accommodation in the Gulf of Mexico deepwater: Withdrawal or inflation, autochthonous or allochthonous? *Gulf Coast Association of Geological Societies Transactions.* 52, 861–869.

Rowan, M. G. (2017) An overview of allochthonous salt tectonics. *Permo-Triassic Salt Provinces of Europe, North Africa and the Atlantic Margins.* 97-114.

Rowan, M. G. & Giles, K. A. (2021) Passive versus active salt diapirism. *AAPG Bulletin.* 105 (1), 53-63.

Rowan, M. G. & Giles, K. A. (2023) Different scales of salt–sediment interaction during passive diapirism. *AAPG Bulletin.* 107 (1), 7-22.

Rowan, M. G., Giles, K. A., Hearon IV, T. E. & Fiduk, J. C. (2016) Megaflaps adjacent to salt diapirs. *AAPG Bulletin.* 100 (11), 1723-1747.

Rowan, M. G., Giles, K. A., Hearon, T. E., Gannaway, C. E. & Fiduk, J. C. (2014) *Megaflaps along the edges of steep diapirs and beneath salt sheets: Models and examples*, *International Conference & Exhibition*

Rowan, M. G., Jackson, M. P. & Trudgill, B. D. (1999) Salt-related fault families and fault welds in the northern Gulf of Mexico. *AAPG Bulletin.* 83 (9), 1454-1484.

Rowan, M. G., Lawton, T. F. & Giles, K. A. (2012) Anatomy of an exposed vertical salt weld and flanking strata, La Popa Basin, Mexico. *Geological Society, London, Special Publications.* 363 (1), 33-57.

Rowan, M. G., Lawton, T. F., Giles, K. A. & Ratliff, R. A. (2003) Near-salt deformation in La Popa basin, Mexico, and the northern Gulf of Mexico: A general model for passive diapirism. *AAPG Bulletin.* 87 (5), 733-756.

Rowan, M. G. & Ratliff, R. A. (2012) Cross-section restoration of salt-related deformation: Best practices and potential pitfalls. *Journal of Structural Geology.* 41, 24-37.

Rowan, M. G. & Vendeville, B. C. (2006) Foldbelts with early salt withdrawal and diapirism: Physical model and examples from the northern Gulf of Mexico and the Flinders Ranges, Australia. *Marine and petroleum geology.* 23 (9-10), 871-891.

Santolaria, P., Granado, P., Wilson, E., de Matteis, M., Ferrer, O., Strauss, P., Pelz, K., König, M., Oteleanu, A. & Roca, E. (2022) From Salt-Bearing Rifted Margins to Fold-And-Thrust Belts. Insights

From Analog Modeling and Northern Calcareous Alps Case Study. *Tectonics.* 41 (11), e2022TC007503.

Saura, E., Ardèvol i Oró, L., Teixell, A. & Vergés, J. (2016) Rising and falling diapirs, shifting depocenters, and flap overturning in the Cretaceous Sopeira and Sant Gervàs subbasins (Ribagorça Basin, southern Pyrenees). *Tectonics.* 35 (3), 638-662.

Schmid, S. & Kissling, E. (2000) The arc of the western Alps in the light of geophysical data on deep crustal structure. *Tectonics.* 19 (1), 62-85.

Schmid, S. M., Fügenschuh, B., Kissling, E. & Schuster, R. (2004) Tectonic map and overall architecture of the Alpine orogen. *Eclogae Geologicae Helvetiae.* 97 (1), 93-117.

Schultz-Ela, D. D. (2003) Origin of drag folds bordering salt diapirs. *AAPG Bulletin.* 87 (5), 757-780.

Schultz-Ela, D. D., Jackson, M. P. & Vendeville, B. (1993) Mechanics of active salt diapirism. *Tectonophysics.* 228 (3-4), 275-312.

Schwartz, S., Gautheron, C., Audin, L., Dumont, T., Nomade, J., Barbarand, J., Pinna-Jamme, R. & van der Beek, P. (2017) Foreland exhumation controlled by crustal thickening in the Western Alps. *Geology.* 45 (2), 139-142.

Schwartz, S., Guillot, S., Tricart, P., Bernet, M., Jourdan, S., Dumont, T. & Montagnac, G. (2012) Source tracing of detrital serpentinite in the Oligocene molasse deposits from the western Alps (Barrême basin): implications for relief formation in the internal zone. *Geological Magazine.* 149 (5), 841-856.

Séranne, M. (1999) The Gulf of Lion continental margin (NW Mediterranean) revisited by IBS: an overview. *Geological Society, London, Special Publications.* 156 (1), 15-36.

Sinclair, H., Sayer, Z. & Tucker, M. (1998) Carbonate sedimentation during early foreland basin subsidence: the Eocene succession of the French Alps. *Geological Society, London, Special Publications.* 149 (1), 205-227.

Sonnette, L., Humbert, F., Aubourg, C., Gattacceca, J., Lee, J.-C. & Angelier, J. (2014) Significant rotations related to cover–substratum decoupling: Example of the Dôme de Barrôt (Southwestern Alps, France). *Tectonophysics.* 629, 275-289.

Soto, J. I., Flinch, J. & Tari, G. (2017) Permo-Triassic Salt Provinces of Europe, North Africa and the Atlantic Margins, Tectonics and Hydrocarbon Potential. Elsevier.

Stampfli, G., Mosar, J., Marquer, D., Marchant, R., Baudin, T. & Borel, G. (1998) Subduction and obduction processes in the Swiss Alps. *Tectonophysics.* 296 (1-2), 159-204.

Stewart, S. (2007) Salt tectonics in the North Sea Basin: a structural style template for seismic interpreters.

Strauss, P., Granado, P. & Muñoz, J. A. (2021) Subsidence analysis of salt tectonics-driven carbonate minibasins (Northern Calcareous Alps, Austria). *Basin research.* 33 (2), 968-990.

Suppe, J., Sàbat, F., Munoz, J. A., Poblet, J., Roca, E. & Vergés, J. (1997) Bed-by-bed fold growth by kink-band migration: Sant Llorenç de Morunys, eastern Pyrenees. *Journal of Structural Geology.* 19 (3-4), 443-461.

Sztrákos, K. & du Fornel, É. (2003) Stratigraphie, paléoécologie et foraminifères du paléogène des Alpes Maritimes et des Alpes de Haute-Provence (Sud-Est de la France). *Revue de micropaléontologie.* 46 (4), 229-267.

Tari, G., Molnar, J. & Ashton, P. (2003) Examples of salt tectonics from West Africa: a comparative approach. *Geological Society, London, Special Publications.* 207 (1), 85-104.

Tavani, S., Bertok, C., Granado, P., Piana, F., Salas, R., Vigna, B. & Muñoz, J. (2018) The Iberia-Eurasia plate boundary east of the Pyrenees. *Earth-Science Reviews.* 187, 314-337.

Teixell, A., Barnolas, A., Rosales, I. & Arboleya, M.-L. (2017) Structural and facies architecture of a diapir-related carbonate minibasin (lower and middle Jurassic, High Atlas, Morocco). *Marine and petroleum geology.* 81, 334-360.

Trudgill, B. (2011) Evolution of salt structures in the northern Paradox Basin: Controls on evaporite deposition, salt wall growth and supra-salt stratigraphic architecture. *Basin research.* 23 (2), 208-238.

Van Der Beek, P. A., Valla, P. G., Herman, F., Braun, J., Persano, C., Dobson, K. J. & Labrin, E. (2010) Inversion of thermochronological age–elevation profiles to extract independent estimates of denudation and relief history—II: Application to the French Western Alps. *Earth and Planetary Science Letters.* 296 (1-2), 9-22.

Vendeville, B. & Jackson, M. (1992a) The fall of diapirs during thin-skinned extension. *Marine and petroleum geology.* 9 (4), 354-371.

Vendeville, B. C. & Jackson, M. P. (1992b) The rise of diapirs during thin-skinned extension. *Marine and petroleum geology.* 9 (4), 331-354.

Warrak, M. (1974) The petrography and origin of dedolomitized, veined or brecciated carbonate rocks, the ‘cornieules’, in the Fréjus region, French Alps. *Journal of the Geological Society.* 130 (3), 229-245.

Warren, J. K. (2016) Evaporites: A geological compendium. Springer.

Worrall, D. & Snelson, S. (1989) Evolution of the northern Gulf of Mexico. *The geology of North America; an overview: Geological Society of America, v. A*. 97-138.

Zurcher, P. (1895) Notes sur la structure de divers points de la région de Castellane. *Bulletin de la Société géologique de France.* 23 (ser. 3), 938-951.